Late Quaternary palaeoenvironments of the southern Cape, South Africa: palynological evidence from three coastal wetlands

Lynne Julia Quick

Thesis Presented for the Degree of

DOCTOR OF PHILOSOPHY

in the Department of Environmental and Geographical Science

UNIVERSITY OF CAPE TOWN

February 2013

Late Quaternary palaeoenvironments of the southern Cape, South Africa: palynological evidence from three coastal wetlands

Lynne Julia Quick

Thesis Presented for the Degree of

DOCTOR OF PHILOSOPHY

in the Department of Environmental and Geographical Science

UNIVERSITY OF CAPE TOWN

February 2013

Abstract

Despite significant advances in palaeoenvironmental research in southern Africa, the late Quaternary palaeoenvironmental history of the region remains incomplete as palaeoclimatic proxy records are temporally and spatially discontinuous. The southern Cape is a key focus area within this region as it encompasses the Fynbos Biome, a global biodiversity hotspot, as well as rare Afrotemperate forest patches and is therefore of great botanical importance. As this area includes the transition from southern Africa's winter rainfall zone to the year-round rainfall zone, it is also important from a climatic perspective.

Palynological records were generated for three coastal wetlands situated on the southern Cape coast plain (SCCP). The sediment core records from vleis at Pearly Beach and Rietvlei Still Bay span ~25 and ~36 ka respectively. Assessed in conjunction with plant biomarker, sedimentological, geochemical and charcoal data, these pollen sequences indicate distinct changes in late Pleistocene and Holocene palaeoenvironments. For example, decreased moisture availability at ~36 ka within the eastern SCCP and from ~22 – 21.5 ka within the western SCCP were identified whereas relatively wetter conditions characterised the whole of the SCCP during the early Holocene. Correlations to changes in Antarctic sea ice presence and its influence on the latitudinal position and/or intensity of the westerly wave belt provides a mechanism for the observed environmental changes during these periods. Further to the east is Vankervelsvlei, a small ombrotrophic depression which is an example of a *schwingmoor* or floating bog, a geomorphological feature that is very rarely found in the Southern Hemisphere. The site is situated in the year-round rainfall zone and is located at the ecotone between the Fynbos Biome and Knysna Afrotemperate Region. A 4 m organic-rich sediment core has yielded a near-basal OSL age of 120 ka. The pollen record exhibits marked changes in forest and fynbos taxa, indicating that there was a greater dominance of afrotemperate forests at the site during the period ~116 – 94 ka. Due to the virtual absence of terrestrial palaeoenvironmental data from the southern Cape covering Marine Isotope Stages five to three, the Vankervelsvlei record represents a particularly important new archive. The variations within this record clearly suggest that glacial-interglacial cycles had a strong impact on the region's vegetation history and climate. In addition, the record has identified discrete periods within which palaeoenvironmental conditions appear to deviate from those associated with the marine isotope stages, providing new insights into the finer-scale climatic and ecological changes within this ecotonal region.

This multi-proxy study provides important insights into the palaeoecology of lowland fynbos, the nature of palaeoenvironmental change on the southern Cape coastal plain and reveals a uniquely extensive palynological record for the Knysna Afrotemperate Region.

Acknowledgements

First and foremost, many thanks are due to my supervisors Mike Meadows and Brian Chase. They have provided a great deal of advice and support to me thoughout the last few years, and without their enthusiasm and passion for palaeoenvironmental research, this thesis and my academic career would not be in existence.

I would also like to thank Mike and Brian for their excellent editorial skills and for all the constructive criticism that has greatly improved the quality of this thesis. I owe thanks to PAST (Palaeontological Scientific Trust), the University of Cape Town's Postgraduate Funding Office and the Bundesministerium für Bildung und Forschung (BMBF) (some of this work forms part of a bilateral - South African/German - project between the University of Cape Town and Friedrich Schiller University of Jena) for generously funding various parts of this reseach. In addition, the financial assistance of the National Research Foundation (NRF) towards this research is hereby acknowledged.

I am very grateful to Andy Carr for collaborating with me and for generating a large quantity of geochemical and plant biomarker data amazingly quickly! This thesis has benefitted significantly from the inferences drawn from this data. Many thanks also go to Mark Bateman who provided the OSL ages for the Vankervelsvlei core. These ages played an instrumental role in the establishment of what has turned out to be a uniquely extensive palynological record.

To my office mates and all my departmental friends and colleagues: thanks for the valuable company, moral support and generally for making the last few years in the EGS department so enjoyable. Special mention needs to be made for Kelly Kirsten, who as a fellow palaeo PhD student has supported me tremendously throughout this endeavour. Thanks also to Jemma Finch and Jared Lodder, fellow pollen people, for the guidance and advice.

Lastly and most importantly, thanks to my mother and brother for their unconditional support and encouragement throughout it all! This thesis is dedicated to my father who fostered my love for Geography and southern African environments.

Lynne Quick
7 February 2013

Table of Contents

List of Figures

List of Tables

1. Introduction

1.1 Quaternary environmental change and the role of southern Africa palaeoenvironments

With the possibility of significant environmental change occurring in the near future, there is a great need to optimise our understanding of the spatial and temporal complexities of both climatic and ecological change. Palaeoenvironmental data contribute to and enhance the theory behind climate dynamics and the responses of biota to these changes and can help to provide a basis for the sustainable management of ecosystems (Meadows, 2001; Lovejoy and Hannah, 2005; Jansen et al., 2007; Meadows, 2012). In addition, palaeoenvironmental inputs into climate models are essential as they can significantly reduce uncertainties within these models; therefore contributing to an improved framework for strategic planners in their efforts to mitigate impacts upon society (IPCC, 2007).

The Quaternary[1] is an important phase in the earth's geological history as it represents the most recent time period and is characterised by high climate variability with large-scale global changes occurring at frequencies of thousands to hundreds of thousands of years (Williams et al., 1998). Unravelling the details of Quaternary environmental change helps to develop a better understanding of the interrelationships of the atmosphere, hydrosphere, biosphere and cryosphere. It provides crucial data and validation for conceptual climate models and allows for the analysis of the roles of earth system processes and orbital forcing mechanisms and controls. Quaternary environmental changes represent the best analogues available for the understanding of present changes and therefore knowledge of the mechanisms for environmental change during this period is a prerequisite for modelling future change.

To this extent, the Northern Hemisphere's Quaternary palaeoenvironmental history has been relatively well-established due to the volume of research conducted over many decades producing an abundance of published papers and datasets. In contrast, palaeoenvironmental evidence for southern Africa remains frustratingly incomplete as palaeoclimatic proxy records are scarce and often discontinuous (Meadows and Baxter, 1999; Chase and Meadows, 2007). Consequently, current palaeoenvironmental data from southern Africa are neither sufficient nor robust enough in terms of

[1] The Quaternary represents the last 2.6 million years (Pillans and Naish, 2004) Although it should be noted that there has been much debate about the exact timing and status of the Quaternary within the geological time scale.

its temporal and spatial resolution to validate long-term climatic projections. Therefore, there is a pressing need for the establishment of new palaeoenvironmental records as well as the re-examination of existing records within this region. Furthermore, the significant advances and refinements in palaeoenvironmental and palaeoecological methodologies that have occurred have mainly been applied to the Northern Hemisphere (e.g. MacDonald et al., 2008). This has resulted in a data set that is spatially unrepresentative of the dynamics of global Quaternary change.

It has been proposed that Southern Hemisphere millennial-scale climate change leads changes in the Northern Hemisphere (e.g. Charles et al., 1996; Blunier et al., 1998; Blunier and Brook, 2001; Chiang et al., 2003; Wunsch, 2003; Chiang and Bitz, 2005; Wyrwoll et al., 2012) suggesting that Southern Hemisphere dynamics potentially act as triggers for glacial-interglacial global-scale climatic and environmental changes. Though the above statement is still a subject of great debate, the fact that southern Africa is influenced by a wide variety of atmospheric and oceanic circulation systems, and therefore occupies an integral position within the Southern Hemisphere, further stresses the importance and relevance of palaeoenvironmental research in this region (Chase and Meadows, 2007).

From an anthropogenic standpoint, southern Africa is extremely important as it is the geographical locality for the speciation events that culminated in the evolution of anatomically and indeed behaviourally modern humans (Marean et al., 2007b; Brown et al., 2009). Determining the environmental context for these events is an essential tool to understand and explain human evolution, behaviour and dispersal patterns (c.f. Blome et al., 2012; Maslin and Christensen, 2007 in Thomas and Burrough, 2012) . This is especially the case for the southern Cape coast due to its rich archaeological history and the fact that modern humans are thought to have originated from this area (e.g. Marean et al., 2007b; Brown et al., 2009; Marean, 2010; Brown et al., 2012).

1.2 The southern Cape coastal plain

Extending from the Bot River (~70 km south east of Cape Town) to Plettenberg Bay and bounded by the Cape Fold Belt mountains, the coastal lowlands that constitute the southern Cape coastal plain (SCCP, Chapter 2) represents the southernmost region of the African continent and encompasses a significant portion of the Fynbos Biome (Figure 1.1). The SCCP not only includes fynbos vegetation types but also encompasses portions of the Albany Thicket Biome and rare afrotemperate forests patches and therefore the SCCP has great significance from a botanical perspective.

The area occupied by the Fynbos Biome (*sensu* Mucina and Rutherford, 2006) is a key focus area within southern Africa as it is recognised as being a global biodiversity hotspot (Myers et al., 2000). It has been predicted that with future climate change major shifts in vegetation distributions are likely to occur which may threaten the high levels of species richness and endemism found within this biome (Hannah et al., 2002; Midgley et al., 2002; Pyke et al., 2005). These predictions are based on the outputs of various bioclimatic models (e.g. Midgley et al., 2002; Midgley et al., 2003) which require the use of palaeobotanical data to test the strength of the projections and validate the climate-vegetation hypotheses inherent within these models. However, the late Quaternary palaeoenvironmental history of this area has yet to be fully established due to the limited number of well-dated published records as well as the discontinuous temporal nature of these records (refer to Chapter 3). For a more complete assessment and possible improvement of these models, additional palaeoenvironmental (especially palynological) data is required to quantify the nature and timing of vegetation shifts (Midgley et al., 2001).

As the SCCP presently encompasses portions of both the year-round and winter rainfall zones (*sensu* Chase and Meadows, 2007; Figure 2.6) and is influenced by tropical and temperate climate dynamics, there is also a great need to understand the extent of past changes in the seasonality of rainfall within this region and its bearing on vegetation change. Therefore due to its botanical importance in terms of biodiversity and its high conservation status as well as its key climatic location within southern Africa, the environmental history of the SCCP needs to be further resolved.

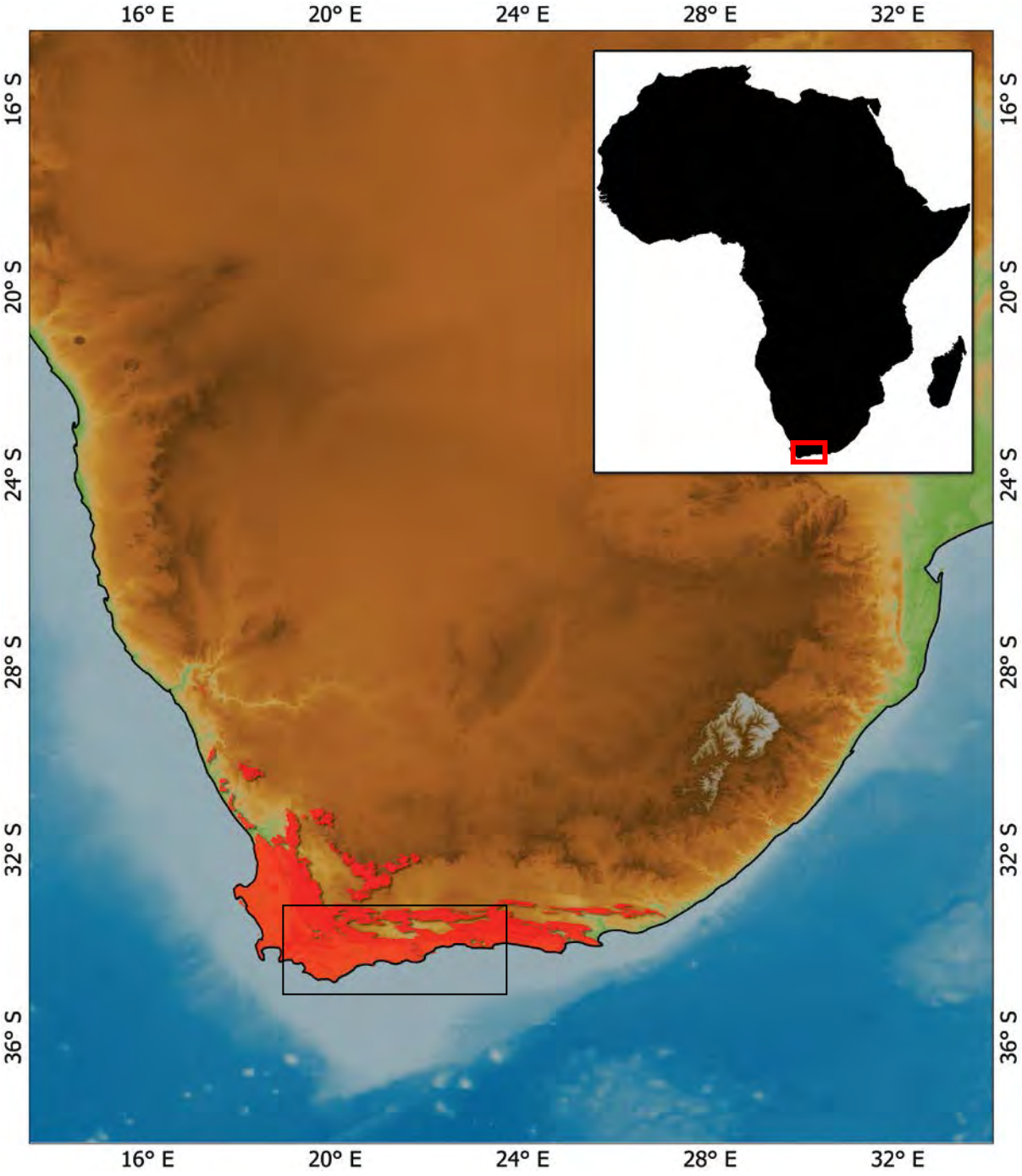

Figure 1.1 The location of the southern Cape coastal plain (thick red and thin black boxes) and the Fynbos Biome (red shaded area) [bathymetry and topography data source: GEBCO www.gebco.com].

Recent work (Quick, 2009; Quick et al., 2011) made use of hyrax middens found in the Cederberg Mountains within the north-western reaches of the Fynbos Biome as a palaeoenvironmental archive. The stable carbon and nitrogen isotope records and pollen data derived from this midden site were able to significantly enhance our understanding of the climatic and ecological changes that occurred during the last 28 000 years within the western mountainous region of the Fynbos Biome. However

very little palaeoenvironmental evidence is currently available for the coastal lowland regions such as the SCCP, which encompass vegetation communities that potentially are more sensitive to environmental change (c.f. Quick et al., 2011). The discrepancy between the relatively rich archaeological record and the dearth of palaeoenvironmental sites located on the SCCP, further stresses the significance of the establishment of new records.

It is often stated that late Quaternary palynological investigations in southern Africa are severely restricted due to the scarcity of suitable environments, such as peat bogs, lakes and wetlands for the accumulation of organic sediments that favour the preservation of pollen grains and other palaeoenvironmental proxy sources (Meadows and Baxter, 1999; Chase and Meadows, 2007). In contrast, several wetland deposits have been identified on the SCCP and, accordingly, the potential for further palaeoenvironmental research in this region is considerable. This study endeavours to expand (both spatially and temporally) the overall palaeoenvironmental record for the SCCP by the establishment of new multi-proxy palaeoenvironmental records and through the critical assessment of previously explored sites within the region. Through the analysis of these sites, it becomes possible to investigate the relationship between changing rainfall seasonality and fynbos vegetation dynamics as well as the different responses of particular vegetation types (fynbos and non-fynbos communities) to environmental changes.

In summary, three factors exemplify the significance of the findings that emanate from this research:

- Greater understanding of the contemporary environments and palaeoenvironments of the southern Cape coastal plain.
- Climatic and palaeobotanical context for understanding the biodiversity found on the southern Cape coastal plain.
- Improved understanding of regional climate dynamics and therefore an improved understanding of potential impacts of predicted climate change on biota.

1.3 Research questions

This thesis engages with the following key research questions:

- What ecological and environmental changes have occurred across the SCCP during the late Quaternary?
- How have climates changed within the SCCP during the late Quaternary and what has been the timing, structure and underlying mechanisms of these changes?

- How do the vegetation histories, as revealed by pollen analysis, compare to previously and presently studied palaeoenvironmental records in the region?
- What might these ecological changes mean in terms of climate change (present and future predictions for the SCCP and the Fynbos Biome)?

1.4 Thesis aim and specific objectives

Multiple lines of proxy evidence per site are analysed, since a multi-proxy approach represents the most rigorous means for the comprehensive understanding of palaeoenvironmental change at both local and regional scales and reduces the interpretative difficulties and relative sensitivities encountered at the individual proxy level.

The primary aim of this study is to investigate the vegetation dynamics and associated environmental conditions on the southern Cape coastal plain over the late Quaternary through the application of pollen analysis.

The following are presented as specific objectives:

- Identify and sample suitable sediment cores within the boundaries of the southern Cape coastal plain;
- Sub-sample deposits in order to establish:
    - accurate high resolution chronologies
    - palynological records of vegetation community changes over time
    - charcoal records to investigate fire regimes within fynbos communities over time
    - sedimentological and bulk geochemical records to provide details relating to the depositional environments of the sediment cores and insights into the nature of the vegetation at the sites
- Reconstruct the palaeoenvironmental conditions for the study sites using the conclusions drawn from the above analyses and use these reconstructions to contribute to the presently limited palaeoenvironmental history of the region.
- Evaluate the conclusions and interpretations drawn from the above analyses by assessing them against the backdrop of previous and presently studied palaeoenvironmental records for the region.
- Place the findings of this study within the broader context of southern African palaeoenvironmental research.

1.5 Thesis structure

Chapter two introduces and defines the southern Cape coastal plain, detailing its geological, geomorphological, climatic and ecological characteristics and therefore provides the contemporary environmental context for this research. Interpretations of palaeoenvironmental evidence from the SCCP is complex due to the high degrees of climatic and ecological heterogeneity (outlined in Chapter two), therefore interpolations beyond the site level cannot always reliably be applied to regional syntheses. A thorough review of the available late Quaternary palaeoenvironmental evidence from the SCCP and neighbouring regions is the focus of Chapter three. Hypotheses relating to the climatic mechanisms responsible for the documented changes are also presented in Chapter three. Chapter four outlines the approach taken in sampling sites on the SCCP. The technique employed in the field to sample these sites is described together with the nature of the specific types of palaeoenvironmental archives found at the sites. The theoretical underpinnings as well as the practical laboratory techniques of the selected palaeoenvironmental proxies, namely; pollen, charcoal, sedimentological, geochemical and geochronological analyses are also outlined in Chapter four. Chapter five presents the results of the multi-proxy analyses; the stratigraphic and sedimentological properties of the cores are described, the chronological results and age models are given and the palynological, microscopic charcoal and geochemical analyses are displayed and described. Interpretation of the new palaeoenvironmental evidence (presented in Chapter five) is the focus of Chapter six. Specific elements largely pertaining to fynbos ecology, which are used to interpret the records, are initially presented, followed by discussions of the overall palaeoenvironmental records for Pearly Beach, Rietvlei Still Bay and Vankervelsvlei. The new palaeoenvironmental information generated for this study is then assessed in relation to the established southern Cape palaeoenvironmental record as well as regional and hemispheric climate change proxies. Chapter seven provides a summary of key findings and general research conclusions, reflects on the aims and objectives of the study and the extent to which they have been achieved and identifies potential future avenues for research in the region.

2. Contemporary southern Cape environments

2.1 Introduction

An understanding of various aspects of the contemporary environments of the southern Cape coastal plain, particularly the role that geology, climate and ecological factors have played in influencing vegetation type and distribution, is essential for creating an environmental context for the study, upon which the palaeoenvironmental evidence can be critically assessed. Details of the local sampling site characteristics are then provided in Chapter 4.

2.2 The southern Cape coastal plain

For the purposes of this study, the southern Cape coastal plain (SCCP) is defined here as the coastal lowlands extending from the Bot River mouth (34° 21.995'S; 19° 6.008'E) in the west to Plettenberg Bay (34° 3.825'S; 23° 21.608'E) in the east and bounded to the north by the mountain ranges of the Cape Fold Belt (Figure 2.1). The geology, atmospheric and oceanic systems, as well as the broad geomorphological features of the SCCP, are outlined below. The vegetation types and ecological considerations of their distributions are discussed within the framework of three botanically-significant subregions of the SCCP, namely the Agulhas Plain (Figure 2.1 A), the Riversdale Plain (B) and the Knysna Afrotemperate Region (C).

2.3 The geological history of the southern Cape

The southern Cape coastal plain is separated from the rest of the continent by the Cape Fold Belt mountains. The Cape Fold Belt consists of a series of parallel folded mountain ranges of quartzites and quartz-rich sandstone with elevations of up to two kilometres (Compton, 2011). These rugged mountains sharply intersect the coast at Cape Hangklip in the west, forming part of the fold syntaxis (Figure 2.1). To the east, there is a broader intersection with the coast between George and Port Elizabeth. The Table Mountain, Bokkeveld and Witteberg Groups form the “Cape Supergroup” of Palaeozoic age (Thwaites and Jacobs, 1985; Marker and Holmes, 2010). The Cape Supergroup was deposited in a passive margin basin as clastic marine shelf deposits after the Late Precambrian to Early Cambrian Saldanian Orogeny and Pan-African depositional cycles had ceased on the Gondwana supercontinent (Partridge and Maud, 2000; Thamm and Johnson, 2006). The Cape Fold Belt was

formed through orogeny of the Cape Supergroup during the Permian and early Triassic (Dingle et al., 1983) (Table 2-1). The coastal plain is cut across the Cape Supergroup rocks as well as various underlying basement rocks including the Precambrian - Cambrian Malmesbury Group (Saldania Belt terranes), the polymetamorphic metasediments of the Kango and Kaaimans Groups (Saldania Belt inliers) and granitic intrusions (the Cape Granite Suite), as well as Cretaceous Enon fanglomerates (Uitenhage Group) (Rozendaal et al., 1999; Thamm and Johnson, 2006; Marker and Holmes, 2010; Figure 2.2).

The origin and development of the coastal plain is thought to be the result of the rifting that led to the break-up of Gondwana and the separation of Africa from South America, India and Antarctica, which is estimated to have occurred between 155 – 135 mya (Dingle et al., 1983; Marker and Holmes, 2010). The Gondwanan break-up event was a fundamental phase in the landscape evolution of the whole of southern Africa with the subsequent processes of rifting, erosion, deposition and warping ultimately creating the broad geomorphic structures visible in the area today.

During the latter stages of this break-up, two processes took place simultaneously: late Cretaceous down faulting of the southern African coastline and flexural uplift of a 'hingeline' separating the interior plateau from the coastal platform forming the Great Escarpment (Partridge and Maud, 1987). Following this, the coastal platform was planed and the Great Escarpment was eroded inland resulting in a modified 'African Surface'[2] (Partridge and Maud, 1987; Partridge and Maud, 2000; Marker and Holmes, 2010). The African Surface manifested itself south of the Cape Fold Belt as the coastal plain and was further modified through the deep incision of rivers that drain southwards off the Cape Fold mountains (Marker and Holmes, 2010).

There is still an ongoing debate as to the exact nature and timing of the development of the escarpment and the adjacent coastal plain, with one school of thought favouring gradual denudation (e.g. King, 1950, 1955) while others suggest initial or delayed rapid denudation of the coastal plain (e.g. Partridge and Maud, 1987; Summerfield, 1996). Recent advances in absolute dating methods and numerical modelling have led some authors to claim that this single-event model of flexural uplift and parallel scarp retreat that initiated the Gondwanan break-up may not play as a significant role as previously thought (Van der Wateren and Dunai, 2001; Burke and Gunnel, 2008).

It appears that the nature and timing of the origins of Great Escarpment and its links to the Cape Fold Belt is complex and still remains a topic of debate. It is clear that there are distinct differences

[2] Alternatively named the African Erosion Surface or African Planation Surface, a composite erosion surface of continental extent generated by the multi-phase cycle of Cretaceous erosion/the terminal result of protracted denudation initiated by the breakup of Gondwana (Burke and Gunnel, 2008).

in the evolutionary and erosional processes on the western and eastern sides of escarpment (Burke and Gunnel, 2008). The coastal plain is geographically partitioned from the subcontinent according to climatic, oceanographic and tectonic regimes and this is especially reflected in the Cenozoic sediments discussed below.

Figure 2.1 The location and overall topography of the southern Cape coastal plain (SCCP).
The SCCP is bounded by the mountains of the Cape Fold Belt (CFB). The lower map is a composite of Spot satellite images for the SCCP (black box in the top map corresponds to the area covered by the satellite images).
Diamond markers indicate the sampling sites Pearly Beach, Rietvlei – Still Bay and Vankervelsvlei (described in detail in Chapter 4).
The blue lines and areas are rivers and dams.
Thin black boxes in lower map are the approximate areas of the Agulhas Plain (A), the Riversdale Plain (B) and the Wilderness embayment (C).
[Spot satellite images source: Fundisa CSIR; Bathymetry: ETOP2; Digital elevation model: SRTM]

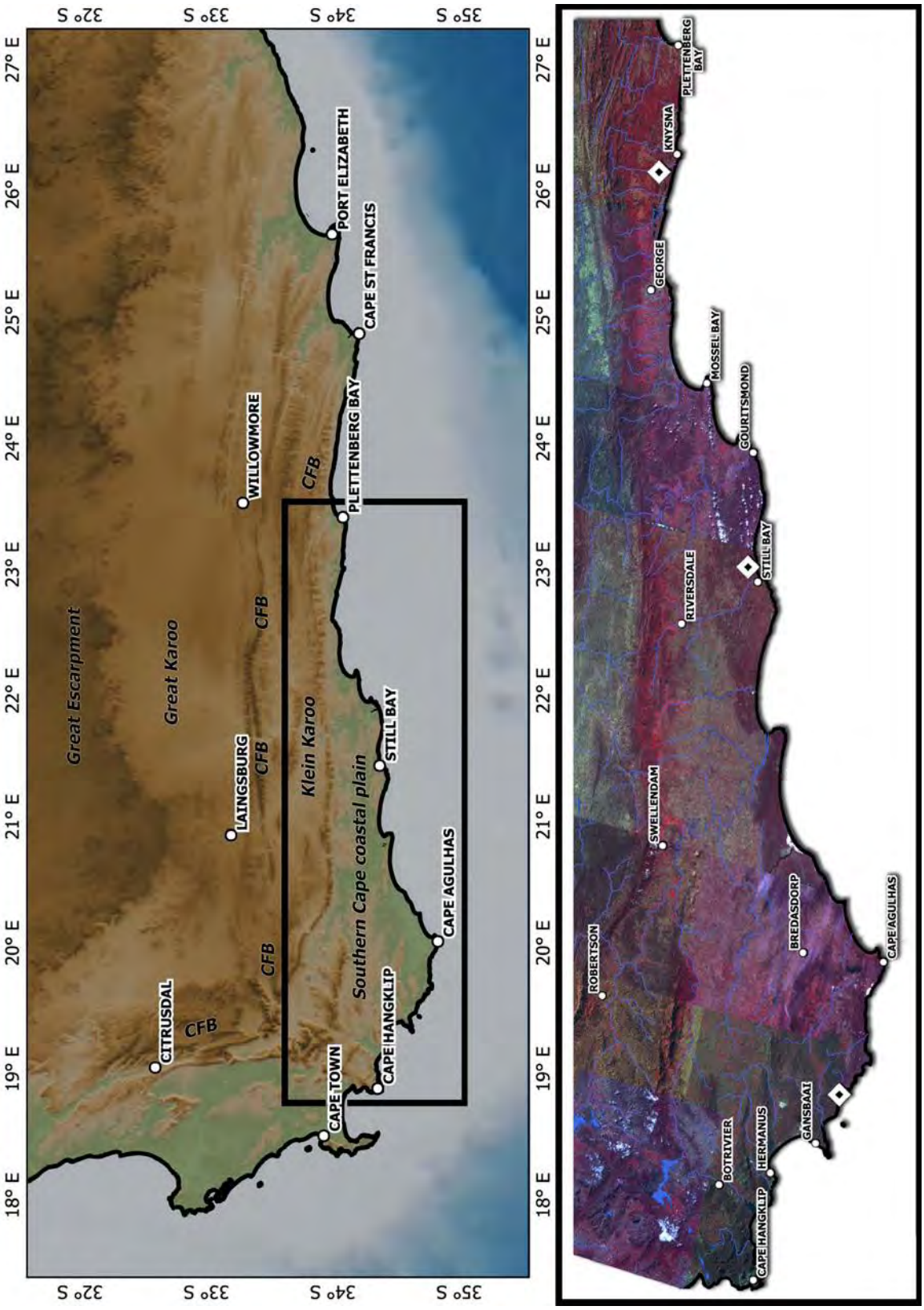

Table 2-1 Summary of the major geological units and geomorphic events for the southern Cape coastal plain (adapted from Partridge and Maud, 1987; Malan and Viljoen, 1990; Partridge and Maud, 2000; Marker and Holmes, 2010).

ERA	Myr	Period or Epoch	Group or Formation and geomorphic events		Primary composition
Cenozoic	0.01	Holocene	Waenhuiskrans Formation	Bredasdorp Group	Semi-consolidated aeolianite
		Upper Pleistocene	Klein Brak Formation		Quartzose sands and conglomerates
		Middle Pleistocene			
		Early Pleistocene			
	1.8	Pliocene	Wankoe Formation		Calcified aeolianite, quartzose sands and conglomerates
	5				
	25	Miocene	Coversands	200 m uplift ↑	
	36	Oligocene	Knysna Formation	200 m uplift ↑	Lignitic sands and lignites
	54	Eocene			
		Palaeocene			
	65		Grahamstown Formation	Coastal platform	Duricrusts of laterite, silcrete and saprolite
Mesozoic	141	Cretaceous	Uitenhage Group	African planation	Sandstone/shale/conglomerates
	200	Jurassic		Gondwana rifting	
	230	Triassic		Cape orogeny	
		Permian			
Palaeozoic		Carboniferous	Witteberg Group	Cape Supergroup	Sandstone/shale
		Devonian	Bokkveld Group		Sandstone/shale
		Silurian			
		Ordovician	Table Mountain Group		Sandstone/shale/tillite
		Cambrian	(Peninsula Formation)		
	550		Cape Granite Suite		Granite, quartz prophyry
	600 - 900	Late Precambrian	Kaaimans & Kango Groups		metasedimentary, metapelites with some quartzite and marble
	700		Malmesbury Group (700 myr)		Shale/mica/schist

Figure 2.2 Geological map of the southern Cape with legend in upper right corner [data source: Council of Geosciences, obtained from African Earth Observatory Network (AEON)].

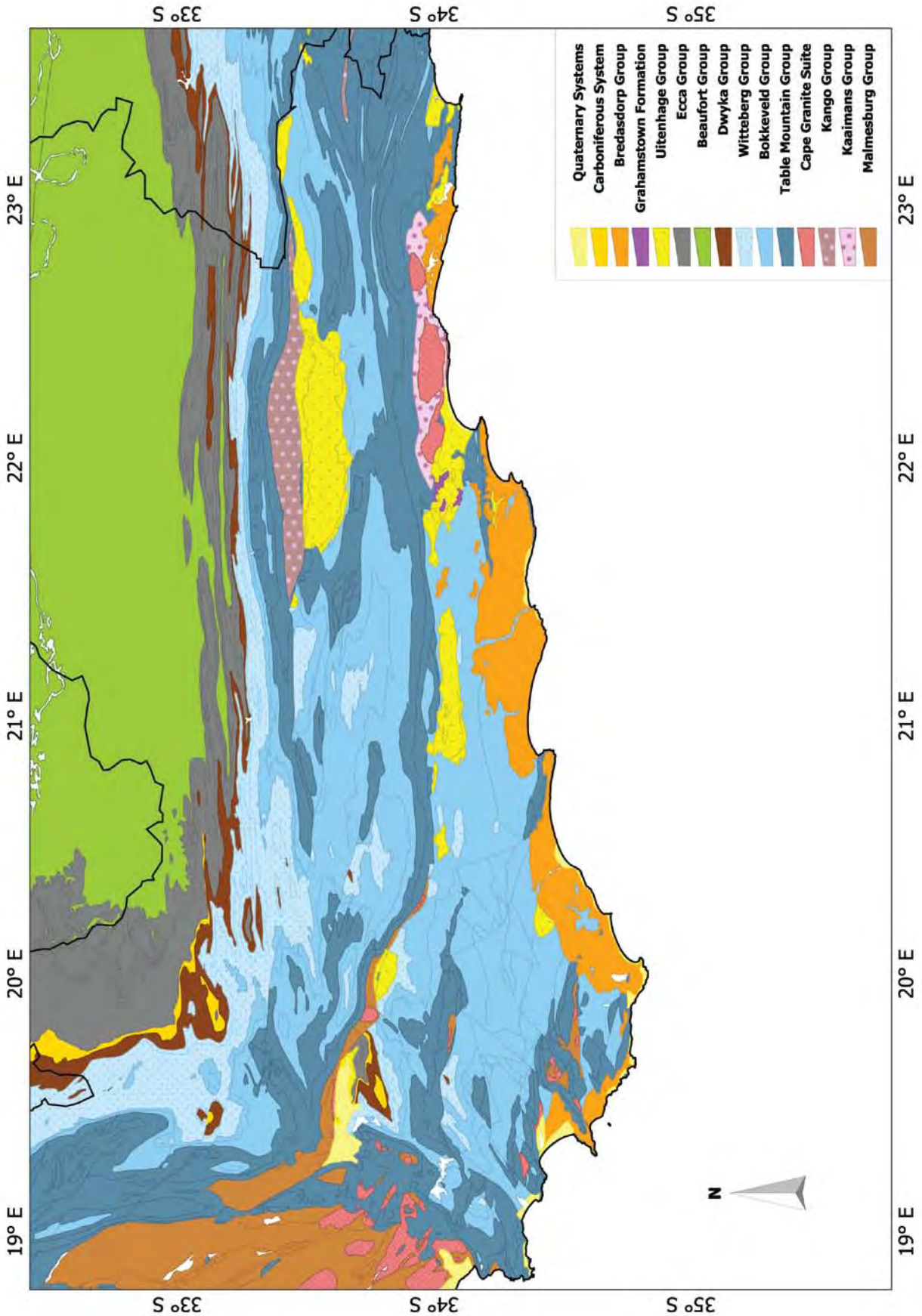

2.3.1 The Cenozoic geology of the southern Cape coastal plain: the Bredasdorp Group

Cenozoic deposits of marine, estuarine, fluvial, lacustrine and aeolian origin are extensively developed along the coastal flanks of southern Africa. The Bredasdorp Group limestones represent the most recent deposits on the southern Cape coastal plain extending from Cape Hangklip to Plettenberg Bay (Figures 2.1 and 2.2). The group refers to all marine and marine-associated Cenozoic sediments exposed on the coastal plain. Malan (1989) defined the Bredasdorp Group as consisting of limestones, calcarenites, calcirudites, conglomerates, coquinites and calcareous sandstones and formally divided the group into five lithostratigraphic units (Figure 2.3).

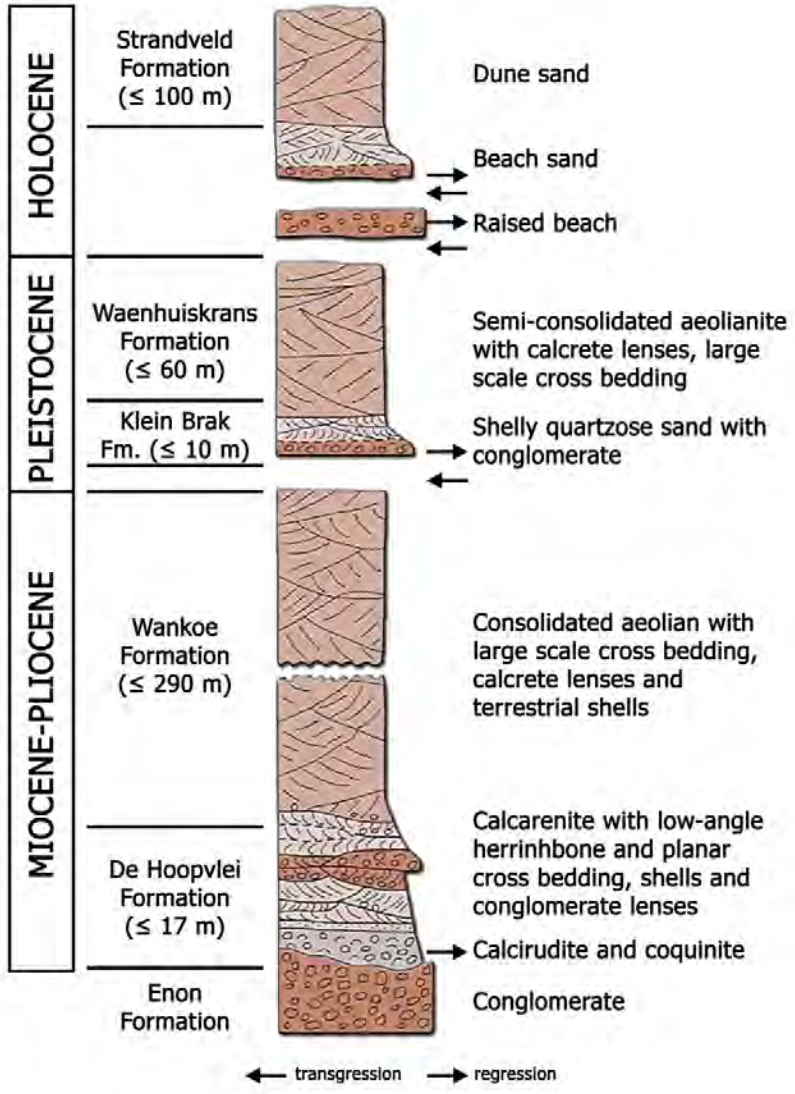

Figure 2.3 Generalised stratigraphic profile of the Bredasdorp Formation (after Roberts et al., 2006; Malan, 1989; 1990).

Siesser (1970) and Malan (1989, 1990) described the Bredasdorp sediments in detail. In general, the group unconformably overlies the Uitenhage Group or the Cape Supergroup strata on the coastal plain and extends up to 25 km inland with the deposits becoming progressively younger seawards (Malan, 1990). The sediments of this group were probably formed through sea level fluctuations on the wave cut platforms of the southern Cape (Malan, 1989; Roberts et al., 2006).

The marine De Hoopvlei Formation is the basal unit of the group and forms narrow outcrops between Bredasdorp and Mossel Bay. It is conformably covered by the aeolian Wankoe Formation (Malan, 1989, 1990). It has retained diverse marine macrofossil assemblages which indicate that deposition of this formation was most probably within a regressive, shallow marine environment (Roberts et al., 2006). The Wankoe Formation is the most extensive of the five lithostratigraphic units and is overlain by either the Klein Brak Formation or unconsolidated aeolian sand (Malan, 1989; Roberts et al., 2006). It outcrops as prominent ridges of calcified dune sand up to 300 m in thickness between Hermanus to Mossel Bay (Roberts et al., 2006). These limestones often support complex karst landforms for example the Canca se Leegte (Marker, 1987). The Klein Brak Formation is a thin deposit which typically lies unconformably on the coastal platform and is overlain by Waenhuiskrans and Strandveld sediments. It is thought to be indicative of marine transgressions within the mid to late Pleistocene (Malan, 1990, Roberts et al., 2006). The Waenhuiskrans Formations rests unconformably on Cape Supergroup rocks or conformably on Klein Brak sediments. This formation was originally presumed to be of Eemian (MIS 5e) age (Malan, 1990), however more recent investigations into its lithology and geological context together with absolute dating has shown that it is predates this interglacial highstand (Roberts et al., 2006). It consists of semi-consolidated sandy sediments with distinct cross-bedding and like the Wankoe Formation, the Waenhuiskrans Formation has been interpreted to have been deposited during periods of enhanced aeolian activity during periods of lower sea levels (Malan, 1990). The most recent dunes that adjoin the present-day coastline represent the Strandveld Formation. These dunes consist of unconsolidated, calcareous sands presumed to be formed during the Holocene (Tinley, 1985).

The Waenhuiskrans and Strandveld Formations are rich in biogenic carbonates and fragments of marine organisms such as comminuted molluscs, echinoderms, coralline algae, bryozoans and benthic foraminifera (Siesser, 1970; Malan, 1990). This indicates a marine origin and calls into question Malan (1990)'s interpretations. In addition, some authors assert that the large dunes associated with these formations could not arise without a proximal littoral sediment source and therefore were most likely formed as a result of relatively high sea levels (Illenberger, 1996; Bateman et al., 2004; Carr et al., 2006a).

2.3.2 Topography and geomorphology

Southern Cape landforms are a product of differential erosion of the underlying and overlying geology (section 2.1) and the responses of the geological units to planation, tectonic activity (uplift) and fluctuations in sea level.

During and directly after the African planation event and within the more recent transgressive-regressive cycles, the resistant TMG formed highlands, headland cliffs, ridges and capes e.g. Cape Hangklip and Cape Agulhas (Figure 2.1). Embayments are carved into more easily eroded Bokkeveld Group shale and Enon Formation conglomerate (Uitenhage Group). Late Cenozoic Bredasdorp Group limestones overlie the above sediments forming a low-relief coastline with log spiral (zeta) bays characterizing the marine interface (Marker and Holmes, 2010). SE-NW trending halfgrabens are responsible for the structural control of these morphologies (Dingle et al., 1983).

Aeolian deposits are an important feature of the landscapes of the southern Cape coastline, boasting a spatially extensive and diverse range of forms from barrier dune systems (e.g. Wilderness embayment), the aeolianites of the Waenhuiskrans Formation and discrete lunette dunes formed at the edges of pans (Bateman et al., 2004; Carr et al., 2006a; Carr et al., 2007; Bateman et al., 2011).

The specific nature of the topography, geomorphology and the soil characteristics for each sampling site are given in Chapter 4.

2.3.3 Offshore bathymetry and shelf deposits

The bathymetry of the continental margin of southern Africa consists of a nearshore rocky platform, the continental shelf, continental slope and the continental rise. The Agulhas Bank forms the southernmost margin of the continental shelf and is the most prominent feature of the offshore region of the coastal platform.

It is a relatively wide (300 km), shallow feature (< 200 km) covering an area of approximately 80 000 km^2 and bounded in the west by the Benguela upwelling region and to the east by the path of the Agulhas Current (Lutjeharms et al., 1996; Figures 2.4 and 2.5). During lower sea level stands, the exposure of large portions of the shelf would have significantly extended the coastal platform. The resultant increased continentality would not have been uniform. For example, during glacial maxima lowstands, the shoreline between Cape Agulhas and Mossel Bay would have been ~100 – 200 km further south than present whereas at Cape Point the coast would only have been ~16 km further southward (Dingle and Rogers, 1972; Figure 2.4). Therefore the difference between the more

steeply-shelved section from Cape Point to Gansbaai/Pearly Beach and the flatter offshore terrain to the east could have led to increased climatic variation across the coastal region.

The Agulhas Bank consists of a series of faulted ridges of Palaeozoic and Precambrian rocks overlain by a thick (up to 6.2 km) Mesozoic-Cenozoic sedimentary sequence (Dingle and Rogers, 1972; Dingle, 1973). The surface sediments of the bank comprise of a mixture of calcareous aeolian sands and muddy alluvial deposits derived from river drainage systems. The calcareous sandy deposits to the east of the Agulhas Bank and adjacent to the coastline most probably provide the sediment source for the Bredasdorp Formation. The nature of the sediments and the topographic structure of the shelf extending out from the Wilderness embayment provide evidence of the presence of relict dune cordons similar to the ones found on land (Birch, 1977; Bateman et al., 2011).

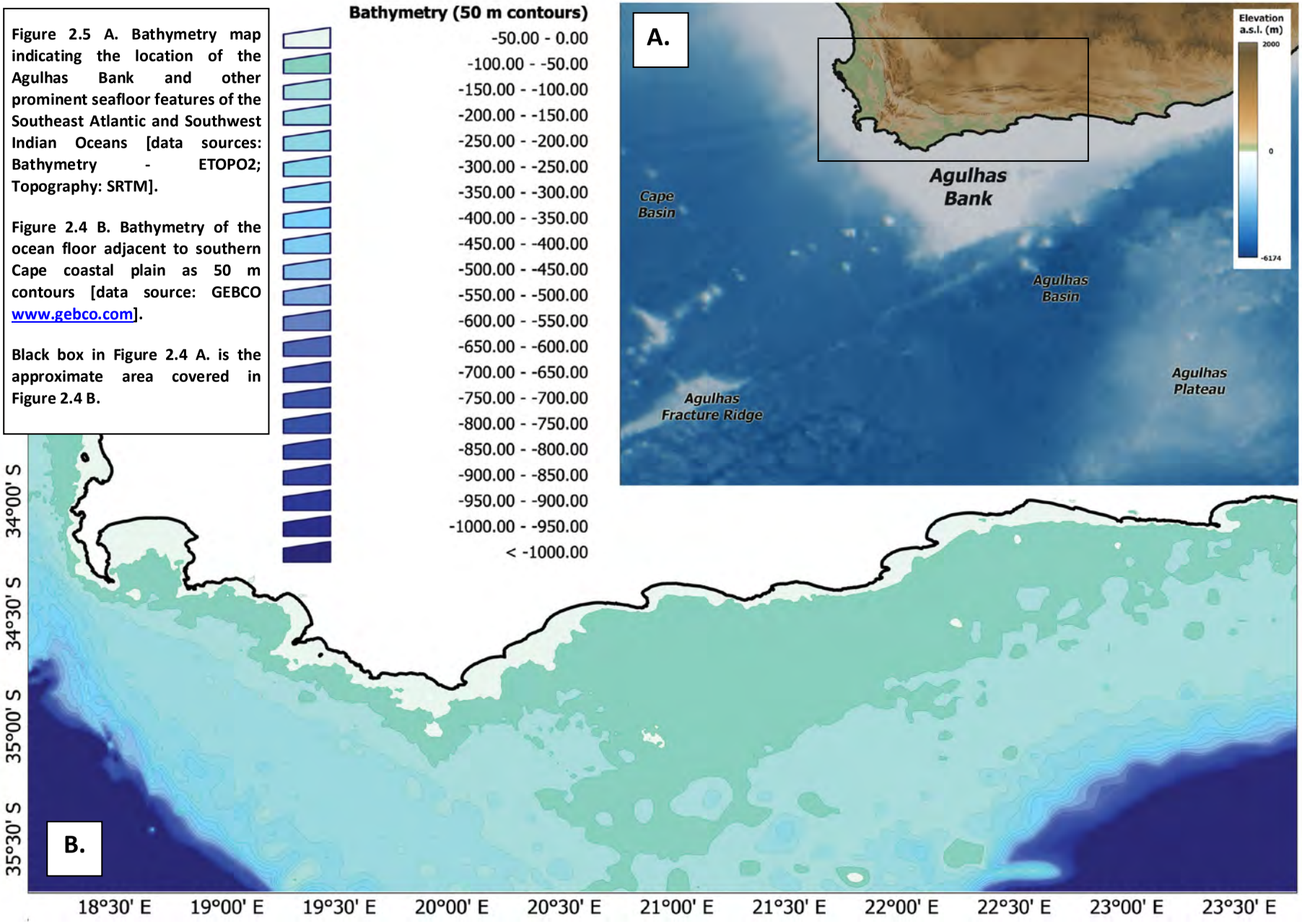

Figure 2.5 A. Bathymetry map indicating the location of the Agulhas Bank and other prominent seafloor features of the Southeast Atlantic and Southwest Indian Oceans [data sources: Bathymetry - ETOPO2; Topography: SRTM].

Figure 2.4 B. Bathymetry of the ocean floor adjacent to southern Cape coastal plain as 50 m contours [data source: GEBCO www.gebco.com].

Black box in Figure 2.4 A. is the approximate area covered in Figure 2.4 B.

2.4 Ocean circulation: the Agulhas Current

Another important feature that significantly influences the climates of the southern Cape coast is the Agulhas Current. This western boundary current carries South Indian Subtropical Surface Water, Antarctic Intermediate Water and some remnants of the Red Sea Water and Tropical Indian Surface Water down the east coast of South Africa then along the Agulhas Bank into the Agulhas Retroflection region (Valentine et al., 1993; Lutjeharms et al., 2001). This flow of warm water provides a source of moisture that creates the humid conditions that exist along the south coast.

At the retroflection, the Agulhas Current turns back on itself flowing eastward as the Agulhas Return Current which may become embedded in the Antarctic Circumpolar Current (Lutjeharms et al., 2001; Rau et al., 2002; Figure 2.5). Within the retroflection loop, warm Agulhas rings are pinched off and enter the northward flowing cold Benguela Current (Figure 2.5). This represents a major mechanism for inter-ocean exchange and has global climatic implications (Lutjeharms, 1996). Models have suggested that this phenomenon may control the rate of thermohaline overturning of the entire Atlantic (Weijer et al., 1999).

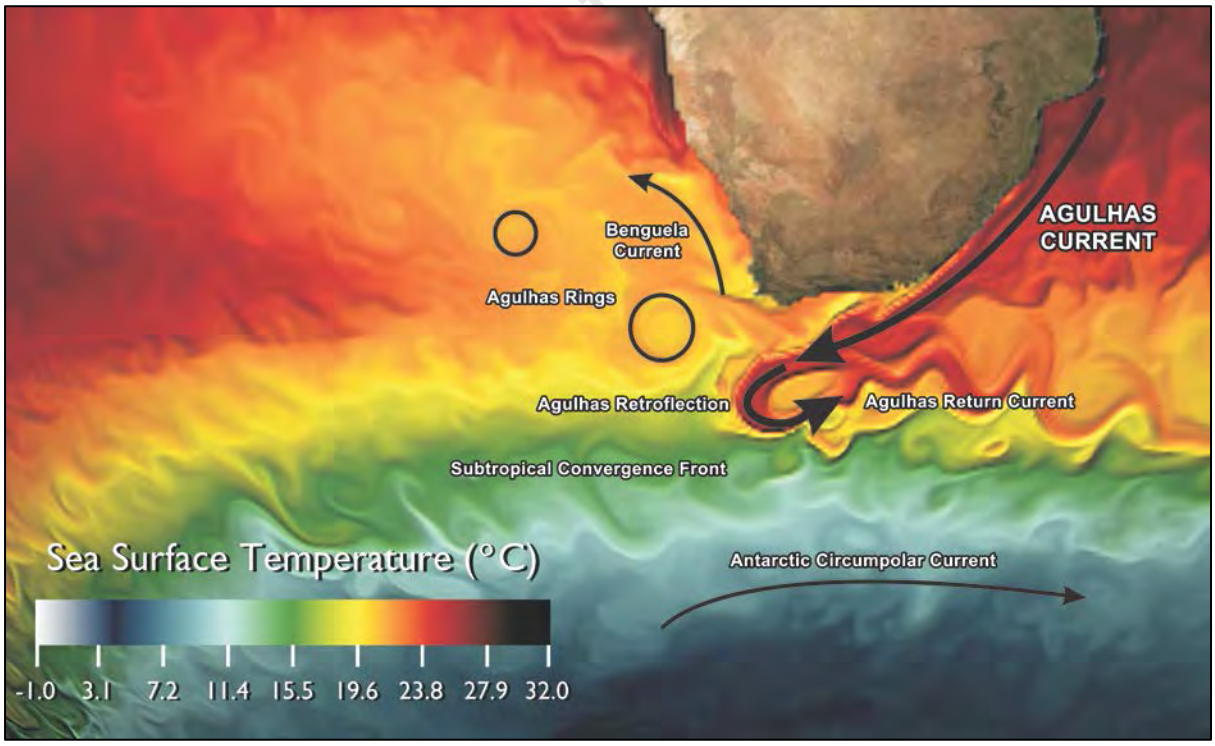

Figure 2.6 The location of the Agulhas Current in relation to other major oceanic circulation systems surrounding southern Africa. [Sea surface temperature image source: http://www.gfdl.noaa.gov/pix/tools_and_data/gallery/gfdlcm24sst.png]

2.5 Contemporary climates

The climates of southern Africa are characterised by a high degree of spatial and temporal variability. This variability is evident on a smaller scale as is exemplified here for the southern Cape coastal plain. Major components of the global atmospheric circulation significantly influence the coastal plain's climate. This has resulted in the region encompassing two different rainfall regimes.

2.5.1 Modern rainfall zones

Southern Africa can be divided into three principal zones according to rainfall seasonality (Tyson, 1986; Figure 2.6). The winter rainfall zone (WRZ) receives the majority of its precipitation during the austral winter (between April and September). It is characterised by a Mediterranean-type climate, with cool, wet winters and warm, dry summers (Tyson, 1986). In contrast, the summer rainfall zone (SRZ) receives the largest proportion of its annual rainfall during the austral summer (October – March). Its climate is one of generally clear dry winters and more humid summers with afternoon thunderstorms and periodic tropical cyclones. Between these two regions lies the year-round rainfall zone (YRZ), a relatively narrow region extending from the north western reaches of South Africa diagonally down to the south coast (Figure 2.6). It receives both winter and summer precipitation. Absolute rainfall amounts are a key determining factor for the shifts in the boundaries of the YRZ. The south coast section is more stable than the semi-hyperarid northern section as it receives greater, and more regular, amounts of rainfall. The northern section of the YRZ is more sensitive to boundary shifts and can be influenced by a single storm event (Chase and Meadows, 2007). The extents and positions of the three zones can be highly variable on an inter-annual level and over longer time periods – e.g. the late Quaternary (Chapter 3).

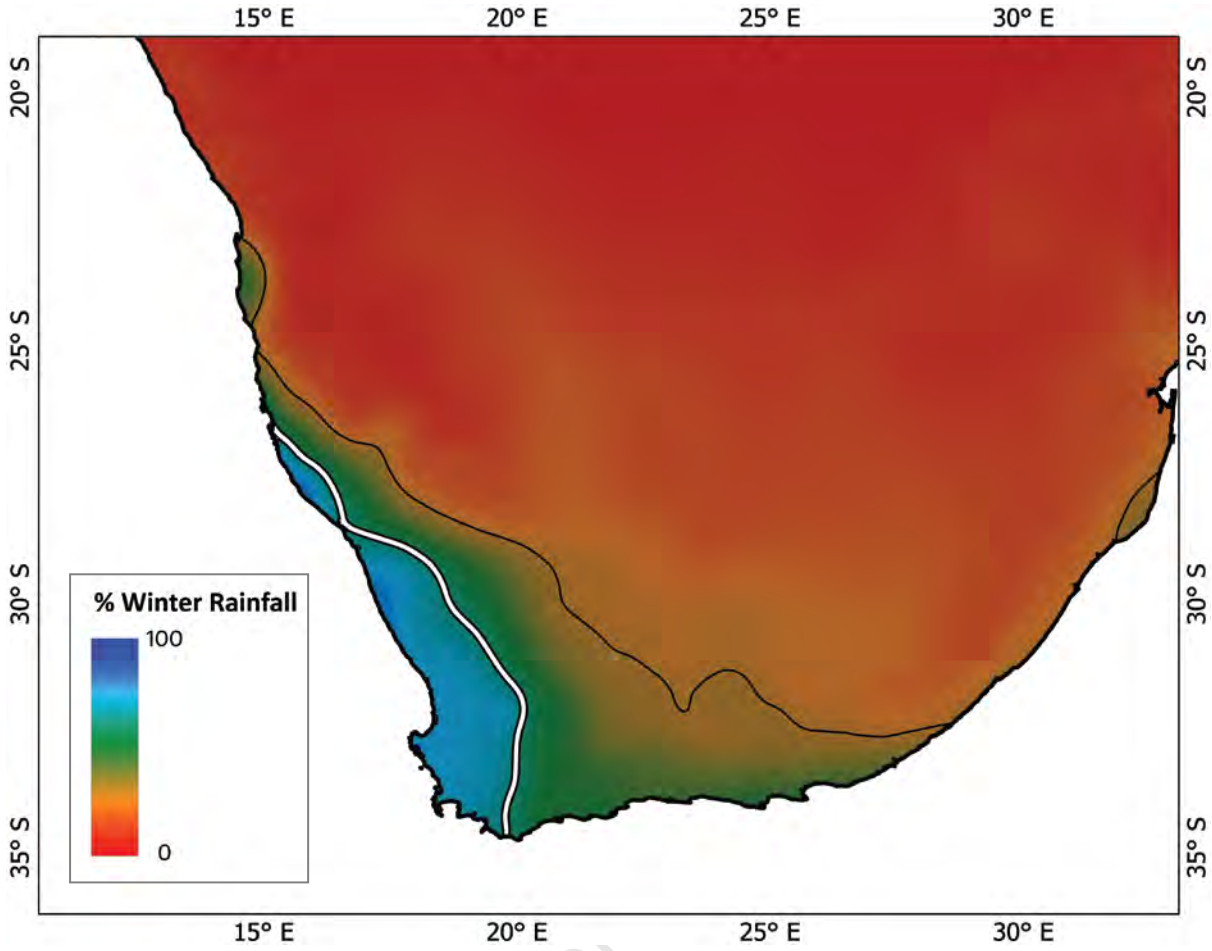

Figure 2.7 Southern African rainfall seasonality: WRZ – Winter rainfall zone, >66% winter rain – to the left of the thick white line; YRZ – Year round rainfall zone 66 – 33% winter rain – between the thick white and thin black lines; SRZ – Summer rainfall zone, <33% winter rain – to the right of the thin black line (*sensu* Chase and Meadows, 2007).

2.5.2 Climate drivers

The seasonal patterning of precipitation that has resulted in these three distinct rainfall zones is a result of the interplay amongst the three dominant atmospheric circulation systems operating in the African sector of the Southern Hemisphere: the westerlies, the subtropical anticyclones and the tropical easterlies (Figure 2.7).

2.5.2.1 The tropical easterlies

In the region between the Northern and Southern Hemisphere's semi-permanent subtropical anticyclones, circulation is controlled by the tropical easterly flows that converge at the thermal equator to form the Inter-Tropical Convergence Zone (ITCZ) (Tyson and Preston-Whyte, 2000). The intensity and position of the ITCZ varies seasonally as a response to the changing strengths of the

easterlies/trade winds. Traditionally, it has been assumed that the ITCZ is responsible for the significant convective activity and major tropical latent heat release over southern Africa (as stated in Lindesay, 1998; Tyson and Preston-Whyte, 2000). However the 'classic' ITCZ paradigm has been revised, with many climatologists recognising that the ITCZ is almost exclusively an oceanic feature and that the rain found within the vicinity of the equator, termed the 'tropical rain belt', is more related to the position of pressure troughs, cool upper atmospheric temperatures and jet stream dynamics than converging trade winds (Nicholson, 2009).

Nevertheless, disturbances in the tropical easterly flow are represented by easterly waves and thermal low pressures[3] (Tyson and Preston-Whyte, 2000; Reason et al., 2006). They are usually associated with tropical convection, the tropical rain belt and the warm moist air from the Indian Ocean that is transported by the easterlies. The easterlies and their related disturbances are the primary mechanism for precipitation in the SRZ. From October to March, easterly flow is enhanced due to a southerly shift in the global circulation systems and the development of a semi-stationary low-pressure system over the continent that results in increased rainfall over the interior.

2.5.2.2 The subtropical anticyclones

The subtropical high pressure belt is a major near-surface feature of the Southern Hemisphere and extends from 23° – 42°S at the extreme limits and on average occurs within 27° – 38°S (Tyson and Preston-Whyte, 2000). Its influence in southern Africa results from three semi-permanent anticyclones: the South Indian Anticyclone (SIA), the continental high and the South Atlantic Anticyclone (SAA). These subtropical high pressure systems strongly influence southern African climates by generating anticyclonic vorticity, suppressing convection and causing clear, dry weather conditions through the enhanced atmospheric stability (Lindesay, 1998). They are associated with large-scale subsidence throughout a deep layer, surface divergence, elevated inversions and little or no rainfall (Lindesay, 1998; Tyson and Preston-Whyte, 2000). In addition, the SAA plays an important role in delimitating the SRZ as it can block easterly flow.

Their influence over the southern Africa as a whole, as well as the adjacent oceans, is particularly strong during Southern Hemisphere winter due to the northward displacement of the SIA and the SAA (Tyson and Preston-Whyte, 2000). In both summer and winter they are responsible for fair-weather conditions along the southern Cape coast. They are also linked to various synoptic-scale

[3] Alternatively referred to as heat lows, non-frontal low pressure systems.

features that contribute to the weather experienced on the SCCP. Of particular importance are ridging anticyclones and blocking highs. Ridging anticyclones originate as extensions of the SAA and are usually situated just off the southern Cape coast on the Agulhas Bank (Hunter, 1987). They form small migratory or bud-off highs when they are cut off from the SAA and then eventually merge with the SIA. Ridging highs associated with a westerly wave at 500 hPa can produce thunderstorms and widespread rainfall over the southern and eastern coasts of South Africa (Tyson and Preston-Whyte, 2000). Like ridging highs, blocking highs originate in the ridge of the SAA and form a migratory high pressure system. They become near-stationary features that can inhibit the west-east progression of mid-latitude cyclones and are associated with the formation of cut-off lows (Hunter, 1987).

2.5.2.3 The temperate westerlies

The atmospheric circulation of the Southern Hemisphere poleward of the subtropical high pressure belt is dominated by the circumpolar westerly winds at both surface and upper atmospheric levels. The area of maximum westerly flow is the upper tropospheric subtropical jet stream which, at its zonal mean, lies at ~40°S in the summer and 30°S in the winter (Newell et al, 1972 and Trenberth, 1981a in Lindesay, 1998).

Transient low pressure systems are embedded in the mean circumpolar westerly flow and follow a northeasterly trajectory in the southern African region of the South Atlantic. They then track southeastward as they approach and pass the continent. These systems account for the bulk of the rainfall in the WRZ (Tyson, 1986). Westerly waves and cold fronts traverse the southern Cape coast with peak frequencies between two and eight days (Lindesay, 1998; Tyson and Preston-Whyte, 2000) and are significant rainfall-producing systems on the SCCP, especially in winter. Cold fronts are associated with distinctive cloud bands, 'backing' winds (shift from northerly to southerly flow), changes in gustiness and wind speed and cold snaps of a few days duration (Tyson and Preston-Whyte, 2000).

Another synoptic scale feature that is associated with westerly flow and forms part of extensive pre-frontal systems is the coastal low. Hunter (1987) found that coastal lows were the most dominant synoptic scale systems on the southern Cape coast. Coastal lows are formed by cyclonic vorticity generated from air descending the escarpment and moving onto the coastal platform. They are decoupled from the upper westerly wave and rely on local topography and strong offshore winds for their formation and persistence. They can originate at any locality along the coast from Namibia to Mozambique but are usually initiated on the west coast and propagate southward or on the south

coast and move eastward and northeastward. All coastal lows produce warm offshore adiabatic airflow ('Berg' wind conditions) ahead of the system and cool onshore air behind it. They are rarely associated with more than light mist or fine drizzle but can develop into a coastal depression bringing more substantial rainfall to the SCCP.

Cut-off lows represent the most intense form of westerly perturbation. These are deep unstable baroclinic systems that originate as an upper westerly trough which becomes cut off over southern Africa by the ridging of the SAA to the south (Lindesay, 1998). They then deepen into closed circulations extending downwards to the surface and becoming displaced out of the westerly flow. Cut-off lows are associated with strong convergence, vertical motion and wide-spread precipitation which have often led to flooding events in South Africa. Cut-off lows that produce heavy rainfalls are most frequent in Autumn (March-May) and Spring (September-November) (Tyson and Preston-Whyte, 2000).

2.5.2.4 Southern meridional flow and tropical-temperate troughs

Southern meridional flow and tropical-temperate troughs (TTTs) are synoptic-scale systems that form as a result of the interactions amongst the tropical easterlies, subtropical anticyclones and the temperate westerlies.

Southern meridional flow occurs when a westerly wave passes eastward over or near the subcontinent and the SAA extends eastward behind the trough forming a ridging anticyclone. The resulting strong surface zonal pressure gradient between the high and low pressure systems can produce southerly onshore airflow (Lindesay, 1998). The upper-level divergence ahead of the trough overlies the surface convergence to the rear of the trough resulting in rainfall along the coast. In winter this synoptic system can generate extremely cold conditions and snow on the Cape Fold Belt mountains. The interaction between an easterly wave or low over southern Africa with a temperate westerly disturbance to the south can produce TTTs. TTTs are associated with distinct meridionally-oriented cloud bands and bring large amounts of rain to the interior primarily in mid-summer during times of maximum tropical convection (Harrison, 1984; Taljaard, 1996). Although predominantly contributing to summer rainfall and variability over the interior (Todd and Washington, 1998; Crétat et al., 2012), when other systems (such as cold fronts or cut-off lows) are embedded in TTTs (often once they have decayed), rainfall is enhanced and reaches the southern Cape coast (Singleton and Reason, 2007; Hart et al., 2012).

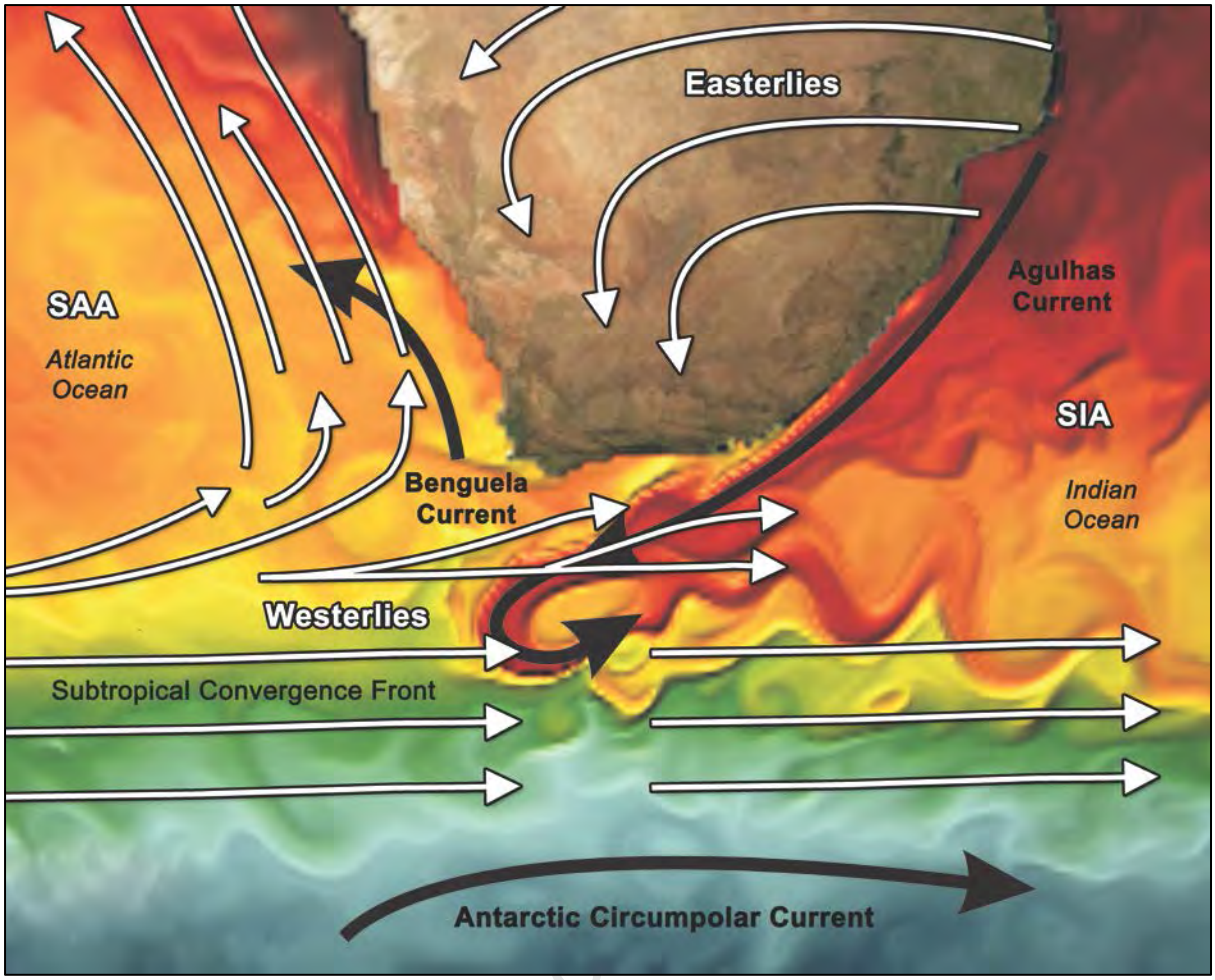

Figure 2.8 A simplified schematic of the major atmospheric circulation types (in white) influencing the SCCP superimposed over the dominant oceanographic circulation (in black). SAA = South Atlantic Anticyclone; SIA = South Indian Anticyclone.

2.5.3 Variations in the mean circulation over southern Africa

The three features mentioned above are embedded within large-scale meridionally-orientated circulation cells that transport mass, heat and water vapour throughout the Southern Hemisphere (Lindesay, 1998). The tropical and subtropical regions are dominated by the thermally direct Hadley Cell which incorporates the easterlies. The cell's ascending branch forms a near-equatorial trough (often linked to the ITCZ) and its descending branch ends in the subtropical ridge of the high pressure belt. The thermally indirect Ferrel Cell lies poleward of the Hadley Cell, in the westerly wind belt, feeding descending air into the subtropical anticyclones and its rising limb forms the Antarctic tough (Lindesay, 1998).

These cells shift latitudinally due to temperature fluctuations which are a result of seasonal variations in solar insolation. Due to this process, the easterlies and the westerlies migrate

northward during the boreal summer and southward during the austral summer. The subtropical anticyclones are strengthened and expand during winter as a result of increased hemispheric temperature gradients and continental cooling. The continental high pressure cell is especially dominant over the interior in winter. During summer, the continental anticyclone is replaced by a weak heat low centred over the central interior which results from higher temperatures and a poleward shift in the mean circulation belts (Tyson and Preston-Whyte, 2000). The presence of a zone of lower pressure over the interior in summer and the associated shifts in the mean circulation belts allows for an increase in easterly flow which generates precipitation within the SRZ.

The intensification and equatorward expansion of the westerlies, the northward movement of the westerly jet stream maximum and the migration of the ITCZ and the tropical rain belt into the Northern Hemisphere during the austral winter causes an increased number of frontal depressions to reach southern Africa (Tyson and Preston-Whyte, 2000; Figure 2.8). Therefore the WRZ receives progressively more precipitation from April through to June/August. Rainfall within the WRZ drops sharply in September as the westerlies weaken and shift poleward (Figure 2.8).

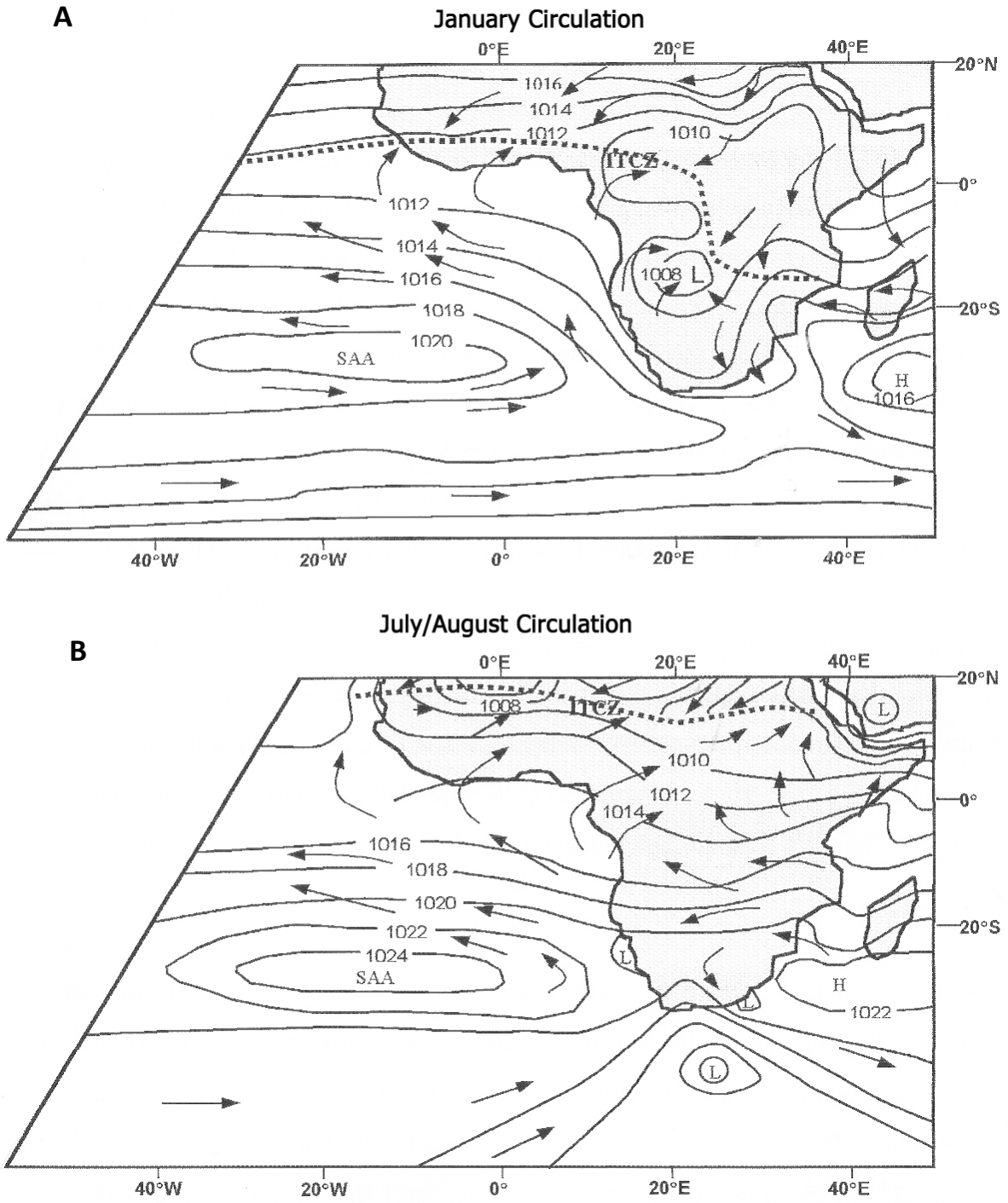

Figure 2.9 Generalised summer (A) and winter (B) atmospheric circulation patterns over Africa. Arrows indicate winds, thin black continuous lines are the pressure fields and the dashed line is the Inter-tropical Convergence Zone (ITCZ). SAA = South Atlantic Anticyclone, H = high pressure cell and L = low pressure cell (adapted from Tyson, 1987).

2.5.4 Climates of the southern Cape coastal plain

The climates of the SCCP are a product of the amalgamation of a wide range of influencing factors from shifts in the large-scale circulation systems to oceanographic and topographic controls.

In terms of the Köppen (1931) climate classification system, the western section of the southern Cape coast plain from Cape Agulhas to Cape Hangklip falls under the class: Csa – summers long dry and hot (Schulze et al., 2007). The central parts of the coastal region from Cape Agulhas to George are classified as BSk –semi-arid cool and dry. Between George and Plettenberg Bay, in the Afrotemperate region, the climate is classified as Cfb - wet all seasons, summers long and cool (Schulze et al., 2007).

2.5.4.1 Spatial variation of precipitation

The southern Cape coastal plain encompasses the transition from the WRZ to the YRZ and therefore strong west – east patterns of variability are evident.

Rainfall along the coast varies in both total amount and seasonality. The weather stations in Figure 2.9 show the major distribution of rainfall across the region. To the west there are clear indications of winter rainfall, while the stations to the east of Cape Agulhas along the coast show less distinct seasonality.

The inland stations at Laingsburg and Willowmore illustrate the significant effect of topography on rainfall amounts (Figure 2.9). The Cape Fold Belt has a strong rain shadow effect, such that atmospheric moisture brought in by westerly flow dynamics does not often penetrate northwards over the mountains. These two stations also demonstrate the change to a bimodal (summer) rainfall regime towards the northeast.

Topographic complexity leads to increased rainfall variability. For example, the presence of the Cape Peninsula and Langkloof and Outeniqua mountains have resulted in increased total amounts of precipitation in the Cape Town and Knysna regions whereas the more homogenously flat Agulhas and Riversdale coastal plains, exemplified here by the Cape Agulhas and Still Bay weather stations, experience lower rainfall totals due to less orographic precipitation.

The Afrotemperate region, which is represented here by the Knysna and Tstisikamma stations, receives elevated overall precipitation (between 600 to over 1000 mm annual average precipitation compared to the Agulhas and Riversdale Plains which receive 445 – 550 mm) throughout the year

with equinoxial maxima. This is due to the area being influenced by disturbances in both the temperate westerlies and the tropical easterlies that are then enhanced through the orographic controls of the surrounding mountains. Orographic uplift (the Outeniqua Mountains) and atmospheric instability of oceanic air masses results in frequently cloudy conditions with high relative humidity, light rain and fog (Martin, 1968; Hunter, 1987).

Figure 2.10 Average monthly rainfall totals (mm) for selected weather stations illustrating how topographic complexity and seasonality affect rainfall across the SCCP [data source: CSAG, 2012].

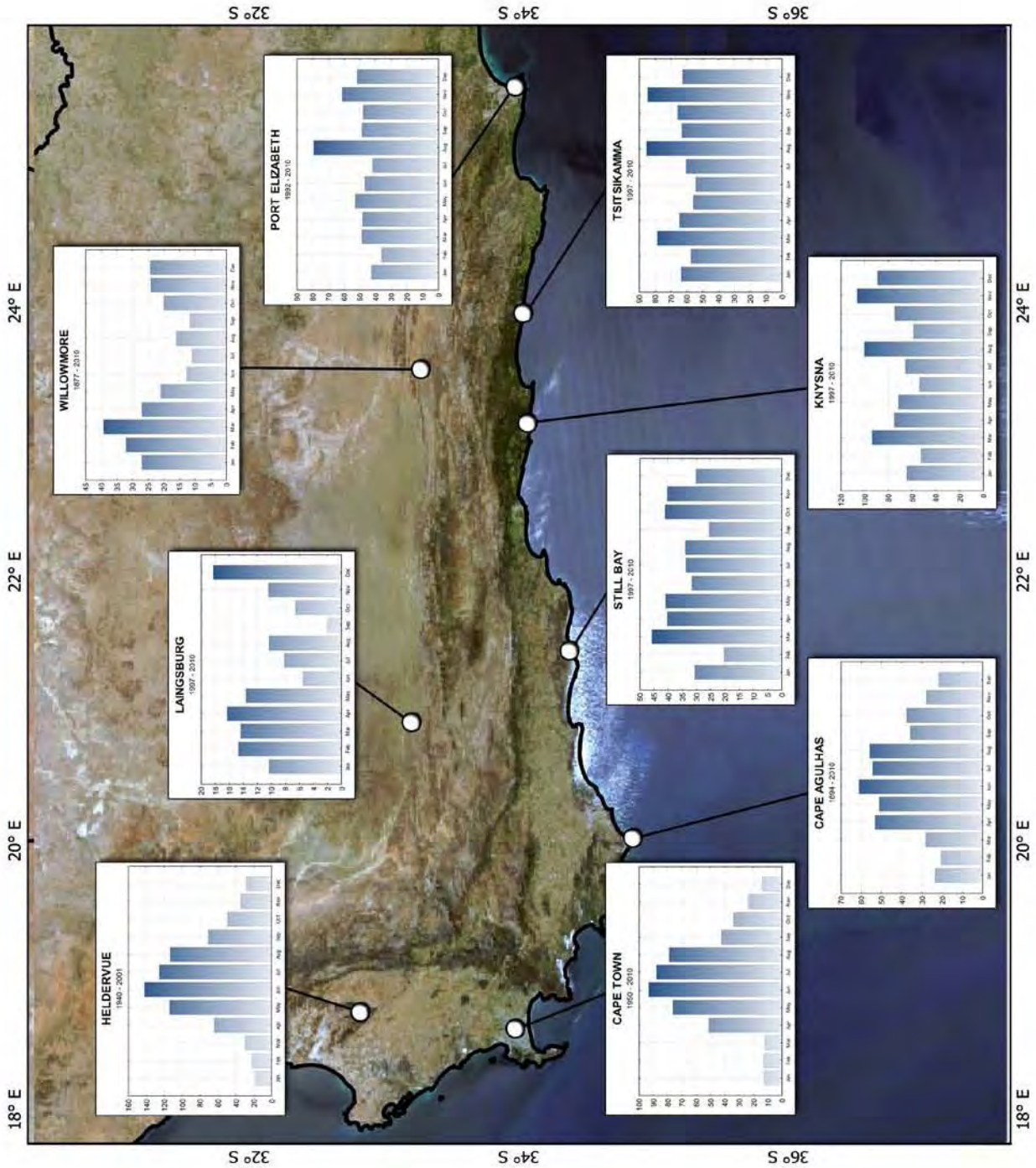

2.5.4.2 Oceanographic controls

The coastal areas of South Africa are greatly influenced by the surrounding oceans and ocean currents. Temperatures along the coast are moderated by the presence of the oceans and contrast significantly with the strong continentality that characterises the climates of the interior.

The cold Benguela Current and its associated upwelling centres encourage atmospheric stability along the west coast and therefore contribute to the region's general aridity. In contrast, the southern Cape coast is influenced by the warm Agulhas Current which provides moisture to the region.

At a subcontinental scale, it has been shown that sea surface temperature (SST) variations in the south Atlantic and south Indian Oceans may have both a local and a remote effect on southern African rainfall variability (Reason, 1998a; Reason, 1998b; Reason and Mulenga, 1999; Washington and Todd, 1999; Lutjeharms et al., 2001; Reason, 2001, 2002; Williams et al., 2011). Locally, SSTs can modulate latent heat fluxes and temperature and pressure gradients (Reason, 1998b; Williams et al., 2011). SST anomalies can also have a remote effect on rainfall variability via changes to the larger scale rain-producing systems such as TTTs (discussed above) (Reason, 1998a; Williams et al., 2011).

2.5.4.3 Winds

In general, easterly winds dominate the southern Cape in summer and northwesterlies or westerlies in winter (Tyson, 1986). The strongest winds recorded along the southern Cape coast are gale-force westerly winds associated with westerly wave disturbances, especially cut-off lows during winter (Hunter, 1987). Gale-force easterlies are prevalent during summer. Like precipitation, the seasonality of winds is more pronounced towards the western regions of the coastal platform.

The configuration of the coastline, the position of the mountain ranges and existence of river valleys result in localised changes to the prevailing winds. For example, there is an abrupt change in wind characteristics between Cape St Blaize and George. The westerly component of the wind is enhanced to the east of Cape St Blaize most probably due to weather systems encountering a mountain range (the Outeniquas) near George.

Immediately along the coast winds typically have a major alongshore flow pattern. Sea breezes are not noticeable whereas land breezes represent a relatively dominant component of southern Cape climates. They are especially prevalent in winter when katabatic winds that blow down river valleys reach the coast are enhanced by westerly wave circulation resulting in cold offshore westerly or

northwesterly winds. During summer, the general flow is reversed generating onshore winds linked to the low pressure cells.

Berg winds, warm, dry adiabatic winds similar to the European foehn winds, are most frequent in winter but can also occur fairly often along the coast at the change of season, in spring and autumn.

Winds with a strong easterly component, such as the gale-force easterlies that dominate in summer, can generate regions of local upwelling along the southern Cape coast if they are strong enough and are associated with appropriate onshore and offshore topography (Schumann et al., 1982; Schumann et al., 1995).

2.5.4.4 Temperatures

In general, southern Cape temperatures are not extreme. The large amount of cloud, the frequent rains and the presence of the Agulhas Current all exercise a moderating effect on the temperatures along the coast. In comparison to the interior, diurnal temperature ranges are small and the mean temperatures of the coldest and warmest quarters of the year are moderate (Figures 2.10 and 2.11).

Mean annual temperatures for the whole of the southern Cape coast are on average around 15 - 18°C with higher temperatures in the central region (from Cape Agulhas to George) and cooler temperatures in the eastern Afrotemperate section (Table 2.2). Minimum temperatures are experienced in June and July (Table 2.2) normally in association with either cut-off lows or cold offshore flow as a result of land breezes. Berg winds are responsible for anomalously high temperatures along the coast (Hunter, 1987).

As Figures 2.11A and 2.11B clearly illustrate, the Cape Fold Belt mountains' higher elevations and topographic complexity reduce temperatures in these regions. Snow and frost are common along these ranges and in the interior but do not occur along the coast.

Table 2-2 Table of monthly mean minimum and maximum temperatures for weather stations along the Cape coast, ordered from east to west (records are averages from at least 10 years of continuous data) [data source: CIP CSAG, 2012].

Month	Cape Town		Hermanus		Cape Agulhas		Still Bay		Cape St Blaize		Knysna		Tsitiskamma		Port Elizabeth	
	Min	Max	Min	Max	Min	Max	Min	Max	Min	Max	Min	Max	Min	Max	Min	Max
Jan	16.0	26.5	16.7	23.8	18.0	24.4	16.4	25.4	18.2	23.8	17.4	25.8	17.4	24.7	17.3	25.6
Feb	16.0	27.0	16.8	23.8	18.3	24.2	16.9	25.5	18.3	23.7	18.0	26.4	17.8	24.9	17.7	26.2
Mar	14.5	25.9	15.6	22.7	17.1	22.8	15.3	24.3	17.1	22.6	16.5	25.3	16.5	23.6	16.1	24.9
Apr	12.2	23.2	13.9	21.0	15.0	20.5	13.1	22.2	15.3	21.4	14.1	23.4	14.5	21.8	13.6	23.3
May	10.0	20.2	12.6	19.7	13.4	19.1	11.2	21.0	13.5	20.3	11.7	21.9	13.0	21.0	10.9	21.9
Jun	8.3	18.2	11.0	18.3	11.7	17.9	9.1	19.4	12.1	19.5	9.4	20.5	11.0	19.7	8.2	20.6
Jul	7.1	17.6	10.2	17.7	11.0	17.1	8.1	18.5	11.3	18.8	8.7	19.7	10.2	19.0	7.6	20.2
Aug	7.7	17.7	10.6	17.6	11.0	17.1	8.6	18.8	11.3	18.6	9.6	19.8	11.0	19.1	9.1	20.0
Sep	9.0	19.3	11.8	18.9	12.1	18.1	9.8	19.7	12.2	18.8	10.8	20.5	12.0	19.5	10.5	20.2
Oct	11.0	21.8	13.5	20.5	13.8	19.6	11.8	21.3	13.7	19.6	13.0	22.0	13.4	20.6	12.7	21.4
Nov	13.2	23.7	14.8	21.7	15.4	21.5	13.4	22.8	15.3	21.0	14.6	23.0	14.9	22.0	14.4	22.8
Dec	15.3	25.4	16.2	23.2	16.9	23.3	15.3	24.5	17.0	22.8	16.5	24.8	16.4	23.6	16.0	24.4

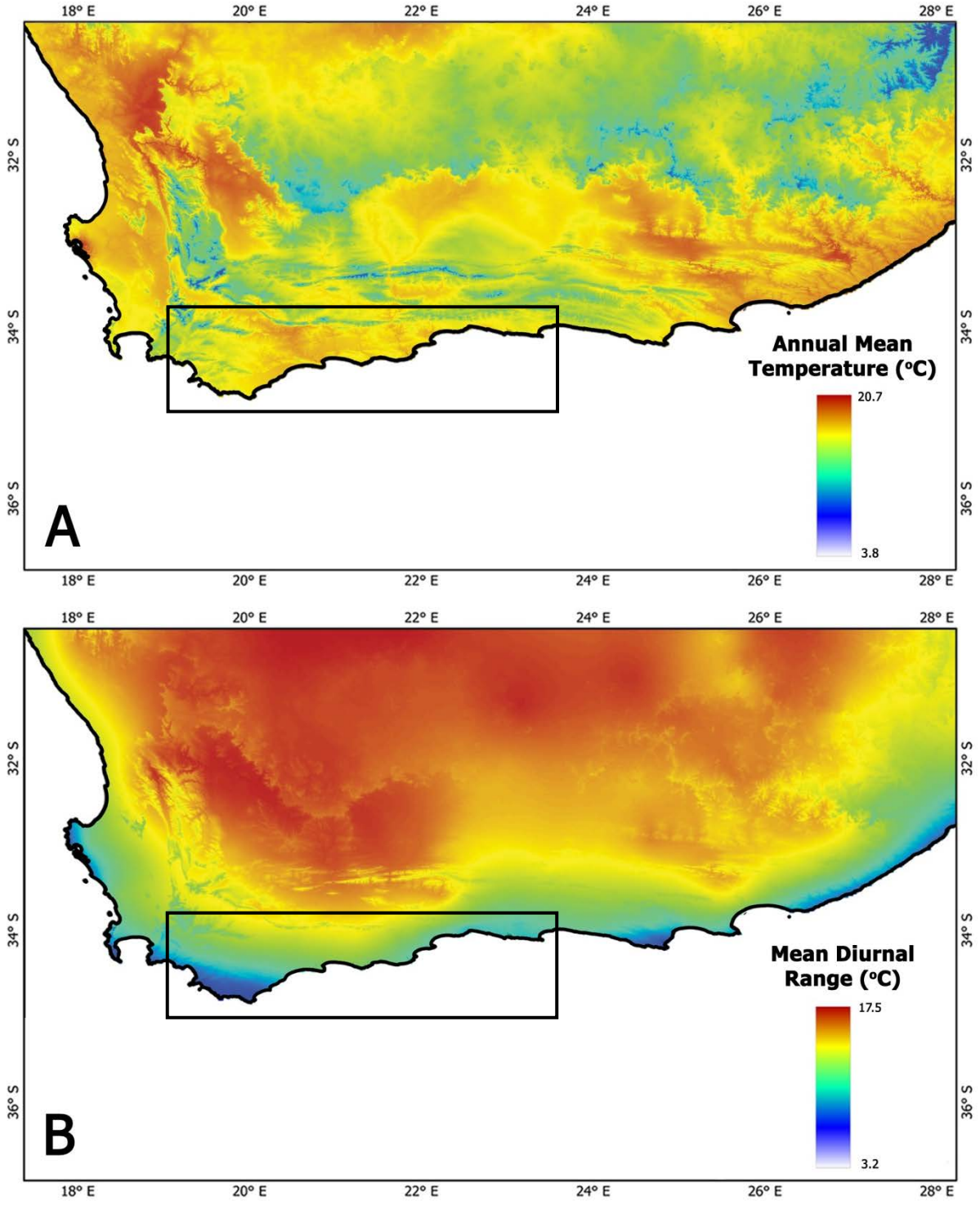

Figure 2.11 Annual mean temperatures (A) and the mean diurnal temperature range (B) [data source: WorldClim 1.4 variables BIO1 and BIO2 (Hijmans et al., 2005)], black boxes = SCCP.

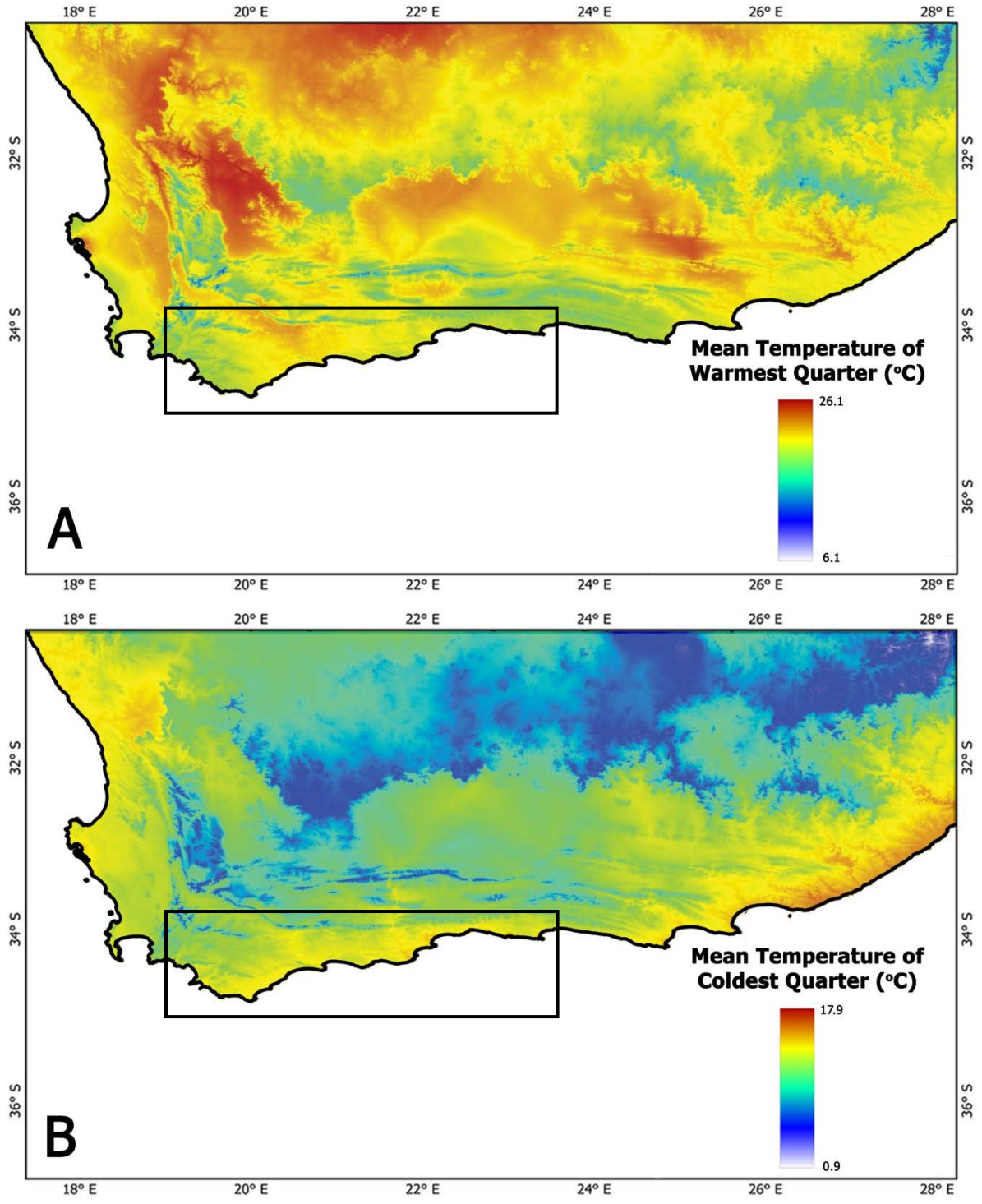

Figure 2.12 Mean temperatures of the warmest (A) and coldest (B) quarters of the year [data source: WorldClim 1.4 variables BIO5 and BIO6, (Hijmans et al., 2005)], black boxes = SCCP.

2.6 The vegetation of the southern Cape coastal plain

The SCCP covers a large proportion of the Fynbos Biome (Figure 2.12), which is the dominant vegetation of the Cape Floristic Region (CFR). The Fynbos Biome *sensu* Mucina and Rutherford (2006) encompasses the following three major vegetation types: fynbos, renosterveld and strandveld.

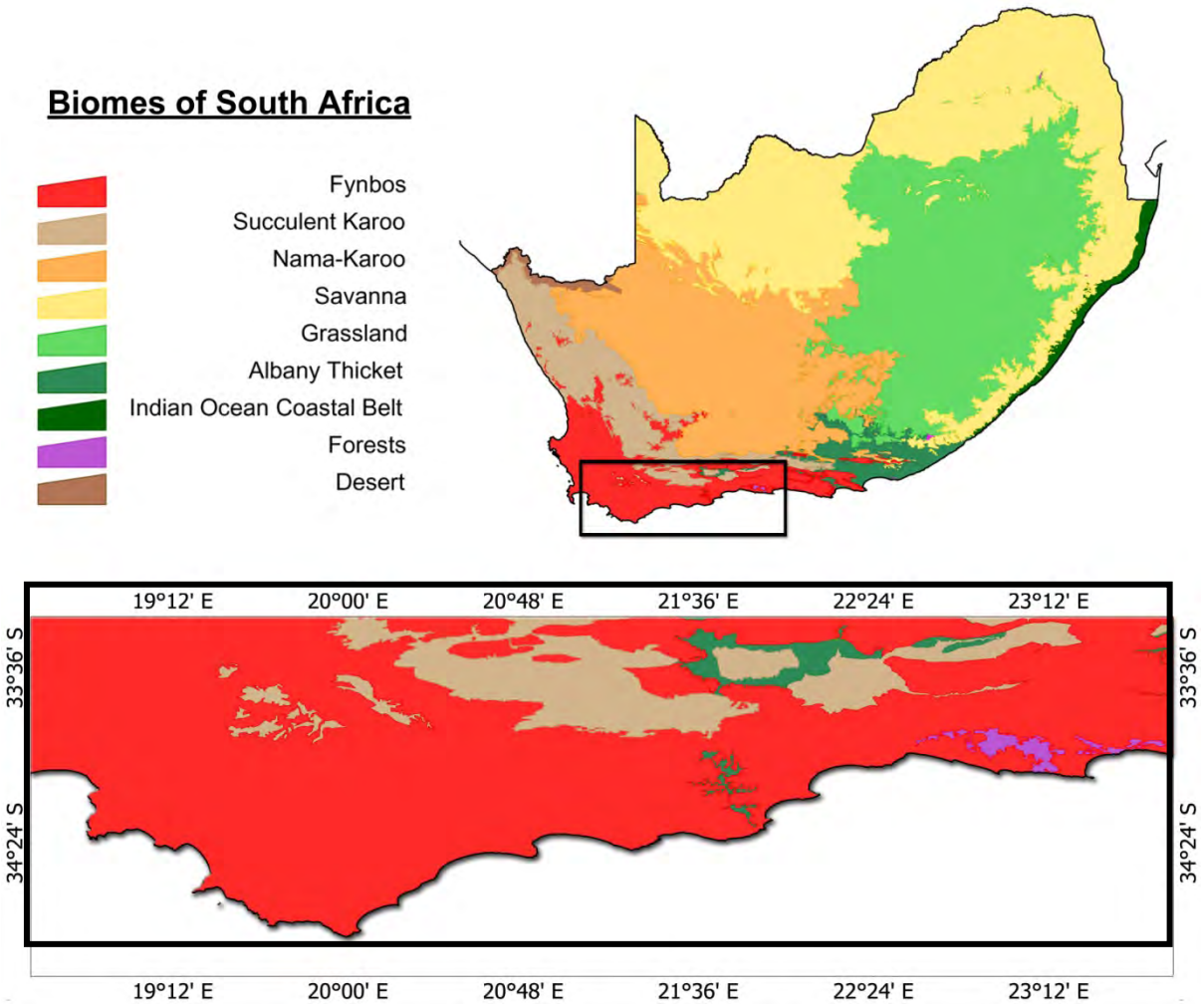

Figure 2.13 Vegetation biomes of South Africa (Mucina and Rutherford, 2006). Black boxes delineate the southern Cape coastal plain.

2.6.1 The Fynbos Biome

The vegetation of the Fynbos Biome and CFR has been subjected to decades of intensive botanical research due to its unique floristic, evolutionary and ecological characteristics as well as its conservation appeal (e.g. Bond and Goldblatt, 1984; Campbell, 1985; Cowling, 1992; Cowling et al., 1995; Cowling et al., 1997a; Goldblatt and Manning, 2000; Mucina and Rutherford, 2006). Fynbos

vegetation represents a broad complex floristic category of diverse evergreen sclerophyllous shrublands characterised by high specific (69%) and generic (16%) endemism (Cowling and Holmes, 1992b; Low and Rebelo, 1996; Goldblatt and Manning, 2002; Mucina and Rutherford, 2006; Verboom et al., 2009).

In terms of life-form categorization, fynbos is uniquely characterised by the co-dominance of hemicryptophytes, chamaephytes and phanerophytes (Rutherford and Westfall, 1986). Structurally, it is characterised by the presence of the following elements:

1. A restioid component (Restionaceae family (Cape Reed)), which replaces grasses on nutrient-poor soils where there is a strong winter rainfall component.
2. An ericoid component: small narrow rolled leaves, mainly the Ericaceae and Asteraceae families but also Bruniaceae, Fabaceae, Rhamnaceae and Thymelaeaceae families.
3. A proteoid component (Proteaceae), which represents the dominant overstorey in fynbos (Table 2-3; Figure 2.12; Cowling and Holmes, 1992b; Cowling et al., 1997a; Mucina and Rutherford, 2006).

Table 2-3 Structural communities within the Fynbos Biome (source: Cowling et al 1997 Table 6.1).

Community[a]	Formation[b]	Differentiating features	Floristics	Distribution[c]	Environment
Fynbos[d] Group: Cape fynbos shrubland					
Grassy fynbos	Low, mid-dense to closed leptophyllous (ericaceous[e] or ericoid[f]) shrubland	High grass cover and a relatively high cover of non-proteoid[f] nanophylls and forbs	Variable: *Themeda triandra, Tristachya leucothrix, Restio triticeus, Leucadendron salignum, Phylica axillaris, Erica* spp., *Helichrysum* spp., *Rhus* spp., etc.	Mainly E but also SI and SC on lower mountain slopes and coastal forelands	Easternmost fynbos (high proportion of summer rain) on finer textured and more fertile soils than other fynbos types
Asteraceous fynbos	Low to mid-high, open to mid-dense, leptophyllous shrubland	Low total cover, often high grass and elytropappoid[g] cover and a high cover of non-ericaceous ericoids	*Elytropappus, Pentaschistis, Phylica, Passerina, Agathosma* and other Rutaceae, *Aspalathus, Restio, Felicia, Hypodiscus, Cliffortia, Maytenus oleoides, Protea nitida*	Throughout the biome except for mountains in E	Occupies the driest fynbos sites on a range of substrata, linking fynbos to karroid shrubland and renosterveld; widespread on coastal forelands on calcareous dunes and on shales and silferricretes where rainfall is <550 mm yr^{-1}; in the mountains, rainfall ranges from 450 to 950 mm yr^{-1} and soil depth averages <0.4 m
Restioid fynbos	Dwarf to tall, mid-dense to closed restioland with a sparse shrub stratum	Highest restioid[f] cover (>60%) and the lowest shrub cover (<30%) of all fynbos types; it has the lowest constancy of tall (>1.5 m) shrubs	Restionaceae, *Tetraria, Leucadendron, Pentaschistis, Phylica, Protea, Stoebe*, etc.	Throughout the biome except for the mountains in E; rare in SC	Occurs where conditions are limiting for shrub growth, owing to either excessive waterlogging or drainage; it occupies more mesic sites than asteraceous fynbos; soils may be deep sands or shallow and rocky; in the mountains restioid fynbos is a feature of dry, north slopes
Ericaceous fynbos	Low to mid-high, closed ericaceous shrubland	Like asteraceous fynbos, a leptophyllous shrubland, but has a high cover of restioids and the shrubs are mainly ericaceous ericoids. Shrub cover and total cover are also higher than asteraceous fynbos	Ericaceae, Restionaceae, Bruniaceae, Penaeaceae, Grubbiaceae, *Tetraria, Leucadendron*	Mostly SW and SC	Largely confined to south-facing and wet (rainfall average of 1500 mm yr^{-1}) slopes of the coastal mountains; soils have a high carbon content, low pH and high fine-particle fraction
Proteoid fynbos	Low to tall, open to closed, proteoid shrubland	Differs from other types by having >10% cover of mid-high to tall, non-sprouting, proteoid shrubs; included also are some communities on the coastal foreland where the canopy proteoids are <1.5 m	*Leucadendron conicum, L. coniferum, L. eucalyptifolium, L. gandogeri, L. laureolum, L. loeriense, L. meridianum, L. rubrum, L. uliginosum, L. xanthoconus, Protea aurea, P. compacta, P. eximia, P. laurifolia, P. lorifolia, P. mundii, P. neriifolia, P. punctata, P. obtusifolia, P. repens, P. susannae,* Restionaceae, Ericaceae, etc.	Throughout the biome except I; relatively rare in NW and E and most extensive in the SC	Like grassy fynbos, proteoid fynbos occurs at lower altitudes and on more fertile soils than other fynbos types; soils are mostly deep, well-drained and derived from a wide range of substrata including colluvial sands and limestone on the forelands; altitude ranges from sea level to 950 m, and rainfall from 400 to 1100 mm yr^{-1}
Closed-scrub fynbos	Mid-high to tall, open to closed, nano-microphyllous shrubland with an open cover of tall restioids	Similar to forest and thicket in the relatively high cover of mesophyllous, non-proteoid woody plants. Differs by having a high cover (>10%) of restioids and a high frequency of ericaceous ericoids	*Meterosideros angustifolia, Brachylaena neriifolia, Calopsis paniculatus, Salix mucronata, Cannomois virgata, Berzelia intermedia, Empleurum serrulatum, Leucadendron salicifolium, Elegia capensis*	Throughout the biome except in the E and I	Associated with well-drained riparian habitats
Non-fynbos Group: Renosterveld and karroid shrubland					
Renosterveld	Low to mid-high, open to mid-dense leptophyllous shrubland, often with an open, grassy understorey	Generally lacks fynbos characteristics (restioids, proteoids, ericaceous ericoids); high cover of elytropappoids, grasses and fleshy-leaved shrubs	*Elytropappus rhinocerotis, Pteronia* spp., *Anthospermum aethiopicum, Dodonaea viscosa, Pentaschistis* spp., *Relhania* spp., *Helichrysum* spp., *Ruschia* spp., *Themeda triandra*	Throughout the fynbos biome on lower mountain slopes, interior valleys and coastal forelands	On fine textured soils usually on the ecotone between fynbos and succulent (karroid) shrubland; very occasionally on quartzite; rainfall mostly <450 mm yr^{-1}

[a] Communities described are at the series level in Campbell's (1985) scheme.
[b] According to Campbell *et al.* (1981).
[c] In relation to the montane regions of Campbell (1985): C, central; E, eastern; I, interior; NW, northwestern; SC, southern coastal; SI, southern interior.
[d] See text for distinction between fynbos and non-fynbos.
[e] Refers to ericoid shrubs belonging to the Ericaceae.
[f] See Table 6.2 for description of growth forms.
[g] Shrubs with scale-like, pubescent leaves; most are species of *Elytropappus* and *Stoebe* (Asteraceae).

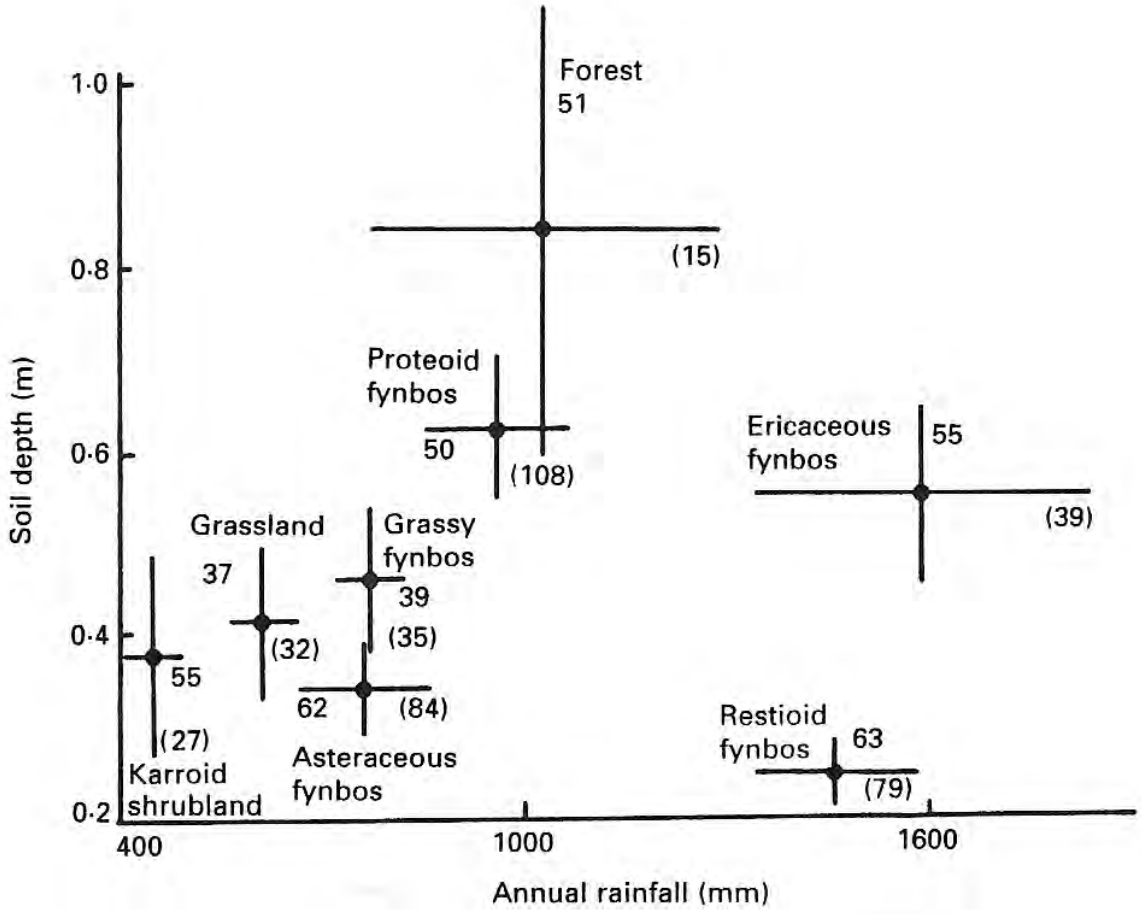

Figure 2.14 Major plant communities of the Fynbos Biome and selected adjacent biomes in relation to annual rainfall (mm) and soil depth (m). Horizontal and vertical lines are the 95% confidence intervals, numbers in figure (no parentheses) is the % winter rainfall, numbers in parentheses are the number of plots per community (source: Campbell and Werger, 1988 redrawn in Cowling et al., 1997).

Several factors have been proposed to be responsible for the distribution of fynbos including: climate (winter rainfall and summer drought), fire regime (intense and recurrent summer fires at intervals between four and 40 years (van Wilgen, 1992) and edaphic controls. Many authors propose that climate and nutrient-poor soils are of greatest significance (Cowling, 1983b; Campbell, 1985; Campbell and Werger, 1988; Richards et al., 1997; Lechmere-Oertel and Cowling, 2001; Mucina and Rutherford, 2006). Rutherford and Westfall (1986) claim that fynbos is climatically distinguished from other biomes by receiving more than 40% of its annual rainfall during the winter months. In comparison to adjacent biomes, soils from within the Fynbos Biome tend to have lower PH values, lower available phosphorous, lower base values and higher clay contents (Cowling et al., 1997a). Edaphic control appears to be especially important in maintaining vegetation boundaries and persistence within the mountainous regions of the Fynbos Biome, while lowland fynbos communities are potentially more susceptible to intermingling and invasion by either different fynbos types or

non-fynbos communities[4] (Cowling and Campbell, 1983; Campbell, 1985; Campbell and Werger, 1988).

Fire is a major driving force in fynbos plant communities, with many fynbos species only regenerating with the release of their seeds after fire (Cowling et al, 1992). Without fire, fynbos communities become senescent and other plant types can invade into the biome (Cowling et al., 1992; Mucina and Rutherford, 2006). An important element with respect to fire and fynbos is changes in the fire season which is thought to be driven by changes in rainfall seasonality and temperature fluctuations (Deacon et al., 1992).

Therefore borders between fynbos and non-fynbos communities are generally maintained through specific combinations of climatic and edaphic controls together with the fire regime.

2.6.2 Southern Cape vegetation

The sampling sites can be broadly attributed to three botanically-significant geographical areas: the Agulhas Plain (A), the Riversdale Plain (B) and the Knysna Afrotemperate forest complex (Figures 2.1, 2.14 and 2.16). The major vegetation groups found within these areas are described below while the specific vegetation units (and dominant species) found at the sites are given in Chapter 4.

2.6.2.1 The Agulhas and Riversdale plains

The Agulhas Plain contains exceptionally high levels of biodiversity (~1 751 species) and endemism (~100 species confined to the area of about 2 160 km^2) (Cowling and Holmes, 1992a; Lombard et al., 1997). Detailed descriptions and classifications for the area have been generated with the predominant vegetation types being identified as fynbos and renosterveld. (Cowling et al., 1988; Cowling and Holmes, 1992a). This coastal lowland plain has been extensively fragmented through the conversion of land for agriculture, the growth of coastal towns and the aggressive spread of invasive alien species resulting in high levels of species vulnerability (Rouget, 2003). Therefore various conservation measures have been fairly extensively investigated and applied (Willis et al., 1996b; Lombard et al., 1997; Heydenrych et al., 1999; Castellani, 2000; Cole et al., 2000; Pence et al., 2003; Rouget, 2003; Joubert et al., 2009; Laubscher and Ndakidemi, 2009; Laubscher et al., 2009).

[4] However the exception is limestone fynbos which is strongly edaphically-constrained.

Despite exhibiting slightly lower species richness and diversity in comparison to the Agulhas Plain (~1 580 species in 2 800 km^2), the Riversdale Plain represents an important area of the Fynbos Biome and CFR as it contains over half of all the limestone fynbos and 88% of dune fynbos (as defined by Moll et al., 1984 and Bohnen, 1986 referenced in Low and Rebelo, 1991). In terms of botanical studies, the Riversdale Plain has received significantly less attention compared to the Agulhas Plain. Only one detailed floristic description has been published for the area (Rebelo et al., 1991) and more recently, a fine-scaled vegetation map has been created (Vlok and De Villiers, 2007).

Figure 2.14 displays the major vegetation groups present on the Agulhas and Riversdale Plains, after which general descriptions of these principal groups are provided.

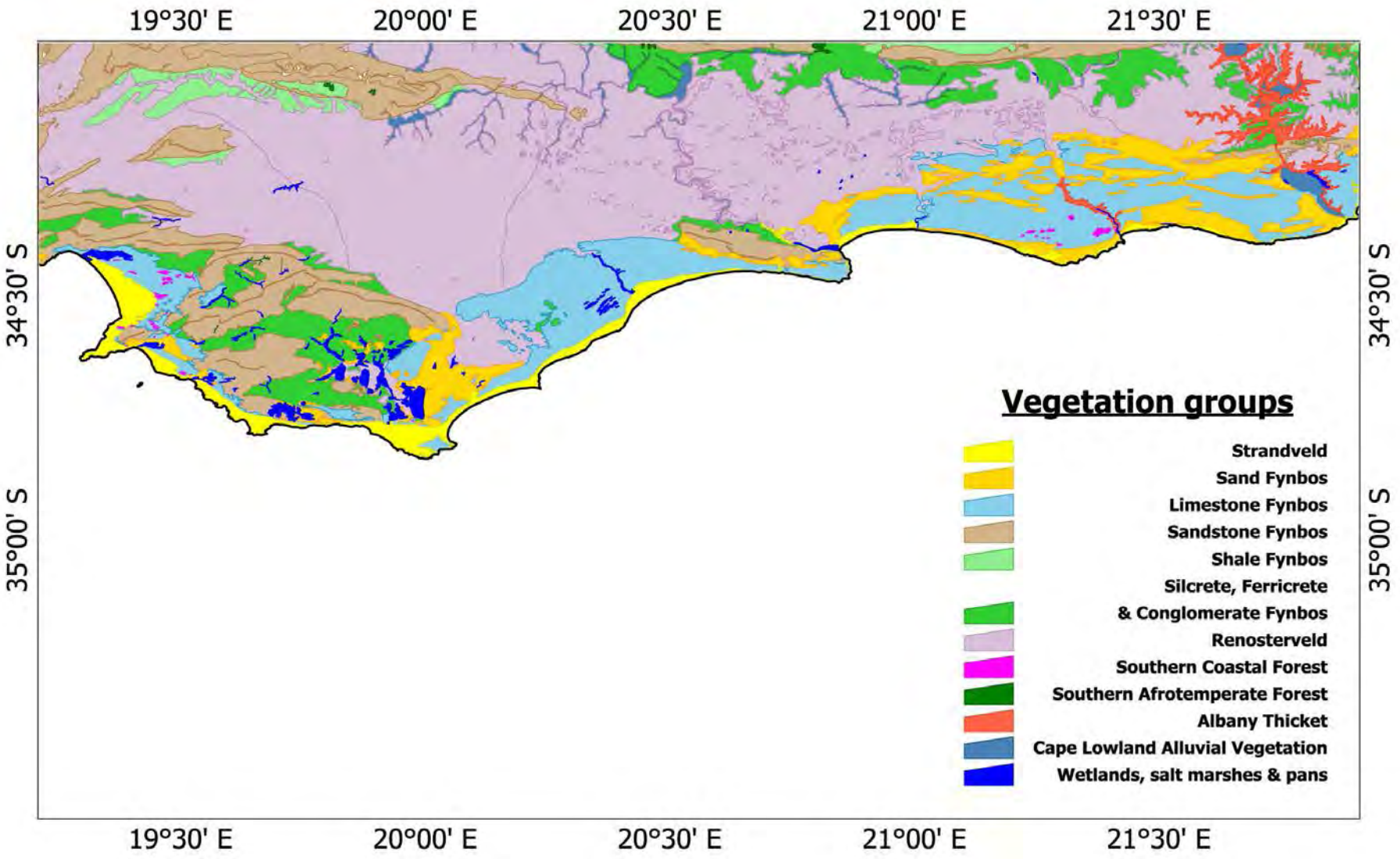

Figure 2.15 Vegetation groups on the Agulhas (A) and Riversdale (B) Plains [data source: Mucina and Rutherford, 2006].

Limestone Fynbos

The differentiation of many of the different fynbos communities on both the Agulhas and Riversdale Plains is largely controlled by edaphic factors (Thwaites and Cowling, 1988a; Cowling, 1990; Rebelo et al., 1991; Lombard et al., 1997; Richards et al., 1997). This is especially the case for limestone fynbos which is only found on the alkaline soils of the Bredasdorp Group limestones and aeolianites. Due to its highly specialised and restricted nature it represents one of the most threatened fynbos vegetation types (Cowling and Holmes, 1992a; Willis et al., 1996b).

Limestone fynbos is compositionally very distinct from other fynbos groups and shares very few species across vegetation unit boundaries. Structurally, limestone fynbos is dominated by asteraceous, restioid and proteoid fynbos with graminoid and ericaceous fynbos being largely absent from this group (Mucina and Rutherford, 2006). Limestone fynbos patches form 'islands' within larger expanses of sand fynbos. The interface between these two groups is often fringed with thicket (strandveld) elements (Mucina and Rutherford, 2006).

As the calcareous substrates upon which limestone fynbos grows were laid down during the Pliocene and Pleistocene marine transgression-regression cycles (section 2.3.1), it has been proposed that this type of fynbos is relatively young (Cowling and Holmes, 1992a; Mucina and Rutherford, 2006).

Sand Fynbos

Sand fynbos is almost exclusively found on the coastal lowlands and is one of the largest groups of fynbos (Mucina and Rutherford, 2006). On the southern Cape coastal plain, sand fynbos generally inhabit the fairly deep, weakly acidic, infertile soils and colluvial sands that surround limestone hills (Cowling, 1990). Proteaceae and Restionaceae are common, while geophytes are fairly rare (Mustart et al., 2003). Sand fynbos can take on any of the five structural forms of fynbos depending on the depth of the water table (Mucina and Rutherford, 2006). Boundaries between sand fynbos and thicket communities are often dynamic with localised fire frequencies and dune topography playing the determining roles in their respective distributions.

Sandstone Fynbos

Sandstone fynbos (synonymous with mountain fynbos) is the largest fynbos group covering one third of the area of the Fynbos Biome (Mucina and Rutherford, 2006). It occurs on high-relief areas of coarse-grained, nutrient-poor substrates derived from TMG sandstones and is therefore predominantly found on the Cape Fold Belt mountain ranges. Consequently, sandstone fynbos is not very prevalent on the southern Cape coastal plain. No sandstone units are found on the Riversdale

Plain although Overberg Sandstone Fynbos does occur on the sandstone hills on the western margins of the Agulhas Plain.

Silcrete, Ferricrete and Conglomerate Fynbos

These three relatively small groups (accounting for less than 5% of the Fynbos Biome) represent intermediate units between sandstone and shale fynbos or sandstone fynbos and renosterveld. They are often underlain by more than one geological type and therefore Mucina and Rutherford (2006)'s classification of these units is somewhat arbitrary.

Southern Coastal Forest

This vegetation group is represented by the Western Cape Milkwood Forests on the southern Cape coastal plain. These scrub forests have a very fragmented distribution along the coast on deep nutrient rich sandy soils over aeolianite or limestone of the Bredarsdorp Group (Mucina and Rutherford, 2006). These forests are low, scrub forest characterised by *Sideroxylon inerme* (white milkwood) and distinctly different from the afromontane/afrotemperate forests discussed below.

Strandveld/Coastal thicket

Strandveld, a medium dense to closed shrubland, is a mosaic of asteraceous or restioid fynbos and subtropical thicket (alternatively named dune thicket or coastal thicket) which generally inhabits calcareous coastal dune areas (Cowling et al., 1997a). Evergreen thicket elements (e.g. *Euclea, Maytenus, Rhus*) either form distinctly separate thicket patches/low forest stands or are intermingled amongst fynbos elements. Strandveld is floristically and structurally very different from fynbos: thicket taxa occur outside the biome[5], have low flammability, fleshy ornithochorous fruits and seedling establishment does not occur directly after fires (Cowling et al., 1997a and references therein; Mucina and Rutherford, 2006). Restionaceae is often present within strandveld, however Proteaceae is absent and Ericaceae taxa are extremely rare (Mucina and Rutherford, 2006).

Dune fynbos represents the seral stage between strandveld and fynbos (predominantly sand fynbos) (Cowling and Pierce, 1988). Dune fynbos occurs over a wide range of habitats including dune ridges where the soils are deep, well-drained, alkaline sands and also shallow sands overlying calcrete. The interplay between fire, succulence (fire-sensitive taxa) and dune topography (affecting the type of soils) regulate the boundaries between sand fynbos and strandveld and result in a spectrum of

[5] Low and Rebelo (1996) included the coastal thickets of the Western Cape as part of the Subtropical Thicket Biome/Albany Thicket Biome.

possible community responses that can vary temporally as well as spatially (Mucina and Rutherford, 2006; Figure 2.15).

On the Agulhas Plain, strandveld can be replaced with Western Cape Milkwood Forests (Cowling et al., 1988).

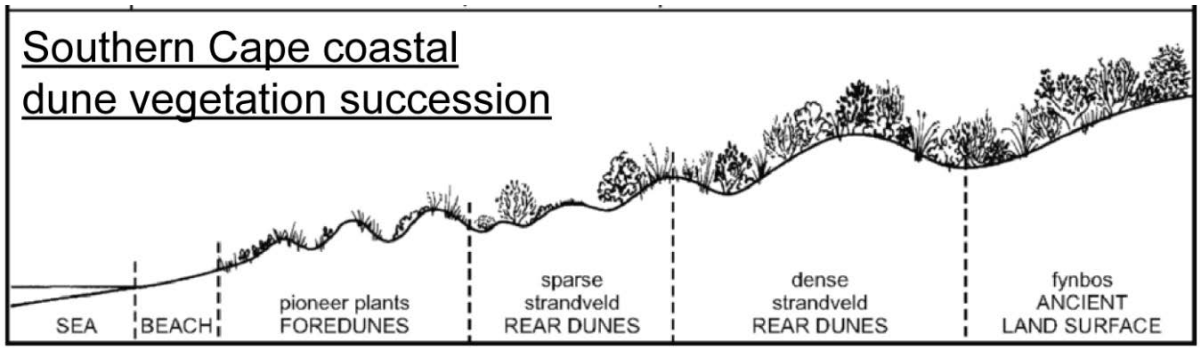

Figure 2.16 Succession from seashore vegetation to strandveld to fynbos (source: Lubke et al., 1997).

Southern Cape Valley Thicket

Southern Cape Valley Thicket is primarily found within the river valleys of the Goekoe River (between Riversdale and Still Bay) and the Gouritz River valley with smaller unmapped patches present within other valleys within the Western Cape (Mucina and Rutherford, 2006). This group represents the westernmost thicket type within the Albany Thicket Biome. It is entirely embedded within renosterveld units with the incidence of thicket patches becoming more prominent east of Riversdale (Mucina and Rutherford, 2006).

It is a dense, woody, semi-succulent and thorny variety of thicket with a wide range of growth forms, a testament to the transitional nature of this vegetation type. *Aloe ferox*, a succulent and rosulate tree, is prominent feature within Valley Thicket.

In general, the separation between the Fynbos Biome and Albany Thicket Biome is tied to seasonality of rainfall with Albany thicket communities associated with areas of lower moisture availability and an increased proportion of summer rainfall. Cowling and Holmes (1992b) claim that summer growth season temperature is the overriding factor controlling this boundary. However, the boundary between Southern Cape Valley Thicket and renosterveld is related to topography and fire. Valley Thicket is limited to fire-free (fire destroys the succulent-rich thicket taxa), steep, highly exposed slopes in valleys containing skeletal soils (Cowling, 1983b).

Renosterveld

Renosterveld is a non-fynbos shrubland or grassland and therefore generally lacks the typical structural fynbos elements outlined above. It is characterised by the dominance of members of the Asteraceae family - specifically one species; *Elytropappus rhinocerotis* (Renosterbos) and has an understorey of Poaceae and geophytes (Boucher and Moll, 1981; Cowling et al., 1997a; Mucina and Rutherford, 2006).

Renosterveld is broadly confined to moderately fertile soils, mainly clays and silts derived from the Malmesbury and Bokkeveld Groups as well as the Karoo Sequence, and is found on the coastal forelands and inland valleys (Low and Rebelo, 1996). On the Agulhas and Riversdale plains this correlates to the areas between the Cape Fold Belt mountain ranges and the limestone lowlands. The boundaries between renosterveld and granite and shale fynbos are often very diffuse (Mucina and Rutherford, 2006). Towards the eastern margins of the southern Cape coast, renosterveld grades into Albany thicket vegetation units where dissected topography prevents the spread of fires (Lombard et al., 1997).

With nearly 85% of south coast renosterveld having been replaced by agriculture, conservation of the remaining fragmented patches of this vegetation type has been afforded great importance in terms of management strategies (Kemper et al., 1999).

2.6.3 The Knysna Afrotemperate Region

Due to the extremely fragmented (archipelego-like) distribution of indigenous forests[6] in South Africa, they should not be classified as a single biome (Mucina and Rutherford, 2006). However, as southern Africa's largest forest complex (Geldenhuys, 1993; Midgley et al., 1997), the afromontane (White, 1978) or rather afrotemperate (Meadows and Linder, 1993; Low and Rebelo, 1996) forests of the southern Cape do qualify as a separate biome in their own right (Rutherford and Westfall, 1986). Mucina and Rutherford (2006) defined the southern Cape forests as one of their zonal vegetation units, the Southern Cape Afrotemperate Forest Type. The largest concentration of this vegetation unit is the Knysna Afrotemperate Region (KAR) which roughly equates to the area extending from 22° E to 24° 30' E (Geldenhuys, 1991) bounded by the coast to the south and the Outeniqua, Langkloof and Tsisikamma mountain ranges to the north (Figure 2.16).

[6] Indigenous forest is defined as: "a generally multilayered vegetation unit dominated by trees (largely evergreen or semi-deciduous), whose combined strata have overlapping crowns and where graminoids in the herbaceous stratum are generally rare (Bailey et al., 1999 as cited in; Mucina and Rutherford, 2006: 586).

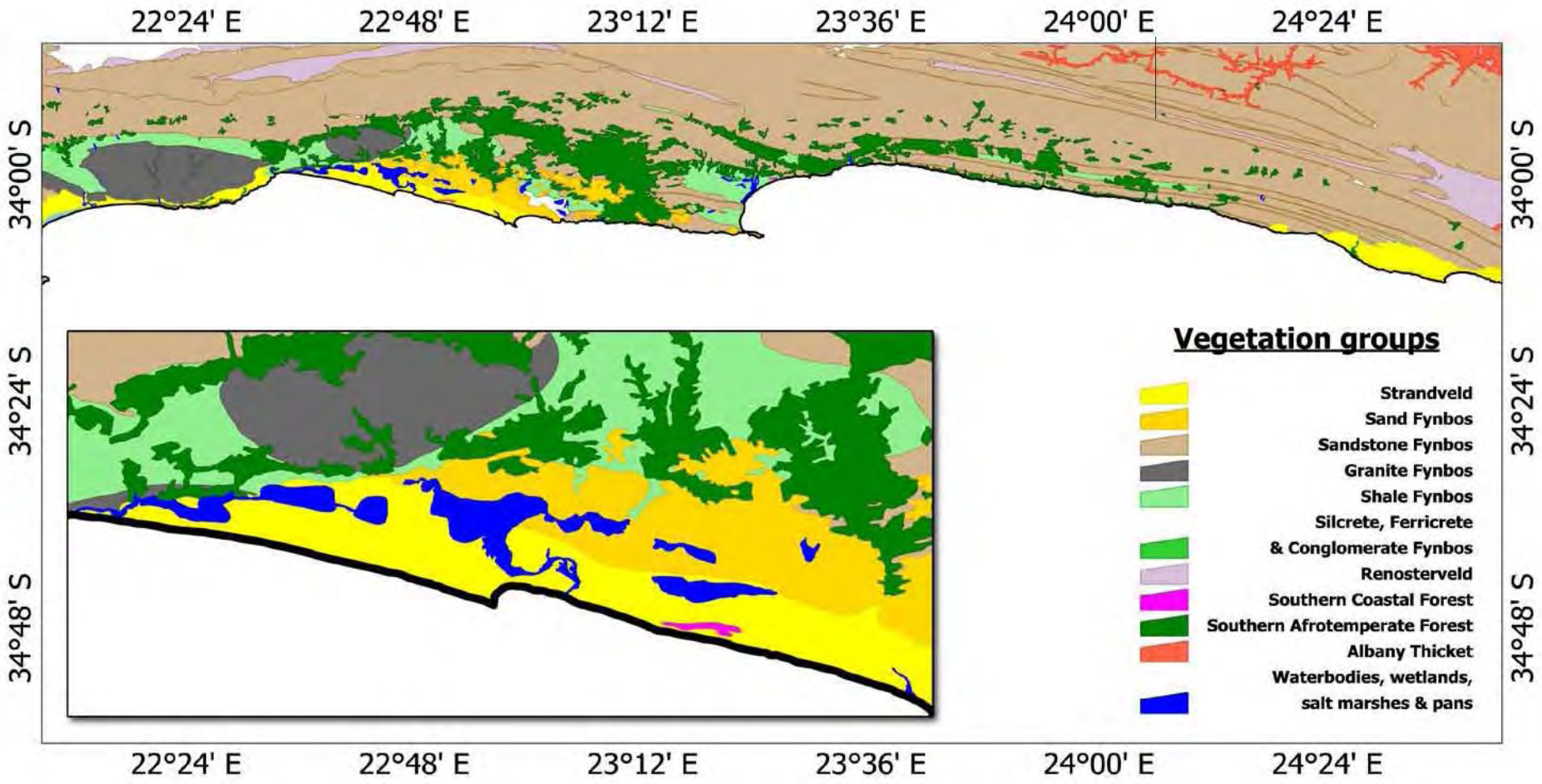

Figure 2.17 The extent of the Southern Afrotemperate Forest complex with the Wilderness embayment as the inset [data source: Mucina and Rutherford, 2006].

This region was originally botanically described by Phillips (1931, as cited in Geldenhuys, 1993) as temperate-form subtropical moist forests. Geldenhuys (1993), building on von Breitenbach (1974) and several other early botanical works, classified the KAR into several subtypes including: high[7] wet forest (comprised mostly of afromontane tree taxa), moist forest, moist to dry forest, dry forest grading into coastal scrub[8] forest (full annotated species list found in Geldenhuys 1993). His structural analysis highlights a clear differentiation between tree and understorey species along altitudinal, topographical and geological gradients. In general, the dominant canopy species of the Knysna forest communities are:

- *Ocotea bullata* (Lauraceae)
- *Olea capensis ssp. marcocarpa* (Oleaceae)
- *Podocarpus falcatus* (Podocarpaceae)
- *P. latifolius* (Podocarpaceae)

(Geldenhuys and MacDevette, 1989 cited in Midgely et al., 1997).

Endemism and speciation levels are both low within the KAR (Phillips, 1931 as cited in Geldenhuys, 1993), as is the case for all South African forests (Figure 2.17).

[7] Stand heights of over 30 m constitutes high forest
[8] Stand heights of ~3 m and below constitutes scrub forest

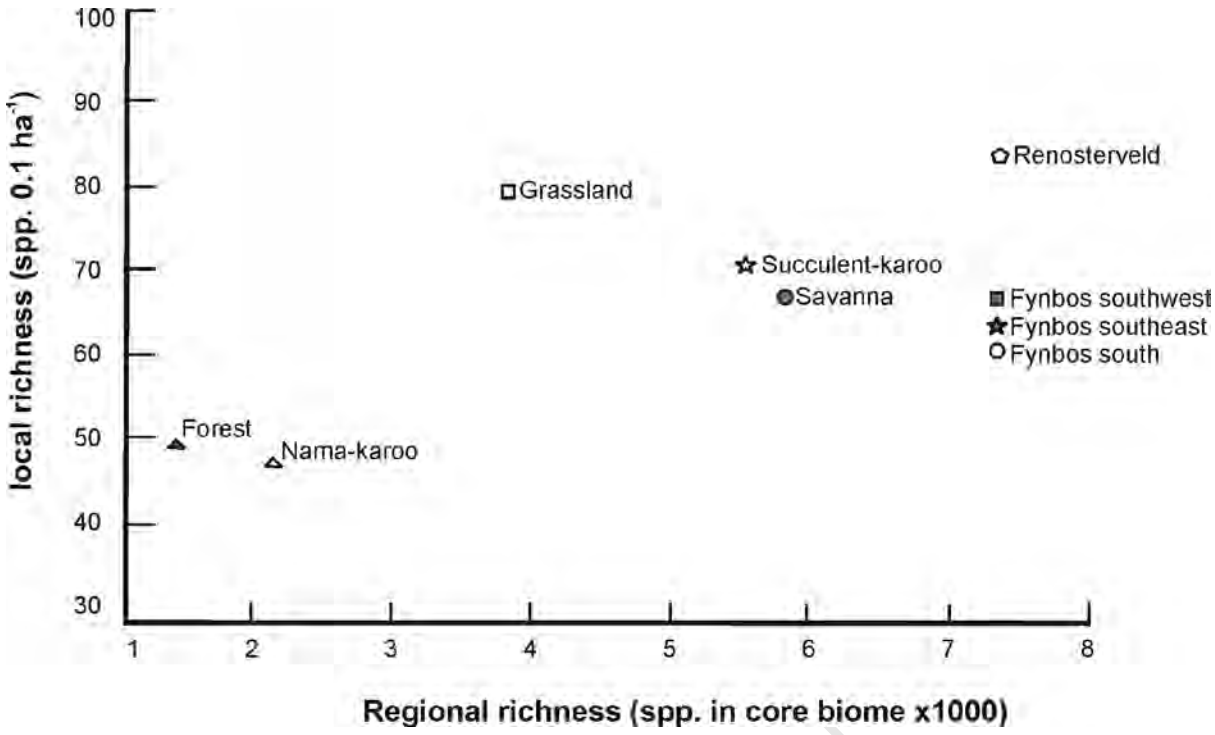

Figure 2.18 Relationship between local richness [mean number of species in 0.1 ha^{-1} plots data from Cowling et al. (1992)] and regional richness [number of species in core biomes, data from Gibbs Russell (1987), Geldenhuys (1992) and Cowling et al. (1997a)] redrawn from Cowling et al. (1997b).

The fynbos/forest boundary

In the KAR region, the 'islands' of forest are embedded within patches of various fynbos types, coastal thicket, southern coastal forest and karroid vegetation resulting in Cowling (1983b) stating that the area "comprises a huge tension zone where four major phytochoria converge" (page 396).

Climate, edaphic controls, topographic complexity, fire regimes and ecological factors such as vegetation succession all appear to influence the distribution of forests to varying degrees over multiple spatial and temporal scales (Cowling, 1983b; Rutherford and Westfall, 1986; Manders, 1990; Cowling and Holmes, 1992b; Geldenhuys, 1997; Mucina and Geldenhuys, 2006).

According to Rutherford and Westfall (1986), ~625 mm of rainfall is generally required for the development of forests, with winter-rainfall areas requiring less than this (525 mm) and summer-rainfall areas greater amounts (725 mm). This condition is currently met in the Knysna region, where orographic rainfall is extremely high ensuring that soil moisture is not limiting for extensive periods of time, with a combination of low seasonality and high absolute precipitation amounts therefore promoting forest establishment (Cowling, 1983b). Some authors claim that the Fynbos Biome is bioclimatically suitable for an expansion of afrotemperate forests (e.g. Manders, 1990; Cowling and Holmes, 1992b; Midgley et al., 1997). However the limited forest distribution and clear boundaries

between fynbos and forest indicates that rainfall amount[9] is a poor differentiating factor for estimating the present boundaries between these two vegetation types.

Forests are normally associated with deeper, more fertile soils than fynbos (Cowling and Holmes, 1992b). However this association is most probably the result rather than the cause of forest establishment: forest can develop on soils that support fynbos with chemical differences resulting from the different plant-induced nutrient cycling processes (Thwaites and Cowling, 1988b; Manders, 1990; Cowling et al., 1997a). Edaphic factors appear to therefore control the rate of forest development but do not govern the extent or the establishment of forests (Manders et al., 1992).

Fire is an extremely important determinant of forest boundaries and forest composition, in general across South Africa and specifically in terms of fynbos-forest boundaries (Cowling et al., 1997a; Midgley et al., 1997). Manders and Richardson (1992) proposed a conceptual model that highlights the importance of fire in maintaining fynbos communities over forest (Figure 2.18). Forest species will encroach upon, and eventually replace, fynbos communities given time and the exclusion of fire.

On a more localised scale, Geldenhuys (1994) suggested that the distribution pattern of forest patches in the Knysna-Tsisikamma area is determined by the interplay between topography and fires specifically associated with berg winds. The topographic configuration of the coastal plain and mountain ranges in this area confines the flow of berg winds which in turn controls the location of fires associated with these hot, dry winds.

Overall, it appears that an increase in total rainfall, reduced seasonality, decreased summer drought and fewer fires will promote forest expansion or enhance the persistence of already established forest patches.

[9] Rainfall seasonality may be more of an important factor than total amount.

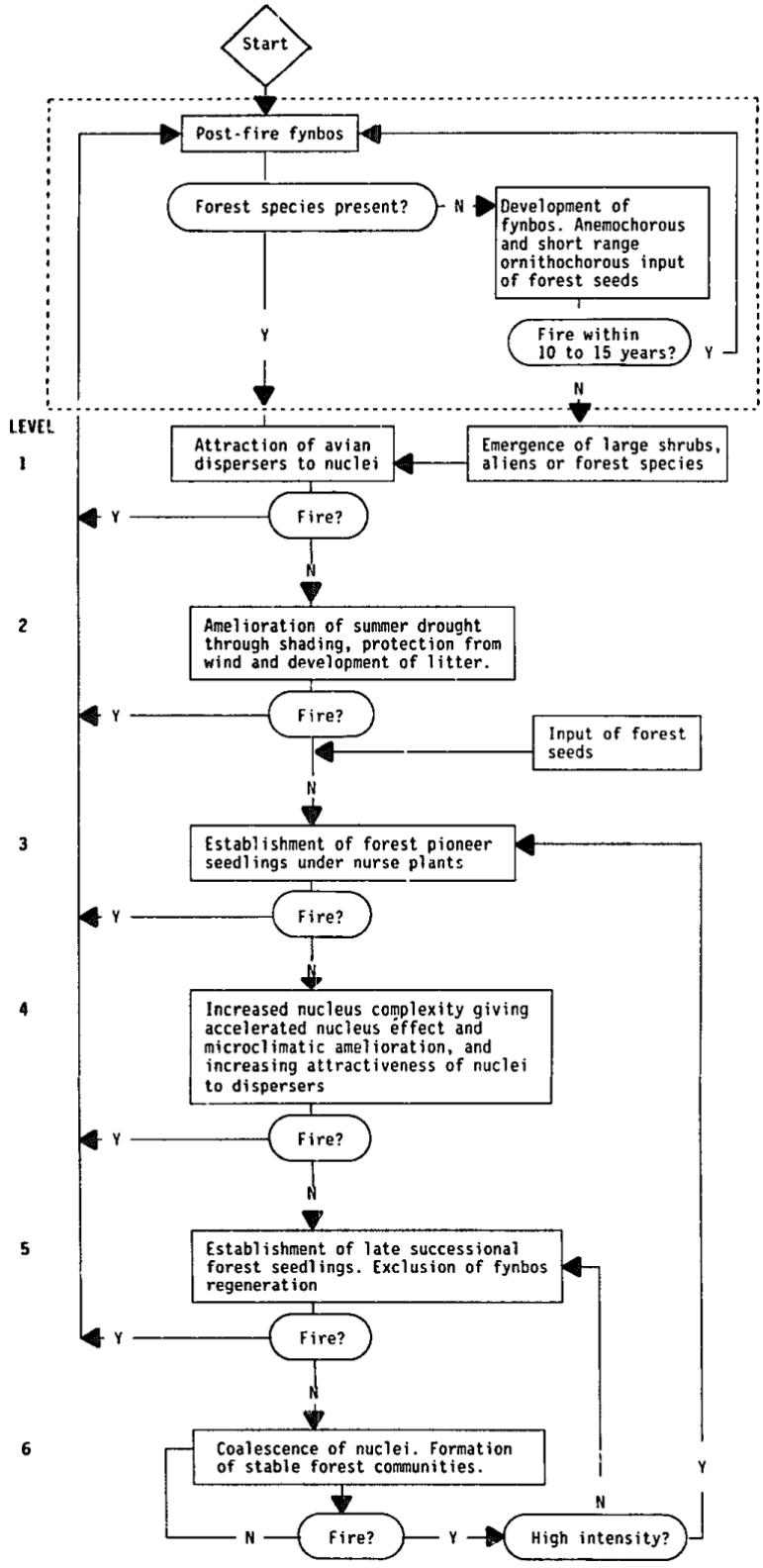

Figure 2.19 A conceptual model of the fire-driven succession between fynbos and forest (source: Manders and Richardson, 1992).

Fynbos communities within the KAR

The distribution of the fynbos units that are presently interspersed with forest patches within the KAR are displayed in Figure 2.16. The strandveld, Sand Fynbos and Southern Coastal Forest groups are outlined within section 2.6.2.1. The region contains relatively large proportions of shale and granite fynbos.

Granite fynbos only accounts for two percent of the overall Fynbos Biome, it is a tall dense form of fynbos often characterised by *Cliffortia* and other spiny-leaved species (Mucina and Rutherford, 2006). It has a distinctive post-fire seral phase dominated by dense stands of Asteraceae and Fabaceae (primarily *Aspalathus*), which lasts for a few years then dies away being replaced by asteraceous, restioid and proteoid fynbos.

Patches of shale fynbos occur from the Groot Brak River Valley through to Plettenberg Bay on Kaaimans Group sediments and abutting granite fynbos outcrops (Mucina and Rutherford, 2006; Figure 2.16). The prominent features of shale fynbos are the relatively high proportions of grasses and herbs.

These two vegetation groups are structurally and floristically similar except that granite fynbos has thicket and scrub forest elements whereas shale fynbos does not (Mucina and Rutherford, 2006).

2.7 Conclusion

This chapter has outlined the general location, geological, climatic, geomorphological and ecological features of the southern Cape coastal plain – providing the contemporary context for the study. The following chapter reviews the current understanding of the palaeoenvironmental history of the region.

3. Late Quaternary palaeoenvironments of the southern Cape

3.1 Introduction

The aim of this chapter is to provide a review and synthesis of the palaeoenvironmental evidence available for the southern Cape coastal plain and neighbouring regions. The late Quaternary palaeoenvironmental history of the SCCP has yet to be fully established mainly due to the limited number of published records for this region (Figure 3.3) and the discontinuous temporal nature of many of these records. Encompassing portions of the modern WRZ and the YRZ, the Fynbos Biome, the Albany Thicket Biome and afrotemperate forests bioregion, the SCCP represents a unique region characterised by high degrees of climatic and ecological heterogeneity. Therefore interpretations of palaeoenvironmental evidence can be complex and interpolations beyond the site level cannot always reliably be applied to regional syntheses.

3.2 Definitions

3.2.1 Ages and time periods

Calibrated radiocarbon ages are cited using the suffix "cal kBP", while uncalibrated ages are reported using the suffix "^{14}C kBP". Ages reported using the suffix "ka" are those generated from optically stimulated luminescence, uranium-series techniques, ^{18}O stratigraphies or a combination of methods (c.f. Chase and Meadows, 2007).

Marine oxygen isotope stages (MIS) are considered in association with the below key episodes and are used to provide chronological structure to the chapter. The review encompasses MIS 5 – MIS 1, with boundaries defined according to Martinson et al. (1987): MIS 6-5 = 128 ka, MIS 5-4 = 74 ka, MIS 4-3 = 59 ka, MIS 3-2 = 24 ka and MIS 2-1 = 12 ka.

The time periods of particular palaeoenvironmental significance discussed in this chapter include: the Last Glacial Maximum (LGM), the last glacial-interglacial transition (LGIT), the Holocene and the Holocene Altithermal (HA). The LGM is the period within which global ice coverage reached its maximum and represents the time whereby glacial environmental conditions were the most developed. The 'Environmental Processes of the Ice-Age Land, Ocean, Glaciers Programme' (EPILOG) (Mix et al., 2001; Clark and Mix, 2002) defines the LGM as the period from 24 – 18 ka. Even though the LGM is considered a global event; its regional expressions varied, with maximum ice presence

and extent peaking at different times in the Northern and Southern Hemispheres (Gersonde and Zielinski, 2000; Dyke et al., 2002; Crosta et al., 2004; Stuut et al., 2004). The last glacial – interglacial transition (LGIT) encompasses the transition between the LGM and the Holocene roughly between 18 – 11.5 ka. The LGIT does not represent a smooth transition period but instead corresponds to a dynamic climate phase. The Holocene is the interglacial period covering the last ~11 500 years (Mayewski et al., 2004). The warmest part of the Holocene is referred to as the HA, and Chase and Meadows (2007) tentatively define this period as spanning from 8 – 4 ka in southern Africa.

3.2.2 Geographical extent of the review

The SCCP, as defined in Chapter 2, is climatically complex as it encompasses the transition between the WRZ and the YRZ. As climate boundaries are inherently dynamic, these precipitation boundaries most likely would have changed over the time period relevant to this study. Therefore, this chapter not only examines the existing palaeoenvironmental sites found within the boundaries of the SCCP, but also includes all sites within the modern YRZ and sites that would potentially be included within an expanded WRZ.

The hypothesis developed for this study is centred on the varying influence of winter-rainfall bearing systems along the southern Cape coast. Due to the relatively limited number of sites in the SCCP, in order to develop a comprehensive palaeoenvironmental framework, key evidence from the west coast, Namibia and marine cores from both the Benguela and Agulhas current regions are also reviewed.

3.3 Previous southern African palaeoenvironmental reviews

The majority of previously published syntheses of southern African palaeoenvironmental evidence date to the 1990s or earlier and therefore do not include the latest developments within the field (e.g. Deacon and Lancaster, 1988; Partridge et al., 1990; Partridge, 1997; Meadows and Baxter, 1999; Partridge et al., 1999). Many of these review papers have either focussed narrowly on one specific subregion and have consequently built broader regional syntheses on localised assumptions, or have conflated palaeoenvironmental evidence from differing climatic and biogeographical regions into generalised syntheses (e.g. Partridge, 1990). This has been a necessary consequence of the limited number of records but was sometimes accompanied by the assignment of inappropriate climatic regional boundaries and inaccurate associations with ecological boundaries. For example,

the establishment of a more precise delineation of the boundaries of the WRZ (c.f. Chase and Meadows, 2007) highlights the fact that the area covered by the WRZ is distinctly different from the winter rainfall area as defined by Meadows and Baxter (1999), as well as the limits of the Fynbos Biome. A further problem affecting review and individual site papers is that the same type of evidence can be interpreted differently by different authors.

Archaeological sites represent a valuable source of palaeoenvironmental information. However, the practice of assigning archaeological units to certain age periods using relative methods and erroneous assumptions relating to climate states (as outlined in Chase, 2010) has led to much confusion and misinformation. Many of these problems have stemmed from the difficulties of establishing robust chronologies. Radiocarbon dating is limited to a functional range of roughly 40 – 50 ka and is not a reliable technique for accurately dating certain open-system carbonates, which are prevalent in southern Africa (Geyh and Eitel, 1998; Chase and Meadows, 2007). However the application of single grain OSL techniques to archaeological deposits (e.g. Jacobs et al., 2008a; 2008b) has greatly improved chronologies and provides great potential for the generation of more robust records in the future. A further consideration is that archaeological deposits can be inherently biased as their taphonomy is complex and may reflect anthropogenic collections/selections. Therefore, despite the large variety of terrestrial data available, many of these sources can be complex as regards to palaeoenvironmental reconstructions as they are of uncertain climatic significance.

More recently, comprehensive evaluations of the available records have been produced by Chase and Meadows (2007), with a focus on the WRZ of southern Africa; Gasse et al. (2008), a review of equatorial and southern African records for the period 30 – 10 ka with more emphasis on the equatorial and marine records than on the southern African region; Chase (2010), a palaeoenvironmental contextualisation of the southern and southwestern Cape archaeological records focussing on MIS 4; Dupont (2011), a review of Middle and Late Pleistocene southern and western African marine records with strong focus on the palynological evidence from these and the links to orbital forcings and Scott et al. (2012), predominantly a summary of a selection of previously published southern African pollen records covering the last 26 ka. These have greatly improved upon the older reviews mainly due to the inclusion of a greater number of marine and terrestrial records with improved chronological controls and calibrations. However, apart from Chase and Meadows (2007) and Chase (2010) (the latter of which only assesses the archaeological records relevant to the Howieson's Poort and Still Bay industries), these new syntheses have not had a strong, or in some cases any, focus on the YRZ or the southern Cape palaeoenvironmental record, emphasising both

the need for a thorough reassessment of the available published records and the need for the establishment of new southern Cape records.

3.4 Palaeoclimatic forcing mechanisms and existing conceptual models

Due to the low spatial and temporal resolution of the aggregate palaeoenvironmental record for southern Africa, the development and application of palaeoclimatic conceptual models have been essential for the contextualisation of individual records.

Chase and Meadows (2007) review the main conceptual models established during the 1960s, 1970s and 1980s (e.g. van Zinderen Bakker, 1967; 1976; Butzer et al., 1978; Lancaster, 1979; Butzer, 1984), which attempt to explain the responses of southern African terrestrial environments to glacial-interglacial climates and the nature of palaeoclimatic changed during these periods. Using atmospheric circulation models developed from observations of present-day climatic variability together with an assessment of the older conceptual models, Tyson (1986) and Cockcroft et al. (1987) produced conceptual models that propose an anti-phase relationship between the WRZ and the SRZ. In general they associated cool/wet and warm/dry conditions with the WRZ and warm/wet and cool/dry conditions with the SRZ. Cockcroft et al. (1987)'s heuristic multi-level model hypothesized that, during glacials, the westerlies intensified and migrated northward resulting in an expanded, more intensified WRZ, while the SRZ experienced net reductions in precipitation related to a weaker Walker Circulation (Cockcroft et al, 1987). During interglacials the opposite occurs: Walker Circulation intensifies, there is an increased dominance of the tropical easterlies and an enhanced tropical rain belt resulting in a larger more humid SRZ with perhaps increased occurrences of TTTs (Cockcroft et al., 1987; Tyson, 1999; Chase and Meadows, 2007).

In terms of forcing mechanisms, orbitally-induced solar radiation is of fundamental underlying importance as it represents the primary control on late Quaternary palaeoclimates on global and hemispheric scales. It has been proposed that obliquity (~41 kyr cycle) and precession (~23 kyr cycle) are the underlying variables that influence Pleistocene and Holocene climates through their impact on the amount and distribution of insolation (Hays et al., 1976; Imbrie et al., 1992; Imbrie et al., 1993; Figure 3.1). Orbital eccentricity also influences climate dynamics in a nonlinear manner over lower frequency, longer (~413 kyr) cycles (Rial, 2004). Furthermore, eccentricity has been identified as a possible driving mechanism behind the 100-kyr glacial-interglacial cycle (Imbrie and Imbrie, 1980). Alternatively the 100-kyr cycle could be more related to internally-driven climate feedbacks with only minor associations with eccentricity and precession (Lisiecki and Raymo, 2007; Lisiecki,

2010) or it could have resulted from the compound effects of obliquity cycles (Huybers and Wunsch, 2005) or a nonlinear combination of eccentricity-modulated precession together with direct climatic forcing (e.g. CO_2 fluctuations and sea ice dynamics) (Imbrie et al., 1993).

The influence of the higher frequency orbital parameters, *viz*. precession (controlling the seasonal distribution of insolation) and obliquity (affecting the amplitude of the seasonal cycle), would have been greater after the last Interglacial (~115 ka) as eccentricity gradually reduced from this point towards a minimum around the LGM (Berger and Loutre, 1991; Figure 3.1). It has been postulated that obliquity forces subtropical and high latitude climate dynamics, whereas the precessional signal is more obviously associated with low latitude (equatorial) forcing (Berger and Loutre, 2004; Dupont, 2011).

Precession influences the position of the tropical rain belt and regulates the intensity of monsoon systems (Kutzbach, 1981) with increased low latitude insolation resulting in stronger monsoons (Kutzbach et al., 2008). Analyses of the sediments from the Tswaing Impact Crater/the Pretoria Saltpan postulated that precession was the dominant control on South African summer rainfall (Partridge, 1993; Partridge, 1997; Kristen et al., 2007). While elements of this particular record has been called into question (c.f. Chase and Meadows, 2007; Chase, 2010; Kirsten et a., 2010), studies conducted in tropical and subtropical eastern Africa and the associated offshore regions do support the notion of strong precessional controls on atmospheric and oceanic circulation over the last ~200 kyr (e.g. McIntyre et al., 1989; Jansen et al., 1996; Mix and Morey, 1996; Schneider et al., 1996; Scholz et al., 2007).

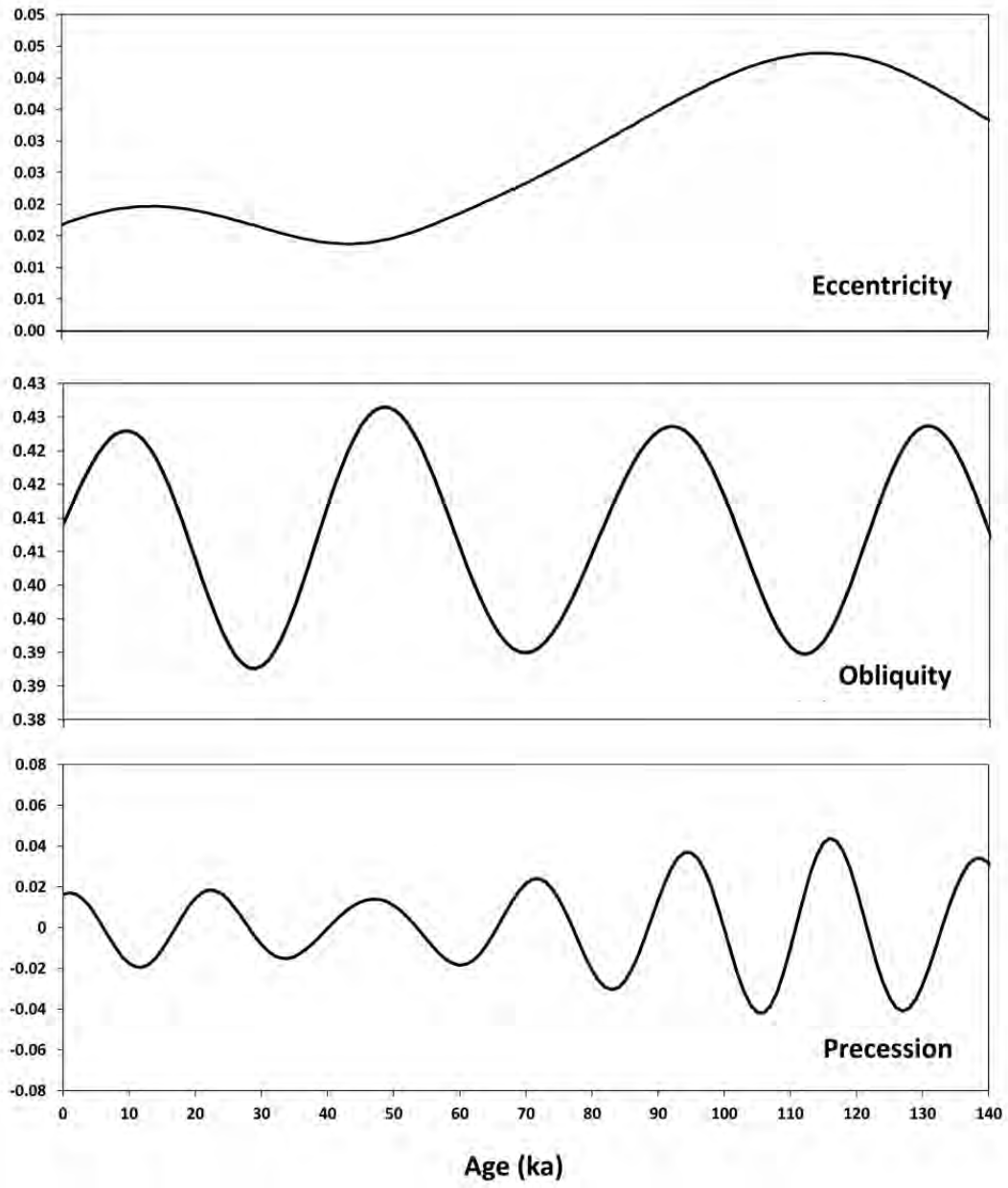

Figure 3.1 The orbital parameters that influence climate dynamics (Laskar et al., 2004; Laskar et al., 2011).

Obliquity controls the insolation gradient between high and low latitudes and therefore affects the atmospheric meridional flux of heat, moisture and latent energy balances and can modulate the strength of the westerlies and subtropical trade winds (Raymo and Nisancioglu, 2003; Lee and Poulsen, 2005). The obliquity signal is clearly important in many of the Southern Hemisphere subtropical and high latitude records (Lorius et al., 1985; Brathauer and Abelmann, 1999; Stenni et al., 2004; Jouzel et al., 2007; Caley et al., 2011). However, it has been argued that this latitudinal insolation gradient contains both obliquity and precession periodicities (Davis and Brewer, 2009; in Caley et al., 2011).

Of particular importance from a southern African perspective is the effect of variations in solar insolation, controlled by the orbital parameters - especially obliquity - on the growth and decay of the polar ice sheets (Imbrie et al., 1993). A strong Northern Hemisphere research focus has led to assertions that Arctic sea ice dynamics, modulated by changes in summer insolation at high latitudes, are the main control of glaciations. However, it has recently been hypothesised that Antarctic sea ice may have had an even greater influence than Northern Hemisphere sea ice during glacial times (Chiang et al., 2003 and Chiang and Bitz, 2005 in Chase, 2010). An expansion of Antarctic sea ice leads to an enhancement of the Southern Hemisphere meridional temperature gradients, forcing Southern Hemisphere oceanic and atmospheric fronts, particularly the subtropical convergence front and the westerlies, to shift northward (van Zinderen Bakker, 1976; Gersonde et al., 2003; Stuut et al., 2004; Stuut and Lamy, 2004; Gersonde et al., 2005; Chase and Meadows, 2007; Figure 3.2). These shifts were, however, not uniform or symmetrical (Stuut et al., 2004).

It appears that correlating individual forcing mechanisms to southern African palaeoclimatic changes is extremely complex since orbital perturbations and sea ice dynamics may account only for some of climatic variability expressed in the records. It seems likely that southern Africa responded both to high latitude Southern Hemisphere forcing and low latitude Northern Hemisphere forcing during different time periods together with different regions of southern Africa responding to different forcings or combinations of forcings (for example refer to sections 3.5.2.2 and 3.5.5).

Certainly from a southern Cape perspective, the direct changes in the main components of the atmospheric and oceanic circulation systems as well as more localised dynamics are thought to contribute more strongly to the regional palaeoclimate records than orbital forcings (Chase and Meadows, 2007; Chase, 2010).

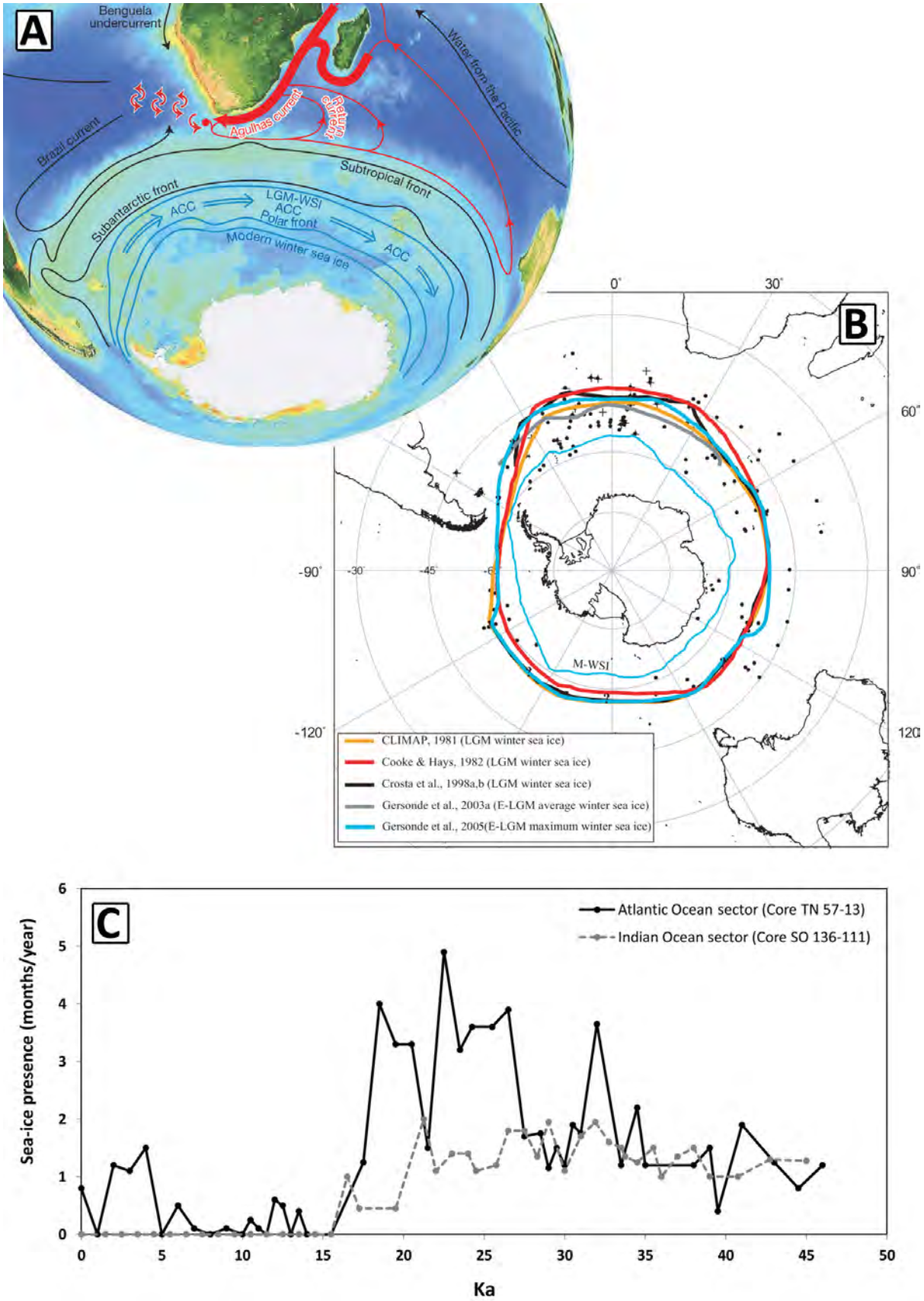
A
Benguela undercurrent
Water from the Pacific
Brazil current
Agulhas Current
Agulhas Return
Subtropical front
Subantarctic front
ACC
LGM-WSI
ACC
Polar front
Modern winter sea ice
ACC
B
0°
30°
60°
90°
120°
-90°
-30°
-45°
-60°
M-WSI
CLIMAP, 1981 (LGM winter sea ice)
Cooke & Hays, 1982 (LGM winter sea ice)
Crosta et al., 1998a,b (LGM winter sea ice)
Gersonde et al., 2003a (E-LGM average winter sea ice)
Gersonde et al., 2005(E-LGM maximum winter sea ice)
C
Atlantic Ocean sector (Core TN 57-13)
Indian Ocean sector (Core SO 136-111)
Sea-ice presence (months/year)
Ka
0
1
2
3
4
5
6
0
5
10
15
20
25
30
35
40
45
50

3.5 The palaeoenvironmental record: proxy evidence from the winter and year-round rainfall zones

This section is a review of the palaeoenvironmental evidence generated from key archaeological and palaeoenvironmental sites located within and beyond the boundaries of the SCCP organised within distinct biogeographical categories. These include:

A. Western lowland sites: west and southwestern coastal sites situated within the modern WRZ.
B. Western montane sites: sites associated with the Cape Fold Belt mountains (or outlying mountain ranges) within the modern WRZ.
C. Eastern lowland sites: coastal plain sites within the modern YRZ.
D. Eastern interior sites: sites situated on the foothills of the eastern arc of the Cape Fold Belt mountains within the YRZ.

Sites that are situated beyond the limits of Figure 3.3 but provide additional insight into the palaeoenvironmental dynamics of the SCCP are discussed in sections 3.5.5 and 3.5.6.

This is followed by a synthesis of the overall record within a chronological framework with particular focus on the key climatic episodes defined in section 3.2.1.

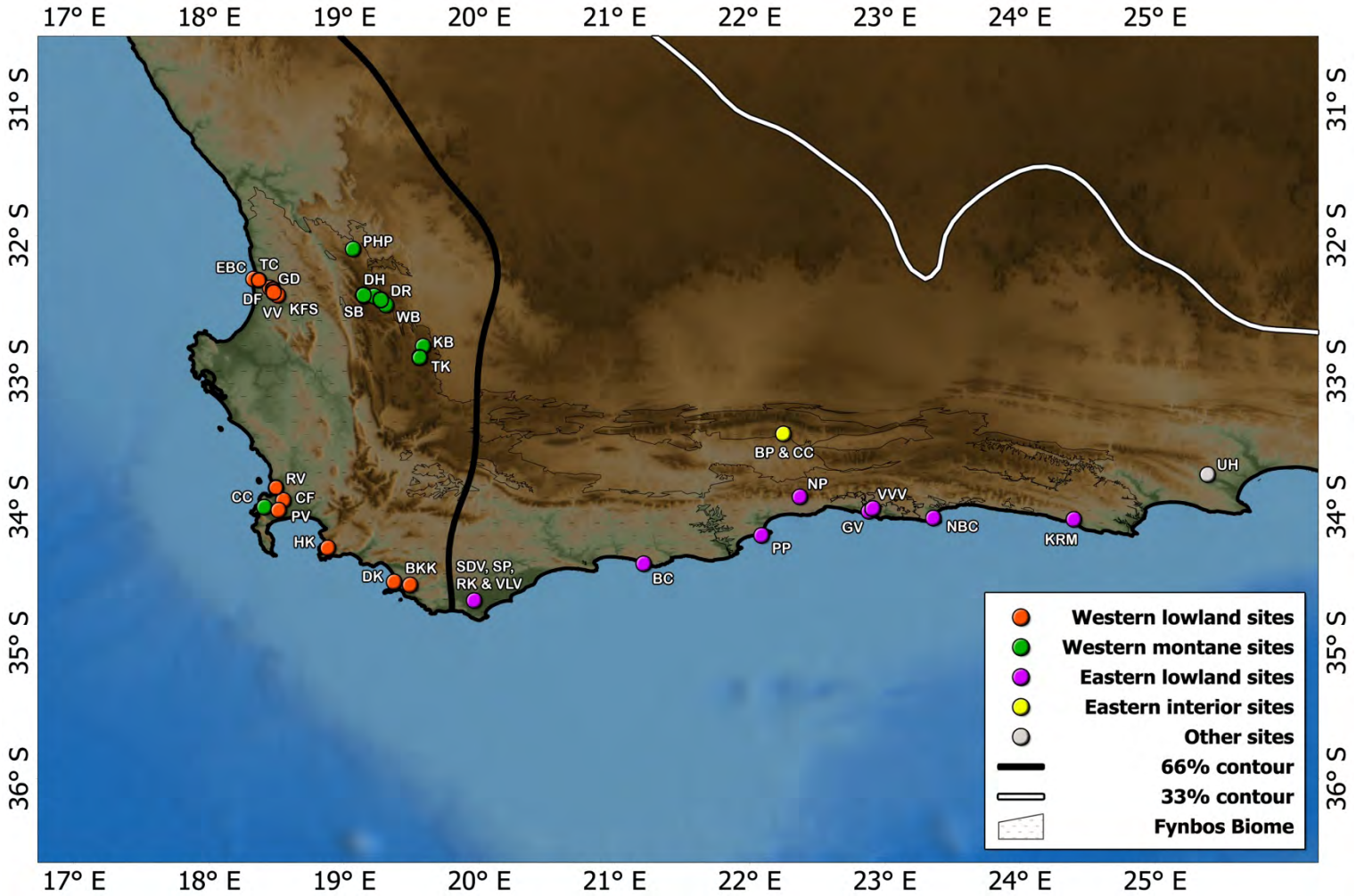

Figure 3.3 Map of palaeoenvironmental archives organised into distinct biogeographical categories. The 66% contour marks the boundary of the WRZ and the 33% contour delineates the boundary between the YRZ and the SRZ. PHP: Pakhuis Pass, DH: Driehoek Vlei, DR: De Rif, SB: Sneeuberg Vlei, WB: Wolfberg, KB: Katbakkies, TK: Truitjes Kraal, EBC: Elands Bay Cave, TC: Tortoise Cave, GD: Grootdrift, VV: Verlorenvlei, KFS: Klaarfontein Springs, RV: Rietvlei, CF: Cape Flats, PV: Princess Vlei, CC: Cecilia Cave, HK: Hangklip, DK: Die Kelders, BKK: Byneskranskop, the Agulhas Plain vleis and lunettes (SDV: Soetendalsvlei, VLV: Voëlvlei, RK: Renosterkop and SP: Soutpan) BC: Blombos Cave, PP: Pinnacle Point, BP: Boomplaas, CC: Cango Cave, NP: Norga peats, GV: Groenvlei, VVV: Vankervelsvlei, NBC: Nelson's Bay Cave, KRM: Klasies River Mouth, UH: Uitenhage. Box indicates SCCP.

3.5.1 Western lowland sites

3.5.1.1 Elands Bay Cave

Most of the significant palaeoenvironmental and archaeological studies situated in this zone are concentrated within the Eland's Bay – Verlorenvlei area. The archaeological site of Elands Bay Cave (EBC) is a northwesterly-facing cave situated on Baboon Point headland on the west coast about 250 km north of Cape Town (Figure 3.3). The area is presently subject to a semi-arid climate and experiences winter rainfall between 200 - 250 mm yr^{-1} (Cowling et al., 1999). The contemporary vegetation is strandveld (Mucina and Rutherford, 2006). Through various analyses of sediments that have preserved the evidence of human occupation in EBC for periods within the late Quaternary, a multi-proxy record of environmental change has been established. However the deposit does not represent a continuous sequence but rather a 'pulsed' record due to the episodic nature of human habitation (Cartwright and Parkington, 1997).

Macrofaunal evidence was examined by Klein and Cruz-Uribe (1987) and Klein (1991). Despite the small assemblage size, the taxa identified in the late Pleistocene levels showed marked differences to those found in Holocene levels. The assemblage for the LGM period included several grazing fauna including two equids and springbok (*Antidorcas marsupialis*) (Klein and Cruz-Uribe, 1987). This type of assemblage usually indicates drier conditions but the associated presence of the hedgehog (*Erinaceus frontalis*), which inhabit areas with annual precipitation between 300 – 800 mm (Smithers 1983: 21) possibly suggests greater moisture availability together with increased grass cover (Klein and Cruz-Uribe, 1987).

In addition, the large size of dune molerat (*Bathyergus suillus*) distal humeri indicates that relatively humid conditions most probably prevailed during the early Holocene (Klein and Cruz-Uribe, 1987; Klein, 1991). It is argued that the increased size of molerat at this time signifies that rainfall values were at least 400 mm/yr^{-1} (Klein, 1991), therefore approximately double what is presently received.

An extensive wood charcoal record has been established for EBC (Cartwright and Parkington, 1997; Cowling et al., 1999; Parkington et al., 2000; Figure 3.4). The section of the record dating to >40 ^{14}C yr kBP (beyond the limits of radiocarbon dating at the time) is dominated by afromontane forest taxa (such as *Kiggelaria africana*, *Podocarpus elongata* and *Myrsine africana*) indicating that conditions during the late Pleistocene were most probably several degrees cooler and somewhat wetter than today (Parkington et al., 2000), albeit that chronological control for this sequence is weak so that a more resolved palaeoenvironmental reconstruction is not possible. The LGM is only represented by three discrete samples; the two samples from around 24 cal kBP show increased

proportions of afromontane forest taxa and therefore could indicate conditions cooler and wetter than present. After the LGM, samples show a reduction in afromontane taxa, with the replacement of these forest elements by mesic thicket taxa (such as *Diospyros glabra,* and *Olea europaea ssp. africana*), proteoid fynbos elements (including *Protea glabra*, *Leucodendron pubescens* and *Erica* spp.), asteraceous shrubland elements (e.g. *Eriocephalus aromata, Aspalathus* sp. and *Passerina glomerata*) and xeric thicket taxa. By ~4.5 cal kBP, asteraceous shrubland and xeric thicket taxa (such as *Euclea racemosa*, *Rhus undulata* and *Ruschia maxima*) dominate the assemblage indicating that the late Holocene was characterized by warmer and drier conditions during which the modern vegetation (strandveld) was established.

In addition to the charcoal record, twelve sedimentary units were suitable for pollen analysis and dated from >40 ^{14}C kBP to 12.5 cal kBP (Baxter, 1996). The pollen assemblage exhibits many similarities to the charcoal results (Parkington et al., 2000). Pollen from the LGM period (represented within this record by samples dating to 23.7 – 20.7 cal kBP) were marked by maximum values of afromontane taxa, with *Kiggelaria*, *Ficus, Salix* and *Podocarpus* occurring only in this zone (Figure 3.5). This zone is also characterised by low frequencies of xeric karroid and strandveld pollen types and relatively high percentages of grass pollen (Baxter, 1996). Consequently, significantly moister and cooler conditions have been inferred from this zone (Baxter, 1996; Meadows and Baxter, 1999; Parkington et al., 2000).

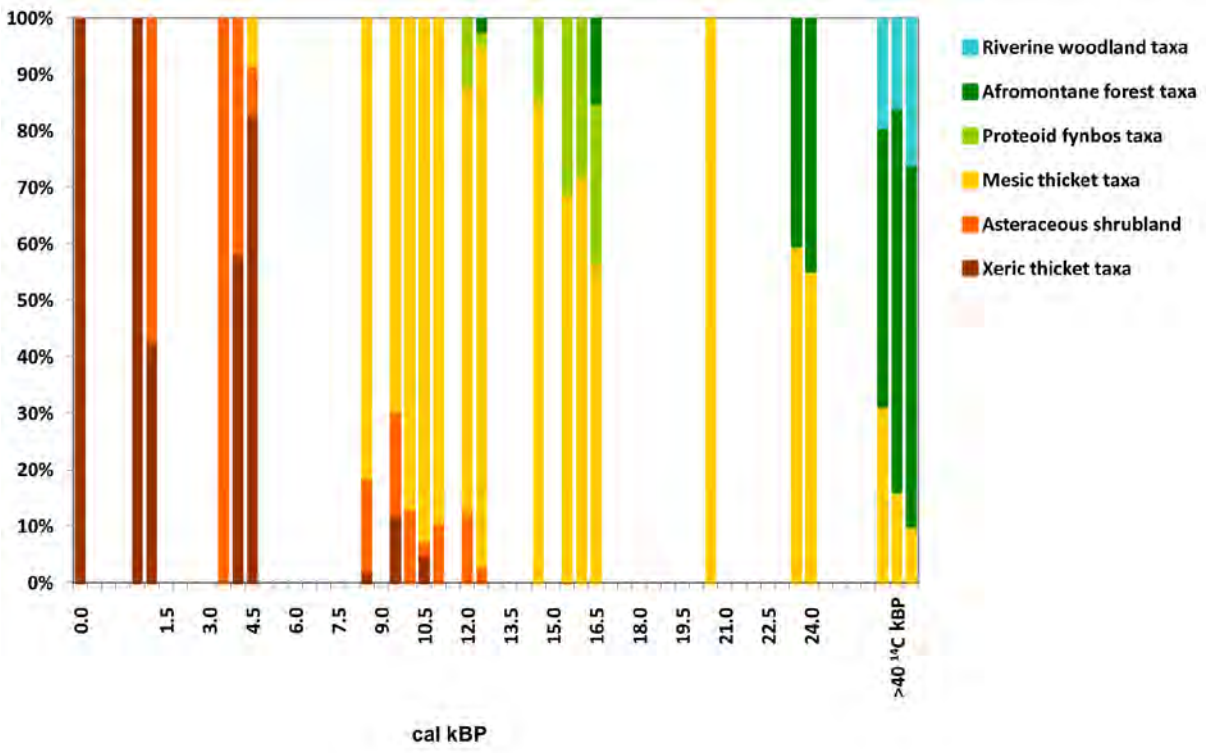

Figure 3.4 The Elands Bay Cave charcoal record, taxa grouped according to general ecological communities (Parkington et al., 2000).

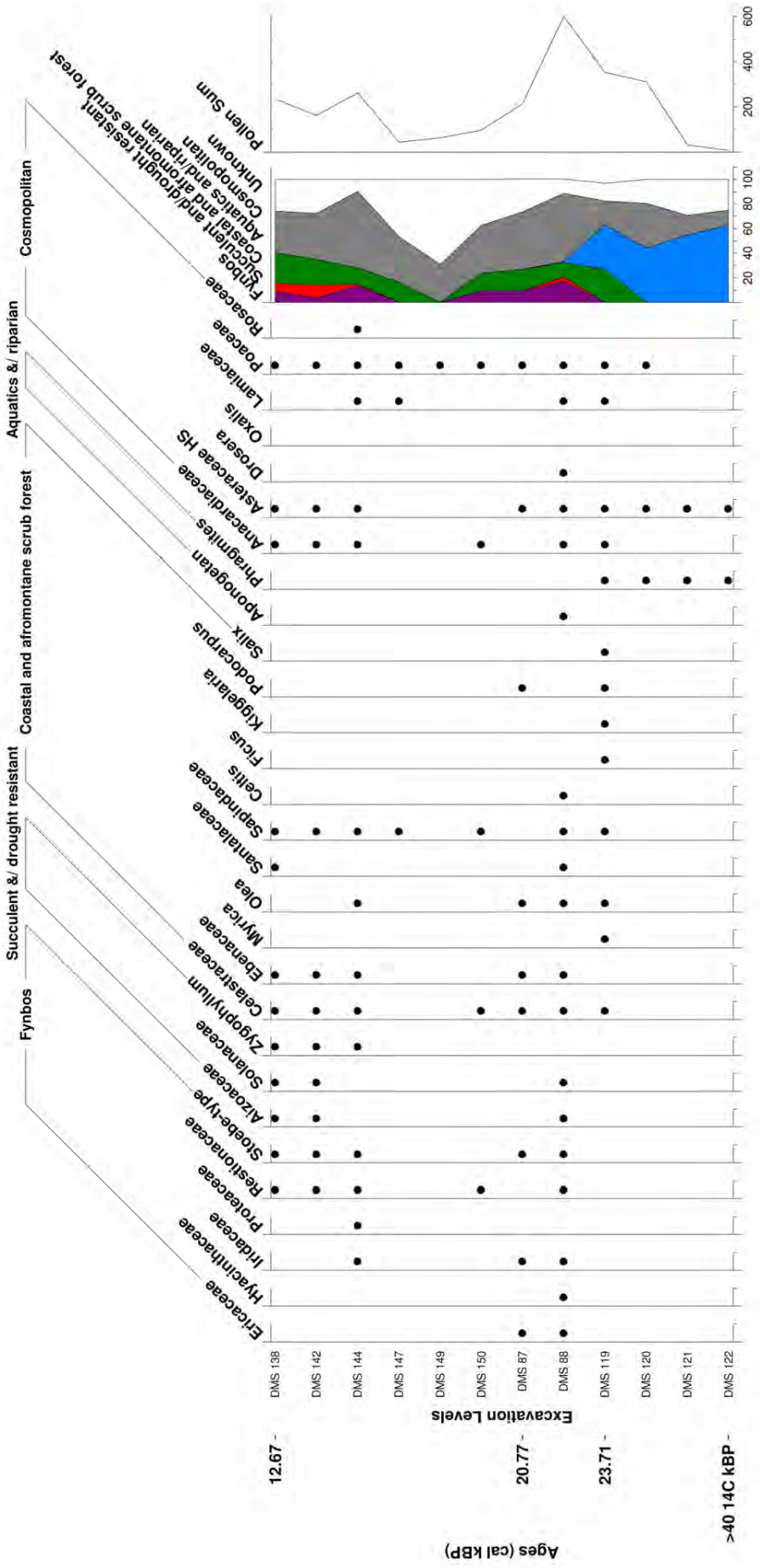

Figure 3.5 The Elands Bay Cave pollen record displayed as a presence pollen diagram (Baxter 1996).

The EBC deposits have also yielded a record associated with changes in the adjacent marine environment. A sea surface temperature (SST) record of the southern Benguela upwelling system was reconstructed using limpet (*Patella granatina* and *P. granularis*) shells from midden deposits using oxygen isotopes and aragonite-calcite ratios (Cohen et al., 1992). Three significant deviations from the modern $\delta^{18}O$ and aragonite values occurred: 12.7 – 11.5 cal kBP, 3.36 cal kBP and 0.55 to 0.51 cal kBP (Cohen et al., 1992; Figure 3.6). These excursions represent periods of decreased SSTs and correspond to periods of global cooling. Of particular interest is the cooling period between 13 cal kBP and 11 cal kBP as this coincides to the Younger Dryas (13 – 11. 5 cal kBP) as observed in the GRIP ice core $\delta^{18}O$ record (Dansgaard et al., 1993).

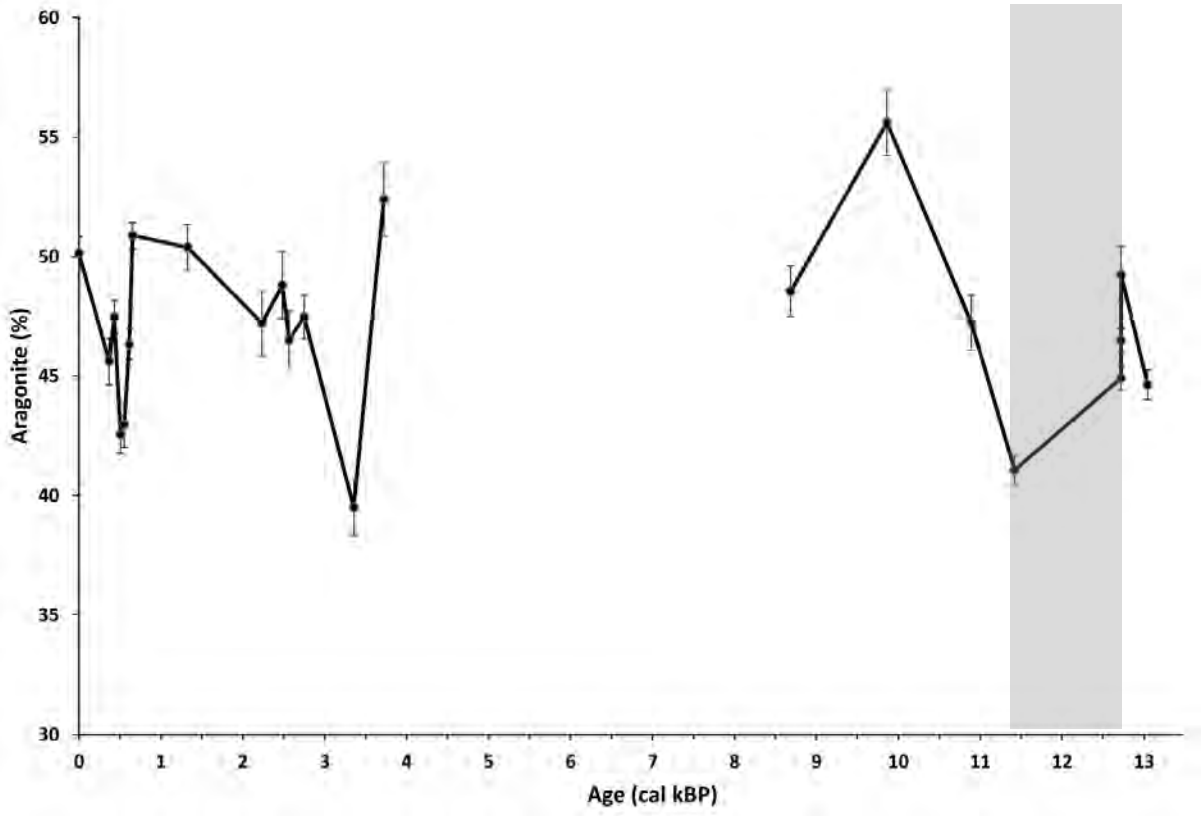

Figure 3.6 Percentage Aragonite from *Patella granularis* shells found at Elands Bay Cave (Cohen et al., 1992). The grey bar represents the period coinciding with the Younger Dryas.

3.5.1.2 Diepkloof Cave

Diepkoof Cave is situated about 10 km inland from the town of Elands Bay and overlooks the Verlorenvlei coastal wetland. It is one of the few sites where the Middle Stone Age (MSA) techno-complexes of Howiesons Poort and Stillbay can be excavated from the same sequence (Rigaud et al., 2006; Henshilwood et al., 2009; Tribolo et al., 2009). These industries are of particular importance

from an archaeological perspective as they have been thought to represent evidence for early modern behaviour (Texier et al., 2010).

There has been very little published palaeoenvironmental evidence from Diepkloof. However Butzer (1979) uses roof spall to infer cooler conditions during portions of the MSA. In addition, the presence of afromontane forest (including *Podocarpus*, *Kiggelaria africana*, *Celtis africana* and *Ficus* sp.) and thicket (e.g. *Diospyros* spp., *Cassine peragua*, *Maytenus* spp. and *Rhus* spp.) taxa at Diepkloof during the period ~65 to 50 ka reflects a much more wooded riverine environment indicating more humid conditions during at least some episodes during the last glacial period than today (Cedric Poggenpoel, *pers. comm.* in Chase and Meadows, 2007; Texier et al., 2010).

3.5.1.3 Verlorenvlei

Near Elands Bay, within the coastal estuarine/lacustrine wetland known as Verlorenvlei, several sediment cores have been analysed providing multi-proxy records of Holocene climatic, hydrological and sea level changes for the area (Baxter, 1996; Meadows et al., 1996; Baxter and Meadows, 1999; Meadows and Baxter, 2001; Stager et al., 2012; Figure 3.3).

The pollen record extracted from the Grootdrift site provides evidence for an arid HA. This is inferred from the increased percentages of xeric taxa (such as Asteraceae and Chenopodiaceae) at the base of the core at ~6.3 cal kBP, indicating that the wider environment most probably experienced more arid conditions than that of today (Meadows et al., 1996). The Grootdrift pollen record indicates greater moisture availability during the late Holocene (Meadows and Baxter, 1999).

The most significant influence on the Grootdrift sediments and the pollen assemblage appears to have been sea level change (Meadows et al., 1996). A composite sea level curve based on proxies from the Grootdrift cores was constructed (Baxter and Meadows, 1999). Evident in this curve, as well as several others studies from the west coast including the archaeological site Tortoise Cave (Yates et al., 1986; Jerardino, 1993; Miller et al., 1993; Jerardino, 1995; Miller et al., 1995), is the mid-Holocene sea level transgression that is generally dated to ~5 – 4 ka and broadly corresponds to the HA (Figure 3.7). After ~4 ka a substantial regression is hypothesised by Meadows and Baxter (1999) and is somewhat evident in some of the other curves but to a lesser extent (Figure 3.7).

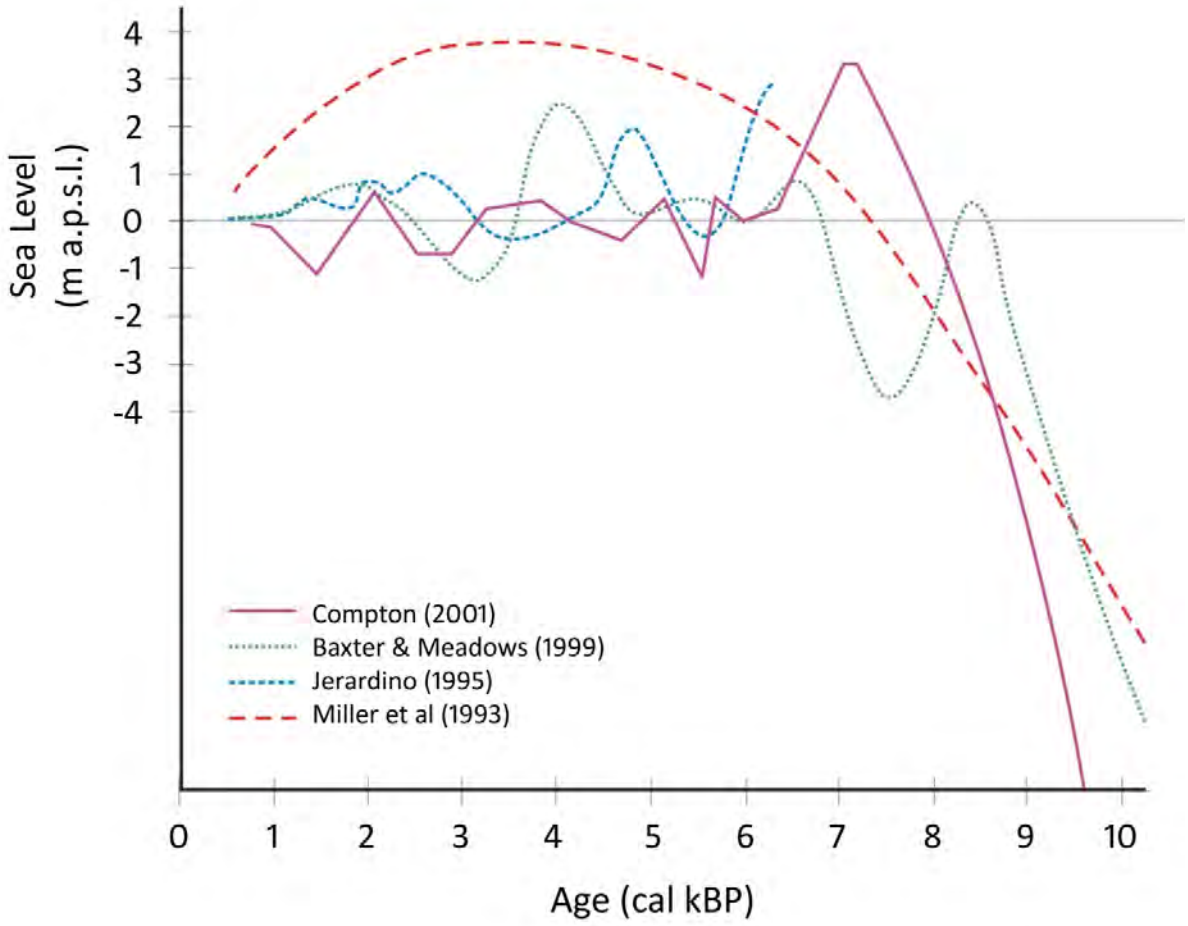

Figure 3.7 A composite of Holocene sea level curves (Chase, 2006).

A six metre core was extracted from Klaarfontein Springs, an artesian spring site about 18 km inland of Elands Bay town (Meadows and Baxter, 2001; Figure 3.3). Pollen from this site further supports the idea of arid conditions prevailing at the HA, with the section covering the period: ~7.5 – 4 cal kBP dominated by Poaceae, Asteraceae and Chenopodiaceae pollen (Meadows and Baxter, 2001). In accordance with inferences made from the Grootdrift record, moister conditions are evident at Klaarfontein from ~4 – 2 cal kBP (Meadows and Baxter, 2001).

A very recent high-resolution study by Stager et al. (2012) uses diatom and sedimentological evidence from three cores taken from Verlorenvlei to infer precipitation changes over the last 1 400 years. They suggest that these variations are strongly coupled to changes in the westerlies and that winter rainfall was relatively enhanced for the period 1.4 – 1.2 cal kBP and within the Little Ice Age (~1400-1800 AD).

3.5.1.4 Rietvlei, Cape Flats and Cape Hangklip

Further south on the Cape Peninsula, Schalke (1973) analysed pollen from several sediment cores extracted from the Cape Flats, Rietvlei basin and Cape Hangklip (Figure 3.3). As a result of sea level fluctuations, variable aeolian activity, changes in the regional hydrology and drainage patterns; these deposits have produced discontinuous palaeoenvironmental sequences (Schalke, 1973). Despite these complexities, marked differences exist between the pollen assemblages dated to >40 – 37 cal kBP and those of the Holocene. The pollen levels relating to the period roughly equivalent to 38 cal kBP in Schalke's (1973) pollen diagrams are dominated by afrotemperate forest taxa (primarily *Podocarpus*) whereas the Holocene sections show a complete absence of forest taxa. The former assemblages are very similar to the modern vegetation communities found in the Knysna area within the YRZ. This suggests that the Cape Peninsula received significantly more effective year-round precipitation during this period than what is experienced today (Chase and Meadows, 2007). However eight out of the eleven of the radiocarbon ages of the Rietvlei and Cape Flats cores should be deemed infinite as they fall beyond the limits of radiocarbon dating abilities at the time and therefore these sequences are of limited use for chronologically-grounded palaeoenvironmental reconstructions.

More recently, the analysis of pollen and charcoal from a sediment core from Princess Vlei on the Cape Flats, has yielded a record of ecological and climate changes during late Holocene as well as evidence of disturbance by colonial settlers since c. 300 years ago (Neumann et al., 2011). Relatively dry conditions are inferred from increases in Aizoaceae, *Crassula*-type and Asteraceae pollen within the basal zone of the sequence, from 4.15 – 3.4 cal kBP. Increases in *Morella*, Cyperaceae and Carpacoce pollen could indicate that wetter conditions prevailed during the period 3.4 – 2.6 cal kBP, followed by inferences of a relatively dry climate from 2.6 – 1.9 cal yr BP. Increased proportions of aquatics such as *Nymphaea* point towards deeper water and wetter conditions for the period 1.9 – 1 cal kBP. The pollen assemblages from the top of the core records increasing levels of human disturbance with elevated proportions of Poaceae, the presence of neophytes such as *Pinus* and *Zea mays* and high charcoal values. It should be noted that this record is hampered by several uncertainties related to the chronology (e.g. difficulty in establishing the relationship between a floating vegetation mat and the sediments below it and age reversals) and due to the fact that the core was extracted over 60 years ago and could possibility have been altered/contaminated prior to analysis.

3.5.1.5 Die Kelders

The major archaeological site of Die Kelders is a sea cave complex about 50 km southeast of Cape Hangklip. Dating the archaeological deposits found at Die Kelders has proved difficult and contentious (Butzer, 2004). The sediments were deposited beyond the range of radiocarbon dating and therefore optically stimulated luminescence (OSL) (Feathers and Bush, 2000) and electron spin resonance (ESR) (Schwarcz and Rink, 2000) dating techniques have been employed to provide more secure chronologies for the proxy records. There is a significant hiatus within the overall sequence, with the Later Stone Age (LSA) deposit (dated to about 2 ka) lying on the much thicker MSA section. Differing assumptions with regard to moisture content and stratigraphic inconsistencies mean that the best age estimate for the MSA late Pleistocene sequence is: 70 – 60 ka (Feathers and Bush, 2000; Klein and Cruz-Uribe, 2000; Schwarcz and Rink, 2000).

The macrofaunal evidence from Die Kelders indicates cooler and wetter conditions than present for the estimated period 70 – 60 ka. Greater humidity is inferred from the presence of southern reedbucks, the increased mean size of the dune molerats (*Bathyergus suillus*), while the large size of the grey mongoose (*Galerella pulverulenta*) implies lower temperatures (Klein and Cruz-Uribe, 2000; Klein et al., 2000). In addition, the presence of extralimital ungulates point to relatively moist and grassier environments (Klein and Cruz-Uribe, 2000). The scenario of cooler and wetter conditions in the MSA is corroborated by the micromammalian evidence, in the form of higher percentages of forest shrews (*Myosorex varius)* and Saunders' vlei rats (*Otomys saundersae)* (Avery, 1982).

3.5.1.6 Byneskranskop

Byneskranskop cave site is situated only about 10 km away from the Die Kelders cave complex (Figure 3.3). LSA layers span the interval between ~15 cal kBP and 0.2 cal kBP covering the lateglacial and Holocene (Schweitzer and Wilson, 1978; 1982). The macrofaunal evidence points towards a trend in decreasing moisture from a relatively wet lateglacial-early Holocene to a drier later Holocene (post-7.3 cal kBP). This is inferred from the significantly larger size of the dune molerat remains during 15 – 11 cal kBP compared to those found within the later Holocene (Klein, 1991). Avery (1993) claims that an increased grass component of the vegetation at Byneskranskop by 7 cal kBP was related to a greater proportion of summer rainfall, suggesting that the year-round rainfall regime would have been established by this point (Chase and Meadows, 2007).

3.5.2 Western montane sites

3.5.2.1 Driehoek and Sneeuberg Vleis, Cederberg

The Cederberg Mountain range is the location for almost all of the upland palaeoenvironmental archives of the western montane sites category.

In the central Cederberg, in one of the highest parts of the range, sediment cores were extracted from wetlands and their pollen contents were analysed (Sugden, 1989; Meadows and Sugden, 1990; 1991). The base of the Sneeuberg Vlei core was dated to ~10.98 cal kBP while the record from Driehoek Vlei, at a slightly lower altitude, covers the last 17.6 cal kBP. From the examination of the pollen assemblages it can be concluded that the overall palaeoenvironmental record obtained from these Cederberg wetland sites is one of stability and that mountain fynbos was the dominant vegetation type throughout the period of sedimentation (Sugden, 1989; Meadows and Baxter, 1999; Figures 3.8 and 3.9).

Despite the fact that the LGM period is not encompassed in the Driehoek record, the steady decline in the abundance of the Clanwilliam cedar (*Widdringtonia cederbergensis*) from the base of the record, has been used to suggest that the climate of the last glacial period may have been more favourable to this endemic tree, therefore indicating that cooler and wetter conditions may have prevailed during the LGM (Sugden and Meadows, 1991, Meadows and Baxter, 1999).

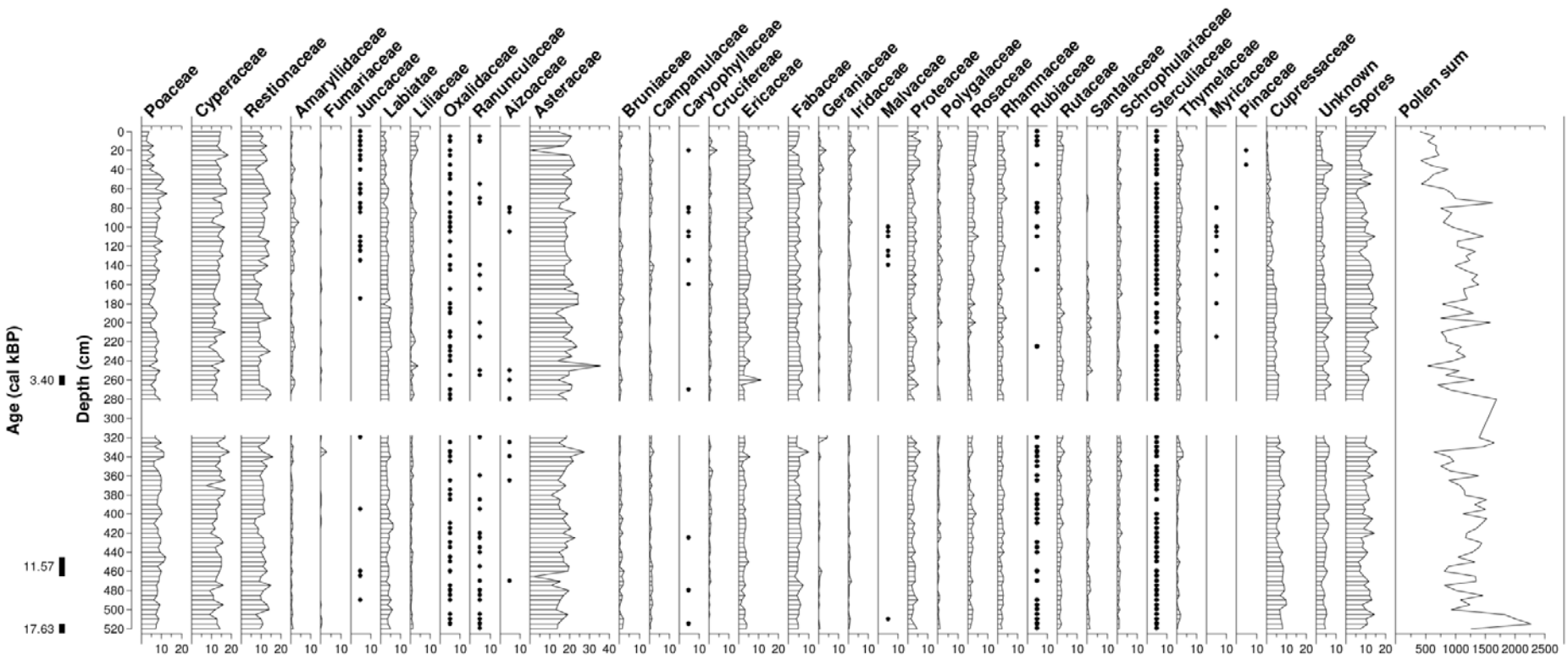

Figure 3.8 The Driehoek Vlei pollen record displayed as a relative percentages pollen diagram with taxa contributing to less than 2% of the total pollen sum presented as presence/absence graphs.

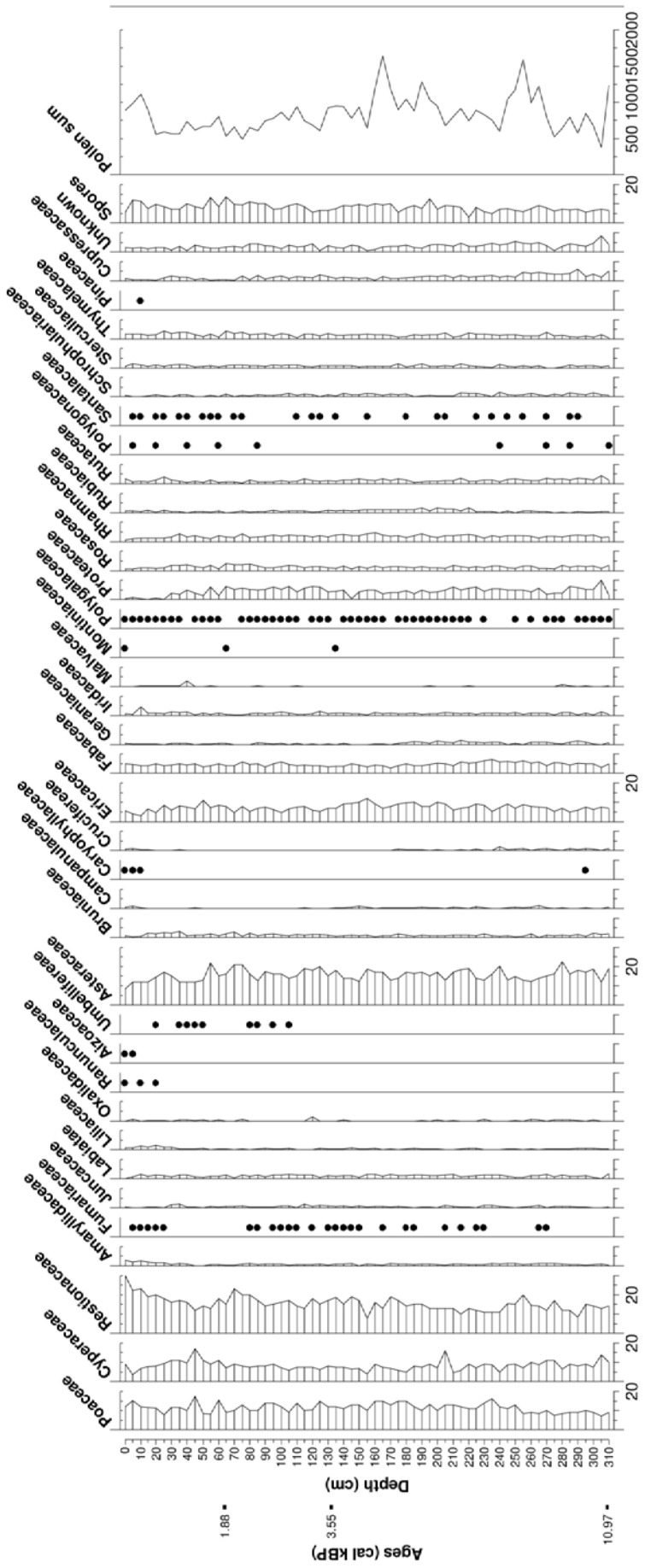

Figure 3.9 The Sneeuberg Vlei pollen record, displayed as a relative percentages pollen diagram with taxa contributing to less than 2% of the total pollen sum presented as presence/absence graphs.

3.5.2.2 De Rif, Cederberg

Stable isotopes and pollen data were generated from two rock hyrax middens (De Rif 1 and 2) extracted from De Rif in the Cederberg, less than 10 km north east of the Driehoek Vlei site (Quick, 2009; Chase et al., 2011; Quick et al., 2011). The high-resolution De Rif 2 (DR-2) carbon and nitrogen records represent a particularly significant contribution to the overall palaeoclimatic history of southwestern Africa, while the pollen record provides key insights into mountain fynbos palaeoecology.

The De Rif records indicate that the last glacial period was generally characterised by increased moisture availability, however the LGM period is punctuated by a discrete arid episode from 22 – 21 cal kBP (Figure 3.10). A significant period of isotopic enrichment, indicating lower moisture availability, is evident during the period 12.7 – 11.5 cal kBP correlating to the Younger Dryas (YD) climatic event (Figure 3.11). The identification of the YD within these records represents the first unequivocal terrestrial manifestation of this event from the southern African subtropics (Chase et al., 2011). The YD signal in the De Rif records is strongly linked to variations in SSTs and upwelling intensity within the Benguela Upwelling system and provides clear evidence of Northern Hemisphere forcing of southern African climates within LGIT period.

Depleted $\delta^{15}N$ and $\delta^{13}C$ values together with peaks in arboreal pollen in De Rif 2 records indicates that the early Holocene was wetter than present especially from ~11 to 10 cal kBP (Figure 3.11). A trend of decreasing moisture availability seems to be evident after this period. The presence of a significant amount of *Dodonaea* pollen in the DR-2 assemblage suggests that the Holocene was characterised by warmer conditions. The De Rif 1 pollen and isotope records signify that relatively minimal environmental change occurred during the late Holocene.

It is clear from the DR-2 isotope records that significant, rapid changes have occurred in the region's climate, but these changes are not reflected as clearly in the pollen records from the De Rif middens or the neighbouring vleis, leading Quick et al. (2011) to conclude that mountain fynbos communities can persist due to high levels of resilience and their strong association with oligotrophic sandstone substrates.

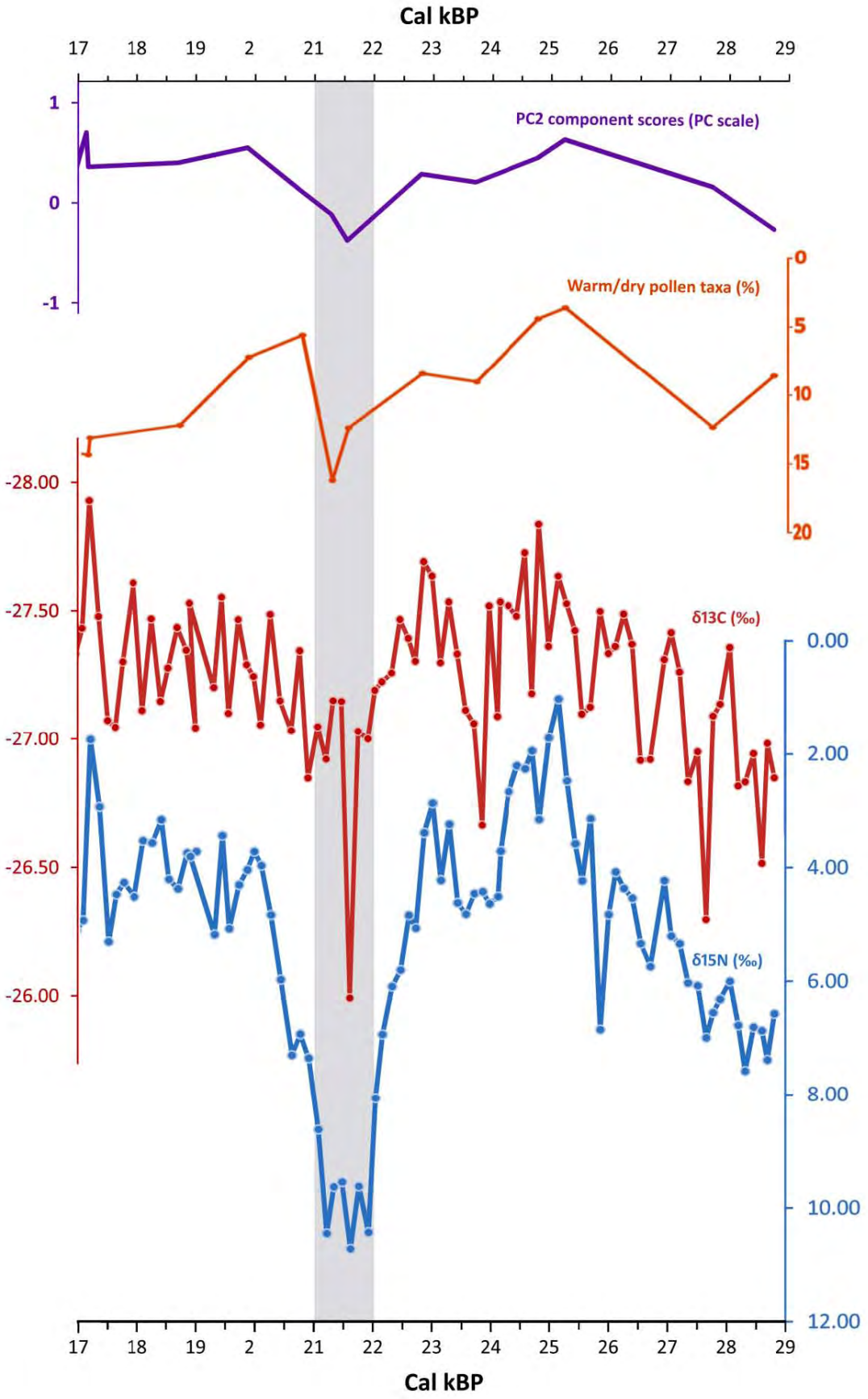

Figure 3.10 The glacial section of the De Rif 2 record (adapted from Quick, 2009).

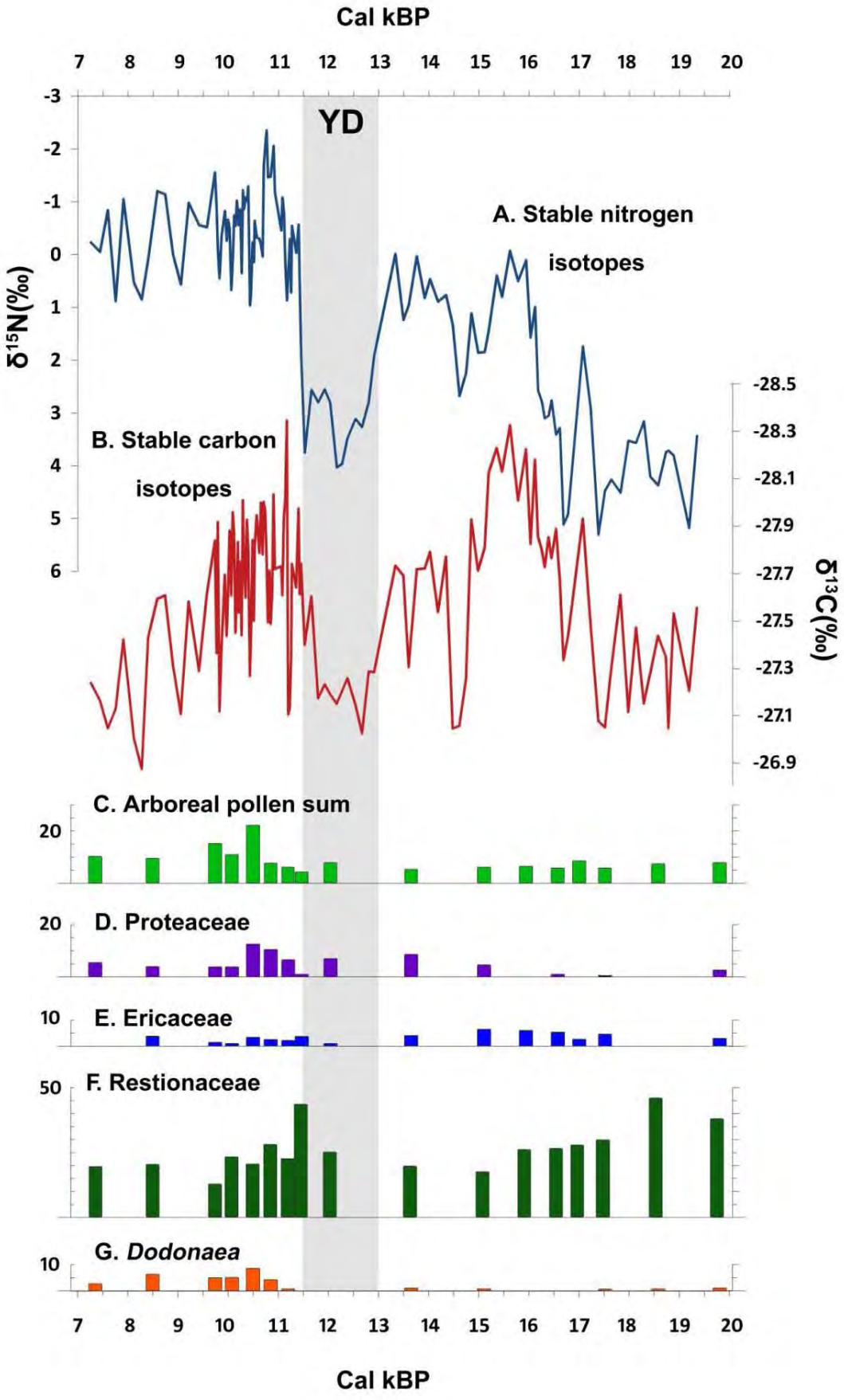

Figure 3.11 The LGIT period of the De Rif 2 record (adapted from Quick et al., 2011).

3.5.2.3 Pakhuis Pass

Towards the northwestern, more xeric, side of the Cederberg, pollen from hyrax midden deposits at Pakhuis Pass were analysed by Scott (1994) and Scott and Woodborne (2007a, b). Greater distinctions between glacial and interglacial environments were inferred from the Pakhuis Pass record in comparison to the extremely muted signals from the vlei records and the variations within the De Rif pollen sequences.

The vegetation during the LGM is characterised by great variability, with fluctuations in *Stoebe* -type pollen and the presence of typical fynbos elements such as Ericaceae, Proteaceae, *Passerina* and *Cliffortia*, as well as elevated levels of Cyperaceae. Holocene vegetation generally consisted of a mosaic of fynbos, thicket and succulent vegetation. Similar to the De Rif 2 pollen sequence, the most prominent change in the Pakhuis Pass assemblage is the sharp increase in *Dodonaea* (from 15.6 cal kBP; Figure 3.12), indicating that post-glacial warming affected both these sites.

In general, the greater variability reflected within the Pakhuis Pass sequence compared to the vlei records (section 3.5.2.1) and the De Rif pollen assemblages (section 3.5.2.2) can be attributed to factors such as the dominating influence of the geology on mountain fynbos (Quick et al., 2011), elevation, rainfall and microclimatic factors. Pakhuis Pass is at a lower elevation (460 m a.s.l.), in the rain shadow of the Cederberg mountains and could possibly have been influenced by greater amounts of summer rainfall during certain periods of the late glacial and Holocene (Scott and Woodborne, 2007a, b), or it could be sensitive to changes in the intensity of winter storms. Pollen within the De Rif middens is almost exclusively composed of mountain fynbos taxa situated on Table Mountain sandstones. Despite also being located on sandstone substrates, a large proportion of pollen incorporated into the Pakhuis Pass midden originated from Karoo vegetation constrained to Bokkeveld Shales and the Karoo Supergroup. Karoid pollen taxa would have become incorporated in the Pakhuis Pass midden due to the site's north-easterly position relative to the Cederberg range, therefore being in closer proximity to the boundary of the Succulent Karoo and the Nama Karoo than De Rif. In addition, if there were greater amounts of summer rain in the past, the drier Pakhuis Pass would have been more affected than De Rif, with the possibility of the Pakhuis Pass region being able to support increased proportions of Karoo vegetation. Due to the higher altitude at De Rif it is likely that this fynbos-dominated zone, which is not close to biome boundaries, was therefore less affected.

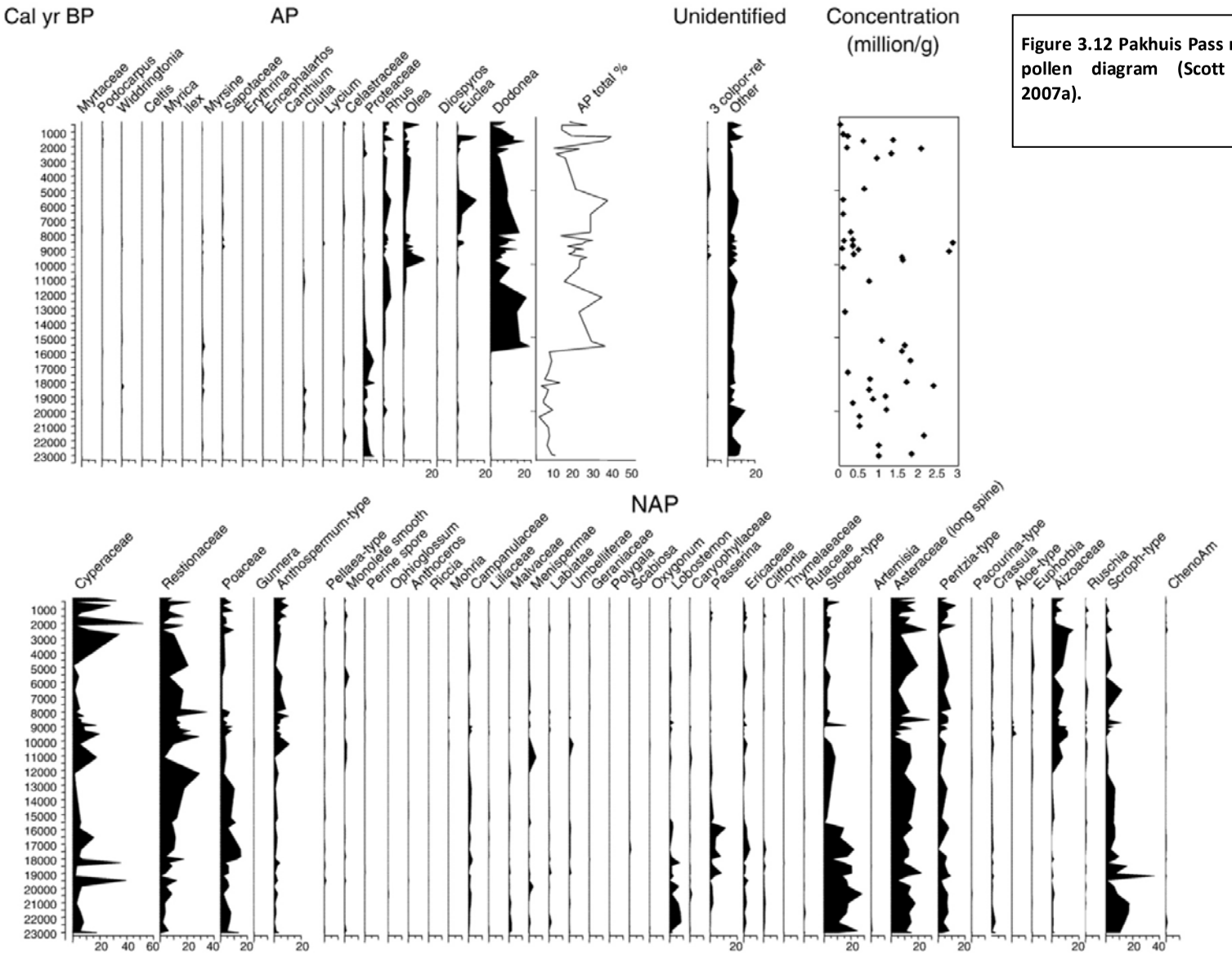

Figure 3.12 Pakhuis Pass relative percentages pollen diagram (Scott and Woodborne, 2007a).

3.5.2.4 Truitjes Kraal and Katbakkies

Truitjes Kraal is a hyrax midden site situated in the southern reaches of the Cederberg, about 17 km southeast of Driehoek. Truitjes Kraal 4 (TK-4) is an 11 cm section of the deposit which has formed within the Holocene over the period ~9.5 – 1.3 cal kBP (Meadows et al., 2010). Pollen and stable carbon and nitrogen analyses were carried out on TK-4, with the results from these analyses concurring that, in general, rather little vegetation change occurred around this site over the Holocene. In spite of the overall conclusion of environmental stability, subtle changes in the pollen frequencies were evident. Slightly greater moisture availability was inferred for the section representing the earlier Holocene as it contained higher frequencies of Poaceae, Ericaceae and arboreal elements as well as relatively depleted $\delta^{13}C$ and $\delta^{15}N$ values (Meadows et al., 2010). The HA and late Holocene are characterised by a minor increase in asteraceous and succulent pollen taxa together with enrichments in $\delta^{13}C$ and $\delta^{15}N$ values, indicating a trend towards more arid conditions (Meadows et al., 2010; Figure 3.13).

Katbakkies Pass in the Swatruggens Mountains, part of the Cape Fold Belt but further south than the Cederberg, is the location of another hyrax midden site. Katbakkies Pass 1 (KB-1) accumulated over a shorter period than TK-4, only covering the late Holocene (~3.7 cal kBP – 0.6 cal kBP) (Meadows et al., 2010). Only very subtle changes in the pollen assemblage for this site are apparent, however, the earlier section (~ 3.7 – 2.4 cal kBP) did contain relatively higher frequencies of Crassulaceae and Euphorbiaceae. Together with slightly elevated $\delta^{13}C$ and $\delta^{15}N$ values, this may indicate warmer and drier conditions during this period (Meadows et al., 2010). A drying trend is also apparent in the stable isotope record from 1.3 cal kBP with increased $\delta^{13}C$ and $\delta^{15}N$ values (Figure 3.13).

Collectively, the pollen and stable isotope records from TK-4 and KB-1 indicate very minimal changes in the vegetation and climatic conditions over the Holocene. There are limitations to the pollen records for TK-4 and KB-1. In particular, the sequence has low taxonomic resolution as a result of pollen identification difficulties as well large sampling intervals which may have resulted in sections containing both warmer/drier and cooler/wetter indicators being conflated in the interpretation. Concordance between the pollen and the isotope records does, however, provide some validation for these records.

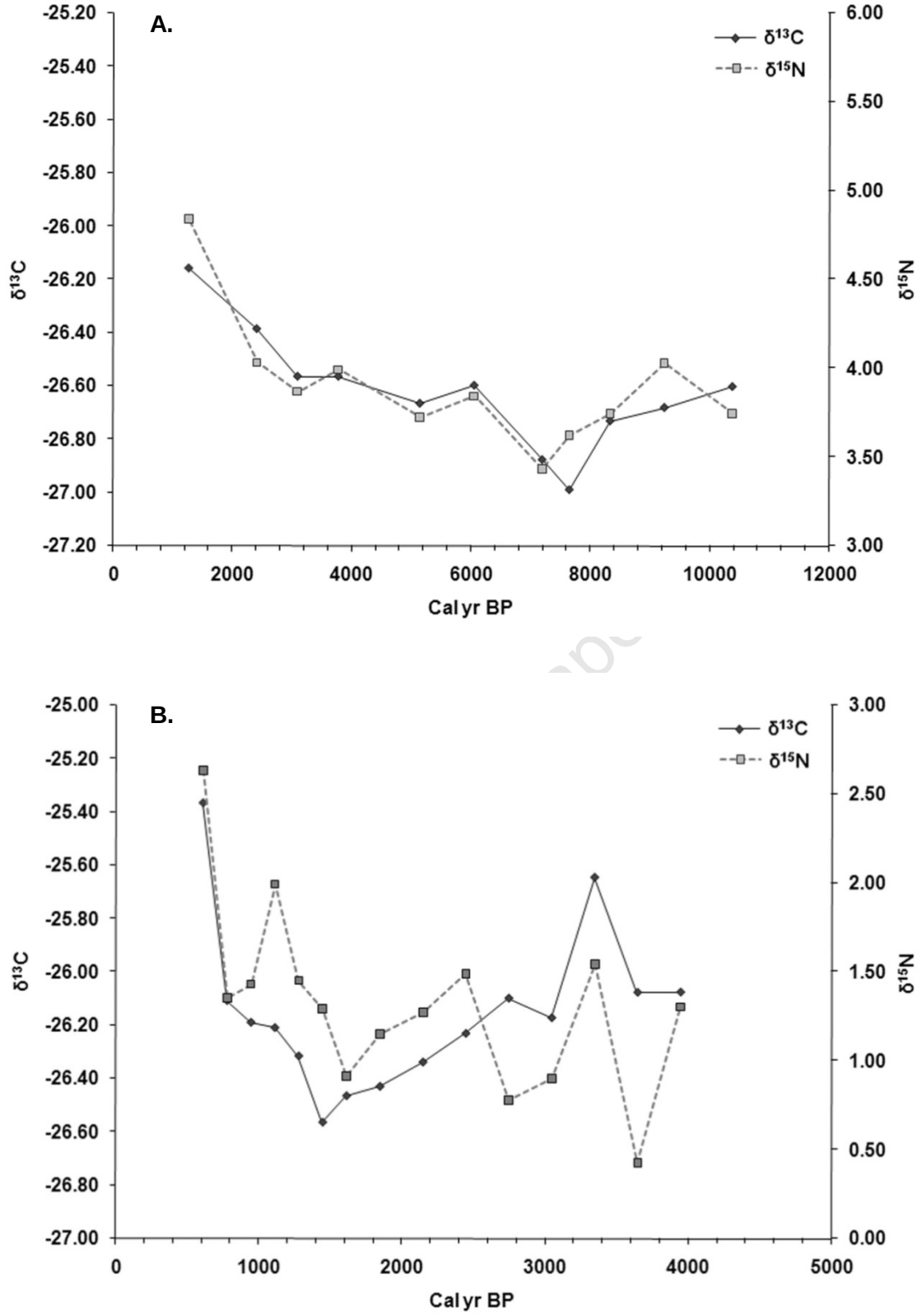

Figure 3.13 Truitjes Kraal 4 (A) and Katbakkies 1 (B) stable isotope data from Meadows et al. (2010).

3.5.2.5 Cecilia Cave, Table Mountain

Baxter (1989) examined pollen from sediments taken from Cecilia Cave, situated at an altitude of approximately 550 m on the eastern side of Table Mountain, on the Cape Peninsula. The sediment deposit found at the rear of the cave accumulated intermittently within part of the Holocene (Meadows and Baxter, 1999). Despite the absence of overarching changes in the pollen frequencies, possible under-representations of arboreal taxa and over-representations of anemophilous pollen, the pollen record obtained from this mountainous site does provide some significant palaeoenvironmental information:

The dominance of Asteraceae pollen together with low absolute pollen concentrations at the base of the pollen record, dated to 8.3 cal kBP, implies that drier conditions most likely prevailed at the site during the HA (Baxter, 1989; Chase and Meadows, 2007). Slightly moister and possibly cooler conditions were inferred from the pollen sequence for the period ~4 – 2 cal kBP due to the presence of Ericaceae combined with an increase in Restionaceae and Iridaceae, and a decrease in Poaceae pollen (Baxter, 1989).

3.5.3 Eastern lowland sites

3.5.3.1 Agulhas Plain pans and lunettes

Sedimentological and palynological investigations were undertaken by Carr et al. (2006a; b) on several pans and their associated lunette deposits situated on the Agulhas Plain (Figure 3.3). Despite the fragmented nature of these archives, they do seem to provide some indications of phases of enhanced aridity and humidity during the late Pleistocene and the Holocene.

OSL ages from the lunettes at Soutpan and Renosterkop reveal that these features developed between ~60 – 45 ka and have been used to infer that drier conditions characterised the Agulhas Plain during this period (Carr et al., 2006a). Further, the orientations of the dunes were used to establish that strong westerly winds prevailed during this period (Carr et al., 2006a).

The discontinuous pollen record from the lacustrine sediments, extracted from the Voëlvlei pan floor, cover the periods >42 – 37.9 cal kBP and ~33.3 cal kBP (Carr et al., 2006b). Substantial increases in Ericaceae and Restionaceae compared to modern vegetation surveys and the recent (~0.3 ka assemblage) suggest increased humidity and cold conditions during this period.

Lunette accretion during the period ~13 – 12 ka was used to infer a shift to drier conditions in the Agulhas Plain region at the end of the glacial period (Carr et al., 2006a). Lunette formation also indicates that the Agulhas Plain experienced multiple phases of increased aridity within the Holocene particularly from 2.8 – 2.6 ka and at 0.7 ka and 0.45 ka. Enhanced humidity has been inferred from the significant and rapid erosion of the inner Voëlvlei lunette by rising water levels around 2 ka (Carr et al., 2006a; b).

It should be noted that the palaeoenvironmental significance of lunette dune accretions have yet to be fully understood (Telfer and Thomas, 2006), and therefore interpretations based on these features remain somewhat speculative.

3.5.3.2 Pinnacle Point

The archaeological work done at Pinnacle Point, a cave complex near Mossel Bay (Figure 3.3), has provided extremely important insights into the behaviour, technological prowess and dietary preferences of early modern humans (Marean et al., 2007a; Brown et al., 2009; Jerardino and Marean, 2010; Marean, 2010; Brown et al., 2012). A wide range of investigations have been carried out at this site including, and not limited to, studies relating to sea level modelling (Fisher et al., 2010), lithics (Schoville, 2010; Thompson et al., 2010), faunal remains (Rector and Reed, 2010; Matthews et al., 2011), micromorphology (Karkanas and Goldberg, 2010), phytoliths (Albert and Marean, 2012) and isotopic content of speleothems (Bar-Matthews et al., 2010). The only records that can be used for palaeoclimatic inferences are the $\delta^{18}O$ and $\delta^{13}C$ isotopes from the Crevice Cave speleothem (Bar-Matthews et al., 2010) and the faunal evidence from PP9C, PP13B and PP30 cave assemblages (Rector and Reed, 2010; Matthews et al., 2011).

The isotope records cover the period ~90 – 53 cal kBP, with Bar-Matthews et al (2010) suggesting that the speleothem $\delta^{18}O$ values were indicative of changes in the relative contribution of summer and winter rainfall. They propose that the southern Cape was influenced by increased summer rainfall during glacials and additionally, that during these periods there was an increased cover of C_4 grasslands near the site (Bar-Matthews et al., 2010; Marean, 2010).

The interpretation of the $\delta^{18}O$ record was based on modern drip water $\delta^{18}O$ values and the $\delta^{13}C$ profile. However deciphering $\delta^{18}O$ signals in speleothems can be extremely difficult as the values are influenced by a complex interplay of various factors including the amount and seasonality of rainfall, atmospheric temperature, the percolation path of the drip water and evaporative effects (Desmarchelier et al., 2000; Treble et al., 2005; Lachniet, 2009; Deininger et al., 2012). In addition,

further consideration needs to be given to the interpretation of the $\delta^{13}C$ signal. As the site is situated within an area that at present, consists of a mosaic of fynbos, strandveld and thicket communities within which CAM type plants can be important elements (e.g. geophytes associated with fynbos and succulents associated with the strandveld and thicket vegetation types) it follows that the $\delta^{13}C$ values most likely do not reflect absolute changes from C_3 to C_4 vegetation ('grasslands' according to Bar-Matthews, 2010) but rather have been influenced subtly by varying amounts of CAM plant inputs and altered through changes in water-use efficiencies (a major determinant of $\delta^{13}C$ in C_3 ecosystems, refer to Chapter 4). Relatively enriched $\delta^{13}C$ values within the section ~74 – 60 cal kBP (MIS 4) and at 80 cal kBP is probably indicative of either increased C_4 or CAM inputs and could possibly signify an increased influence of summer rains to the area.

It is certainly does not seem likely that all (or in fact any) glacial periods were characterised by increases in C_4 vegetation cover (as stated by Bar-Matthews et al., 2010). Indeed, there is evidence for the opposite occurring during the LGM (Talma and Vogel, 1992) with cooler winter growth periods promoting the establishment of C_3 vegetation despite lower CO_2 concentrations (Cowling, 1983b; Meadows and Baxter, 2001; Scott, 2002; Rector and Verrelli, 2010). Whereas the growth and spread of C_4 plants is dependent on warmer temperatures (also promotes the spread of CAM plants) and increased summer rainfall inputs as C_4 plants are generally more efficient under summer growing seasons when temperatures are around 23°C or higher (Vogel, 1978; Vogel et al., 1978; Lee-Thorp and Beaumont, 1995; Scott, 2002).

A further concern is the strong covariance between the $\delta^{18}O$ and $\delta^{13}C$ signals from Crevice Cave, which could indicate that kinetic effects have influenced these records and that the cave system where in fact not in equilibrium, therefore calling into question the reliability of these records as indicators of climatic change.

The faunal records from Pinnacle Point unfortunately do not cover the same period as the isotope sequences and are focussed on the MIS 6/5 boundary. Matthews et al. (2011) infer that warmer and wetter conditions characterised MIS 5e (from ~136 – 120 ka) and that during this time vegetation cover was relatively dense and composed predominately of fynbos. Rector and Reed (2010) propose that vegetation change associated with glacial-interglacial cycles and fluctuating sea levels on the SCCP may have resulted in a complex succession of mosaic communities, composed primarily of C_3 vegetation types and supporting unique mammalian communities.

As sea level changes may have played an important role in the landscape that early humans could inhabit, and thus represent a significant influencing factor on southern Cape palaeoenvironments,

the study by Fisher et al. (2010) is particularly valuable both from an archaeological and palaeoenvironmental perspective. Fisher et al. (2010) used integrated bathymetric datasets, GIS techniques and a relative sea level curve (Waelbroeck et al., 2002) to produce a conceptual 'Paleoscape model' that estimates the position of the southern Cape coastline at increments of 1.5 ka over the last 420 ka. Figure 3.14 A and B displays the relative sea level curve and resultant coastline distances over the relevant time span for this study at Pinnacle Point and Blombos Cave.

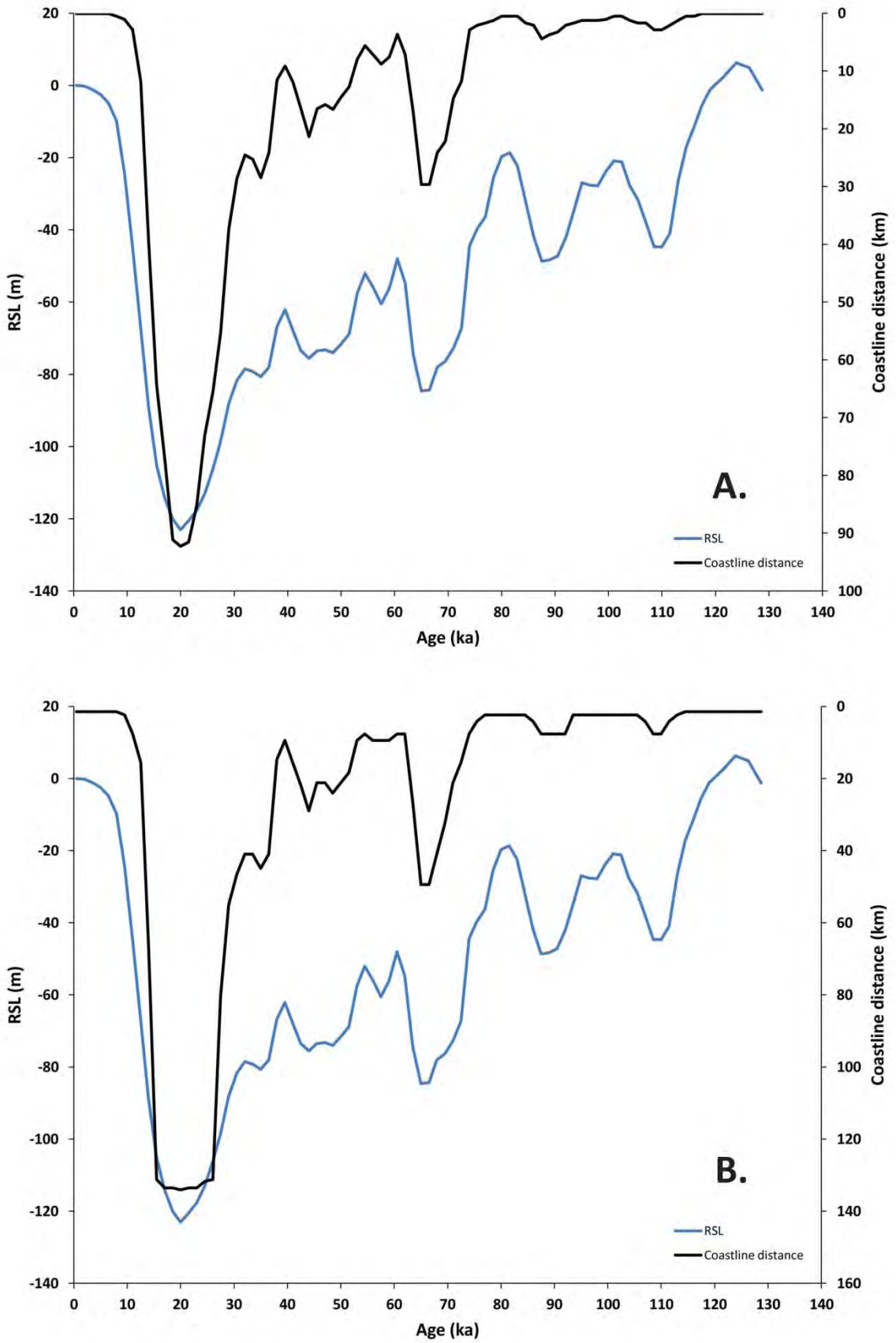

Figure 3.14 The relative sea level (RSL) curve and the estimates of the distances from the coastline for Pinnacle Point (A) and Blombos Cave (B) (Fisher et al., 2010).

3.5.3.3 Norga peat

Palynological analysis was performed on a peat deposit situated in Upper Norga River valley, northwest of the town of George in the southern Cape (Scholtz, 1986; Figure 3.3). The resultant pollen record, while only encompassing the late Holocene and only being supported by three radiocarbon ages, does provide some useful insight into the palaeoenvironments of the afrotemperate region of the southern Cape. Increased moisture availability can be inferred from the initiation of this peat deposit around ~4.5 cal kBP. Conditions from this time until ~2.6 cal kBP appear to have been more favourable than present for the spread of forests, perhaps indicating an increase in summer rainfall and warmer temperatures during this period (Scholtz, 1986). This phase of forest development was interrupted by an episode of increased aridity between ~2.7 – 1.3 cal kBP, within which decreased percentages of forest taxa were recorded (Scholtz, 1986).

3.5.3.4 The Wilderness embayment barrier dunes

The Wilderness embayment comprises of a series of shore-parallel barrier/cordon dunes accompanied by several back barrier/inter-dunal lakes (Illenberger, 1996; Bateman et al., 2011; Figure 4.10). Geochronological analyses performed on the embayment fossilised dunes as well as others found within the southern Cape have shown that coastal dune formation appears to be associated with interglacials and interstadials, with the major control on dune formation being relative sea level (Bateman et al., 2004; Bateman et al., 2011). Bateman et al., 2011, building on earlier work and new OSL chronologies, determined that multiple phases of dune construction occurred during sea level highstands. The Landward Barrier is the oldest of the three main dune formations within the embayment, most likely with an MIS 9 initiation age. Increased stabilisation of this barrier occurred from MIS 5 onwards, once the Middle and Seaward barriers were developed and able to protect it (Bateman et al., 2011). The Middle Barrier OSL ages generally indicate two principal dune sedimentation phases during the penultimate interglacial (MIS 7e and MIS 7a) and last interglacial (MIS 5). A large cluster of OSL ages from the Seaward Barrier are also associated with MIS 5. From the end of MIS 5 through to MIS 2, the lowering of sea levels restricted onshore barrier dune construction by cutting off the sediment supply (Waelbroeck et al., 2002; Bateman et al., 2011). Holocene dune sedimentation occurred after the mid-Holocene highstand with OSL ages clustering around ~3.7 – 2.4 and ~1.7 – 0.6 ka (Bateman et al., 2011).

3.5.3.5 Groenvlei

Martin (1968) established a pollen sequence from a 6.3 m core taken from the eastern end of Groenvlei, one of the interdunal lakes in the Wilderness embayment 20 km east of the Norga site. The sequence covers about ~9 cal kBP with the basal units prior to ~7.8 cal kBP being characterised by limited afrotemperate forest taxa and the dominance of Asteraceae (high spine variety) and dry fynbos elements (Martin, 1968). Around 7.8 cal kBP Martin (1968) uses the presence of peat deposition and an increased abundance of forest taxa to infer an expansion of the afrotemperate forests under humid conditions. This phase was however short-lived as from 7.6 cal kBP (6870 ± 160 yr ^{14}C) to 1.8 cal kBP (1905 ±60) increases in dry fynbos and coastal dune pollen types indicate increased aridity. The last phase of forest expansion was evident around 1.8 cal kBP followed by indications of forest retreat just prior to the arrival of the first European settlers (Martin, 1968).

It should be noted that the evidence for expansions and restrictions of afrotemperate forest derived from the Groenvlei pollen record may be complicated by the influence of shifting sand dunes and marine transgressions and may therefore not directly indicate increases or decreases in moisture availability.

3.5.3.6 Vankervelsvlei

Due to the establishment of a new record from Vankervelsvlei with stronger chronological controls (this study), a re-evaluation of Irving's (1998) pollen records from Vankervelsvlei is now possible. This site is therefore excluded from this review and is instead discussed in conjunction with the new evidence in Chapter 6.

3.5.3.7 Nelson Bay Cave

Nelson Bay Cave is a late MSA and LSA archaeological site on the Robberg Peninsula, Plettenberg Bay (Figure 3.3.). Faunal remains were only preserved in the LSA deposits covering the period ~21.65 cal kBP (18.1 ± 5.5 ^{14}C kBP) to 6.17 cal kBP (5.38 ± 0.65 ^{14}C kBP)(Inskeep, 1972; Klein, 1972a; Fairhall and Young, 1973). Klein (1972a, b, 1980, 1983) analysed the mammalian faunal remains and reported that significant variation existed between the LGM and the Holocene assemblages. A wide variety of grazers dominated the record from ~21.65 cal kBP to ~14 cal kBP while increased abundances of browsers were recorded from ~14 cal kBP to 6.17 cal kBP. These findings were thought to reflect the presence of an increased grass component of the vegetation on the more exposed coastal platform

during the low sea level stands of the LGM. Although the disappearance of many of the larger grazing ungulates within the Lateglacial – early Holocene sections of the record may be attributed to human behaviour rather than ecological (and climatic) change (Rector and Verrelli, 2010). However, Faith's (2011) dietary mesowear analysis does corroborate Klein's earlier work. In addition, the micromammalian record established by Avery (1982) also supports Klein and infers that the LGM at Nelson Bay Cave was characterised by a cooler and drier climate.

3.5.3.8 Klasies River Mouth

Klasies River Mouth is an archaeological cave site near Cape St Francis (Figure 3.3) and is renowned for being one of only few sites which contain anatomically modern human remains in MSA deposits (Singer and Wymer, 1982; Rightmire and Deacon, 1991; Grine et al., 1998; Rightmire et al., 2006). The deposits mainly cover a broad, discontinuous age range of ~115 – 40 ka determined from a number of different dating techniques (e.g. Grün et al., 1990 ; Feathers, 2002). The age of the deposits relating to the Howieson's Poort (HP) techno-complex was widely debated prior to the establishment of a more robust chronology by Jacobs et al. (2008a) (~66 - 58 ka).

There is very limited evidence that can be used definitively to infer palaeoenvironments. Deacon (1984b) employed correlations between shellfish remains and browsing antelope to suggest that during MIS 5, warmer periods were associated with an increase in moisture. High marine shell concentrations (MSC) was used by Thackeray (1988; 1992, 2007) to infer that the MSA I and MSA II stratigraphic units (MIS 5) were associated with higher sea levels after which decreases in MSC indicated a lowering of the sea level across the HP (2007, 1992). Klein (1976) claimed that the increased abundance of grazers within the macrofaunal record indicated colder drier conditions for late MIS 5/early MIS 4. Through the analysis of the micromammalian remains, Avery (1987) suggests that the vegetation mosaic within the vicinity of Klasies River was similar to that of the present for most of the sequence however the HP section was associated with more open, grassier vegetation and moist conditions.

In terms of the assessment of the microfaunal and macrofaunal remains, implicit assumptions were made that decreased species diversity and an increase in grazing animals over browsing automatically related to colder glacial periods and *vice versa* (Klein, 1976; Avery, 1987). Rector and Verrelli (2010) warn against the use of relative abundances of species and MNIs (minimum number of individuals) as used by Klein (1976) when analysing macrofaunal assemblages. Their re-

examination of macrofaunal evidence (taking the full range of species identified, analysing the "community composition of assemblages") from multiple MSA sites across the Western Cape and has shown that glacial periods are in fact not associated with an increased proportion of grazers in the community. Therefore indications of a spread of grasslands during glacial periods may be a misinterpretation of the record. A final precaution as to the reliability of the analyses of the ungulate assemblages from Klasies River Mouth relates to the original excavation methods used and the possible biases associated with them (outlined in Bartram and Marean, 1999; Faith, 2011).

3.5.4 Eastern interior sites

Only three sites fall within this category and they are all concentrated in the Cango Valley, near Oudtshoorn in the Klein Karoo.

3.5.4.1 Boomplaas Cave

Boomplaas Cave is situated on a low limestone hill (part of the foothills of the Swartberg Mountains) about 60 m above the floor of the Cango Valley. A wide variety of evidence has been amassed from this site including macrofaunal (Klein, 1978), microfaunal (Avery, 1982), pollen and macrocharcoal (Deacon et al., 1984; Scholtz, 1986). As the lower lithological members 'BOL', 'OCH' and 'LOH' all dated to beyond the limits of radiocarbon dating, chronological control on these portions of the record has been problematic. However, the recent initiatives to better constrain the southern African MSA industries (e.g. Jacobs et al., 2008a) have shed further light on the HP identified in Boomplaas's facies. The majority of the HP artefacts were concentrated in the 'OCH' member, likely dating to ~66 – 58 ka (Miller et al., 1999; Jacobs et al., 2008a). No charcoal was examined within this layer, although ferricrete nodules were identified and interpreted as indicating increased rainfall (Deacon et al., 1984). Klein's (1984) study of the macrofaunal remains revealed that the levels roughly equating to MIS 4-3 (~66 – 24 ka) were characterised by increased numbers of *Pelea capreolus* (a montane browser) and Alcelaphini (grazers associated with grassland and more open environments)(Klein, 1984). Klein (1983, 1984) inferred cool moist conditions from these assemblages. These interpretations were corroborated by the microfaunal evidence, specifically the relative abundance of the cold tolerant Saunders' vlei rat (*Otomys saundersae*) and the forest shrew (*Myosorex varius*, favouring moist habitats)(Avery, 1982; Deacon et al., 1984).

Charcoal evidence for the BOL and OPL members (approximately attributed to ~55 ka to 37.5 cal kBP) was interpreted by Scholtz (1986) as indicating significantly drier and colder conditions.

However this interpretation is primarily based on what is referred to as the "stunted, spindly growth form" of the plants and not on the taxa identified. Due to the small sample size, the antiquity of the material and the minimum piece diameter (MPD) value, this interpretation should be viewed with caution. The assemblages for this period in fact resemble the lateglacial assemblages which were associated with cool but very wet environments (cf. Chase and Meadows, 2007). Scholtz's (1986) charcoal assemblage Zone B, dating from ~37.5 to 25.5 cal kBP, provides indications of cool, wet environments and a dominance of winter rainfall.

The LGM is represented in Zone C (~25.5 – 21.3 cal kBP) and was characterized by very low species diversity and the absence of tree taxa (Scholtz, 1986). It is dominated by a variety of asteraceous taxa and Ericaceae indicating that conditions were cold and particularly dry (Deacon et al., 1984; Scholtz, 1986). Both the macrofaunal and microfaunal records corroborate Scholtz's claim of a cold dry LGM with greater proportions of grazers prior to ~14 cal kBP (therefore grassier environments), the absence of the reddish-grey musk-shrew (*Crocidura cyanea*), the mean size of the red musk-shrews (*Crocidura flavescens*) and the increased presence of bush Karoo rats (*Otomys unisculcatus*)(Avery, 1982; Klein, 1980).

The lateglacial and early Holocene charcoal assemblages reflect a conspicuous increase in the plant diversity with a replacement of asteraceous shrubland taxa with woodland taxa indicating that while still cool, environments were characterised by highly effective rainfall (Scholtz, 1986; Chase and Meadows, 2007). In contrast, samples dated to ~7.3 cal kBP point towards warm, dry conditions at the HA in association with increased episodes of drought (Scholtz, 1986). The absence of drought-tolerant and cold-resistant taxa for the late Holocene (~2 – 3 kBP) section signifies that warm, mesic conditions occurred during this period, while xylem analysis suggests an increase in summer rainfall perhaps signifying the development of a year-round rainfall regime (Scholtz, 1989; Chase and Meadows, 2007).

3.5.4.2 Cango Cave speleothem and Uitenhage Aquifer temperature records

The $\delta^{18}O$ signal from a speleothem extracted from the Cango Caves (Figure 3.15) shows no clear systematic difference between the glacial and interglacial periods and includes a substantial hiatus from ~16 – 6 cal kBP (Talma and Vogel, 1992). However the palaeotemperature curve derived from the combination of the $\delta^{18}O$ values with the $\delta^{18}O$ content of a nearby confined aquifer does document that the LGM was on average 6°C cooler than present and records post-glacial warming after the LGM and generally warmer temperatures during the Holocene.

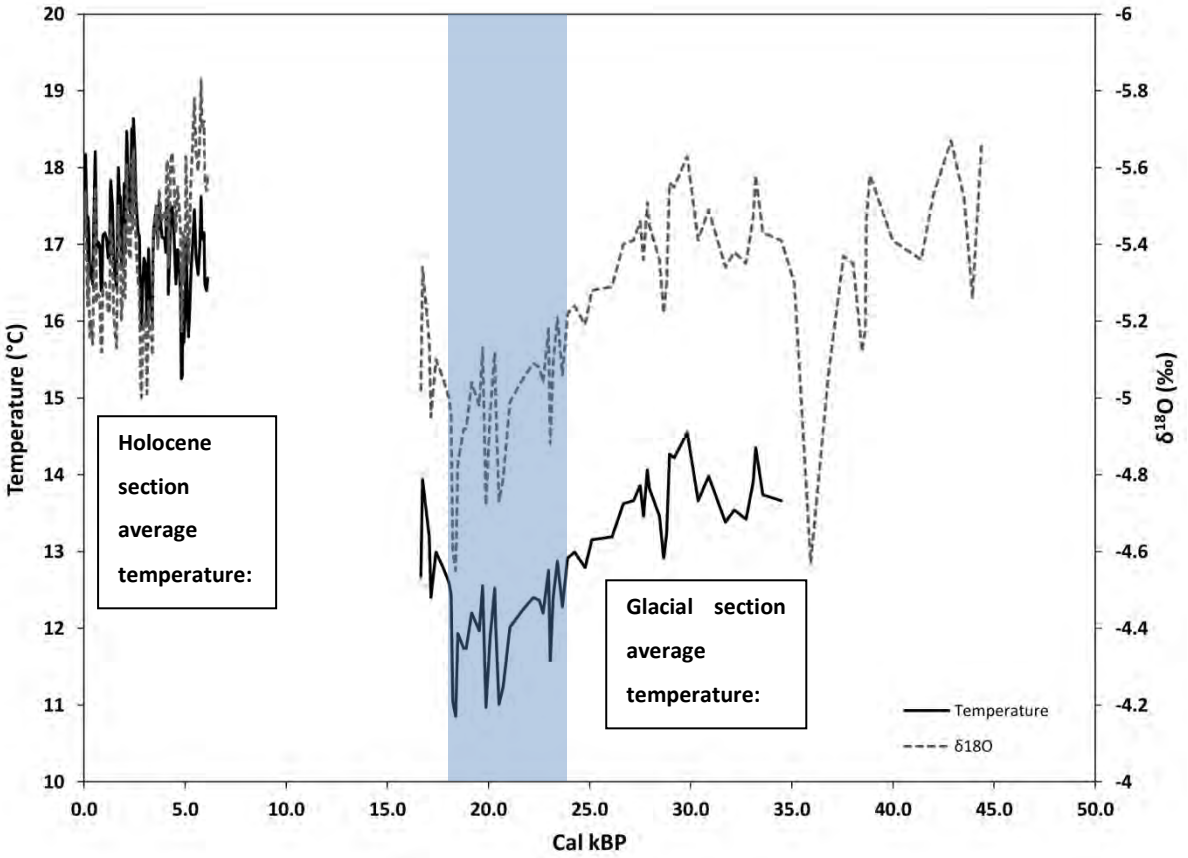

Figure 3.15 The $\delta^{18}O$ and resultant temperature record from the Cango Cave speleothem (Talma and Vogel, 1992). Shaded blue box is the Last Glacial Maximum period.

The Uitenhage Aquifer, an artesian aquifer situated further towards the southeast than Cango Cave (Figure 3.3), reflects similar temperature trends to the Cango Cave record, recording a 5.5 °C cooling at the time of the LGM compared to present with evidence for the initiation of post-glacial warming around 18 – 17 cal kBP (Heaton et al., 1986; Stute and Talma, 1998). Despite the lower sampling resolution, increased temperatures (~2-3 °C higher than present) characterising the HA, are clearer to identify within the Uitenhage record in comparison to the Cango Cave curve. In addition, the presence of a 'neoglacial' period is evident within the Uitenhage record with temperatures of about 3 °C lower than present recorded for the period 4 – 2 cal kBP (Figure 3.16). Further support of these relatively broad trends can be found in the record from Stampriet in Namibia (Stute and Talma, 1998) and all of these data show marked similarities to Antarctic temperature curves, with rises in temperature from approximately 17 ka (Chase and Meadows, 2007).

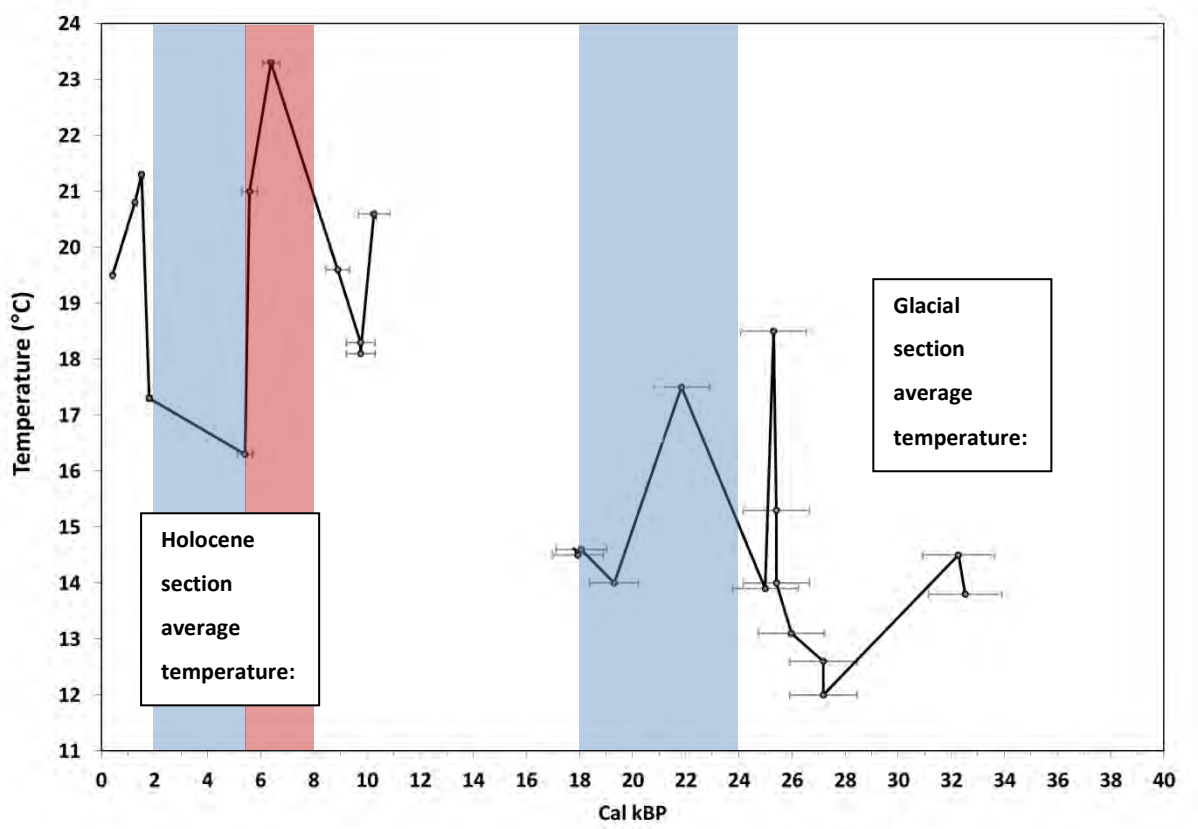

Figure 3.16 The Uitenhage Aquifer recharge temperature record (dissolved N_2/Ar method), blue shaded bars signify phases of cooling whereas the red shaded bar indicates a warmer phase (Stute and Talma, 1998).

3.5.5 Namibian and west coast offshore records: the western margin of southern Africa

Sites inland and off the coast of Namibia and Angola provide additional insight into the palaeoenvironmental history of the WRZ.

Boegoeberg 1 is a brown hyena den located on the west coast of South Africa approximately 450 km north of EBC. The large size of black-backed jackal (*Canis mesomelas*) bones together with the presence of two extralimital ungulates, the blue wildebeest (*Connochaetes taurinus*) and the southern reedbuck (*Redunca arundinum*), have been interpreted as being indicative of cooler temperatures and increased rainfall during the period roughly equivalent to late MIS 5/early MIS 4 to ~41 cal k BP (Klein et al., 1999). However the chronology for this record is extremely tentative.

Although only consisting of four samples, the results of pollen analysis from a hyrax midden deposit extracted from the Brandberg Massif in northern Namibia indicate that the vegetation during the late Pleistocene differed markedly from the current arid vegetation (Scott et al., 2004). In comparison to the two Holocene samples and the modern pellets sample, the samples dating to ~35.5 cal kBP and ~20 cal kBP contained elevated percentages of *Olea*, *Artemisia*, *Stoebe*-type and

fern spores and reduced proportions of succulent desert taxa (e.g. Aizoaceae and *ChenoAm*-type). Therefore this assemblage indicates that conditions during the glacial period were cool with increased humidity around the LGM (Scott et al., 2004). Geomorphological data derived from a variety of studies within the Namib Desert (e.g. Vogel and Visser, 1981; Beaumont, 1986; Teller and Lancaster, 1986 in Chase and Meadows, 2007) support the assertions of increased humidity during the last glacial period.

High resolution stable carbon and nitrogen isotope records from hyrax middens from northwestern Namibia indicate that the mid – late Holocene was characterised by phases of aridity while wetter conditions are evident for much of the early Holocene (Chase et al., 2009; Chase et al., 2010). Strong correlations are observed between these isotope records and a proxy for SSTs and upwelling strength from the Benguela upwelling system (Farmer et al., 2005) highlighting the tight coupling between terrestrial and marine records within this region (Chase et al., 2010). Using the trends in the nitrogen isotopes and their similarities with both low-latitude Southern and Northern Hemisphere records, Chase et al. (2010) claim that rather than precession driving changes in low latitude climate, high-latitude Northern Hemisphere forcing is the dominant control on tropical and subtropical African climate during the Holocene (Figure 3.17).

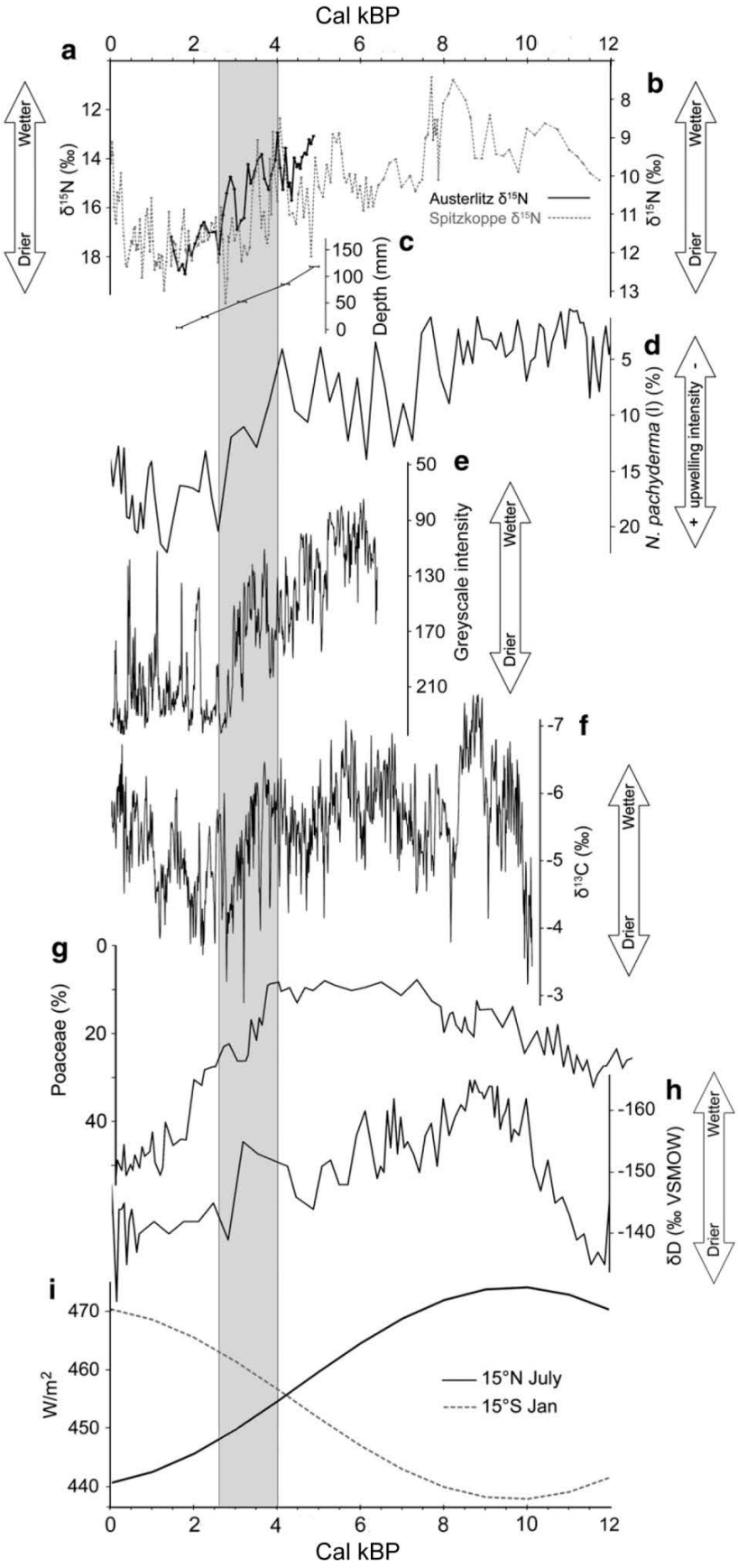

Figure 3.17

Chase et al., 2010 Figure 2 (page 39): Comparison of δ15N records from the Austerlitz hyrax midden (a) with δ15N records from the Spitzkoppe hyrax middens (b) (Chase et al., 2009), N. pachyderma (left coiling) percentages from the Benguela upwelling region (d) (Farmer et al., 2005), Cold Air Cave speleothem grey scale measurements (e) (Lee-Thorp et al., 2001), Cold Air Cave speleothem δ13C values (f) (Holmgren et al., 2003), the percentage of grass pollen at ODP Site 1078 off the coast of central Angola (g) (Dupont et al., 2008), δD values from plant waxes in marine core GeoB 5518-1 off the Congo River mouth (h) (Schefuß et al., 2005), and summer insolation at 15°N and 15°S (i) (Berger and Loutre, 1991). Panel c shows the age-depth curve for the Austerlitz hyrax midden.

Marine cores off the Angolan and Namibian coasts have provided important evidence of long term climate change for the region (Little et al., 1997b; Shi et al., 2000; Shi et al., 2001; Stuut et al., 2002; Rommerskirchen et al., 2006; Dupont et al., 2008). Of particular significance are the pollen results from two marine cores GeoB1023-5 (Shi et al., 2000) and GeoB1711-4 (Shi et al., 2001) which reflect maximum frequencies in Restionaceae pollen from 32 – 23 cal kBP (Figure 3.18) indicating greater moisture availability than present. In addition peaks in Restionaceae pollen together with Ericaceae have been used to infer that the WRZ expanded along the western escarpment during the LGM (as reviewed and displayed in Dupont, 2011). However as Restionaceae was not found in the Brandberg pollen assemblages this assertion is equivocal.

The peaks in Restionaceae pollen in the GeoB cores are followed by gradual declines until ~19 cal kBP for GeoB1023-5 and ~15 cal kBP for GeoB1711-4, after which the frequencies drop off rapidly to negligible values (Shi et al., 2000, 2001; Figure 3.18). Increases in desert, semi-desert and temperate pollen taxa in GeoB 1023-5 (Shi et al., 2000) from ~21 – 17.5 cal kBP correspond to lowered SSTs in association with enhanced upwelling (Kim et al., 2002).

It should be noted that the authors' interpretations of the pollen data derived from the above marine cores have been brought into question (Scott et al., 2004; Chase and Meadows, 2007). The changes to the pollen assemblages from these cores were most probably a response to variations in windiness as well as pollen transport regimes rather than a direct function of temperature and precipitation changes at the core sites. An increase in windiness would have resulted in more remote (often more mesic) taxa being brought to the sites whereas a decrease in windiness would have resulted in greater proportions of local xeric taxa being incorporated into these offshore assemblages. In addition, there are many taphonomical biases affecting pollen transport regimes over the continent with changing wind directions bringing different types of pollen from different parts of the continent to the core sites. Consequently, the overall pollen sequences are a result of a complex combination of these factors together with actual vegetation changes and therefore this data is susceptible to multiple interpretations until further evidence can be supplied.

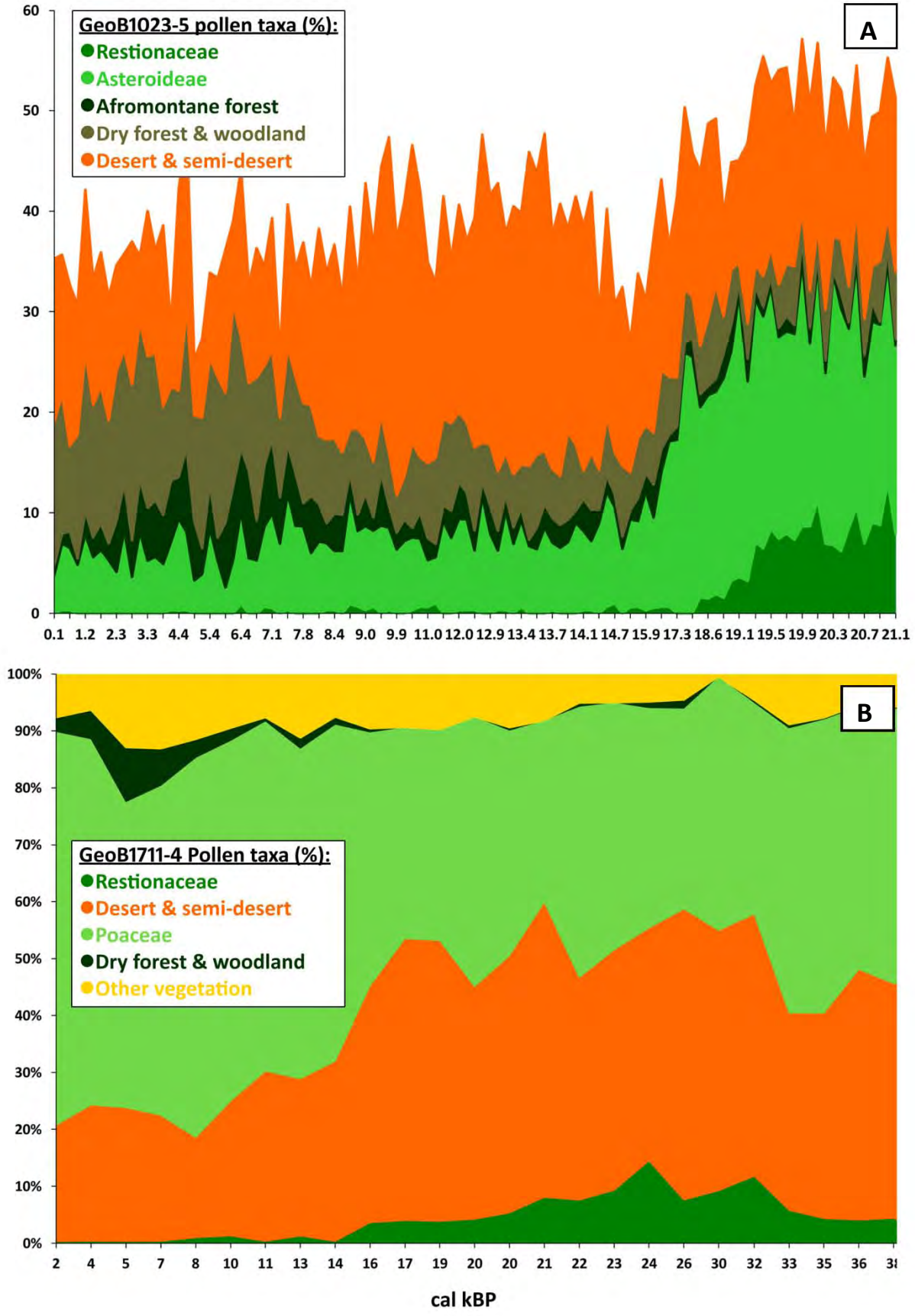

Figure 3.18 Pollen taxa percentages from cores GeoB1023-5 (A) and GeoB1711-4 (B) (Shi et al., 2000, 2001).

Particle size analysis on sediments extracted from marine core MD962094 provide key insights into the behaviour of the southeastern trade winds and their influence on southern Africa palaeoenvironments over the last 300 kyr (Stuut et al., 2002). End-member modelling of the particle size distributions revealed that the southeastern trade winds intensified during glacials when compared to interglacials though teleconnections with the movement of the Antarctic polar and subtropical convergence front (STC) (Stuut et al., 2002; Figure 3.19). These dynamics resulted in relatively drier conditions along the northern west coast during interglacials and increased humidity during glacials. The trade wind proxy shows similar variability to Little et al.'s (1997a; b) trade-wind-induced upwelling intensity record.

From Stuut et al.'s (2002) aridity index (Figure 3.19) it appears that the northern west coast was particularly dry at ~117 cal kBP in association with decreased trade wind intensities. This was followed by a series of significantly wetter periods, particularly at~ 83 cal kBP, between 69 – 59 cal kBP (MIS 4) and during the LGM.

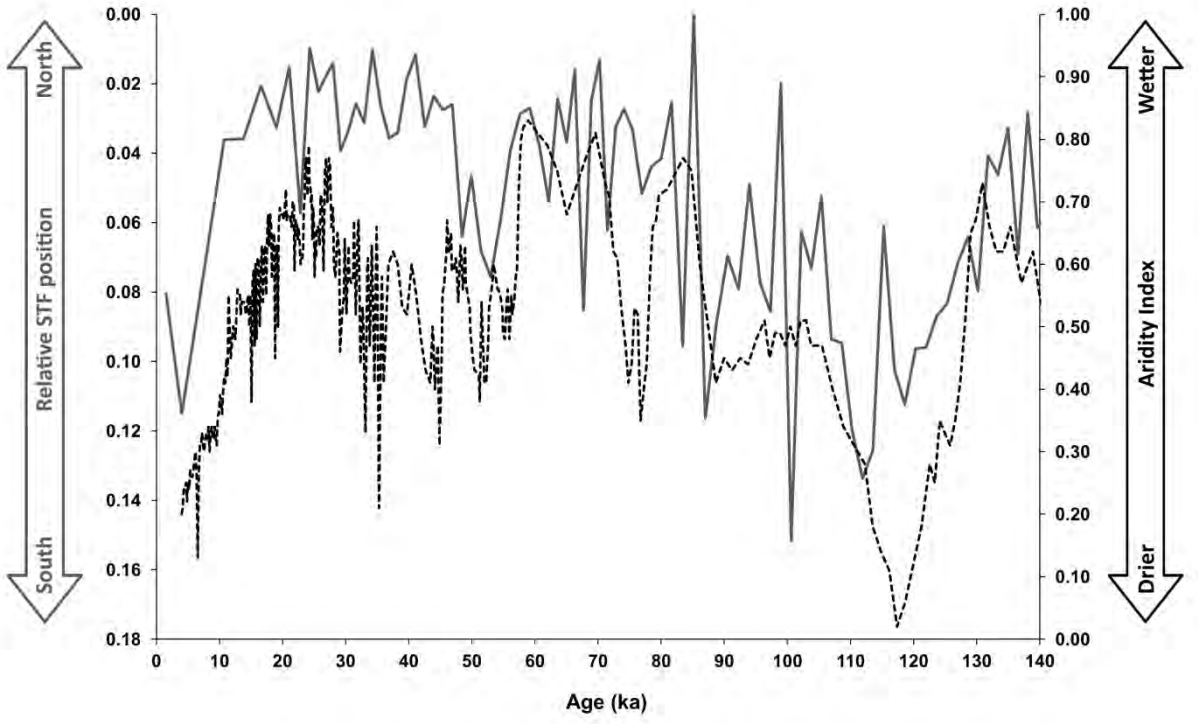

Figure 3.19 Relative position of the subtropical convergence front (STC) (in grey) (Peeters et al., 2004) and Stuut et al.'s (2002) Aridity Index for the northern west coast region derived from end member modelling from the proportion of fluvial sediments from core MD962094 (dotted black line).

3.5.6 Marine records of Agulhas Current dynamics

Agulhas Current dynamics (primarily its temperature and competence) represents an extremely significant influencing factor on southern Cape climates (Tyson, 1986; Reason, 2001; Chase, 2010). However, due to the nature of the bathymetry of the southern Cape, very few marine Quaternary palaeoenvironmental records exist for the region. Nevertheless, marine cores situated within the Cape basin (towards the west) and the upstream region of the Agulhas Current (towards the north east) are able to provide key insights into how the system has changed in the past and how it has affected southern Cape palaeoclimates.

Of the Cape basin records, Peeters et al.'s (2004) 550-kyr Cape Basin Record (CBR) (the product of splicing planktonic foraminifera data from cores GeoB-3603-2 and MD96-2081) is of particular importance as it has been used to infer changes in both the flow of the Agulhas Current and the shifts in the position of the STC (Figure 3.19). This record exhibits strong glacial-interglacial variations (the 100 kyr cycle) with reduced proportions of the foraminiferal assemblage associated with Agulhas leakage, known as Agulhas leakage fauna (ALF) characterising the glacial periods (Peeters et al., 2004). The low contribution of ALF during glacials indicates a weaker communication between the Indian and the Atlantic Oceans and is thought to be linked to concomitant expansions of Antarctic sea ice, northward shifts in the STF and enhanced strength of the westerlies (Peeters et al., 2004; Bard and Rickaby, 2009; Biastoch et al., 2009). In contrast, during interglacials ALF contributions are greater, Agulhas leakage is enhanced in response to the southward movement of the STC and the reduced influence and poleward shift of the westerlies (van Zinderen Bakker, 1976; Cockcroft et al., 1987; Chase and Meadows, 2007; Biastoch et al., 2009). The warmer SSTs associated with general interglacial conditions (and the southward shift of the STC) resulted in increased advection of moisture over the southern Cape. It is thought that during these periods under the reduced influence of the westerlies, the southern Cape would have been subjected to enhanced extra-tropical cyclones and easterly wave dynamics (Reason, 2002).

It has been highlighted by Caley et al. (2011) that the studies from the Cape basin have produced conflicting results (e.g. Peeters et al., 2004; Martínez-Méndez et al., 2008). This is most likely the result of the great complexity of this area primarily a result of the formation of Agulhas rings, the influence of the Benguela Current and lateral shifts in the Agulhas retroflection. However Caley et al.'s (2011) 800-kyr SST and sea surface salinity (SSS) records from the upstream "precursor" region of the Agulhas Current largely corroborates the theories incorporated within the CBR.

In addition, both the CBR and Caley et al.'s (2011) record contain strong obliquity signals, indicating that Agulhas Current dynamics may be primarily driven by obliquity rather than a tropical climate mechanism (precession).

3.6 Palaeoenvironmental synthesis for the southern Cape coastal plain

A severe limiting factor for many of the published SCCP palaeoenvironmental records has been the failure to establish robust chronologies. Owing to this, there are very few terrestrial records for MIS 5 – late MIS 3. The studies that are available have been conducted primarily from an archaeological perspective and consequently there has been relatively limited focus on palaeoenvironmental reconstructions.

As subsections 3.5.1 - 3.5.4 illustrates, the evidence for the SCCP is also spatially discontinuous with differing responses to climate change occurring due to the influence of different rainfall regimes and altitudinal variations. Despite the somewhat sparse evidence presently available, in conjunction with evidence outlined in subsections 3.5.5 and 3.5.6, it is possible to conclude the following:

Exceedingly limited information is available for the Last Interglacial period. Global temperatures and sea levels were both elevated and using inferences from Klasies River Mouth, Pinnacle Point and the Wilderness barrier dune chronologies; sea levels do appear to have been high along the southern Cape with warm phases associated with increased moisture (Deacon, 1984; Bateman et al., 2011; Matthews et al., 2011). This period was most likely associated with increased summer rainfall within the area encompassed by the modern YRZ, an assertion that is supported by the Agulhas Current records (subsection 3.5.6). Furthermore, the Namibian offshore records exhibit trends of increased aridity and have been used to infer a diminished westerly influence and increased easterly flow during MIS 5 (Little et al., 1997a; Shi et al., 2001; Stuut et al., 2002; Chase and Meadows, 2007).

Chase (2010) provides a thorough review of the southern Cape palaeoenvironmental history for MIS 4 and concludes that the whole of the SCCP was characterised by more humid conditions as a result of an increased influence of the westerlies, warm SW Indian SSTs and increased linkages between tropical and temperate systems (e.g. TTTs). This hypothesis is strongly supported by the available evidence from both the western and eastern portions of the SCCP (Avery, 1982; Deacon et al., 1984; Avery, 1987; Avery et al., 1997; Klein et al., 1999; Klein and Cruz-Uribe, 2000) and the offshore records (e.g. Shi et al., 2001; Stuut et al., 2002; Peeters et al., 2004).

MIS 3 is very poorly represented in the overall SCCP palaeoenvironmental record and as a result there are only vague hints as to what the environment may have been like during this period. There is some evidence for colder and wetter conditions within the WRZ for certain parts of MIS 3 (Schalke, 1973; Klein et al., 1999; Scott et al., 2004; Quick, 2009) and from Boomplaas (Avery, 1982; Klein, 1983; Deacon et al., 1984; Klein, 1984). Supported by evidence from the SRZ (Allott, 2006; Sievers, 2006; Clark and Plug, 2008; Hall et al., 2008; Wadley et al., 2008; Holzkämper et al., 2009), Chase (2010) proposes that the transition from MIS 4 to MIS 3 was characterised by aridity with a drop in SW Indian Ocean SSTs (van Campo et al., 1990) resulting in decreased moisture availability within the SRZ. Figure 3.19 highlights that there is a brief drier period at the onset of MIS 3 (and a southward shift in the STC) followed by wetter conditions associated with a northward shift in the STC. Similar inferences were made by Carr et al., (2006a, b) and a strong C_3 signal (if reliable, perhaps indicating increased fynbos presence and a dominance of winter rainfall) is evident from the Crevice Cave isotope records (Bar-Matthews et al., 2010). Therefore it appears that MIS 3 was generally associated with reductions in summer rainfall and perhaps an expanded and more intense WRZ.

With comparatively more records covering the last glacial period, palaeoenvironmental conditions can be described in greater detail and the differences between the coastal and montane regions and the WRZ and YRZ areas appear with improved clarity. The coastal lowlands and montane regions of the WRZ seem to have been generally subjected to cool conditions with increased moisture availability (Schalke, 1973; Parkington et al., 2000; Scott and Woodborne, 2007b; Quick, 2009). Information obtained from the marine cores together with evidence from the Brandberg (Scott et al., 2004) and the Namib desert (Lancaster, 2002) provides further support for greater moisture availability along the western margin of southern Africa during the last glacial period (section 3.5.5). However, the evidence from the Cederberg suggests that the climate during the LGM was more complex than a ubiquitous increase in moisture availability. Prior to 22 cal kBP the climate was indeed cooler and wetter but from ~22 – 21 cal kBP conditions were distinctly more arid (Figure 3.10) after which there was a return to increased moisture availability (Scott and Woodborne, 2007b; Quick, 2009).

Temperatures are confirmed to have been cooler during the LGM with southern Cape palaeotemperature records indicating temperatures of ~6 – 5 °C cooler than present (Heaton et al., 1986; Talma and Vogel, 1992). However, in contrast to the WRZ, these cooler conditions appear to have been associated with increased aridity within the eastern subregions/YRZ section of the SCCP (Avery, 1982, 1983; Butzer et al., 1984; Klein, 1980, 1983, 1984).

These patterns of palaeoclimatic change can be explained by changes in the relative strength and positions of the westerlies and easterlies. An expansion of Antarctic sea ice would have led to the intensification and/ or expansion of the westerly wave belt (with a concomitant northward shift in the STC) resulting in more frequent or intense frontal systems which would have produced increased rainfall along the western and northern parts of southern Africa (Stuut et al., 2002; Chase and Meadows, 2007; Figure 3.2). Whereas the opposite would result in the discrete period of aridity identified within the De Rif record (Figures 3.2 C and 3.10). The occurrence of the peaks in Restionaceae within cores GeoB 1023-5 and GeoB 1711-4 (Shi et al., 2000, 2001) is consistent with the hypothesis of a northward extension of the WRZ during this period, although increases in trade winds and long-distance transport of pollen cannot yet be eliminated as a possible alternative explanation.

Towards the eastern side of the SCCP, lower sea levels would have exposed a large proportion of the Agulhas Bank perhaps creating a more continental climate regime with the potential for the establishment of no-analogue vegetation communities. Reduced summer rainfall due to less effective monsoonal influences and perhaps the blocking of an expansion of the winter rainfall into the region through an enhanced/expanded continental anticyclone (Chase and Meadows, 2007), would account for the drier conditions at Nelsons Bay Cave and Boomplaas.

Alternatively, the notion of drier conditions within the eastern parts of the SCCP may be a product of the region receiving reduced summer rainfall combined with more seasonal winter rainfall (and not absolute reductions in precipitation) (c.f. Chase and Meadows, 2007). Therefore it is possible that the whole of the SCCP was under a relatively homogenous winter rainfall regime. The establishment of higher resolution records from the eastern subregion of the SCCP is required to fully establish the characteristics of, and driving mechanisms for, climate change during the LGM period.

The transition from the glacial period into the Holocene does not appear to have been a smooth one with great variability evident within the available records. However in general, for the LGIT period and early Holocene, the SCCP was characterised by warmer conditions associated with phases of increased moisture availability (Martin, 1968; Schalke, 1973; Klein, 1972a, b, 1980, 1983, 1984, 1991; Scholtz, 1986; Klein and Cruz-Uribe, 1987; Avery, 1993; Parkington et al., 2000; Scott and Woodborne, 2007a; Chase et al., 2009, 2010, 2011; Meadows et al., 2010).

The eastern subregion of the SCCP may have received maximum effective precipitation within the deglacial period (from ~17 – 14 cal kBP) as a result of enhanced winter rainfall with increasing amounts of summer rainfall which would have led to a greatly reduced and less intense dry season

(Scholtz, 1989; Chase and Meadows, 2007). Whereas, the northwestern region of southern Africa experienced increased aridity from about ~15 cal kBP (inferred from the decline in Restionaceae within GeoB1023-5 and GeoB1711-4 and the increase in xeric taxa) (Shi et al., 2000, 2001). A decrease in moisture moving out of the glacial period is most probably as a result of the declining influence of the westerlies (associated with the southward movement of the STC) and a contraction in the extent of the WRZ (Stuut et al., 2002; Peeters et al., 2004; Chase and Meadows, 2007).

The identification of a dry YD episode within the De Rif records further highlights the complexity of palaeoenvironmental change within this region and together with the Namibian hyrax midden records (Chase et al., 2009, 2010) strongly suggest a dominance of northern hemispheric forcing of southwestern Africa from this period into the Holocene (Chase et al., 2011).

The HA was generally associated with warmer and drier conditions, increased aeolian activity and elevated sea levels across the whole of the SCCP (Klein, 1984; Scholtz, 1986; Baxter, 1989; Meadows and Sugden, 1990, 1991; Meadows and Baxter, 1999, 2001; Chase and Thomas, 2007; Scott and Woodborne, 2007a, b; Meadows et al., 2010). A decrease in the amount and/ or the intensity of frontal systems associated with a southward shift (or contraction) in the westerlies most likely was responsible for this drying trend (Chase and Meadows, 2007).

With a relatively higher number of sites, many of which are more finely temporally resolved, the late Holocene palaeoenvironmental record is better resolved but certainly complex. For the western lowland region, temperatures during the late Holocene were similar to present day but have been interpreted to be associated with greater moisture potential between ~4 – 2 cal kBP (Meadows and Baxter, 1999, 2001). Conversely the Elands Bay Cave charcoal assemblage for the late Holocene consists entirely of xeric thicket and asteraceous shrubland taxa and has therefore been used to infer warmer and drier conditions. However, this section of the record is only represented by five sample levels and, since this type of vegetation exists naturally in the region today, it is probably more accurate to state that conditions at that time were broadly similar to the present day.

Evidence from the western montane sites also exhibit possibly conflicting results. The Pakhuis Pass record suggests that the late Holocene was generally warm and dry but included phases of greater moisture availability (Scott and Woodborne, 2007a, b). However the central and southern Cederberg sites (Driehoek Vlei, Sneeuberg Vlei, De Rif 1 and Katbakkies) mainly record very minimal environmental change. The pollen record from Cecilia Cave provides some indications of cooler and moister conditions for the period ~4 -2 cal kBP.

The initiation of the formation of the Norga peat deposit at ~4.5 cal kBP together with the presence of increased forest taxa within the pollen record between ~4.5 – 2.6 cal kBP (Scholtz, 1986), indicates greater moisture availability perhaps as a result of more aseasonal rainfall. This was followed by what appears to have been a brief period of aridity from ~2.7 – 1.3 cal kBP, within which forest taxa percentages decreased (Scholtz, 1986) and lunette dune development occurred on the Agulhas Plain (Carr et al., 2006a). A final phase of forest establishment within the Knynsa region was thought to begun around 1.8 cal kBP (Martin, 1968) and 1.3 cal kBP (Scholtz, 1986).

The majority of the records indicate that the first half of the late Holocene was associated with increased moisture availability which most likely can be attributed to the reassertion of the westerlies after the HA. The phases of forest expansions during the late Holocene probably indicate that the year-round rainfall climate regime was firmly established along the southern Cape coast.

3.7 Conclusion

This chapter illustrates that despite the discontinuous and often poorly-dated nature of many of the available records, a fairly comprehensive body of information does exist, that, if carefully assessed, provides key insights into the palaeoenvironmental history of the SCCP. Furthermore, what is clearly evident is that the SCCP represents an extremely complex region that has not responded in a uniform or globally-representative way to past climate change. As the region is subjected to changes in both tropical and temperate systems controlled by a variety of forcing mechanisms over differing spatial and temporal scales, it is not possible to reconstruct SCCP palaeoenvironments directly from these forcing mechanisms (e.g. Antarctic temperature, Agulhas SSTs). Therefore the data presented (Chapter 5) and discussed (Chapter 6) within this study represent important new records that further elucidate the nature of palaeoenvironmental change within three different areas of the SCCP.

4. Methodological Approach

4.1 Introduction

In order to reconstruct southern Cape palaeoenvironmental conditions, deposits that incorporate and preserve multi-proxy evidence in stratified sequences were required. The following chapter outlines the approach taken in sampling sites along the southern Cape coast. The technique employed in the field to sample these sites is described together with the nature of the specific types of palaeoenvironmental archives found at the sites. The theoretical underpinnings as well as the practical laboratory techniques of the selected palaeoenvironmental proxies, namely; palynomorphs, charcoal, sedimentological, geochemical and geochronological analyses are then outlined.

4.2 Site selection

To investigate vegetation dynamics along the southern Cape coast, sites were selected along a west-east transect which crosses the contemporary WRZ boundary (Figure 4.1). It was envisioned that sampling along this axis would make it possible to investigate the relationship between changing rainfall seasonality and fynbos vegetation dynamics as well as the different responses of particular vegetation types (fynbos and non-fynbos communities) to environmental changes.

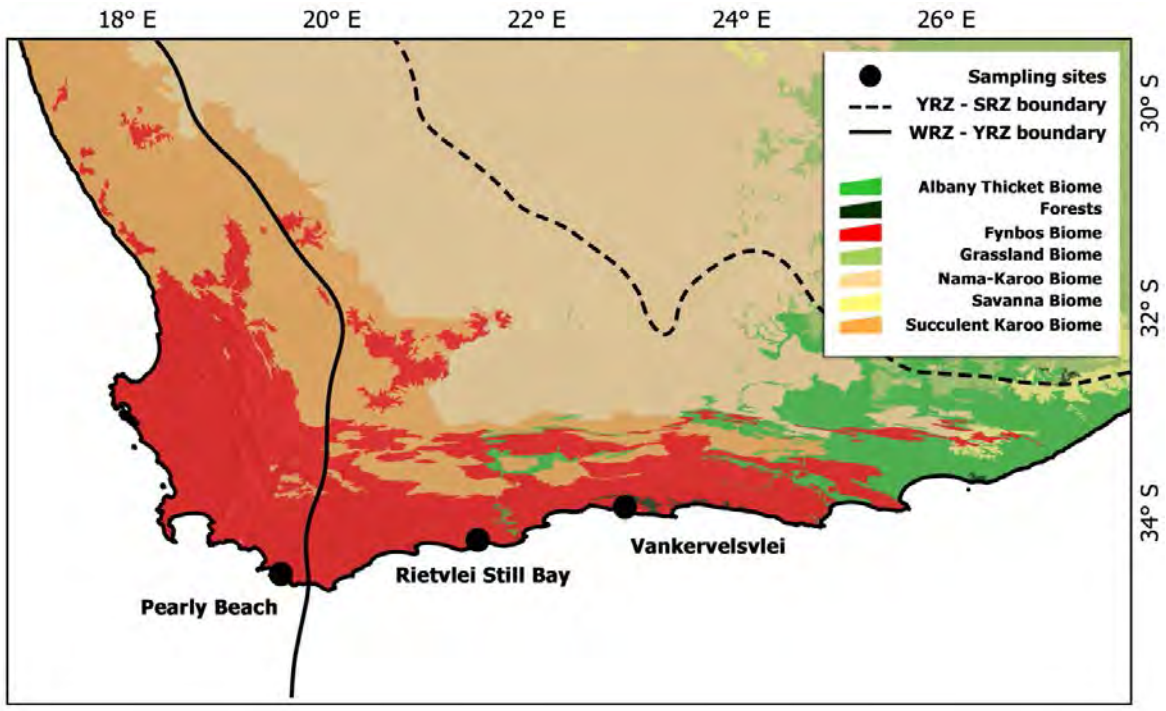

Figure 4.1 The location of the sampling sites in relation to the rainfall zone boundaries and South Africa's major biomes.

Site selection was dictated by the identification of deposits that were likely to contain well-preserved organic matter suitable for palynological analysis. Despite the often-stated scarcity of these types of deposits in southern Africa, the southern Cape has a relative wealth of potential sites. Various types of wetlands including vleis[10] and lakes are present within the landscapes of the southern Cape coast and are identifiable on aerial photographs and satellite imagery (e.g. Figure 2.1). However, the majority of these sites are unsuitable as they are subjected to strong seasonal drying which prevents the preservation of pollen and other palaeoecological proxies.

It was determined that the sites that would most likely contain preserved organic material and have potentially extensive sediment deposits were perennially wet environments. Two vleis with these characteristics were identified: Pearly Beach Marsh at Pearly Beach and Rietvlei near Still Bay (Figure 4.1).

Pearly Beach Marsh is situated well within the contemporary winter rainfall zone, within the mega-diverse Fynbos Biome (refer to Chapter 2) and more specifically falls within the region that has been informally declared the "hottest" of biological hotspots in the world (Cowling, 1996; Willis et al.,

[10] South African terminology for perennial or ephemeral shallow lake/marsh.

1996a; Jones et al., 2002; Goos, 2009) (Figure 4.1). Therefore the wetland is in an excellent position to record past vegetation and climatic dynamics in the core of the modern WRZ.

Rietvlei, ~200 kms to the east of Pearly Beach is also within the CFR/Fynbos Biome but is located within the year-round rainfall zone, a climatic transition zone between the WRZ and the SRZ. It is not only an important location from climatic and ecological perspectives but is also of great significance due to its close proximity to key archaeological sites *viz.* Blombos Cave and Pinnacle Point. A study exploring the application of plant biomarker analysis and geochemistry to palaeoenvironmental studies was conducted by Drs A. Carr, A. Boom, B. Chase and D. Roberts using sediment cores extracted from Rietvlei (Carr et al., 2010a). Therefore there was further incentive to generate palynological data for this site as it was hoped that this study would corroborate and strengthen the biomarker and geochemical findings, creating a robust multi-proxy record.

Irving and Meadows (1997) identified Vankervelsvlei, a small sediment-filled depression near the town of Knysna, as an example of what is known as a *schwingmoor* or floating bog. Such a landform is very rare in the Southern Hemisphere[11] and, since it supports an extensive organic-rich sedimentary sequence, it holds great potential to provide detailed palaeoenvironmental evidence. This site is situated in the YRZ and is located at the ecotone between fynbos vegetation and the Knysna Afrotemperate Region (Figure 4.1; section 2.6.2.2). The past distribution of afrotemperate forests remains the subject of an ongoing palaeoecological debate (Phillips, 1931; van Daalen, 1980; Geldenhuys, 1994). The establishment of an extensive palynological record has the potential to shed further light on the proposed past expansion of afrotemperate forests in the region.

Although a palynological study has already been conducted at Vankervelsvlei (Irving, 1998), the re-sampling carried out for this study was warranted due to refinements in radiometric dating techniques (the inclusion of optically stimulated luminescence ages) together with the implementation of a more extensive and thorough pollen analysis.

4.3 Vlei sediments as palaeoenvironmental archives

Closed lake or vlei sediments provide excellent records of past environmental change as they archive a wide spectrum of palaeoenvironmental data, both spatially and temporally, in stratified sequences. They therefore have been extensively used as a standard tool for the reconstruction of

[11] Floating vegetation mats have been identified at Braamhoek (Norström et al., 2009), Princess Vlei (Neumann et al., 2011) and within the Okavango Delta ('floating sudds') (Ellery et al., 1990) however these have not been classified as *schwingmoors*.

Quaternary palaeoenvironments. Despite the limited availability of these systems due to the semi-arid to arid climates in the region, wetland sites have contributed greatly to the palaeoenvironmental history of southern Africa especially in terms of palynological evidence (e.g. Schalke, 1973; Meadows and Sugden, 1990; Meadows and Sugden, 1991; Scott et al., 1991; Baxter and Meadows, 1999; Meadows and Baxter, 2001; Scott and Nyakale, 2002; Carr et al., 2006b; Finch and Hill, 2008; Norström et al., 2009). Palaeoenvironmental studies using vlei sediments have become significantly more reliable due to improvements in radiometric dating, including the application of OSL dating to inorganic matter within the sediment profiles, and the inclusion of new lines of evidence (e.g. plant biomarkers).

4.4 Peat bogs as palaeoenvironmental archives

Throughout the last century peat bogs[12] have comprehensively been used in the Northern Hemisphere as a valuable archive for climatic and environmental change(Chambers et al., 2012). A remarkably wide range of proxies have been developed to reconstruct palaeoenvironmental parameters using peat sediments (a list of these parameters can be found in Chambers et al. (2012).

On a global scale, peat formation is predominately a result of low oxygen availability which is commonly associated with permanently waterlogged environments (Moore, 1989). It is therefore not surprising that peat bogs are an unusual feature in arid to semi-arid South Africa and only occur in relative abundance in the more tropical coastal plain of northern KwaZulu-Natal (Thamm et al., 1996; Grundling et al., 1998; Finch and Hill, 2008; Ellery et al., 2012).

As mentioned above, Vankervelsvlei is an example of a specific type of bog called a *schwingmoor*[13] or quaking bog. These are typically found in parts of Europe, eastern North America and Canada as their development is primarily a result of glacial processes: melting blocks of ice form over steep-sided kettle holes which subsequently can evolve into schwingmoors (Moore, 2002). They originate from oligotrophic lakes that are slowly colonized by floating rafts of vegetation that extend from the edges of the lake and coalesce at the centre. Over time, the vegetation mat thickens and can eventually even support terrestrial plant species (Warner, 1993; Moore, 2000, 2002). In terms of their hydrological classification quaking bogs can transition between rheotrophic (fed by rain and groundwater flow) and ombrotrophic (exclusively rain-fed) systems. However a permanent

[12] Acidic mires, mires are peat-forming wetlands.
[13] Literal translation is 'swinging bog'.

ombrotrophic system is established once the vegetation mat covers the entire water body and becomes sufficiently elevated.

The occurrence of this type of bog in the southern Cape represents a unique opportunity to gain insight into the development and ecology of such a rare system in the Southern Hemisphere.

4.5 Vibracoring

To extract undisturbed, continuous sequences from the selected sediments deposits most efficiently and effectively, a portable vibracorer was used. The vibracoring system (adapted from Lanesky et al., 1979 and Smith, 1984; detailed methodology found in Baxter, 1996) consists of a poker vibrator (powered by a small petrol engine) clamped to an aluminium core tube (length: 6 m, diameter: 7.5 cm) (Figure 4.2). The vibrator imparts high-frequency, low-amplitude standing waves along the length of the tube. This vibration liquefies the sediments at the base of the core tube making it possible for the sediment to be drawn into the tubing, ready for retrieval using a winch, pulley and tripod system (Figure 4.2). Provided that the sediments are to some degree saturated by water, vibracoring can be used to sample a wide range of depositional environments, making it a particularly versatile coring system (Baxter, 1996; Glew et al., 2001).

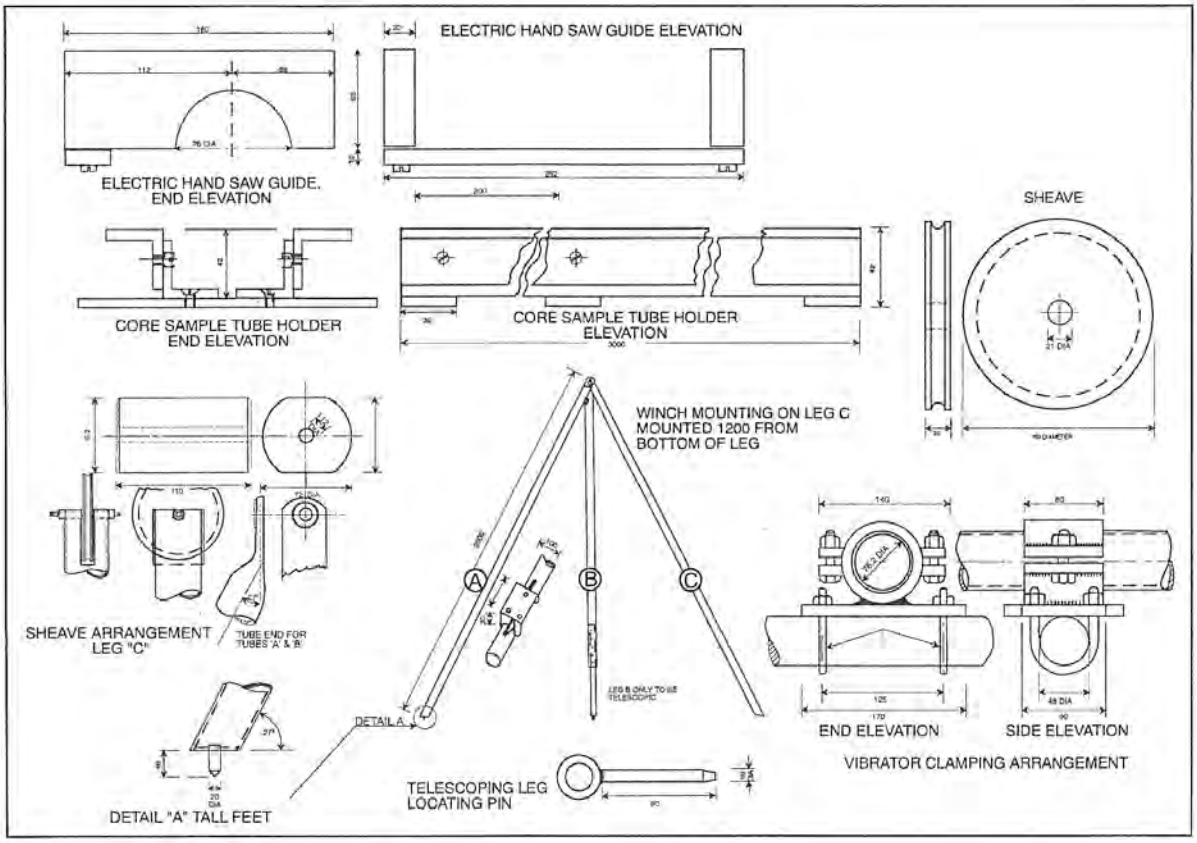

Figure 4.2 The schematic layout of the department of Environmental and Geographical Science's vibracoring system (Baxter, 1996).

Vibracoring was specifically chosen as the most suitable coring technique for the following reasons:

- The vibracorer that was employed (owned by the department of Environmental and Geographical Science, University of Cape Town) has been successfully utilised for the extraction of sediments from various environments throughout South Africa over the last 20 years (e.g. Meadows and Sugden, 1991; Baxter, 1996; Irving, 1998; Baxter and Meadows, 1999; Norström et al., 2009).
- Other coring techniques (such as hand augers and pistons) are unable to penetrate through sand lenses which are common features of southern Cape wetland substrates.
- It is possible to extract extensive sequences, beyond the depth limitation of a single aluminium tube, by riveting tubing together. This technique proved particularly useful for the retrieval of cores from Vankervelsvlei.
- As less vertical force is required in comparison to other corers, the diameter of the core tube can be wider. It has been reported that wider core diameters have produced better penetration and extraction ratios (Thompson et al., 1991 and Smith, 1987 in Glew et al.,

2001). The wide diameter is extremely advantageous as multiple analyses can be conducted on single cores as there is sufficient material available.

- The samples are extracted as continuous sediment sequences, a great advantage over other corers that require overlapping sections to be taken (e.g. Russian corer).
- As sediments are sealed within the aluminium tubes they are not exposed to light and can therefore be sampled subsequently for luminescence dating.

After retrieval, the sediment cores are split open in the laboratory, initially under darkroom conditions enabling them to be sampled for luminescence dating. Following this, sequential sub-sampling took place at regular intervals along the length of the cores for pollen and charcoal (combined within one sample), sedimentological, plant biomarker, geochemical and radiocarbon analyses.

4.6 Sampling sites

This section describes the location and nature of each of the three sampling sites, giving details on the local geology, geomorphology, climate and ecology found at each site.

4.6.1 Pearly Beach

A single sediment core (Pearly Beach 1, 34° 40.155'S; 19° 31.665'E, 5 m a.s.l.) was extracted in 2007 from Pearly Beach Marsh. The vlei is located less than two kilometres from the coastal village of Pearly Beach, which lies about 200 km southeast of Cape Town (Figure 4.3). The wetland derives its source of water from the confluence of the Groot Hagelkraal and Klein Hagelkraal Rivers. The Groot Hagelkraal River flows from higher elevations northeast of the site to form a system of valley bottom wetlands and hill-slope seeps north of the R43 road (Figure 4.3). To the south of the R43, it converges with the channelized Klein Hagelkraal River. Further downstream, the river broadens out over a depression forming the Pearly Beach Marsh, after which it narrows into a small slow-flowing river which opens into a shallow lagoon on the beach.

The Groot Hagelkraal River catchment is predominantly situated on the *Groot Hagelkraal* farm, a registered private nature reserve and a South African Nature Foundation Natural Heritage Site which has been reported to be the location of the world's "hottest" biodiversity hotspot and foremost conservation priority in the CFR (Cowling, 1996; Willis et al., 1996a; Jones et al., 2002). The coastal

waters to the southwest of the site have the highest level of marine endemism found in southern Africa (Goos, 2009).

Geology, geomorphology and soils

The vlei is situated on a low-lying undulating coastal plain which is bounded to the north by limestone ridges (Bredarsdorp Formation) and Table Mountain sandstone outcrops of Peninsula Formation. Transverse coastal dunes, extensively invaded by alien vegetation, stretch along the southern and western boundaries of the wetland adjacent to the ocean. Relict deflated Pleistocene parabolic dunes can be identified within the landscape towards the northwest and southeast of the site.

The coastal area is underlain by unconsolidated aeolian calcareous Quaternary sediments of the Strandveld Formation with partially consolidated calcrete lenses found in some patches along the coast and further inland (Gresse and Theron, 1997). Alluvium deposits characterise the wetlands including the Pearly Beach Marsh.

Figure 4.3 Pearly Beach coring site location and local vegetation. Black box in (A) is the approximate area covered in (B).

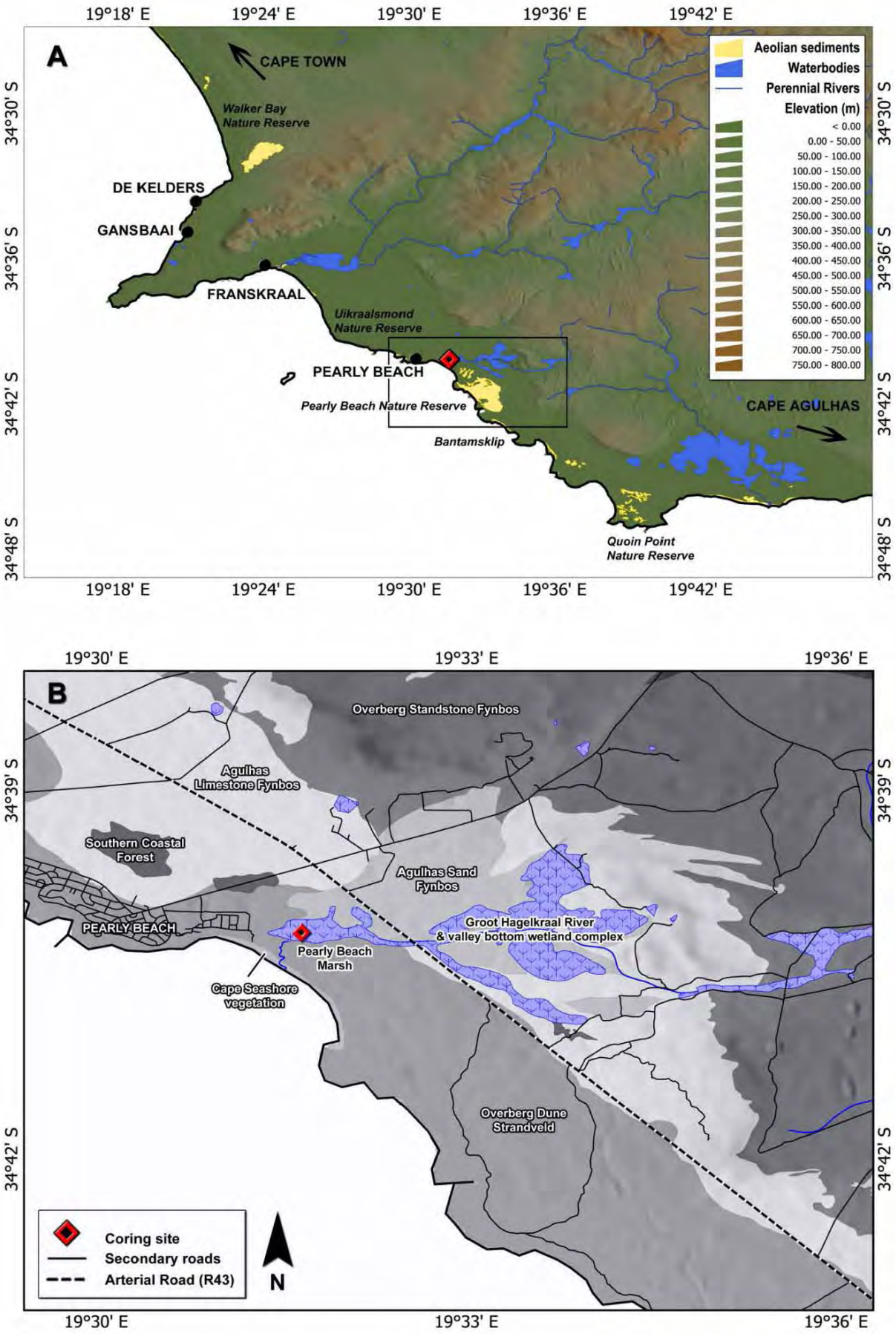

On the sandstone ridges, soils are shallow, alkaline and calcareous whereas the lower slopes are characterised by more acidic, colluvial soils with evidence of early stages of podsolisation (Cowling et al 1988b). The coastal sands are associated with younger and deeper calcareous, alkaline soils in comparison to the soils found in the slopes. Low (2011) determined that soil patterns in the area correlate well with different plant communities with a clear separation between calcareous and non-calcareous habitats.

Climate

Pearly Beach lies within the boundaries of the WRZ and therefore receives the majority of its precipitation in the winter months of June, July and August.

Average rainfall for the nearest stations at Hermanus and Cape Agulhas is 482 mm a^{-1} and 469 mm a^{-1} respectively. The 8-month(January – August 2008) total for Bantamsklip (Figure 4.3) was 881 mm, substantially higher than the surrounding stations, however as this is a very short measurement time the value is not statistically reliable (GIBB, 2010; Climate Systems Analysis Group, 2012; Figures 4.4 and 4.5).

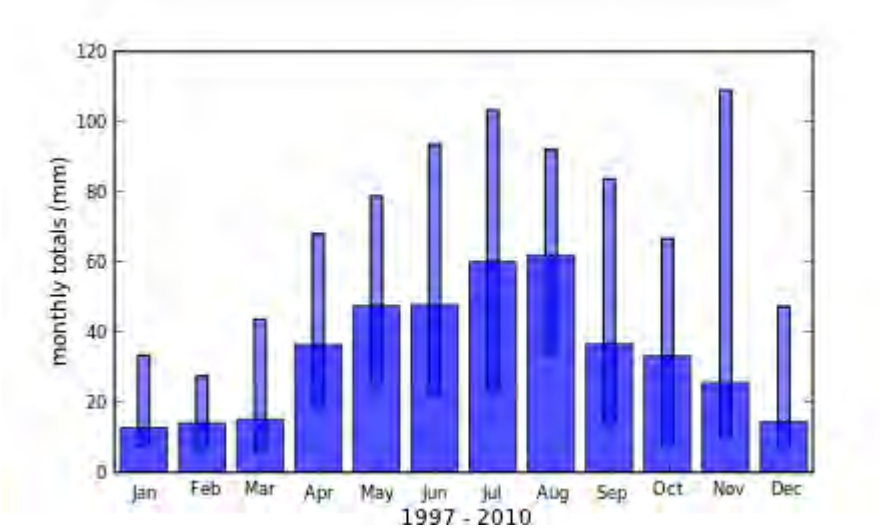

Figure 4.4 The annual cycle of monthly rainfall (mm) for Hermanus. Wide bars indicate the median monthly rainfall for the climate period. Narrow bars indicate the 10th to 90th percentile range of monthly rainfall for each month during the climate period (Climate Systems Analysis Group, 2012).

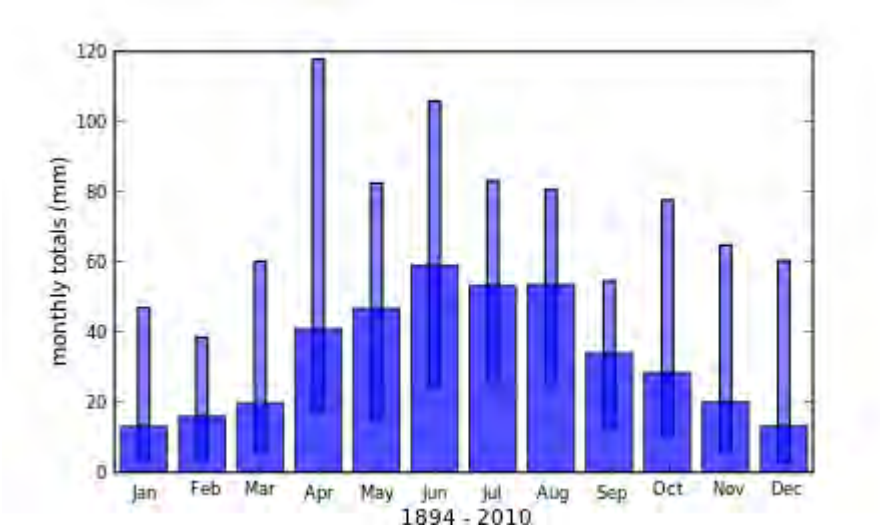

Figure 4.5 The annual cycle of monthly rainfall (mm) for Cape Agulhas. Wide bars indicate the median monthly rainfall for the climate period. Narrow bars indicate the 10th to 90th percentile range of monthly rainfall for each month during the climate period (Climate Systems Analysis Group, 2012).

Winds vary seasonally and are predominantly either easterly or westerly (Figure 4.6), typically with an alongshore flow pattern. During winter there is an increase in the frequency of east-northeasterly winds. An increase in the frequency and strength of westerly winds occurs during summer months with a greater number of moderate to strong winds (5-10 m/s) being observed. Autumn is the calmest period with low wind speeds (GIBB, 2010).

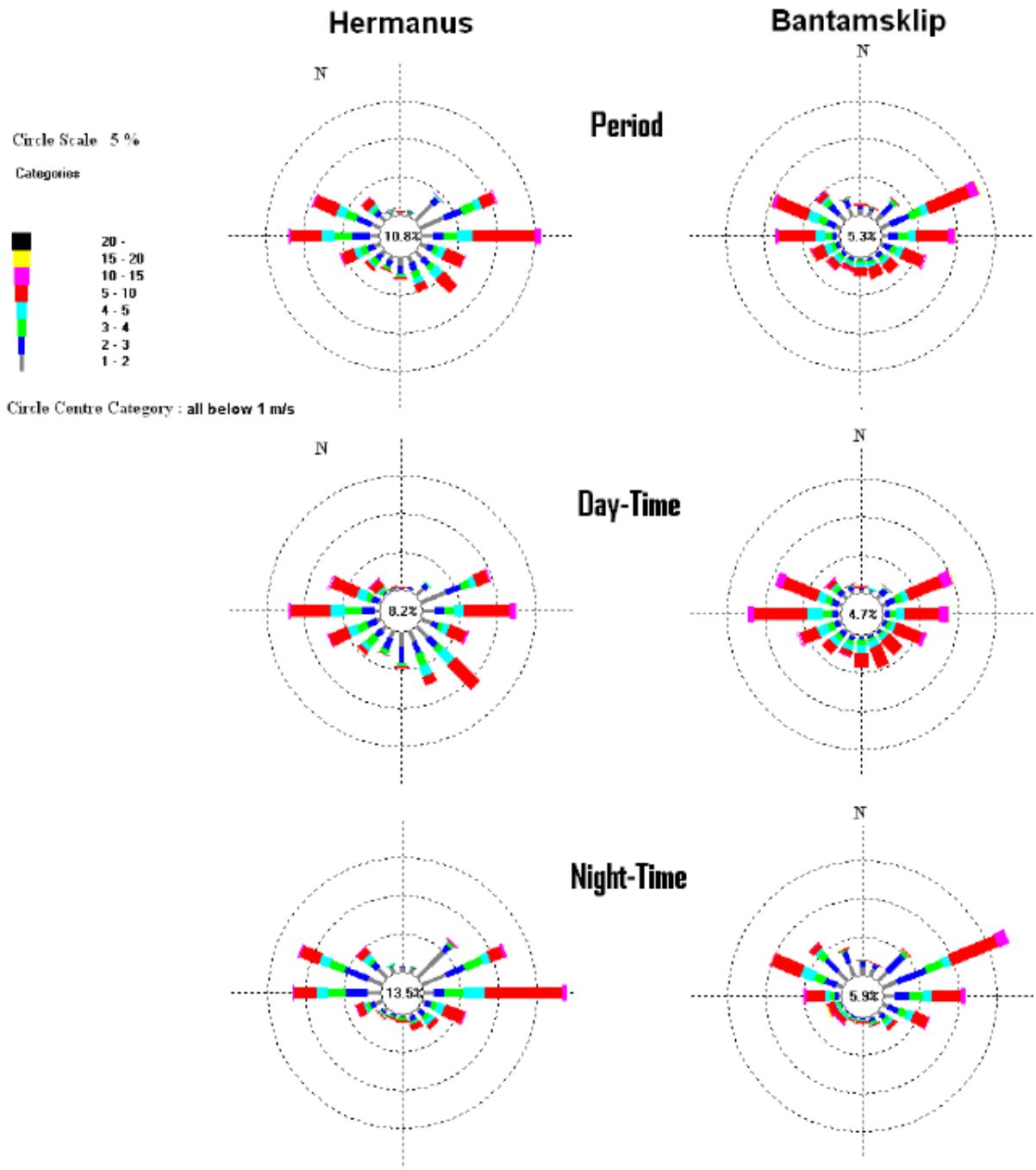

Figure 4.6 Wind roses for Hermanus and Bantamsklip (GIBB, 2010).

Temperatures are moderate with an overall monthly-averaged daily mean of 17 °C (calculated from the 8 month observation period)(GIBB, 2010; Table 4-1). Snow has not been recorded at Pearly Beach and frost appears to be absent from the area as well.

Table 4-1 Dry bulb temperature observations at Bantamsklip for January 2008 – August 2009 (GIBB, 2010).

Month	Daily Average (℃)	Daily Maximum (℃)	Daily Minimum (℃)
January	20.3	30.1	11.9
February	20.2	32.7	10.2
March	19.4	33.2	8.9
April	17.0	33.2	9.5
May	16.2	30.5	7.9
June	14.0	26.0	6.2
July	13.1	26.8	4.5
August	13.4	27.9	3.6
September	13.8	32.4	2.8
October	15.6	25.5	5.8
November	17.0	28.4	8.1
December	19.4	29.1	8.6

Contemporary vegetation

Six vegetation types were identified within the general vicinity of the sampling site.

Agulhas Limestone Fynbos can be found along fragmented patches inland of the site on the Bredasdorp Formation limestones (Figure 4.3B). This vegetation type grades into Agulhas Sand Fynbos on the deeper sands directly north of the site. It is the smallest but most diverse of the limestone vegetation units in the Fynbos Biome (Mucina and Rutherford, 2006). This mid-high, moderately dense shrubland unit contains tall, emergent proteoids and is characterised by the presence of *Protea obtusifolia* and *Leucadendron meridianum*. It occurs on the crests and midslopes of limestone outcrops and ridges throughout the Southern Overberg (Mustart et al., 2003; Mucina and Rutherford, 2006). Other typical taxa found in the area include: *Leucadendron patersonii* (endemic), *Mimetes saxatilis, Ischyrolepis leptoclados* and *Ficinia truncata* (limestone endemic). There are also many endemic ericoids present (especially from the Rutaceae family). The following are characteristically found within limestone fynbos: *Diosma guthriei, D. haelkraalensis, Euchaetes longibracteata, E. meridionalis, Erica calcareophila, E. mariae, E. spectabilis, Jamesbrittenia calciphila, Metalasia calcicola, Muraltia lewisae, Phylica selaginoides, Euryops linifolius* and the geophytes: *Freesia caryophyllacea, Lachenalia muirii and Watsonia fergusoniae* (Cowling et al., 1988; Mustart et al., 2003; Mucina and Rutherford, 2006)

Agulhas Sand Fynbos (structurally defined as neutral sand proteoid fynbos) occurs on the boundaries of limestone outcrops, on the low-lying coastal plains, and supports tall medium dense shrubland with some emergent tall shrubs (Mucina and Rutherford, 2006). Proteoids that characterise this

vegetation type are *Protea susannae, Leucadendron coniferum* and *Leucospermum penduculatum* (Mustart et al., 2003). Other important taxa include: *Metalasia densa, Passerina corymbosa, Amphithalea tomentosa, Cliffortia ferruginea, Elytropappus rhinocerotis, Erica discolour, E, plukenetii subsp. lineata, E. rhopalantha, Spatalla ericoides* (Hagelkraal endemic), *Leucadendron linifolium, Morella quercifolia, Serrucia nervosa* with graminoid elements: *Cynodon dactylon, Elegia filacea, E. recta, E. tectorum, Hypodiscus albo-aristatus, Restio triticeus, Thamnochortus erectus* and *T. insignis* (Mucina and Rutherford, 2006). This vegetation type is considered to be vulnerable in terms of conservation, with 27% transformed mainly due to alien plant infestation and cultivation (Mucina and Rutherford, 2006).

Overberg Sandstone Fynbos is found encircling the limestone outcrops where Table Mountain sandstones are exposed (Figure 4.3). These acidic lithosol soils support moderately tall, dense restioid, proteoid and ericoid shrublands, however it is predominantly structurally defined as proteoid fynbos (Mucina and Rutherford, 2006). Typically, the proteoids emerge to about 1.5 m, over an understorey of ericoid-leaved shrubs, restioids and occasionally sedges. Key species include *Erica plukenetii*, *Leucadendron xanthoconus*, *Leucospermum cordifolium*, *Protea compacta*, *P.longifolia* and *Restio* cf. *triticeus* (Low, 2011).

Overberg Dune Strandveld can be found on the coastal dunes. It is structurally defined as dune asteraceous fynbos and comprised mainly of ericoid shrubs (other than Erica species) (Mucina and Rutherford, 2006). Important taxa include: *Metalasia muricata* (most dominant), *Ischyrolepis eleocharis, Agathosma collina, Muraltia satureoides, Passerina ericoides, Chrysanthemoides monilifera, Helichrysum dasyanthemum, Otholobium fruticans, Pelargonlum betulinum* and *Salvia Africana-lutea* (Mustart et al., 2003). Thicket shrubs (especially *Rhus glauca, Euclea racemosa* and *Olea exasperata*) are reported to be common within this vegetation type, however these were not identified during the vegetation survey carried out in 2011 due to the overwhelming presence of alien invasives.

Cape Seashore Vegetation inhabits the area just above the high water line and on the mobile dunes bordering on the littoral zone. This area is dominated by the grasses *Ehrharta villosa and Thinopyron distichum* and the succulent shrubs *Tetragonia decumbens* and *Carpobrotus acinaciformis*. Other important taxa include: *Arctotheca populifolia, Cynodon dactylon, Bassia diffusa, Dasispermum suffrucosum, Senecio elegans, Silene undulata, Hebenstreitia cordata, Thesidium fragile* and *Passerina rigida*. The more stabilised dunes half a kilometre away from the littoral zone are vegetated predominantly by *Chrysanthemoides monilifera*.

There are isolated patches of Southern Coastal Forests to the north and west of the site. These patches are dominated by *Sideroxylon inerme* (Sapotaceae). Other trees and shrubs present in these patches include: *Cassine maritime, C. peragua, Maytenus procumbens, Olea capensis, O. exasperate, Polygala myrtifolia, Pterocelastrus tricuspidatus*, *Zygophyllum morgsana* and *Rhus laevigata* (Mucina and Rutherford, 2006; Mustart et al., 2003). The understorey is comprised of vines and climbers including *Asparagus asparagoides, Cineraria geifolia, Cynanchum obtusifolium* and *Solanum quadrangulare*.

The Pearly Beach Marsh and the wetlands that are encompassed within the upper reaches of the Groot Hagelkraal River fall into Mucina and Rutherford (2006)'s Cape Lowland Freshwater Wetlands azonal vegetation type which has been classified from a conservation perspective as vulnerable. Cowling (1996) botanical assessment of the whole Groot Hagelkraal wetland system determined that 800 species were present in the area with a high proportion (2.6 %) being local or regional endemics "this must rank as amongst the most extreme concentrations of point endemism anywhere in the world" (page 12).

The vlei is dominated by *Phragmites australsis* and *Juncus kraussii* and *J. capensis. Scirpus nodosus* sedges form dense stands along the margins of the vlei while *Schoenoplectus scipoideus*, *Typha capensis* and *Isolepis prolifer* inhabiting the open water and shallower margins. Also present within the wetland: *Zantedeschia aethiopica, Chironia decumbens*, *Ornithogalum thyrsoides, Helichrysum dasyanthum* and geophytes *Gladiolus tristis*, *Spiloxene aquatica*, *Watsonia meriana* and *Ixia* species as well as true aquatics including *Aponogeton distachyos* and *Nymphaea* species.

The coastal plain especially to the south of the R43 road on the dunefields have been heavily invaded by alien vegetation, predominately *Acacia cyclops* (rooikrans) and to a lesser degree *A. saligna* and *Leptospermum laevigatum*. These woody invasives have formed dense thickets surrounding the wetland.

4.6.2 Rietvlei, Still Bay

Rietvlei is an elongated wetland that is approximately 3.5 km long and 100 m wide, running parallel to the shoreline. It is situated on the Riversdale coastal plain around 8 km east of the town of Still Bay (Figure 4.7).

Two vibracoring field excursions to Rietvlei in 2008 and 2009 yielded a total of three sediment cores: RVSB-1, RVSB-2 and RVSB-3. Rietvlei Still Bay 2 (RVSB-2, 34° 21.249'S; 21° 32.127'E, 17 m a.s.l.) had the greatest potential for the generation of a multi-proxy palaeoenvironmental record.

Geology, geomorphology and soils

The wetland occupies a distinct topographic depression between two shore-parallel coastal barrier dunes and therefore most probably originated as an interdunal slack lake (Roberts et al., 2008). While both categorised within the Cenozoic Bredasdorp Group, the landwards barrier is calcified aeolianite of the Wankoe Formation which was established in the Neogene whereas the seawards barrier was formed during the Last Interglacial sea level highstand (~125 ka) and is derived from the Waenhuiskrans Formation (Roberts et al., 2008). The seaward barrier is being rapidly eroded by high-energy wave action forming steep sea cliffs, with vertical extents of as much as 70 m. The whole area is underlain by Bokkeveld Group mudrocks (part of the Cape Supergroup). Alluvial silty sands characterise the Rietvlei wetland with the aeolianites immediately to the south and southeast of the site comprising of medium-grained, moderately sorted calcareous limestones (Roberts et al., 2008). The limestone outcrops to the north of the site are associated with shallower alkaline calcareous soils with occasional calcrete lenses. Fey (2010) classifies the soils of the region as cumulic soils which are immature soils derived recently from their parent material.

Roberts et al. (2008) determined that these coastal aeolianites were rich in faunal remains and trace fossils suggesting that the site was most probably a valuable water source throughout the late Pleistocene and Holocene.

Figure 4.7 Rietvlei coring site location and local vegetation. Black box in (A) is the approximate area covered in (B).

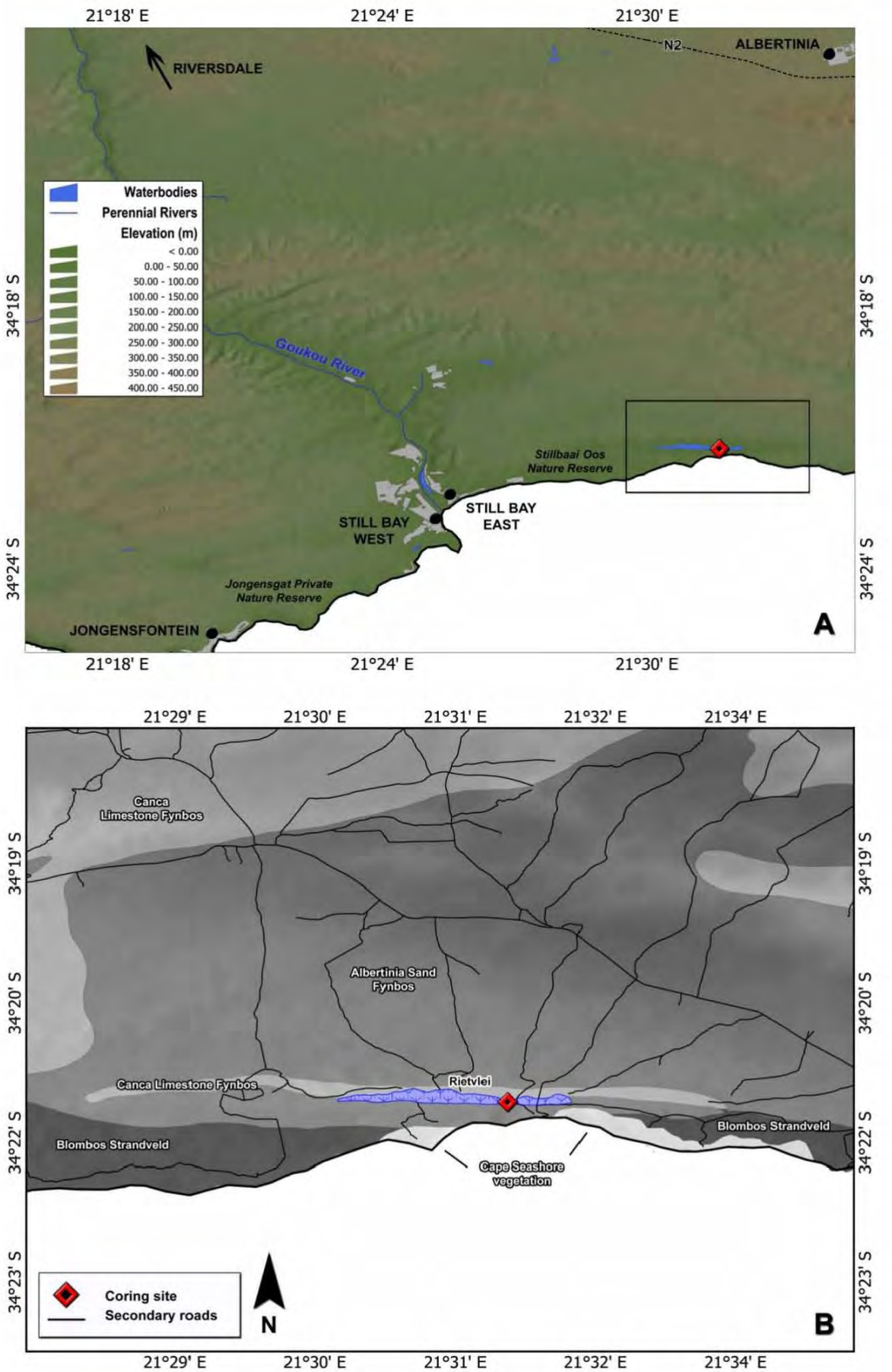

Climate

Rainfall at Still Bay is distributed in a relatively uniform pattern throughout the year as it lies within the YRZ, although annual totals average only 414 mm; the climate is therefore classified as semi-arid (Climate Systems Analysis Group, 2012). Figure 4.8 confirms the low precipitation values, especially for January and February and indicates that the distribution of rainfall is slightly bi-modal with peaks in autumn and spring.

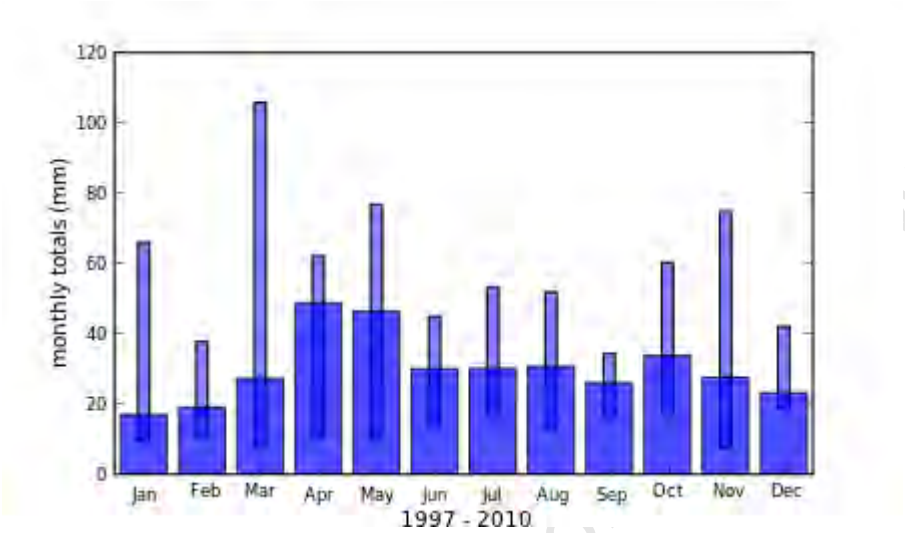

Figure 4.8 The annual cycle of monthly rainfall (mm) for Still Bay. Wide bars indicate the median monthly rainfall for the climate period. Narrow bars indicate the 10th to 90th percentile range of monthly rainfall for each month during the climate period (Climate Systems Analysis Group, 2012).

The dominant winds are north westerlies and south easterlies varying with the season. The maximum wind speed can reach up to 10.7 m/s in east south east direction and 8.7m/s in the northwest direction (Figure 4.9).

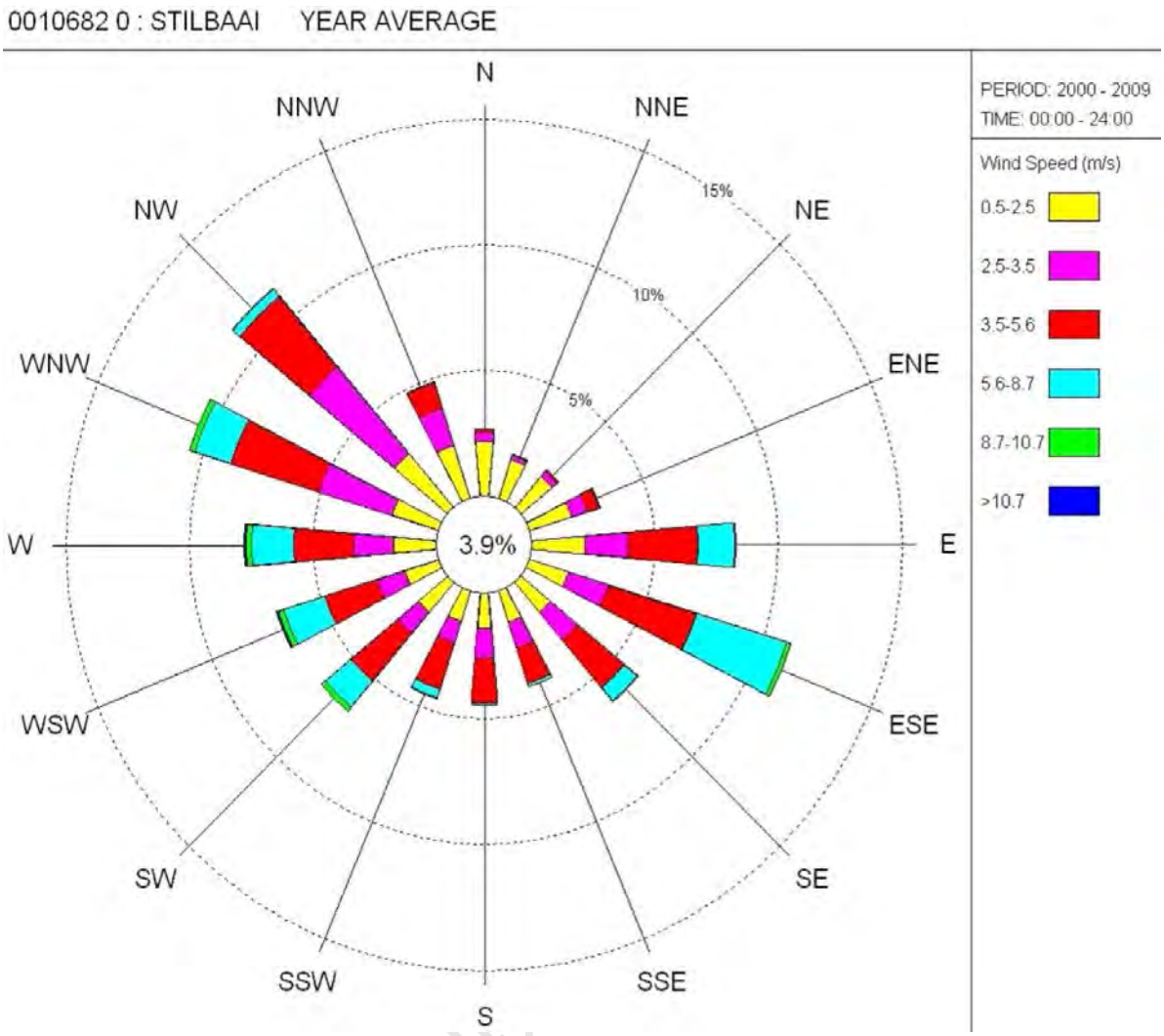

Figure 4.9 Wind rose for Still Bay, displaying the annual average wind speeds and direction for the period 2000 – 2009 [data source: South African Weather Service, found in Swartz (2010)].

The maximum average day temperature is 25.8°C in the summer and can drop to a minimum of 9.4°C at night in the winter (Table 4-2).

Table 4-2 The monthly averaged minimum and maximum temperatures for Still Bay for 2009 [data source: South African Weather Service, found in Swartz (2010)].

Month	Ave T_{max} (℃)	Ave T_{min} (℃)
January	24.8	16.5
February	25.6	16.8
March	25.8	15.5
April	23.1	13.9
May	21.9	11.8
June	20.4	11.1
July	20.8	9.9
August	20.3	9.4
September	20	9.9
October	21.4	12.5
November	23	13.5
December	23.9	14.3

Contemporary vegetation

Many of the vegetation types that presently surround the Rietvlei wetland are the same as, or very similar to, those found in the vicinity of the Pearly Beach site (Figures 4.3 and 4.7).

The calcareous ridge immediately to the north of Rietvlei is dominated by the endemic-rich limestone proteiod fynbos (Mustart et al., 2003). Mucina and Rutherford (2006) classify this as Canca Limestone Fynbos which is floristically similar to Agulhas Limestone Fynbos (details of which can be found in section 4.6.1).

Albertina Sand Fynbos is found bordering the patches of limestone fynbos, it is more extensive than the limestone fynbos and is concentrated within the valleys and on the coastal plain. It is structurally defined as proteoid fynbos and characterised by medium to tall open shrublands (Mucina and Rutherford, 2006). Taxa identified on patches below the limestone ridges near the site include: *Cassine peragua* subsp. *peragua, C. maritima, Pterocelastrus tricuspidatus, Leucadendron eucalyptifolium, L. meridianum, Metalasia densa, Protea repens, P. susannae, P. obtusifolia,*

Passerina corymbosa, P. rigida, Aspalathus calcarea, Muraltia ciliaris, Aspalathus calcarea, Eriocephalus paniculatus, Phylica ericoides, P. parviflora, Cliffortia stricta, Polygala myrtifolia, Helichrysum crispum and *Thamnochortus insignis*.

To the south of the site, the coastal dune crests and landward slopes are vegetated by dune thicket, comprising of a high cover of tall non-proteoid trees and shrubs and a high presence of fleshy-leaved shrubs (Rebelo et al., 1991; Mustart et al., 2003). This vegetation type is characterised by the co-dominance of *Euclea racemosa* and *Olea exasperata*. Other noteworthy taxa found within this unit include: *Sideroxylon inerme, Zygophyllum morgsana, Rhus crenata, R. longispina, R. glauca, Pterocelastrus tricuspidatus, Cassine maritime* and *C. peragua* subsp. *barbara*. The thicket elements form a mosaic with dune asteraceous fynbos[14] on the neutral sands to the southwest and southeast of the site (Rebelo et al., 1991; Mucina and Rutherford, 2006). This vegetation unit comprises of elements which are predominantly ericoid shrubs other than *Erica* species (Rebelo et al., 1991). Taxa characteristic of this vegetation type include the following tall shrubs: *Metalasia muricata, Chrysanthemoides monilifera, Cussonia thyrsiflora, Grewia occidentalis, Maytenus procumbens, Morella cordifolia, Tarchonanthus littoralis, Passerina rigida, Salvia africana-lutea, Aspalathus alopecurus, Eriocephalus africanus* var. *africanus*; succulents: *Zygophyllum morgsana, Osteospermum fruiticosum, Crassula nudicaulis, C. pubescens, Euphorbia mauritanica, Carpobrotus acinaciformis, Crassula expansa, Pelargonium peltatum* and graminoids: *Cynodon dactylon, Ehrharta delicatula, E. villosa var. villosa, Ficinia indica, F. lateralis, F. ramosissima, Thamnochortus erectus*.

The immediate littoral zone is sparsely vegetated, due to the steep scree slopes. However elements of Mucina and Rutherford (2006)'s azonal vegetetation community Cape Seashore vegetation were identified including: *Tetragonia decumbens*, *Carpobrotus acinaciformis, Arctotheca populifolia, Cynodon dactylon, Dasispermum suffrucosum, Passerina rigida, Drosanthemum hispidum* and *Othonna dentata*.

The wetland itself is extensively covered by *Phragmites australis*. Also present within the floating mat of emergent vegetation are various Juncaceae, Cyperaceae, Apiaceae and Araceae species as well as true aquatic elements such as *Aponogeton*.

[14] Mucina and Rutherford (2006)'s 'Blombos Strandveld' vegetation unit includes both dune thicket and dune asteraceous fynbos.

4.6.3 Vankervelsvlei

Vankervelsvlei (or Van Kervel's vlei named after the first mayor of the nearby town of George) is situated approximately 9 km to the east of the coastal village of Sedgefield and about 15 km west of the Knysna (Figure 4.10). It is located at an elevation of 150 m a.s.l and lies a few kilometres inland of the coastal lake of Groenvlei (studied by Martin, 1968). The site is on the timber company B.G. Bison's property, only accessible with special permission by the plantation management either from the Ruitgevlei - Karatara road that leads off the N2 national road at Groenvlei or from the Buffelsbaai/Blackwaters River Lodge turnoff further towards Knysna (Figure 4.10).

Fieldwork campaigns were undertaken in 2009 and 2010 and a total of four cores were successfully extracted: VVV09, VVV10.1, VVV10.2 and VVV10.3. Vankervelsvlei 2010 #1 (VVV10.1, 34° 0.743'S; 22° 54.251'E, 153 m a.s.l.) was deemed the most promising of the four from a palynological perspective.

Geology and geomorphology

Vankervelsvlei is situated on the landward edge of the Wilderness embayment area (Illenberger, 1996; Bateman et al., 2011). The wetland is a ~0.5 km^2 irregular-shaped depression surrounded by a stabilised aeolian dune cordon/barrier, the 'Landward barrier' *sensu* Illenberger (1996)(Figure 4.11). Bateman et al. (2011) determine that the age of the Landward barrier to be approximately 241 – 221 ka. Palaeozoic (Ordovician – Silurian) Penninsula Formation sandstones and quartzites of the Table Mountain Group (Cape Supergroup) presumably underlie the Middle to Late Pleistocene dune systems and the coversands of Mid-Miocene to Pliocene age (Marker and Holmes, 2002; Parsons, 2009; Carr et al., 2010d; Marker and Holmes, 2010; Bateman et al., 2011).

Figure 4.10 Vankervelsvlei coring site location and local vegetation. Black box in (A) is the approximate area covered in (B).

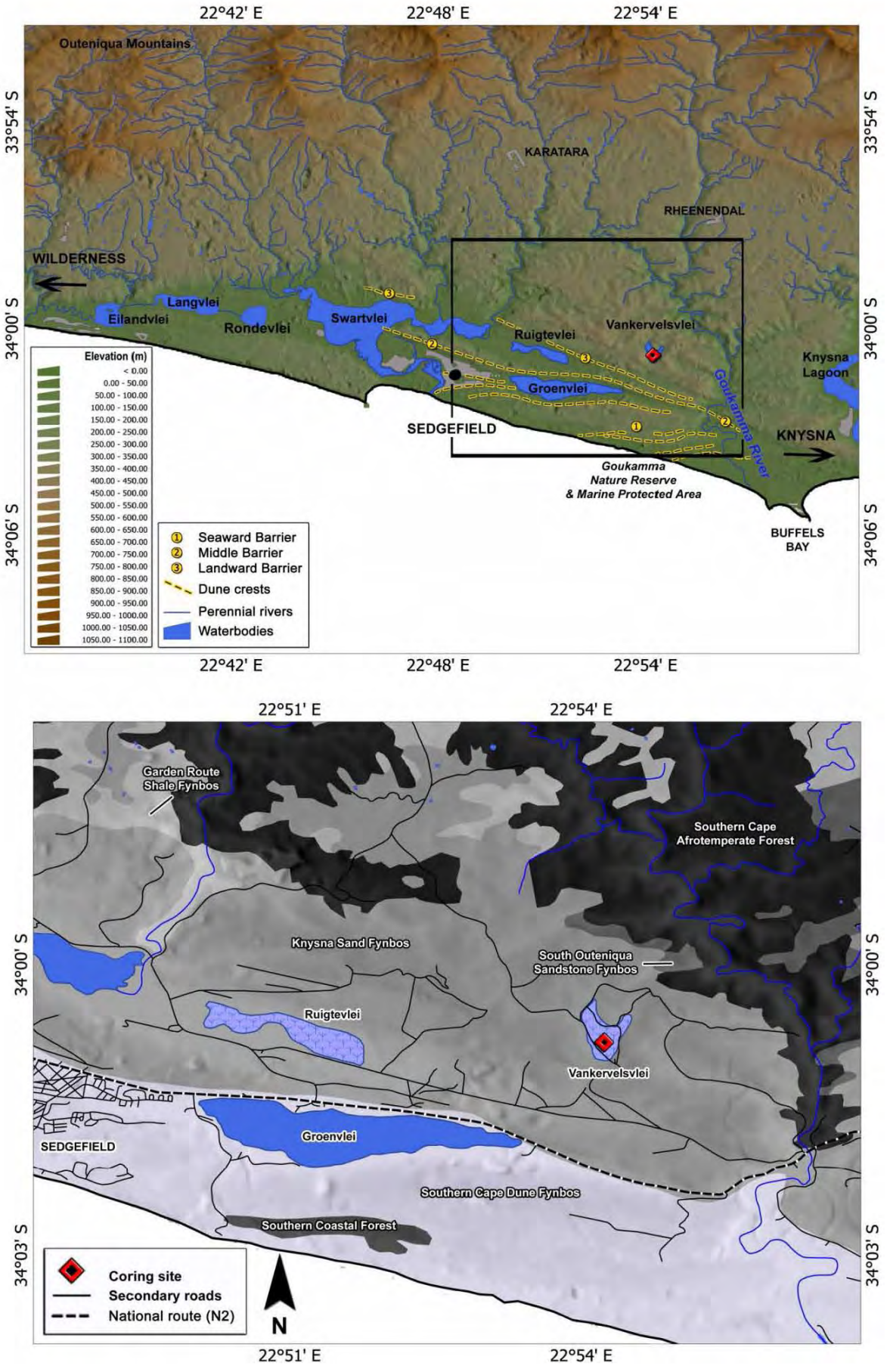

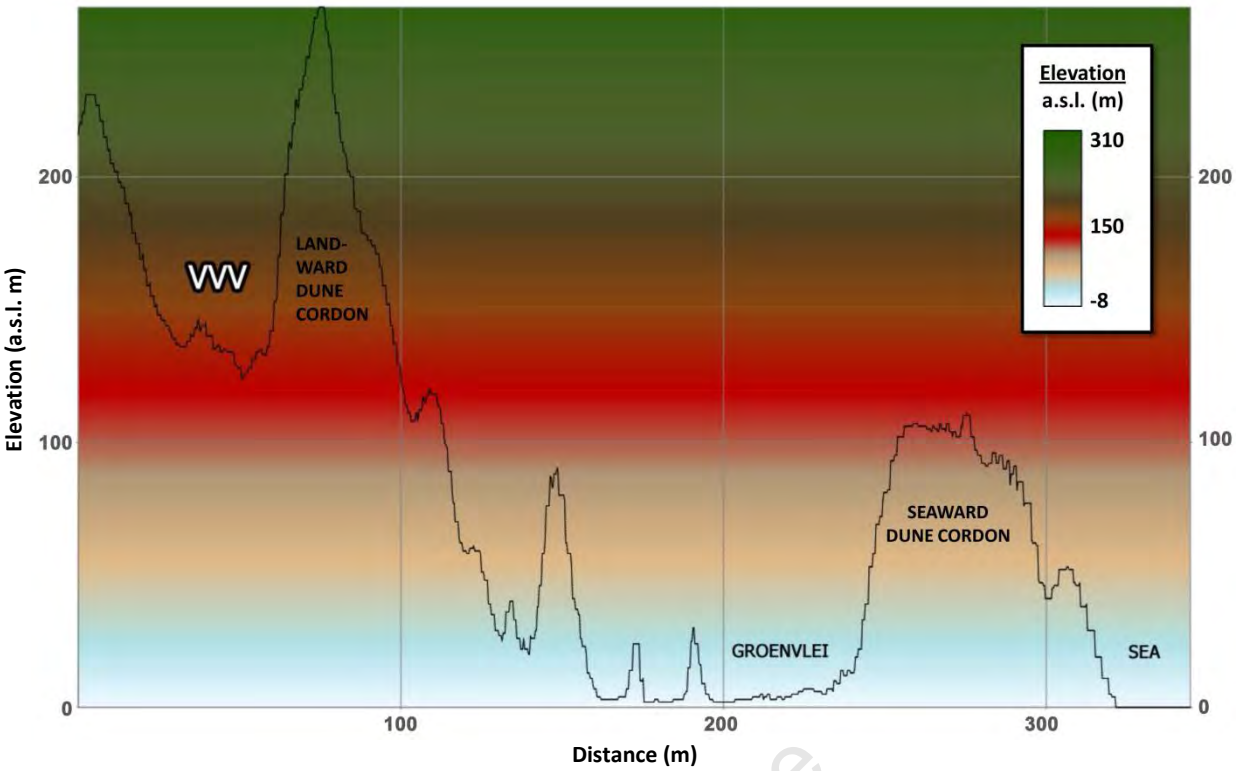

Figure 4.11 A longitudinal profile illustrating the Vankervelvlei (VVV) basin in relation to some of the major geomorphological features in the area [data source: SRTM digital elevation model].

There is no open water currently present as the surface of the wetland is completely covered by a dense mat of Cyperaceous vegetation extending to a depth of roughly two metres below the surface (Irving, 1998; Figure 4.12). The vegetation mat is well established, densely fibrous and able to support substantial weight. This was verified during various fieldwork campaigns in 1992, 1996, 2009 and 2010 where the mat was able to support a number of field workers together with several hundred kilograms of vibracoring equipment.

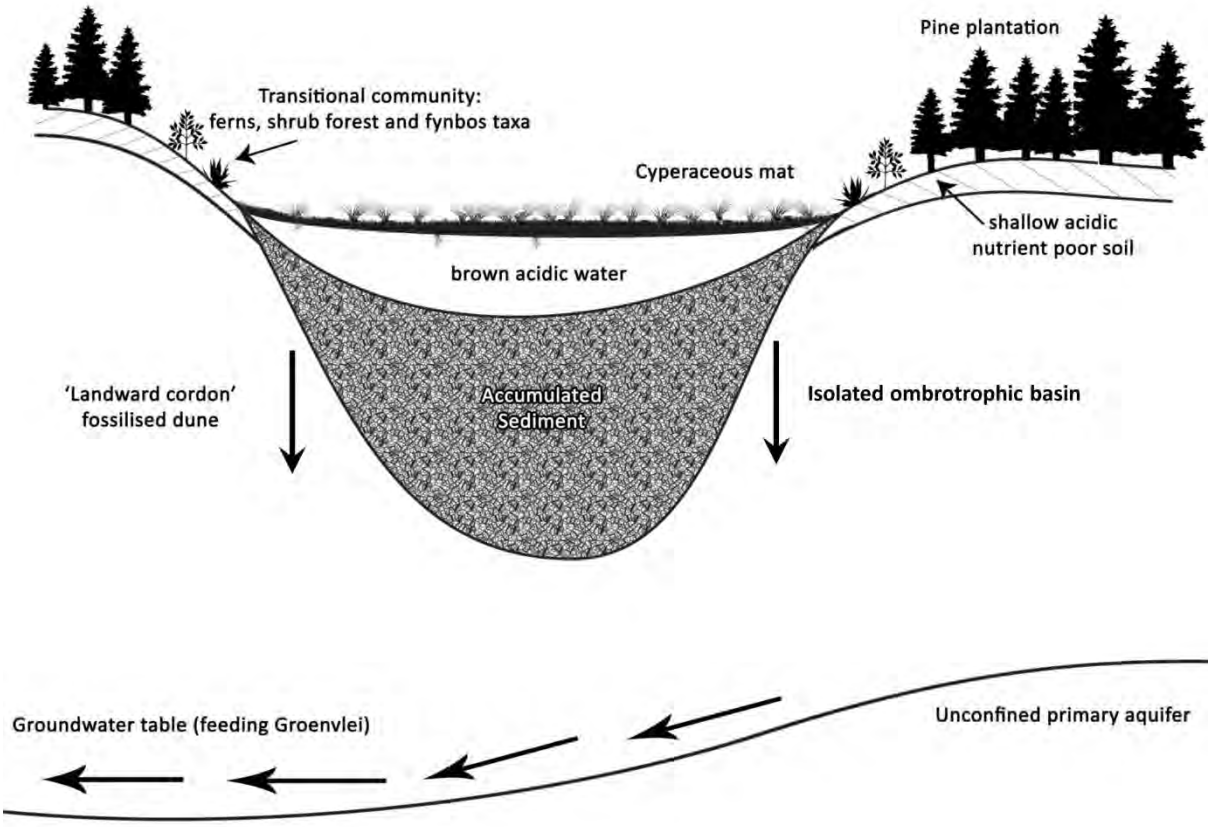

Figure 4.12 A schematic representation of the Vankervelsvlei basin.

Roets et al. (2008) proposed that a hydrological link between Vankervelsvlei and Groenvlei existed, with both water bodies being recharged through the Table Mountain Group Aquifer. Parsons (2009) convincingly refuted the Roets et al. (2008) theory, asserting that the available topographical, geological, geohydrological and hydrochemical data provides no evidence in support of their model. Therefore it appears that Vankervelsvlei is an ombrotrophic system with no surface inflows or outlets and is fed exclusively by rainfall. As it is situated in the YRZ the wetland is continually recharged.

Vankervelsvlei most probably originated as an open water near-coastal back barrier lake formed behind the Landward barrier at some point after the dune cordon's stabilisation within MIS 9 – MIS 7 and persisted as a doline in response to solution of interstitial calcium carbonate (Irving and Meadows, 1997). The depression filled up over time with the accumulation of organic material and variations in the amount and type of aquatic vegetation growing in and around the water body. Irving and Meadows (1997) propose that the floating mat of vegetation covered the catchment

about 3 cal kBP. Hydroseral succession from open lake to ombrotrophic bog was probably driven by changes in climate and or sea level together with changes in local environmental/sedimentological processes and groundwater recharge.

Climate

Vankervelsvlei receives rainfall throughout the year and has a total average amount of 906 mm a^{-1} (based on the Knysna station data), which is considerably higher than the values for Pearly Beach and Still Bay (Climate Systems Analysis Group, 2012). In general, south westerly winds predominate in the region.

Temperatures are generally uniformly mild (annual averages between 13 - 20°C) throughout the year with few extreme maximum temperatures (Figure 4.14). However, berg wind conditions which are especially prevalent during the winter months result in anomalously high temperatures. Frost rarely occurs as temperatures are very infrequently below 4°C. Snow can occur, although it is restricted to high peaks over 1000 m a.s.l. (van Daalen, 1980).

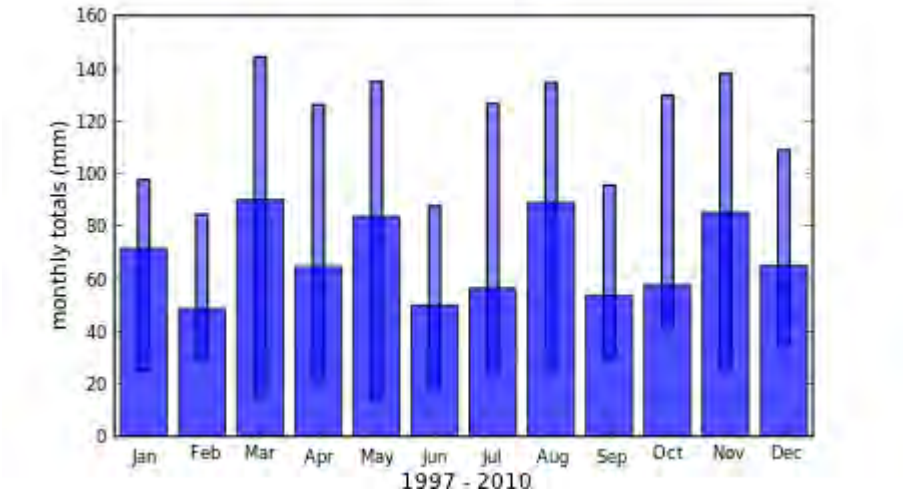

Figure 4.13 The annual cycle of monthly rainfall (mm) for Knysna. Wide bars indicate the median monthly rainfall for the climate period. Narrow bars indicate the 10th to 90th percentile range of monthly rainfall for each month during the climate period (Climate Systems Analysis Group, 2012).

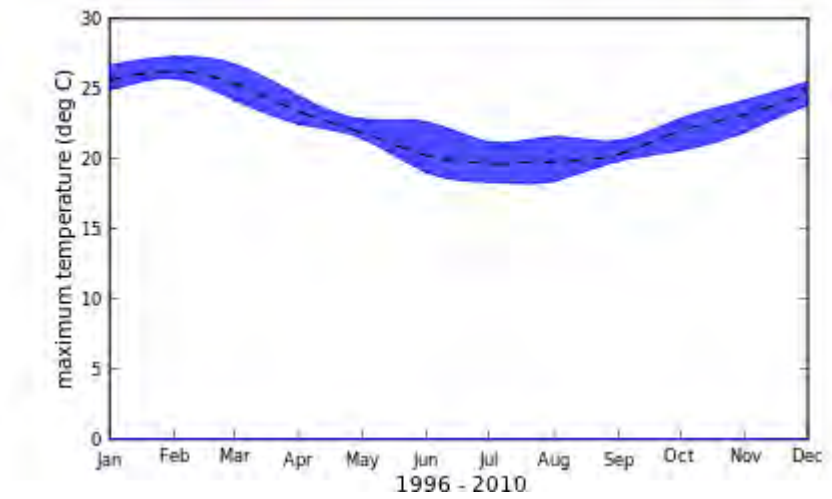

Figure 4.14 The annual cycle of monthly mean maximum daily temperatures for Knysna. The blue envelope represents the 10th percentile to 90th percentile inter-annual range (Climate Systems Analysis Group, 2012).

Contemporary vegetation

The steep slopes surrounding the catchment are entirely vegetated by exotic pine trees (*Pinus*) as part of the P.G. Bison plantation. Along the margins of the vlei are fynbos-dominated pioneer communities including the species of *Passerina, Erica, Leucadendron* and restios. Scrub forest elements such as *Cassine, Euclea and Kiggelaria* are present within the transitional areas between the pine plantations and the wetland. As mentioned above, the wetland is entirely covered by a floating vegetation mat predominantly consisting mainly of Cyperaceae with some Pteridophytes (ferns) and Bryophytes (mosses).

Beyond the catchment, Knysna Sand Fynbos inhabits the stretch of coastal flats to the north of the Wilderness lakes to the Knysna lagoon region, however more than 70% of this vegetation unit has been transformed into pine and gum plantations, cultivated land and urban sprawl (Mucina and Rutherford, 2006). Therefore this unit has been poorly researched. The patches that do remain consist of dense, moderately tall microphyllous shrublands. Important shrubs taxa include: *Cliffortia linearifolia, Leucadendron eucalyptifolium, Metalasia densa, Passerina corymbosa, Anthospermum aethiopicum, Berzilia intermedia, Clutia rubicaulis, Erica diaphana, E. glandulosa* subsp. *fourcadei, E. glumiflora, E. sessiliflora, Helychrysum aspermum, Muraltia squarrosa, Protea cynaroides* and *Stoebe plumosa*.

Southern Cape Dune Fynbos is found south of the N2 road to the coast, on the coastal dune cordons and is characterised by sclerophyllous shrubs with a rich restio undergrowth. The dominant shrubs include *Olea exasperata*, *Phylica litoralis* and a variety of *Rhus* species with *Ischyrolepis eleocharis*

being the most prominent restioid feature. Thicket taxa such as *Pterocelastrus tricuspidatus, Rhus lucida* and *Sideroxylon inerme* have recently (last 100 years) invaded the fynbos shrubs on these dunes.

Patches of Southern Afrotemperate Forest can be found to the north of Vankervelsvlei and within the Goukamma River kloofs (Mucina and Rutherford, 2006). This unit is discussed in section 2.6.2.2. Small patches of South Outeniqua Sandstone Fynbos are also found north and northeast of the site and is characterised by tall open to medium dense shrubland with medium dense, medium tall shrub understorey (Mucina and Rutherford, 2006).

Garden Route Shale Fynbos is found in the Karatara and Rheenendal areas and like the previous unit, represents the interface between fynbos, scrub forest and true afrotemperate forest. These patches are structurally defined as tall dense proteoid and ericaceous fynbos. *Virgilia oroboides* is prominent at the actual boundary between forest and fynbos.

4.7 Sample analyses

4.7.1 Pollen analysis

Pollen analysis, also referred to as palynology, is the study of the structure and formation of pollen grains and spores as well as their dispersal and their preservation under certain environmental conditions (Moore et al., 1991). The first true Quaternary palynological research was published by Lennart von Post in 1916 using pollen from Swedish peatlands to infer climatic changes (Manten, 1967; Jansonius and McGregor, 1996; Bennett and Willis, 2001). Palynology still remains the principal method available to determine the responses of vegetation to environmental change over various spatial and temporal scales (Faegri and Iversen, 1989; Bennett and Willis, 2001).

It is one of the most widely used techniques for the reconstruction of Quaternary environments (Birks, 1981; Faegri and Iversen, 1989; Moore et al., 1991; Lowe and Walker, 1997; Williams et al., 1998; Chambers, 2002). Fossil pollen data are used for a variety of Quaternary applications including geochronology, biostratigraphy, palaeoecology, palaeoclimatology and archaeology (Traverse, 2008). It is also a powerful tool for more applied fields such as forest management, nature conservation and ecosystem restoration as the pollen record is able to disentangle long-term natural variability from the impact of human activities on the landscape (Birks, 1996; Bennett and Willis, 2001; Seppa and Bennett, 2003; Willis and Birks, 2006; Willis et al., 2007).

The diverse range of studies mentioned above is possible because of the extraordinary preservation characteristics of the outer layer of the pollen grain, the exine. The exine consists of material called sporopollenin, which is resistant to microbial decay, "possibly the most inert organic compound known" (Traverse, 2008: 59). This outer layer preserves pollen grains in ancient deposits and sediments when almost all other organic materials are reduced to unrecognisable components (Lowe and Walker, 1997). A second important trait of pollen grains is the distinct identifiable variations in the sculpting of the exine (Moore et al., 1991). These two characteristics of pollen grains *viz.* the preservation and sculpting of the exine make it possible to use palynology as a powerful empirical tool to reconstruct vegetation histories.

The reliability of palynology as a palaeoenvironmental tool is a function of:

- the robust preservation of pollen grains and their resistance to decay,
- the wide dispersal of pollen grains and their presence in a broad range of environments such as lakes, peat deposits, soils, colluvium, alluvium, estuarine deposits, ocean floor and faecal material,
- the abundant production of pollen grains,
- the relative ease of identification as a result of the distinctive structural patterning of the exine,
- and the direct link between the identification of pollen grains and the parent plant (Faegri and Iversen, 1989; Moore et al., 1991).

Pollen grains are viewed under the light microscope and their correct identification hinges on discriminating between various structural types and sculpting types of the exine and, less reliable but sometimes indicative, features such as shape and size (Chambers, 2002). Preparation of samples for mounting on microscope slides is performed in the laboratory (refer to the subsection 4.7.1.2).

For this study, the application of pollen analysis to the selected southern Cape sediment cores makes it possible to infer the compositional changes in plant communities and, through this, palaeoenvironmental reconstructions of the prevailing conditions over the period of accumulations were produced.

Incorporation into sediment deposits: mechanisms and source areas

Pollen is incorporated in vlei sediments through a range of mechanisms e.g. pollen rain, surface runoff, soils of the catchment and locally growing aquatic plants (Delcourt and Delcourt, 1991;

Moore et al., 1991; Figure 4.15). However pollen rain, that is pollen brought to the site through atmospheric transport predominantly from above the tree canopy, generally outweighs the other sources in terms of its relative contribution to the overall pollen estimation (Jackson, 1990)[15].

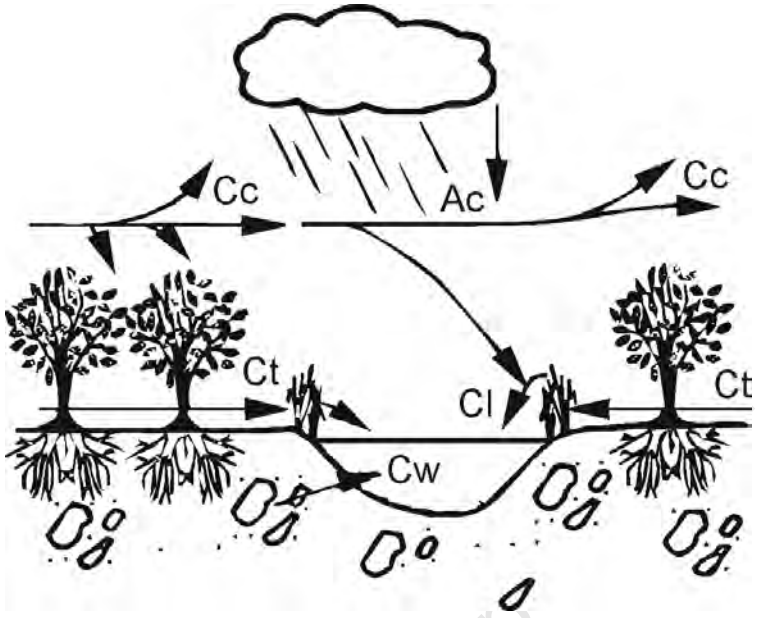

Figure 4.15 Sources of pollen deposited in a vlei: Cc – canopy transported component, Ac – atmospheric component ('pollen rain'), Cl – local wetland component, Ct – trunk space transported component and Cw – water transported component (including discharge through soils) [redrawn from McDonald (1996) which was after Moore et al. (1991)].

Sediment deposits from vleis record both regional and local pollen signals. Both of which are important as they provide different lines of evidence: past hydrological conditions can be inferred from the local aquatic pollen signal whereas the regional signal can provide insight about the surrounding vegetation communities.

Features such as catchment size and shape, topography and geology influence the specific nature of pollen influx and sedimentation (Moore et al., 1991; Hjelle and Sugita, 2011). Consequently, the relative contribution of regional and local pollen within a sediment core is related to the size and nature of the individual wetland catchment (Jackson, 1990; Delcourt and Delcourt, 1991). Various theoretical (largely model simulations) and empirical investigations have been undertaken to determine the influence of catchment sizes on pollen source area (e.g. Prentice, 1985; Jackson, 1990; Sugita, 1993, 1994; Sugita et al., 1999; Bunting et al., 2004; Sugita, 2007b, a). From these studies it appears that in general, small catchments have smaller pollen source areas and higher pollen abundance than larger catchments with local pollen signals often overrepresented in small

[15] However in some cases, the local wetland component can dominant a pollen sequence e.g. reed mats.

basins (Seppa and Bennett, 2003). Models quantifying this relationship have certainly enhanced the vegetation reconstructions; however empirical studies have indicated significant inconsistencies and deviations from these model simulations mostly relating to pollen dispersal characteristics and the complex nature of real ecosystem dynamics (Jackson and Kearsley, 1998; Seppa and Bennett, 2003).

Careful examination of the specific contemporary environment of the selected wetland sites is therefore necessary before accurate inferences of vegetation dynamics can be made using fossil pollen data.

Overcoming palynological limitations

General palynological shortcomings including difficulty of identifying pollen to genus and species levels, the inherent differential production and dispersal (e.g. the differences between wind and insect pollination), as well as differences in accumulation and preservation of pollen types need to be taken into account when interpreting pollen evidence. Great emphasis should be placed on the careful evaluation of the spatial representation of both pollen records as well as individual taxa. In addition, it is critical to determine the relationships between modern vegetation changes, their causal factors and their relation to the pollen record. This together with the application of the "indicator approach" can minimise the impact of the more intrinsic limitations of the technique listed above.

It has been established that a combination of a few prominent "indicator" taxa can be characteristic of certain vegetation types and environmental conditions (Meadows and Sugden, 1991; Scott and Cooremans, 1992). The so-called indicator approach therefore uses the presence (or absence) of indicator taxa, whose modern ecological tolerances are well understood as a basis for reconstructing palaeoenvironments (Birks, 1981, 1980, Birks and Birks, 2005, Birks, 2005). This approach assumes that the limiting conditions in the past were the same as they are today, an assumption which most probably holds for the time period in question (i.e. the late Pleistocene and Holocene periods).

To identify the ecological controls and main climate dependencies of specific indicator taxa bioclimatic modelling is used. Predictive modelling of species environmental requirements and their geographic distributions using maximum entropy techniques within the programme *MaxEnt* (Phillips et al., 2006) and GIS taxa-climate analyses was used to determine the specific ecological constraints of the selected indicator pollen taxa.

Cognisance of the general limitations to the method, application of the approaches outlined above together with the incorporation of other palaeoecological and sedimentological analyses (detailed below) has produced robust palaeoenvironmental reconstructions for the three sites in question.

4.7.1.1 Subsampling

Subsampling interval and subsample size was dependent on stratigraphic complexity and the degree of precision required for change detection. Subsampling was initially done at a coarse resolution (~10 cm), and then if changes were evident more directed subsampling at finer resolutions (2 to 5 cm) were performed (Moore et al, 1991). Sections for subsampling were cleaned and a scalpel was used to extract subsamples, all cuts were made in a direction horizontal to the axis of the core to avoid contamination at any given level of sediment with material from a position above or below its own (Moore et al., 1991). Care was taken to avoid subsampling sections in contact with the aluminium tubes. Subsamples for microfossil analysis were placed in air-tight plastic vials ready for chemical treatment (section 4.7.1.2).

4.7.1.2 Laboratory procedures and chemical treatment

The extraction of palynomorphs from sediment subsamples follows standard palynological methods aimed at the concentration of pollen grains and the removal, disintegration and dissolution of the non-pollen matrix (Moore et al., 1991) with specific adaptations for dense media separation from Nakagawa et al. (1998). Pollen is extracted from samples through 30% HCl treatment to remove carbonates followed by 10% KOH digestion to disaggregate the samples and remove humic acids. Following this, heavy liquid mineral separation using $ZnCl_2$ at a specific gravity of 1.88 is used to separate the pollen grains from the mineral fraction (Faegri and Iversen, 1989; Moore et al., 1991; Nakagawa et al., 1998). For samples with a high clay content, HF treatment was used to remove all siliceous material. Finally, all samples were acetolysised and mounted in *Aquatex* (aqueous mounting agent). Three slides were produced per sample. Figure 4.16 provides a summarised flow chart of the steps involved whereas the detailed laboratory procedure can be found in Appendix A.

To determine absolute counts and pollen concentrations, *Lycopodium* spores are added (Stockmarr, 1973). These spores are added prior to physical and chemical processing so as to ensure even losses amongst fossil and exotic grains during processing.

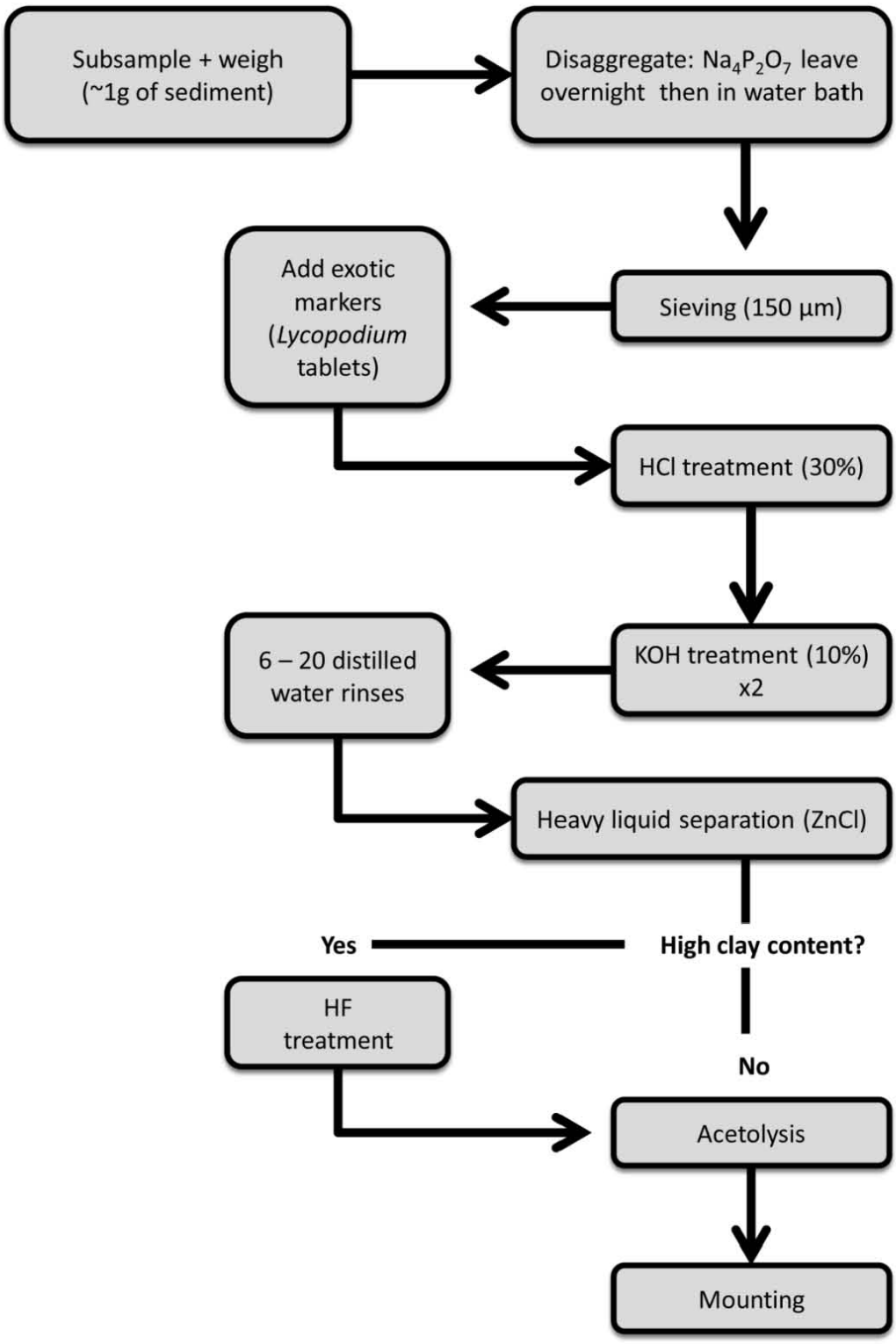

Figure 4.16 A flow chart of the pollen analysis laboratory procedure employed for this study.

4.7.1.3 Counting and identification

As pollen counts are only samples of the overall amount of pollen under consideration, there are statistical uncertainties inherent within them (Bennett and Willis, 2001). These uncertainties are reduced with greater pollen counts. Pollen counting is particularly time consuming therefore a balance needs to be established between time spent and the level of uncertainty. Counts of between 250 and 350 pollen grains have routinely been conducted and deemed statistically significant for various studies in South Africa (e.g. Scott, 1987; Scott, 1994; Meadows et al., 1996; Meadows and Baxter, 2001; Scott and Nyakale, 2002). Bennett and Willis (2001) recommend that to reduce errors sufficiently, counting should be to a minimum of 300 grains with ideal count size being 500 grains.

Therefore pollen counts of 500 grains per sample were carried out using a *Zeiss Axiostar Plus* microscope at a magnification of 400x for routine identification and 1000x for specific identification. Spores and other non-pollen palynomorphs were also counted but not included in the total pollen sum. When pollen concentrations were very low, counting was discontinued after scanning and counting all traverses from 3 slides for an individual sampling level.

Identification of pollen taxa was made possible using the Cape Town Collection of Pollen reference slide, photograph and key card collection housed in the department of Environmental and Geographical Science at the University of Cape Town as well as van Zinderen-Bakker's reference book collection (van Zinderen Bakker, 1953, 1956; van Zinderen Bakker and Coetzee, 1959; Welman and Kuhn, 1970) and Scott (1982). The computer software *Polycounter* version 2.5.3 (Nakagawa, 2007) was used to increase the efficiency of the counting procedure.

4.7.1.4 Data representation and analysis

The results of the pollen and charcoal analyses for each site are presented graphically in the form of standard pollen diagrams using the *Psimpoll* software package version 4.27 (Bennett, 1993 - 2009), within which the data can be plotted against stratigraphic layer (Troels-Smith lithology), depth and calibrated radiocarbon ages. CONISS (Constrained Incremental Sum of Squares) (with square root transformation) was used in *Psimpoll* to divide each data set into pollen assemblage zones (Grimm, 1987).

Various multivariate numerical techniques have been use over the last few decades to display, summarise and interpret pollen data. To reduce multidimensional pollen data to lower dimensions

and reveal the underlying structure within the data, ordination techniques such as principal component analysis (PCA), correspondence analysis (CA) and detrended correspondence analysis (DCA) have been applied (e.g. Birks 1986; Prentice 1978, 1980, Anderson, 1992, Seppa, 1996). For testing and identifying specific factors influencing the variation in pollen data, constrained ordination approaches of redundancy analysis and canonical correspondence analysis have been used (e.g. Odgaard, 1992; Lotter and Birks 1993, Odgaard and Rasmussne 2000, Nielsen and Odgaard 2004). Detailed reviews of palaeoecological (including palynological) data analysis techniques are found in various works by Birks (e.g. 1986, 1992, 1995, 1998, Birks and Birks, 1980).

For this study, a DCA was initially performed on each pollen dataset in the programme *CANOCO* for Windows (version 4.51) and *CanoDraw* for Windows (version 4.1) (ter Braak and Smilauer, 1997). This was to calculate the length of the environmental gradient in order to determine the most appropriate ordination technique *viz.* unimodal or linear. If the DCA results revealed gradient lengths below 3, a PCA was then carried out, following the recommendation by Leps and Smilauer (2003). If gradient lengths were long (greater than 4) then the data are considered too heterogeneous with too many taxa deviating from the assumed model of linear response; in such cases, therefore, unimodal methods such as DCA, CA or CCA are deemed most appropriate (Leps and Smilauer, 2003).

4.7.2 Microscopic charcoal analysis

Charcoal or charred particles are carbon derived products from the incomplete combustion of plant material and can be easily preserved with the fossil record as it is resistant to oxidation and microbial decay (Patterson et al., 1987; Scott and Damblon, 2010; Mooney and Tinner, 2011). Microscopic charcoal analysis was originally developed as a means to rapidly identify and count charcoal fragments as the use of thin sections prepared from charcoal from archaeological deposits was deemed too time consuming (Figueiral and Mosbrugger, 2000). The method has since been used in a wide array of studies from ecosystem changes to biomass burning and its influence on global carbon cycles (Tinner and Hu, 2003; Daniau et al., 2012). The quantification of the accumulation of microscopic charcoal fragments (<100 µm in length) preserved in lake sediments and other palaeoecological archives is commonly used to investigate the occurrence and nature of past fires (Clark, 1984; Patterson et al., 1987; Tinner et al., 1999; Tinner and Hu, 2003; Sadori and Giardini, 2007; Conedera et al., 2009; Mooney and Tinner, 2011). As fire plays an integral role in fynbos ecology (Cowling, 1992), the combination of charcoal and pollen analyses holds great

potential for the elucidation of the relationships between fire regimes, vegetation changes and climate.

Microscopic charcoal particles are incorporated into sedimentary deposits in a similar manner to pollen grains *viz.* aeolian transport and saltation. Charcoal that is preserved in sediments reflects a combination of different scales of fire source areas including local (within watershed), extra-local (just outside watershed), regional and extra-regional (continental or even global) (Clark, 1988; Morrison, 1994; Conedera et al., 2009). However a range of studies reviewed in Conedera et al. (2009) suggest that microscopic charcoal is most likely derived from sources within 20 – 100 km radii of the site, with lake environments holding the potential for greater charcoal source areas in comparison to small peat bogs (Mooney and Tinner, 2011). Due to the degree of uncertainty inherent in charcoal analysis, which is predominantly the result of limited research into charcoal size dynamics and transport mechanisms, there are a number of key assumptions that underlie the interpretation of microscopic charcoal analysis data:

- Charcoal peaks are considered to be above background values of charcoal concentrations.
- Primary dispersal of charcoal occurring during or soon after the fire event contributes to the majority of microscopic charcoal found in sedimentary deposits (as opposed to secondary dispersal such as run-off).
- Large particles are considered to represent local fires as they are not transported long distances, whereas smaller particles are able to travel extensive distances away from the source of the fire.
- Microscopic charcoal fragments are a reliable source to interpret past fires regimes.

The laboratory preparation and chemical treatments employed for the extraction of pollen (section 3.7.1.2) also preserves charcoal, making it possible to count charcoal particles and pollen grains simultaneously. Tinner and Hu (2003) investigate two methods of quantifying charcoal presence in sediments and concluded that both methods (area measurements and particle counts) produced similar trends. Therefore the particle count technique was used as it represents the fastest and most reliable method (Tinner and Hu, 2003). Charcoal particles were identified and counted on all microscope slides produced. Only particles that were black, opaque and angular were considered charcoal fragments (Patterson et al., 1987; Mooney and Tinner, 2011). Charcoal fragments were classified and counted according to three size groups based on the longest axis of each fragment; 10 – 50 µm, 50 – 100 µm and >100 µm. Particles less than >75 μm^2 (or ~ 10 µm long) were not counted due to the risk of false identification as they may be mistaken for other objects such as pyrite or

plant material (Mooney and Tinner, 2011). Absolute charcoal abundances were calculated in the same manner as pollen concentrations using exotic *Lycopodium* spores (Stockmarr, 1973).

4.7.3 Sedimentological analysis

Particle size distributions are used to indicate the composition of sediments and can, under some circumstances, provide information on the nature of the environments within which the sediments were deposited or formed. However, direct interpretations of hydrological and depositional environments from particle size data are often not very useful and can be fairly ambiguous (Teller and Last, 1990b; Last, 2001). Therefore it is best to use particle size distributions more as descriptive measures and not as interpretative ones.

Particle size analysis for the Pearly Beach and Vankervelsvlei cores[16] were conducted at the Department of Geography, Friedrich-Schiller-University, Jena, Germany. Subsamples of ~5 g were pre-treated to remove organic material by adding 5 ml of 10% hydrogen peroxide (H_2O_2) left overnight then shaken in a water bath at 80^0C for two hours. This procedure was repeated using 30% H_2O_2. To remove carbonates, 5 ml of 10% hydrochloric acid (HCl) was added followed by 5 ml sodium pyrophosphate ($Na_4P_2O_7$) used as a deflocculant agent.

After pre-treatment, the particle size distributions were detected using a *Beckman Coulter LS 13 320 Laser Diffraction Particle Size Analyzer*, the single wavelength Aqueous Liquid Module (ALM). This model can measure grains in the range of 0.375 - 2000 µm. The LS 13 320 software package presents the results (three runs per sample) and calculates statistical properties for the distributions including mean and median grain size, sorting, kurtosis and skewness.

Laser diffraction particle size analysis was chosen as the most accurate and efficient means to measure the grain size distributions as there are many advantages of using this technique instead of the more traditional sieve-pipette methods. These advantages include: the ability to measure a wide range of grain sizes including clay and silt fractions, smaller amounts of sediment are required (0.5 – 5 grams *vs.* > 10 grams for the sieving method) and laboratory efficiency and the rapidity of measurement (runs take 60 seconds) makes it possible to produce multiple measurements for individual samples (Konert and Vandenberghe, 1997; Beuselinck et al., 1998).

Laser diffraction size analysis is based on the forward scattering of monochromatic light and determines the grain size of a particular particle as a function of the cross-sectional area of that

[16] The particle size analysis for the Rietvlei Still Bay core was conducted by Dr. A.S. Carr at the University of Leicester's Geography department and followed a similar methodological approach.

particle. Therefore the results can be affected by variations in particle mineralogy and morphology. For this reason, it has been reported that laser diffraction may underestimate the clay fraction (>2 μm) in comparison to measurements from sieving methods (Beuselinck et al., 1998; Di Stefano et al., 2010). However it still remains a far superior technique in relation to classic sieve, pipette and sedimentation methods.

4.7.4 Geochemical analysis

The analysis of 'bulk[17]' geochemical variables such as Total Organic Carbon (TOC), elemental TOC/TN ratios and stable carbon isotopes ($\delta^{13}C$) can be used to ascertain the sources of organic matter (OM) contained within sediments. As both production and preservation of OM are affected by environmental change, these geochemical variables can also assist in the understanding of palaeoenvironmental conditions (Meyers, 1997). Bulk identifiers of OM origins represent an integrated signal of all the OM components within the sediments which can prove to be beneficial, however it also has the potential to be misleading as soil forming processes can be complex.

4.7.4.1 Total organic carbon

The concentration of TOC is a generic measure of overall organic content in sediments. It represents the fraction of OM that escaped re-mineralization during sedimentation and integrates the different origins of OM, delivery routes, depositional processes and amount of preservation (Meyers, 2003).

TOC is determined by weight ratios and is therefore affected by the particle size composition and nature of sediments (Meyers, 2003). The addition of a pre-treatment step to remove carbonates minimises the risk of TOC concentrations by the dissolution of carbonate minerals in sediments.

4.7.4.2 Stable carbon isotopes

Isotopes are naturally occurring forms of the same chemical element that differ in the number of neutrons in their nucleus. Stable isotopes are isotopes that do not undergo radioactive decay. Stable isotopes of the same element have the same chemical characteristics. The mass differences ('heaviness') of isotopes, a result of the difference in the number of neutrons in the nucleus, affect

[17] Bulk refers to measurements utilising the entire sediment sample, instead of isolating specific size fractions or compounds.

reaction rates and bond energies. These differences result in partial separation of the light isotopes from the heavy ones during chemical reactions, a process known as isotope fractionation (or isotopic discrimination). As a consequence of the fractionation process, substances often develop unique isotopic compositions or signatures (ratios of heavy to light isotopes) that may be indicative of the nature and source of the substance or of the processes that formed it (Dawson and Brooks, 2001). Stable isotope analyses have been successfully applied in a wide variety of botanical, plant physiological, archaeological and ecological studies (West et al., 2006).

Stable isotopes are expressed as 'δ' values in parts 'per mil' (‰) enrichments or depletions relative to a standard of known composition (the PDB marine limestone for carbon and atmospheric (AIR) N, for nitrogen) (Fry, 2006). δ values are calculated by the following generalized equation:

$$\delta\ (‰) = \left(\frac{R_{sample}}{R_{standard}} - 1\right) * 1000$$

where "R" is the ratio of the heavy to light isotope in the sample or standard.

A positive δ value means that the sample contains more of the heavy isotope compared to the standard, known as an 'enriched' signal, while a negative δ value means that the sample contains less of the heavy isotope than the standard, therefore a 'depleted' signal (Dawson and Brooks, 2001).

The isotopic ratio of an element in a system not only reflects the source ratio of the element, but also any fractionation that may occur within the system or across its boundaries. These stable isotope ratios act as recorders or tracers in biotic and abiotic molecules, as δ values provide specific isotopic signatures that can be used to "…trace the movements of nutrients, particles and organisms across landscapes and between components of the biosphere, and to reconstruct aspects of dietary, ecological and environmental histories" (West et al., 2006: 408).

Stable carbon isotopic signatures of vegetation

The stable carbon isotopes ^{12}C and ^{13}C are unevenly distributed among and within different components of ecosystems. The distribution of these isotopes can reveal information about the physical, chemical and metabolic processes involved in carbon fractionations (Farquhar et al., 1989a; Farquhar et al., 1989b).

Stable carbon fractionation is well documented in plants (Smith, 1972) and is a result of the photosynthetic process, which is dictated by the pattern of photosynthesis in which the plant species is engaging (O'Leary, 1981; Farquhar et al., 1989a; Cerling et al., 1991; Dawson and Brooks, 2001). The stable carbon isotope compositions of terrestrial, marine and freshwater plants are distinctly different because they assimilate their carbon from different sources (Mackie et al., 2005).

Terrestrial plants use either C_3 (Calvin), C_4 (Hatch-Slack) or CAM (Crassulacean acid metabolism) photosynthetic pathways, which all have different mechanisms of processing atmospheric CO_2 and consequently have different $\delta^{13}C$ values (Smith and Epstein, 1971) (Table 4-3). During photosynthesis, C_3 plants form a three carbon molecule, while C_4 and CAM plants form a four carbon molecule (Smith, 1972). In high temperature or strong sunlight conditions or periods of lower CO_2 concentrations, C_4 and CAM plants are photosynthetically more efficient than C_3. C_3 plants include trees, shrubs and temperate grasses whereas tropical grasses are C_4 species. CAM plants are mostly succulents. In southern Africa, C_3 plants are more abundant in the WRZ (and at high elevations e.g. the Drakensberg Mountains) and include fynbos, while C_4 grasses are more common in the YRZ (Vogel et al., 1978; Scott, 2002; Stock et al., 2004; Cordova, 2013).

Terrestrial plants are depleted in ^{13}C relative to their carbon source, the atmosphere and the $\delta^{13}C$ standard - PBD (Park and Epstein, 1961). During photosynthesis, plants discriminate against ^{13}C and preferentially fix more ^{12}C CO_2 (Park and Epstein, 1961). The average $\delta^{13}C$ value of C_3 plants is approximately -27 ‰ and the average $\delta^{13}C$ value of C_4 plants is about -13 ‰ (O'Leary, 1981; Sternberg and DeNiro, 1983; Ehleringer et al., 1997; Ehleringer and Cerling, 2001)(Table 4-3).

CAM plants have $\delta^{13}C$ values varying between C_3 to C_4 values: 'obligate' CAM plants, which operate by fixing CO_2 at night, have $\delta^{13}C$ values similar to C_4 plants (Pate, 2001). Whereas, 'facultative' CAM plants – species that can shift between C_3 and CAM type photosynthesis depending on the conditions – have $\delta^{13}C$ values similar to C_3 plants when under well-watered conditions but under dry or saline environments they have values resembling C_4 plants (Farquhar et al., 1989a; Pate, 2001).

Plants inhabiting marine environments utilise marine dissolved inorganic carbon (from dissolved bicarbonate) and bulk organic matter from marine sediments have enriched $\delta^{13}C$ values ranging from -19 ‰ to -22 ‰ (Meyers, 1997; Mackie et al., 2005). Whereas, freshwater aquatic plants utilise dissolved CO_2 and therefore have more depleted $\delta^{13}C$ values (full range -10‰ to -50‰ , average of -27‰ (Mackie et al., 2005 and references therein)and can be indistinguishable from terrestrial $\delta^{13}C$ signatures (Meyers, 1994, 1997). The assessment of C/N ratios (discussed in the next subsection) in

conjunction with $\delta^{13}C$ values allows better discrimination between freshwater aquatic and terrestrial plant sources of OM (Figure 4.17).

Table 4-3 Summary of principal differences in carbon isotope discrimination and water-use efficiency (Pate, 2001; Mackie et al., 2005; Lamb et al., 2006).

	$\delta^{13}C$ (‰) range	$\delta^{13}C$ (‰) average	WUE (mL H2O transpired per g dry matter gain)	Characteristics
Freshwater algae^	-26 to -30	-27		
Aquatic plants	-10 to -50	-27		Utilise dissolved CO_2 (or bicarbonate)
C_3 plants (e.g. fynbos)	-20 to -32‰	-27	400 – 600	Use Calvin Cycle with Rubisco* to fix CO2 in leaf. Perform best at moderate temperatures and light intensities.
C_4 plants (e.g. tropical grasses)	-9‰ to -14‰	-13	200 – 300	Use PEP carboxylase to fix CO_2 in leaf. More efficient water users than C_3 plants especially at high temperatures.
CAM/C3 plants (e.g. succulents)	Same as C4 plants when operating in CAM mode and close to C3 plants when in C3 mode		50 (when in CAM mode)	Fix CO2 at night using PEP carboxylase. Succulent and very slow growing in CAM mode. Can convert to C3 when water is available and/ salinity is reduced.

***Rubisco = ribulose-1,5-bisphosphate carboxylase/oxygenase**
^In a C_3-dominated environment

Plant carbon isotope signatures are also influenced by water-use efficiency[18] (WUE) (Farquhar and Richards, 1984). Plants can optimise the trade-off between gaining carbon and losing water by controlling leaf stomatal aperture. In general, water-stressed plants have smaller/closed stomatal openings, retain water well and have a high WUE resulting in enriched $\delta^{13}C$ values (Farquhar et al., 1989b; Fry, 2006). More depleted $\delta^{13}C$ values are associated with plants with larger stomatal openings and poorer WUE, often indicating ample water supplies (Farquhar and Richards, 1984; Farquhar et al., 1989b; Fry, 2006).

[18] WUE: the efficiency with which plant dry matter is laid down relative to amounts of water which the plant transpires – measured in terms of water transpired per unit dry matter gain (Pate, 2001).

Carbon isotopic composition of C_3 vegetation has been shown to correlate negatively with rainfall over continental and landscape gradients (Ehleringer and Cooper, 1988; Ehleringer et al., 1992; Stewart et al., 1995; Schulze et al., 1998; Miller et al., 2001). This relationship is principally due to the effect of water availability on ^{13}C discrimination in leaves of C_3 plants (Farquhar et al., 1989a; Farquhar et al., 1989b) which then translates to community and landscape scales (Kaplan et al., 2002). However the relationship between $\delta^{13}C$ and precipitation (or any other measure of water availability) is not constant at the community level (Schnyder et al., 2006). Therefore the $\delta^{13}C$ values from plants have not been found to reliably show any significant direct relationship with environmental factors such as temperature (Smith, 1972) or precipitation (Swap et al., 2004).

Application to core sediments

The carbon isotopic composition of organic matter within bulk sediment samples can be used to infer changes in C_3 and C_4 plant abundances over time and the rate and magnitude of environmental processes (Cerling et al., 1991; Meyers, 2003). Although either differential preservation or mineralization of soil components with different $\delta^{13}C$ values does lead to gradual shifts in soil ^{13}C content (normally slight enrichments), on average there is little fractionation of respired CO_2 and therefore $\delta^{13}C$ values in soil organic matter can reflect plant $\delta^{13}C$ signatures (McPherson et al., 1993; Schwartz et al., 1996; Bowman et al., 2004; Liu et al., 2005; Fry, 2006; Laskar et al., 2010)

The dominance of these vegetation types in the landscape varies as a function of temperature, precipitation and seasonality, and atmospheric CO_2 concentrations (Ehleringer et al., 1997). Therefore the differences in the ecological tolerances between C_3 and C_4 plants can be determined from their carbon isotope signals.

In summary, the $\delta^{13}C$ signal recorded in core sediments can provide a spatially integrated indicator of the changing dominance of either C_3 or C_4 vegetation in the landscape over time. More specifically, $\delta^{13}C$ variations in sediments from a predominately C_3 ecosystem, such as fynbos dominated areas (Vogel, 1978) can signify changes in plant water-use efficiencies.

One limitation of analysing bulk organic matter samples is that it is difficult to determine the spatial scale of the derived isotopic record making it difficult to distinguish whether the signal represents local heterogeneity of vegetation or more widespread shifts in plant community type (Gilson et al 2004; Scott 2002). A further consideration is the potential alteration of the integrated $\delta^{13}C$ signal through the influence of CAM plants.

4.7.4.3 Organic C/N ratios

TOC/TN ratios[19], in conjunction with $\delta^{13}C$ values, are frequently used to distinguish between algal and terrestrial plant origins of organic matter extracted from sedimentary sequences (Meyers, 1994 and references therein ; 1997, 2003; Mackie et al., 2005).

Bacteria and algae have TOC/TN ratios that are distinct from terrestrial vegetation with algae typically having low TOC/TN ratios (between 4 and 10), while terrestrial plants have much higher values (greater than 20) (Meyers, 1994; Lamb et al., 2006; Figure 4.17). The distinction arises because terrestrial plants contain lignin and are cellulose-rich, whereas aquatic plants are protein-rich which increases their nitrogen levels (Meyers, 1994).

TOC/TN ratios can generate misleading indications of organic matter provenance due to the selective degradation of OM components during early diagenesis (Meyers, 1994, 1997). (Sediment diagenesis has little influence on $\delta^{13}C$ in organics (Lamb 2004; Lamb et al., 2006)). Microbial immobilisation of nitrogenous material by bacteria and the remineralisation of carbon can potentially result in lower TOC/TN ratios in soils. However, bacteria contain a high level of labile compounds and decompose more rapidly than terrestrial plants and therefore become a less significant component of bulk organic TOC/TN samples (Lamb et al., 2006). Further, subaqueous sediments appear to not be affected by this phenomenon (Meyers, 1994). Alternatively the preferential degradation of labile nitrogenous compounds could result in higher TOC/TN values (Meyers and Lallier-vergés, 1999; Das et al., 2008). Therefore bulk TOC/TN ratios may reflect both organic matter preservation as well as provenance (Carr et al., 2010a).

[19] Determined from elemental analysis of organic matter.

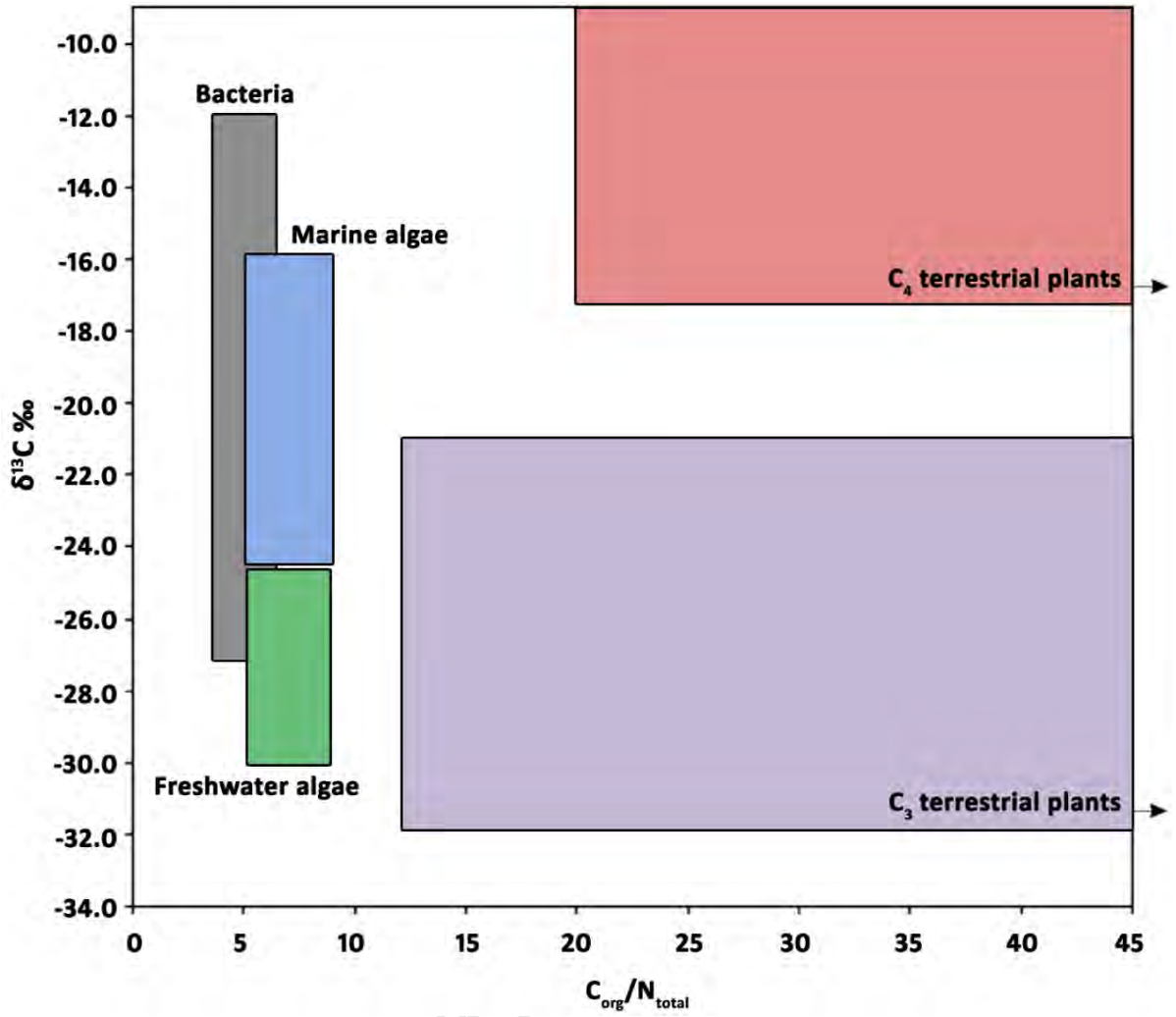

Figure 4.17 The relationship between $\delta^{13}C$ and the C/N ratio (adapted from Mackie et al. 2005; Lamb et al. 2006).

4.7.4.4 Laboratory procedures

Bulk geochemical analyses were performed on subsamples from Pearly Beach 1 and Rietvlei Still Bay 2 by Dr. A.S. Carr at the University of Leicester. TOC, TN and $\delta^{13}C_{TOC}$ were determined using a *SerCon ANCA GSL* elemental analyser interfaced to a *SerCon Hydra 20–20* continuous flow isotope ratio mass spectrometer. For the determination of the TOC and $\delta^{13}C_{TOC}$, samples were pre-treated with 10% HCl to exclude any inorganic carbon potentially derived from carbonate associated with the near-by coastal dune systems. All analyses were carried out in triplicate with a typical precision of ~0.05%.

4.7.5 Establishing chronologies

4.7.5.1 Radiocarbon dating

Radiocarbon dating is the most widely applied dating technique for the Holocene and late Pleistocene periods, providing reliable and accurate temporal controls for palaeoenvironmental studies. It was therefore employed to obtain absolute independent chronologies for the sediment cores in question.

Radiocarbon dating determines ages of carbonaceous materials using the radioisotope Carbon-14. Carbon-14 (^{14}C) is produced in the upper atmosphere mainly as a result of the interaction of cosmic ray neutrons with Nitrogen-14 atoms (Muscheler et al., 2004; Fairbanks et al., 2005). ^{14}C mixes rapidly throughout the atmosphere to form carbon dioxide and enters the global carbon cycle. As it reacts with the Earth's carbon reservoirs (atmosphere, oceans and biosphere) it decays (Fairbanks et al., 2005). Plants and animals assimilate ^{14}C from carbon dioxide or through the food chain. During their lifetimes their ^{14}C content is in equilibrium with the ^{14}C concentration of the atmosphere. However, as soon as a plant or animal dies the metabolic uptake of carbon ceases. Hereafter its ^{14}C content will decrease at a constant rate determined by the law of radioactive decay (Fairbanks et al., 2005; Walker, 2005). In 1949 Willard F. Libby and his colleagues were the first to measure this rate of decay. They determined that ^{14}C decays exponentially through a series of half-lives of 5568 ±30 years, later this was corrected to 5730 ±40 years (Higham, 1999; Walker, 2005; Figure 4.18).

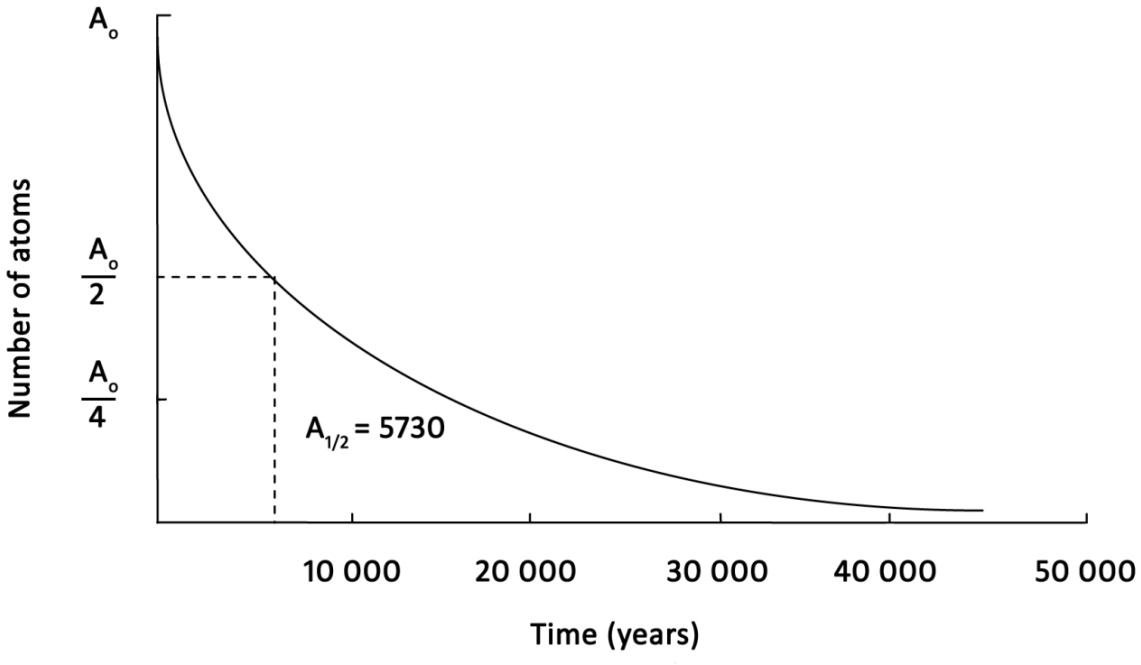

Figure 4.18 The radiocarbon decay curve (adapted from Walker, 2005).

It is therefore possible to calculate age determinations by measuring the ^{14}C concentration or residual radioactivity currently present within a sample, using the rate of ^{14}C decay curve to establish the number of decay events per gram of carbon and comparing this to modern levels of activity (1890 wood corrected to 1950 AD) (Higham, 1999). The limit of measurement using this technique is conventionally around 45 – 50 kBP (eight half-lives), beyond this point other dating techniques must be employed (see section 4.7.5.2) (Walker, 2005).

Two main approaches of radiocarbon measurement exist: beta counting and accelerator mass spectrometry (AMS). Beta counting (either by gas proportional counting or liquid scintillation counting) detects and measures the β emissions from ^{14}C atoms. The rate of emissions reflects the residual level of ^{14}C activity within the sample. Whereas, AMS uses particle accelerators as mass spectrometers to separate the ^{14}C isotopic signal from that of the other isotopes within the sample and is then able to count the relative number of ^{14}C atoms (Walker, 2005). AMS has many advantages when compared to the 'conventional' radiometric techniques. The quantity of material required is substantially smaller (0.1 – 2 mg compared to 0.5 – 2 g), measurement times are reduced (a couple of hours instead of a few days) and it is 1000 – 10 000 times more sensitive than decay counting (Jull and Burr, 2006; Hua, 2009). A further advantage of AMS is that it measures the two stable carbon isotopes – carbon 12 and carbon 13 and can therefore determine $\delta^{13}C$ which is used to

evaluate the level of isotopic fractionation, a potential source of error in ^{14}C analysis. The establishment of AMS techniques has therefore been of great significance to palaeoenvironmental and archaeological research with the increased precision and smaller sample sizes making it possible to continually push the boundaries of this dating technique.

An important consideration is that atmospheric ^{14}C ($\Delta^{14}C$) has not remained constant in the past as it is affected by variations in the geomagnetic field and solar activity as well as major changes within and among the Earth's active carbon reservoirs (Kitagawa and van der Plicht, 1998; Fairbanks et al., 2005; Walker, 2005; Lal and Charles, 2007; Hua, 2009). Modulations in the $\Delta^{14}C$ record appear to be on both short and long time scales; with deep ocean circulation changes and/or solar activity causing significant variations in $\Delta^{14}C$ between 11 – 15 kBP and geomagnetic field fluctuations causing changes over longer times scales (Fairbanks et al., 2005). There is also variation in $\Delta^{14}C$ concentrations between the Northern and Southern Hemispheres. This is the result of the larger expanse of ocean in the Southern Hemisphere compared to the Northern Hemisphere. Differences in the atmosphere-ocean CO_2 exchanges between the hemispheres lead to uneven distributions of ^{14}C in the troposphere (McCormac et al., 2002). This non-constant inter-hemispheric offset is observed when dating terrestrial organic materials in the Southern Hemisphere with the resultant radiocarbon ages usually being older than those in the Northern Hemisphere (McCormac et al., 2002).

As the calculation of conventional ^{14}C ages assumes that the $\Delta^{14}C$ has been constant (Stuiver and Polach, 1977), radiocarbon calibration is essential (Fairbanks et al., 2005; Reimer et al., 2009). Radiocarbon calibration transforms radiocarbon ages to calendar ages and accounts for the variations in $\Delta^{14}C$ over time (Fairbanks et al., 2005). Calibration is a critical step for any study that aims to compare ages from different sites or calculate rates of change. Numerous global and hemispheric calibration curves based on independent absolute data such as tree rings (dated by dendrochronology) or combinations of absolute datasets have been constructed over the last few decades (e.g. Pearson and Stuiver, 1986; Stuiver and Becker, 1993; Stuiver, 1998; McCormac et al., 2004; Reimer et al., 2004a; Fairbanks et al., 2005; Hughen et al., 2006; Weninger and Jöris, 2008; Reimer et al., 2009). The current internationally-ratified calibration curve for Northern Hemisphere terrestrial material is IntCal09 covering the period 0 – 50 cal kBP (Reimer et al., 2009) and the Southern Hemisphere[20] curve is SHcal04 (McCormac et al., 2004). For this study Holocene ages were calibrated by means of version 6.0.1 of the *CALIB* programme (Stuiver and Reimer, 1993) using the SHcal04 (McCormac et al., 2004). The SHcal04 calibration curve was selected as it is the most

[20] The Southern Hemisphere is defined as south of the thermal equator or the Intertropical Convergence Zone (ITCZ) rather than the geographic Equator.

suitable curve for Southern Hemisphere Holocene *viz.* for ages between 0 – 11 cal kBP (McCormac et al., 2004). McCormac et al. (2004) recommends that the SHcal04 curve should not be used for ages beyond 11 cal kBP (due to larger changes in the inter-hemispheric offset). For ages beyond this point, the IntCal09 curve (Reimer et al., 2009) will be used with a Southern Hemisphere correction of 56 ± 24.

Reservoir effects resulting from the differences in the apparent ages of surface and bottom waters need to be identified and corrected for in all marine records prior to calibration (Kitagawa and van der Plicht, 1998; Hughen et al., 2004; Hua, 2009). Freshwater lakes may also be affected by reservoir effects as lake sediments can appear older than contemporaneous terrestrial samples if the sediments incorporate ^{14}C-deleted carbon sources such as dissolved inorganic carbon (TDIC) and carbonates from limestones (Geyh et al., 1998). The reservoir effect within lakes (known as the hard-water effect) is often a function of the ratio of the water volume (related to depth) and the surface area and can therefore vary significantly with time (Geyh et al., 1998). However, as peat and vlei/wetland sediments primarily consist of locally grown plants that decay *in situ* their ^{14}C content remains in equilibrium with $\Delta^{14}C$ and therefore it is unlikely that a reservoir effect would be present (Blaauw et al., 2004).

4.7.5.2 Laboratory procedures and considerations

Subsamples of approximately 1 g were taken from relevant depths from the three sediment cores and sent to *Beta Analytic Inc* for AMS radiocarbon dating using a tandem accelerator system in order to construct high resolution age-depth models.

Contamination can occur if younger or older carbon is incorporated into the sample material. If this is not accounted for, the ages will be anomalous with errors increasing with the sample age (Walker, 2005). External sources of contamination include: percolation of humic acids, inclusion of carbon from rootlet penetration, reworking of macrofossils within sediments, bioturbation and detrital carbonate contamination (Walker, 2005; Blockley et al., 2007). In order to minimise contamination samples are pre-treated prior to analysis. *Beta Analytic* follows two protocols to remove contaminants: physical and chemical pre-treatment. The first step involves increasing the surface area of samples, crushing solid chunks, shredding fibrous material, dispersing sediments and removal of roots and rootlets. After which HCl is applied to the samples to ensure the absence of carbonates.

Beta Analytic was instructed to date the 'bulk organic fraction' (the organic material that remains after sieving the sediment through < 180 micron sieves) for all samples despite the presence of intact macro-plant remains within some of the samples. Analysing the plant fraction instead of the organic fraction could be considered a better choice as it represents a more unique event in time and can be additionally treated with alkali to remove any humic acids present. However, the risk of this material constituting rootlets which could be extraneous together with the need to remain consistent meant that it was deemed best to only date the organic fractions.

4.7.5.3 Luminescence dating

In addition to the application of AMS dating, it was possible to obtain Optically Stimulated Luminescence (OSL) ages from the sediment cores due to the presence of sand-rich units. This supplementary dating method provided increased chronological control and made it possible to date material beyond the limit of radiocarbon dating.

OSL determines the time since quartz or feldspar grains within a sediment sample were last exposed to sunlight (Huntley et al., 1985; Stokes, 1999; Walker, 2005). Sediments are exposed to a constant flux of ionising radiation (the environmental dose rate or annual dose) from the radioactive decay of uranium-238 (^{238}U), ^{235}U, ^{232}U (and their daughter products) and potassium-40 (^{40}K). Quartz and feldspar minerals act as dosimeters by recording their exposure to this radiation flux. Samples with these minerals contained within them emit light when stimulated by light (or heat with respect to thermoluminescence). The burial dose (the equivalent dose or palaeodose) can be measured using OSL and is proportional to the amount of luminescence emitted since the minerals were last exposed to heat or light. Ages are calculated by measurements of the equivalent dose and the annual dose – the present day annual ionising dose rate using this equation:

$$Age\ (ka) = \frac{equivalent\ dose}{annual\ dose}$$

OSL dating has been effectively employed to establish chronologies for the Wilderness barrier dunes (Bateman et al., 2004; Carr et al., 2007; Bateman et al., 2008; Carr et al., 2010b; Bateman et al., 2011) as well as other sections of the southern Cape coast (Carr, 2004; Carr et al., 2006a; Roberts et al., 2009). OSL ages for Rietvlei and Vankervelsvlei were produced by Prof. M.D. Bateman at the Sheffield Centre for International Dryland Research at the University of Sheffield. Detailed descriptions of the methods used to determine the dose rates and equivalent doses as well as

techniques employed to limit potential errors (such as water content and partial bleaching) can be found in Bateman et al. (2004; 2011) and Carr et al. (2007; 2010b).

4.7.5.4 Age-depth modelling

Age-depth models estimate the ages of depths within sediment deposits by using the limited numbers of 'absolute' dated ages (predominantly ^{14}C ages) available and by making assumptions about the type of deposit, the sedimentation rate and the calibration curve (Blockley et al., 2007). Various types of age-models can be applied to palaeoenvironmental data with the majority of researchers employing linear interpolations between known ages (Blaauw, 2010). As calibrated radiocarbon ages have predominately irregularly-shaped probability density distributions they should not be limited to single point values with symmetric errors (Telford et al., 2004b; Blaauw and Christen, 2005; Blaauw, 2010). If single estimates have to be used they should be derived from weighted means or medians as these describe the distribution better than intercept-based methods (Telford et al., 2004b). Bayesian age models are at the forefront of age modelling as they have been shown to minimise the uncertainties of isolated ages, leads and lags through the application of advanced, robust and flexible numerical methods (Blaauw and Christen, 2005; Blockley et al., 2007; Blaauw, 2010). However existing Bayesian age-depth modelling methods do not add extra value to datasets that rely on a minimum number of ages (Blaauw, 2010).

Ideally a large number of ages (e.g. 24 for a Holocene sequence (Telford et al., 2004a)) are needed for precise statistically robust approximations to be modelled, however owing to constraints on budget, time and availability of appropriate material this is often not feasible. As all age-depth models have inherent errors (Blockley et al., 2007; Blaauw, 2012), the goal should be to establish the most parsimonious age model possible by incorporating all information available e.g. ^{14}C and OSL ages, sedimentation rates and stratigraphic markers. To this end, the software *CLAM* (Classic Age Modelling) (Blaauw, 2010) was used to develop suitable age-depth models for the Pearly Beach, Rietvlei and Vankervelsvlei cores. *CLAM* is integrated into *R* – an open source statistical environment (Team, 2011), standard code supplied by Blaauw (2010) was implemented together with the following parameters:

- The Southern Hemisphere calibration curve SHCal04 was used for the Holocene *viz.* ages between 0 – 11 cal kBP (McCormac et al., 2004).

- Late Pleistocene ages (beyond 11 cal kBP) were calibrated using INTCAL09 with a Southern Hemisphere correction of 56 ± 24 years applied to the uncalibrated ages (McCormac et al., 2004; Reimer et al., 2009).
- Iterations of 10 000.
- Linear interpolation was used to develop the models.
- OSL ages with their uncertainties were added to the models as 'calibrated' ages.

In CLAM the highest posterior density probabilities are not normalised to 100% which differs from other programmes e.g. *CALIB* (Stuiver and Reimer, 1986-2010; Stuiver and Reimer, 1993). The Monte Carlo method is used to calculate confidence intervals for undated depths. Confidence levels are calculated at two standard deviations (95%) to account for the asymmetric multimodal distribution (Blaauw, 2010).

4.8 Conclusion

Despite the problems that still exist relating to taxonomy and taphonomy, pollen analysis remains the leading technique for palaeoenvironmental reconstructions that focus on vegetation histories. The establishment of multi-proxy investigations has great potential to reduce the errors that are associated with individual analyses, with the hope that a commensurate number of lines of evidence will provide the greatest amount of insight.

This chapter has illustrated how the application of palynology, microscopic charcoal and geochemistry to sediment core material provides detailed information on past vegetation communities and climate-induced variability for a given location. The results of these well-defined analyses for the three sites in question are presented in the next chapter.

5. Palaeoenvironmental evidence from the southern Cape coast

5.1 Introduction

Having described the contemporary environments of the three coastal wetlands, the southern Cape palaeoenvironmental context, the laboratory and analytical methods employed, results of the multi-proxy analyses are now presented. The cores are initially described in terms of their stratigraphic and sedimentological properties. The chronological results and age models are then given, followed by the presentation and description of the palynological, microscopic charcoal and geochemical analyses, grouped according to pollen assemblage zones. New late Quaternary palaeoenvironmental evidence for the southern Cape coast is therefore the focus of this chapter.

5.2 Pearly Beach

5.2.1 Stratigraphy and sedimentology

The stratigraphy of the 250 cm core from Pearly Beach Marsh, labelled 'Pearly Beach 1' (PB-1), is displayed in Figure 5.1 while the result of the laser particle size analysis is presented in Figures 5.2, 5.3 and Appendix C.

The particle size analysis shows that the overall particle size distribution is positively skewed with the core predominantly comprising of sands and silty sands (Figures 5.2 and 5.3). Three distinct zones of pale coarser-textured sands are found at the top (0 – 25 cm), middle (130 – 160 cm) and base (235 – 250 cm) of the core. These sections contain moderate amounts of rootlets and plant fragments. They are bounded by relatively homogeneous organic-rich silty sands. The exception being a thin lens of light-coloured coarser sand situated between 175 and 180 cm.

The core consists of moderately well sorted sediments except for the section between 20 cm and 100 cm which is very poorly sorted and contains increased finer-grained sediments such as greater proportions of silt and clay (Figures 5.2 and 5.3). A further section where the sediments are poorly sorted is within the thin sand lens between 175 and 180 cm. This thin sand lens could possibly represent a period of less inundation, increased sediment exposure and reduced water levels.

As mentioned in Chapter 4 section 4.73, direct interpretations of hydrological and depositional environments from particle size data can be fairly ambiguous (Teller and Last, 1990a; Last, 2001). However the clear changes between the darker and lighter sands and silty sands most likely does indicate significant changes in the past sedimentological environment at Pearly Beach.

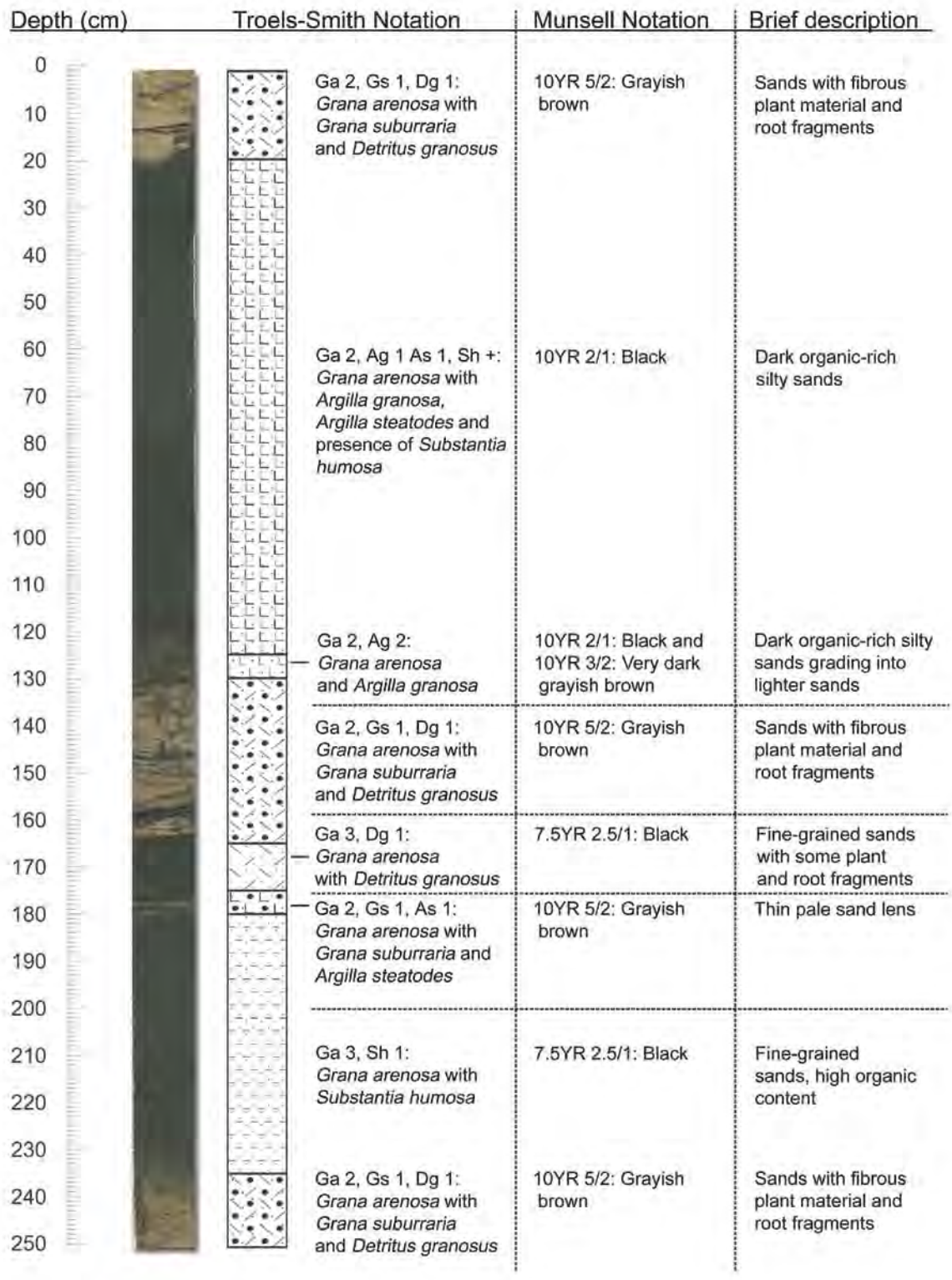

Figure 5.1 Stratigraphic description of Pearly Beach 1 (PB-1) employing the Troels-Smith sediment composition notation (Troels-Smith, 1955) and the Munsell Colour notation.

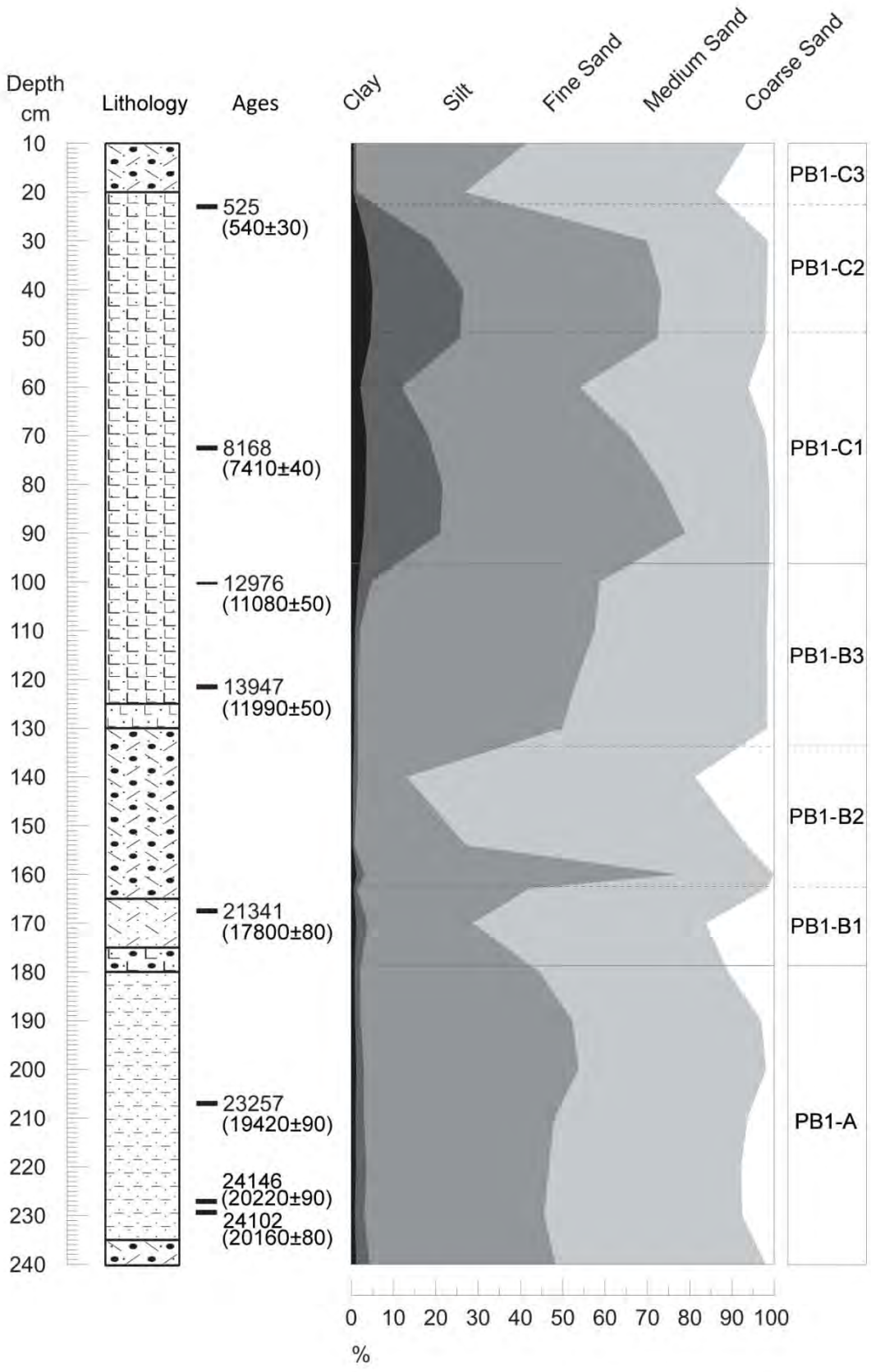

Figure 5.2 Pearly Beach 1 particle size analysis summary diagram displaying percentages of clay (0 – 2 µm), silt (2 – 20 µm), fine sand (20 – 200 µm), medium sand (200 – 500 µm) and coarse sand (500 – 2000 µm). Median probability calibrated ages are displayed above uncalibated ages and errors (in parentheses), pollen assemblage zones are indicated to the far right.

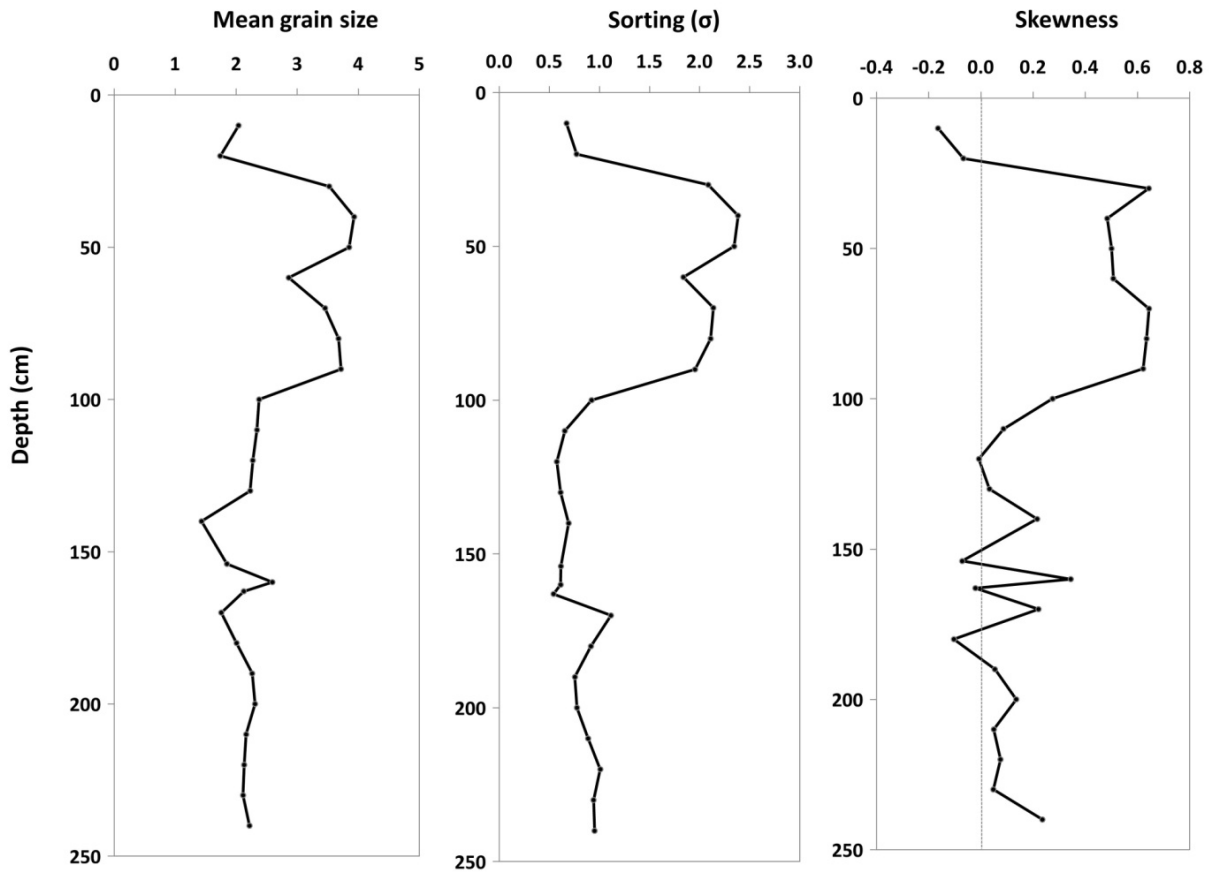

Figure 5.3 Pearly Beach 1 grain size distribution statistical parameters (ϕ) (Folk and Ward, 1957 method calculated in *Gradistat* version 8 Blott 2010).

5.2.2 Chronology and sediment accumulation

The results of the radiocarbon analysis and the calibration of these results are presented in Table 5.1. The age-depth model for the core was established following the methodologies outlined in the previous chapter (section 4.7.4) and is displayed in Figure 5.4. The model includes a depositional hiatus from 130 – 160 cm; given the current number of radiocarbon ages available either side of this, together with the limited amount of organic material, it is not possible to more accurately resolve the ages represented by this sand layer. Therefore the most appropriate solution is to exclude this section from the study until further chronological control can be achieved.

The core spans the period ~25 cal kBP to present with a break in sedimentation between ~21 cal kBP – 14.5 cal kBP (the hiatus mentioned above) and therefore encompasses the whole of the Holocene and sections of the late Pleistocene.

The top 20 cm of the core could not be dated as very little organic matter is present; the top of the sequence was therefore assumed to date roughly to present day.

Despite the appearance of a slight reversal between the two ages near the base of the core, their calibration curves are extremely similar and therefore, taking into account the error estimates, represent essentially the same age range (Figure 5.5).

Sedimentation accumulation rates for the Holocene and early glacial sections (0 – 100 cm) are relatively consistent (although this may be an artefact of the limited number of radiocarbon ages) with an average rate of 0.63 mm yr^{-1}. Sedimentation rates are greatly increased for the late Pleistocene sections with an average rate of 2.45 mm yr^{-1} between 100 and 130 cm and 2.15 mm yr^{-1} between 160 and 250 cm.

Table 5-1 Pearly Beach 1 radiocarbon and calibrated ages.

Sample ID	Laboratory ID	Average depth (cm)	Measurement method	14C age yr BP	1 sigma error	Calibration data	95.4 % (2σ) cal age range	Relative area under distribution	median probability
PB1-A	Beta-298974	23.0	AMS	540	30	SHCal04	cal BP 502 - 548	1	525
PB1-F	Beta-305128	72.5	AMS	7410	40	SHCal04	cal BP 8030 - 8224 cal BP 8233 - 8313	0.796895 0.203105	8168
PB1-H	Beta-311274	100.5	AMS	11080	50	INTCal09	cal BP 12753 - 13117		12976
PB1-B	Beta-298973	121.5	AMS	12102*	55.5	INTCal09	cal BP 13794 - 14120	1	13947
PB1-C	Beta-298972	167.5	AMS	17856*	83.5	INTCal09	cal BP 20969 - 21566	1	21341
PB1-E	Beta-305127	207.0	AMS	19476*	93.1	INTCal09	cal BP 22673 - 22859 cal BP 22862 - 23617	0.102195 0.897805	23257
PB1-D	Beta-298971	227.3	AMS	20276*	93.1	INTCal09	cal BP 23889 - 24469	1	24194
PB1-G	Beta-308917	229.8	AMS	20216*	83.5	INTCal09	cal BP 23860 - 24426	1	24136

AMS = Accelerated mass spectrometry

SHCal04 (McCormac et al., 2004); INTCal09 (Reimer et al., 2009)

***Adjusted for recommended SH offset of 56 +/- 24 (McCormac et al., 2004)**

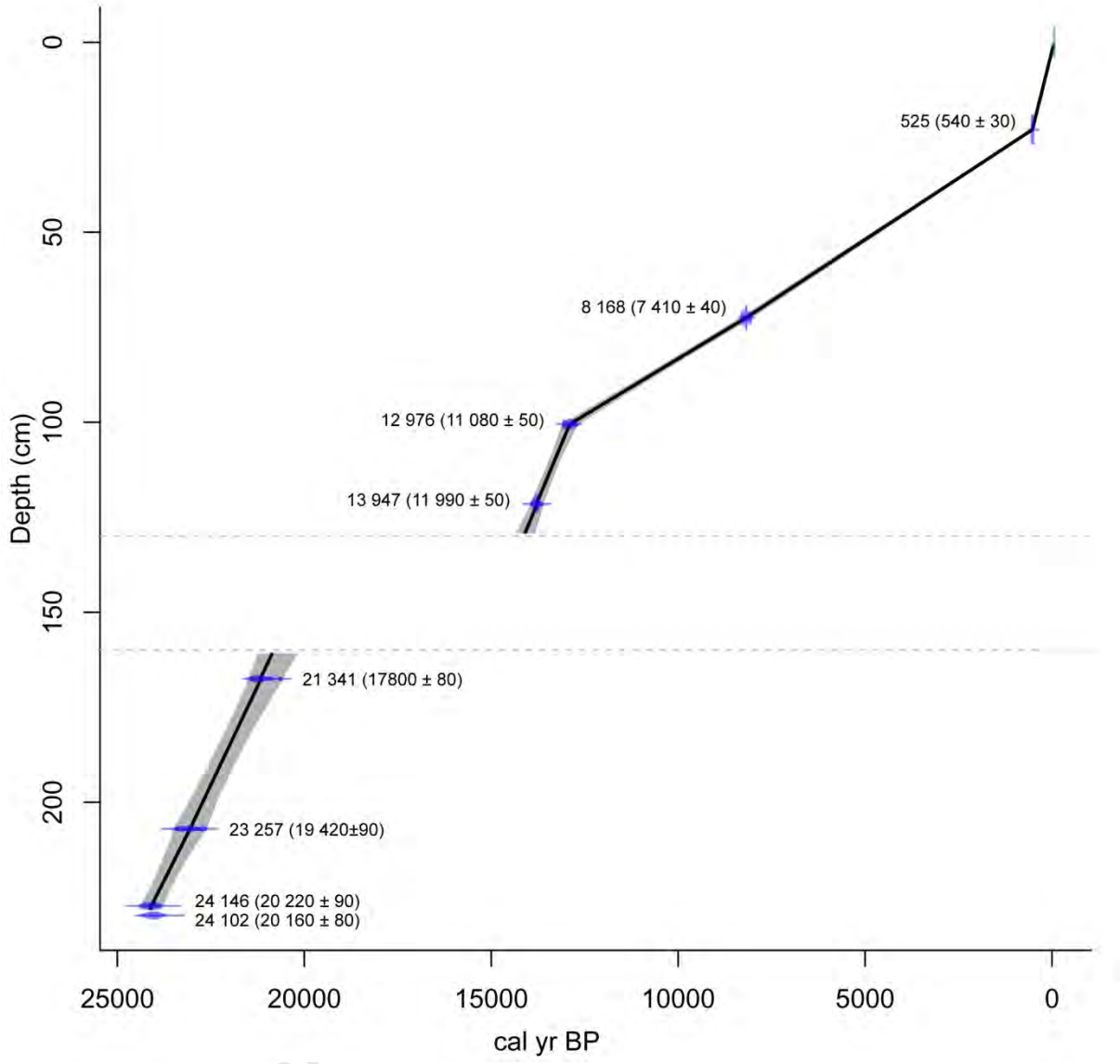

Figure 5.4 Age-depth model for Pearly Beach 1, generated in *R* using *CLAM* (Blaauw, 2010) and taking into account a hiatus between 130 and 160 cm and the surface as -56 cal yr BP (2006 AD; the date the core was extracted). The median probability calibrated ages are labelled and the uncalibrated ages with errors are provided in parentheses. Grey envelopes show the 95% confidence intervals, blue histograms indicate the ^{14}C calibrated distribution using SHCal04 (McCormac et al., 2004) or IntCal09 (Reimer et al., 2009) (see Table 5-1).

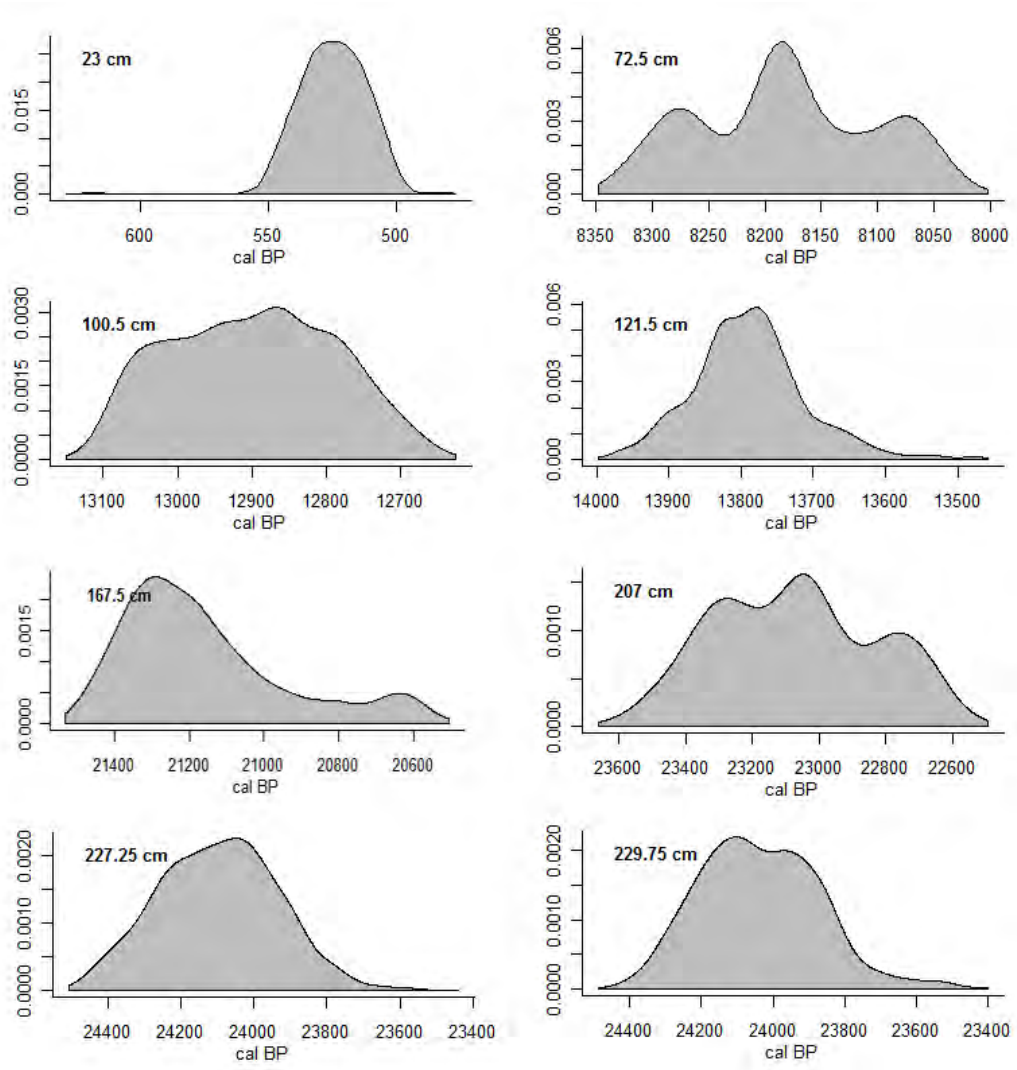

Figure 5.5 Calibration curves for Pearly Beach's eight radiocarbon ages.

5.2.3 Pollen and microscopic charcoal analyses results

A total of 78 samples were taken for pollen and microscopic charcoal analysis, however 20 of these contained too low concentrations of pollen grains to produce reliable, statistically-robust counts. On average, counts of 500 grains were carried out on the remaining 58 samples (see Appendix D for absolute counts). For low concentration levels, a minimum of three slides were counted in full.

Pollen concentrations were variable ranging between 1.74×10^3 and 3.32×10^4 grain g^{-1} with an average of 1.20×10^4 grain g^{-1}, which is lower than some of the montane hyrax midden sites within the Fynbos Biome (Scott and Woodborne, 2007a; Meadows et al., 2010; Quick et al., 2011) and Vankervelsvlei 2010 (section 5.4.3) but similar to Rietvlei Still Bay 2 (section 5.3.3).

The overall assemblage is dominated by lowland fynbos taxa (e.g. Proteaceae, Ericaceae, Restionaceae and *Cliffortia*) together with local aquatic/riparian vegetation and more cosmopolitan pollen taxa (such as Asteraceae high spine variety and Poaceae). The major changes evident within the pollen sequence are described below.

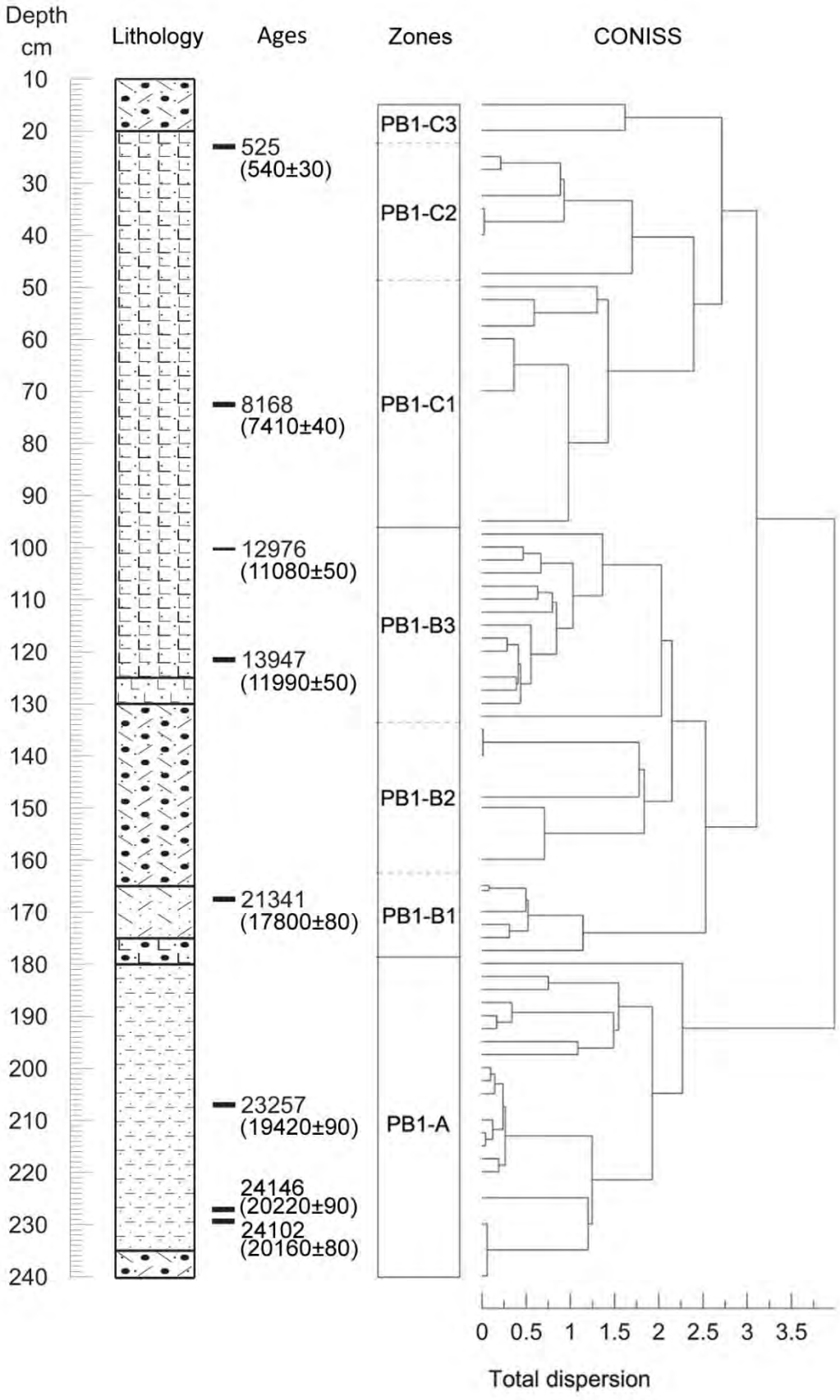

Figure 5.6 The results of CONISS displaying pollen assemblage zones for Pearly Beach 1.

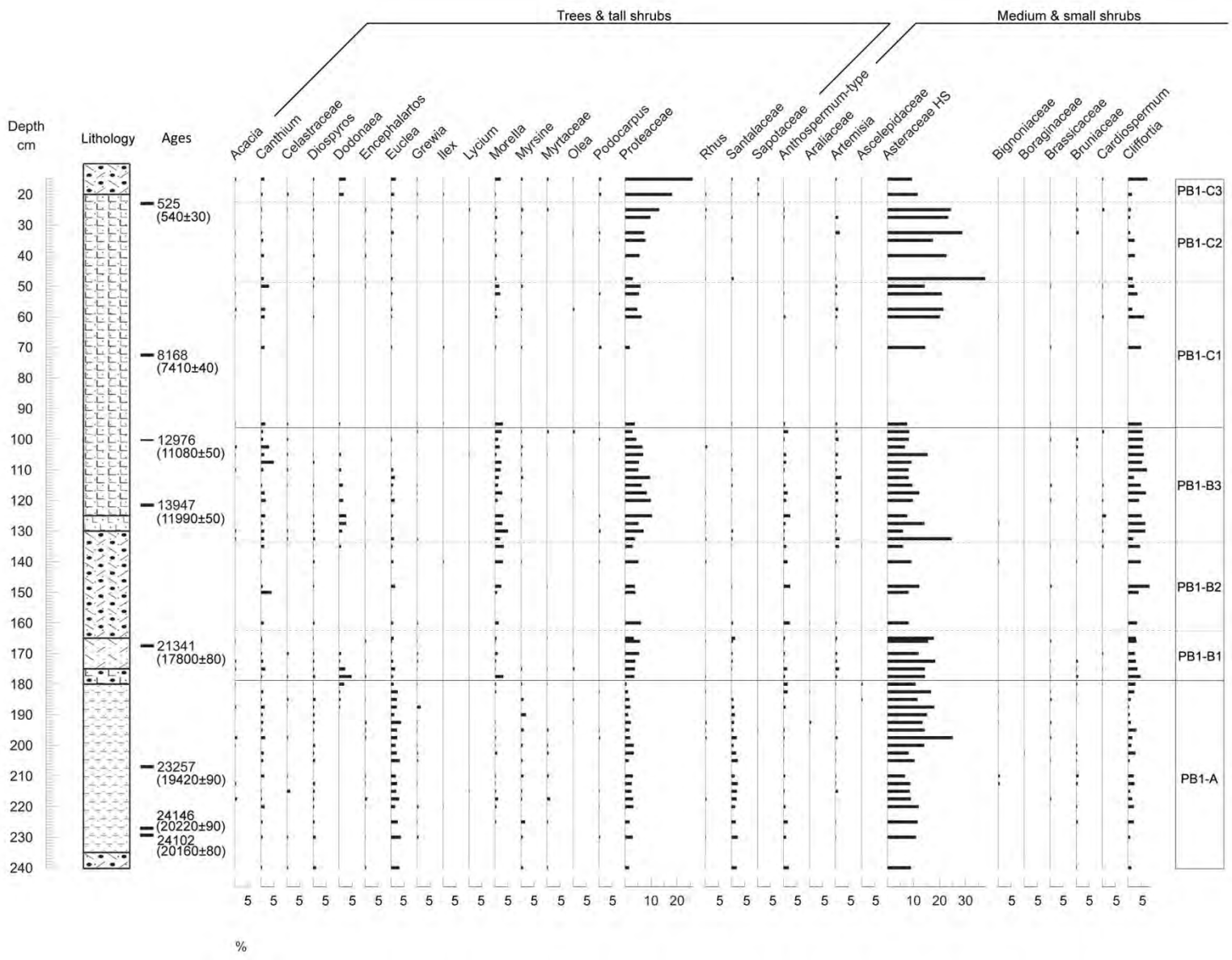

Figure 5.7 Comprehensive relative percentages pollen diagram for Pearly Beach, taxa grouped according to general growth form (page 1 of 4).

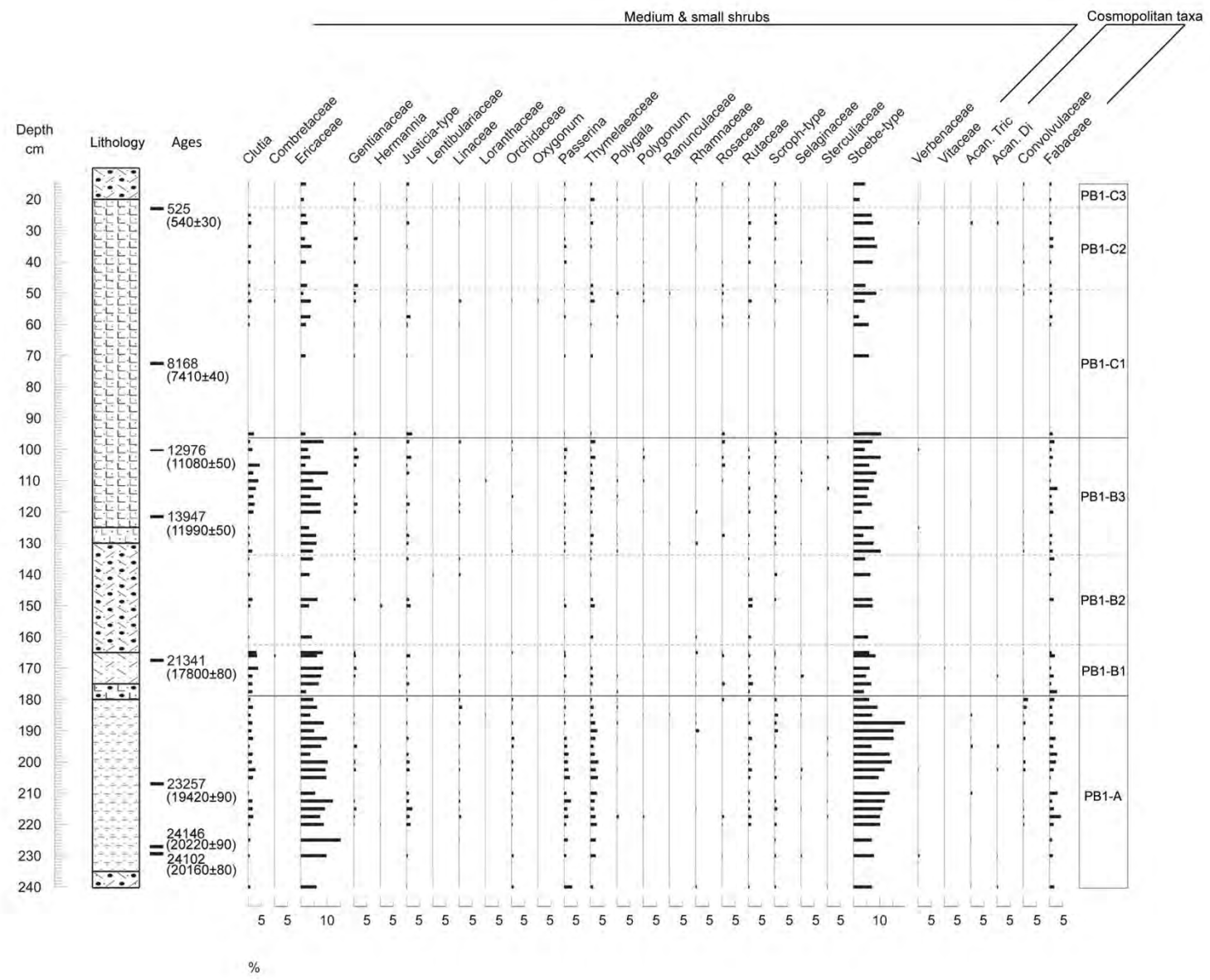

Figure 5.8 Comprehensive relative percentages pollen diagram for Pearly Beach, taxa grouped according to general growth form (page 2 of 4).

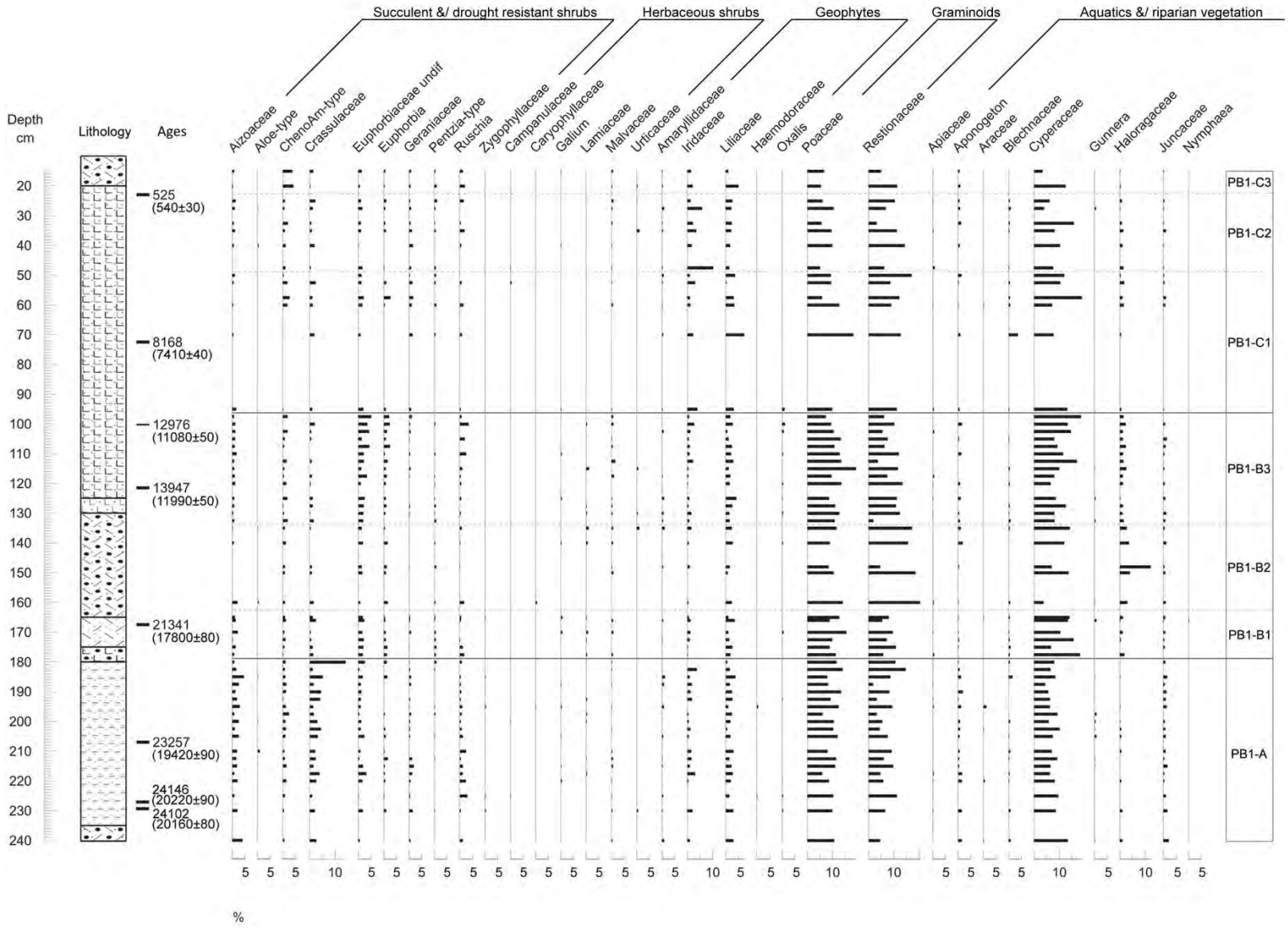

gure 5.9 Comprehensive elative percentages ollen diagram for Pearly each, taxa grouped ccording to general rowth form (page 3 of 4).

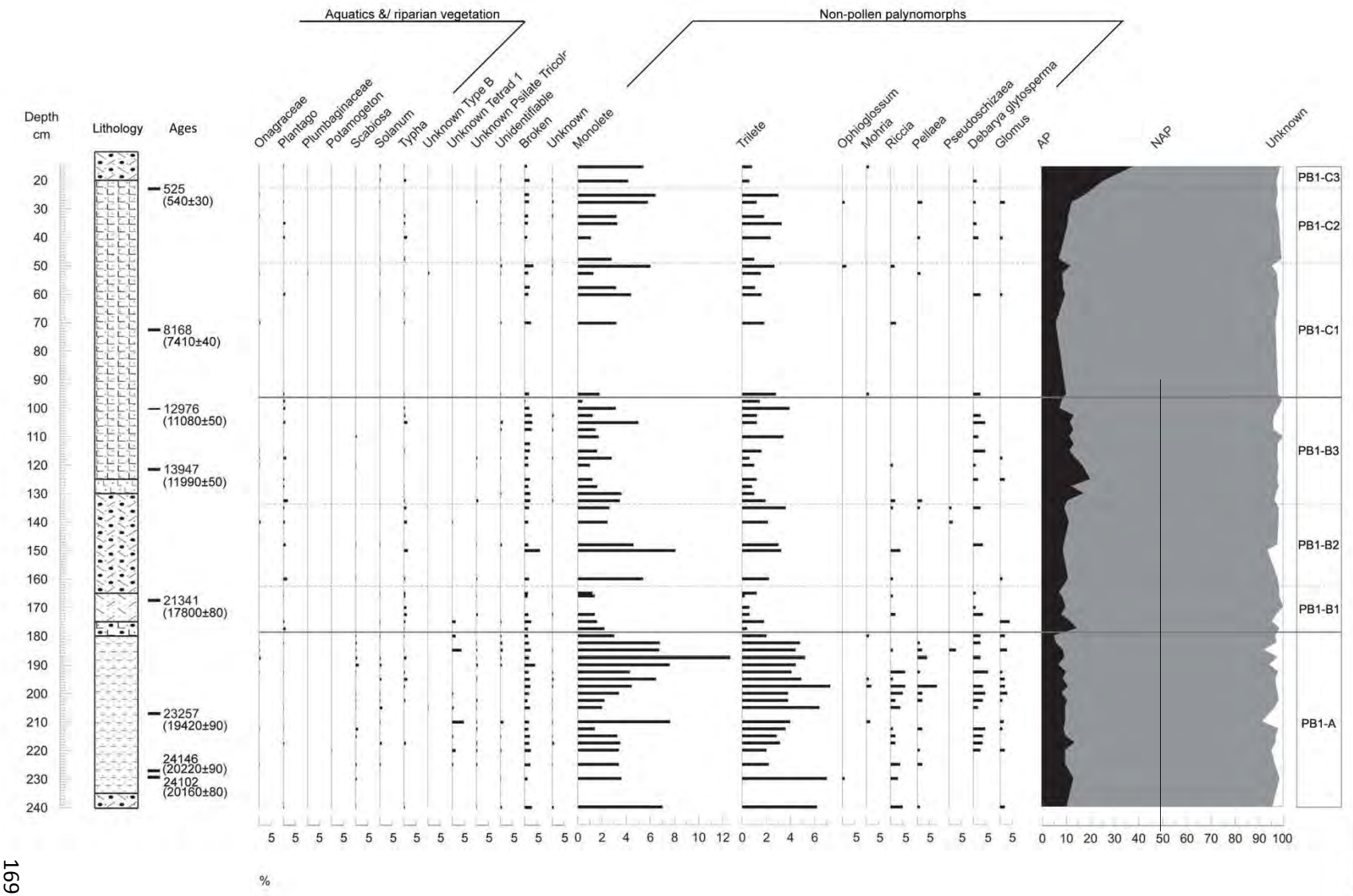

Figure 5.10 Comprehensive relative percentages pollen diagram for Pearly Beach, taxa grouped according to general growth form, non-pollen palynomorphs as percentages relative to the total pollen count (page 4 of 4).

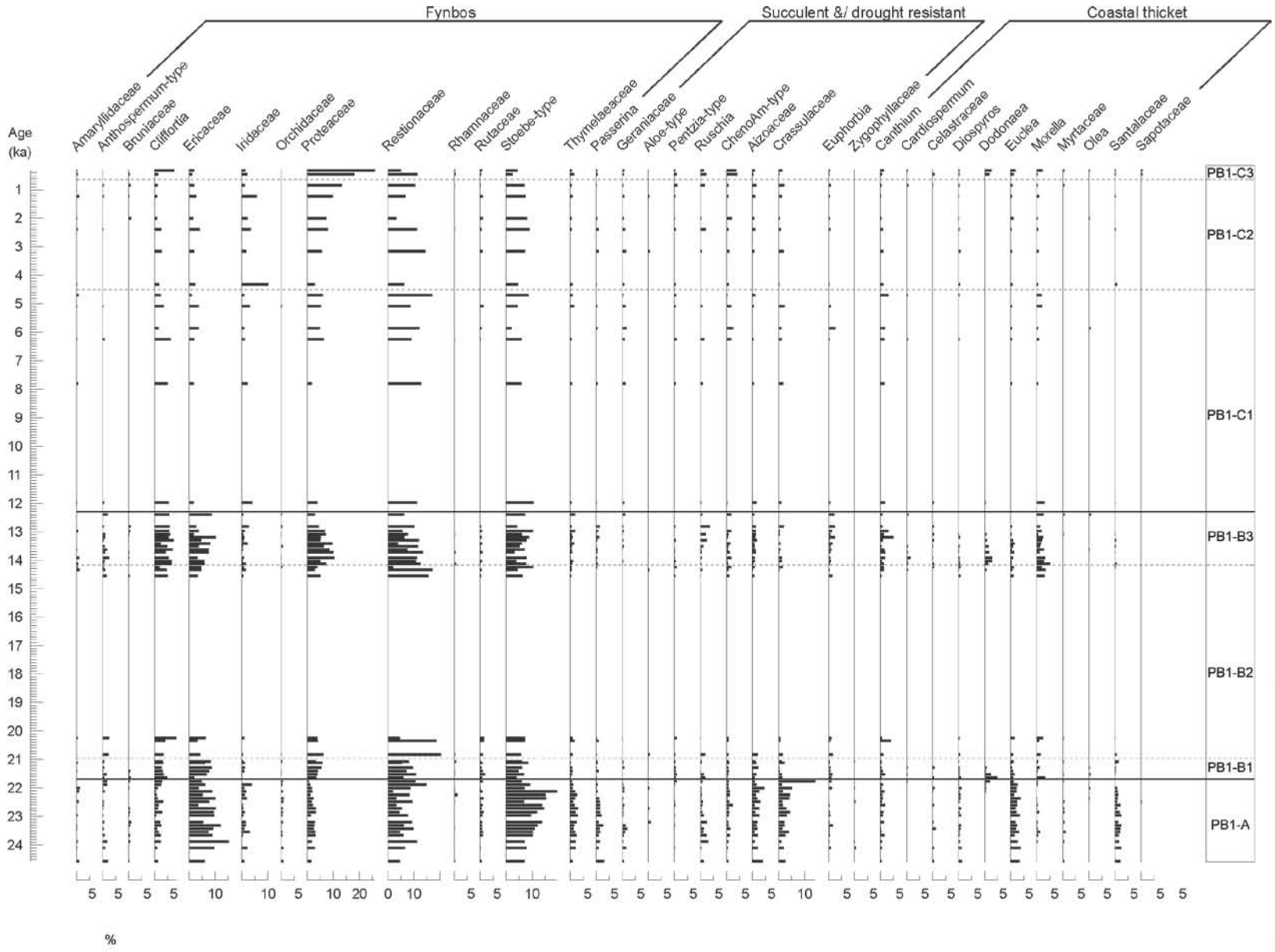

Figure 5.11 Relative percentages pollen diagram for Pearly Beach, selected taxa grouped according to ecological affinities and plotted against interpolated age (page 1 of 2).

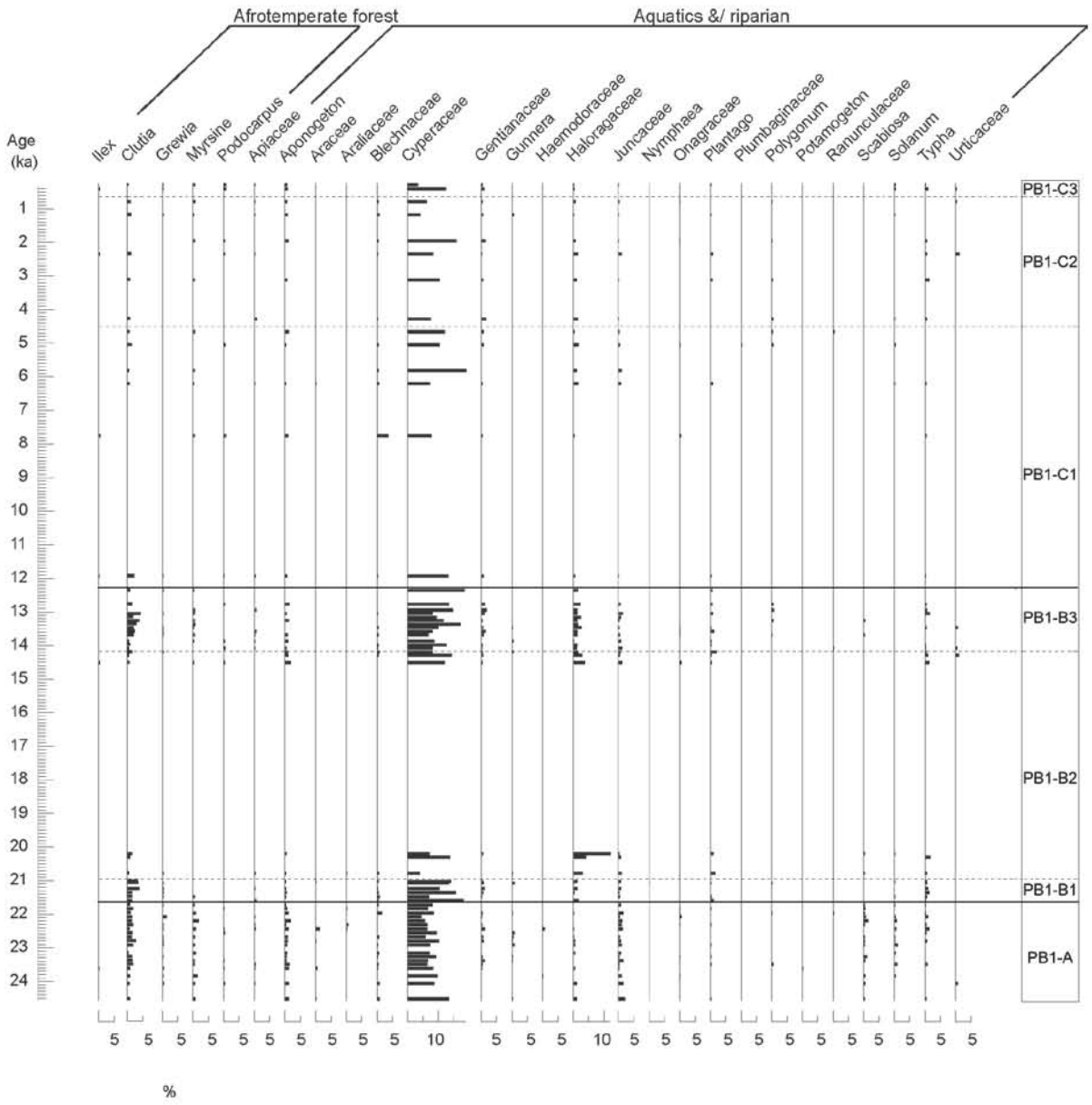

Figure 5.12 Relative percentages pollen diagram for Pearly Beach, selected taxa grouped according to ecological affinities and plotted against interpolated age (page 2 of 2).

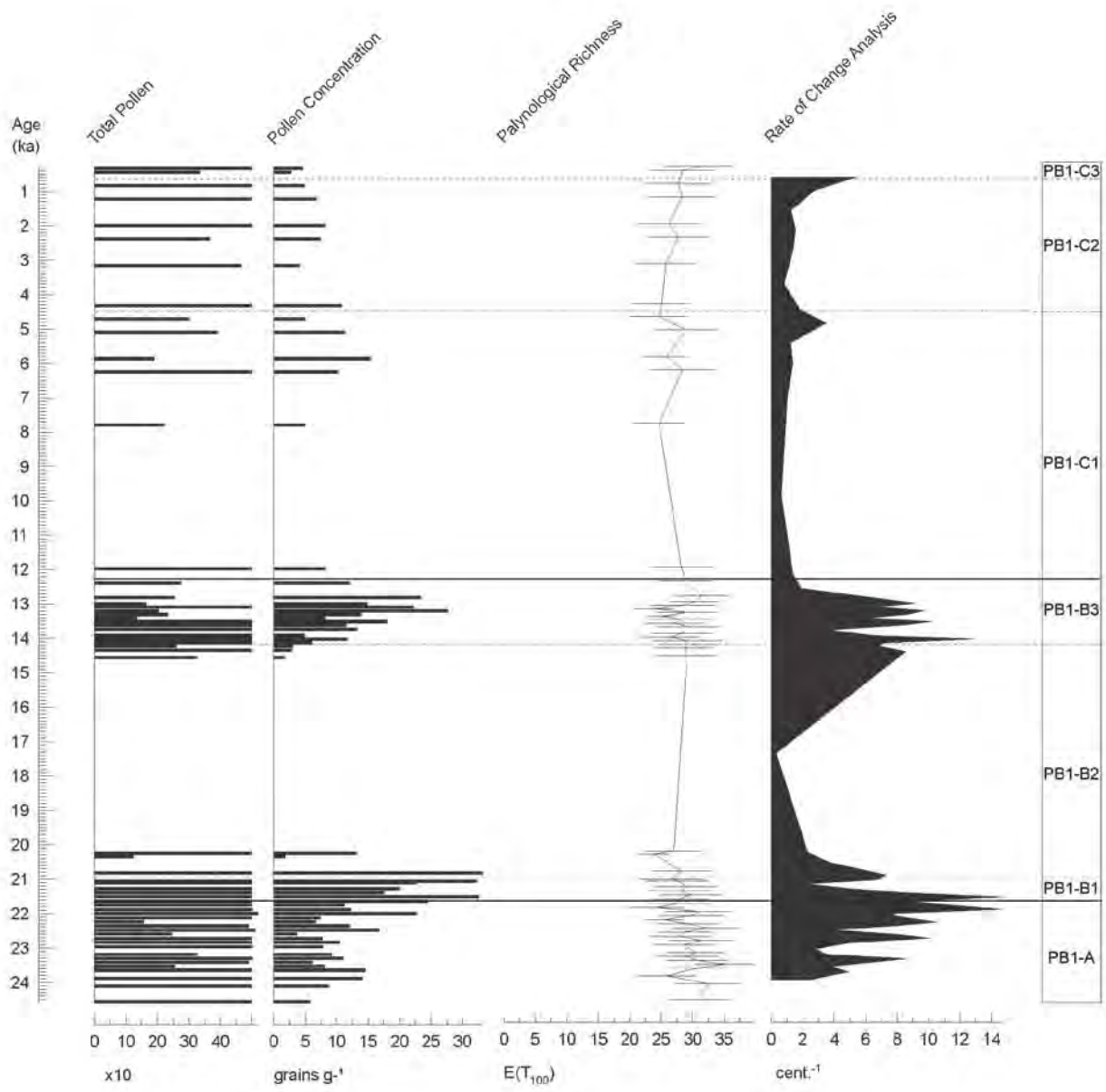

Figure 5.13 Pearly Beach total pollen counts, pollen concentrations and the palynological richness and rate of change analyses results.

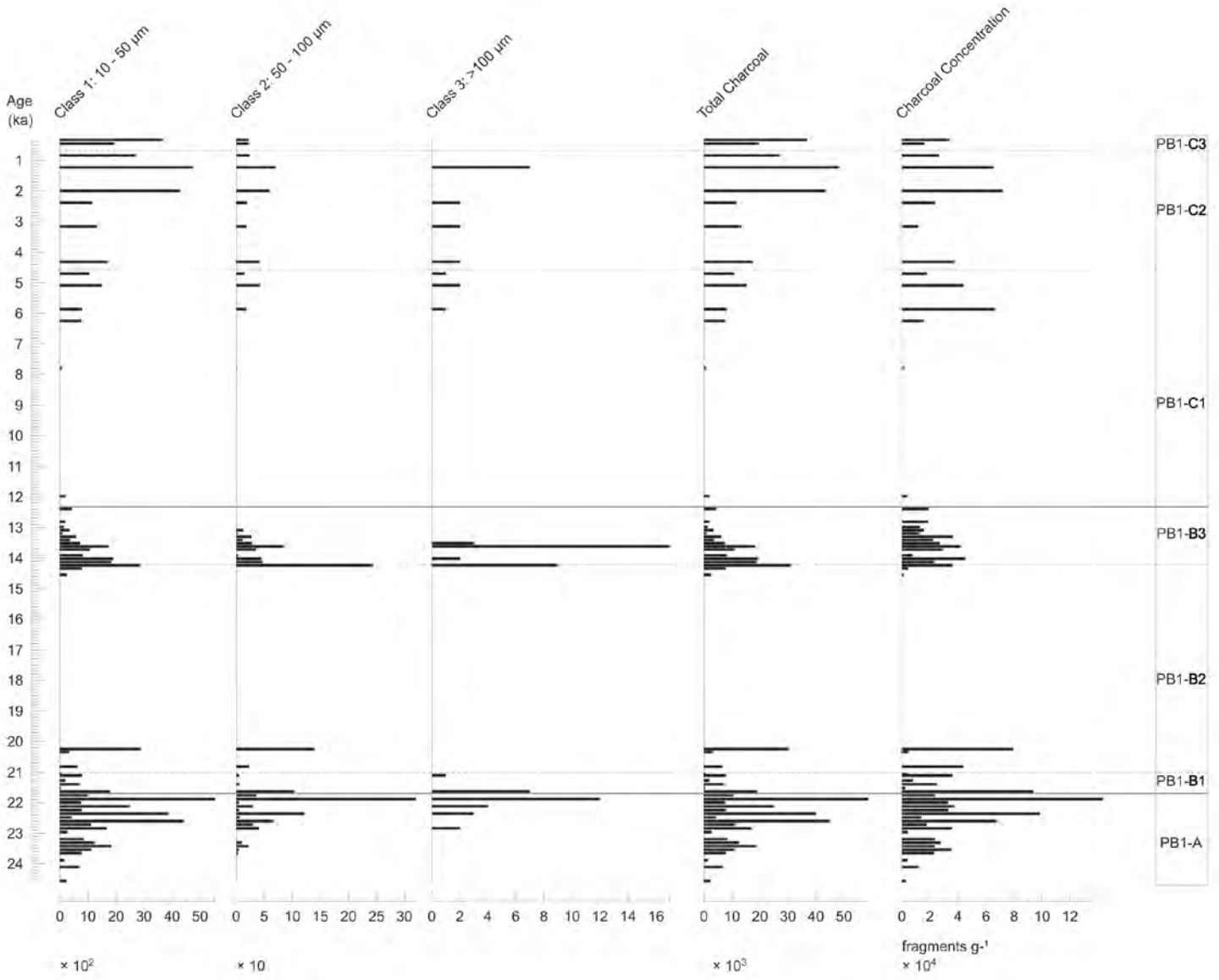

Figure 5.14 Results of Pearly Beach's microscopic charcoal analysis, displaying the three size classes counted, total charcoal (sum of the three classes) and charcoal concentrations (calculated in a similar manner to pollen concentrations using the exotic marker counts).

Zone PB1-A: 240 – 181 cm; approximately 24.8 – 21.8 cal kBP

Relatively high percentages (~10%) of Ericaceae characterise this zone with the largest peak (15%) for the sequence found at 225 cm/~23.9 cal kBP. *Stoebe*-type (which includes various *Stoebe* and *Elytropappus* spp.) proportions are also fairly high, increasing towards the top of PB1-A. Proteaceae and *Cliffortia* percentages are both lowest for the sequence within this zone. There are relatively low proportions of undifferentiated high-spine Asteraceae except for peak at 197.5 cm/~22.6 cal kBP. Local aquatics and riparian taxa are moderately high but decrease towards the top of the zone. A prominent feature of PB1-A is the greatly increased percentages of fern and Bryophyte spores (monolete, trilete, *Riccia* and *Pellaea* types). Coastal thicket taxa are either absent or present at low proportions throughout, except for *Euclea* and Santalaceae types. Poaceae and Restionaceae percentages remain relatively consistent at ~10% throughout the zone.

Charcoal is very low at the base with only small (Class 1) fragments present however both amounts and concentrations reach their highest levels for the sequence at the top of the zone.

Zone PB1-B: 181 – 96 cm; approximately 21.8 – 12.2 cal kBP

This zone is divided into three subzones which are described below.

Subzone PB1-B1: 181 - 162 cm; approximately 21.8 – 21.0 cal kBP

The pollen composition of first level within this subzone, the sample at 21.8 cal kBP, differs significantly from PB1-A and the rest of PB1-B. The most prominent feature of this level is the remarkably large peak in Crassulaceae (14%).

Other succulent/drought resistant taxa are present but at low percentages at 21.8 cal kBP. In comparison to PB1-A, *Anthospermum*-type and *Dodonaea* exhibit slight increases for this level. There are significant reductions in charcoal, pollen concentration, arboreal pollen (low percentages and absence of many trees and tall shrubs, lowest percentage of Proteaceae for the whole sequence), *Stoebe*-type, fern and Bryophyte spores and local aquatic/riparian pollen (extremely low or absence except for Cyperaceae).

The rest of the subzone is characterised by continued low proportions of arboreal pollen except for peaks in *Dodonaea* and *Myica* at the base of PB1-B1. There are increases in percentages of fynbos taxa (especially Proteaceae and *Cliffortia*) except for *Stoebe*-type which remains low throughout the subzone. Ericaceae percentages are very low near the base of the subzone but increase to relatively

high proportions at the top of the subzone. Cyperaceae percentages are significantly elevated from 21.6 cal KBP to the top of the subzone. Aquatics are slightly increased from 21.6 – 21 cal kBP in comparison to PB1-B. *Clutia* increases from 1.6% at 21.6 cal kBP to over 3% towards the top of the zone.

Pollen concentrations are high especially at the top and bottom of the zone. Charcoal counts and concentrations are very high at the base and then decrease significantly towards the top of PB1-C.

Subzone PB1-B2: 162 – 133 cm

This subzone represents the sand layer on uncertain age discussed in section 5.2.2.

A few levels within this subzone were devoid of pollen with the remaining levels reflecting very low pollen concentrations. In general, there are significantly elevated percentages of Restionaceae (20% at the base, the highest for the sequence) and lower frequencies of arboreal pollen are found within this subzone.

The sample at 148 cm is considerably different from the rest of those within PB1-B2 and is characterised by peaks in Ericaceae, *Cliffortia*, Haloraginaceae (12%, highest for the sequence), monolete spores, pollen and charcoal concentrations together with reductions in Cyperaceae and Restionaceae.

Subzone PB1-B3: 133 – 96 cm; approximately 14.2 – 12.2 cal kBP

Zone PB1-B3 exhibits increases in arboreal pollen taxa, notably elevated percentages of Proteaceae and the reappearance of *Dodonaea*. Other coastal thicket taxa are present in slightly higher proportions than in previous zones. The majority of the fynbos taxa are also present throughout this subzone. There is a significant peak in high-spine Asteraceae at the base of PB1-B3. In general, *Stoebe*-type, Poaceae and Restionaceae all remain relatively high (~8 – 12% each) throughout the subzone.

Charcoal amounts and concentrations taper off towards the top of the subzone, except for a peak in large charcoal fragments (Class 3) at 117.5/ ~13.6 cal kBP (highest amount in the sequence). Pollen concentrations increase towards the top of PB1-B3.

Zone PB1-C: 96 – 0 cm; approximately 12.2 – 0 cal kBP

PB1-C encompasses the Holocene and is divided into three subzones.

Subzone PB1-C1: 96 – 49 cm; approximately 12.2 – 4.5 cal kBP

Pollen grains are not preserved between 92.5 and 62.5 cm except for at 70 cm where pollen concentrations are very low. Pollen concentrations increase from 60 cm/ ~6.2 cal kBP towards the top of the subzone. Arboreal pollen taxa are either at very low percentages or absent from PB1-C1. Asteraceae high spine variety percentages are elevated at the top of this subzone, whereas Ericaceae frequencies are greatly reduced in comparison to previous zones. Poaceae reaches its highest percentage (18%) at 70 cm/~7.8 cal kBP whereas Cyperaceae and charcoal concentration peaks at 57.5 cm/ ~5.9 cal kBP.

Zone PB1-C2: 49 – 22 cm; approximately 4.5 – 0.65 cal kBP

Asteraceae high spine is highest for the sequence (38%) at the base of the subzone after which it decreases towards the top. Proportions of Restionaceae, Cyperaceae and *Stoebe*-type fluctuate throughout the subzone but in general are relatively high. Ericaceae and *Cliffortia* frequencies are low throughout this subzone. There is a steady increase in Proteaceae pollen towards the top of PB1-C2. Monolete and trilete spores also rise towards the top of the zone. At the base of PB1-C2 there is a significant peak in Iridaceae. Charcoal peaks whereas pollen concentrations decrease towards the top.

Zone PB1-C3: 22 – 0 cm; approximately 0.65 – 0 cal kBP

The most prominent feature of this subzone is the significantly elevated percentages of Proteaceae (up to 26%, the highest for the sequence). There are peaks in *Cliffortia*, monolete spores and charcoal fragments (Class 1) at the top of the subzone. *ChenoAm*-type percentages are relatively high throughout zone in comparison to all other zones. There is an increase in coastal thicket with the first appearance of Sapotaceae pollen (most likely *Sideroxylon inerme*) and slightly elevated percentages of *Euclea*, *Dodonaea* and *Morella*. Cyperaceae (together with other aquatic/riparian taxa) and Restionaceae proportions drop off at the top of the subzone. High-spine Asteraceae, Poaceae and pollen concentrations are all relatively low throughout the subzone.

5.2.4 Multivariate data analyses

The statistical analyses described below were performed on a subset of the pollen data. A selection of 20 ecologically sensitive taxa was chosen for the analyses (Table 5-2).

The initial detrended correspondence analysis (DCA) revealed gradient lengths well below 3 (the longest gradient length was 1.146) therefore a principle component analysis (PCA) was undertaken (Leps and Smilauer, 2003). The pollen taxa data was standardized and square-root transformed. The ordination was centred by taxa and scaling was focused on inter-sample distance.

Table 5-2 A selection of ecologically sensitive pollen taxa for statistical analyses.

Selected pollen taxa	General ecological affinity
Aponogeton	aquatic/riparian
Araceae	aquatic/riparian
Blechnaceae	aquatic/riparian
Gunnera	aquatic/riparian
Haloragaceae	aquatic/riparian
Cliffortia	fynbos
Ericaceae	fynbos
Passerina	fynbos
Proteaceae	fynbos
Stoebe -type	fynbos
Podocarpus	forest
Dodonaea	thicket
Sapotaceae	thicket
Celastraceae	thicket
Morella	thicket
Aizoaceae	succulent/drought resistant
Crassulaceae	succulent/drought resistant
Euphorbia	succulent/drought resistant
Geraniaceae	succulent/drought resistant
Ruschia	succulent/drought resistant

Table 5-3 Summary table displaying the Principal Component Analysis (PCA) results for Pearly Beach 1.

Principal component axes	1	2	3	4	Total variance
Eigenvalues	0.314	0.127	0.086	0.082	1
Cumulative percentage variance of species data	31.4	44.1	52.7	60.9	
Total sum of squares in species data	283.6				
Total standard deviation in species data TAU	0.494				

The results of the PCA indicate that PCA axis 1 (PC1) and axis 2 (PC2) account for ~31% and ~13% respectively of the total variability (Table 5-3). The subsequent principal components do not explain significant percentages of the variance. Figure 5.15 is a distance biplot of the PCA scores displaying the relationship between the taxa and samples (ages) on PC1 and PC2. The relative distance between samples is related to the differences in pollen taxa composition of those samples. The positions of the taxa arrows indicate the correlation with the samples with short distances representing high correlations between taxa and samples.

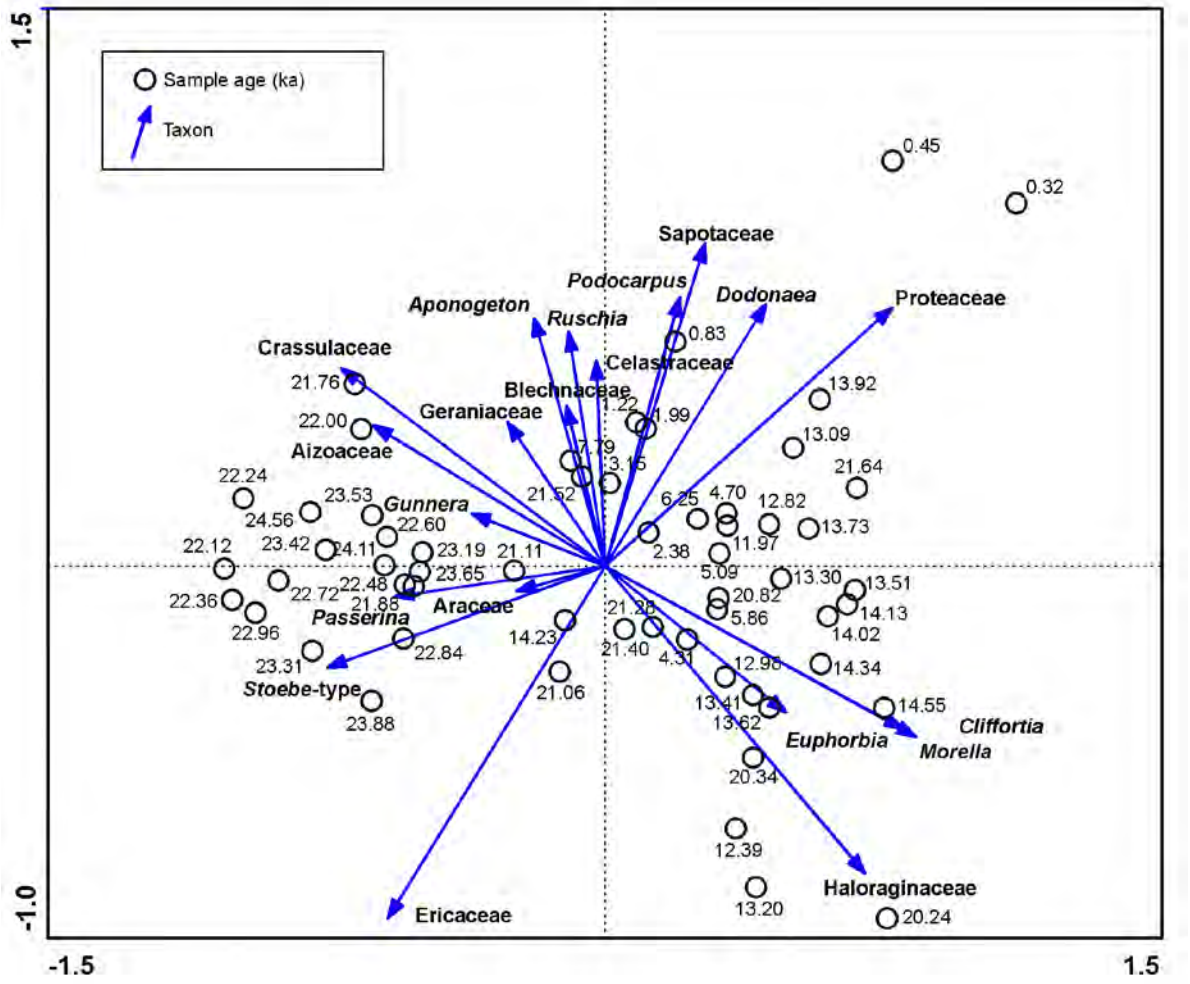

Figure 5.15 Ordination biplot mapping the taxa and sample ages scores for Pearly Beach 1.

The samples that have the most distinctly different pollen compositions in relation to the rest of the dataset are those at the very top of the sequence (0.45 and 0.32 cal kBP). These levels are dominated by increased arboreal taxa (especially Proteaceae). The Holocene samples reflect a strong association with coastal thicket as represented here by Sapotaceae, Celtrastraceae and *Dodonaea*.

The majority of the samples representing pollen assemblage zone PB1-A (the early last Glacial, prior to 21.7 cal kBP) are clustered together and are associated with the vector arrows of *Passerina*, *Stoebe*-type, Araceae and *Gunnera*. Samples at 22 cal kBP and 21.7 cal kBP are grouped very closely with Crassulaceae and Aizoaceae, reflecting the relative dominance of these taxa within the pollen compositions of these samples.

5.2.5 Geochemical results

Total organic carbon (TOC), is generally low (in comparison to Rietvlei Still Bay 2's range, see section 5.4.4). TOC varies between 0.2 to 4.6 % with lowest values (below 1%) from 118 to 143 cm (~13.4 – 14.5 cal kBP) and from 228 cm/~23.8 cal kBP to the base (Figure 5.16). Peaks occur at 168 cm (~21 cal kBP), 88 cm (~10 cal kBP) and 33 cm (1.3 cal kBP). Total nitrogen (TN) follows a similar trend to that of TOC except for a drop at 178 cm (21.4 cal kBP).

Bulk $\delta^{13}C_{TOC}$ data strongly reflect the C_3 vegetation surrounding the site ranging between -22 and -25.6 ‰ (Figures 5.16 and 5.17). There is little variability in the $\delta^{13}C_{TOC}$ values except for a relative enrichment coincident with a peak in TOC at 88 cm (~10 cal kBP).

The ratio of TOC to TN, as mentioned in Chapter 4 (section 4.7.4) is an indicator of the biological provenance of the TOC and can be relevant to the interpretation of the $\delta^{13}C$ signal. This ratio does not vary significantly throughout the core with most values being between 10 and 35 (Figures 5.16 and 5.17). However there are significantly elevated values for the sand layer hiatus (between 148 and 158 cm) and the thin sand lens at 178 cm. The lowest values for the core are found at the top of the sequence (within pollen assemblage subzone PB1-C3) and between 143 – 118 cm (~14.5 – 13.4 cal kBP, within PB1-B) and could indicate organic matter within these samples were marine or algal in origin as the ratios were below 10 (Figure 5.17). Pollen assemblage subzone PB1-B2 shows the greatest diversity of TOC/TN ratio values (Figure 5.17).

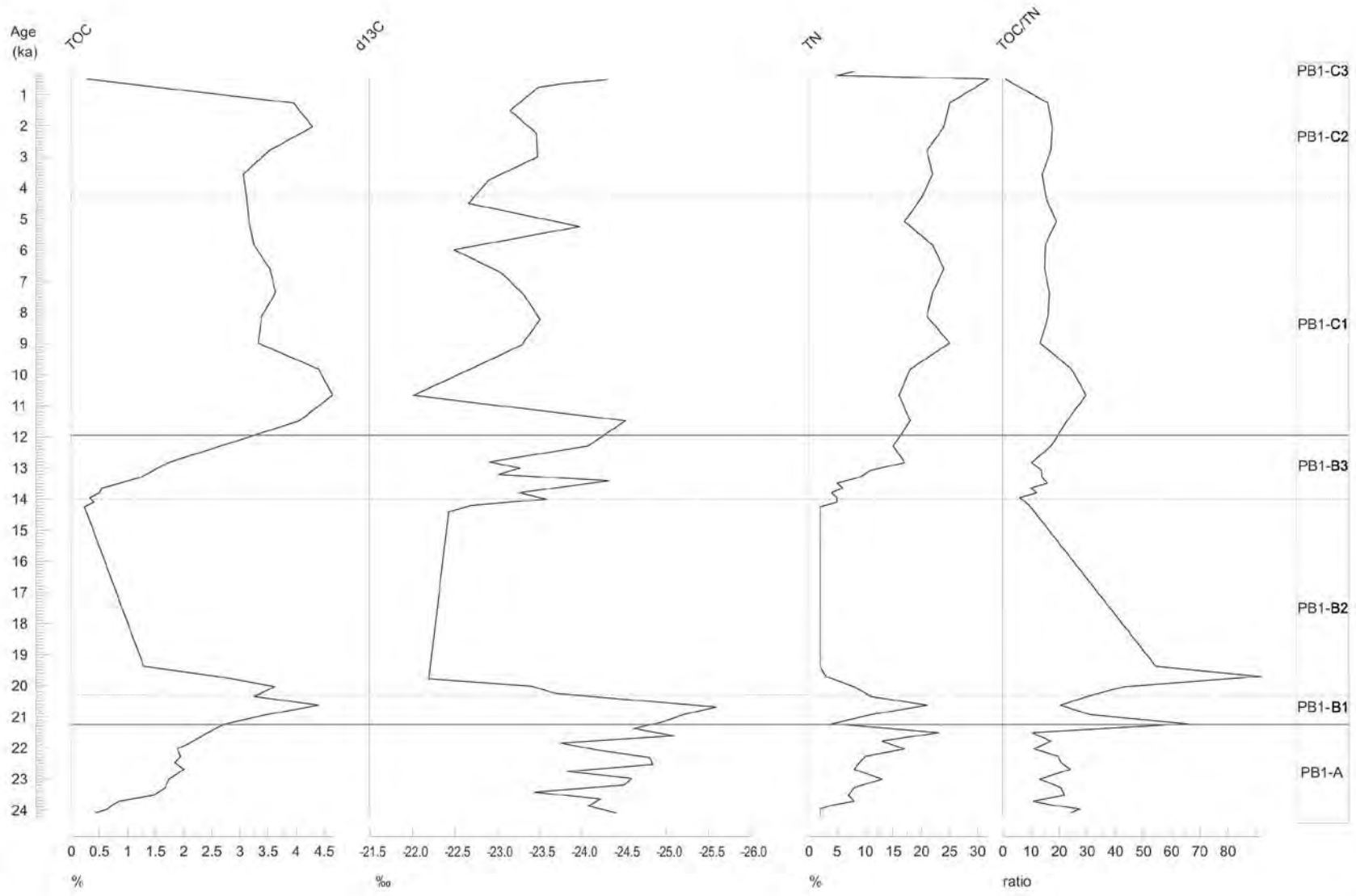

Figure 5.16 Variation in total organic carbon (TOC), $\delta^{13}C$, total nitrogen (TN) and the ratio TOC/TN for the PB-1 core.

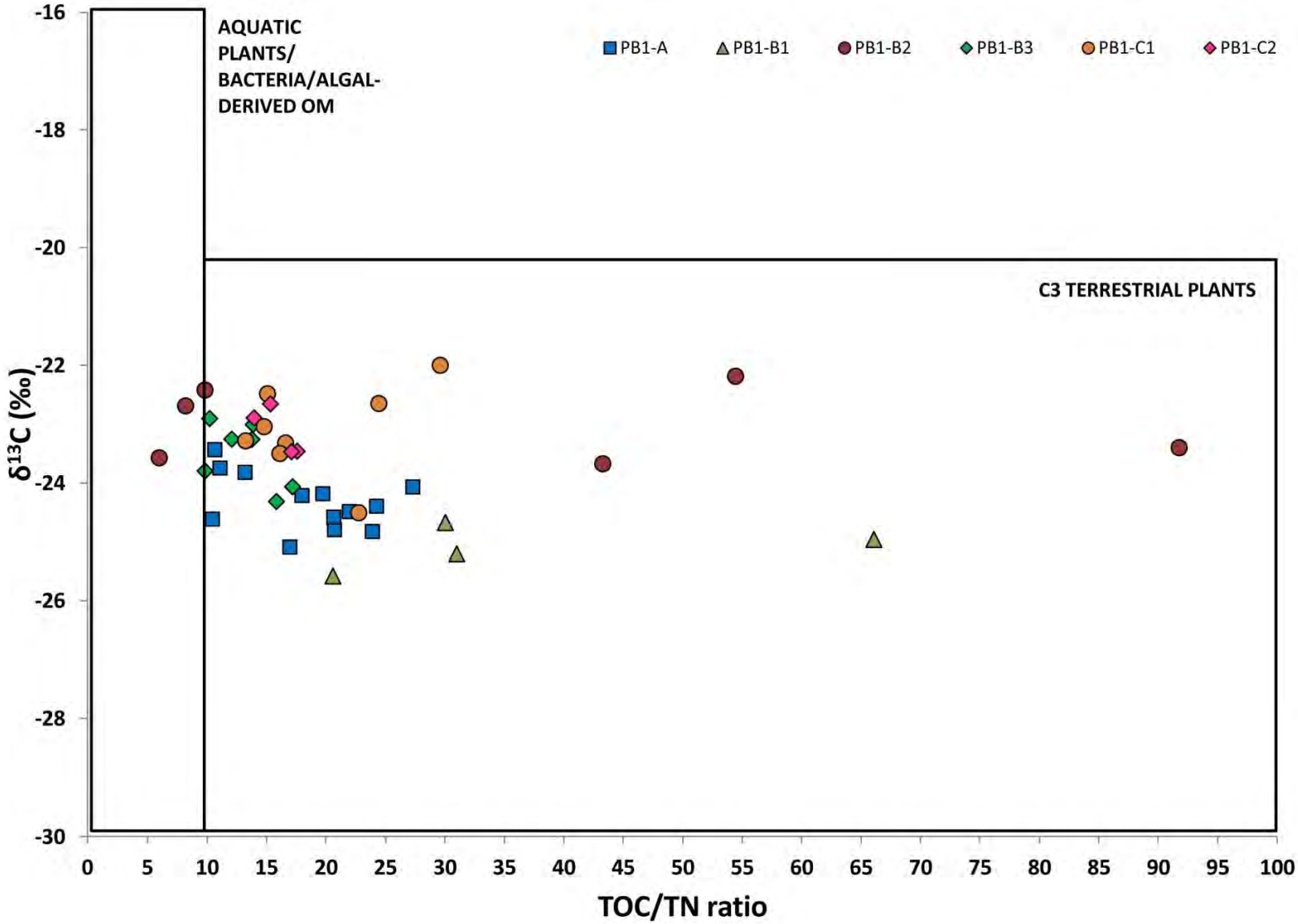

Figure 5.17 Plot of the relationship between $\delta^{13}C_{TOC}$ and TOC/TN grouped according to pollen assemblage zone for Pearly Beach 1

5.3 Rietvlei Still Bay

5.3.1 Stratigraphy and sedimentology

A stratigraphic description of the Rietvlei Still Bay 2 (RVSB-2) core is given in Figure 5.18, together with the laser particle size analysis results (Figure 5.19 and 5.20 and Appendix F).

The 360 cm core consists primarily of poorly-sorted silty sands with slight increases in the clay and silt fractions at 130 cm and 270 – 330 cm (Figure 5.19). The 80 – 330 cm section is distinctly different from the rest of the sequence comprising of pale carbonate-rich sediments with feint orange mottles.

The top 70 cm of the core contains abundant macro-plant remains predominantly of *Phragmites australis*. Mollusc shells and fragments of other marine micro-fauna were found throughout most of the core and are especially evident between 150 and 280 cm.

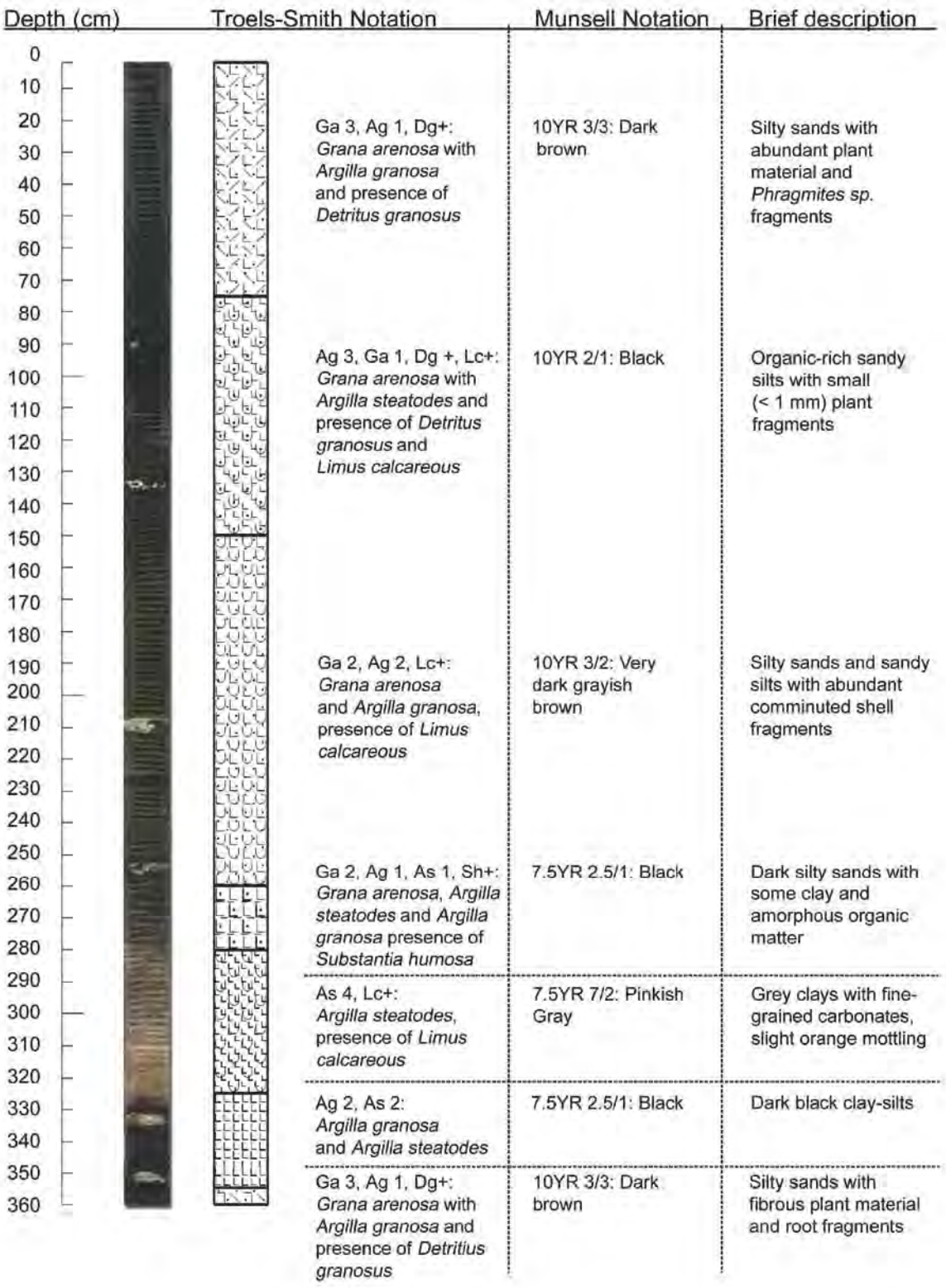

Figure 5.18 Stratigraphic description of Rietvlei Still Bay 2 (RVSB-2) employing the Troels-Smith sediment composition notation (Troels-Smith, 1955) and the Munsell Colour notation.

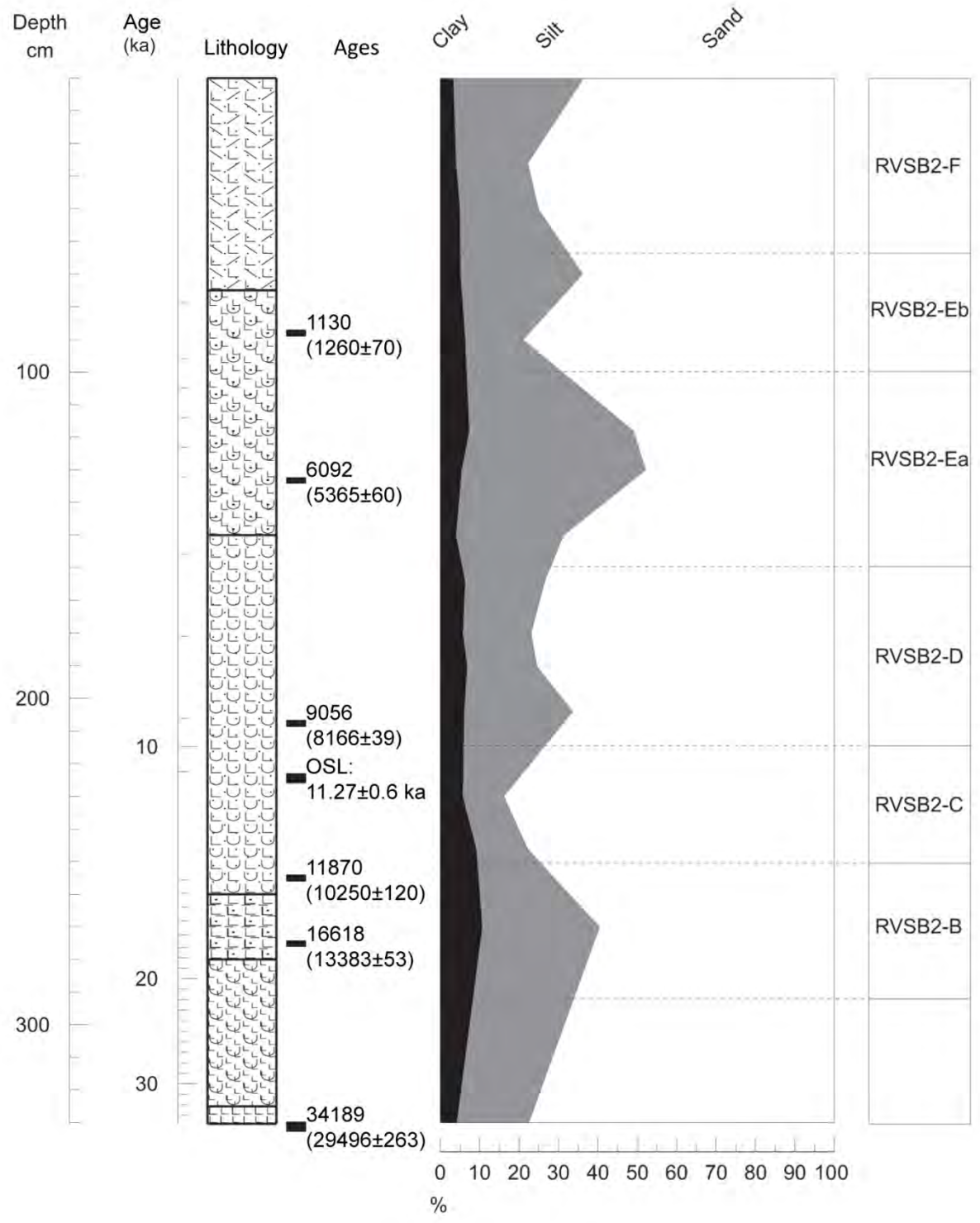

Figure 5.19 Rietvlei Still Bay 2 (RVSB-2) particle size analysis summary diagram displaying percentages of clay (0 – 2 µm), silt (2 – 20 µm) and sand (20 – 2000 µm) [data source: Dr A. Carr].

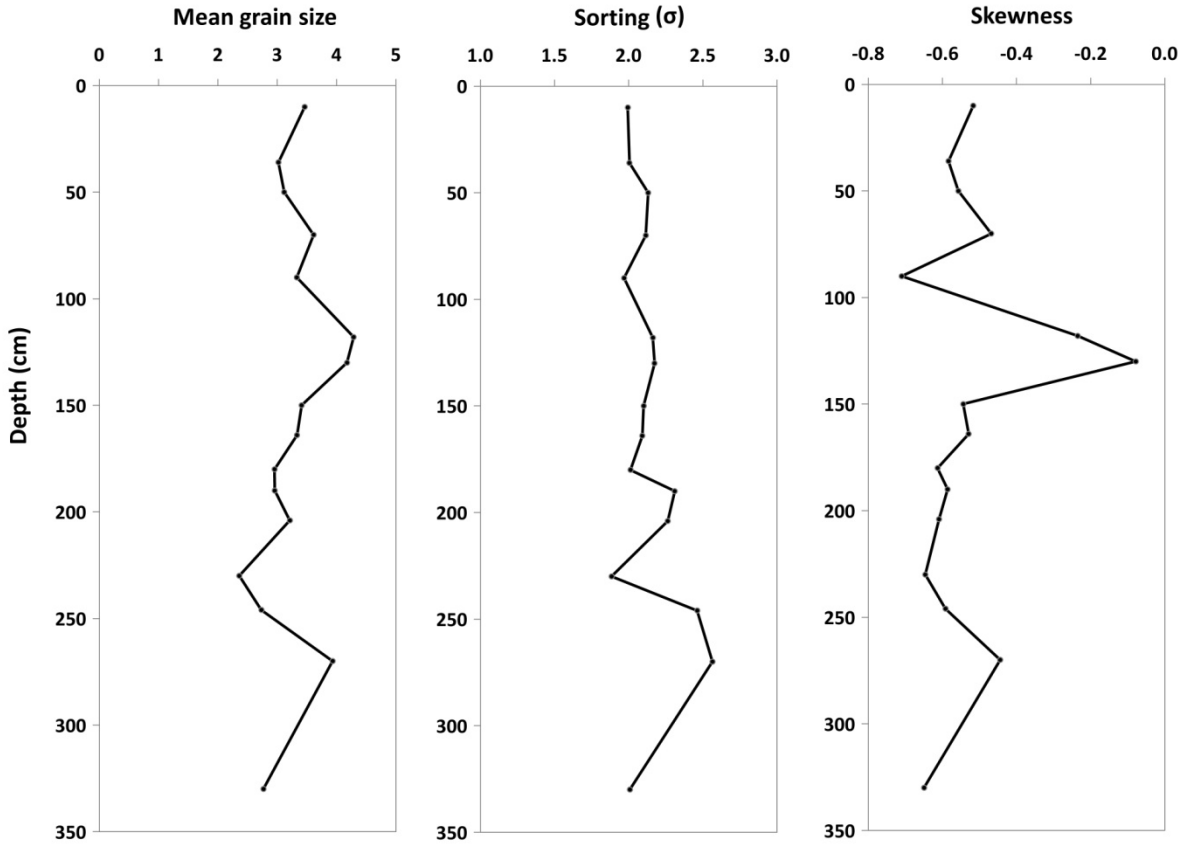

Figure 5.20 Rietvlei Still Bay 2 (RVSB-2) grain size distribution statistical parameters (ϕ) [data source: Dr A. Carr].

5.3.2 Chronology and sediment accumulation

The radiocarbon ages together with an OSL age and their calibration data are presented in Table 5-4. Much like Pearly Beach's radiocarbon results, there is a small reversal between the two ages from near the base of RVSB-2 (Figure 5.21). Given the larger errors associated with conventional radiocarbon dating in comparison to AMS, these two samples have very similar 2 σ calibrated age ranges (Table 5-4, Figure 5.22). Therefore an average of these two ages was used for interpolations of sample ages.

The results therefore indicate that RVSB-2 spans the period ~33 ka to present, encompassing the Holocene and the LGIT. The orange mottles evident within 270 – 330 cm section most probably represent minor oxidation which could be a result of shallow-water conditions in the wetland or sub-aerial exposure of the sediment during that period (Carr et al., 2010a). It is thus possible that this section may encompass a break in deposition (Figure 5.21).

Table 5-4 Rietvlei Still Bay 2 (RVSB-2) radiocarbon and calibrated ages.

Laboratory ID	Average depth (cm)	Measurement method	14C age yr BP	F14C ± 1 σ	1 sigma error	Calibration data	95.4 % (2σ) cal age range	Relative area under distribution	median probability	Date (2σ) range (AD)	OSL age (ka)	OSL age error (ka)
UBA-19735	2.5	AMS	Greater than modern^	1.0103 ± 0.0048		Wellington				1955 - 1957		
A-14939	88.0	GPC	1260		70.0	SHCal04	cal yr BP 977 – 1 274	1	1130			
A-15438	133.0	GPC	5365		60.0	SHCal04	cal yr BP 5 936-6 215 cal yr BP 6 240-6 271	0.948000 0.052000	6092			
UBA-18048	207.5	AMS	8166		39.0	SHCal04	cal yr BP 8799-8802 cal yr BP 8807-8825 cal yr BP 8871-8878 cal yr BP 8977-9145 cal yr BP 9166-9254	0.000857 0.010763 0.004020 0.908147 0.076213	9056			
	224.5	OSL									11.27	0.6
A- 14938	255.0	GPC	10250		120.0	SHCal04	cal yr BP 11 366 – 11 137 cal yr BP 11 393 – 12 245 cal yr BP 12 265 – 12 375	0.001590 0.946000 0.052500	11870			
UBA-19737	274.5	AMS	13439*		58.18*	INTCAL09	cal yr BP 16 195 - 16 881	1	16618			
UBA-19736	331.5	AMS	29552*		264.09*	INTCAL09	cal yr BP 33 441 - 34 738	1	34189			
A- 14937	351.5	GPC	27686*		1135.25*	INTCAL09	cal yr BP 30 363 – 34 622	1	32280			

AMS = Accelerated mass spectrometry
GPC = Gas proportional counting
OSL = Optically stimulated luminescence
^Modern = 1950 AD
F14C = fraction modern
The age range for the greater than modern sample was calculated from the Wellington dataset (Manning and Melhuish, 1994) available from *CALIBomb* (Reimer and Reimer, 2010; http://calib.qub.ac.uk/CALIBomb/frameset.html) (Reimer et al., 2004b)
SHCal04 (McCormac et al., 2004); INTCal09 (Reimer et al., 2009)
***Adjusted for recommended SH offset of 56 +/- 24 (McCormac et al., 2004)**

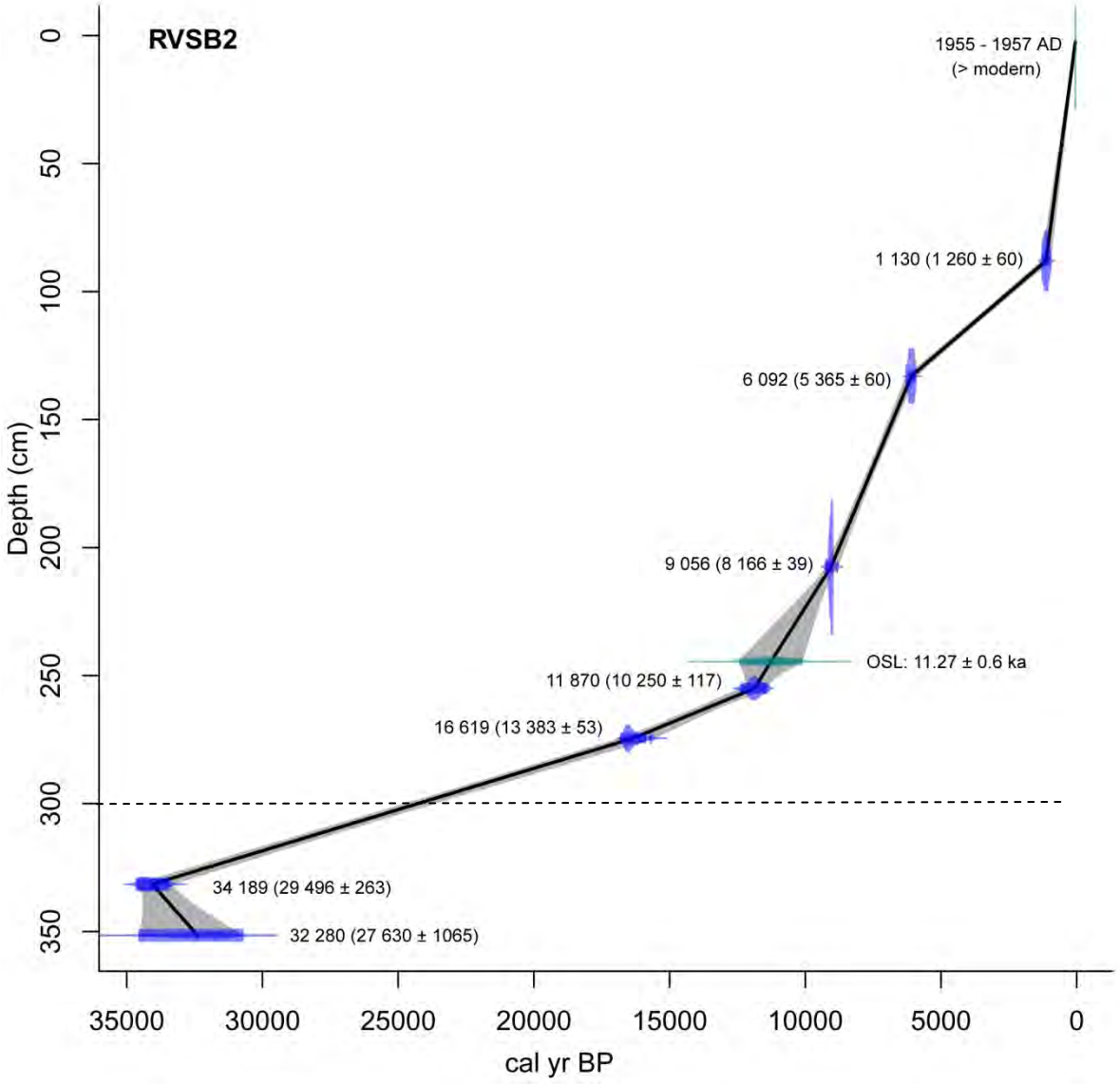

Figure 5.21 Age-depth model for Rietvlei Still Bay 2, generated in R using CLAM (Blaauw, 2010). The median probability calibrated ages are labelled and the uncalibrated ages with errors are provided in parentheses (apart from the first age range which is the greater than modern sample's AD date range). Possible hiatus at 300 cm. Grey envelopes show the 95% confidence intervals, dark blue histograms indicate the ^{14}C calibrated distribution using SHCal04 (McCormac et al., 2004) or IntCal09 (Reimer et al., 2009) and the light blue histogram indicates the OSL age distribution (see Table 5-4).

The age-depth model (Figure 5.21) indicates that sedimentation rates were relatively high for the Holocene (0 – 255 cm) with an average rate of 0.29 mm yr^{-1}. This is in comparison to the 0.04 mm yr^{-1} average sedimentation rate for the late Pleistocene section (255 - 340 cm). The top 88 cm has the highest sedimentation rate - 0.79 mm yr^{-1}. In general, accumulation rates are lower than those established for Pearly Beach.

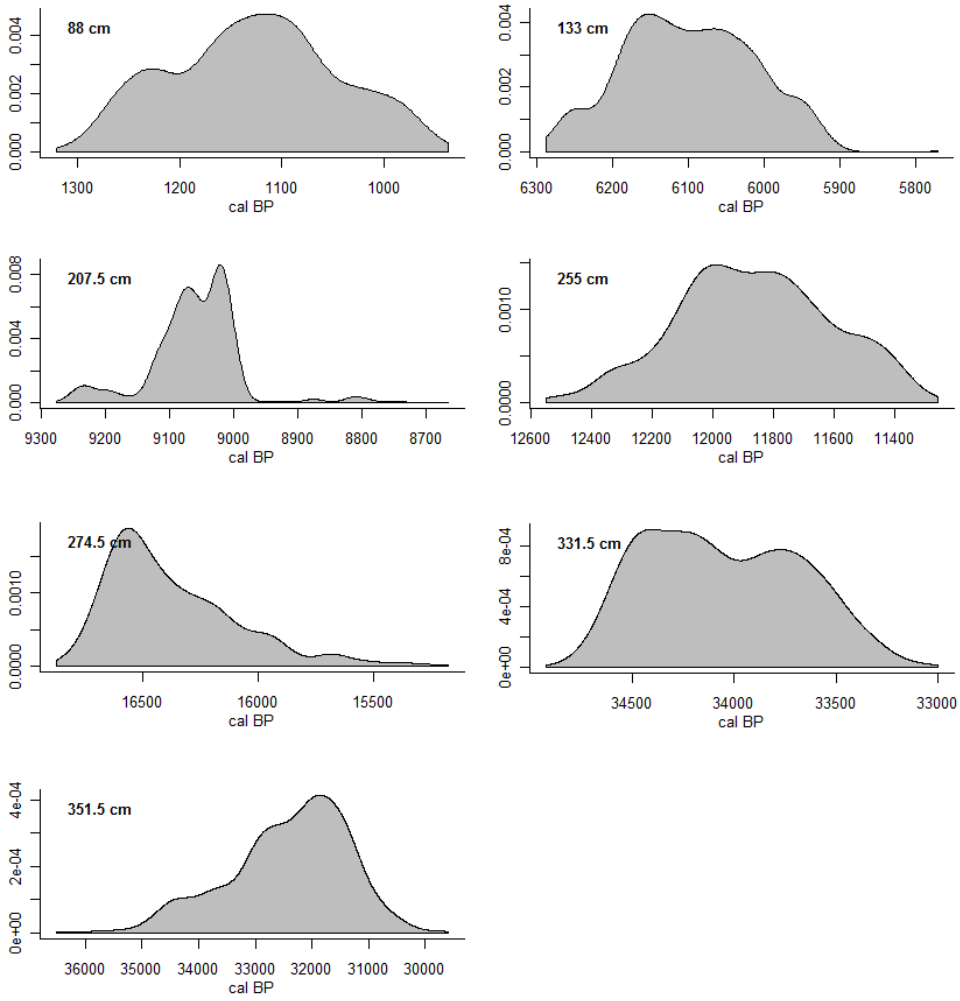

Figure 5.22 Calibration curves for RVSB-2's radiocarbon ages.

5.3.3 Pollen and microscopic charcoal analyses results

A total of 86 samples were processed for pollen and microscopic charcoal analysis, however 28 of these were either devoid of pollen altogether or contained too low concentrations. For the remaining 58 samples, an average of 500 grains was counted per level (see Appendix G for absolute counts).

Pollen preservation was variable with relatively high pollen concentrations (mean = $7.2x10^4$ grains g^{-1}) found within the top 2.2 m of the core, after which concentrations dropped considerably towards the base. The two sections of the core that contained inadequate pollen concentrations for analysis were from 220 – 260 cm and 270 – 330 cm, corresponding to the base of a sand layer and a calcareous/clay-rich zone. Pollen concentrations appear to correlate well with the geochemical variables and indicate that pollen preservation is strongly associated with the depositional environment.

The pollen and charcoal results are presented below as relative percentage diagrams (Figures 5.24 – 5.32). To assist interpretation, all of these diagrams (as well as the grain size and geochemical data) are divided into pollen assemblage zones using the statistical output of CONISS (Grimm, 1987) (Figure 5.26).

The overall pollen record from RVSB-2 indicates that there are distinct differences between the glacial and interglacial pollen assemblages, with the record reflecting changes in the local environmental conditions of the wetland as well as shifts in regional vegetation communities. These differences are described within the pollen assemblage zones below.

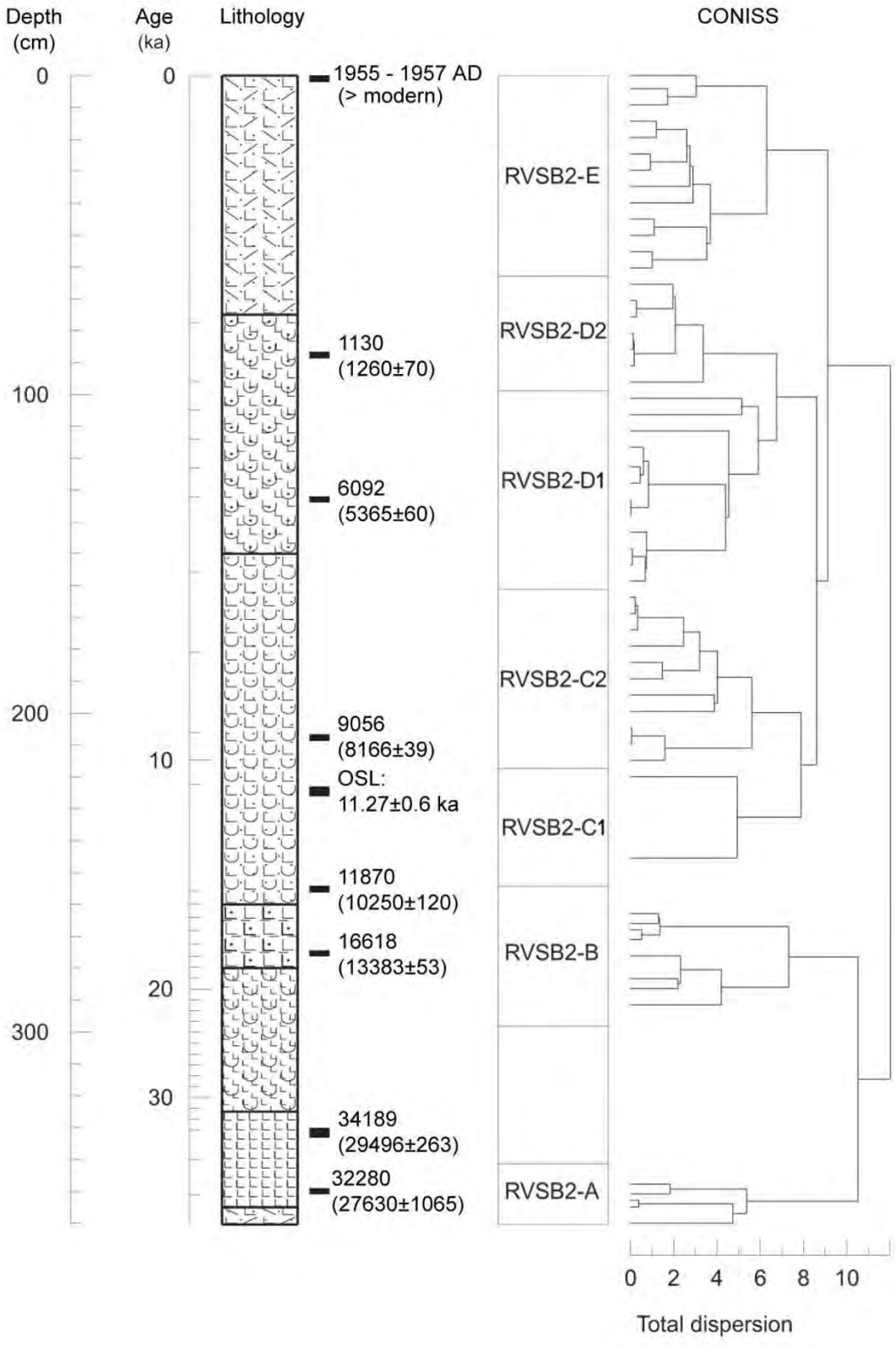

Figure 5.23 The results of CONISS displaying pollen assemblage zones for RVSB-2.

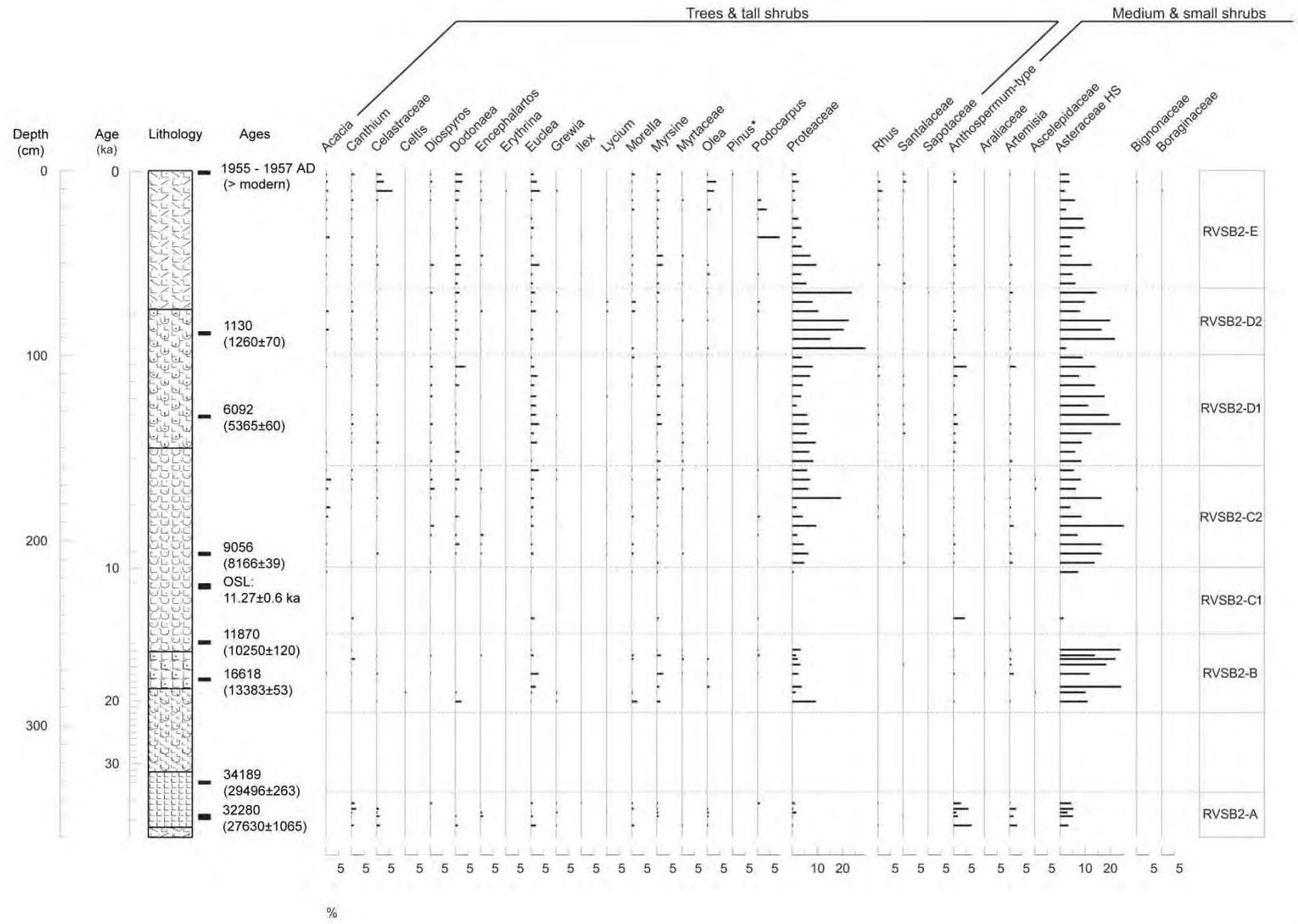

Figure 5.24 Comprehensive relative percentages pollen diagram for RVSB-2, taxa grouped according to general growth form. *Neophtye pollen type. (page 1 of 5).

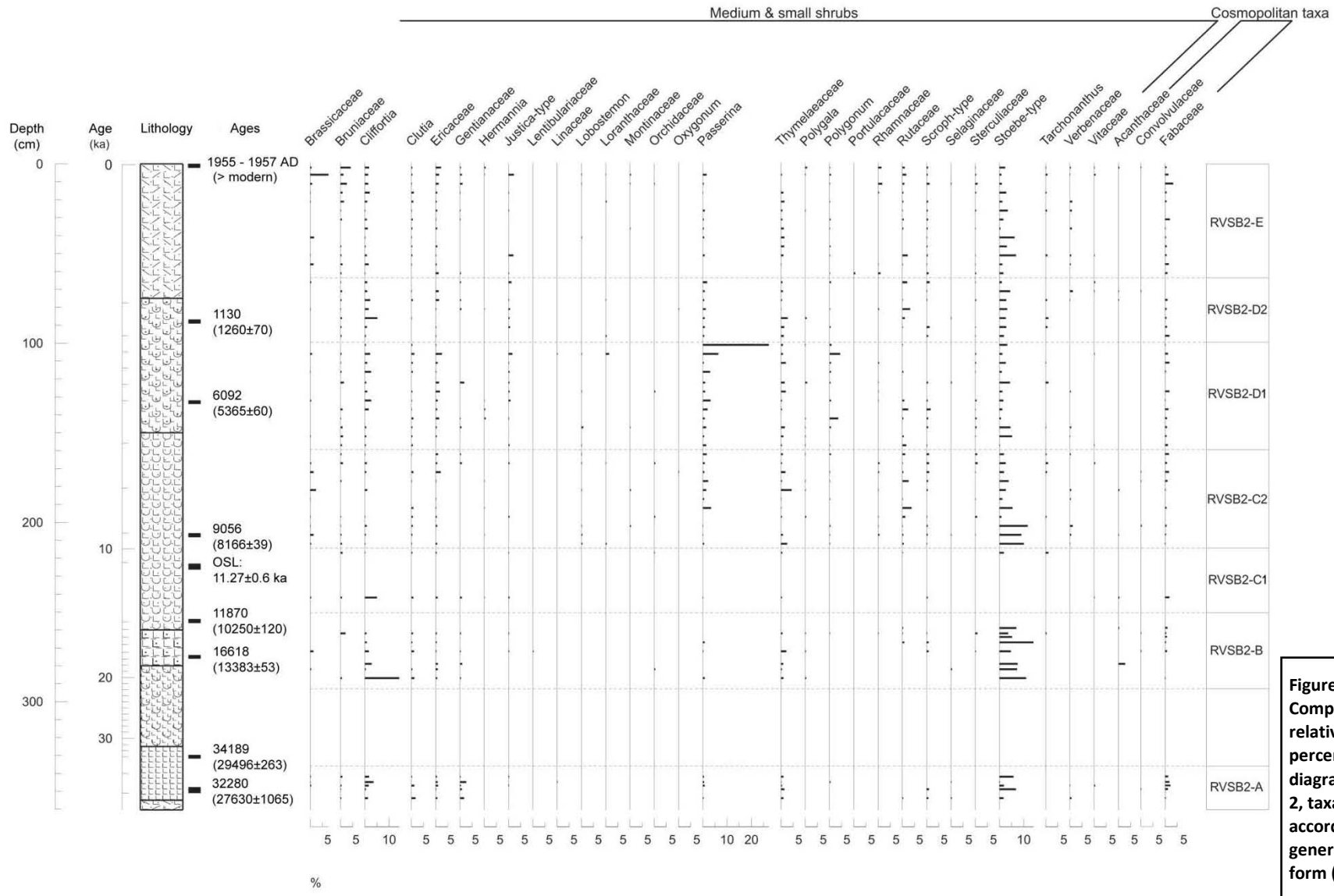

Figure 5.25 Comprehensive relative percentages pollen diagram for RVSB-2, taxa grouped according to general growth form (page 2 of 5).

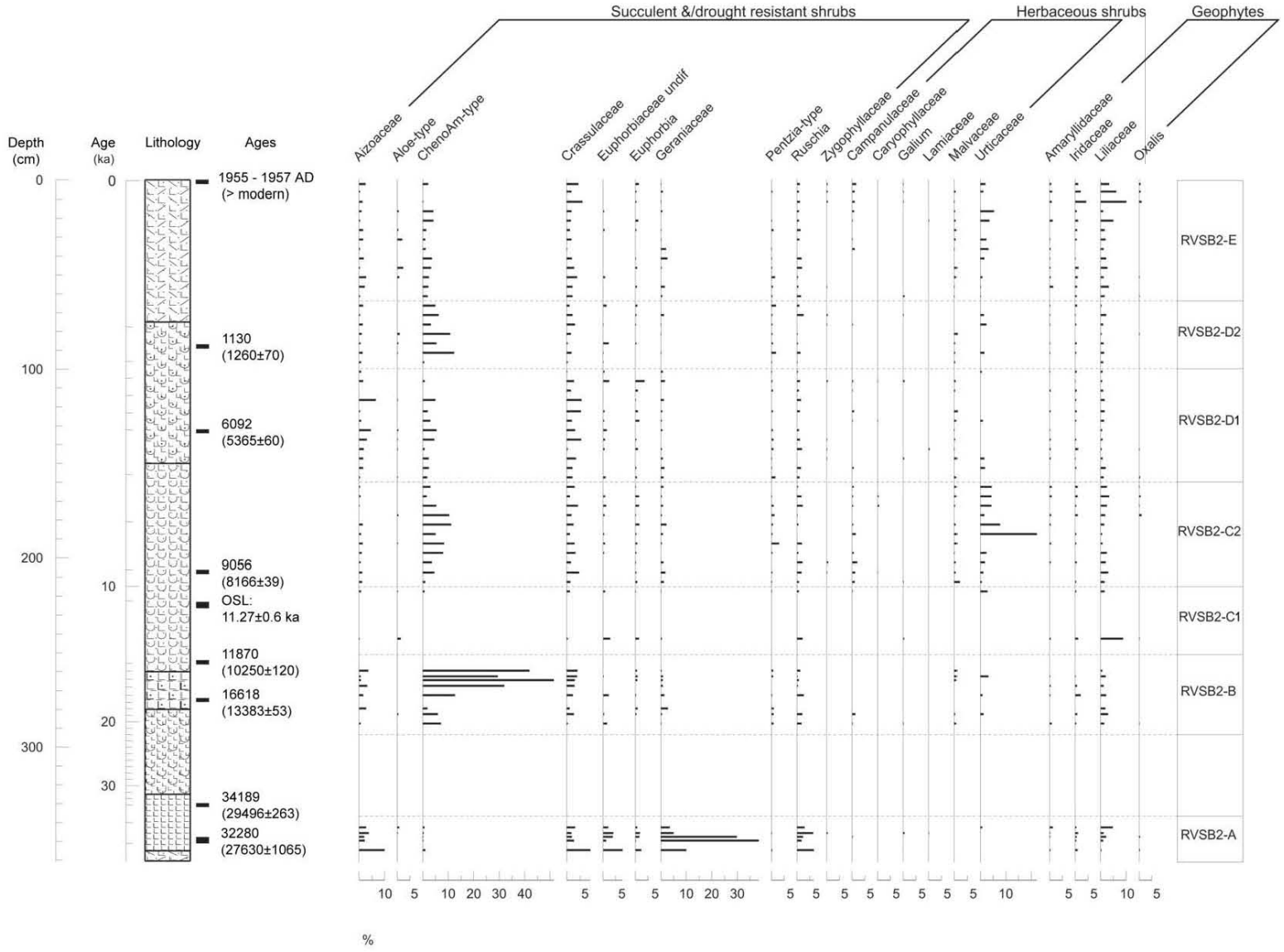

Figure 5.26 Comprehensive relative percentages pollen diagram for RVSB-2, taxa grouped according to general growth form (page 3 of 5).

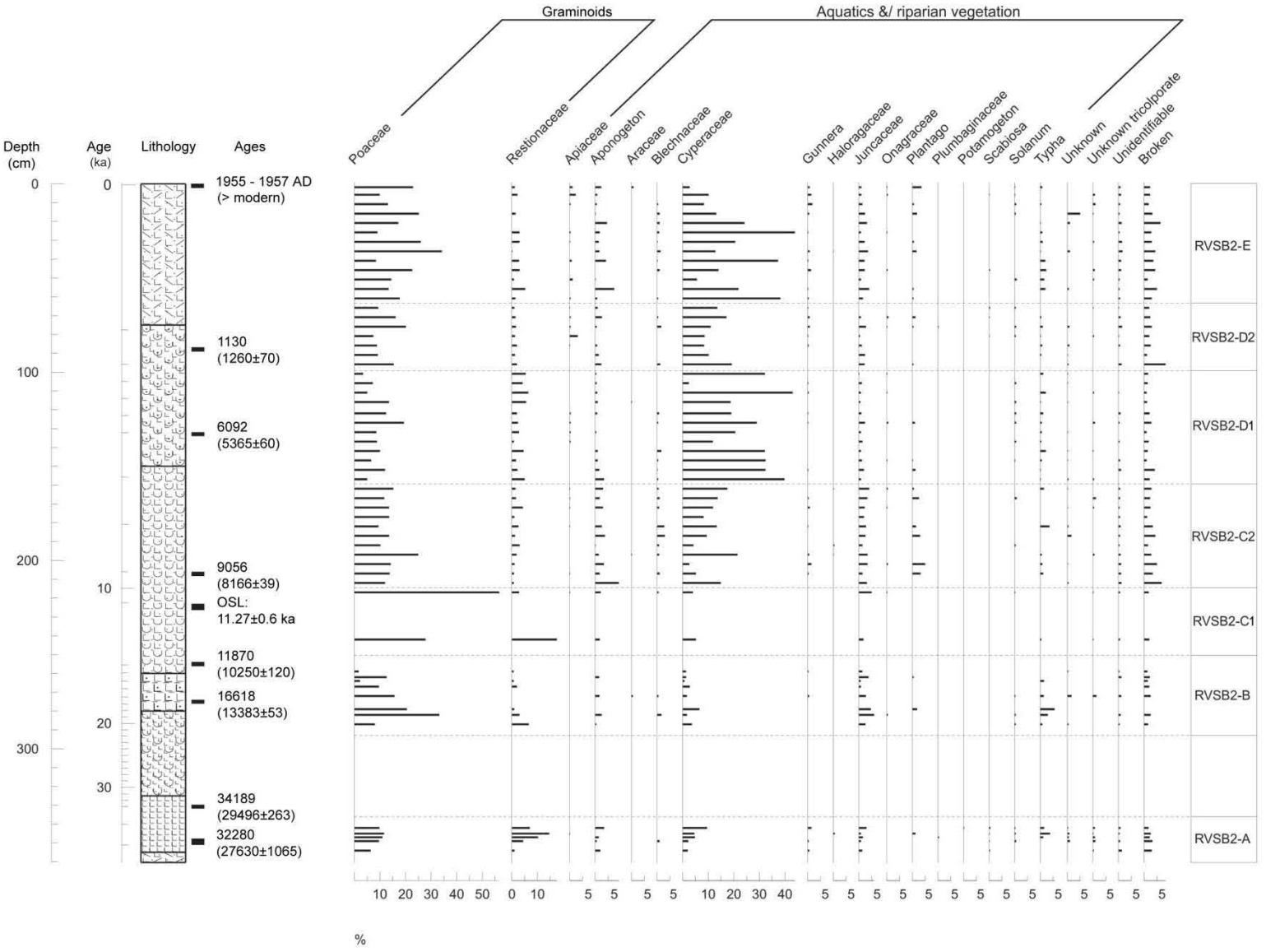

Figure 5.27 Comprehensive relative percentages pollen diagram for RVSB-2, taxa grouped according to general growth form (page 4 of 5).

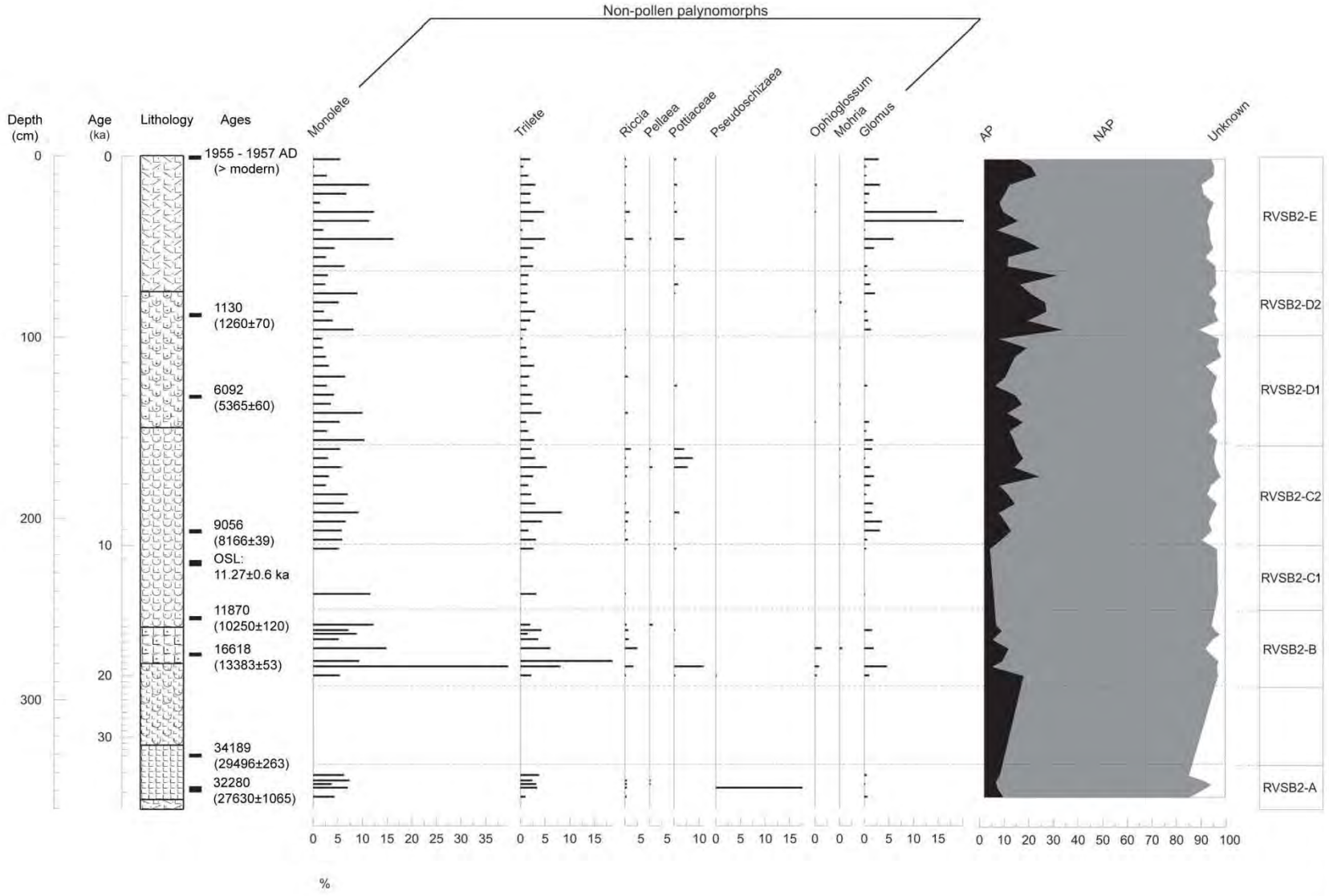

Figure 5.28 Comprehensive relative percentages pollen diagram for RVSB-2, non-pollen palynomorphs as percentages relative to the total pollen count (page 5 of 5).

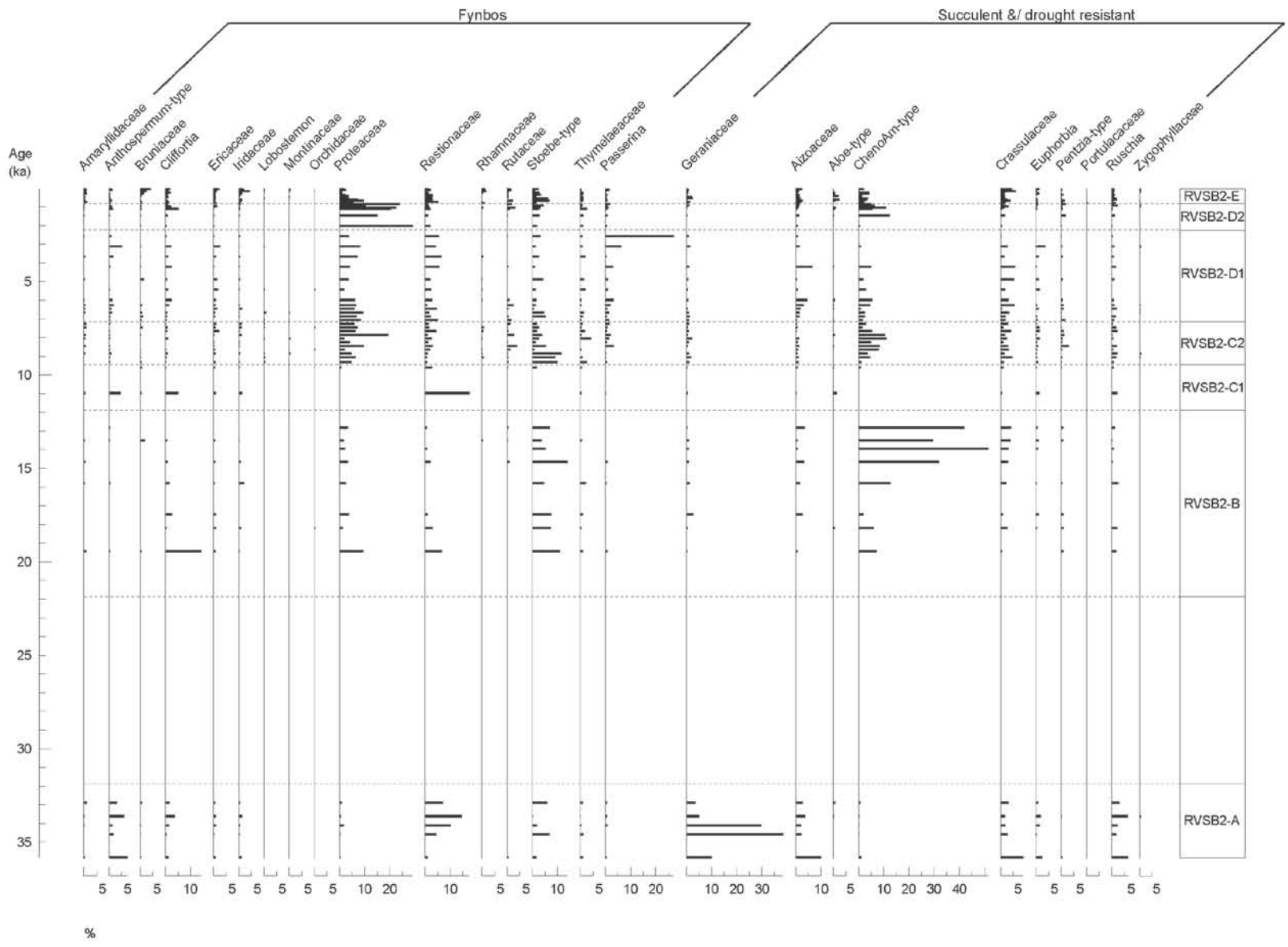

Figure 5.29 Relative percentages pollen diagram for RVSB-2, selected taxa grouped according to ecological affinities and plotted against interpolated age (page 1 of 2).

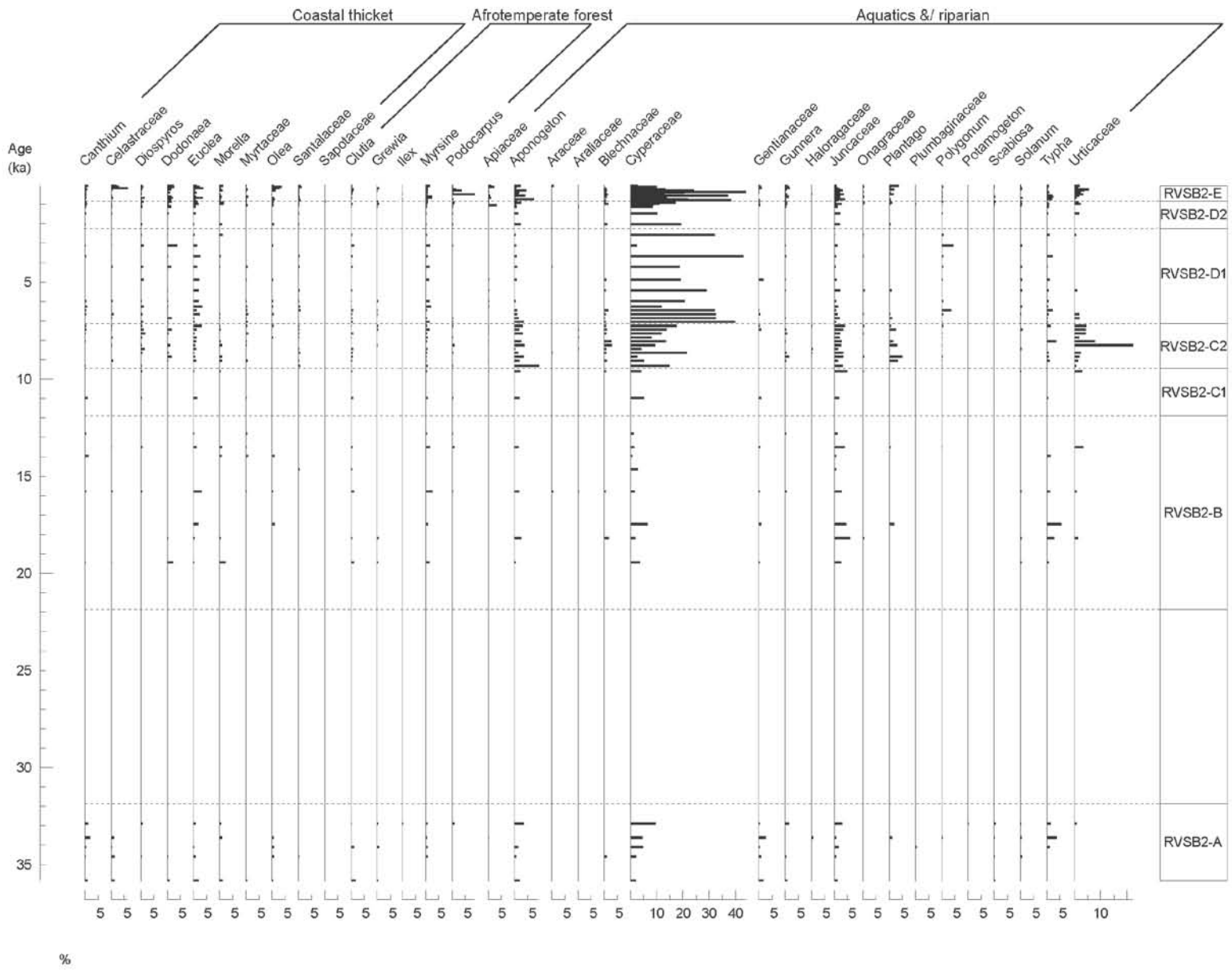

Figure 5.30 Relative percentages pollen diagram for RVSB-2, selected taxa grouped according to ecological affinities and plotted against interpolated age (page 2 of 2).

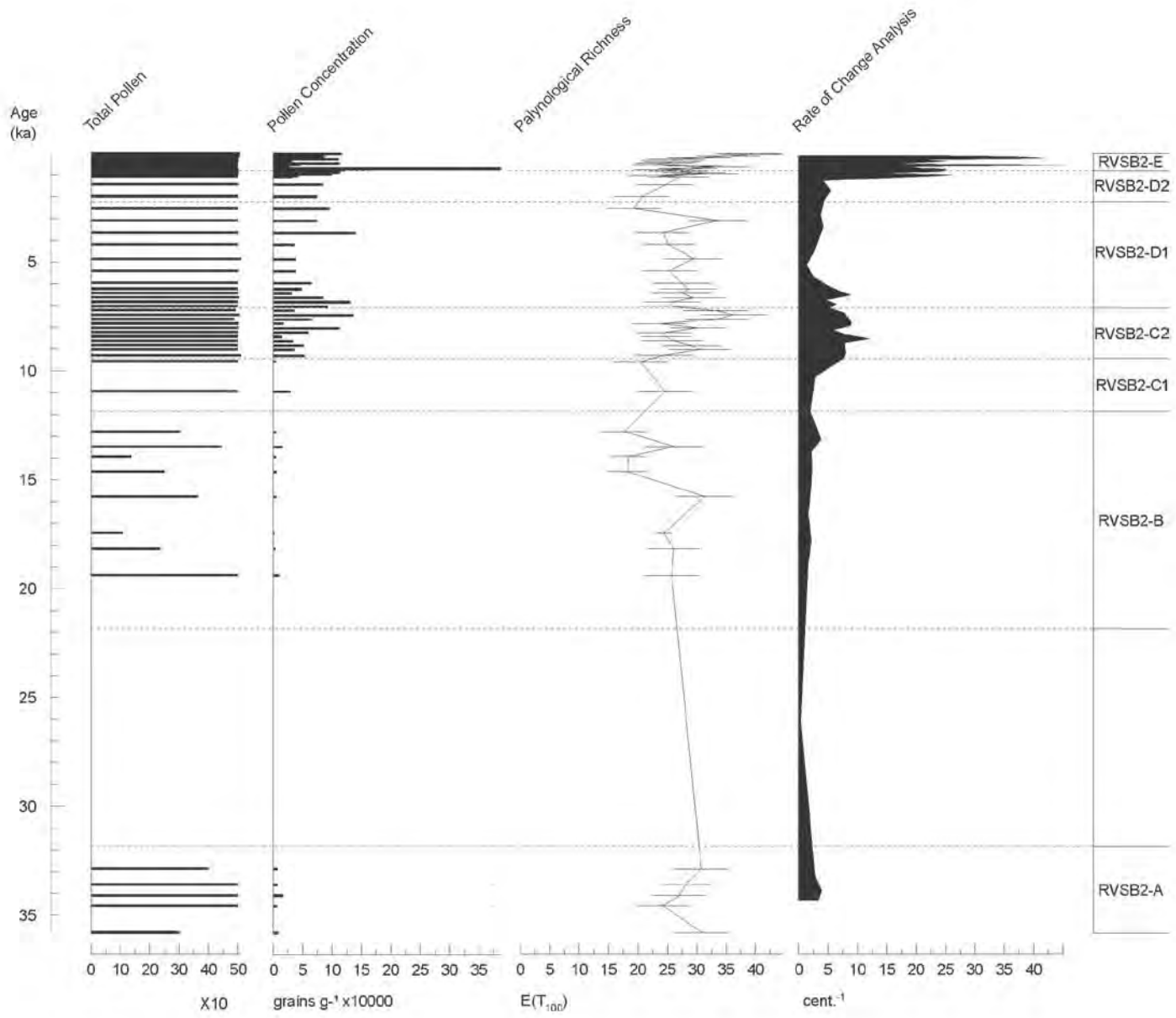

Figure 5.31 RVSB-2 total pollen counts, pollen concentrations and the palynological richness and rate of change analyses results.

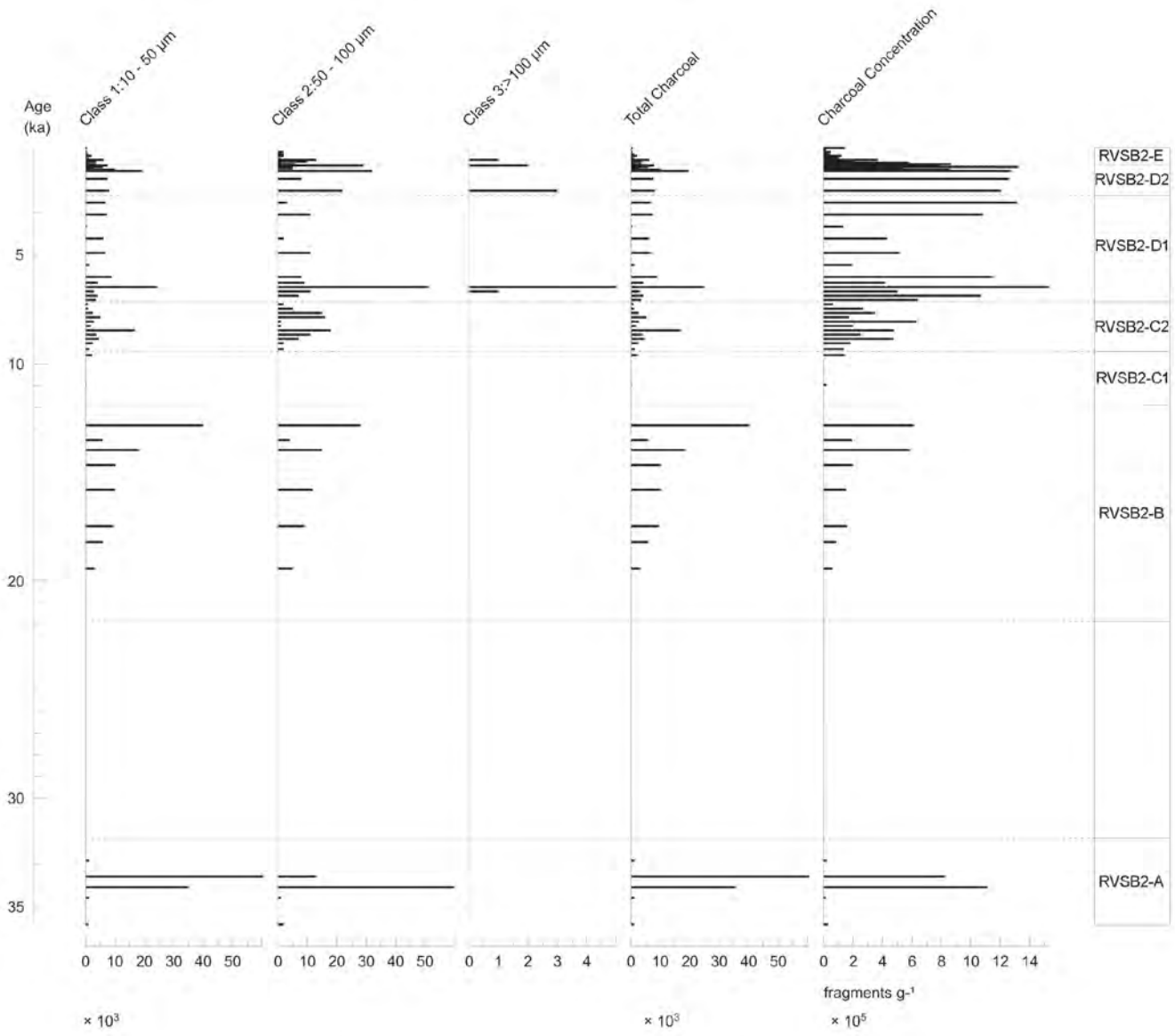

Figure 5.32 Results of RVSB-2's microscopic charcoal analysis, displaying the three size classes counted, total charcoal (sum of the three classes) and charcoal concentrations (calculated in a similar manner to pollen concentrations using the exotic marker counts).

Zone RVSB2-A: 360 – 342 cm; approximately 35.8 – 32.8 ka

This zone is characterised by reductions in local wetland taxa such as Cyperaceae and Juncaceae. Concurrently, there are significant increases in succulent and/ drought resistant taxa with peaks in Aizoaceae (10%), Crassulaceae (9%), Euphorbia undifferentiated (8%) and *Ruschia* (7%) at the base of the zone. Geraniaceae reaches exceptionally high percentages (30 – 38%) between 349 – 347 cm/~34.6 – 34.1 ka. *Artemisia* and *Anthospermum*-type are also relatively high throughout RVSB2-A in comparison to the other zones.

Fynbos taxa and arboreal pollen percentages are both reduced, with particularly low proportions of Proteaceae (less than 1%) at the base of the zone. There are lower proportions of Asteraceae (high spine variety), *Stoebe*-type and Poaceae in this zone compared to RVSB2-B. Restionaceae percentages are generally elevated relative to the majority of the other zones.

There are moderate amounts of monolete and trilete spores present within RVSB2-A together with an extremely high peak in *Pseudoschizaea* (18%) at 349 cm/~34.6 ka. Charcoal amounts (for all three classes) and concentrations are particularly high in the middle of the zone, while pollen concentrations are low throughout RVSB2-A.

Zone RVSB2-B: 287 – 252 cm; approximately 19. 4 – 11.6 ka

The dominant taxa in RVSB2-B are high spine Asteraceae, *Stoebe*-type and *ChenoAm*-type. *ChenoAm*-type reaches exceptionally high percentages (30 – 50%) between 267 – 259 cm/~14.7 – 12.8 ka. *Cliffortia* and Proteaceae are generally low except for small peaks (10 – 15%) at the base of the zone. Restionaceae and Cyperaceae are particularly low throughout RVSB2-B, whereas other local wetland taxa such as Juncaceae and *Typha* exhibit relatively high percentages. Poaceae percentages are moderately high in comparison to the previous zone, especially at 282 cm/~18.2 ka where it reaches 33%. Monolete spores also peak at 282 cm/~18.2 ka, reaching its maximum level for the sequence (40%). In addition, trilete spores are relatively high throughout the zone with a maximum percentage of 19% at 279/~17.5 ka.

Charcoal amounts and concentrations are low at the base of RVSB2-B and increase steadily towards the top. Similar to the previous zone, pollen concentrations remain very low, whereas palynological richness increases with peaks at 272 cm/~15.8 ka and 262 cm/~13.5 ka.

Zone RVSB2-C: 252 – 162 cm; approximately 11.6 – 7.2 ka

This zone is divided into two subzones described below.

Subzone RVSB2-C1: 252 – 217 cm; approximately 11.6 – 9.6 ka

This subzone only encompasses two levels within which sufficient pollen has been preserved; these are at 242 cm/~11 ka and 217 cm/~9.6 ka. RVSB2-C1 is characterised by extremely high percentages of Poaceae pollen especially at the ~9.6 ka where this taxon reaches 57%. Arboreal taxa and local wetland aquatic/riparian taxa are either absent or at very low percentages within this subzone. *Stoebe*-type also reaches its lowest percentages for the sequence within RVSB2-C1. There are peaks in *Anthospermum*-type, *Cliffortia* (5%), Liliaceae (8%) and monolete spores at ~11 ka. Restionaceae is also high (18%) at ~11 ka dropping considerably to 3% at ~9.6 ka. High spine Asteraceae percentages are low for both levels in comparison to the adjacent zones. Charcoal is almost entirely absent from RVSB2-C1. Pollen concentrations are low as is palynological richness, especially for the sample at ~9.6 ka.

Subzone RVSB2-C2: 217 – 162 cm; approximately 9.6 – 7.2 ka

There are increases in arboreal pollen percentages with Proteaceae peaking (19%) at 177/~7.8 ka. Asteraceae, high spine variety, peaks in the middle of RVSB2-C2 and tapers towards the top of the subszone. A similar trend is evident for charcoal amounts and concentrations. *Stoebe*-type proportions are elevated from the base to 202 cm/~8.8 ka, whereas *ChenoAm*-type percentages are relatively high throughout the whole subzone. Local aquatic/riparian taxa are moderately high. Cyperaceae generally increases towards the top of RVSB2-C2, exhibiting two discrete peaks at the base (15%) and at 197 cm/~8.6 ka (21%). There is a significant peak (22%) in Urticaceae at 187 cm/~8.2 ka. Poaceae percentages are fairly consistent at about 10 – 15% except for a peak at ~8.6 ka. Pollen concentrations are greatly increased compared to the previous two zones and RVSB2-C1 and unevenly increases towards the top of RVSB2-C2. Palynological richness is relatively high throughout the subzone.

Zone RVSB2-D: 162 – 66 cm; approximately 7.2 – 0.8 ka

This zone is divided into two subzones described below.

Subzone RVSB2-D1: 162 – 100 cm; approximately 7.2 – 2.5 ka

The most distinguishing features of RVSB2-D1 are a large peak in *Passerina* (27%) at the top of the

subzone and generally very high Cyperaceae percentages, especially at the top (30%) and bottom (40%) of RVSB2-D1.

Proteaceae percentages are reduced in comparison to the previous zone and subsequent subzone (RVSB2-D2). Similar to RVSB2-DC2, high spine Asteraceae peaks in the middle of this subzone. *Dodonaea* reaches its highest percentage (4%) near the top of the zone. Other coastal thicket taxa are slightly elevated for the zone (e.g. *Euclea*) in comparison to previous zones. The peak in *Dodonaea* coincides with small peaks in *Anthospermum*-type, *Artemisia*, *Euphorbia* and Euphorbiaceae undifferentiated. Aizoaceae and Crassulaceae are relatively elevated throughout most of this subzone. Restionaceae proportions are slightly higher at the top of the zone while Poaceae percentages remain fairly consistent except for a peak (20%) at 127 cm/~5.4 ka.

Charcoal concentrations are high for most of the zone with peaks in all three classes at 142 cm/~6.5 ka. Pollen concentrations generally increase towards the top of the zone with two large discrete peaks at 152 cm/~6.9 ka and 111 cm/~3.7 ka.

Subzone RVSB2-D2: 100 – 66 cm; approximately 2.5 – 0.8 ka

Proteaceae percentages are particularly high, between ~10 – 30 %, for the majority of this subzone. High spine Asteraceae and *ChenoAm*-type percentages are both relatively high for all but the bottom level. *Stoebe*-type and Poaceae frequencies are both somewhat consistent. There is a small peak (5%) in *Cliffortia* percentages at 86 cm/~1.1 ka.

Arboreal pollen and Restionaceae percentages are lower than the other subzone. Cyperaceae proportions are also reduced in comparison to adjacent zones.

Charcoal concentrations are very high for this subzone while palynological richness and pollen concentrations both increase towards the top of RVSB2-D2.

Zone RVSB2-E: 66 – 0 cm; approximately 0.8 – 0 ka

Coastal thicket taxa such as Celastraceae, *Dodonaea*, *Euclea* and *Olea* are present in greater proportions especially at the top of the zone. Proteaceae percentages are considerably lower in comparison to the previous zone. Asteraceae, high spine variety, and Restionaceae both taper towards the top of RVSB2-E. Percentages of the geophytes Liliaceae and Iridaceae are low at the base and peak at the top of the assemblage, coinciding with increases in Bruniaceae, Brassicaceae

and Crassulaceae. *Stoebe*-type proportions are generally low except for two small peaks near the base. There is a peak in *Podocarpus* at 36 cm/~0.5 ka. Poaceae percentages are generally elevated reaching especially high values from the middle to the top of the zone. There is an increase in local wetland taxa with significant peaks in *Aponogeton*, *Plantago* and Cyperceae. Monolete spores amounts are also high for RVSB2-E.

Charcoal amounts are generally low with concentrations dropping towards the top of the zone. Pollen concentrations are extremely high at the base of zone reaching $3.9x10^5$ grains g^{-1} with increasing palynological richness towards the top of the assemblage.

5.3.4 Multivariate data analyses

The multivariate analyses were carried out on a selection of 20 ecologically sensitive taxa extracted from the overall RVSB-2 pollen dataset (the same subset that was used for Pearly Beach's statistical analyses, Table 5-4).

The preliminary DCA revealed gradient lengths below 3 (the longest gradient length was 1.53) therefore a PCA was performed (Leps and Smilauer, 2003). The species data was standardized and square-root transformed. The ordination was centred by species and scaling was focused on inter-sample distance.

Table 5-5 A summary table displaying the Principal Component Analysis (PCA) results for RVSB-2.

Principal component axes	1	2	3	4	Total variance
Eigenvalues	0.266	0.136	0.103	0.087	1
Cumulative percentage variance of species data	26.6	40.2	50.5	59.2	
Total sum of squares in species data	427.4				
Total standard deviation in species data TAU	0.607				

The first three principle components account for just over 50% of the variance (Table 5-5). A large proportion of the samples are grouped fairly close to the local wetland taxa: *Aponogeton*, Blechnanceae, Araceae, *Gunnera*, Haloraginaceae as well as *Podocarpus* and Ericaceae (all indications of increased moisture availability) (Figure 5.33). Many of the early Holocene samples (mainly pollen assemblage zone RVSB2-D) and the 19.42 ka sample are clustered along the Proteaceae, Sapotaceae and *Dodonaea* and *Passerina* vectors. The last five samples of the sequence

that cover the period ~36 – 33 ka are positioned away from the central cluster and close to the vectors for Geraniaceae, Crassulaceae and *Ruschi*a.

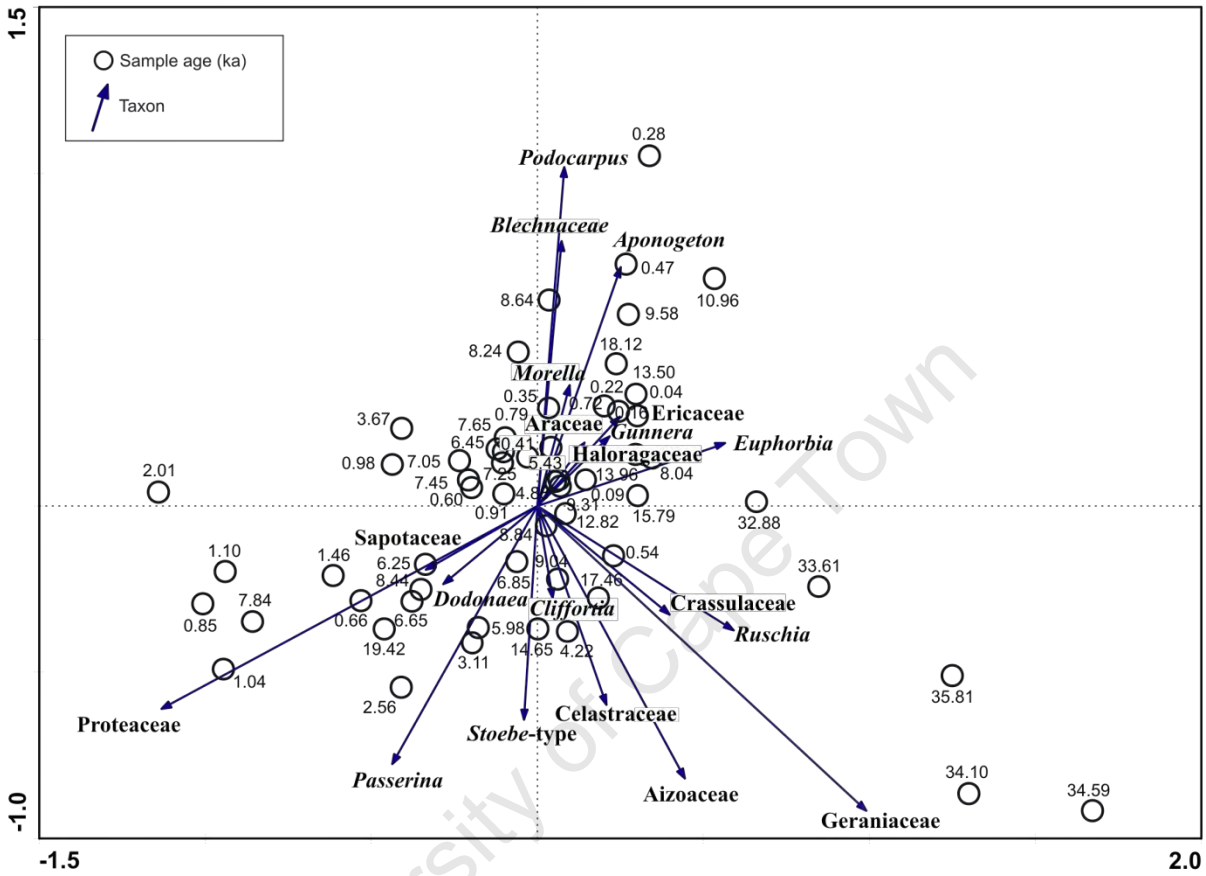

Figure 5.33 Ordination biplot mapping the taxa and sample ages scores for RVSB-2.

5.3.5 Geochemical results

TOC varies quite substantially between 0.5 and 30 %. In general, percentages are higher within the top 200 cm of the core, with particularly high values evident for pollen assemblage zone RVSB2-D. The lowest TOC amounts were recorded for zones RVSB2-B, RVSB2-C and the region of the core devoid of pollen between RVSB2-A and RVSB2-B. TOC recovers within zone RVSB2-A to reach 19% at 348 cm/~34.3 ka. Low values are also evident from short periods between 120 and 112 cm (~4.7 – 3.8 ka) and 36 to 48 cm (~0.6 – 0.6 ka). TN follows a similar trend to TOC and has a range between 0.02 and 2.06 % (Figure 5.34).

Bulk $\delta^{13}C_{TOC}$ values are generally within the typical range for C_3 vegetation (-28 to -20‰) however there is considerable variability throughout most of the sequence (Figure 5.34). The overall dataset

varies over a range of 8.7‰ which is appreciably greater than Pearly Beach's range of 4.1‰. Significant depletions in $\delta^{13}C_{TOC}$ are found from 348 and 342 cm (~34.3 ka – 32.9 ka), 202 – 142 (~8.8 – 6.5 ka) and at 94 cm/~1.8 ka. Zone RVSB-2E is characterised by relatively enriched $\delta^{13}C_{TOC}$ values. Two other sections that are notably more enriched include the base of the sequence and the sample from 322 cm (~28 ka).

TOC/CN remains relatively constant for the top 200 cm of the core, fluctuating around an average of 16. The lower section is characterised by greater variability with values ranging from 6.7 to 58.2. TOC/TN values rise steadily from zone RVSB2-B to RVSB2-A reaching a maximum (58.2) for the sequence at 342 cm/~32.9 ka.

Apart from four data points, all TOC/TN values are greater than 10 indicating that the organic matter within the core was derived from vascular plants and not algae (Figure 5.35).

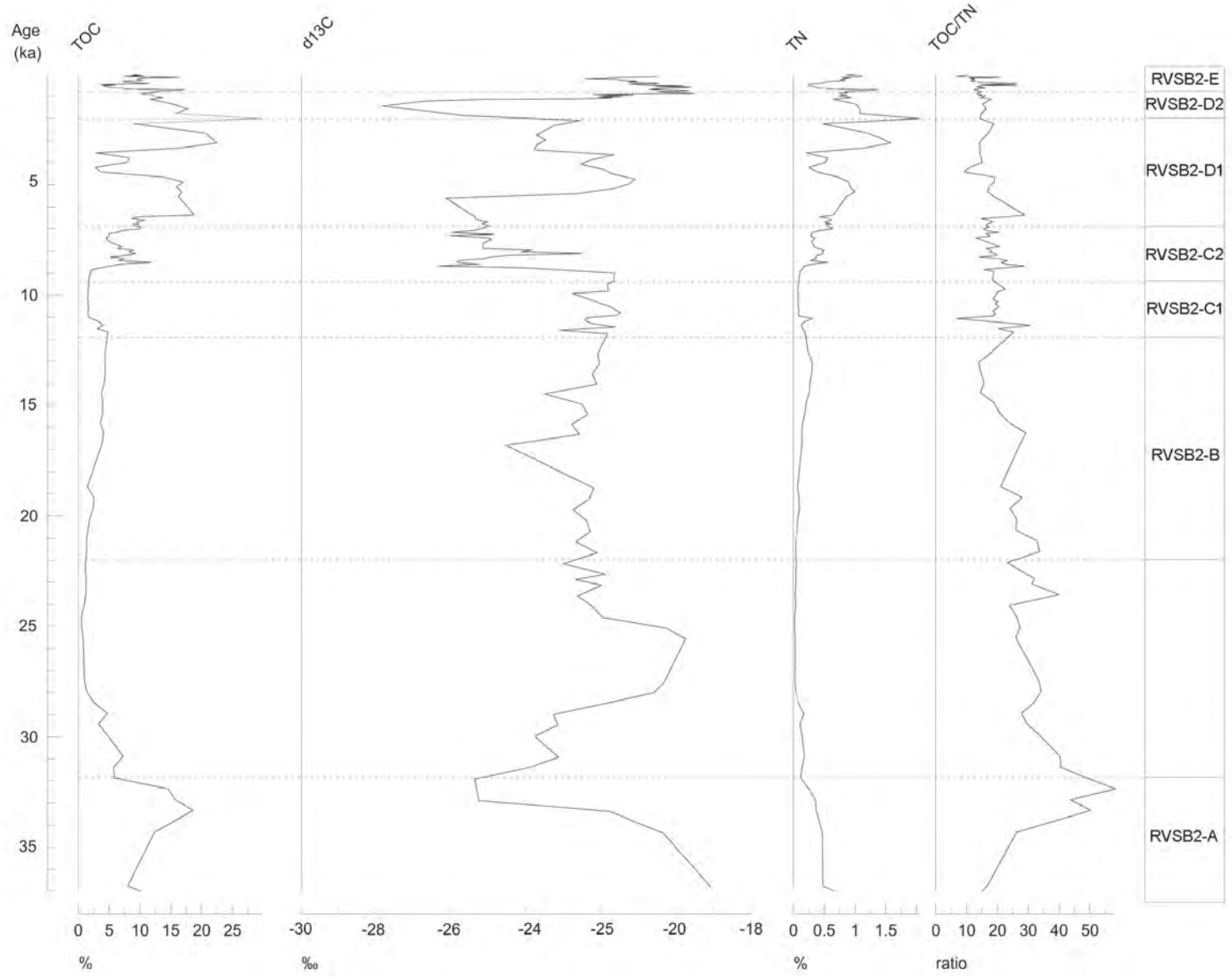

Figure 5.34 Variation in total organic carbon (TOC), $\delta^{13}C$, total nitrogen (TN) and the ratio TOC/TN for the RVSB-2 core.

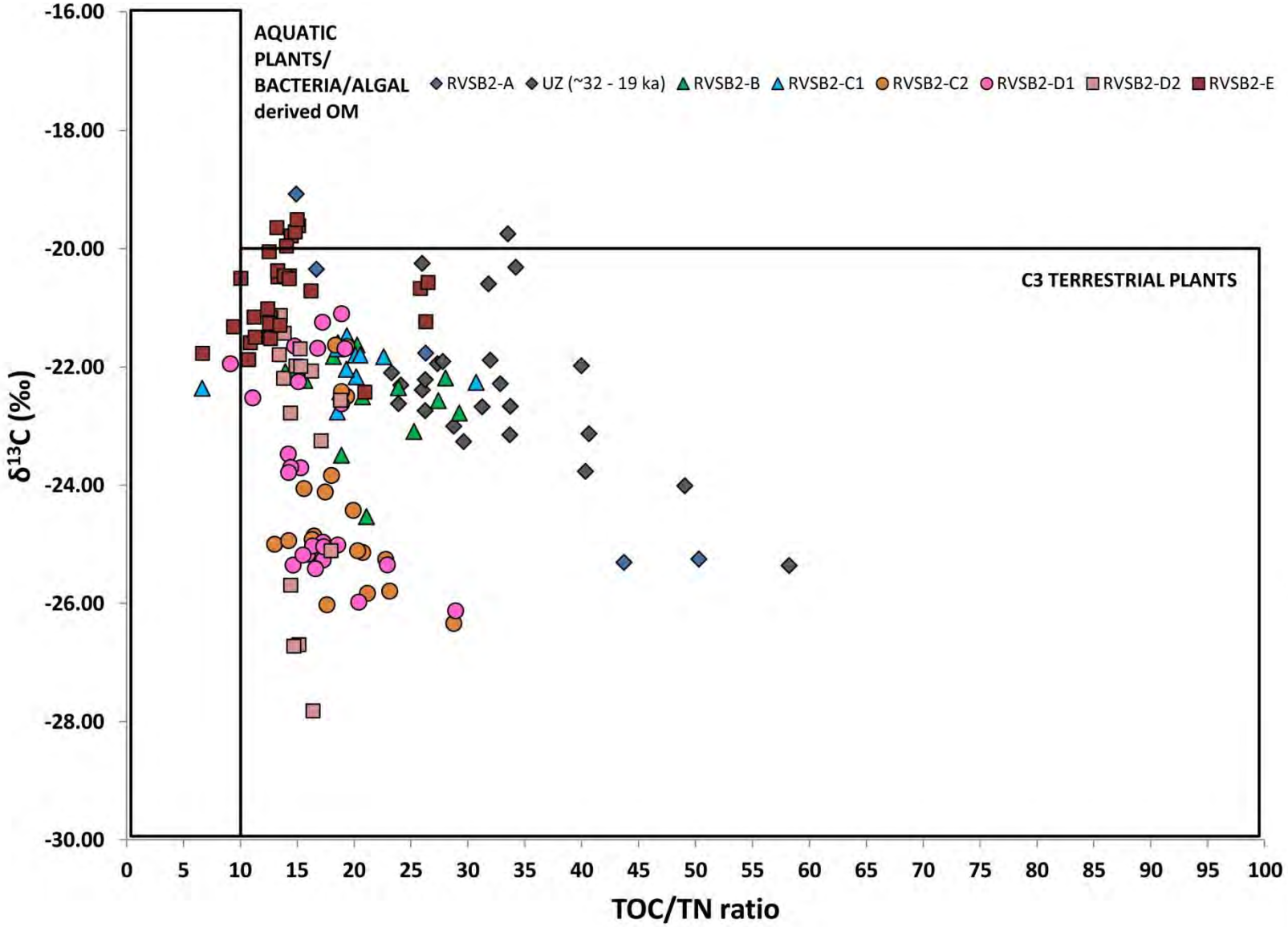

Figure 5.35 Plot of the relationship between $\delta^{13}C_{TOC}$ and TOC/TN grouped according to pollen assemblage zones for RVSB-2 (UZ is the unassigned zone between ~32 – 19 ka which is devoid of pollen).

5.4 Vankervelsvlei

5.4.1 Stratigraphy and sedimentology

'Vankervelsvlei 2010 #1' (VVV10.1) is 400 cm in length and contains sediments that exhibit marked changes in colour and composition (Figures 5.36, 5.37 and 5.38).

VVV10.1 predominately consists of poorly sorted clayey silts and fine-grained silty sands with increased proportions of clay in comparison to PB-1 and RVSB-2: VVV10.1 has an average clay content of ~20% while PB-1 and RVSB-2 contain two and six percent respectively. The mean grain size and skewness parameters (Figure 5.39) also indicate that VVV10-1 sediments are finer (larger positive values on the ϕ scale) than PB-1 and VVV10-1.

The root mat is composed of roughly 10 cm of dense Cyperaceous roots, stems and detritus. The sediment unit from the water layer interface to ~25 cm consists of highly organic material that could be considered to be peat. This unit contains a large proportion of fibrous root material and identifiable plant fragments. The dark organic-rich sediments are fine-grained with a high clay content and very small proportions of medium or coarse sand (Figure 5.37).

From 30 – 60 cm there is a slight increase in coarse-grained material with a small peak in medium-grained sand, this grades into finer-grained lighter grey clays which exhibit slight orange mottling. The section from ~90 cm to ~335 cm is dominated by dark, organic-rich silty clays with small plant fragments (Figures 5.37 and 5.38).

There is a significant increase in coarse-grained particles (primarily the medium sand fraction) between 335 and 350 cm. This section is comprised of very poorly sorted, dark brown silty sands with mottles of paler sands. The bottom stratigraphic unit has proportions of clay and silt similar to the section between 90 and 335 cm however it is much lighter in colour.

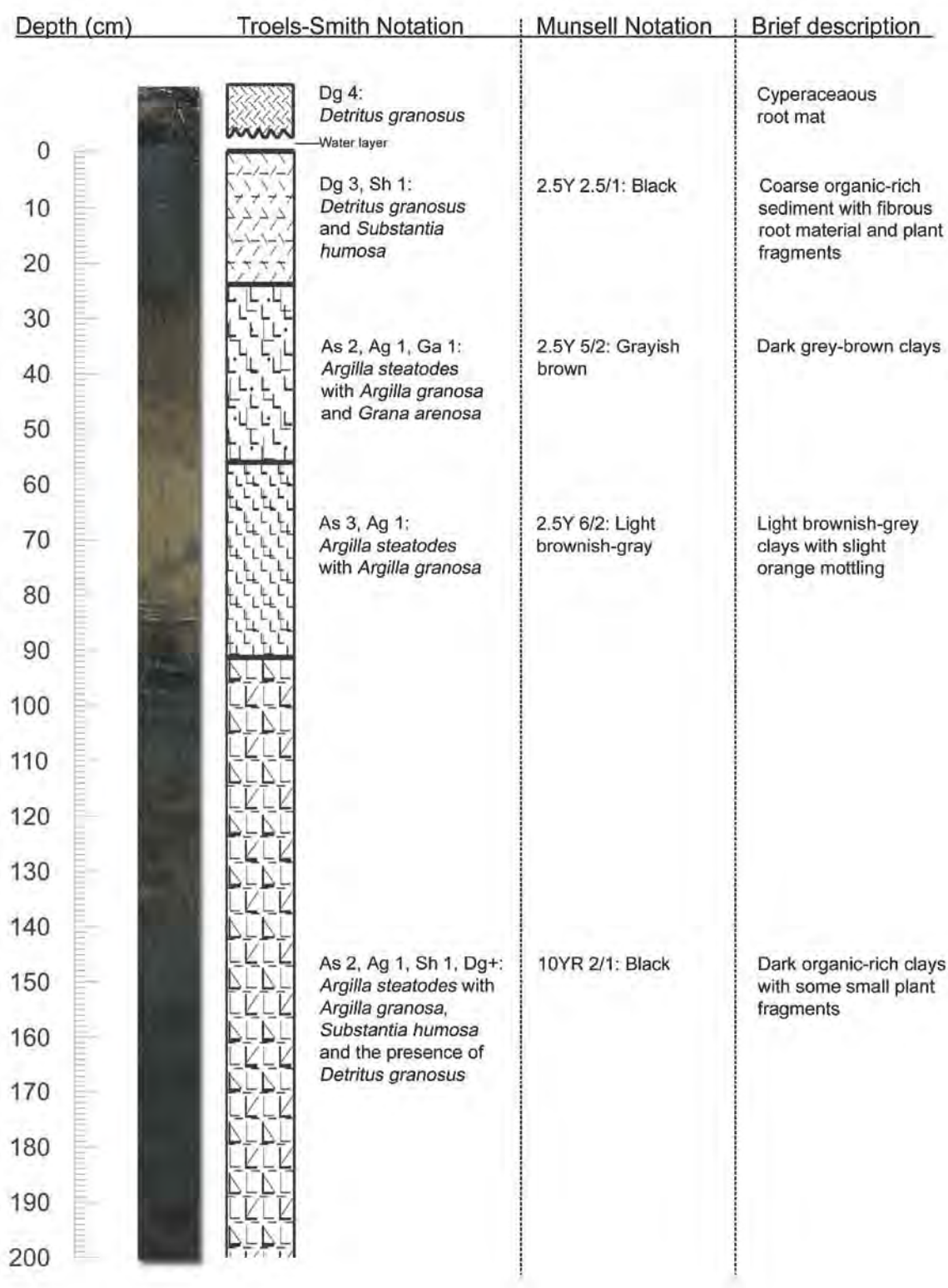

Figure 5.36 Stratigraphic description of Vankervelsvlei 2010 #1 (VVV10.1) section A (0-200 cm) employing the Troels-Smith sediment composition notation (Troels-Smith, 1955) and the Munsell Colour notation.

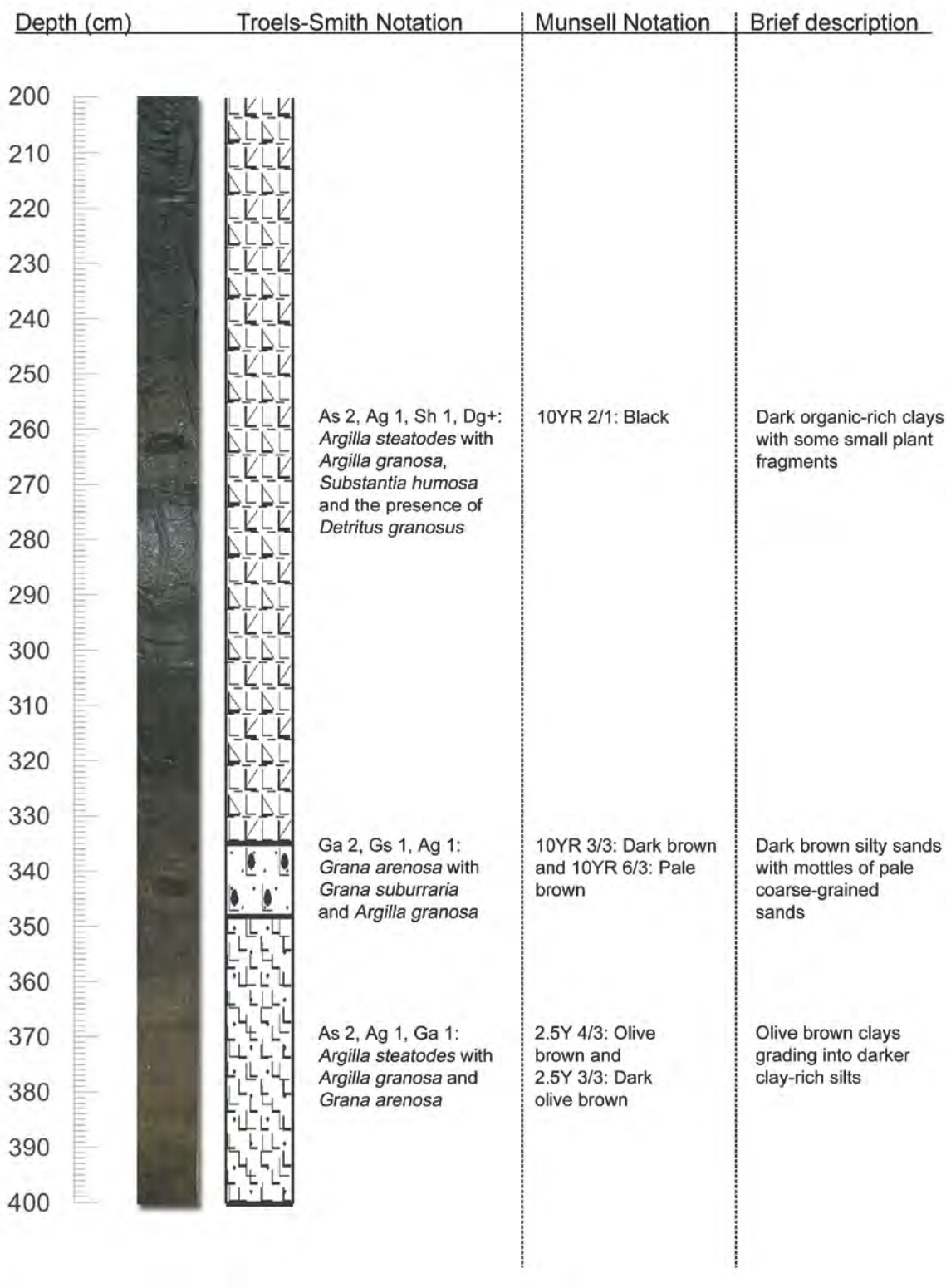

Figure 5.37 Stratigraphic description of Vankervelsvlei 2010 #1 (VVV10.1) section B (200 - 400 cm) employing the Troels-Smith sediment composition notation (Troels-Smith, 1955) and the Munsell Colour notation.

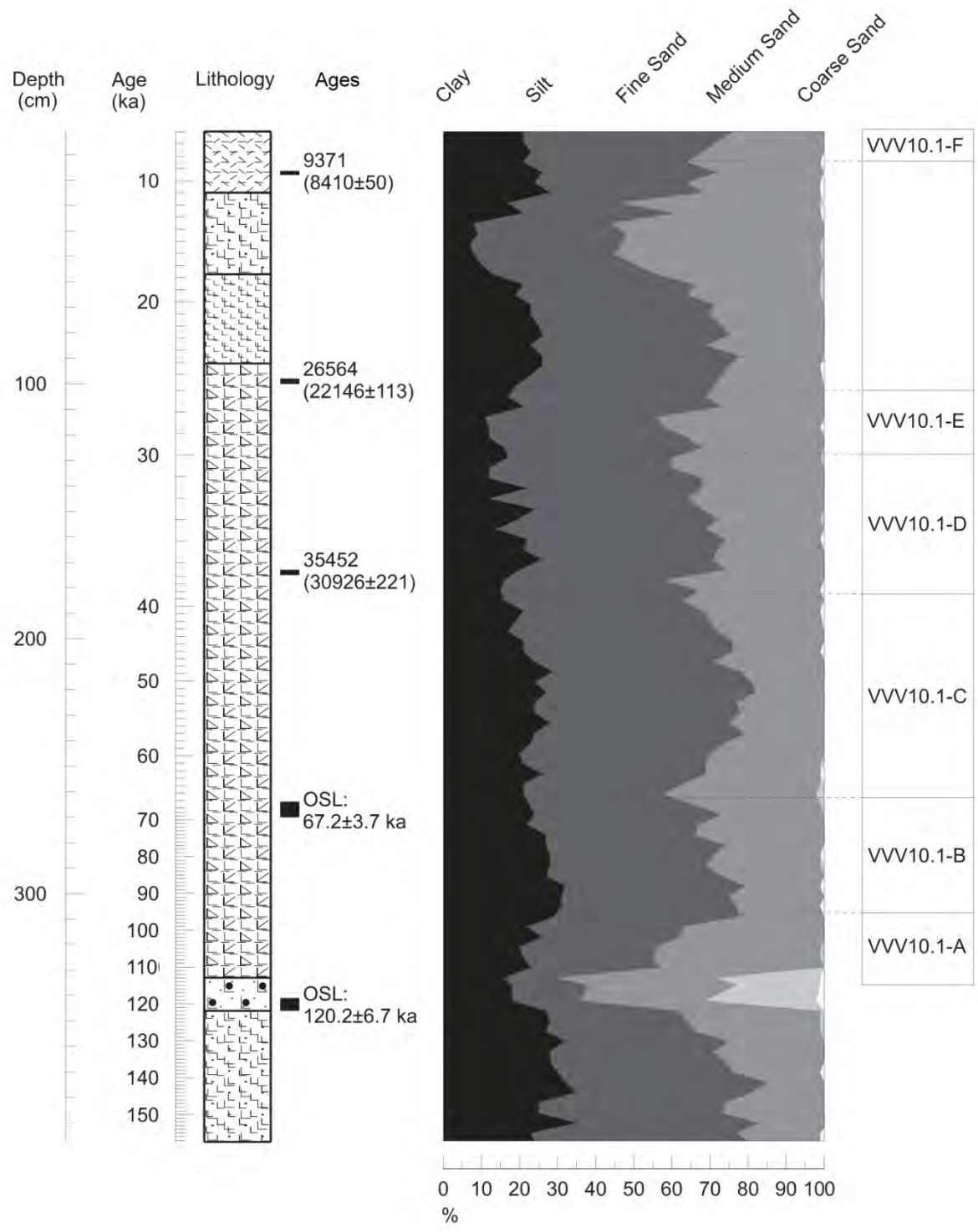

Figure 5.38 Vankervelsvlei 2010 #1 (VVV10.1) particle size analysis summary diagram displaying percentages of clay (0 – 2 µm), silt (2 – 20 µm), fine sand (20 – 200 µm), medium sand (200 – 500 µm) and coarse sand (500 – 2000 µm)(data source: Bürger (2011)).

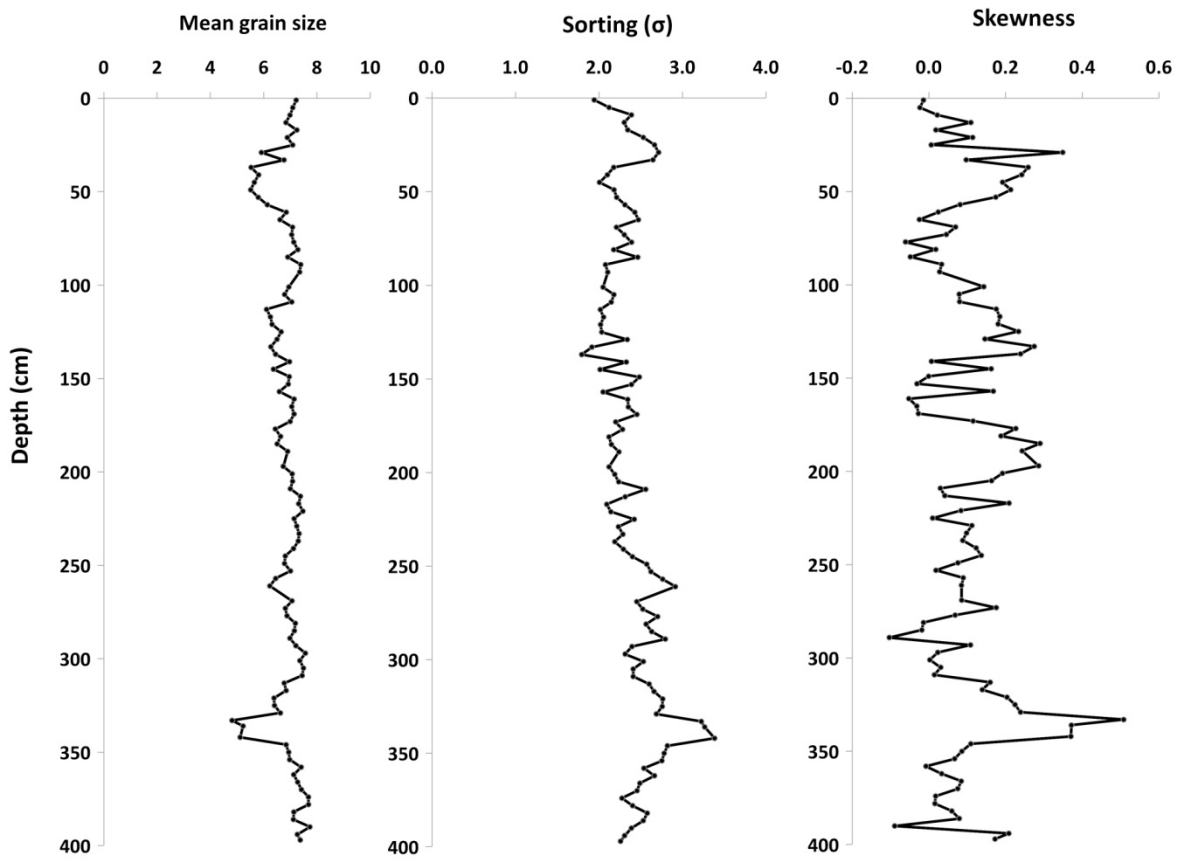

Figure 5.39 VVV10.1 grain size distribution statistical parameters (ϕ) (Folk and Ward, 1957 method calculated in Gradistat version 8 Blott 2010).

5.4.2 Chronology and sediment accumulation

Six radiocarbon and two OSL ages were obtained for VVV10.1 (Table 5-6). The age-depth model is presented in Figure 5.40. Three radiocarbon ages were considered to be outliers and were excluded from the age-depth model (Figure 5.40).

Beta-294326 is reported as greater than 43 500 ^{14}C yr, as the measured ^{14}C activity was extremely low and almost identical to the background signal, it was therefore deemed an infinite age. The age reversal at 271 cm (Beta-292545) is unknown but could be attributed to bioturbation, root contamination or contamination during either subsampling or the laboratory analysis process. The inclusion of an extremely small amount of modern carbon could significantly affect the measurement especially for late Pleistocene ages (Briant and Bateman, 2009). The OSL age Shfd-12016 fits fairly well within the model and therefore provides some substantiation for the exclusion of Beta-292545. Beta-292546 was taken from the base of the core and therefore contamination may have occurred through the sediment retrieval process.

Sediment accumulation initiated around ~5.7 cal kBP and the base of the core has an interpolated age of ~160 ka (Figure 5.40). Therefore VVV10.1 encompasses the latter part of the Holocene, the LGIT and the late Pleistocene extending into MIS 5. However, as the next section outlines, pollen is not found throughout the core and therefore the record is discontinuous.

Sediment accumulation rates were relatively high for the upper 173 cm, with average rates of 0.48 mm yr^{-1} for the section between 0 and 99 cm and 0.84 mm yr^{-1} for the section between 99 and 173 cm. This is in comparison to the lower section of the core that is characterised by average sedimentation rates of 0.29 (173 – 266 cm) and 0.14 mm yr^{-1} (266 – 400 cm).

Table 5-6 Vankervelsvlei 2010 #1 (VVV10.1) ages.

Laboratory ID	Average depth (cm)	Measurement method	14C age yr BP	1 sigma error	Calibration data	95.4 % (2σ) cal age range	Relative area under distribution	median probability	OSL age (ka)	OSL age error (ka)
Beta-292542	17.3	AMS	8810	50	SHCal04	cal BP 9143 - 9174 cal BP 9209 - 9217 cal BP 9242 - 9493	0.024856 0.004145 0.970999	9371		
Beta-292543	99.0	AMS	22146*	113	INTCal09	cal BP 26112 - 27068 cal BP 27324 - 27443	0.986231 0.013769	26564		
Beta-292544	174.0	AMS	30926*	221	INTCal09	cal BP 34902 - 35710 cal BP 35756 - 36284	0.637661 0.362339	35452		
Shfd-12016	267.0	OSL							67.2	3.7
Beta-292545	271.0	AMS	19706*	93	INTCal09	cal BP 23219 - 23906	1	23575		
Beta-294326	272.5	AMS	>43500							
Shfd-11116	343.5	OSL							120.2	6.7
Beta-292546	392.0	AMS	33866*	261	INTCal09	cal BP 37720 - 39504	1	38759		

AMS = Accelerated mass spectrometry
OSL = Optically stimulated luminescence
SHCal04 (McCormac et al., 2004); INTCal09 (Reimer et al., 2009)

***Adjusted for recommended SH offset of 56 +/- 24 (McCormac et al., 2004)**

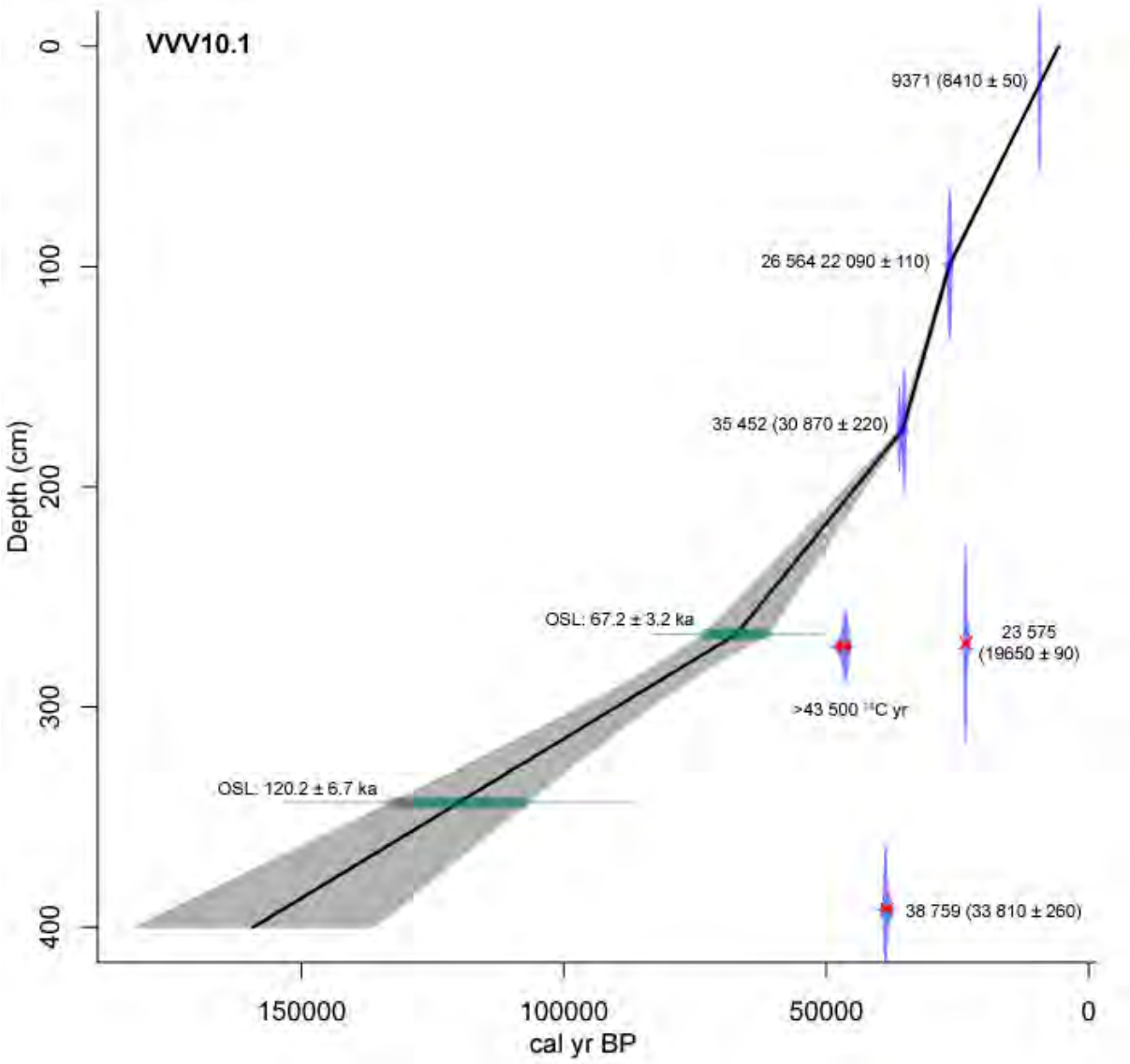

Figure 5.40 Age-depth model for VVV10.1, generated in R using CLAM (Blaauw, 2010). Ages with red stars have been considered to be outliers. The median probability calibrated ages are labelled and the uncalibrated ages with errors are provided in parentheses. Grey envelopes show the 95% confidence intervals, dark blue histograms indicate the ^{14}C calibrated distribution using SHCal04 (McCormac et al., 2004) or INTCal09 (Reimer et al., 2009) and light blue histograms show the OSL age distributions (see Table 5-6).

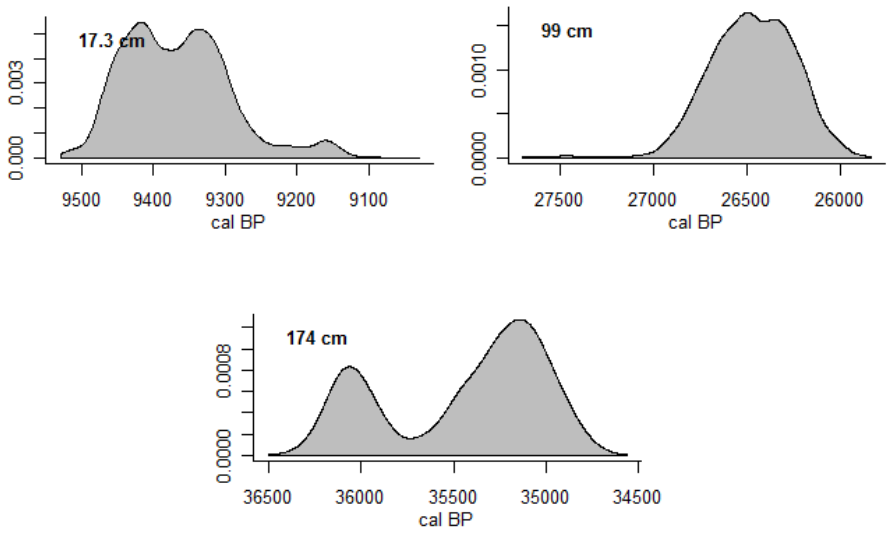

Figure 5.41 Calibration curves for the three radiocarbon ages from VVV10.1 (excluding ages that were deemed outliers).

5.4.3 Pollen and microscopic charcoal analyses results

Seventy nine samples were processed for pollen and microscopic charcoal analyses, however only 43 of these samples contained sufficient concentrations of pollen.

No pollen grains were found in subsamples from 15 - 100 cm, encompassing the whole of the light grey clay layer (section 5.4.1). Pollen was also not preserved from 340 to the base of the core correlating to the sand lens and the olive-brown clay-rich basal unit. The relatively homogeneous, organic-rich sediment layer between 100 and 340 cm contained very high concentrations of pollen (mean: 5.84×10^5 and maximum: 3.38×10^6, exponentially higher than PB-1 and RVSB-2).

The pollen and charcoal results are presented below as relative percentage diagrams (absolute counts found in Appendix J), with the full range of pollen taxa presented against depth (Figures 5.43 – 46) and a selection of ecologically significant taxa presented against age (Figures 5.47 – 5.48). All diagrams are divided into pollen assemblage zones using the statistical output of CONISS (Grimm, 1987) (Figure 5.42).

The overall pollen record from VVV10.1 reflects marked differences between the two Holocene samples and the rest of the core. Fynbos taxa are present throughout most of the record; however there are distinct appearances and fluctuations in certain afrotemperate forest taxa that could be indicative of changing forest-fynbos dynamics. These differences are described within the pollen assemblage zones below.

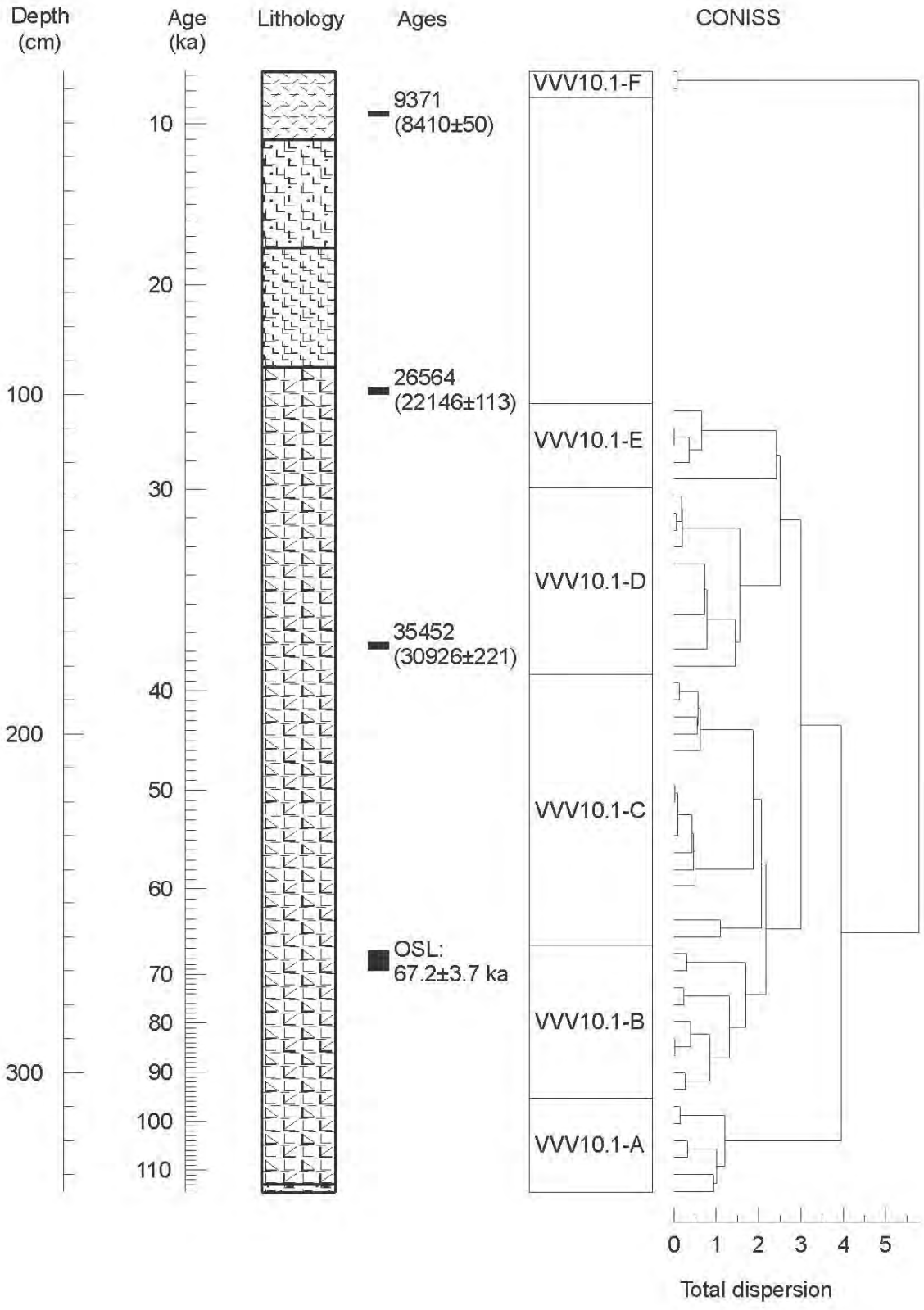

Figure 5.42 The results of CONISS displaying pollen assemblage zones for VVV10.1.

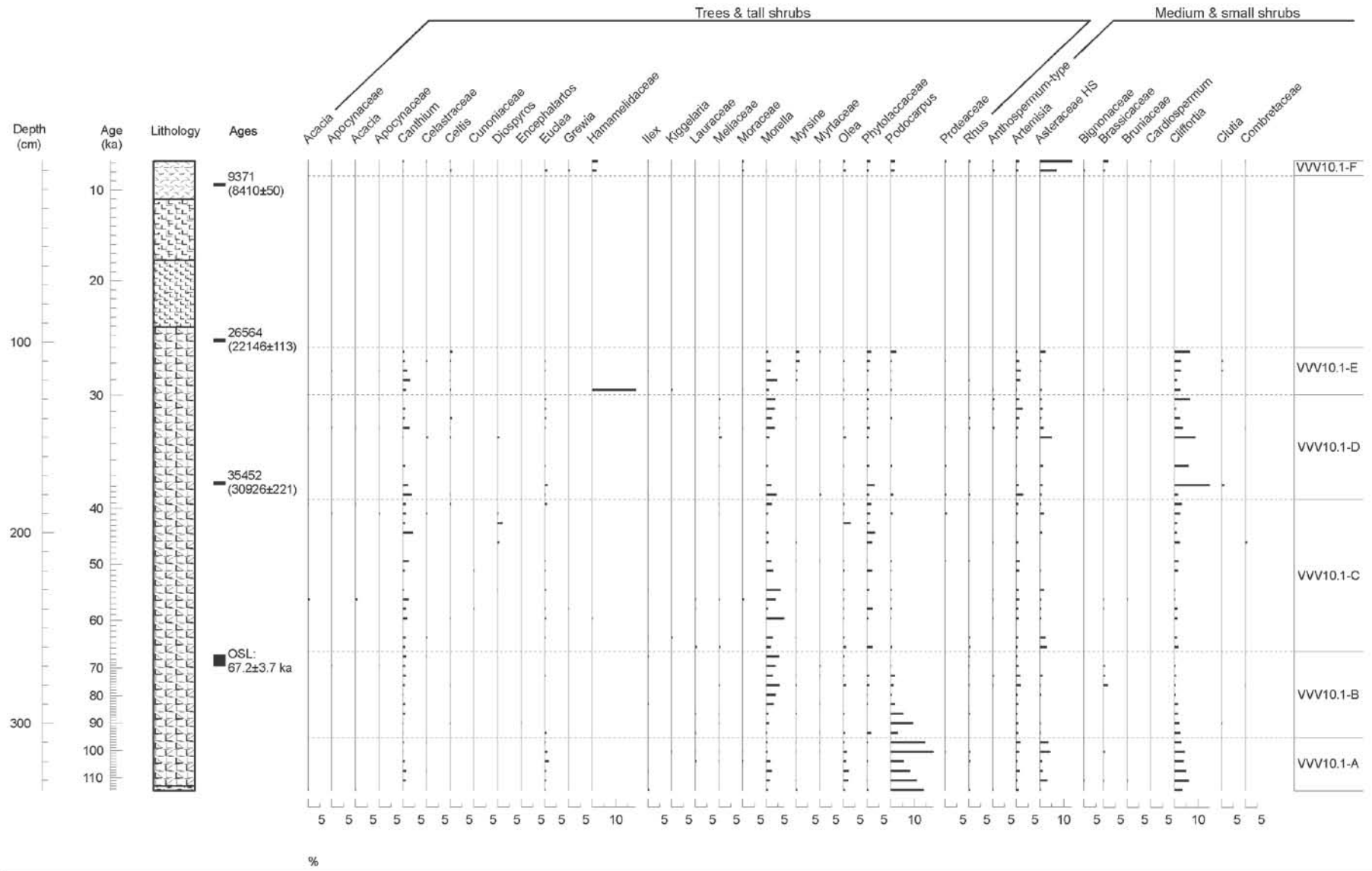

Figure 5.43 Comprehensive relative percentages pollen diagram for VVV10.1, taxa grouped according to general growth form (page 1 of 4).

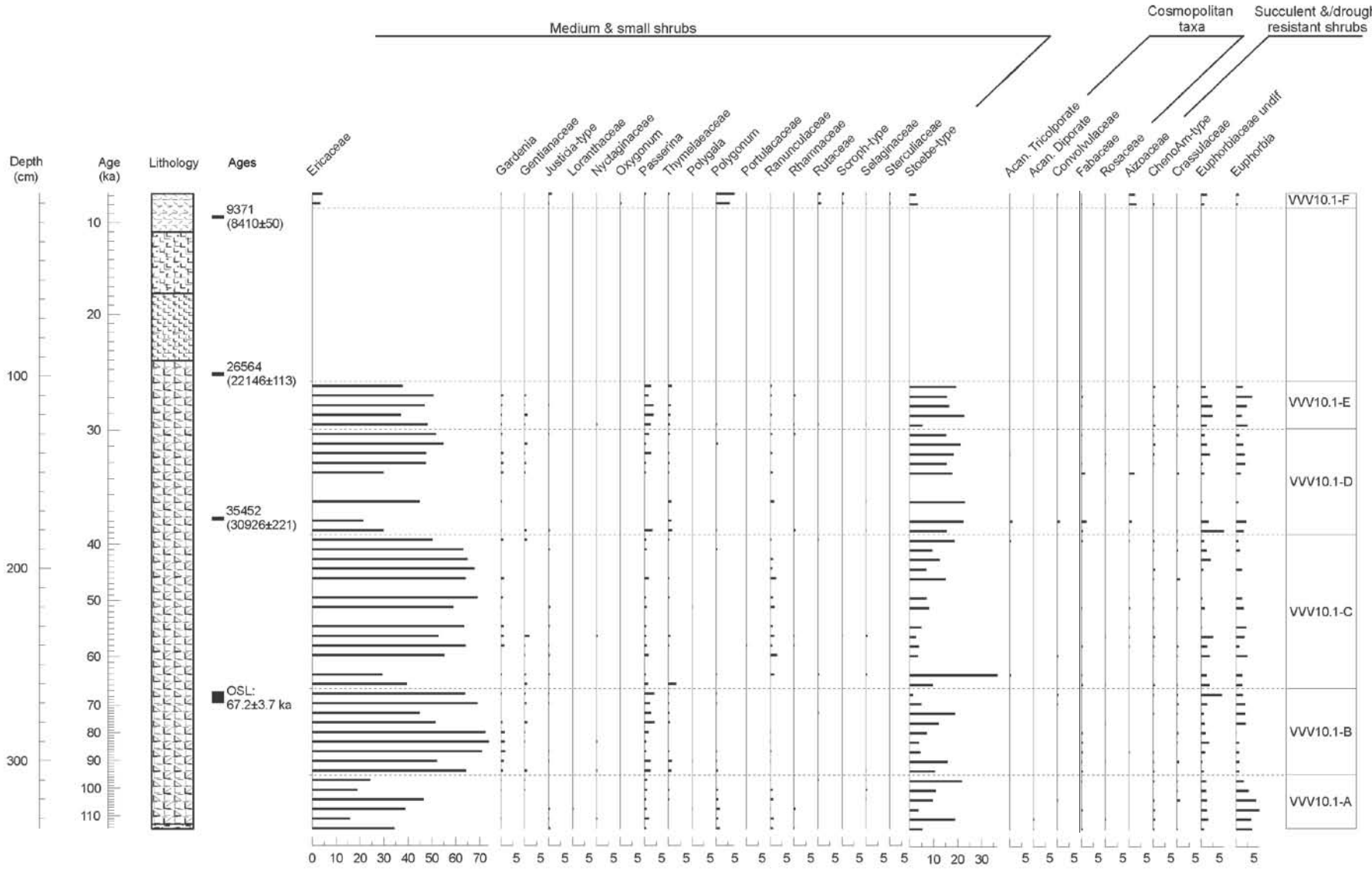

Figure 5.44 Comprehensive relative percentages pollen diagram for VVV10.1, taxa grouped according to general growth form (page 2 of 4).

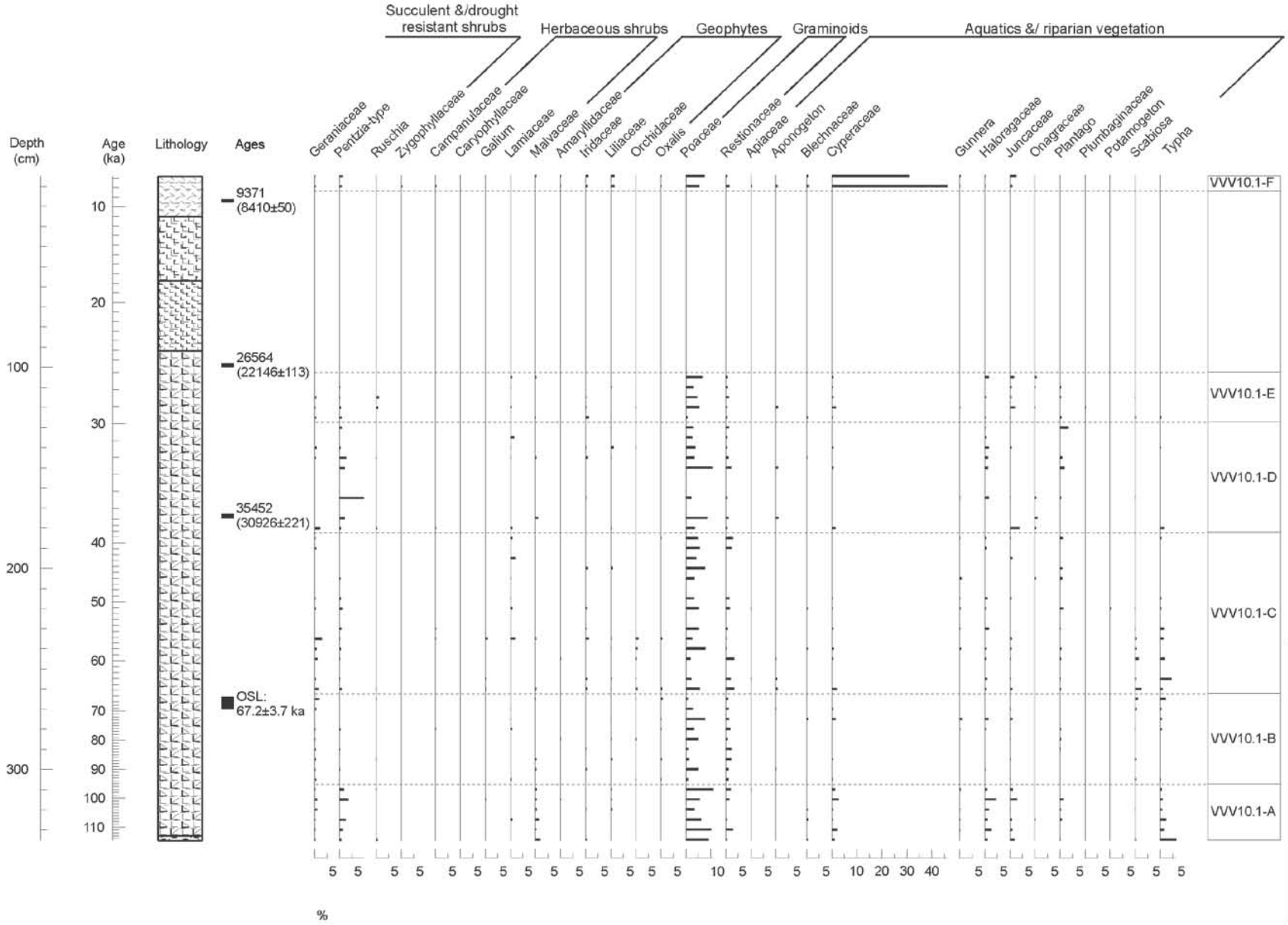

Figure 5.45 Comprehensive relative percentages pollen diagram for VVV10.1, taxa grouped according to general growth form (page 3 of 4).

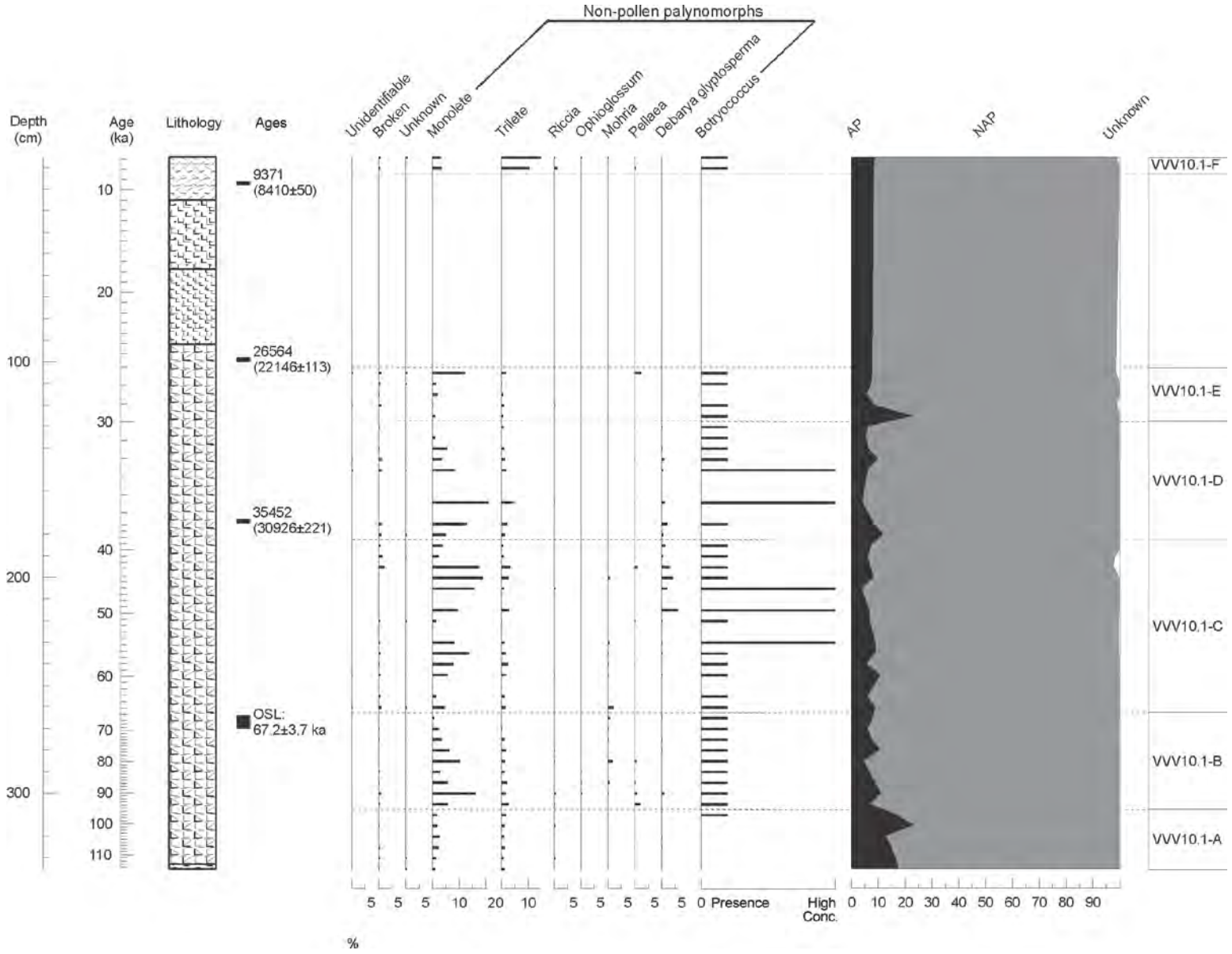

Figure 5.46
Comprehensive relative percentages pollen diagram for VVV10.1, AP is arboreal (trees and tall shrubs) pollen sum, NAP is the sum of all non-arboreal pollen (page 4 of 4).

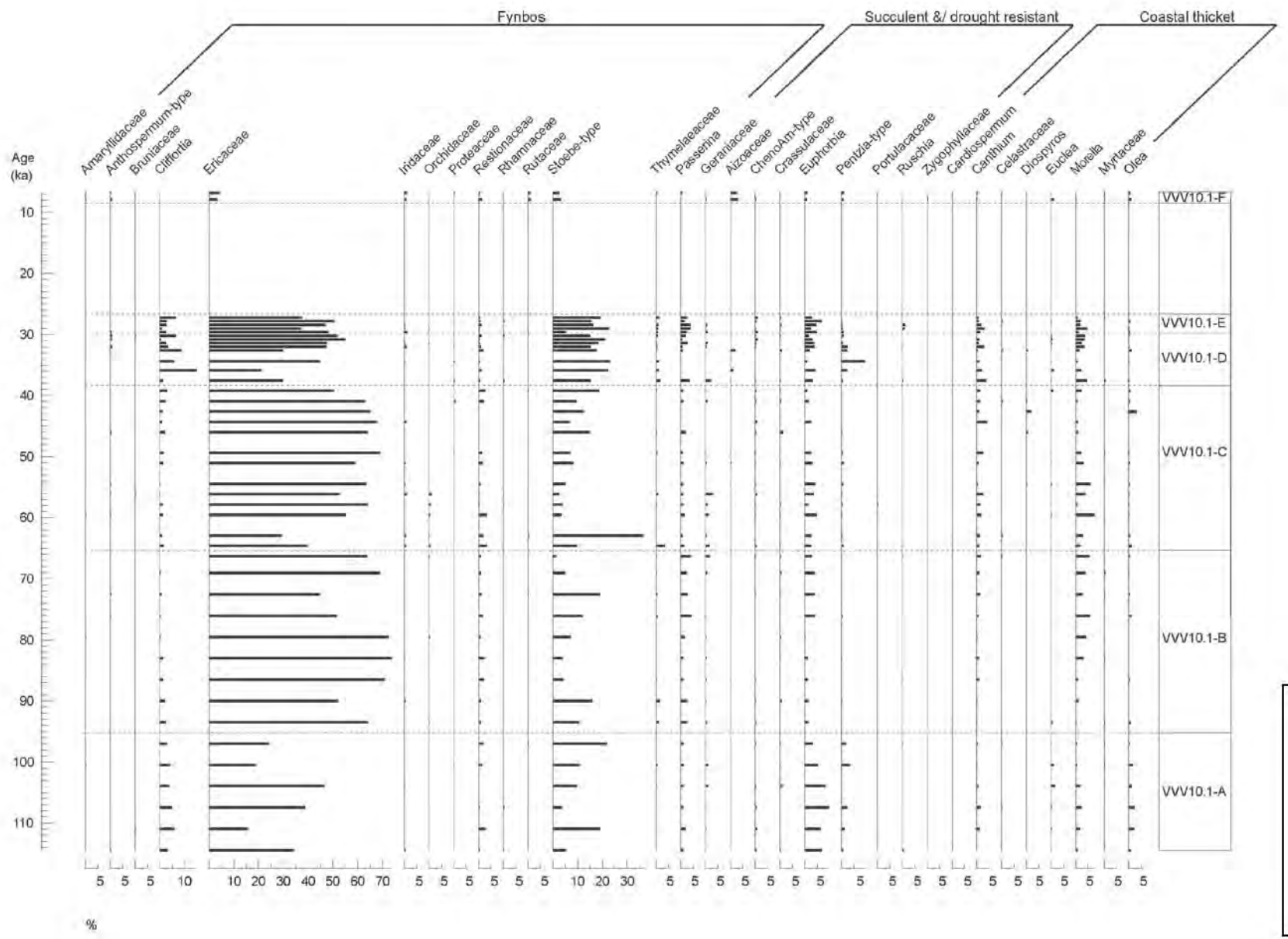

Figure 5.47 Relative percentages pollen diagram for VVV10.1, selected taxa grouped according to ecological affinities and plotted against interpolated age (page 1 of 2).

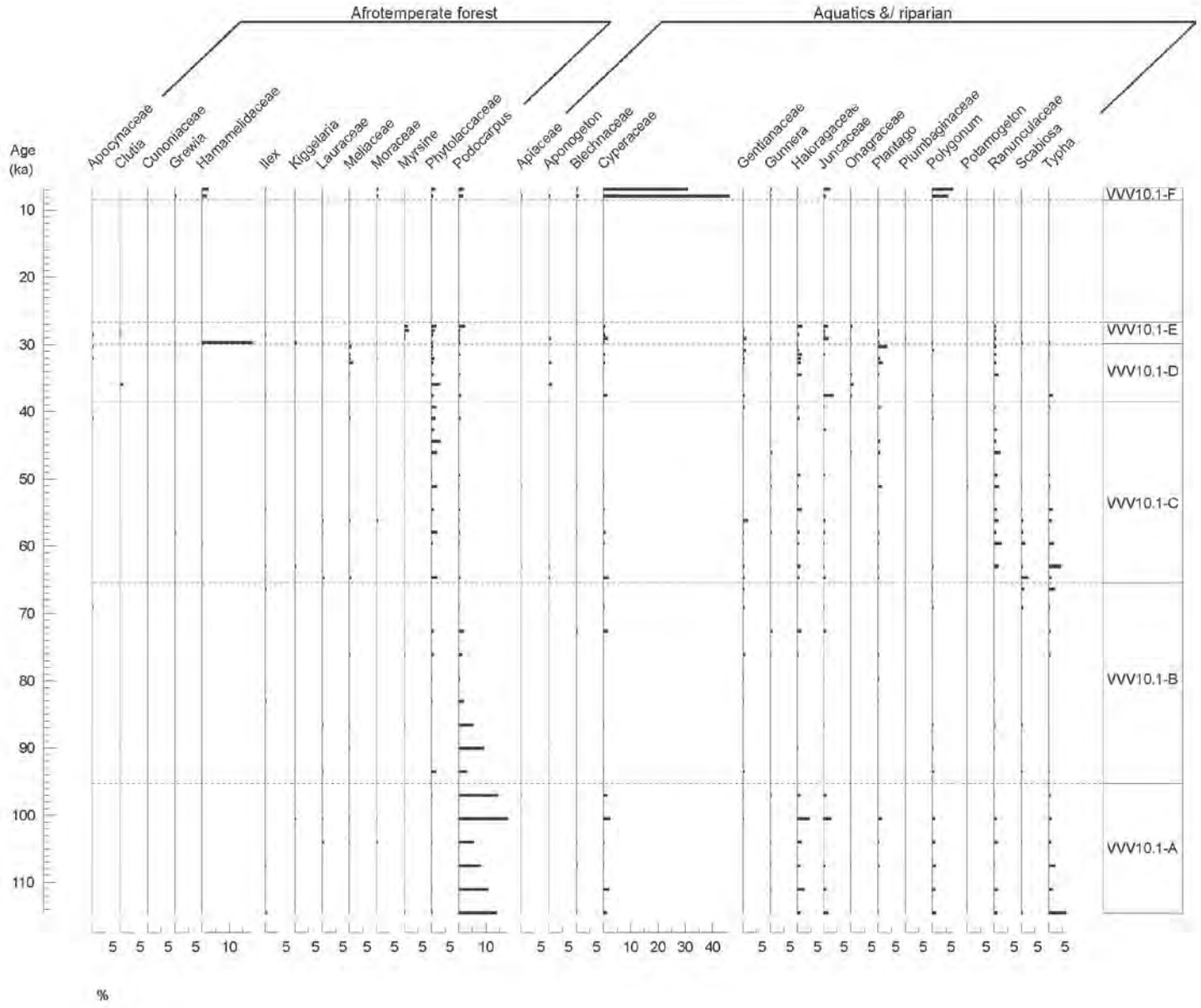

Figure 5.48 Relative percentages pollen diagram for VVV10.1, selected taxa grouped according to ecological affinities and plotted against interpolated age (page 2 of 2).

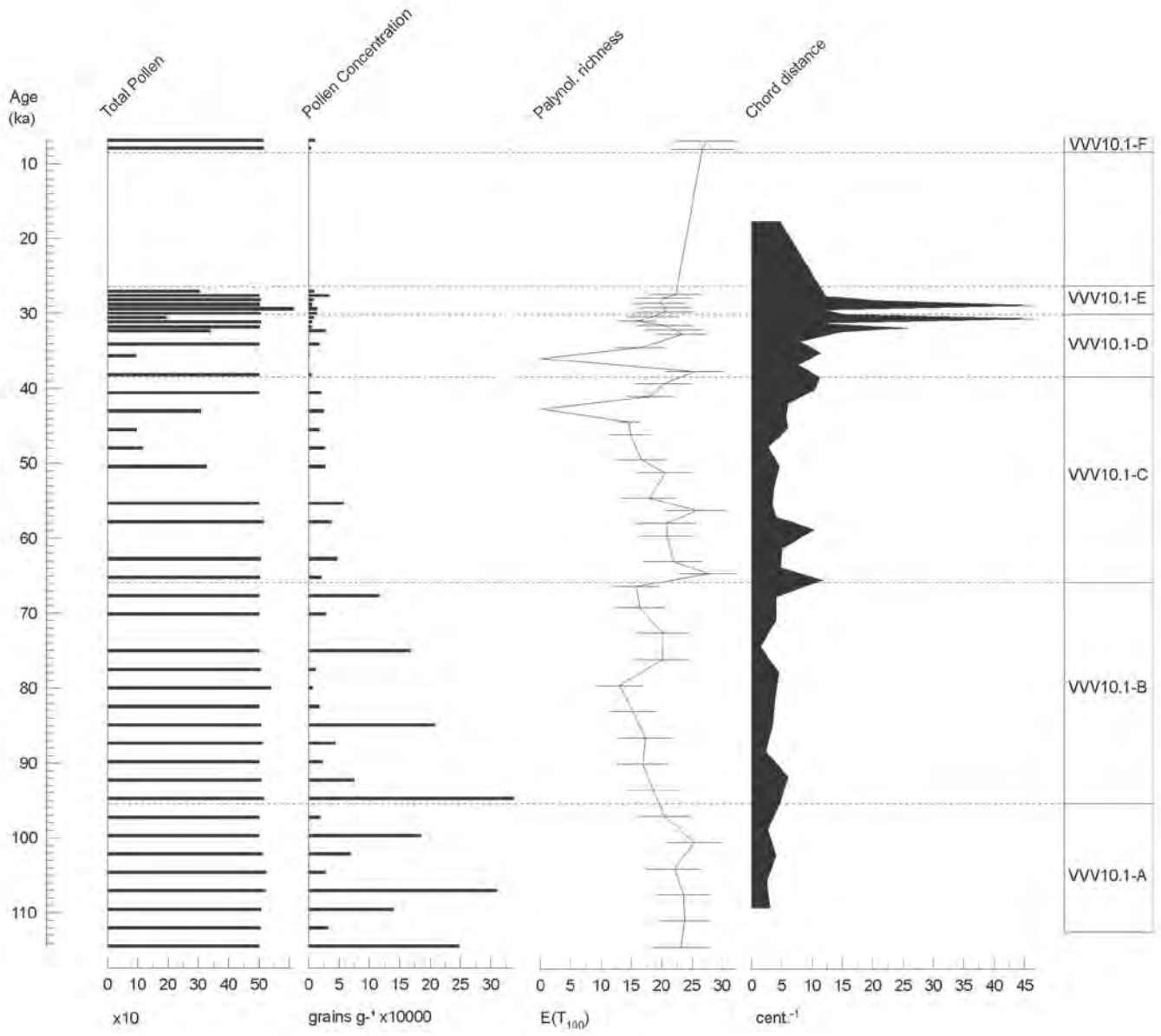

Figure 5.49 VVV10.1 total pollen counts, pollen concentrations and the palynological richness and rate of change analyses results.

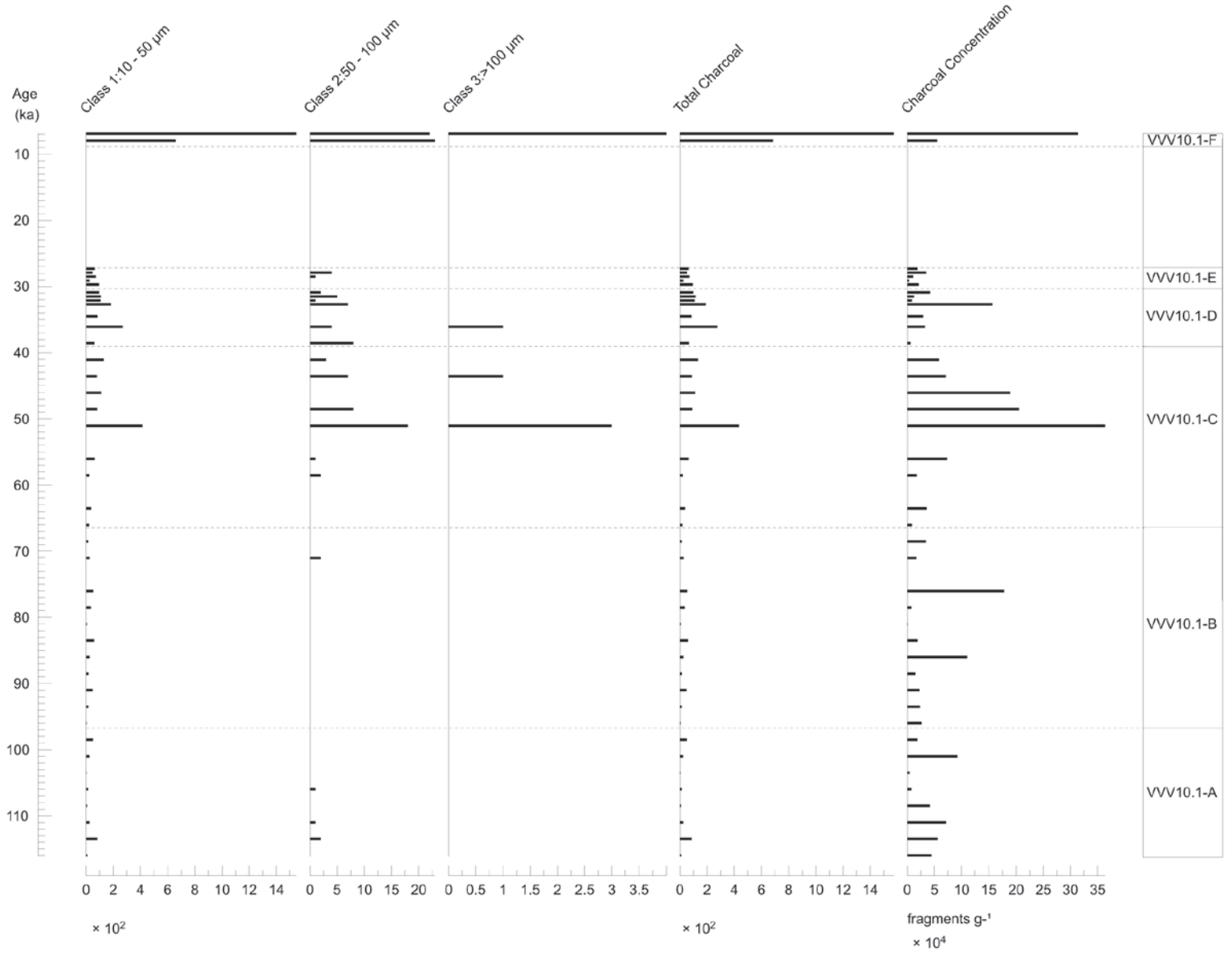

Figure 5.50 Results of VVV10.1's microscopic charcoal analysis, displaying the three size classes counted, total charcoal (sum of the three classes) and charcoal concentrations (calculated in a similar manner to pollen concentrations using the exotic marker counts)

Zone VVV10.1-A: 335 – 308 cm; approximately 116 – 95. 2 ka

This zone is characterised by a significant presence of *Podocarpus,* percentages of this taxon reach 18%, the highest for the sequence at 315 cm/~100.5 ka. Lauraceae, another afrotemperate forest taxon, is also present within VVV10.1-A, albeit at very low percentages (less than 1%).

Many thicket tree elements are present within the zone including *Canthium*, *Euclea*, *Morella* and *Olea*. *Pentzia*-type and *Euphorbia* percentages are relatively high, with the latter reaching 10%, the highest percentage of this taxon within the record, at ~107.5 ka.

Ericaceae, while on average accounting for over 30% of the total pollen per level, is reduced in comparison to zones VVV10.1-B and VVV10.1-C. *Cliffortia* percentages are in general relatively elevated but decrease towards the top of the zone. *Stoebe*-type and Poaceae proportions are both moderately high with peaks near the top and bottom of the zone.

Local aquatic/riparian pollen taxa are generally at low frequencies within VVV10.1-A however there are small peaks in Haloragaceae, Juncaceae and *Typha*. Monolete and trilete spore percentages are low throughout the zone as is charcoal. Pollen concentrations are variable with extremely high values being reached in some samples within this zone.

Zone VVV10.1-B: 308 – 263 cm; approximately 95.2 – 65. 5 ka

Ranging from 45 – 74%, Ericaceae percentages are exceptionally high for this zone. *Podocarpus* and *Cliffortia* percentages both decline towards the top of VVV10.1-B, while *Morella* proportions increase at the top. Similar to the previous zone, Lauraceae is present but at very low percentages.

Euphorbia and Euphorbiaceae undifferentiated are low at the base of the zone and increase towards the top with a relatively large peak (~9%) in the latter. *Passerina* is present throughout VVV10.1-B with slightly increased percentages towards the top of the zone. Peaks in *Stoebe*-type percentages are relatively high and peaks in this taxon are found at 275 cm/~72.5 ka and at the base.

Elevated percentages of Poaceae sporadically occur within this zone, whilst local aquatic/riparian taxa percentages are relatively consistently low. There is a peak in the percentage of monolete spores near the base of VVV10.1-B after which percentages decline towards the top.

Charcoal fragments and concentrations are, like the previous zone, very low. Alternatively, pollen concentrations are extremely high, reaching the maximum for the sequence at ~86.5 ka.

Zone VVV10.1-C: 263 – 183 cm; approximately 65.5 – 38.4 ka

There is a slight drop in the proportions of Ericaceae at the base of the zone; however from 245 cm/~59.5 ka to the top of the zone percentages match the high values present in the previous zone. This zone together with VVV10.1-A and VVV10.1-B are the only zones that contain Lauraceae pollen. Phytolaccaceae, another afrotemperate forest taxon, is present at low percentages (~2-4%) throughout the majority of this zone.

At the base of the zone, *Stoebe*-type pollen is at its maximum value (37%) for the sequence, after which they drop sharply to below 5% then rise steadily towards the top of the zone. Restionaceae proportions are very slightly elevated in comparison to the previous zones.

Aquatic/riparian pollen percentages are fairly low with the exception of *Typha* which exhibits a small peak (4%) at the base of the zone. The other principal constituents of the zone include *Euphorbia*, Euphorbiaceae undifferentiated, Poaceae, *Canthium* and *Morella*.

Monolete spores percentages are variable but generally increase towards the top of the zone. The zygospore *Debarya glyptosperma* is present within the top section of this zone and green algae *Botryococcus* colonies were highly concentrated within samples located within the middle section of VVV10.1-C.

Charcoal fragments are low except for peaks in all three size classes and concentrations at 205 cm/~46 ka. Some levels within this zone were either devoid of pollen or contained too low concentrations (e.g. from 209 – 190 cm/~47.3 – 40.9 ka); for the levels that did contain pollen, concentrations steadily drop towards the top of the zone.

Zone VVV10.1-D: 183 – 128 cm; approximately 38.4 – 30 ka

Like all previously described zones, Ericaceae dominate the spectra, although percentages are somewhat decreased especially at the base of the zone (26%). The second most dominant pollen taxon within this zone is *Stoebe*-type, percentages of which do not fluctuate much throughout the zone.

Cliffortia reaches its highest percentage (15%) for the sequence at the base of VVV10.1-D. Asteraceae high spine variety, *Pentzia*-type and Poaceae are at low proportions except for peaks in Asteraceae high spine and *Pentzia*-type near the middle of the zone and Poaceae near the base and at 150 cm/~32.6 ka. *Canthium, Morella, Euphorbia*, Euphorbiaceae, Phytolaccaceae are present intermittently throughout the zone at low proportions.

Spore amounts are low except for a fairly significant peak (8%) in monolete spores at 32.6 ka. Overall pollen concentrations are low, with some levels containing no pollen. Charcoal fragments are higher in comparison to VVV10-A and VVV10-B but not as high as the previous zone.

Zone VVV10.1-E: 128 –103 cm; approximately 30 – 27 ka

The most distinguishing feature of this zone is the large peak (18%) in Hammeladicaceae at 125 cm/~29.7 ka. Ericaceae is once again the most dominant taxon, ranging from 37% to over 50%. *Stoebe*-type percentages are relatively high for much of the zone (average of 18%) except for at the base where it represents only 5%.

Canthium, Morella, Passerina, Euphorbia, Euphorbiaceae undifferentiated and Poaceae are present at low percentages throughout the zone. There is a small discrete peak in *Podocarpus* at the top of VVV10.1-E whereas *Cliffortia* rises steadily towards the top.

Monolete and trilete spore percentages are very low except for a relatively large peak in monolete spores at the top of VVV10.1-E. Both charcoal fragments and pollen concentrations are low throughout the zone.

Zone VVV10.1-F: 11 – 0 cm; approximately 8 – 5.8 ka

This uppermost zone only encompasses two levels within which enough pollen was preserved, at 10 cm/~7.9 ka and 5 cm/~6.9 ka. The zone is dominated by an overwhelming increase in Cyperaceae percentages, accounting for 46% and 31% of the two levels. Other aquatic/riparian taxa are slightly more prevalent within this zone especially *Polygonum* which reaches nearly 8% at the top of the zone.

In comparison to the rest of the sequence, Ericaceae percentages are extremely low (3-4%), while Asteraceae high spine variety reaches its maximum (~14%) for the record at the top of VVV10.1-F. *Stoebe*-type percentages are greatly reduced in comparison to the previous two zone and *Cliffortia* is entirely absent from VVV10.1-F.

Forest taxa are fairly low or absent from this zone, except for Hammeladicaceae and *Podocarpus* which are present within both levels at around 1-2%. Thicket taxa are also either at very low percentages or absent from this zone.

While being absent or at very low proportions (below 1%) from the previous zones, Aizoaceae is

present within both levels of VVV10.1-F at 2.5 and 3% respectively. Poaceae remains relatively consistent throughout the zone and comparable to the other zones.

Monolete spore proportions are lower than VVV10.1-E whereas trilete spores are significantly increased for this zone. Charcoal fragments and concentrations are exceptionally high, particularly for the top level and especially for the largest size class. Pollen concentrations are as low as the VVV10.1-D and VVV10.1-E amounts.

5.4.4 Multivariate data analyses

The multivariate analyses were carried out on a selection of 20 ecologically sensitive taxa extracted from the overall VVV10.1 pollen dataset (Table 5-7).

Table 5-7 A selection of ecologically sensitive pollen taxa for statistical analyses.

Selected pollen taxa	General ecological affinity
Aponogeton	aquatic/riparian
Blechnaceae	aquatic/riparian
Gunnera	aquatic/riparian
Haloragaceae	aquatic/riparian
Cliffortia	fynbos
Ericaceae	fynbos
Passerina	fynbos
Proteaceae	fynbos
Stoebe -type	fynbos
Cunoniaceae	forest
Hamamelidaceae	forest
Lauraceae	forest
Podocarpus	forest
Celastraceae	thicket
Morella	thicket
Aizoaceae	succulent/drought resistant
Crassulaceae	succulent/drought resistant
Euphorbia	succulent/drought resistant
Pentzia -type	succulent/drought resistant
Ruschia	succulent/drought resistant

Similar to PB-1 and RVSB-2, the DCA performed on VVV10.1 subset revealed gradient lengths below 3 (the longest gradient length was 1.364) therefore a PCA was undertaken (Leps and Smilauer, 2003). The pollen taxa data was standardized and square-root transformed. The ordination was centred by taxa and scaling was focused on inter-sample distance.

Table 5-8 Summary table displaying the Principal Component Analysis (PCA) results for VVV10.1.

Principal component axes	1	2	3	4	Total variance
Eigenvalues	0.36	0.18	0.149	0.07	1
Cumulative percentage variance of species data	36	54	68.9	75.9	
Total sum of squares in species data	378.3				
Total standard deviation in species data TAU	0.663				

The first four principle components account for ~76% of the variance; however the eigenvalues of the last two principal components are low (especially principal component four) and do not explain significant proportions of the variance (Table 5-8). Therefore the results of the first two principal components were the focus of this analysis. Figure 5.51 represents a distance biplot of the PCA scores displaying the relationship between the taxa and samples (ages) on principal component 1 (PC1) and principal component 2 (PC2).

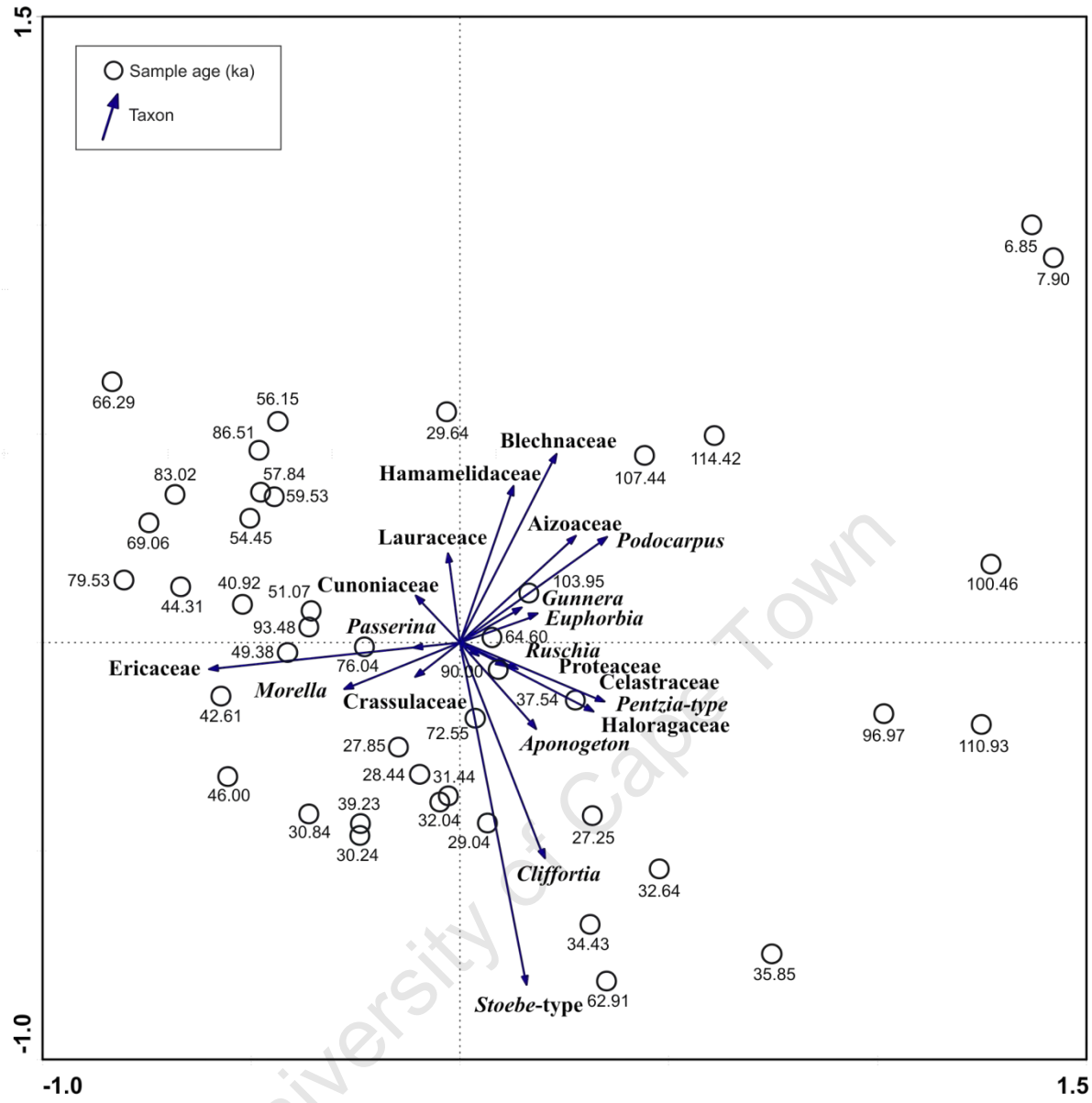

Figure 5.51 Ordination biplot mapping the taxa and sample ages scores for VVV10.1.

Not surprisingly, the two Holocene samples are furthest away from the main cluster. Many of MIS 5 samples are also separate from the main cluster while samples with ages 103.95, 107.44 and 114.42 are aligned to the *Podocarpus* and Aizoaceae vectors. *Stoebe*-type and *Cliffortia* vectors are in similar positions with the majority of the 'LGM' glacial samples clustered in their vicinity. The majority of the remaining samples are clustered loosely around the Ericaceae vector.

5.5 Conclusion

This chapter has presented the particle size, pollen, microscopic charcoal and geochemical data derived from PB-1, RVSB-2 and VVV10.1. Although these three sediment cores do not represent continuous sequences, they do provide important palaeoenvironmental information for some of the key late Quaternary chronozones including: MIS 5, the early glacial, the LGM, the LGIT and the Holocene.

Pearly Beach 1's location within the WRZ is strongly reflected in the overall dominance of fynbos taxa within the palynological record and the clear C_3 vegetation signal evident in the $\delta^{13}C$ data. The significant deviations evident within the particle size, pollen, microscopic charcoal and geochemical data for the thin sand layer at 175 – 180 cm is of particular importance as this section represents the core of the last glacial period. The significance of the PB-1 record in relation to regional and hemispheric climate change is discussed in detail within the next chapter.

The data from RVSB-2 while comparable to PB-1, exhibit much great variability (especially the geochemical data) which indicate the more transitional nature of the site, at the boundary between the WRZ and the YRZ.

The data derived from Vankervelsvlei are considerably different from that generated from the Pearly Beach and Rietvlei sediment cores. This is primarily due to the nature of the site itself (a small catchment), its location in the Knysna Afrotemperate Region and the time period encompassed within the VVV10.1 record.

Synthesised palaeoenvironmental records for each site are presented in the following chapter, together with specific discussions of the significance of these records in relation to fynbos ecology and the overall southern Cape palaeoenvironmental record.

6. A palaeoenvironmental synthesis for the southern Cape coastal plain

6.1 Introduction

Chapter 6 initially discusses the key underpinnings used to interpret the records, largely pertaining to modern bioclimatic tolerances of taxa and fynbos ecology. This is followed by the presentation of the overall palaeoenvironmental records for Pearly Beach, Rietvlei Still Bay and Vankervelsvlei. The new palaeoenvironmental information generated for this study is then assessed in relation to the established southern Cape palaeoenvironmental record as well as regional and hemispheric climate change proxies.

6.2 Bioclimatic tolerances of pollen taxa

In order to determine which pollen taxa were the most climatically sensitive, without relying upon preconceived notions of ecological significance, the modern bioclimatic tolerances of all the pollen taxa counted were established. It is a key assumption that over the time periods in question, taxa would not have been genetically modified and sensitivities to changes would not have changed (Bennett, 1996). Therefore the resultant modern bioclimatic envelopes can be used for the purposes of aiding palaeoenvironmental interpretations.

The full set of results of the *MaxEnt* modelling and GIS taxon-climate distribution analyses (taxa distribution data source: SANBI, 2003; GIS climate data source: Hijmans et al., 2005) is given in Appendix B. The most noteworthy results in terms of extreme climate tolerances are presented and discussed below.

Crassulaceae had the lowest minimum mean annual precipitation (MAP), while the following taxa all had minimum MAP values below 10 mm: Aizoaceae, *Euphorbia*, Poaceae (very wide spatial and climatic distribution), Geraniaceae and Zygophyllaceae. The highest minimum MAP values (both above 300 mm) were associated with the forest taxa Hamamelidaceae and *Olinia*. Other taxa with high minimum MAP values included thicket taxa: *Morella*, Sapotaceae (*Sideroxylon inerme*, the only species of this family that is found in the region) and *Canthium*, as well as one aquatic: *Nymphaea* (Figure 6.1).

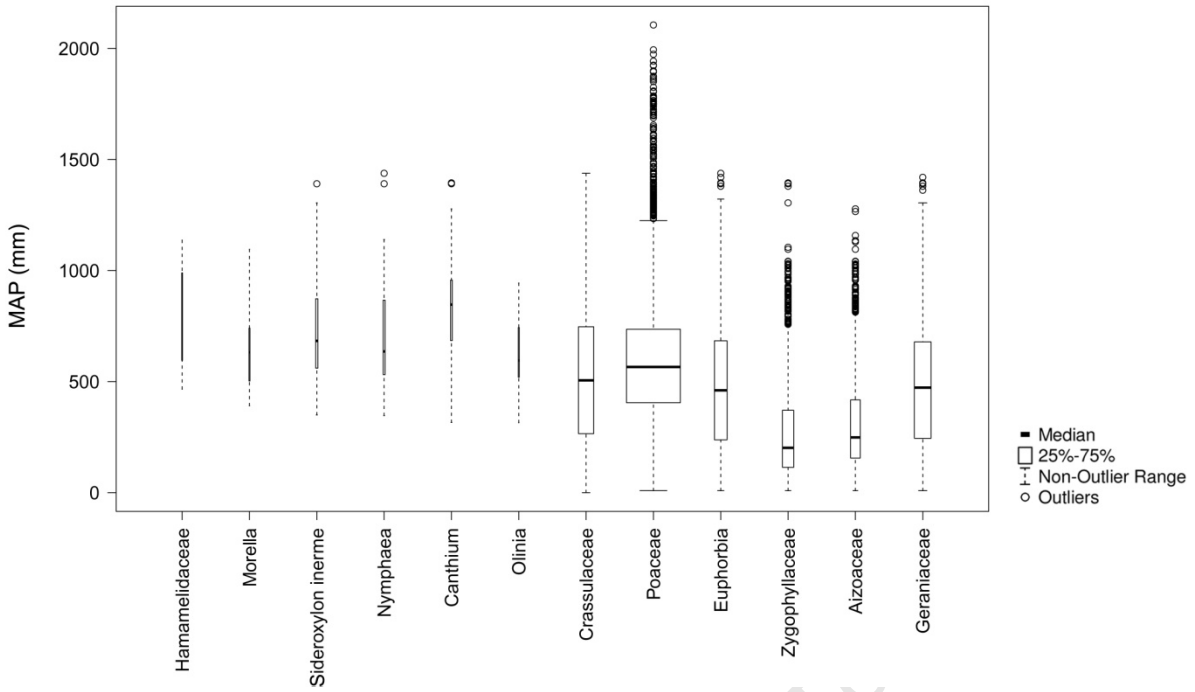

Figure 6.1 Box plots of the highest and lowest minimum mean annual rainfall values (mm); width of boxes is proportional to the square roots of the number of observations.

The assessment of the total amount of winter rainfall (sum of the precipitation for the months of June, July and August) against the overall MAP provides a rudimentary indication of which taxa are reliant on predominantly winter rainfall (Appendix B, Figure 6.2). The taxa with the highest values (above 30%) include: Haemodoraceae, Bruniaceae, *Lobostemon*, Restionaceae, *Stoebe*-type, Proteaceae, Ericaceae, *Cliffortia* and Rutaceae. These fynbos taxa most probably also require a relatively cool growing season (testament to their C_3 photosynthetic abilities) which is likely to be associated with winter rainfall.

The only three taxa with high values for the variable Precipitation of Driest Quarter were the forest taxa Cunoniaceae, Hamamelidaceae and *Olinia* (Appendix B) and therefore appear to be least drought tolerant.

In terms of temperature tolerances, most taxa are found within areas where the Mean Temperature of the Coldest Month is below 0°C except for the following: *Dodonaea, Canthium, Cardiospermum,* Haemodoraceae, *Cliffortia, Sterculia,* Cunoniaceae, Hamamelidaceae and *Olinia* (Figure 6.3).

Figure 6.2 A line plot of the percentage of winter rainfall for all pollen taxa.

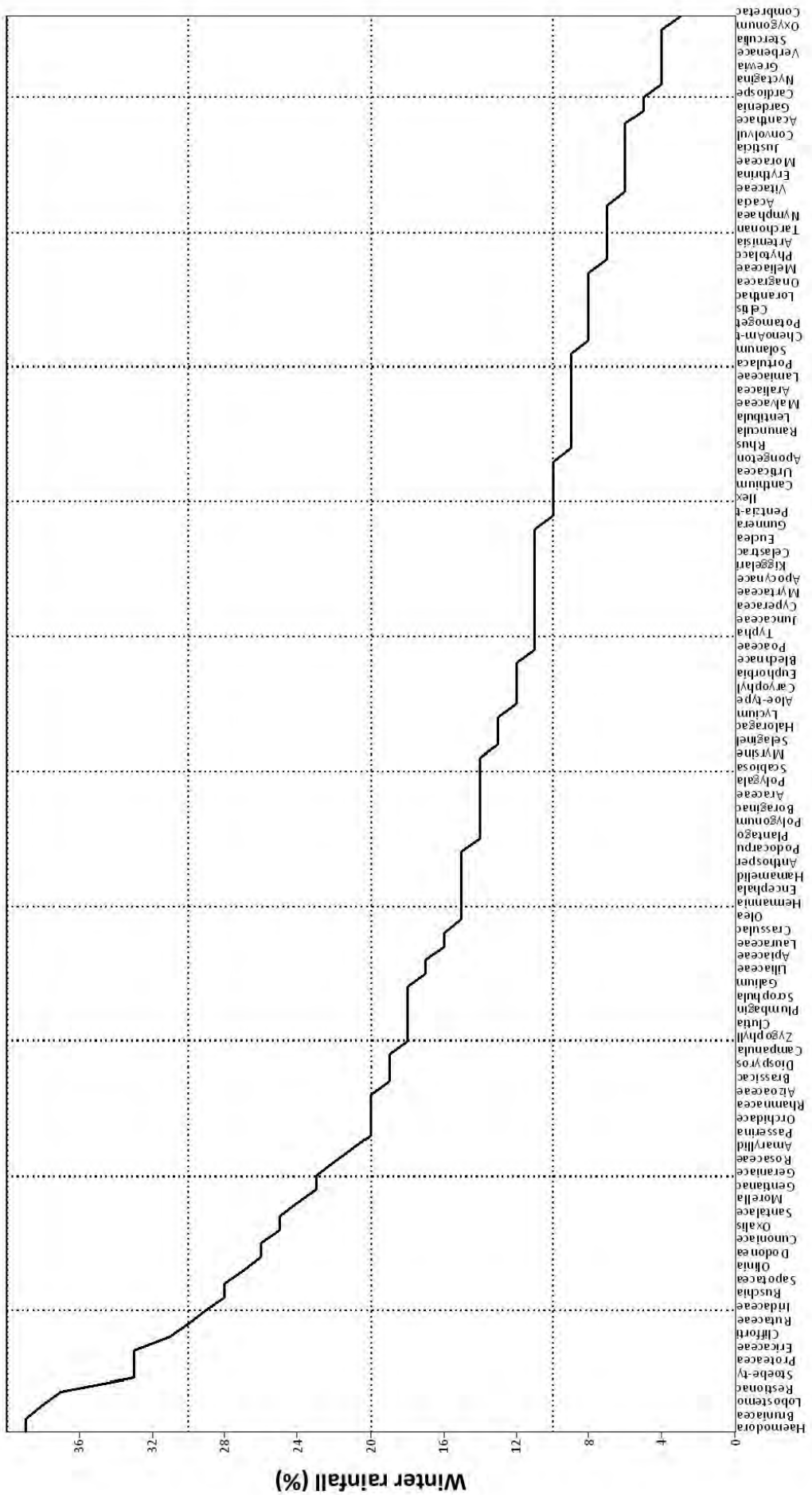

Figure 6.3 Box plots of mean temperature of coldest month (MTCM) for each pollen taxon; width of boxes is proportional to the square roots of the number of observations.

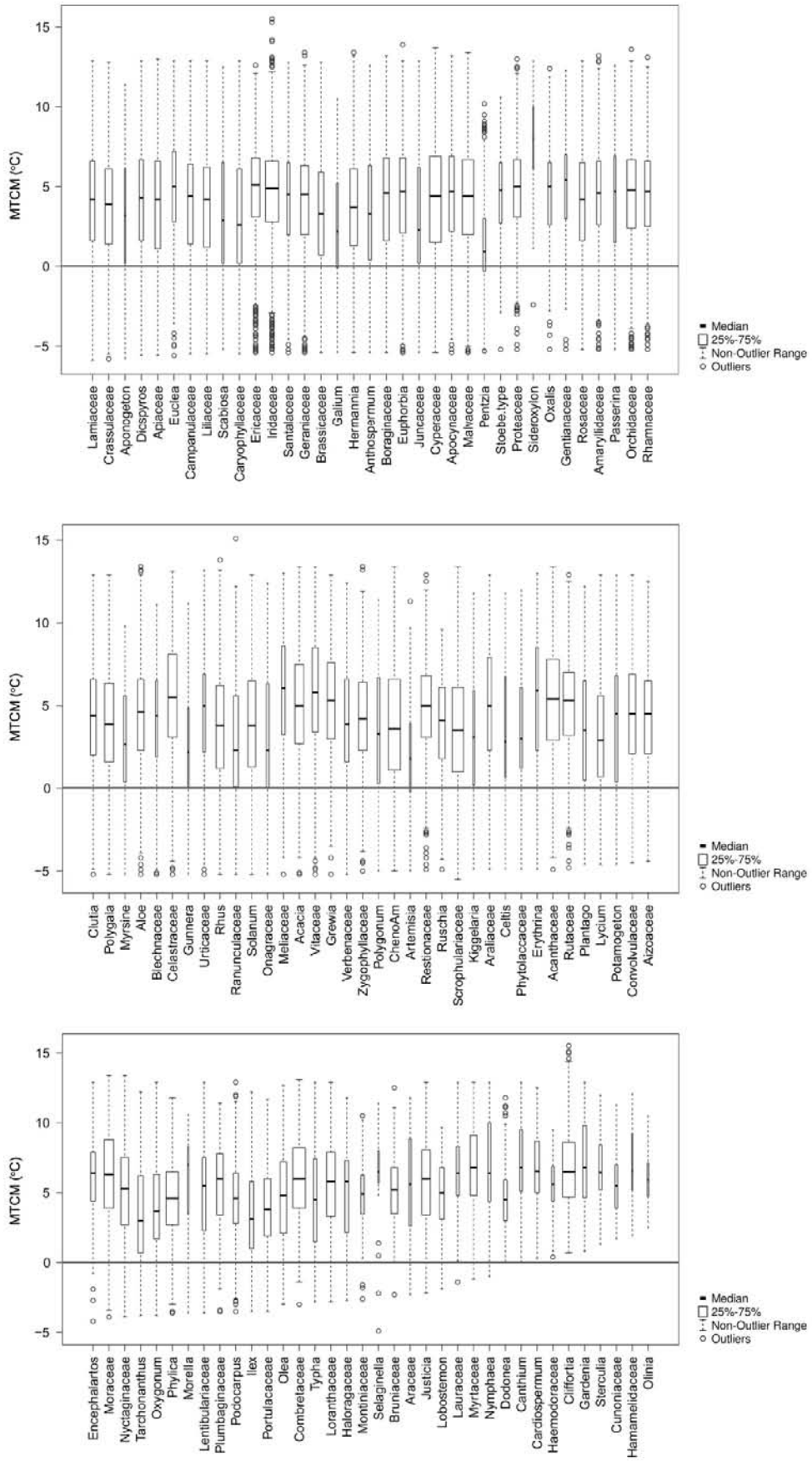

Table 6-1 provides a summary of the analyses discussed above, presenting the most climatically sensitive taxa, based on their modern bioclimatic distributions (Appendix B) and an evaluation of the available literature (cited in Appendix B). They are used as indicator taxa and, in some cases indicator groups, within this chapter.

Table 6-1 Climatically sensitive indicator taxa.

Cold tolerant taxa	Cold intolerant taxa	Drought tolerant	Drought intolerant	Winter rainfall
Ericaceae	*Pentzia* -type	Crassulaceae	Hammelidiaceae	Haemodoraceae
Gunnera	*Dodonaea*	Aizoaceae	Cunoniaceae	Bruniaceae
	Canthium	*Euphorbia*	*Canthium*	*Lobostemon*
	Cardiospermum	Geraniaceae	*Gunnera*	Restionaceae
	Hamamelidaceae	Zygophyllaceae	*Morella*	*Stoebe* -type
			Sapotaceae	Proteaceae
			Myrsine	Ericaceae
				Cliffortia
				Rutaceae

These indicator categories can only be used tentatively as the overall modern distributions of the individual taxa are complex. Further work, beyond the scope of this study, is required to fully elucidate the mechanisms and thresholds of each taxon in question.

6.3 Geochemical evidence portrays the ecological differences between Pearly Beach and Rietvlei Still Bay

The stable carbon isotope ratios derived from the Pearly Beach and Rietvlei Still Bay sediment cores reveal the differing ecological settings of the two sites. PB-1 has a $\delta^{13}C_{TOC}$ range of c. 4 ‰ whereas RVSB-2's range is close to 9 ‰ (Figure 6.4). The narrower spread evident within the PB-1 record reflects a strong C_3 vegetation signal, which would be expected for a fynbos-dominated location. Therefore the more subtle fluctuations in the PB-1 $\delta^{13}C_{TOC}$ record could be attributed to adjustments in water-use efficiencies and reveal changes in moisture availability at the site (as outlined in Chapter 4). Consequently, the record can be divided into two sections: the glacial section from ~25 – 13 cal kBP within which $\delta^{13}C_{TOC}$ values are generally more depleted, reflecting enhanced moisture availability, and the section from ~13 – 1.3 cal kBP which generally indicates conditions that were not as humid as the glacial period. At 10.8 cal kBP the $\delta^{13}C_{TOC}$ value is highly enriched, corresponding to a break in the pollen record and perhaps providing further substantiation for a more xeric phase.

However, as the site does not represent an exclusively C_3 ecosystem (being influenced by the presence of coastal thicket/strandveld which include CAM plants, karroid elements which include CAM and C_4 species and renosterveld which includes a higher cover of C_4 grasses than fynbos vegetation types (Vogel et al., 1978; Cowling, 1983a)) and as the $\delta^{13}C$ record is derived from bulk organic matter, the signal is complex and perhaps not as indicative of regional climatic change as the $\delta^{13}C$ records derived from hyrax middens (e.g. Chase et al., 2011).

The greater variability evident within the RVSB-2 $\delta^{13}C_{TOC}$ record emphasizes the site's position within a more transitional area encompassing fynbos, coastal thicket/strandveld and Albany Thicket communities (Chapter 2). It appears that the RVSB-2 $\delta^{13}C$ record is therefore more sensitive and/ or responsive to changes in comparison to the PB-1 record. The non-fynbos vegetation types potentially include greater proportions of C_4 and CAM plants leading to phases whereby the $\delta^{13}C_{TOC}$ values are more enriched. This is particularly evident from ~37 – 34 ka (A), ~28.5 – 25.5 ka (B) and ~0.85 – 0 ka (D) (Figure 6.5). The first and last of these examples correspond to periods in the pollen record where the thicket sum percentages are relatively high and fynbos taxa percentages are generally low (Figure 6.5). The most depleted $\delta^{13}C_{TOC}$ value for the sequence is found at 1.35 ka, which is bounded by periods where fynbos taxa (especially Proteaceae) percentages are high (Figure 6.5 (C)). Despite the high degree of variability inherent within both the geochemical and palynological records, and the multitude of factors that could have influenced the $\delta^{13}C$ signal, a fairly coherent pattern between the two is evident for much of the overall RVSB-2 record.

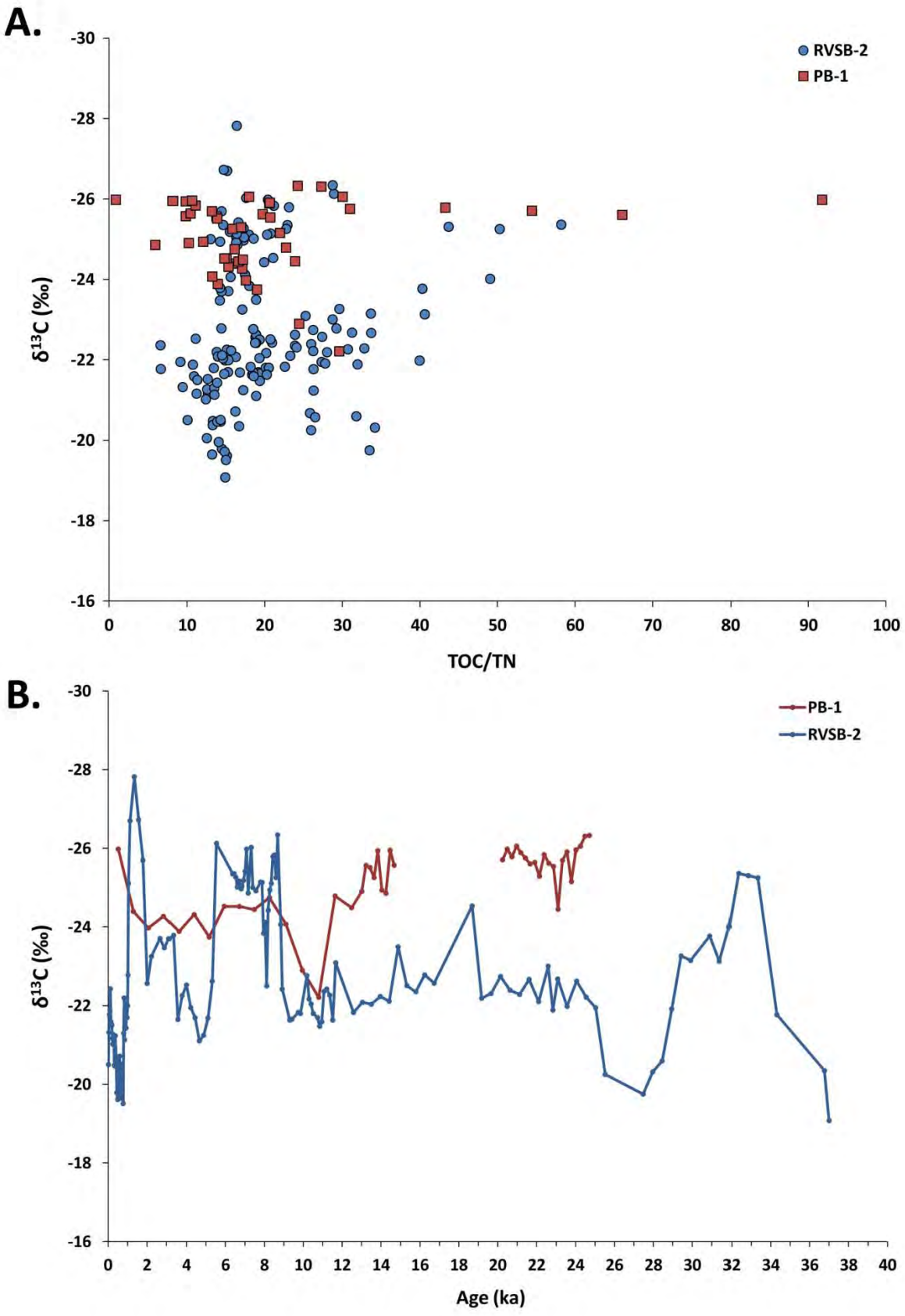

Figure 6.4 A comparison between the geochemical data from Pearly Beach 1 and Rietvlei Still Bay 2. A: the $\delta^{13}C_{TOC}$ values plotted against the TOC/TN ratio, B: the $\delta^{13}C_{TOC}$ data against age.

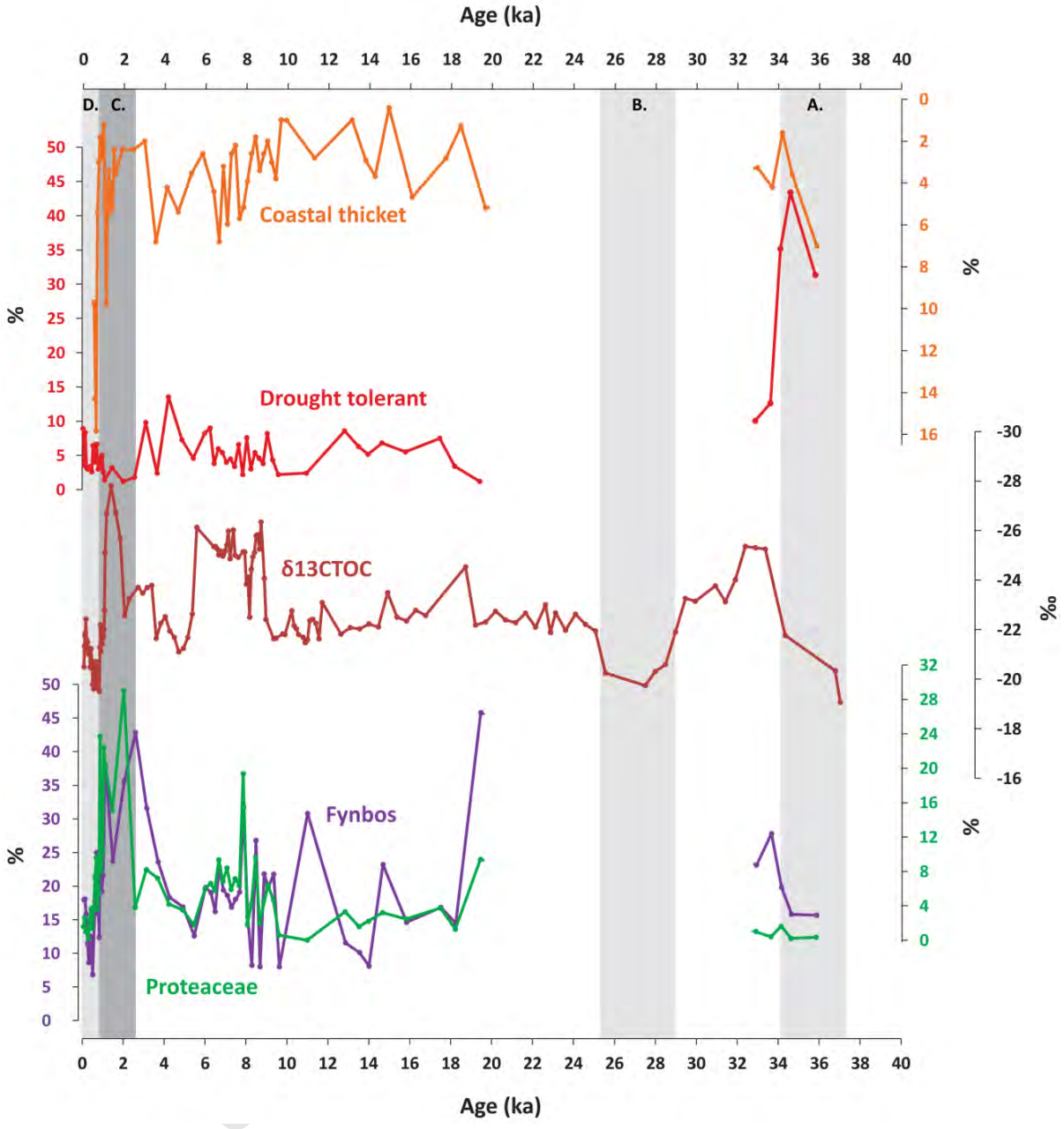

Figure 6.5 A comparison between the RVSB-2 $\delta^{13}C_{TOC}$ and certain elements of the palynological record.

6.4 The relationship between fire and vegetation compositional change

As outlined in Chapter 4, microscopic charcoal counts and concentrations can be used to determine fire regimes and can provide important insight into the association between vegetation change and fire.

As the pollen and microcharcoal records from Pearly Beach, Rietvlei Still Bay and Vankervelsvlei all represent discontinuous time series within which samples often encompass fairly large segments of time (e.g. over 500 years), statistical analyses such as redundancy analysis (RDA) and cross correlation analysis were not plausible or possible. Despite the inability to describe the fire-vegetation relationships quantitatively, certain more obvious trends relating to fire (as inferred from charcoal concentrations) and vegetation types are clearly evident in all three records.

Pearly Beach's pollen and charcoal data reinforce the established contemporary ecological theory governing fynbos and coastal thicket/strandveld and the pivotal role fire plays in determining the dominance of each within a landscape (discussed in Chapter 2). Figure 6.6 illustrates how peaks in charcoal concentrations are often associated with reductions in thicket, whereas when the thicket taxa sum is relatively high there are lower charcoal concentrations. For example, at ~21.9 cal kBP, from ~6 – 5 cal kBP and from ~ 2 – 1 cal kBP peaks in charcoal, signifying increased fire frequencies, correspond to reductions in the thicket sum (Figure 6.6). The opposite occurs from ~14 cal kBP – 12 cal kBP and at ~4.7 cal kBP. The negative correlation between fire frequencies and thicket presence does not exist for all sections of the record largely due to the overarching influence of climate change and the general complexity and imperfect temporal resolution inherent within the datasets. This is especially apparent at ~21.6 cal kBP, when presumably specific climatic conditions promoted both higher fire frequencies and increased thicket.

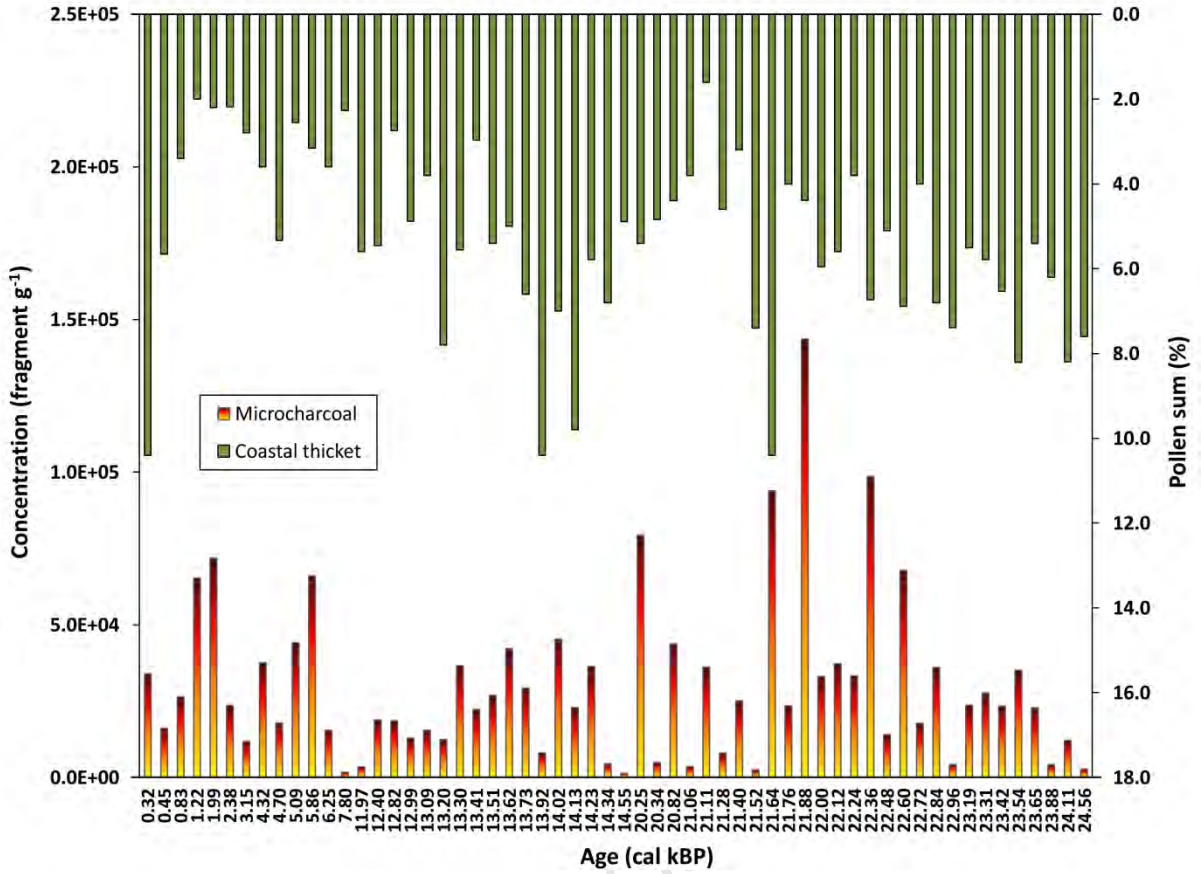

Figure 6.6 Sum of the pollen percentages of coastal thicket taxa and charcoal concentrations for the Pearly Beach 1 record.

The fire-thicket pattern is also reflected in the Rietvlei Still Bay records (Figure 6.7) and is particularly evident for pollen assemblage zone (PAZ) RVSB2-A, from ~7.5 - 6 ka and ~2.5 – 0.9 ka. A combination of climatic change (changes in the amount and seasonality of rainfall and increased temperatures) and prolonged reductions in fire frequencies could be responsible for the significantly higher percentages of thicket taxa within the most recent section of the record (PAZ RVSB2-F).

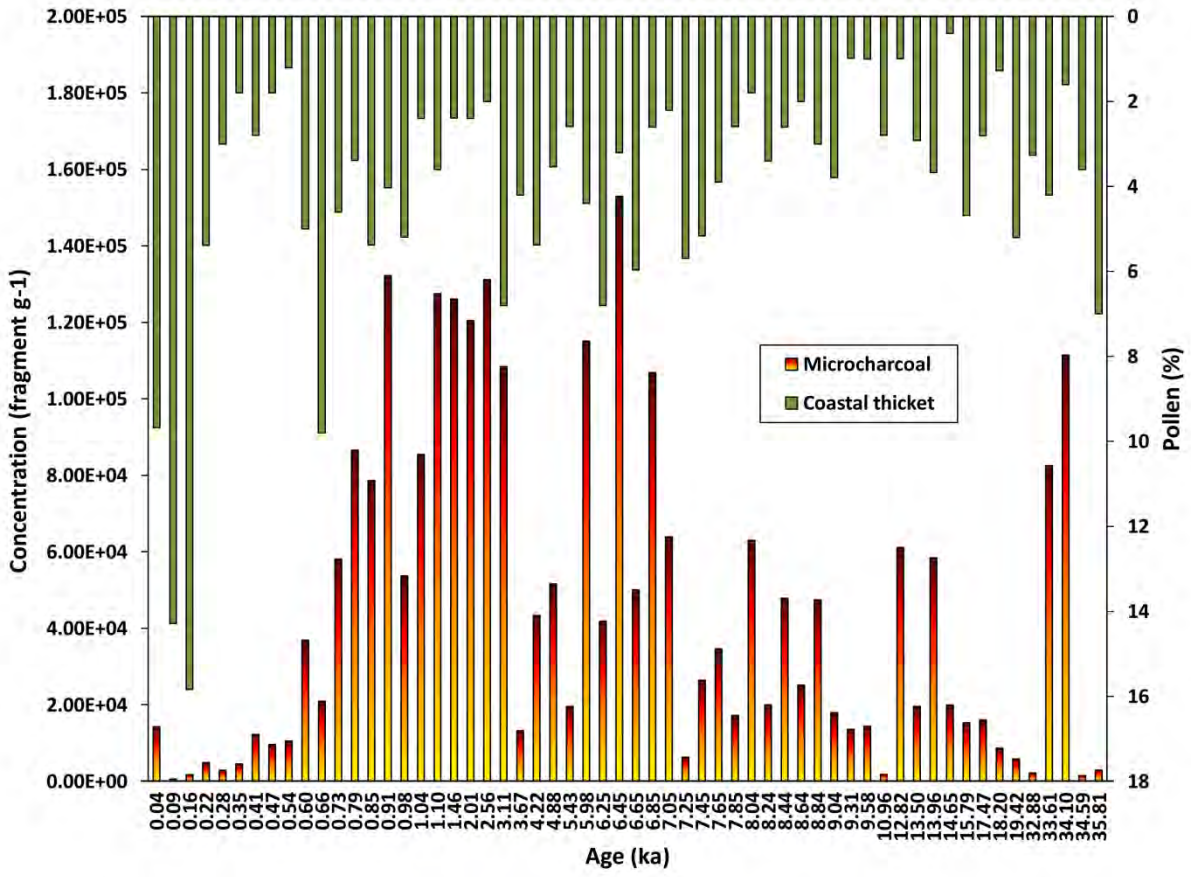

Figure 6.7 Sum of the pollen percentages of coastal thicket taxa and charcoal concentrations for the Rietvlei Still Bay 2 record.

In terms of the Vankervelsvlei record, the above trends are not as clear as fire plays an important role in both fynbos-thicket and fynbos-afrotemperate forest dynamics and all three vegetation groups are encompassed within the VVV10.1 record. Figure 6.8 does confirm that fynbos and fire are relatively well coupled for most of the VVV10.1 record.

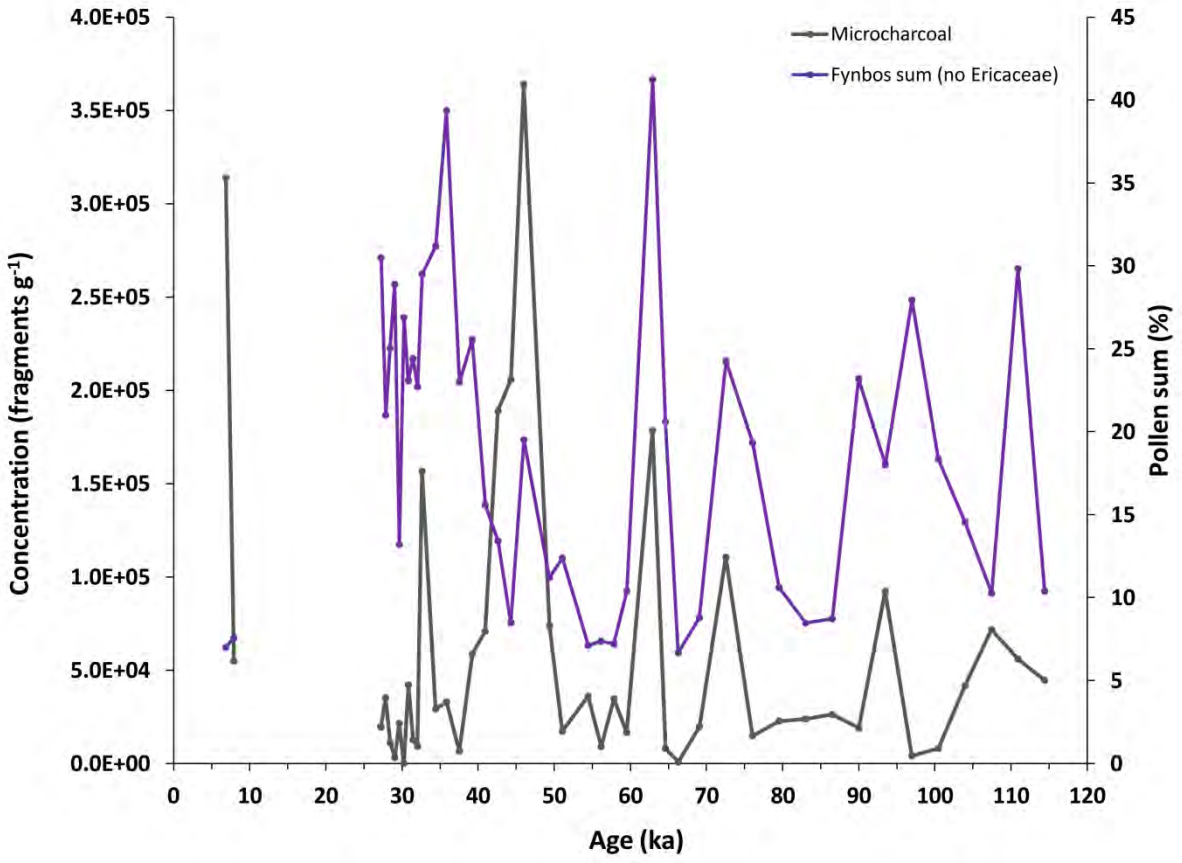

Figure 6.8 A comparison between the sum of the fynbos taxa and microcharcoal concentrations from the VVV10.1 record (Ericaceae percentages were excluded from the fynbos sum as they were disproportionately high).

There appears to be stronger direct linkages between the thicket sum and charcoal concentrations than that of the afrotemperate forest sum and microcharcoal record (Figure 6.9). For example, the two largest peaks in microcharcoal (at ~46 ka and 6.9 ka) correspond to very low coastal thicket sums. Incidentally both of those examples are where the fynbos-fire correlation is not apparent. The underrepresentation of forest taxa within the pollen record may be obscuring this correlation.

Both thicket and forest sums are high for the earliest part of the sequence (from ~114 – 97 ka) while charcoal concentrations are relatively low. However, fire most likely did not drive vegetation change within this MIS 5 section but was more a consequence of the climate regime at the time.

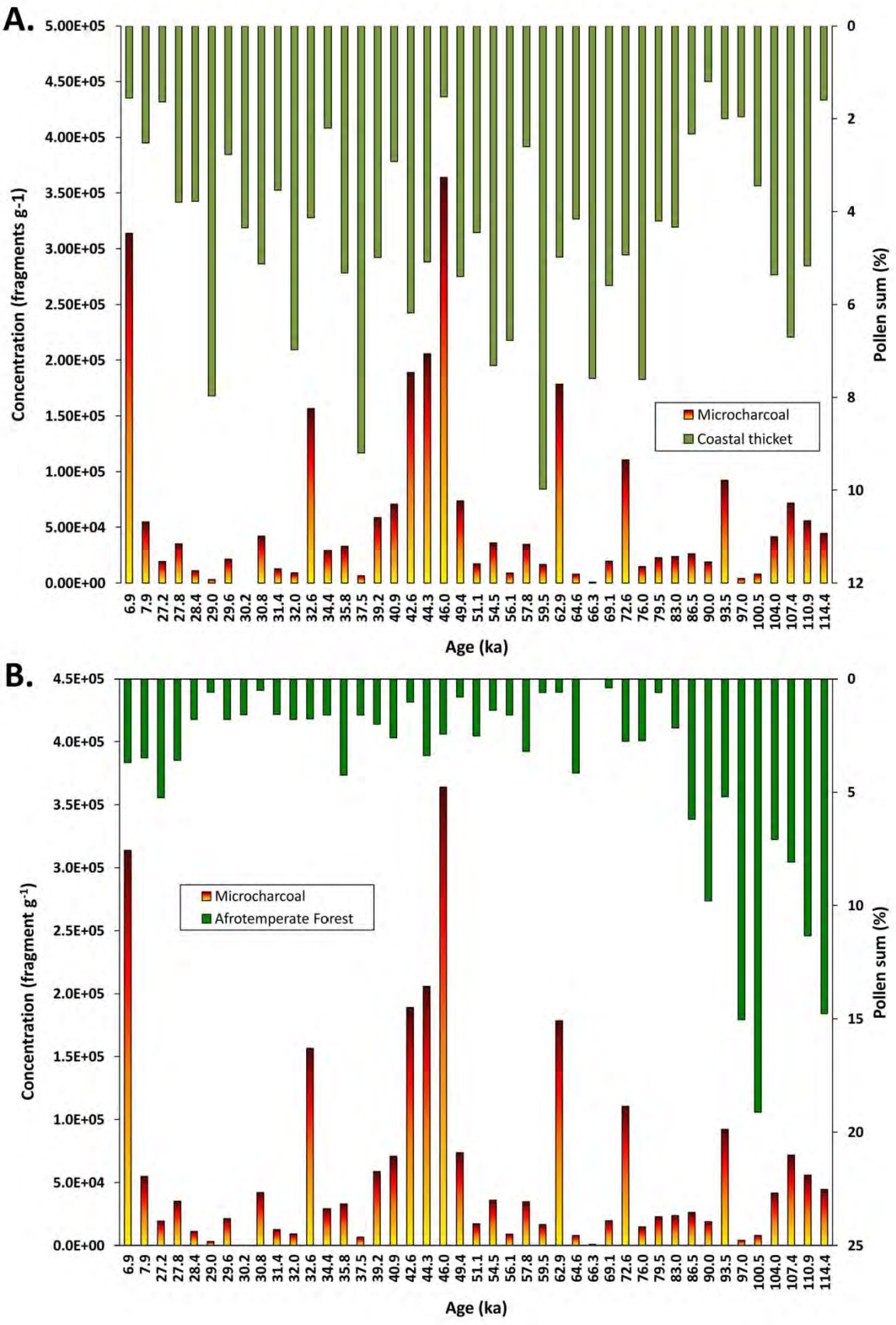

Figure 6.9 A comparison between the sum of the pollen percentages of coastal thicket taxa and microcharcoal concentrations (A) and the sum of the pollen percentages of afrotemperate forest taxa and charcoal concentrations (B) for the Vankervelsvlei 10.1 record.

Fire frequencies certainly exhibit strong ties to vegetation compositional changes for all three records, albeit to varying degrees and over disparate time periods. Climate change directly and indirectly affects both vegetation change and fire regimes. However, the exact nature of the relationships between climate, vegetation and fire cannot be fully elucidated as it is difficult to disentangle which factor drives the observed changes. For example: Does climate change (temperature, moisture and winds) directly affect vegetation change and fire regimes (direct control on fuel flammability and ignition probability) independently? Or are the changes in fire frequencies a result of changes in vegetation type (e.g. changes in fuel characteristics)? Or have changes in fire regimes promoted the establishment of certain vegetation types (e.g. fynbos) over others (e.g. thicket)? It is perhaps most likely that there are combinations of all of the above scenarios embedded within the three records under discussion. Increased chronological control and finer-scale subsampling resolutions together with a better understanding of charcoal source areas are needed to fully explore this line of investigation.

6.5 Palaeoenvironmental reconstructions

An inherent limitation of pollen analysis is the difficulty of identifying taxa down to species level, resulting in the possible reduction of information content in comparison to what could in fact be finer-scale species compositional changes. However, the identification of key indicator taxa and indicator groups together with the statistical analyses and the supplementary proxy data make it possible to reconstruct palaeoenvironmental conditions at each site.

6.5.1 Pearly Beach

Further analysis of the PCA results for PB-1 reveals the possibility that principal component 1 (PC1) may be most strongly related to relative temperature. Taxa such as *Stoebe*-type, Crassulaceae, Ericaceae and *Passerina* are negatively loaded on PC1 while *Dodonaea*, *Euphorbia*, *Morella* and *Sapotaceae* have positive loadings. *Dodonaea* is particularly temperature sensitive and generally is not present where temperatures are below 0°C (Figure 6.3). While the modern bioclimatic analysis (Appendix B) does indicate that many of the other taxa that are associated with positive loadings can tolerate colder conditions, they are relatively less tolerant than a large proportion of the rest of the dataset.

High negative scores for PC1 therefore appear to be associated with colder conditions whereas high positive scores could indicate warmer conditions at the site (Figure 6.10). In a similar manner, it is inferred that PC2 is a measure of the moisture availability at Pearly Beach with high negative scores relating to wetter conditions (e.g. negative scores for *Morella*, *Cliffortia*, *Haloraginaceae* and *Podocarpus* and positive scores for Crassulaceae, Aizoaceae, Geraniaceae and *Passerina*).

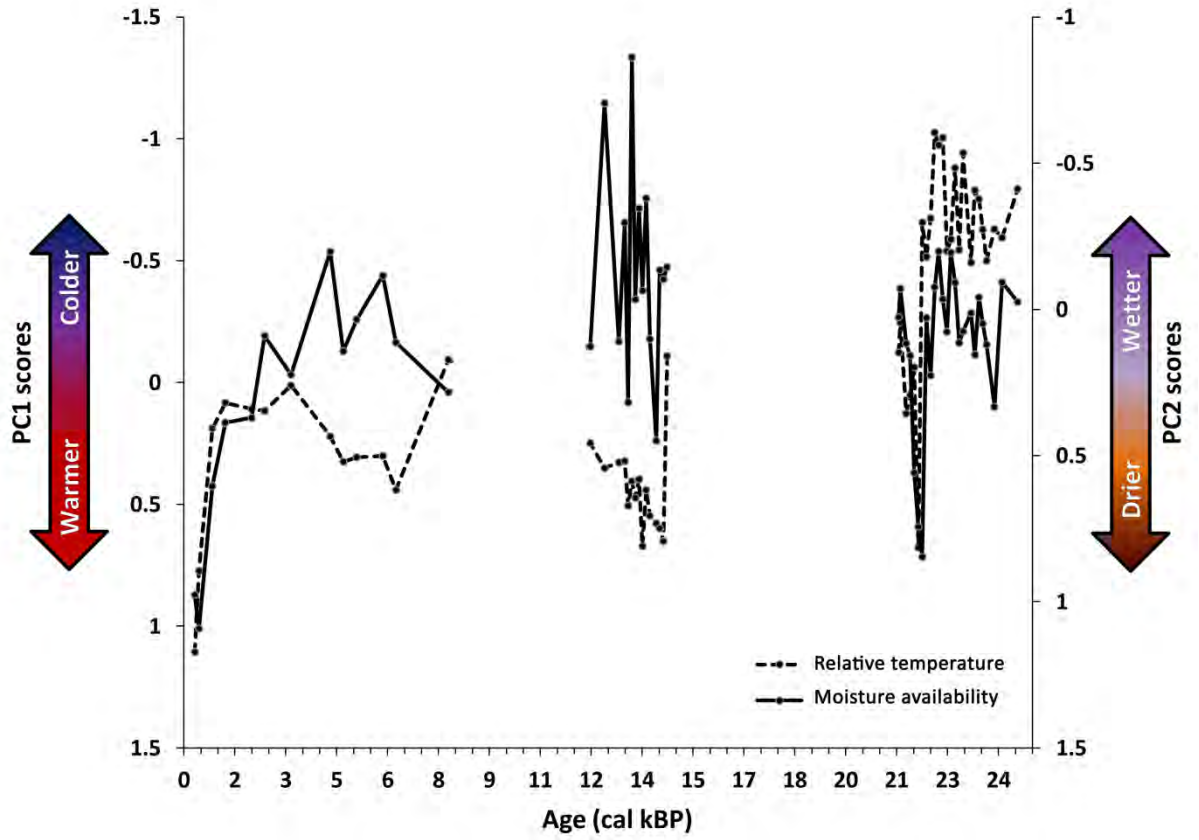

Figure 6.10 Principal Component 1 and 2 (PC1 and PC2) scores against age, PC1 is likely related to relative temperature and PC2 possibly indicates changes in moisture availability at the site.

Gas chromatography mass spectrometry (GC/MS) was applied to extractable (soluble) lipid samples taken from the PB-1 sediment core to determine amounts and proportions of biomarkers characteristic of plant leaf waves (specifically n-alkanes) and to perform compound specific $\delta^{13}C$ measurements. While pyrolysis gas chromatography mass spectrometry (Py-GC/MS) was applied to samples from RVSB-2 (this approach is similar to that applied to the PB-1 samples however the outputs are more complex to interpret as they are products (fragmentations) of the pyrolysis process and may not have been alkanes/alkenes in the original macromolecular material – A.S. Carr *pers comm.*). The biomarker analyses were performed by Dr. A. S. Carr and Dr. A. Boom at the

University of Leicester (details of the methodology for the GC/MS (PB-1) and the Py-GC/MS (RVSB-2) can be found in Carr et al., 2010c) and these data, while not the specific focus of this thesis, provide significant additional insight as to the palaeoenvironmental contexts of both Pearly Beach and Rietvlei, therefore warranting its inclusion within this chapter.

GC/MS and Py-GC/MS are used to characterise complex macromolecular organic matter in order to assess the preservation and provenance of sediment organic matter (Schwark et al., 2002; Meyers, 2003; Carr et al., 2010a). Diagnostic indices calculated from the plant biomarker datasets provide a perspective on palaeolimnological contexts and can aid palaeoenvironmental reconstruction (Vancampenhout et al., 2008; Carr et al., 2010a; Kouli et al., 2012).

The average chain length of long-chain (C_{27} – C_{33}) n-alkanes can be used as an indicator of moisture availability. This indicator is less likely to be influenced by local aquatic plant contributions (which have shorter chain lengths (C_{23} – C_{25})) than the overall average chain length parameter. Lower values on this scale are potentially indicative of increased moisture availability, either due to a shift in plant type or a shift in the type of lipids the plants are synthesising (A.S. Carr *pers comm*.). A project led by Dr. Carr is currently investigating biomarker signatures from typical plants found within the Fynbos and Succulent Karoo Biomes, preliminary results confirming that longer average chain lengths of n-alkanes in the C_{27} – C_{33} range are correlated with lower rainfall in the context of these biomes.

The 'P_{aq}' index, developed by Ficken et al. (2000), is a ratio reflecting the non-emergent aquatic macrophyte input to lake sediments relative to the input from emergent aquatic and terrestrial plants. It is commonly used to determine increased aquatic inputs within sedimentary sequences and is calculated by means of the following equation:

$$P_{aq} = \frac{(C_{23} + C_{25})}{(C_{23} + C_{25} + C_{29} + C_{31})}$$

The P_{aq} ratio was established from a limited survey of n-alkyl lipids extracted from aquatic macrophytes from four open water lakes in Kenya and therefore has not been tested extensively or applied directly to South African vlei environments with limited or no open water. Consequently interpretations from this parameter remain tentative. However, the P_{aq} ratio appears to correlate with the average chain length (C_{27} – C_{33}) index (Figure 6.11). Both indices reveal that sections of the Holocene are characterised by distinct increases in moisture availability associated with a greater contribution from aquatic and/riparian inputs. Furthermore the P_{aq} index and the percentages of aquatic pollen exhibit similar trends (Figure 6.12). The similarities between the two diagnostic

biomarker indices and PC2 scores provide further evidence of coherence between the pollen and biomarker data.

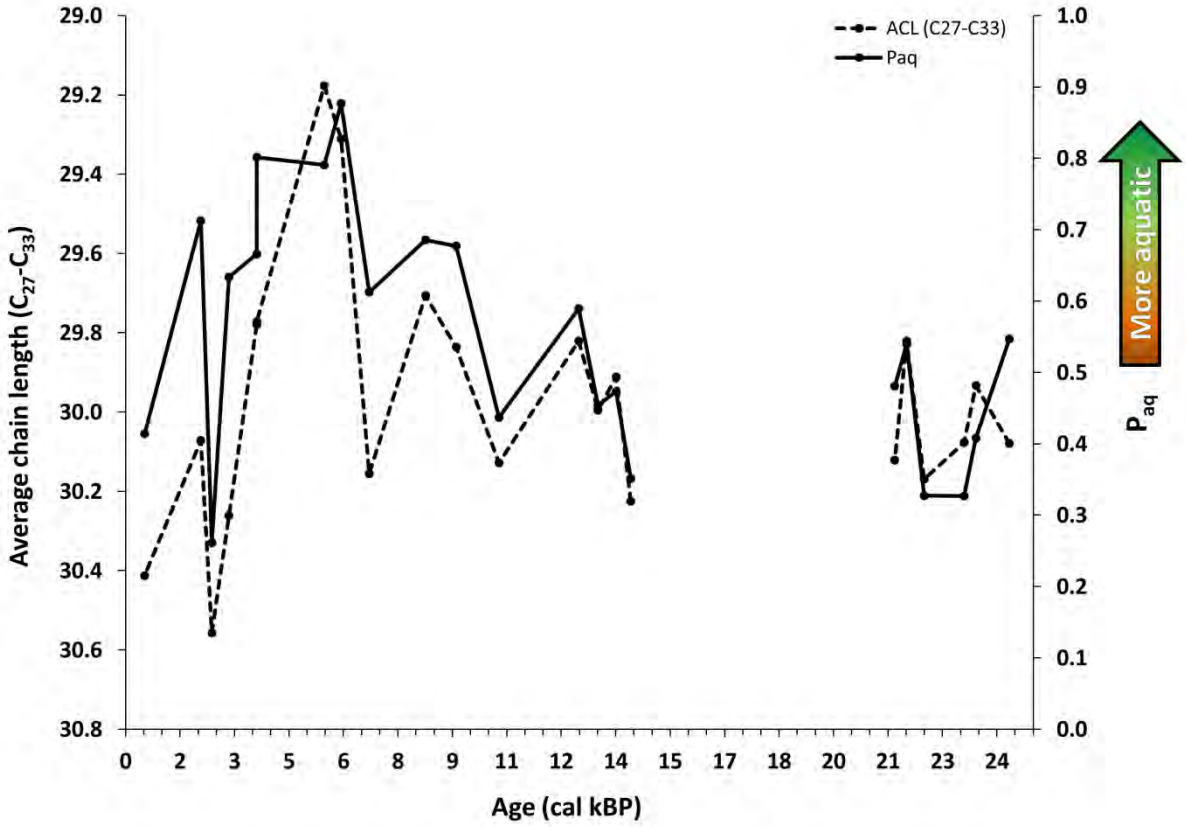

Figure 6.11 Average chain length of long chain n-alkanes (C_{27} – C_{33}) and the P_{aq} (proportion aquatic) parameter (Ficken et al., 2000) (A. Carr unpublished data).

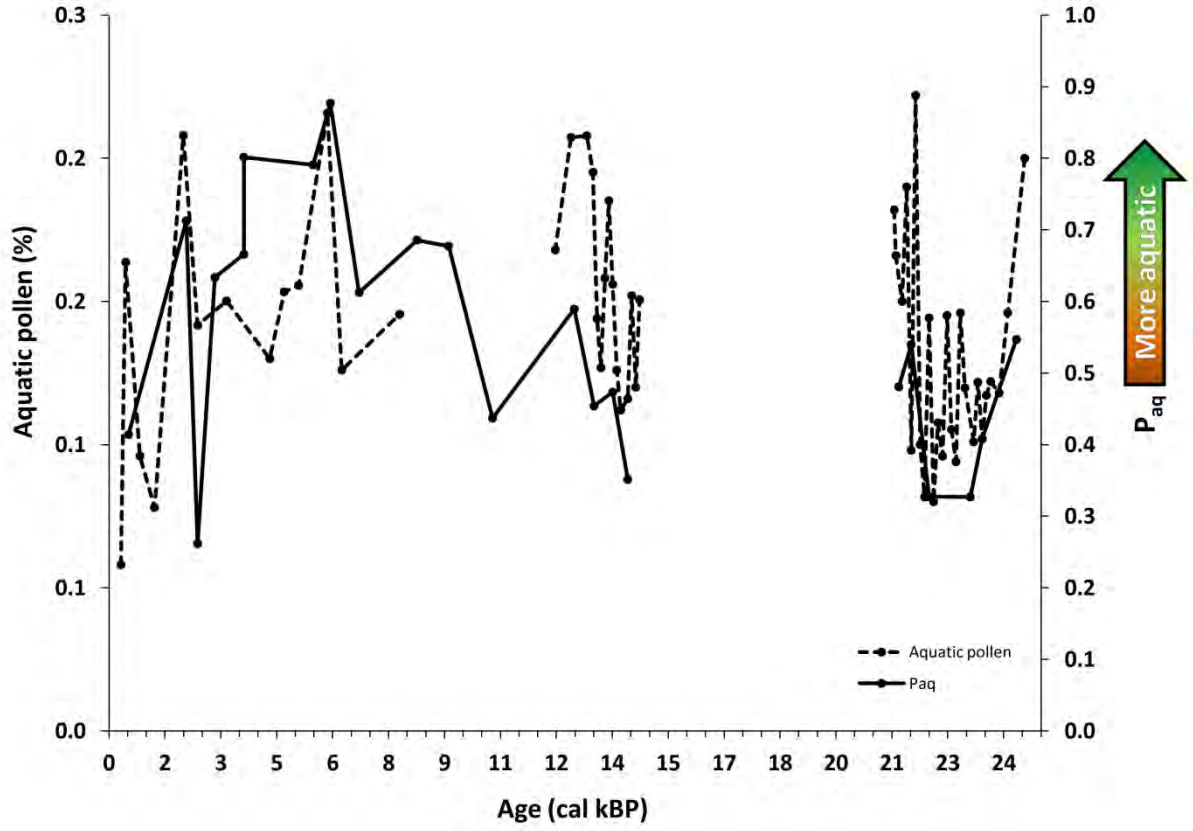

Figure 6.12 The P_{aq} parameter values (A. Carr unpublished data) compared to the sum of aquatic pollen taxa for PB-1.

The assessment of all proxy evidence derived from the Pearly Beach sediment core allows for the following palaeoenvironmental reconstruction for the period ~25 – 0 cal kBP.

Figure 6.13 A comparison of selected elements from the Pearly Beach pollen and geochemical records.

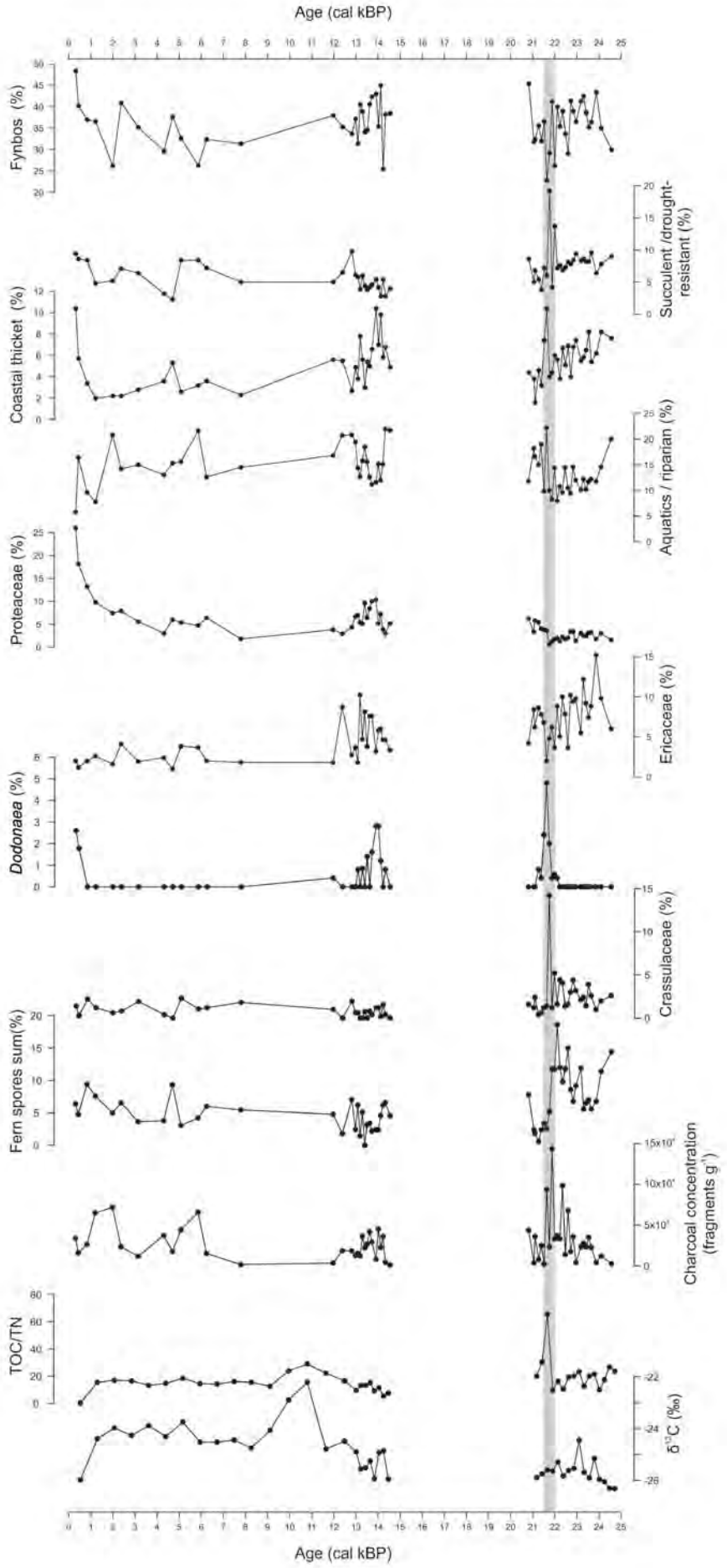

The last glacial section (~25 – 21 cal kBP)

The pollen record indicates that typical fynbos elements (Proteaceae, Ericaceae, Restionaceae, *Stoebe*-type, *Cliffortia* and *Passerina*) were present at the site between ~25 cal kBP and 22 cal kBP. Increased proportions of the cold tolerant taxa Ericaceae and *Stoebe*-type together with relatively elevated percentages of aquatic/riparian taxa (predominantly Cyperaceae, but also presence of *Aponogeton* and Juncaceae) and afrotemperate forest taxa signify that this period was characterised by increased moisture availability and cold temperatures. Further indications of colder and wetter conditions are the greatly increased amounts of fern spores (especially at 22.1 cal kBP) and the more depleted $\delta^{13}C$ signal (Figure 6.13). The moisture availability and relative temperature indices derived from the PCA analysis (Figure 6.10) confirm the above inferences.

An abrupt deviation from the previous conditions is evident for the brief period between 22 cal kBP and 21.5 cal kBP (Figure 6.13 grey shaded area). Although this episode is only represented by very few data points, all lines of proxy evidence are in agreement and indicate that this discrete phase was characterised by a fairly dramatic increase in aridity, possibly also associated with a rise in temperatures:

There is a peak in the succulent/drought resistant taxa sum, primarily a response to a substantial increase in one taxon, *viz.* Crassulaceae, which is generally an indicator of more xeric conditions (Figure 6.13). As the peak in the Crassulaceae is coincident with discrete increases in *Dodonaea* and significant reductions in Ericaceae, *Stoebe*-type, arboreal pollen (absence of many trees taxa and the lowest percentage of Proteaceae for the whole sequence) and fern spores, it is likely that conditions were drier and warmer than the rest of the glacial period. Once again this is also evident within the PCA results as there are strong indications of decreased moisture availability from 21.8 cal kBP to 21.5 cal kBP and a spike in the relative temperature at 21.6 cal kBP.

Charcoal concentrations are exceptionally high at ~21.9 cal kBP coincident with a stronger fynbos presence and slightly before the peak in *Dodonaea* (~21.6 cal kBP) (Figure 6.13), demonstrating that the contemporary ecological dynamics associated with fynbos, fire and coastal thicket elements (introduced in Chapter 2 and discussed in more detail in section 6.4) remain an important mechanism within the palaeoecological record.

The geochemical subsample at ~21.6 cal kBP is strongly indicative of increased terrestrially-derived organic matter inputs as its TOC/TN ratio is exceptionally high in comparison to the rest of the dataset (Figures 5.19 and 6.13).

It therefore appears that, during this period, the Pearly Beach Marsh was less well developed as a wetland and more exposed and that the surrounding vegetation consisted of mainly thicket elements as opposed to fynbos. Environmental conditions were relatively warmer and drier than both the preceding and subsequent glacial sections.

After this brief warmer and drier phase, the remaining section of the last glacial recorded in the PB-1 core (PAZ PB1-B1) appears to be most favourable for the preservation of pollen as pollen concentrations are very high. This period is once again dominated by relatively high percentages of Ericaceae in association with increases in other fynbos taxa, aquatic/riparian pollen and a significant peak in afrotemperate pollen taxa (at ~21.3 cal kBP). Drought resistant and/ succulent taxa and thicket taxa are all relatively low. PC1 indicates wetter conditions and there is a peak in TOC at ~21.2 cal kBP denoting an increase in OM content. Consequently it appears that humid conditions from ~21.5 – 21 cal kBP led to the establishment of increased afrotemperate forest elements within an overall mosaic of fynbos.

The sand layer

The geochemical data from the sand layer between 162 and 133 cm exhibits the greatest extremes with some samples inferring the presence of terrestrially-derived OM (very high TOC/TN ratios) while others having the lowest TOC/TN ratios for the sequence, an indication of enhanced aquatic or algal OM input (see Figure 5.20, PAZ PB1-B2). The pollen and charcoal records reflect a similar chaotic pattern with a large peak in Haloragaceae, high proportions of Restionaceae and one discrete peak in charcoal fragments.

All proxy evidence indicates that this sand layer is an anomaly as it has less stratigraphic integrity than the rest of the core or has been formed as a result of higher accumulation rates and therefore exhibits higher variability. It could either have been deposited instantaneously as one event perhaps as a result of downstream flooding of the Groot Hagelkraal River or accumulated more gradually over time. As the stratigraphy remains somewhat intact (the fine layers of dark, more organic-rich sediments and plant detritus embedded within the sand layer remain horizontally deposited) and gravel-sized particles are absent from the grain size distribution, it is more likely that this layer was formed within a less high-energy environment than that created by a flooding event. The origin of the sand is probably the coastal dunes surrounding the site. Lower vegetation cover on the dunes and/or changes in the wind regime could potentially have resulted in increased exposure and mobilisation of the dunes. Without dating the individual organic-rich lenses, the time frame involved

cannot be determined and therefore this section is deemed to be of limited palaeoclimatic significance.

The LGIT section (~14 – 11.5 cal kBP)

From ~14.2 cal kBP to 12.2 cal kBP (PAZ PB1-B3) the record is characterized by the dominance of fynbos taxa with notably elevated percentages of Proteaceae and Restionaceae, signifying a shift from ericaceous to more proteoid and restioid fynbos types. There is also a peak in the afrotemperate forest sum; however this is mainly due to an increase in *Clutia* pollen percentages which most probably implies the increased presence of scrub forest rather than full afrotemperate forest. The coastal thicket sum is fairly high for this period with the reappearance of *Dodonaea* and increases in *Morella* and *Canthium*. Succulent/drought resistant taxa percentages are low expect for a peak at ~12.8 cal kBP and the persistent presence of Euphorbiaceae which could represent thicket/strandveld elements and perhaps relate to an increase in temperatures.

The vegetation surrounding the wetland, which was fairly well developed, therefore consisted of a mosaic of fynbos and coastal thicket with some scrub forest elements. The greater dominance of arboreal taxa was most probably a response to rising temperatures, increases in moisture availability and perhaps elevated CO_2 (trees generally have greater carbon demands than grasses, herbs and shrubs (Bond et al., 2003 and references therein)).

Charcoal frequencies were generally low for most of this period except for a peak in the large charcoal fragments (Class 3) at ~13.6 ka. This peak most likely represents a localised fire in the vicinity of the vlei (refer to section 4.7.2) and therefore has little bearing on the regional environmental record.

The Holocene (~11.5 – 0 cal kBP)

The poor pollen preservation within the early Holocene (from ~11.9 cal kBP to 7.8 cal kBP) corresponds with increased proportions of clay and silt in the core. General causes of degradation and loss of pollen grains such as oxidation, temperature, pH and bacterial activity may be responsible for the absence of adequate numbers of pollen grains within this section. The geochemical and plant biomarker data for this period are somewhat inconclusive. A high TOC value for the sample as 10.8 cal kBP could suggest increased organic inputs and possibly humid conditions whereas the relatively enriched $\delta^{13}C$ signal, a lower P_{aq} value and increased proportion of longer

chain lengths could indicate decreased moisture availability in association with increased proportions of terrestrially-derived OM.

Pollen is better preserved for the mid-Holocene (from ~7.8 cal kBP to 4.5 cal kBP) and for the late Holocene. Ericaceae percentages are greatly reduced for the whole of the Holocene section, most likely in response to the increased overall temperatures that are characteristic of interglacial periods. *Stoebe*-type pollen proportions are also reduced, however not as significantly as Ericaceae. Proteaceae steadily increases from the mid-Holocene towards the top of the sequence reaching very high proportions within the late Holocene. The afrotemperate forest sum is lowest for the Holocene section in comparison to the LGIT and the glacial period. It should be noted, however, that afrotemperate forest trees are often underrepresented in pollen assemblages and forest elements may have actually been more dominant in the landscape but low pollen production masks this in the pollen record.

In terms of the biomarker data, there is a significant increase in the proportion of shorter chain lengths and a high P_{aq} values from ~5.9 – 5.5 cal kBP, coinciding with a peak in aquatic/riparian pollen and suggesting that wetland productivity was high. At the same time, Proteaceae percentages are low, while Restionaceae percentages, pollen and charcoal concentrations are all relatively elevated. The PCA results indicate moderately warmer and wetter conditions from ~6.0 – 4.5 cal kBP.

After the peak at ~5.9 – 5.5 cal kBP, the biomarker indices indicate that more terrestrially-derived OM was once again dominant. Asteraceae high-spine variety exhibits a marked increase at ~4.3 ka. Scott and co-authors (e.g. Scott and Woodborne, 2007b) have related this taxon to decreased moisture availability; however the cosmopolitan nature of this taxon limits robust environmental inferences.

The most recent period within the sequence (PAZ PB1-H, 0.4 – 0 ka) is characterised by a significant increase in the thicket sum indicated by the presence *Dodonaea, Euclea, Morella* and Sapotaceae (*Sideroxylon inerme*) (Figure 6.13). *ChenoAm*-type percentages are relatively high and, given that this taxon is comprised of a large proportion of halophytic species, this could indicate a strong salt marsh component to the vlei during this period. The local aquatic/riparian sum is comparatively low for this section, while Proteaceae percentages are exceptionally high. The biomarker and PCA results suggest decreased moisture availability and increased temperatures. The warmer conditions characterising the late Holocene, in association with elevated CO_2, probably resulted in the increase in woody thicket elements. Lower charcoal concentrations (low amounts of Class 2 charcoal and

absence of Class 3), implying reduced fire frequencies, may have promoted the establishment of thicket stands in amongst proteoid fynbos. A similar vegetation mosaic is currently present at Pearly Beach. However the fynbos, coastal thicket and rare patches of southern coastal forest are rapidly being replaced by dense stands of alien vegetation (particularly *Acacia* species) and wild flower farming (predominantly the cultivation of *Protea* species).

6.5.2 Rietvlei Still Bay

Analysis of the PCA results from Rietvlei Still Bay yielded no clear correlations between the selected taxa scores and environmental parameters. Little additional palaeoenvironmental information can therefore be inferred from the statistical analysis. The greater variability observed within the Rietvlei pollen record (with pollen taxa representative of multiple types of vegetation) in comparison to the Pearly Beach (strongly dominated by fynbos) may be obscuring these results.

The initial biomarker data for RVSB-2 is published in Carr et al. (2010). The summary of the pyrolysis-GC/MS data in terms of the same parameters used for Pearly Beach is shown as Figure 6.14, while Figure 6.15 presents the DCA factor scores from Carr et al. (2010) that give some indication of the extent of OM preservation and the degree to which the organic matter is either more terrestrial- or algal-derived.

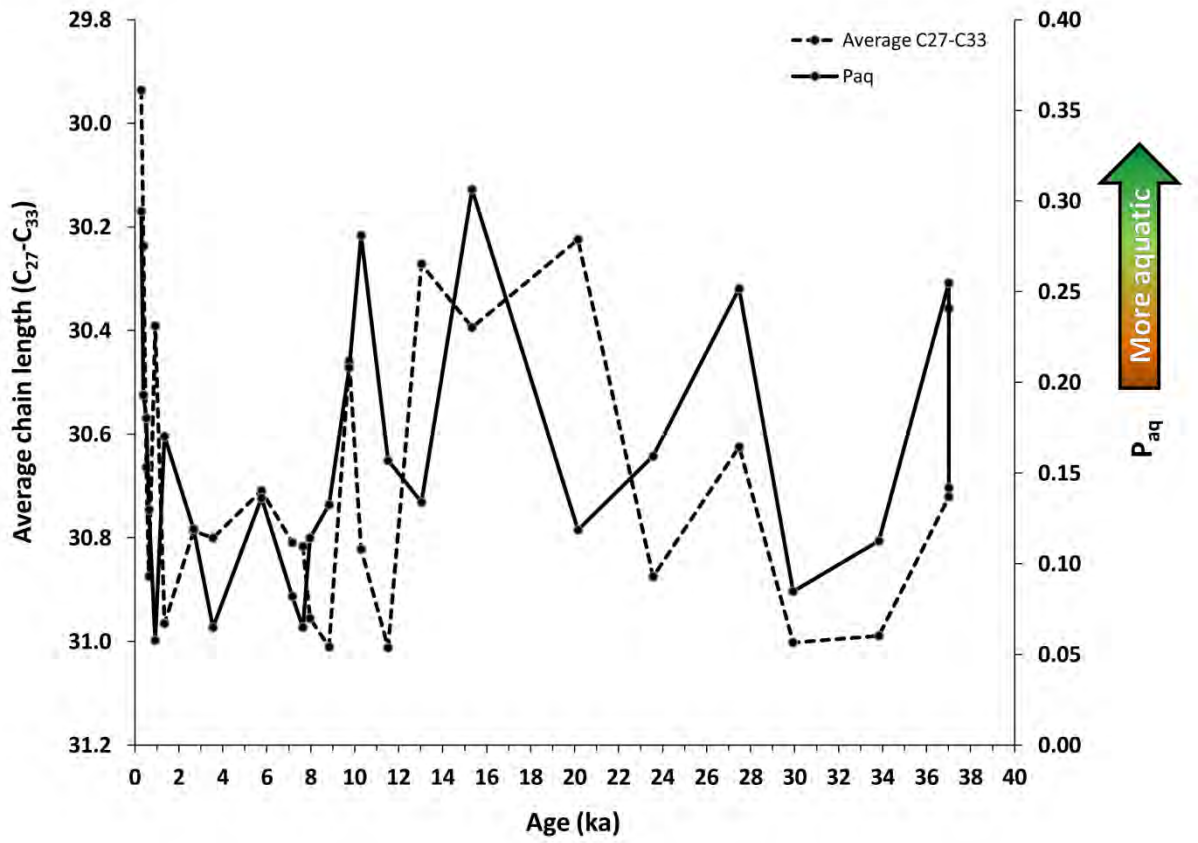

Figure 6.14 Average chain length of long chain n-alkanes (C_{27} – C_{33}) and the P_{aq} (proportion aquatic) parameter (Ficken et al., 2000) for the RVSB-2 core (Carr et al., 2010a and A. Carr unpublished data).

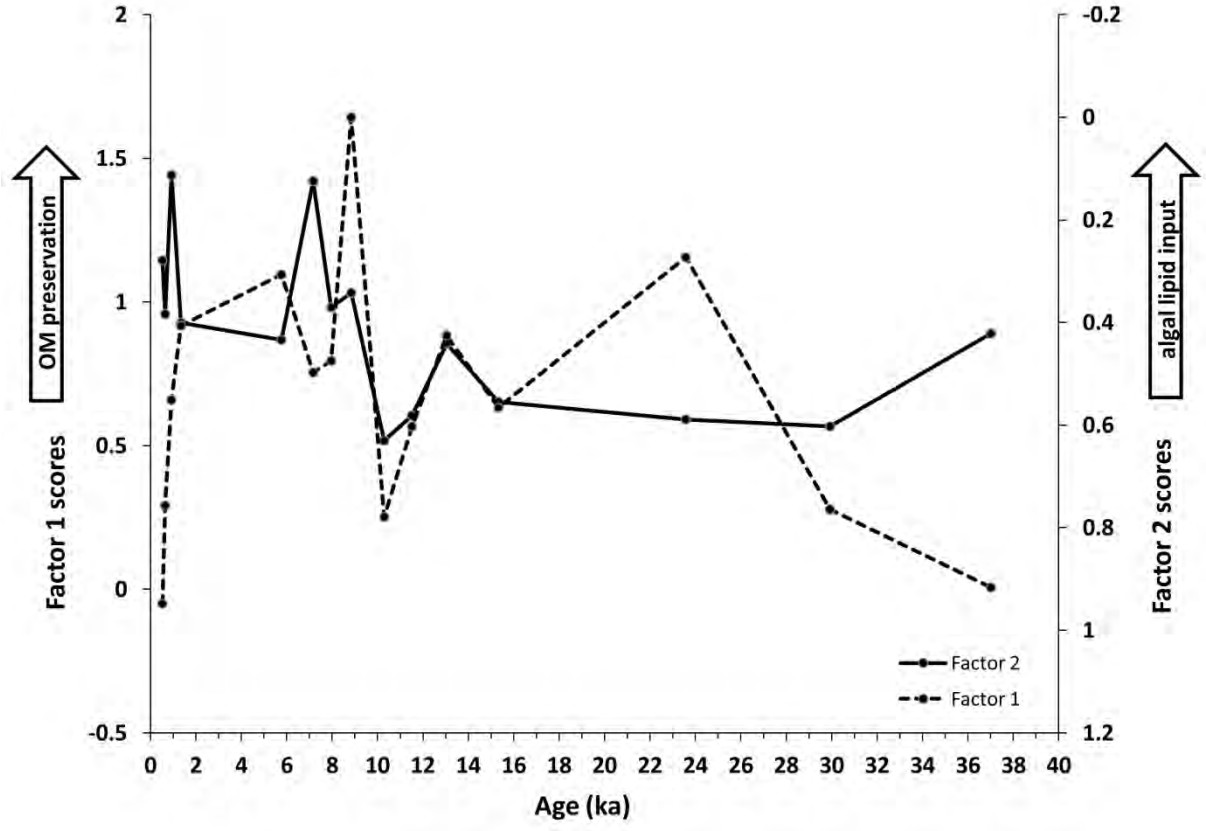

Figure 6.15 RVSB-2 biomarker DCA sample scores for the first two factors from Carr et al. (2010). Factor 1 indicates the extent of organic matter preservation and Factor 2 relates to algal and terrestrial lipid inputs.

The evaluation of the pollen, microscopic charcoal, geochemical and plant biomarker data has resulted in the following palaeoenvironmental reconstruction for Rietvlei for the period 36 – 0 ka.

Figure 6.16 A comparison of selected elements from the Rietvlei Still Bay 2 pollen and geochemical records.

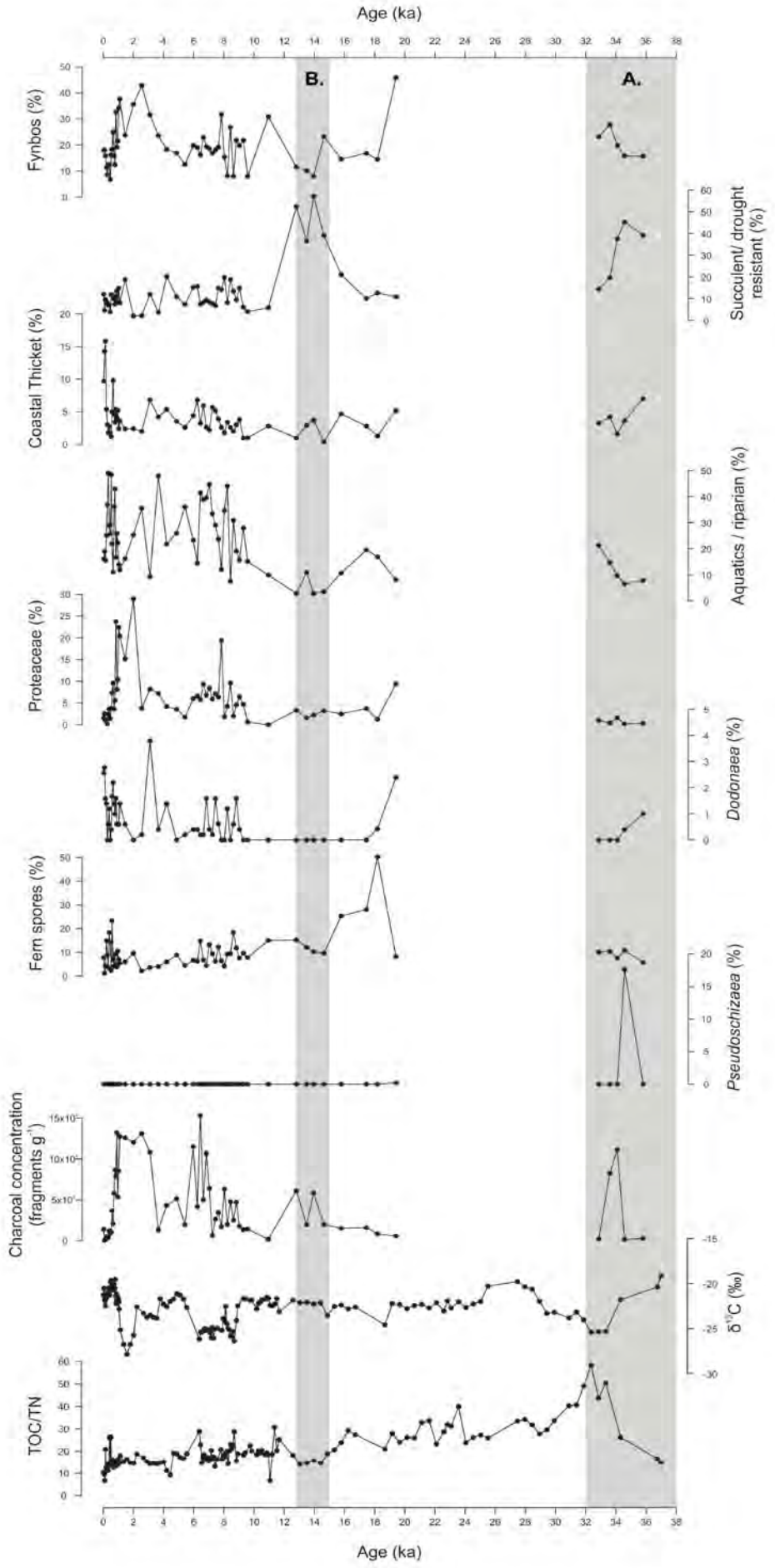

The MIS 3 section (~36 – 32 ka)

In general this period is represented by very low pollen concentrations. While the local aquatic and/ riparian sum is reduced, particularity for the period between ~36 – 35 ka, wetland conditions appear to have still prevailed at the site. Fynbos elements are either low or absent from the section, with the exception of Restionaceae and *Anthospermum*-type which are relatively elevated. The sum of all the succulent and/ drought resistant taxa is fairly high with increases in Aizoaceae, Crassulaceae, Euphorbiaceae, *Ruschia* and especially high percentages of Geraniaceae.

The TOC/TN ratios indicate a stronger influence of terrestrially-derived OM for most of this phase. The data point at the base of the sequence (~36 ka) falls outside the traditionally-constrained C_3 plant envelope in terms of $\delta^{13}C_{TOC}$ values (Figures 5.38 and 6.16), which could perhaps reflect the increased contribution of C_4 grasses and/or the CAM succulent vegetation (e.g. Aizoaceae, *Ruschia*, Crassulaceae and *Euphorbia*) that is evident within the pollen record.

Scott (1992) suggests that the presence of *Pseudoschizaea* shells/spores within sediments could in some instances indicate local seasonal drying. The combination of increased succulents and/drought resistant taxa, a very prominent peak in *Pseudoschizaea*, increased charcoal amounts and concentrations and a less developed wetland environment indicates that conditions were more xeric than present during the earliest part of the record (Figure 6.16 grey shaded area A). Vegetation surrounding the vlei consisted of a greater dominance of succulents, drought resistant shrubs and more cosmopolitan shrubs such as *Anthospermum* and *Artemisia* with limited to no tree and tall shrub elements (which could be a result of drought stress, fire or both these elements).

Depleted $\delta^{13}C_{TOC}$ values and relatively high TOC from ~35 - 32 ka in conjunction with increased percentages of aquatics and/ riparian pollen signifies relatively improved wetland conditions with increased moisture availability and better OM preservation for the latter part of this section.

The late MIS 3 to early MIS 2 section (~32 – 19 ka)

No pollen has been found in the pale carbonate-rich section of the core, which spans from ~32 ka to ~19 ka. These sediments have very low TOC levels and the biomarker data indicate the presence of highly degraded OM. Relative enrichments within the $\delta^{13}C_{TOC}$ sequence during this time are indicative of decreased moisture availability, perhaps resulting in the vlei drying out. Further substantiation for desiccation of the wetland environment is the minor oxidation (slight orange

mottling) of the sediments within this section which could signify shallow-water conditions or sub-aerial exposure (Carr et al., 2010).

The LGIT section (~19.4 – 11.5 ka)

Fynbos (particularly Proteaceae, *Cliffortia* and *Stoebe*-type) percentages, local wetland taxa percentages and fern spore counts are all greatly increased from the recommencement of the pollen record at ~19.4 to ~17.5 ka. Thereafter the proportions of these groups drop substantially for much of the rest of this section. The strong fynbos dominance at ~19.4 ka appears to have influenced the $\delta^{13}C_{TOC}$ record which reflects a more depleted signal relating to the stronger contribution of C_3 vegetation at the site.

It therefore appears that there was a short period of enhanced moisture availability at the beginning of this section promoting the dominance of fynbos vegetation within the region. This is followed by increasing signs of aridity up until the boundary with the Holocene. Decreased moisture availability is especially evident from ~15 – 13 ka, where *ChenoAm*-type reaches exceptionally high percentages (30 – 50%) and charcoal (all classes and concentration) peaks (Figure 6.16 grey shaded area B).

No pollen is preserved for the Younger Dryas chronozone (12.9 – 11.5 ka). However, a distinct decrease in OM preservation and a rise in more terrestrially-derived lipid inputs (Figure 6.5) provide evidence for an even greater decrease in moisture availability during this chronozone in comparison to the previous phase.

The Holocene (11.5 – 0 ka)

The early Holocene is characterised by enhanced wetland productivity inferred from significant increases in OM preservation and greater proportions of algal-derived OM. Lower $\delta^{13}C_{TOC}$ values are accompanied by elevated fynbos and aquatic and/riparian pollen and decreased succulent and/ drought resistant taxa, suggesting an increase in moisture availability during this period (Figure 6.16).

In the mid-Holocene (~7 – 4 ka) section lower proportions of fynbos and aquatic/riparian taxa suggest drier conditions relative to the early Holocene. OM preservation and algal inputs are also reduced at this time.

The late Holocene section is characterised by greater variability with discrete episodes of increased wetland productivity (e.g. from ~3 – 1 ka) and increases in fynbos (e.g. at ~2.6 ka). Contemporary vegetation with a dominant coastal thicket/strandveld component appears to be established around 0.7 ka.

6.5.3 Vankervelsvlei

6.5.3.1 Further interpretation of VVV10.1 PCA results

Examination of the PCA taxa loadings from Vankervelsvlei indicates the possibility that PC1 is primarily a measure of relative temperature, as an especially high negative loading is associated with Ericaceae. *Morella* and *Passerina* (taxa that are also able to tolerate cold conditions) and *Pentzia*-type (a cold intolerant taxon, contemporarily associated with high temperatures) attained the highest positive loadings on PC1 (Figure 6.17).

It is unclear as to whether PC2 (explaining only half as much of the variance as PC1) is related to any particular environmental parameter. Despite high variability, PC2 follows a similar trend to PC1 when plotted against interpolated ages (with the exception of the two Holocene data points). However the taxa loadings do not appear to be grouped according to any clear bioclimatic parameter and PC2, therefore, is not considered useful for the palaeoenvironmental reconstruction presented below.

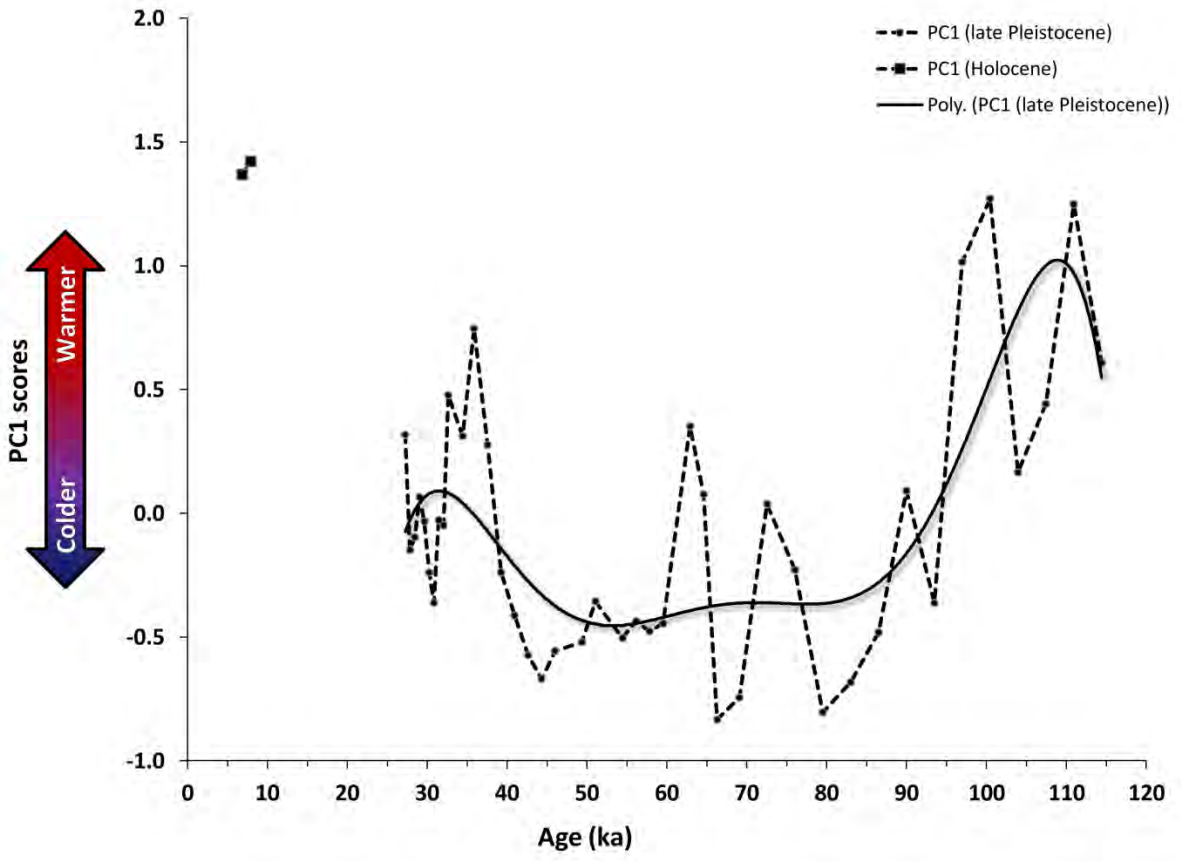

Figure 6.17 VVV10.1 PC1 scores indicating changes in temperature at the site.

6.5.3.2 Other records from Vankervelsvlei

Several sediment cores have been extracted from Vankervelsvlei over the last 20 years (Table 6-2). However, poor chronological control and inconsistencies together with the lack of continuous pollen preservation have meant that up until this study, limited reliable palaeoenvironmental evidence has been generated.

Table 6-2 A summary of all sediment cores extracted from Vankervelsvlei. *Includes all ages even those deemed outliers. #Based on the re-analysis of VVVA and VVVB's chronology and not that used within Irving (1998).

Core	Year of extraction	Ages*	Age range of pollen record#	Analyses	Reference
VVVA	1992	4 ^{14}C ages	3.3 - 56.7 cal kBP	pollen, particle size (sieve)	Irving and Meadows (1997); Irving (1998)
VVVB	1996	4 ^{14}C ages	7.3 - 103.6 ka	pollen, particle size (sieve), geochemistry (inorganic)	Irving and Meadows (1997); Irving (1998)
VVV09	2009	-	-	particle size (laser), geochemistry (organic and inorganic)	-
VVV10.1	2010	6 ^{14}C ages; 2 OSL ages	6.9 - 116 ka	pollen, particle size (laser)	Burger (2011); this study
VVV10.2	2010	3 ^{14}C ages		-	-
VVV10.3	2010	-	-	-	-

Owing to the irregular shape and depositional character of Vankervelsvlei and the different extraction locations (Figure 6.18), the stratigraphies of the six cores are complex and do not all contain analogous sediment units. VVV09 is largely comprised of fairly inorganic clays and fine to medium sands and most likely has been influenced by its close proximity to the sides of the basin. VVV10.2 and VVV10.3 are shorter (185 and 210 cm respectively) and less compacted cores which contain fairly homogeneous, highly organic sediments with large quantities of plant detritus and rootlets. Two of the radiocarbon ages obtained for VVV10.2 are from a single near-basal subsample. AMS analyses were performed on both fractions of the subsample; the bulk organic sediment and identifiable plant material. Reassuringly, these returned similar ages (Table 6-3), which average to 7.4 cal kBP. The sample from 106 cm is associated with an age of 8 cal kBP. This reversal is perhaps a result of rootlet penetration, calling into question the future usefulness of this core. As ages have yet to be procured for VVV10.3 very little can be ascertained from this core at present.

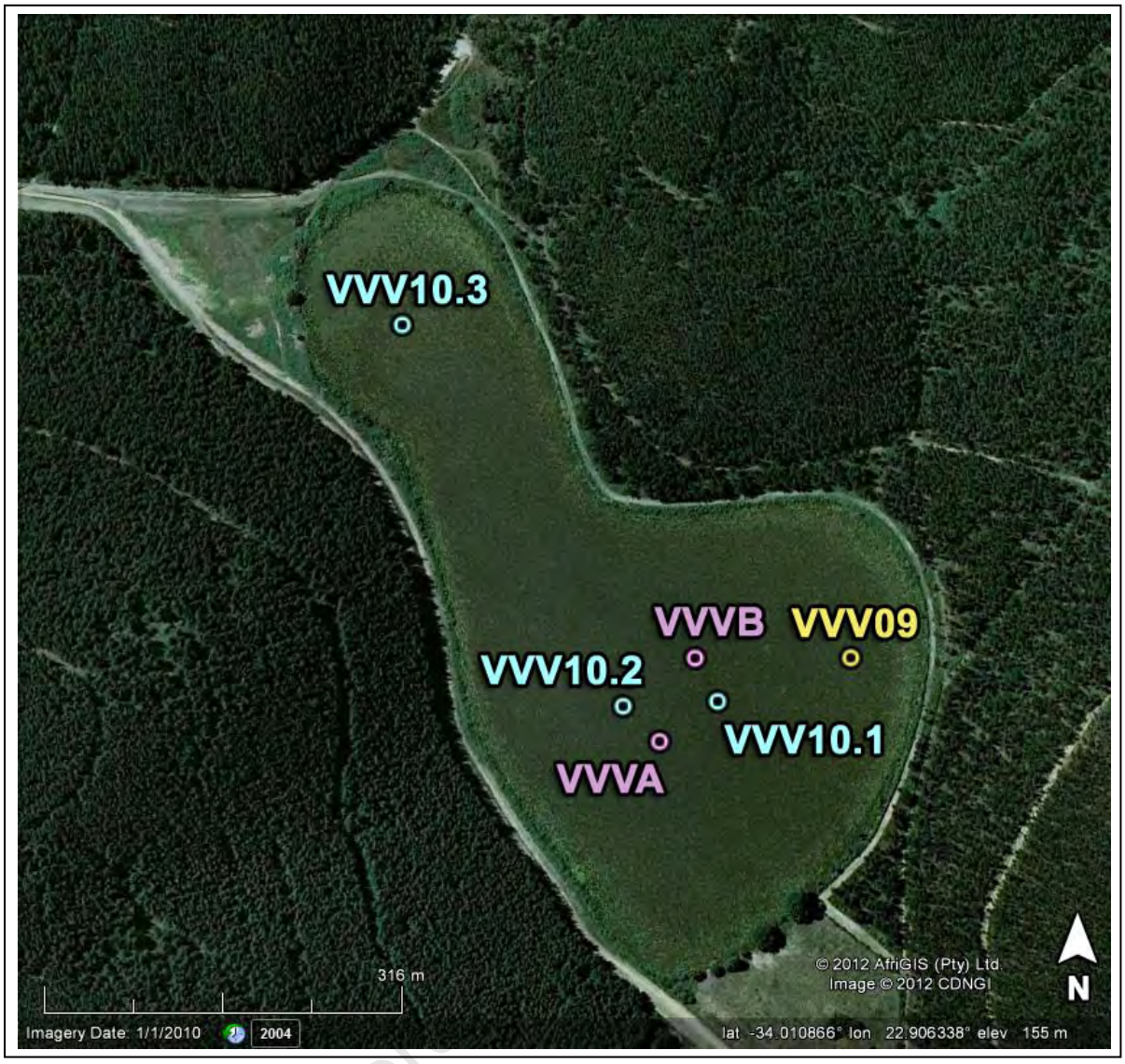

Figure 6.18 The location of all sediment cores extracted from the Vankervelsvlei basin, VVA and VVB (Irving and Meadows, 1997; Irving 1998), VVV10.1 (this study), VVV10.2 and VVV10.3 (not analysed) [image source: Google Earth 2004].

Similarities in the stratigraphies of VVVA, VVVB and VVV10.1 are certainly evident (Figure 6.21). The radiocarbon ages from these cores (Irving and Meadows, 1997) were calibrated and age-depth models were produced (Table 6-3, Figures 6.19 and 6.20). As Pta-6361 and Pta-7259 are close to ~40 000 yr BP, the limit of radiocarbon dating at the time, these ages were excluded from the respective age-depth models. Pta-7124 is associated with a significantly high error (Table 6-3) and has also been excluded from the age-depth model (it is possible that contamination occurred at some point during either the sampling, subsampling or analysis phases, discussion on the repercussions of the inclusion of an extremely small fraction of modern carbon is found in Chapter 5).

A possible relative palynological chronological marker is the sudden rise in *Podocarpus* which is an easily identifiable pollen grain and therefore confidence is placed in the similar pattern present in both VVVB and VVV10.1. The age-depth model presented in Figure 6.20 takes into account the similarities in the stratigraphies between VVVB and VVV10.1 (e.g. the distinct light grey clay layer with orange mottles) and incorporates the *Podocarpus* marker at 86.5 ka.

Laboratory ID	Core	Average depth (cm)	Measurement method	14C age yr BP	1 sigma error	Calibration data	95.4 % (2σ) cal age range	Relative area under distribution	median probability
Pta-6583	VVVA	11.0	GPC	3170	60	SHCal04	cal BP 3161 - 3194 cal BP 3197 - 3466	0.030508 0.969492	3331
Pta-6585	VVVA	410.0	GPC	7130	40	SHCal04	cal BP 7794 - 7814 cal BP 7817 - 7979	0.028626 0.971374	7898
Pta-6584	VVVA	503.5	GPC	19556	221	INTCal09	cal BP 22594 - 23907	1	23346
Pta-6361	VVVA	697.5	GPC	39956	1000	INTCal09	cal BP 42483 - 45363	1	43919
Pta-7258	VVVB	21.0	GPC	7240	60	SHCal04	cal BP 7240 - 7872 cal BP 7928 - 8165	0.963028 0.036972	8004
Pta-7130	VVVB	120.5	GPC	19356	211	INTCal09	cal BP 22457 - 23660	1	23051
Pta-7259	VVVB	379.5	GPC	38456	1100	INTCal09	cal 41342 - 44523	1	42889
Pta-7124	VVVB	524.0	GPC	31656	1200	INTCal09	cal BP 33616 - 38942	1	36273
Beta-292547	VVV10.2	106.0	AMS	7230.0	50	SHCal04	cal BP 7895 - 7895 cal BP 7927 - 8071 cal BP 8085 - 8159	0.040890 0.840824 0.118287	7992
Beta-292548	VVV10.2 - sediment fraction	177.0	AMS	6530	50	SHCal04	cal BP 7273 - 7474	1	7378
Beta-293399	VVV10.2 - plant fraction	177.0	AMS	6490	50	SHCal04	cal BP 7261 - 7433	1	7357

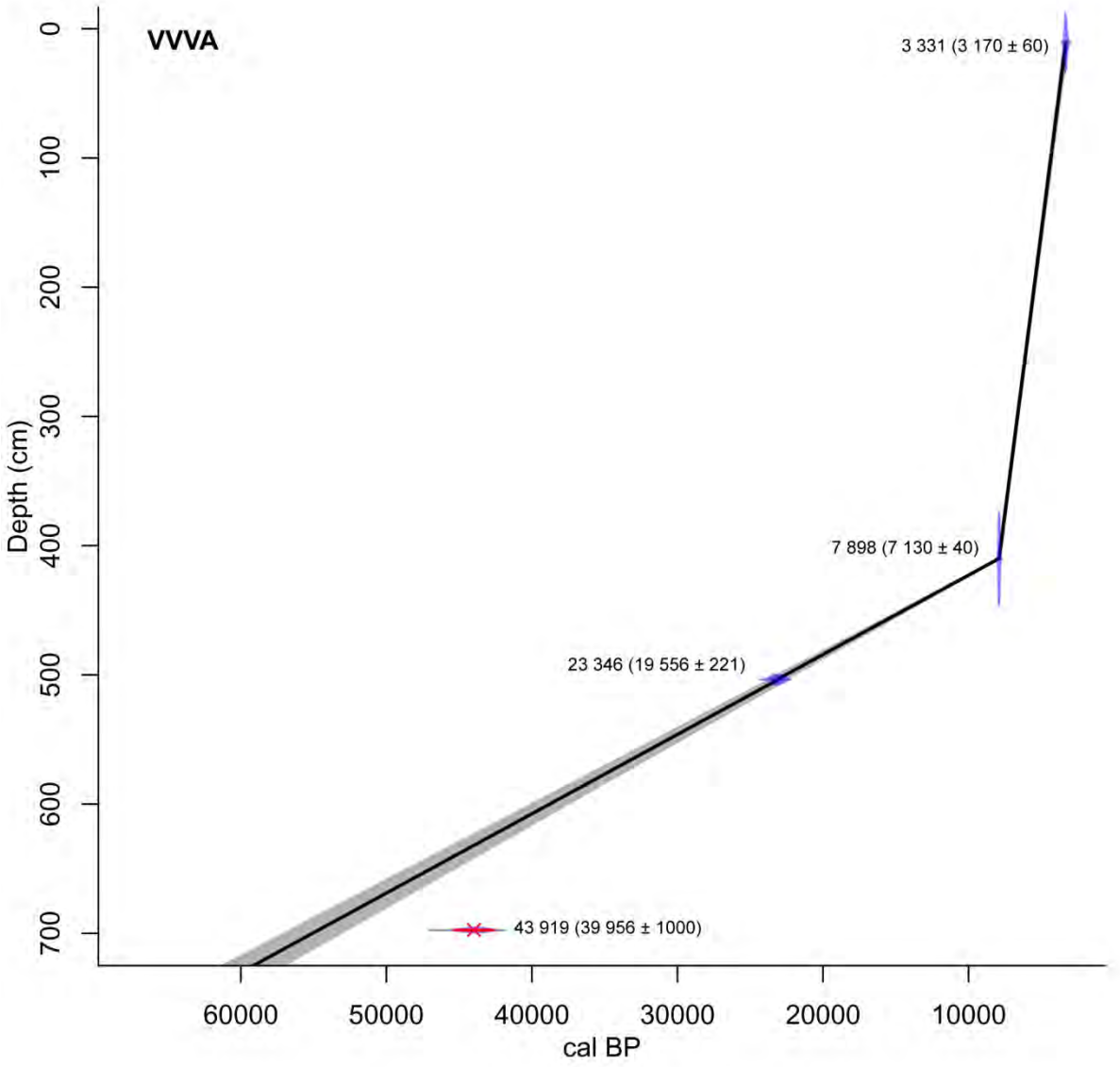

Figure 6.19 Age-depth model for VVVA generated in R using CLAM (Blaauw, 2010). The median probability calibrated ages are labelled and the uncalibrated ages with errors are provided in parentheses. Grey envelopes show the 95% confidence intervals, blue histograms indicate the ^{14}C calibrated distribution using SHCal04 (McCormac et al., 2004) or IntCal09 (Reimer et al., 2009) (see Table 6-3). Red stars indicate those ages that were deemed outliers.

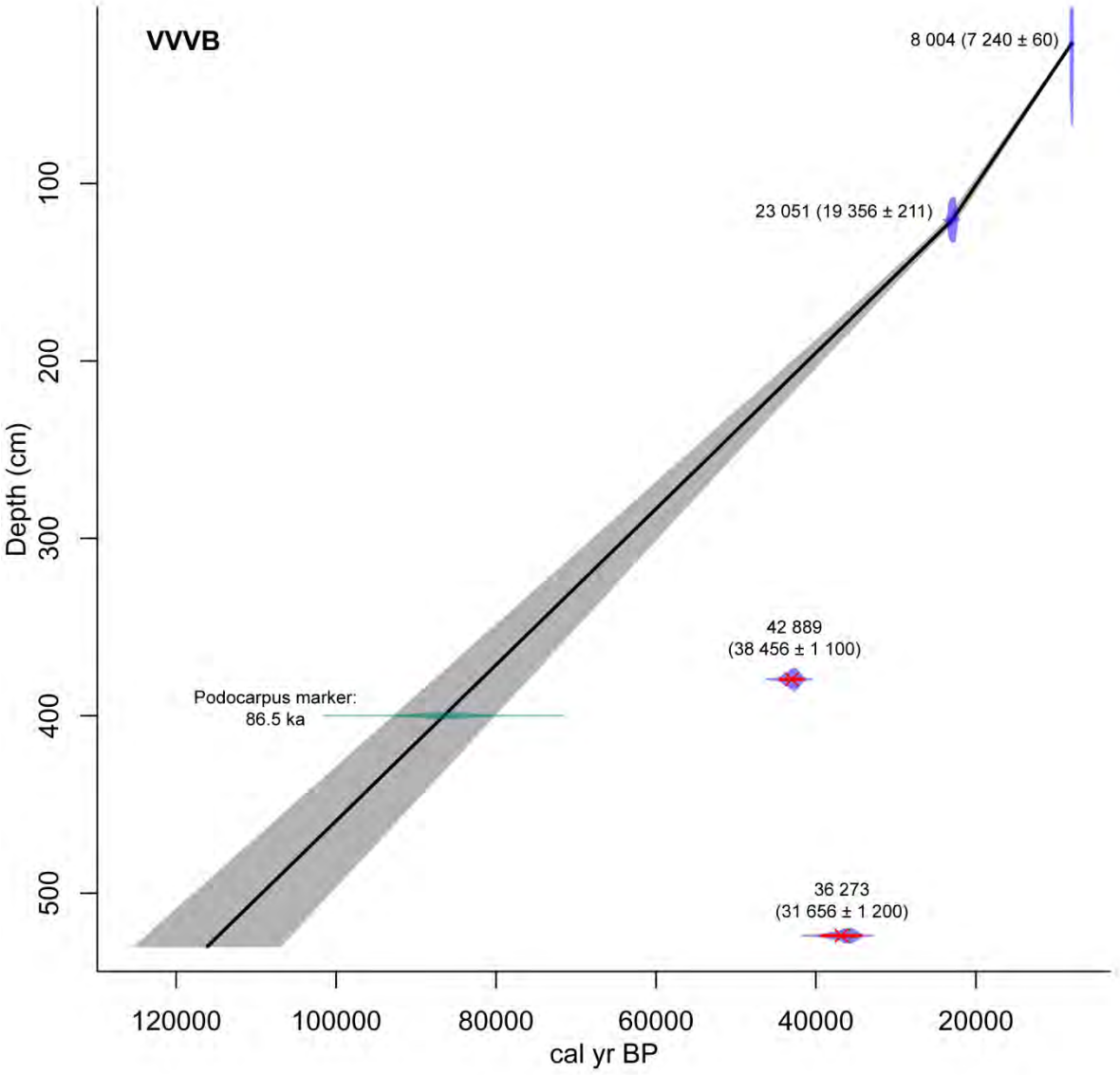

Figure 6.20 Age-depth model for VVVB, generated in R using CLAM (Blaauw, 2010) with the inclusion of the *Podocarpus* marker tied to VVV10.1 (discussed in section 6.5.3.2). The median probability calibrated ages are labelled and the uncalibrated ages with errors are provided in parentheses. Grey envelopes show the 95% confidence intervals, blue histograms indicate the ^{14}C calibrated distribution using SHCal04 (McCormac et al., 2004) or IntCal09 (Reimer et al., 2009) (see Table 6-3). Red stars indicate those ages that were deemed outliers.

Unfortunately the pollen records from VVVA and VVVB (Irving, 1998) are characterised by high counts of 'broken/obscured' grains, low total counts (~350 grains per level) and low taxonomic resolution (Figures 6.22 – 6.24). Only 36 and 33 taxa were identified within VVVA and VVVB respectively. Almost all the taxa identified are at family level which severely hampers palaeoecological interpretations. For example, it is uncertain as to whether Rosaceae refers to *Cliffortia*, Ebenaceae to either *Diospyros* or *Euclea* and Anacardiaceae to *Rhus*. A further limitation to these records is the low subsampling resolution; as it was a pilot study, pollen subsamples were only extracted and analysed at every 25 cm and subsamples were rather large (~5 cm^3).

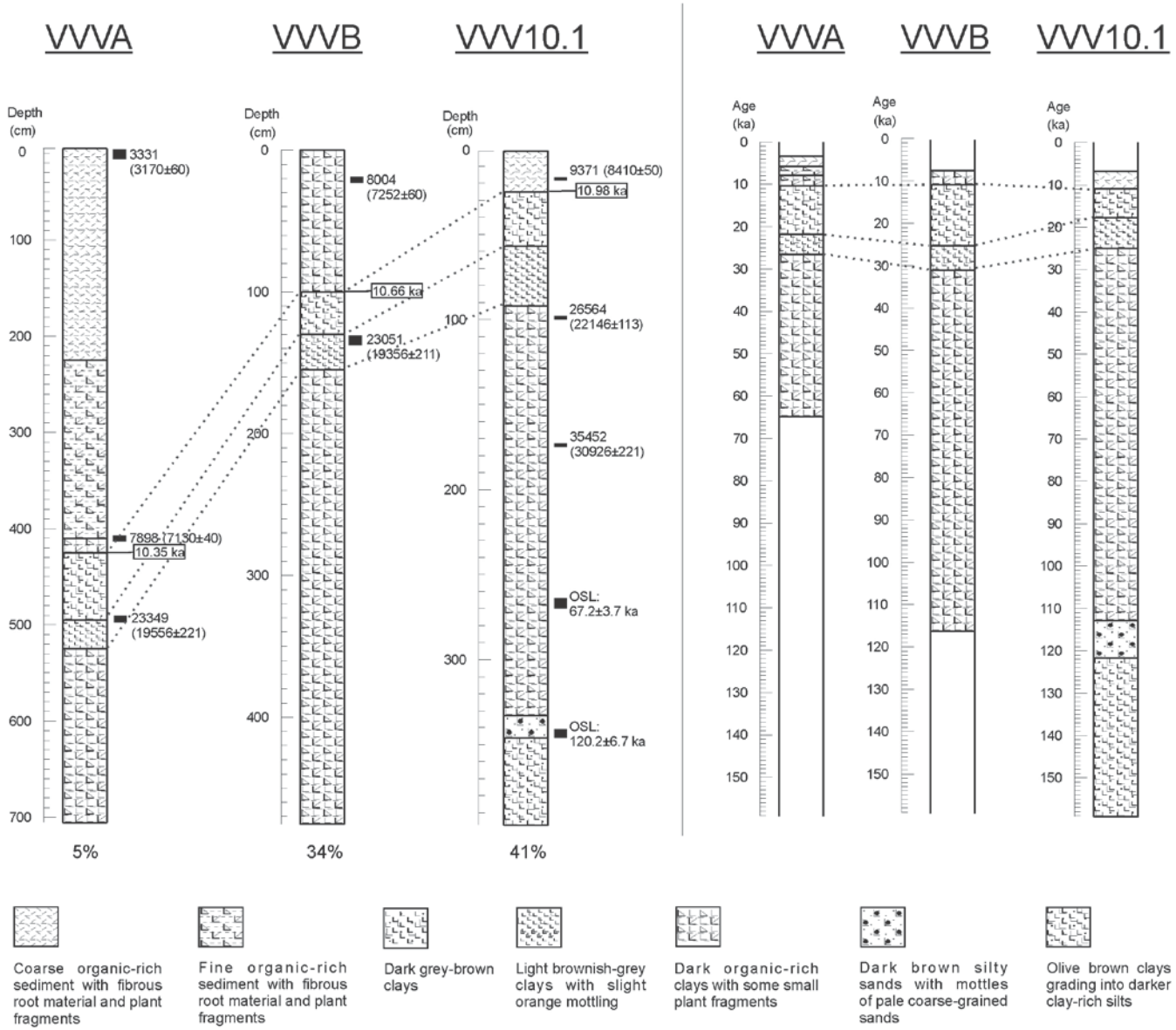

Figure 6.21 A comparison of VVVA, VVVB and VVV10.1's stratigraphies according to depths (left) and modelled age interpolations (right).

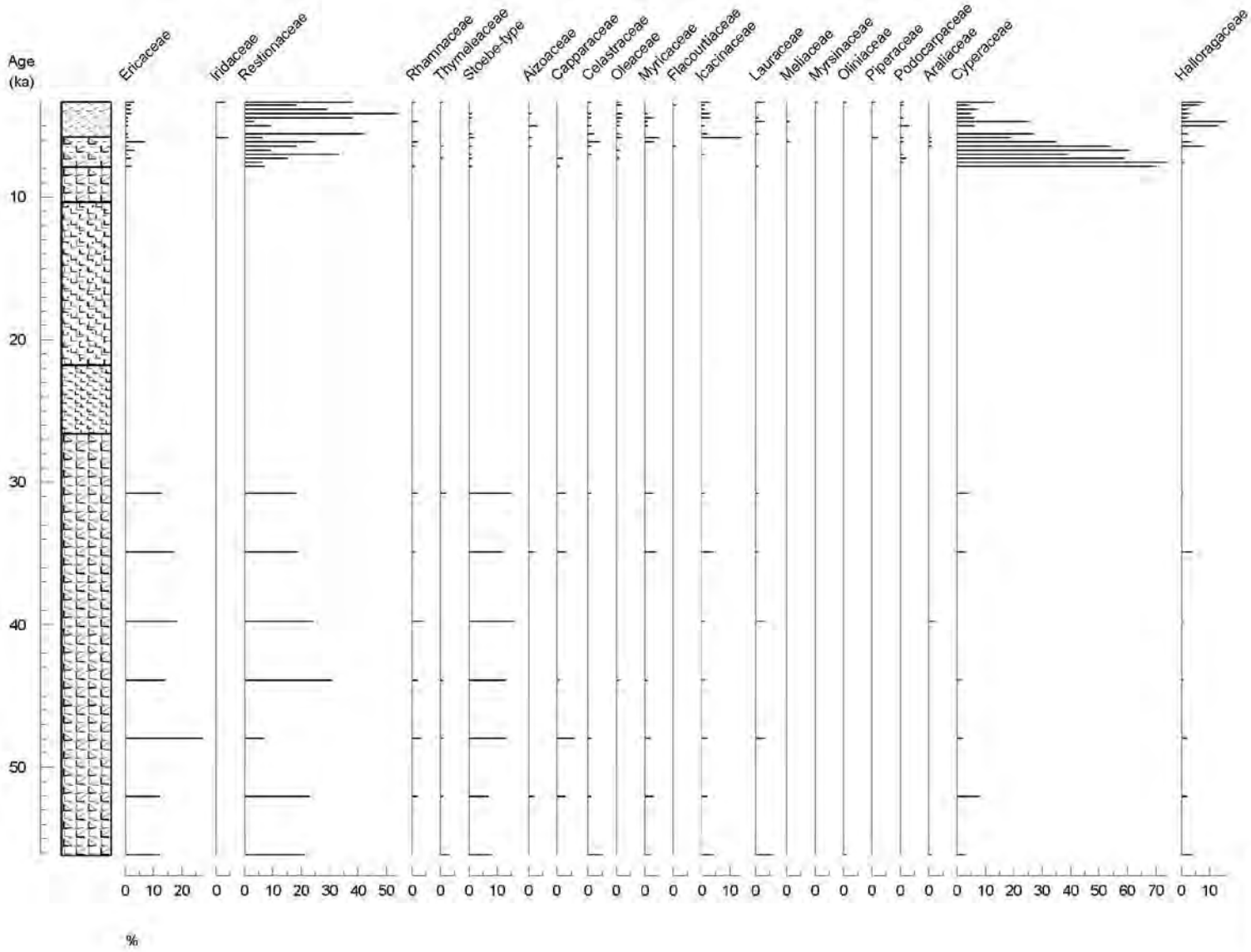

Figure 6.22 Relative percentage pollen diagram for VVVA (page 1 of 2).

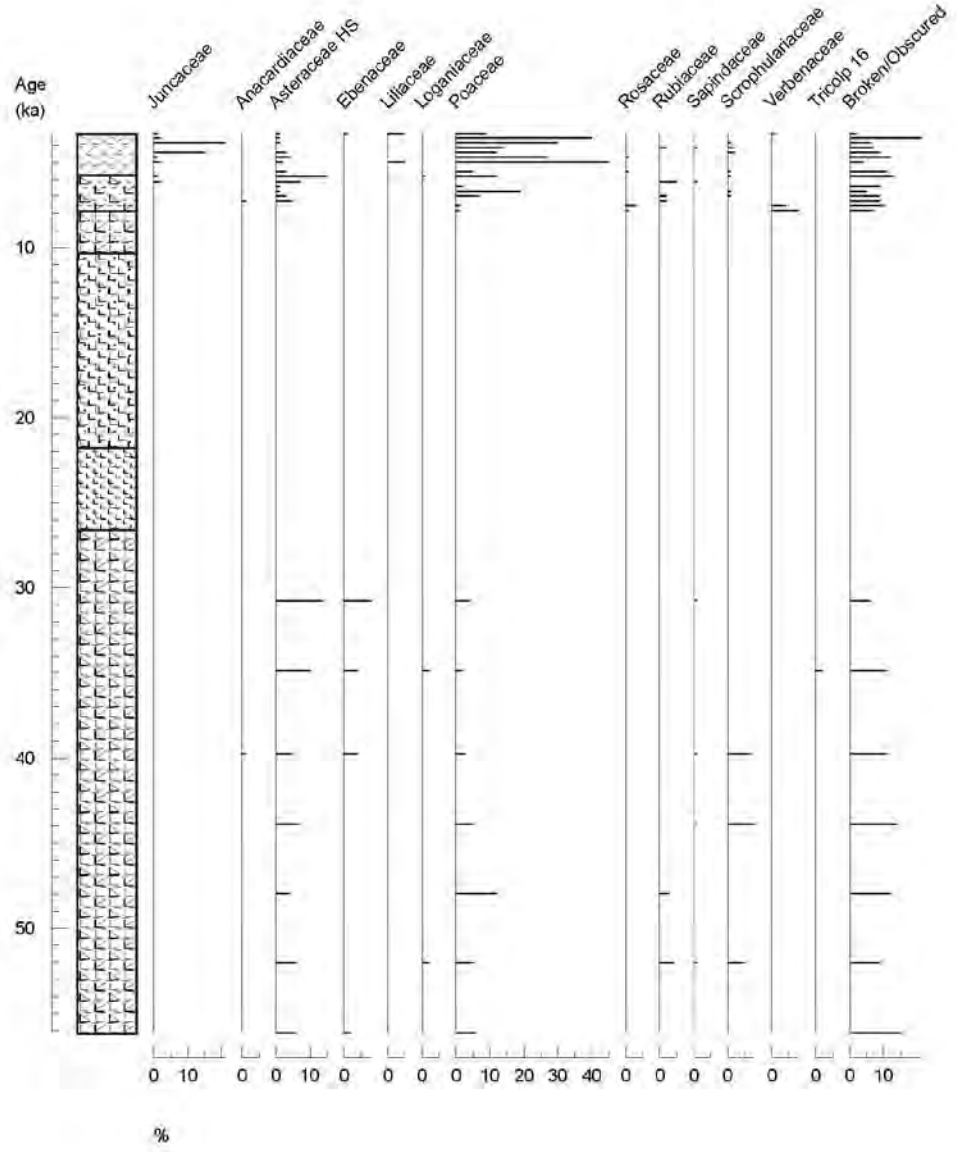

Figure 6.23 Relative percentage pollen diagram for VVVA (page 2 of 2).

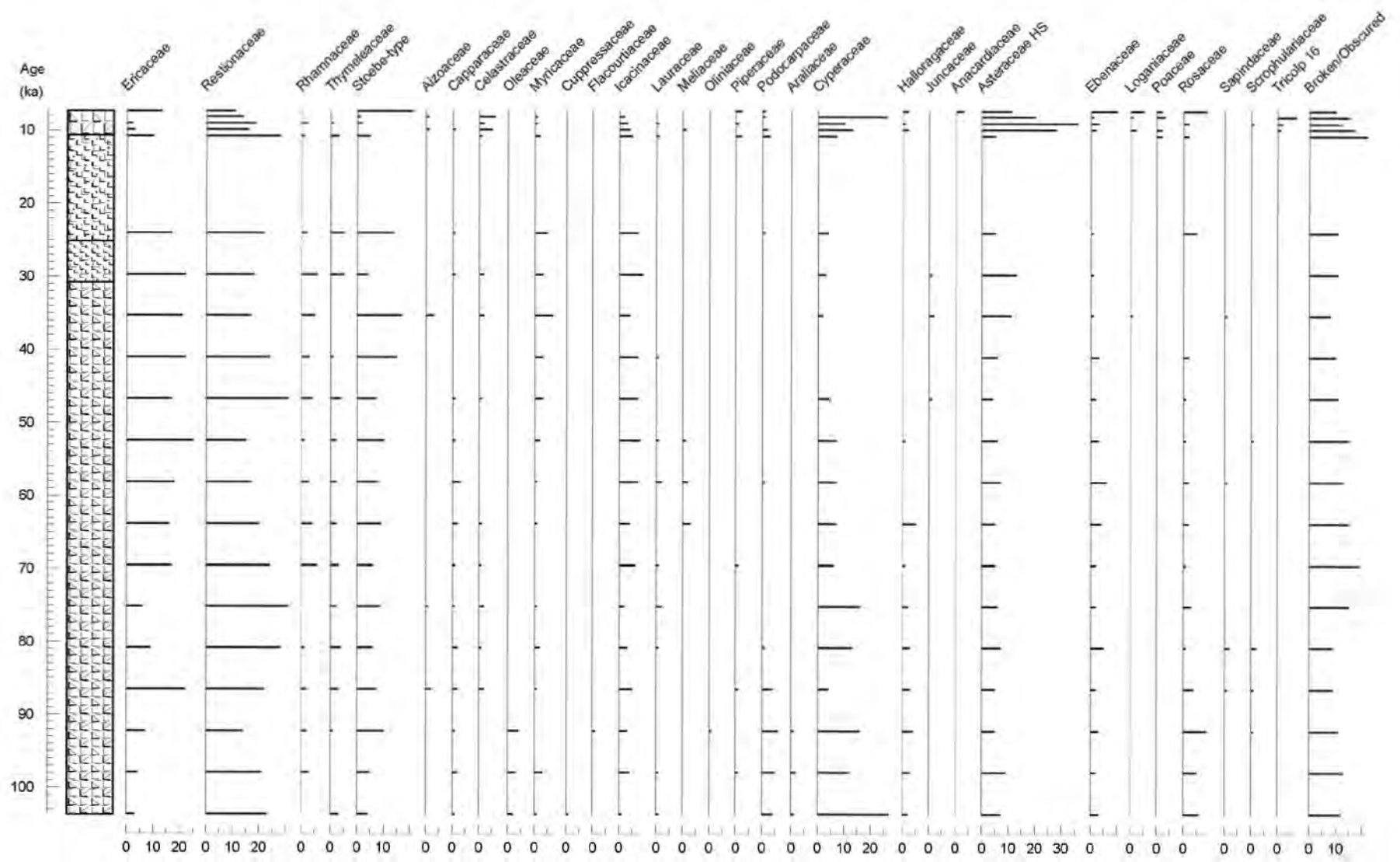

Figure 6.24 Relative percentage pollen diagram for VVVB.

In addition to the production of the pollen records for VVVA and VVVB, Irving (1998) also investigated contemporary pollen assemblages in and around Vankervelsvlei (Figure 6.25). Noteworthy outcomes of this study included: confirmation of the underrepresentation of many afrotemperate forest taxa (with the exception of *Podocarpus*), the highest concentrations of Ericaceae pollen were found in the open transition zone between the vlei and the forest and Cyperaceae pollen concentrations within the vegetation mat samples were dominant but not as overwhelmingly high as expected.

Figure 6.25 Pollen percentages counted from six surface soil samples (Irving, 1998), with the exclusion of *Pinus*. The category 'Transition zone' refers to a sample taken from the area between the edge of the vlei and the surrounding pine plantation.

6.5.3.3 Palaeoenvironmental reconstruction

The pollen records for VVVA and VVVB do, to some extent, support the findings from VVV10.1. However, due to the concerns raised in the previous section and the limited and somewhat tentative new chronological models associated with these records, the following reconstruction relies almost exclusively upon the results from VVV10.1 (therefore all pollen references and interpretations are referring to the VVV10.1 record unless stated otherwise).

There are marked differences between the Holocene pollen assemblage and the late Pleistocene assemblages. Fynbos elements are present throughout all three records with especially high percentages of Ericaceae within the late Pleistocene, indicating that ericaceous fynbos dominated or was the dominant understorey within this period. There are distinct appearances and fluctuations in certain afrotemperate forest taxa that do indicate changes in forest-fynbos dynamics.

Pollen was not preserved from ~156 – 114 ka and from ~27 – 8 ka. The basal stratigraphical unit (from ~156 – 124 ka) and the section from ~27 – 8 ka are both characterised by decreasing organic matter content and increased clay fractions and correspond to the MIS 6 and MIS 2 sea level lowstands (Waelbroeck et al., 2002; Bateman et al., 2010). Lowering sea levels and the climatic mechanisms behind them may have therefore resulted in decreased sediment deposition and reduced system productivity.

The section from ~124 - 114 ka, corresponding to MIS 5e, associated with a marine transgression, comprises of poorly sorted dark brown and paler-coloured sands with a discrete and significant increase in coarse-grained particles. Most of the Wilderness embayment was submerged during this time and therefore Vankervelsvlei would have been much closer to the coast or perhaps even being inundated itself.

Figure 6.26 A comparison of selected pollen taxa and climatic and ecological indicator taxa groups from the VVV10.1 record. The winter rainfall curve is the sum of the winter rainfall indicator taxa (Table 6.1), the cold intolerant curve is the sum of the cold intolerant indicator taxa (Table 6.1) and the aquatics/riparian curve is the sum of the local wetland taxa with the exception of Cyperaceae.

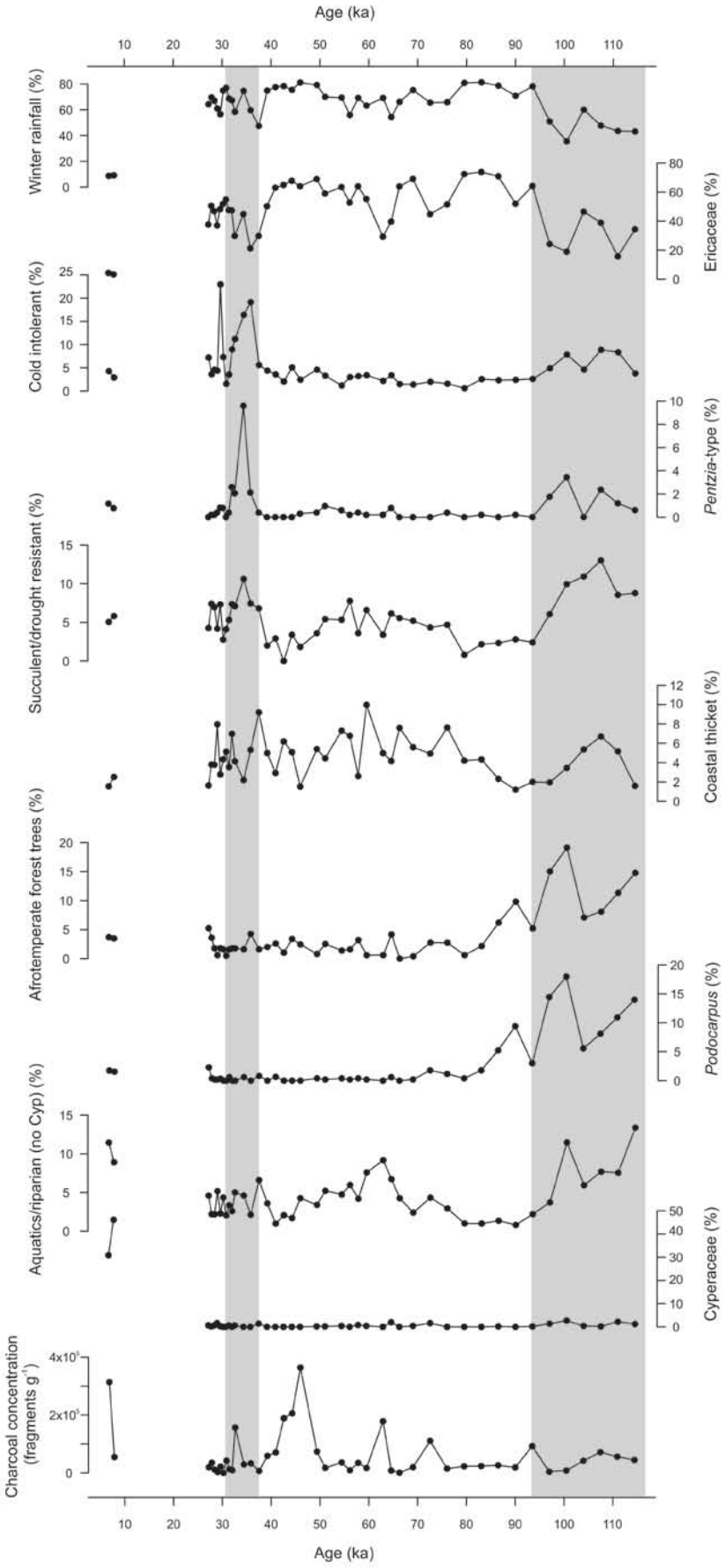

The MIS 5 section (~116 – 74 ka)

The significant increases in *Podocarpus* pollen percentages (mirrored in the VVVB record) and the presence of other forest taxa such as Lauraceae, Moraceae and Meliaceae suggest that the vegetation surrounding Vankervelsvlei during the earlier substages of the MIS 5 section (d, c and b) was characterised by greater afrotemperate forest cover (Figure 6.26 grey shaded area A). With the exception of *Podocarpus*, which is anemophilous and has more widely dispersed pollen aided by its bissacate pollen morphology, many forest trees are often underrepresented within the pollen record, being mostly dispersed through zoophily and therefore having less mobile pollen morphologies (Phillips, 1931; Geldenhuys, 1993). Consequently, the presence of an array of forest tree taxa during this period, even in very low percentages, does appear to be of significance. Many other arboreal elements such as the following coastal thicket taxa; *Canthium*, *Euclea*, *Morella* and *Olea* are present during this time with the overall arboreal sum peaking at ~100 ka. Fynbos elements are still recorded but the overall sum of this group is reduced in comparison to the subsequent sections.

Generally high PC1 scores, increased values for the cold intolerant group and relatively lower Ericaceae percentages (also evident in the VVVB record) all provide clear indications of increased temperatures for the period from ~115 – 94 (PAZ VVV10.1-A, Figure 6.26). Increased drought tolerant taxa (which peaks at ~100 ka) could signify that warmer temperatures were associated with somewhat drier conditions. Conversely, wetter conditions could be inferred from the increased arboreal sum and more specifically the greater dominance of afrotemperate forest taxa. However, the increased arboreal presence may not be a response to greatly increased moisture availability but rather a consequence of elevated CO_2 levels or reduced seasonality of rainfall (Bond and Midgley, 2000). To further complicate the above reconstruction, the higher percentages of succulent/drought resistant taxa in combination with the presence of coastal thicket elements could indicate a closer proximity to the coast and not aridity. The higher proportions of *Euphorbia* and Euphorbiaceae undiff. could substantiate this, as Euphorbiaceae has previously been associated with increased dune mobility and coastal dune vegetation (Schalke, 1973).

Low percentages of the largely riparian Cyperaceae (the main constituent of the contemporary vegetation mat covering Vankervelsvlei) suggest that the wetland was more open, perhaps

representing a back barrier lake. Further evidence in support of this assertion is the absence of the green algae *Botryococcus* (an indication of stagnant or shallow water bodies (Medeanic, 2006))[21].

From ~94 – 74 ka, there are suggestions of increased moisture availability (rise in the drought intolerant sum) and decreased temperatures (more negative PC1 scores) at the site. Exceptionally high percentages of Ericaceae are found from ~87 – 80 ka (absolute counts are highest for the VVV10.1 record at ~83 ka and there is a peak in Ericaceae percentages at ~87 ka in the VVVB record) coincident with a drop in drought tolerant taxa. Some afrotemperate elements are still present although *Podocarpus* percentages drop off almost entirely by ~80 ka (and by ~75 ka in VVVB) while fynbos percentages are elevated during this period (Figure 6.26).

Pollen concentrations are highly variable for the whole of this section with exceptionally high concentrations achieved at ~87 ka, indicating that conditions were optimal for the preservation of organic matter and palynomorphs at this time, or perhaps the water body was enlarged allowing for greater pollen abundances (Seppa and Bennett, 2003).

In summary, the pollen record from ~116 ka to ~94 ka indicates that afrotemperate forest was dominant within the landscape surrounding Vankervelsvlei. Fynbos elements are much less prominent in comparison to the glacial period and most likely represented understorey components or heathland patches which were surrounded by forest. Microscopic charcoal fragments are particularly low for the whole of this section, low fire frequencies perhaps allowing for the greater establishment of forest elements over fynbos communities (discussed further in section 6.4). In addition, coastal thicket elements are present indicating that there were transitional scrub forest and thicket pockets, probably established on nearby coastal dunes. The increased temperatures and decreased fire frequencies would have promoted the greater establishment of these communities. The latter part of this section, from ~94 – 74 ka, sees a shift to decreased temperatures, increased moisture availability and a greater dominance of fynbos. These conditions persist into MIS 4.

MIS 4 (~74 – 59 ka)

This section is dominated by fynbos with relatively high proportions of Ericaceae, *Stoebe*-type, slightly elevated percentages of Restionaceae, and the presence of *Cliffortia*. The afrotemperate forest taxa sum is very low. There are minor increases in some of the aquatic/riparian taxa,

[21] Although there are conflicting accounts as to the palaeoecological significance of *Botryocuccus* as these green algae colonies has been reported to be present under very variable conditions, including both deep open water and shallow stagnant pools (Cook et al., 2011).

specifically a peak in *Typha* at ~63 ka. This peak is coincident with a drop in Ericaceae (both absolute counts and percentages) and a dramatic rise in the *Stoebe*-type pollen and a peak in charcoal concentrations.

Therefore it appears that fynbos communities, as in the latter phase of the last section, were more established than forest stands, and that conditions were moderately wet and cool.

The MIS 3 section (~59 – 27 ka)

The transition from MIS 4 to MIS 3 is marked by a peak in the drought tolerant group, decreased percentages of fern spores and aquatics and an increase in thicket elements, all of which allude to decreasing moisture availability across this boundary. There is also a reduction in pollen concentrations with no pollen being preserved for the sample corresponding to ~61 ka, near the boundary between these two stages.

A further fairly prominent peak in succulent/drought resistant taxa occurs at ~56 ka coincident with a drop in fynbos taxa percentages and a peak in *Morella*. The drying trend at Vankervelsvlei appears to be sustained for much of MIS 3; however greater environmental variability is evident with perhaps an increase in the seasonal drying out of the wetland or lowering of water levels. Evidence for this is the low pollen concentrations and lack of pollen within a few of the subsamples, the decreased percentages of aquatics and riparian pollen, the extremely high concentrations of *Botrycoccus* and the presence of *Debarya glyptosperma* (peak at ~49.4 ka). *Debarya glyptosperma* (De Bary 1858; Wittrock, 1987) usually occurs within shallow pools and has been linked to the desiccation of local habitats and decreases in regional precipitation (Ellis and Van Geel, 1978; Cook et al., 2011).

An exceptionally high peak in the largest microcharcoal class is found at ~46 ka probably indicating the occurrence of a fire within the immediate vicinity of Vankervelsvlei.

In general, moisture availability appears to increase towards the end of this stage with a drop in the drought tolerant index at 42.6 ka. However there is a warmer, drier period between ~39 – 32 ka where the succulent/drought resistant sum peaks, Ericaceae percentages drop and there is an increased presence of thicket elements (Figure 6.26 grey shaded area B). Fynbos dominance is re-established after this phase in association with an isolated peak in Hammelidaceae pollen at 29.6 ka, a drought intolerant taxon. The Hammelidaceae pollen most likely represents *Trichocladus crinitus* or *T. ellipticus* both of which are forest understorey woody shrubs (Geldenhuys, 1993).

Overall, environmental conditions for this section appear to be quite variable with generally decreased moisture availability characterising the first half of MIS 3. Ericaceae percentages and PC1 scores remain high for this period and therefore low temperatures appear to be sustained until about 36 ka. After which, there are temperature spikes with increases in cold intolerant taxa around 36 ka and 29.5 ka and a peak in *Pentzia*-type at 34 ka (Figure 6.26).

The wetland was not as well developed compared to the preceding stages with indications of shallower water levels. Afrotemperate forest elements are generally low for much of this stage and fynbos remains the dominant vegetation type within the surrounding landscape. Hints of wetter and cooler conditions are evident from about 29 ka to the end of this section.

The MIS 3/2 section (~27 – 11.5 ka)

No pollen was preserved for this section. Sand peaks at ~12, 13 and 16 ka and signs of oxidation perhaps indicate seasonal drying out of the vlei occurred. The sediment colour and composition certainly points to a lack of OM preservation and therefore it is not surprising that pollen was not preserved.

The early Holocene section (~10.5 – 6.9 ka)

As the Holocene only encompasses two levels from VVV10.1 (at 7.9 ka and 6.9 ka), only a tentative reconstruction can be made for this period.

High percentages of Cyperceae characterise all three records (VVV10.1, VVVA and VVVB) around ~8 ka, suggesting that the floating vegetation mat was at least partially, if not entirely, covering the vlei by this stage. There are also increases in other aquatic/riparian taxa during this time and trilete spore counts are significantly elevated.

Arboreal pollen, both afrotemperate and thicket trees, are either fairly low or absent from this section. Ericaceae percentages are much lower than in the late Pleistocene assemblages (evident for all three records). *Stoebe*-type and *Cliffortia* are also both greatly reduced. Asteraceae (high-spine variety) reaches its maximum at the top of VVV10.1 (also particularly high percentages of Asteraceae high-spine recorded in VVVB from ~9.8 – 8.1 ka), indicating a shift from ericaceous fynbos to more asteraceous fynbos.

Exceptionally high charcoal fragments and concentrations indicate that fire frequencies were greatly increased during the Holocene section in comparison to the late Pleistocene sequence.

The reduced percentages of Ericaceae and extremely high PC1 scores confirm the expected warming within the Holocene. The establishment of the Cyperaceous vegetation mat covering the wetland's surface reduced the local wetland taxa source areas (Bunting and Tipping, 2004).

The mid- to late Holocene section (~6.9 – 3.3 ka)

The only record covering this period is VVVA and therefore there is limited evidence upon which to base any palaeoenvironmental interpretations. The pollen assemblage from VVA reflects reduced Cyperaceae and Asteraceae percentages, slight increases in other aquatics and high proportions of Restionaceae and Poaceae pollen. Forest elements are present however the composition indicates the presence of scrub forest or coastal thicket rather than the afrotemperate type. The vegetation surrounding Vankervelsvlei during the mid- to late Holocene therefore appears to be dominated by graminoid elements, with perhaps restioid fynbos dominating the landscape.

6.6 Palaeoenvironmental synthesis

This section discusses the evidence obtained from the investigated sites in relation to the overall palaeoenvironmental record for the southern Cape coastal plain (Chapter 3). Emphasis is placed on key palaeoclimatic 'events' and attempts are made to identify the major driving mechanisms behind the observed changes, both within a southern African and southern hemispheric context.

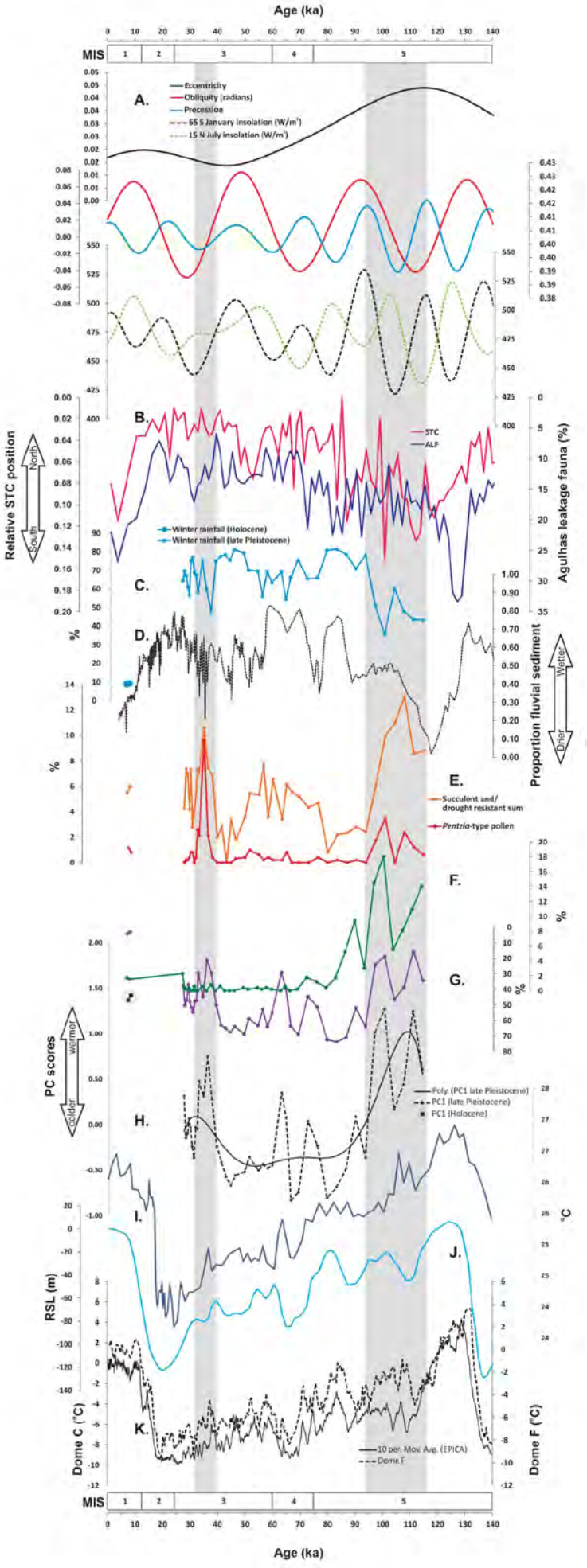

Figure 6.27

A. Variations in orbital and insolation parameters: eccentricity (Laskar et al., 2011), obliquity, precession, mean monthly January insolation at 65 °S and mean monthly July insolation at 15 °N (Laskar et al., 2004).

B. Changes in the relative position of the Subtropical Convergence (STC) and the percentage of Agulhas leakage fauna from the Cape basin record (Peeters et al., 2004).

C. The sum of the winter rainfall indicator taxa from the Vankervelsvlei 2010 sediment core (VVV10.1).

D. Variations in the proportion of fluvial sediment in the Namibian marine core MD962094 indicating changes in terrestrial humidity (Stuut et al., 2002).

E. The sum of succulent and/ or drought resistant pollen taxa percentages (orange) and the percentages of *Pentzia*-type pollen (red) in VVV10.1.

F. VVV10.1 *Podocarpus* pollen percentages.

G. VVV10.1 Ericaceae pollen percentages (note reversed y-axis).

H. VVV10.1 Principal Component 1 scores.

I. Sea surface temperature (SST) stack from the precursor/upstream region of the Agulhas Current (marine core MD962048) (Caley et al., 2011).

J. Relative sea level curve (Waelbroeck et al., 2002).

K. Temperature variations at Dome C (Cowling, 1983a; Jouzel et al., 2007) and Dome F (Kawamura et al., 2007) in Antarctica.

6.6.1 MIS 5 (~128 – 74 ka)

Pollen was not preserved in the VVV10.1 for MIS 5e (~128 - 115 ka) when temperatures and SSTs were greatly increased and sea levels were thought to be comparable to or higher than present, perhaps leading to inundation of the Wilderness Embayment (Deacon et al., 1984; Waelbroeck et al., 2002; Carr et al., 2010b; Bateman et al., 2011; Matthews et al., 2011; Figure 6.27 and references therein). The Vankervelsvlei pollen and charcoal records for the period ~116 – 94 ka indicate that there was a greater dominance of afrotemperate forests in the vicinity of the site (Figure 6.27 F), temperatures were increased[22] (Figure 6.27 E, G and H) and winter rainfall influences were reduced (Figure 6.27 B and C).

As outlined in both Chapters 2 and 3, the Agulhas Current plays a very significant role in modulating climate along the southern Cape coast. Agulhas Current SSTs influence the strength and dominance of the SRZ with increased SSTs resulting in increased summer rainfall (Jury et al., 1993; Jury, 1995; Reason and Mulenga, 1999) and increased advection of moisture over the southern Cape. Data from Dupont (2011) indicates that this contemporary relationship between SSTs and summer rainfall appears to hold for the last 350 ka, at least for north-eastern South Africa. The Vankervelsvlei records corroborate this finding for the southern Cape, illustrating that during much of MIS 5, when Agulhas SST's were relatively high; afrotemperate forest taxa percentages were elevated and winter rainfall-reliant fynbos taxa were reduced suggesting that there was an increased dominance of summer rainfall at the site (Figure 6.27).

The driving mechanisms for these interglacial conditions are tied to changes in the position of the STC, as a southward displacement of the STC (Figure 27 B) would have resulted in a reduced influence and poleward shift of the westerlies, subjecting the southern Cape to enhanced easterly flow (van Zinderen Bakker, 1976; Cockcroft et al., 1987; Chase and Meadows, 2007; Biastoch et al., 2009; Chase, 2010; Figure 6.27 and references therein). The combination of reduced westerly dynamics and enhanced easterly flow would have decreased summer drought and the incidence of berg winds (due to a change in the winter wind systems) resulting in lower fire frequencies and promoting the establishment of afrotemperate forests at the expense of fynbos communities.

Further substantiation for the reduced influence of the westerlies during this period is evident within the Namibian offshore records (manifesting as an increase in aridity) (Little et al., 1997a; Shi et al., 2001; Stuut et al., 2002; Chase and Meadows, 2007; Figure 6.21 D). Despite assertions of strong links between Agulhas Current SSTs and Antarctic temperatures (e.g. Caley et al., 2009) there appears to

[22] Relative to the rest of the Pleistocene section of the record and comparable to the Holocene.

be some disparity between these records for the MIS 5d – b section where Antarctic temperatures decrease more rapidly compared to the Agulhas SSTs and VVV10.1's PC1 scores (Figure 6.27 H, I and K).

For the latter part of the MIS 5 section (from ~94 – 74 ka) of the Vankervelsvlei record there is a shift to decreased temperatures, increased moisture availability and a greater dominance of fynbos. These conditions persist into MIS 4 and coincide with increases in winter rainfall and northward shifts in the STC (Figure 6.27).

6.6.2 MIS 4 (~74 – 59 ka)

Data from Vankervelsvlei generally supports the findings from previously established records from both the western and eastern sections of the SCCP, and the offshore records, that suggest that MIS 4 was characterised by humid conditions as a result of an increased influence of the westerlies, warm SW Indian SSTs (relative to the LGM) and increased linkages between tropical and temperate systems (Avery, 1982; Deacon et al., 1984; Avery, 1987; Avery et al., 1997; Klein et al., 1999; Klein and Cruz-Uribe, 2000; Shi et al., 2001; Stuut et al., 2002; Peeters et al., 2004; Chase, 2010). However, the pollen and charcoal results from VVV10.1 do indicate that there was a slight deviation for these cooler and wetter conditions at ~63 ka where rises in charcoal concentrations, decreases in Ericaceae percentages and lower PC1 scores point towards a brief warmer and drier phase, coinciding with a discrete peak in Agulhas SSTs and a drop in sea levels (Figure 6.27).

6.6.3 MIS 3 (~59 – 24 ka)

This stage is rather poorly represented in the established palaeoenvironmental record. There are indications of colder and wetter conditions within the WRZ section of the SCCP (Schalke, 1973; Klein et al., 1999; Scott et al., 2004; Quick, 2009) and from Boomplaas (Avery, 1982; Klein, 1983; Deacon et al., 1984; Klein, 1984) for at least some parts of MIS 3. Colder conditions are certainly evident within the VVV10.1 record from the start of MIS 3 until ~40 ka (Figure 6.27 G and H).

Indications of decreased moisture availability inferred from multiple lines of evidence from the VVV10.1 record for the earliest part of MIS 3 are consistent with the arid phase that marks the boundary between MIS 4 and MIS 3 (Chase, 2010; further details in Chapter 3). This coincides with decreased winter rainfall indicator sum percentages and a brief southward shift in the STC (Figure 6.27 B and C).

Particularly high percentages of the winter rainfall indicator taxa sum (Figure 6.27 C), synonymous with a strong dominance of fynbos, and greatly increased charcoal concentrations (Figures 6.8 and 6.26) point towards enhanced winter rainfall at Vankervelsvlei from ~50 – 40 ka. Northward shifts in the STC at this time further support the assertion of an expanded and more intense WRZ during this period.

A significant deviation from the above environmental conditions occurred from ~39 to ~32 ka, manifesting as a discrete phase of increased aridity and warmer temperatures, recorded in both the Vankervelsvlei and Rietvlei Still Bay records. Evidence for this 'event' is summarised below (and presented in Figures 6.16 and 6.27):

The Vankervelsvlei record:

- Increases in cold intolerant taxa with a very large peak in *Pentzia*-type pollen at ~34.4 ka
- Lower percentages of Ericaceae pollen from ~39.2 – 32 ka (especially low at ~36 ka)
- High PC1 scores from ~38 – 32 ka
- Decreasing percentages of the winter rainfall indicator sum culminating in a low at ~37.5 ka
- Relatively high percentages of succulent/drought resistant sum from ~37.5 – 32 ka

The Rietvlei Still Bay record:

- Increased percentages of drought tolerant taxa from ~36 – 34 ka
- Fynbos pollen taxa percentages are relatively low
- Increased charcoal amounts and concentrations
- Decreased aquatic/riparian pollen percentages, more terrestrially-derived OM (especially at ~36 ka) and enriched $\delta^{13}C_{TOC}$ values all indicate a less developed wetland environment

These findings coincide with a discrete peak in the Agulhas Current SSTs within the overall trend of decreasing temperatures towards the LGM minima (Figure 6.27 I), indications of increased aridity from offshore Namibia (Figure 6.27 D) and increases in the ALF (Peeters et al., 2004; Figure 6.27 B) (it would be expected that increases in the ALF would be linked to southward shifts in the STC, however this is does not seem to be the case).

This arid phase may have resulted from the prevention of the penetration of winter rainfall systems into the eastern section of the SCCP, a scenario that could also explain the anomalous warm, dry phase at ~63 ka and the environmental conditions in the YRZ during the LGM, as discussed in more detail in the next subsection.

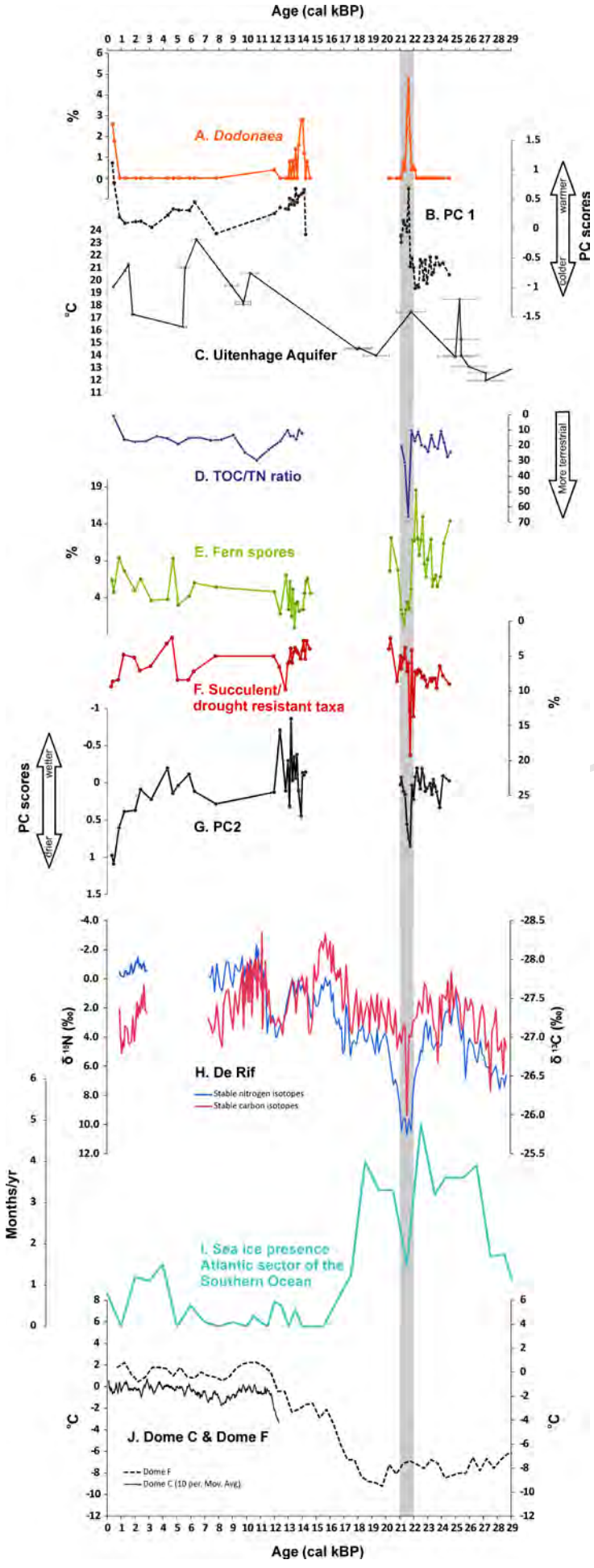

Figure 6.28

A. Percentages of *Dodonaea* pollen in the Pearly Beach 1 sediment core (PB-1).

B. PB-1 Principal Component 1 scores.

C. The Uitenhage Aquifer inferred temperature record (Stute and Talma, 1998).

D. PB-1 TOC/TN ratios.

E. PB-1 fern spore percentages.

F. The sum of the succulent and/ or drought resistant pollen taxa percentages(note reversed y-axis).

G. PB-1 Principal Component 2 scores.

H. The De Rif 2 (DR-2) stable carbon and nitrogen isotope records (Quick, 2009).

I. Sea ice presence within the Atlantic sector of the Southern Ocean (Stuut et al., 2004)

J. Temperature variations at Dome C (Jouzel et al., 2007) and Dome F (Kawamura et al., 2007) in Antarctica.

6.6.4 The LGM (~24 – 18 ka)

The greatest differences between the western (modern WRZ) and the eastern (modern YRZ) subregions of the SCCP appear to exist within the LGM.

It is unfortunate that no pollen was preserved for this period in either the Rietvlei Still Bay or the Vankervelsvlei cores. The lack of pollen preservation together with the sedimentological, geochemical and plant biomarker data generated for VVV10.1 and RVSB-2 strongly suggests that these wetland systems were markedly less productive. This was most likely caused by significantly drier, windier and colder conditions, an assertion supported by other records from the eastern subregion of the SCCP (e.g. Avery, 1982, 1983; Butzer et al., 1984; Klein, 1980, 1983, 1984).

Pollen is preserved in the Pearly Beach record from ~25 – 21 cal kBP with the overall multi-proxy record indicating that most of this period was characterised by the dominance of coastal fynbos vegetation in association with generally increased moisture availability (in relation to the late Holocene section) and decreased temperatures. Therefore the Pearly Beach record generally supports the established theory that the WRZ and the western margin of southern Africa was subjected to cooler and wetter conditions during the last glacial period (Schalke, 1973; Parkington et al., 2000; Lancaster, 2002; Scott et al., 2004; Chase and Meadows, 2007; Scott and Woodborne, 2007a, b; Quick, 2009).

However, these conditions were abruptly interrupted by a brief period of significantly decreased moisture availability, perhaps also associated with relatively elevated temperatures, from ~22 – 21.5 cal kBP. The evidence from the PB-1 record for this phase is summarised below and highlighted in Figure 6.28.

- Charcoal concentrations are exceptionally high at 21.9 cal kBP
- Peak in succulent/drought resistant taxa sum at 21.8 cal kBP, which is primarily composed of extremely high percentages of Crassulaceae
- High PC1 and PC2 scores from 21.8 – 21.5 cal kBP
- A considerable decrease in fern spores from 21.8 to 21.1 cal kBP
- Relatively increased percentages of *Dodonaea* at 21.6 cal kBP
- Lowest value for the fynbos sum at 21.6 cal kBP
- A significant reduction in Ericaceae pollen at 21.6 cal kBP
- A high TOC/TN ratio value at 21.6 cal kBP, indicating increased terrestrially-derived OM inputs

Therefore it appears that environmental conditions at Pearly Beach at this time were distinctly more arid than the previous and subsequent glacial sections of the record, providing crucial support to the findings from De Rif (Quick, 2009), the only other record that documents this climatic excursion (Figure 6.28). The indications of relatively warmer temperatures could be supported by the isolated rise in temperatures in the Uitenhage Aquifer record (Stute and Talma, 1998; Figure 6.28 C).

Once again, SCCP climates appear to be strongly forced by the dynamics of the climate systems originating in the high southern latitudes. Cold Antarctic temperatures, modulated by reduced eccentricity, reductions in summer insolation at high Southern Hemisphere latitudes and an obliquity minimum (Figure 6.27 A), enabled the growth and significant expansion of Antarctic sea ice from ~29 – 17.5 cal kBP (Figures 6.28 I). This resulted in northward shifts in the STC and the intensification and/ or expansion of the westerlies (Stuut et al., 2004; Chase and Meadows, 2007). Therefore, in general, the more frequent and/or intense frontal systems would have produced increased rainfall along the western and northern parts of southern Africa, accounting for the inferences of increased moisture availability in the WRZ records. Whereas a significant retreat in sea ice, such as that recorded at ~21.5 cal kBP (Stuut et al., 2004; Figure 6.28 I), would result in a poleward shift in the STC and the fronts and therefore, barring the attenuating influence of other moisture-bearing systems, a reduction in rainfall at both De Rif and Pearly Beach.

The key drivers underlying climate variability towards the eastern side of the SCCP, the area presently under a year-round rainfall regime, are less clear. Within the established overall palaeoenvironmental record there is a strong bias towards the WRZ with very few eastern/YRZ sites encompassing the LGM. The evidence that is available sharply contrasts that of the WRZ and points towards drier conditions characterising the LGM. A scenario proposed earlier within this chapter (subsection 6.4.3) could account for the aridity. The significantly lower sea levels during the LGM (Figure 6.27 J) would have resulted in an extended coastal plain which could have altered local atmospheric dynamics to the extent that an enhanced and/or expanded continental anticyclone blocked the penetration of winter rainfall systems to the eastern SCCP (Cowling et al., 1999; Carr et al., 2006; Chase and Meadows, 2007). Furthermore, decreased Agulhas Current SSTs (Figure 6.27 I) would have led to decreased advection of moisture over the adjacent coastal areas which in turn would have resulted in the reduced incidence of weather systems such as cut-off lows and ridging anticyclones, features that are responsible for a large portion of present-day rainfall (Chapter 2).

Therefore, despite an intensified and/or expanded winter rainfall towards the southwest, the combination of the above mentioned factors together with reduced summer rainfall meant that the

wetter conditions experienced within the western SCCP did not translate to the eastern SCCP during this period.

6.6.5 The LGIT (~18 – 11.5 ka)

The Vankervelsvlei sediment cores are devoid of pollen for much of this section. The sand peaks found at ~12, 13 and 16 ka could tentatively indicate seasonal drying out of the vlei (possibly in association with windier conditions) during the LGIT. The RVSB-2 pollen record recommences at ~19.4 ka with increased percentages of fynbos taxa, local wetland taxa and fern spores; all indicating increased moisture availability up until ~17.5 ka. From this point there are increasing signs of more xeric conditions, especially evident from ~15 – 13 ka within which *ChenoAm*-type pollen reaches remarkably high percentages. As this taxon is halophytic, high percentages could also indicate an increased marine influence at the site perhaps linked to rising sea levels. No pollen is preserved for the YD; however the biomarker data provide some evidence for substantially reduced moisture availability.

Towards the west, inferences from the Pearly Beach record indicate mesic conditions in association with a fairly well developed wetland system and increases in arboreal elements from ~14.6 cal kBP to ~12 cal kBP. These findings support the notion of a predominantly wet LGIT (however not as wet as parts of the LGM) within the WRZ (Schalke, 1973; Klein, 1991; Avery, 1993).

The evidence from the three new sites presented in this study together with the previously established records (Chapter 3) appears to indicate that the transition from the LGM into the Holocene was characterised by great variability throughout the SCCP. With peaks in *Dodonaea* at ~19 ka, ~14 ka and ~16 ka at Rietvlei Still Bay, Pearly Beach and Pakhuis Pass respectively and rising temperatures in the Cango Cave record, one aspect that is not in dispute is that temperatures during the LGIT were generally warmer than those of the LGM[23] (Talma and Vogel, 1992; Scott and Woodborne, 2007a, b).

The evidence from Rietvlei Still Bay of increased moisture availability between ~19 ka and ~17.5 ka together with rising sea levels could perhaps suggest that the blocking continental anticyclone that was dominant during the LGM weakened, allowing for the penetration of frontal systems towards the east (sea ice presence remained high until 17.5 ka; Stuut et al., 2004; Figure 6.28 I). However these fronts perhaps did not extend as far eastwards as Vankervelsvlei and therefore this site remained relatively arid.

[23] Apart from brief deviations such as during the YD.

The post-glacial warming resulted in a sharp decrease in sea ice presence from 17.5 ka and the establishment of a more poleward position for the STC, severely reducing the influence of high latitude southern hemispheric climatic dynamics on the SCCP. Northern Hemisphere/North Atlantic forcing mechanisms were then able to exert more control on the western subregion of the SCCP from the LGIT onwards (Chase et al., 2009, 2010, 2011). To this extent, increased southeast Atlantic SSTs resulting in increased potential evaporation and moisture could be responsible for the generally wetter conditions at Pearly Beach from ~14 – 12 ka. While the reduced winter rainfall after 17.5 ka could account for the more xeric conditions at Rietvlei Still Bay with the YRZ only becoming a prominent feature during the Holocene.

In order to fully establish the complex nature of environmental change on the SCCP during the LGIT and ascertain the causal mechanisms behind these changes, new higher resolution palaeoenvironmental records are needed, especially for the eastern subregion.

6.6.6 The Holocene (~11.5 – 0 ka)

In terms of the vegetation composition characteristics, the records suggest that there was a clear shift from ericaceous fynbos in the late Pleistocene to other structural types of fynbos (proteoid, restioid and asteraceous) in the Holocene. These changes, together with increases in coastal thicket/strandveld elements (mainly within the late Holocene), are most likely a response to generally warmer interglacial conditions, elevated CO_2 concentrations, changes in rainfall amounts and seasonality and changes in fire regimes.

At all three sites there was inadequate pollen preservation for much of the immediate transition period between the late Pleistocene and the Holocene and the early Holocene (from ~12 ka – 9 ka). The geochemical and plant biomarker data point towards decreases in OM production. Therefore this period seems to have been associated with decreased wetland productivity and perhaps more xeric environments.

The Rietvlei Still Bay, Vankervelsvlei and, to a lesser extent, Pearly Beach records document phases of significantly increased moisture availability within the period ~9 ka to 7 ka, supporting evidence from many other records across the SCCP (e.g. Scholtz, 1986; Avery, 1993; Scott and Woodborne, 2007a; Chase et al., 2009, 2010, 2011; Meadows et al., 2010; Quick et al., 2011) of a wetter early Holocene. During this time Cyperaceous vegetation mats were most likely established on both Rietvlei and Vankervelsvlei, indicating shifts to more advanced hydroseral phases in response to greater amounts (and perhaps more aseasonal) rainfall.

Prominent microcharcoal peaks are present within all three records between ~7 – 5 ka, suggesting that fire frequencies were increased at these sites during the mid-Holocene. This coincided with indications from the RVSB-2 records of increased aridity, which supports the concept of a warmer and drier HA (Klein, 1984; Scholtz, 1986; Baxter, 1989; Meadows and Sugden, 1990, 1991; Meadows and Baxter, 1999, 2001; Chase and Thomas, 2007; Scott and Woodborne, 2007a, b; Meadows et al., 2010). In contrast, the Pearly Beach pollen and plant biomarker data reflect relatively wet conditions but only for a very brief period (5.9 – 5.5 cal kBP). Both before and after this there are indications of moderately drier conditions with decreased percentages of aquatic/riparian pollen percentages and a significant peak in Asteraceae (high spine variety) at 4.3 cal kBP. A further consideration is that the enhanced wetland productivity from 5.9 – 5.5 cal kBP may, at least to some an extent, be the result of sea level-induced changes in groundwater levels and therefore not a response to wetter regional conditions but rather rising sea levels.

Despite possible increases in the amount of summer rainfall/the initiation of the YRZ (as implied by Avery, 1993), a southward shift in the STC around 4 ka (Peeters et al., 2004; Figure 21 B) with concomitant changes in the strength and/ or position of the westerly belt, resulted in decreased winter rainfall. This, together with enhanced evaporation (as a result of higher temperatures) is most likely responsible for the overall trend of increased aridity recorded across the SCCP (Chase and Meadows, 2007).

The late Holocene is characterised by greater variability with discrete episodes of increased wetland productivity and moderately wetter conditions (e.g. from 0.54 – 0.28 in the RVSB-2 record) as well as phases of increased aridity (e.g. 0.45 – 0.32 in the PB-1 record), which is similar in some ways to the findings of Carr et al. (2006b) and Scholtz (1986). It is also possible that the increased variability or 'spikiness' evident in both these records during the late Holocene in comparison to the late Pleistocene sections are artefacts of the higher accumulation rates and/ or temporal subsampling resolutions.

The Pearly Beach and Rietvlei records do not have chronologies of sufficiently high resolution to precisely constrain or characterise late Holocene palaeoclimatic events such as the Little Ice Age (LIA), and therefore these finer-scale phases are not addressed within this discussion. However the expectation might be that the WRZ would be generally wetter during the LIA, as proposed by Stager et al. (2012).

It is clear that, with the establishment of the YRZ and Holocene vegetation reorganisations, very different ecological and climatic dynamics characterised Pearly Beach and Rietvlei, a feature which is

especially evident in the late Holocene. For example, Proteaceae percentages steadily increase from 4.3 cal kBP towards the top of PB-1, reaching exceptionally high proportions from 0.4 – 0.3 cal kBP. Coinciding with the high Proteaceae presence are significant increases in coastal thicket taxa, reduced fire frequencies and low percentages of aquatics/riparian pollen, supporting the inferences from the biomarker and PCA results of warmer and drier conditions. In contrast, RVSB-2 records a significant rise in Proteaceae and charcoal concentrations from ~2 – 0.85 ka. After this phase, Proteaceae percentages drop off almost completely while coastal thicket proportions rise dramatically towards the top of the sequence. The differences in community structures at these two sites are most likely a result of differing fire regimes and the nature of Proteaceae. While the growth and establishment of most, almost all, thicket taxa are generally retarded by fire (with the coeval inverse relationship between coastal thicket and charcoal providing substantiation for the existence of this phenomenon at both Pearly Beach and Rietvlei Still Bay), different Proteaceae species can respond in different ways to fire, that is, different fire intervals, seasonality and intensities (Bond, 1984; Bond et al., 1984; Bowen, 1991; Midgley et al., 2011).

The reassertion of the westerlies after the HA could be responsible for the wetter phases in the Pearly Beach record and the increased Proteaceae percentages (in conjunction with increases in other winter rainfall/fynbos indicator taxa) in the Rietvlei Still Bay record. While the combined increases in winter and summer rainfall led to more humid periods within the eastern subregion of the SCCP, resulting in wetter more aseasonal rainfall (Scholtz, 1986) and phases of greater dominance of afrotemperate forest within the Knysna region (Martin, 1968).

6.7 Conclusion

Due to the virtual absence of terrestrial palaeoenvironmental data from the southern Cape covering MIS 5 to MIS 3, the Vankervelsvlei record represents a particularly important new archive. The variations within this record clearly suggest that glacial-interglacial cycles had a strong impact on the region's vegetation history and climate. In addition, the VVV10.1 record has identified discrete periods within which palaeoenvironmental conditions appear to deviate from those associated with the marine isotope stages (e.g. at 36 ka), providing new insights into the finer-scale climatic and ecological changes within this ecotonal region. The relative dominance of easterly and westerly flow has greatly influenced both the Vankervelsvlei and Rietvlei records. Furthermore, the changes in the Agulhas Current SSTs and their link to Southern Ocean dynamics, primarily through variations in the position of the STC, provide a key mechanism for the recorded changes.

Interpretations of previously established palaeoenvironmental records for the WRZ have generally pointed towards a LGM that was homogeneously and consistently cooler and wetter than present day (Chapter 3). However, the evidence from Pearly Beach (this thesis) and De Rif (Quick, 2009) suggest that there was a greater degree of variability, with this period being punctuated by a discrete arid episode from 22 – 21.5 ka. Correlations to changes in Antarctic sea ice presence and its influence on the latitudinal position and/or intensity of the westerly wave belt provides the mechanism for the observed environmental changes during this period.

Being influenced by a variety of factors including rainfall amount and seasonality, atmospheric and oceanic temperatures, atmospheric CO_2, sea levels and ocean currents, the climatic and vegetation history for the southern Cape coastal plain is certainly complex. The three new records presented within this study provide greater insight into the complex nature of the palaeoenvironments of the SCCP and appear to exhibit similar variability to key Southern Hemispheric palaeoclimatic proxy records, thereby placing southern African palaeoenvironments within the broader hemispheric climate change dynamics of the late Quaternary.

7. Conclusions

7.1 Introduction

By analysing the pollen, charcoal, sedimentological and geochemical data derived from the Pearly Beach, Rietvlei Still Bay and Vankervelsvlei sediment cores, this study has produced multi-proxy records that represent significant contributions to the late Quaternary palaeoenvironmental history of the southern Cape coastal plain. This chapter begins with a summary of the key findings that emanated from this research and places these findings in the context of the overall southern Cape palaeoenvironmental record. An assessment as to how the findings from this study can provide insight into current and future vegetation change on the SCCP is then presented. This is followed by a review of the original aim and objectives (as presented in Chapter 1) and concludes with a brief outline of future research directions.

7.2 Summary of key findings

This study highlights the fact that the southern Cape coastal plain holds great potential for palaeoenvironmental research. Given that it encompasses the transition between the winter and the year-round rainfall zones and is of great botanical importance, it was considered that the SCCP would be particularly sensitive to past climate and vegetation change. By producing three new records that document changes in vegetation community structures and inferred climatic changes, the resulting research confirms the accuracy of the above statement. The combination of several lines of proxy evidence for each site has resulted in robust palaeoenvironmental reconstructions and consequently a cohesive picture has emerged as to what the environments were like on the SCCP over certain periods within the last glacial-interglacial cycle.

Due to the virtual absence of terrestrial palaeoenvironmental data from the southern Cape covering MIS 5 to MIS 3, the establishment of the VVV10.1 record represents a particularly important outcome of this study. The VVV10.1 record makes it possible to reassess the previous work done by Irving and Meadows (Irving and Meadows, 1997; Irving, 1998) and create a more comprehensive understanding of the nature of the Vankervelsvlei basin and the overall vegetation changes that occurred at the site over the last ~116 ka.

Microscopic charcoal counts and concentrations were used to determine fire regimes and, in association with the pollen records, it proves possible to examine vegetation-fire relationships at the three sites over the time periods under investigation. The findings from Pearly Beach and Rietvlei reinforce the established contemporary ecological theory governing fynbos and coastal thicket and the pivotal role fire plays in determining the dominance of each within a landscape. A combination of climatic change (changes in the amount and seasonality of rainfall and increased temperatures) and prolonged reductions in fire frequencies were generally responsible for significantly higher percentages of thicket taxa within these records. The strong linkages between fire and fynbos are also evident within the VVV10.1 record and fire frequency therefore represents an important factor responsible for modulating fynbos-forest dynamics.

Wetland records are perhaps less indicative of regional climatic fluctuations as, for instance, hyrax midden records, but the stable carbon isotope ratios derived from the Pearly Beach and Rietvlei Still Bay sediment cores do reveal the differing ecological settings of the two sites: Pearly Beach exhibits a strongly fynbos-dominated signal whereas Rietvlei Still Bay's $\delta^{13}C_{TOC}$ record emphasizes the site's position within a more transitional area encompassing fynbos, coastal thicket/strandveld and Albany Thicket communities.

7.2.1 The southern Cape coast palaeoenvironmental record

The Vankervelsvlei pollen record indicates a greater dominance of afrotemperate forests in the vicinity of the site during the period ~116 – 94 ka in association with temperatures at least as warm as or warmer than the Holocene and reduced proportions of winter rainfall. Correlations with the Agulhas SST record (Caley et al., 2011) and the Cape Basin Record (Peeters et al., 2004) suggest causal mechanisms for these interglacial conditions indicating that, with a southward displacement of the STC, the westerlies would have shifted poleward, subjecting the southern Cape to enhanced easterly flow (van Zinderen Bakker, 1976; Cockcroft et al., 1987; Peeters et al., 2004; Chase and Meadows, 2007; Biastoch et al., 2009; Chase, 2010; Caley et al., 2011).

The Vankervelsvlei record reflects a shift to decreased temperatures, increased moisture availability and a greater dominance of fynbos from ~94 – 74 ka. These conditions persist into MIS 4, supporting the findings from previously established records from both the western and eastern subregions of the SCCP, and the offshore records, that suggest that MIS 4 was characterised by humid conditions as a result of an increased influence of the westerlies, warm SW Indian SSTs and increased linkages between tropical and temperate systems (Avery, 1982; Deacon et al., 1984; Avery, 1987; Avery et al.,

1997; Klein et al., 1999; Klein and Cruz-Uribe, 2000; Shi et al., 2001; Stuut et al., 2002; Peeters et al., 2004; Chase, 2010).

In general, the eastern subregion of the SCCP appears to have been subjected to enhanced winter rainfall during MIS 3, as the Vankervelsvlei record is characterised by high percentages of the winter rainfall indicator taxa sum (especially from ~50 – 40 ka). This suggests that the WRZ was intensified and/or expanded during this time, associated with northward shifts in the STC (Peeters et al., 2004). However, a significant change in environmental conditions appears to have taken place around ~36 ka. Various lines of evidence from both the Vankervelsvlei and Rietvlei Still Bay records indicate that conditions at this time were considerably more arid than either preceding periods or the present. This situation coincides with a discrete peak in the Agulhas Current SSTs, indications of increased aridity from offshore Namibia and increases in the ALF (Stuut et al., 2002; Peeters et al., 2004; Caley et al., 2011). This arid phase may have resulted from the prevention of the penetration of winter rainfall systems into the eastern section of the SCCP by an enhanced continental high (as suggested by Chase and Meadows, 2007), however further evidence is needed to fully test this hypothesis.

The lack of pollen preservation together with the sedimentological, geochemical and plant biomarker data generated for VVV10.1 and RVSB-2 suggests that xeric conditions characterised the eastern SCCP during the LGM. This assertion is supported by various other records indicating that the LGM was drier, windier and colder than present (e.g. Avery, 1982, 1983; Butzer et al., 1984; Klein, 1980, 1983, 1984). In contrast, the evidence from Pearly Beach generally supports the established theory that the western subregion of the SCCP (modern WRZ) and the western margin of southern Africa was subjected to cooler and wetter conditions during the last glacial period (Schalke, 1973; Parkington et al., 2000; Lancaster, 2002; Scott et al., 2004; Chase and Meadows, 2007; Scott and Woodborne, 2007a, b; Quick, 2009). However, it appears that LGM conditions within the western subregion of the SCCP were not homogeneously and consistently cooler and wetter than present. Evidence from Pearly Beach and De Rif (Quick, 2009) indicates that this period was punctuated by a discrete phase of significantly decreased moisture availability from 22 – 21.5 ka. Correlations to changes in Antarctic sea ice presence and its influence on the latitudinal position and/or intensity of the westerly wave belt provides the mechanism for both the generally enhanced moisture availability within the LGM as well as the discrete arid episode from 22 – 21.5 ka.

The evidence from the three new sites presented in this study, together with the previously established records (Chapter 3), appears to indicate that the transition from the LGM into the Holocene was characterised by great variability throughout the SCCP. The Pearly Beach record supports the notion of a moderately wet LGIT within the WRZ (Schalke, 1973; Klein, 1991; Avery,

1993). Evidence from Rietvlei also indicates increased moisture availability from ~19.4 – 17.5 ka. However after this period there are increasing signs of more xeric conditions and indications of rising sea levels, especially from ~15 – 13 ka. No pollen is preserved for the period coinciding with the YD; however the biomarker data provide some evidence for substantially reduced moisture availability. The Vankervelsvlei records were generally devoid of pollen for much for the LGIT with prominent sand peaks found at ~12, 13 and 16 ka signifying that the vlei was probably subjected to drier and/or windier conditions. These conditions were most likely a consequence of post-glacial warming which resulted in rising sea levels (perhaps leading to a weakening of the blocking continental anticyclone) and sharp decreases in Antarctic sea ice presence from 17.5 ka, resulting in the establishment of a more poleward position of the STC. Therefore the influence of high latitude southern hemispheric climatic dynamics on the SCCP would have been reduced. Consequently, Northern Hemisphere/North Atlantic forcing mechanisms were then able to exert more control on the western subregion of the SCCP from the LGIT onwards (Chase et al., 2009, 2010, 2011).

Evidence from the three new records generally supports past findings of increased moisture availability within the early Holocene and the existence of a warmer drier HA (Klein, 1984; Scholtz, 1986; Baxter, 1989; Meadows and Sugden, 1990, 1991; Avery, 1993; Meadows and Baxter, 1999, 2001; Chase and Thomas, 2007; Scott and Woodborne, 2007a, b; Chase et al., 2009, 2010, 2011; Meadows et al., 2010; Quick et al., 2011). However, finer-scale changes are evident within the Pearly Beach and Rietvlei records that stand in contrast to the above generalisations. For example, the Pearly Beach pollen and plant biomarker data reflect relatively wet conditions for a brief period within the HA (from 5.9 – 5.5 cal kBP).

The late Holocene is characterised by greater variability with discrete episodes of increased wetland productivity and moderately wetter conditions (e.g. from 0.54 – 0.28 in the RVSB-2 record) as well as phases of increased aridity (e.g. 0.45 – 0.32 in the PB-1 record). Contemporary vegetation structures consisting of mosaics of coastal thicket/strandveld elements and various fynbos communities appear to have been established at both Pearly Beach and Rietvlei Still Bay during the late Holocene. These changes are most likely a response to the generally warmer interglacial conditions, elevated CO_2 concentrations, changes in rainfall amounts and seasonality and changes in fire regimes.

Despite the discontinuous nature of all three palynological records, the positions of the sites along a longitudinal gradient and the multi-proxy approach undertaken in this study, make it possible to compare and contrast palaeoenvironmental conditions from the western/modern WRZ and the eastern/modern YRZ subregions of the SCCP. The variability within the three records clearly suggests that glacial – interglacial cycles had a strong impact on the region's vegetation history and climate

and that high Southern Hemisphere latitude climate dynamics coupled with Agulhas SST fluctuations were most likely responsible for much of the documented changes. In addition, the new records have identified discrete periods within which palaeoenvironmental conditions appear to deviate from those associated with the marine isotope stages (e.g. at 36 ka), providing new insights into the finer-scale climatic and ecological changes on the SCCP.

7.3 The implications of past vegetation community changes in the face of future anthropogenic climate change on the southern Cape coastal plain

This section attempts to answer the last key research question presented in Chapter one relating to how the insights gained from this study might contribute to the understanding of how present and future climate change may impact on the vegetation communities on the SCCP.

7.3.1 The Knysna Afrotemperate Region

The Vankervelsvlei record sheds further light on the fynbos-forest debate within the KAR, highlighting the mosaic nature of the KAR vegetation and establishing the antiquity of the coexistence of both fynbos and forest elements. This study, to some extent, disproves the contention that, in the past, afrotemperate forests covered the entire region from Knysna to the Cape Peninsula, that human intervention was solely responsible for forest decline and that the patchiness of the current forest distribution is relictual (Phillips, 1931; van Daalen, 1980).

Furthermore, the VVV10.1 data offers insights into the response of fynbos and forest vegetation to fluctuating environmental conditions over a vast period of time - the longest vegetation history yet produced for the KAR. The increased presence of afrotemperate forest taxa during MIS 5 d-c points to the likelihood that, during periods of increased absolute rainfall (as well as perhaps more aseasonal precipitation), warmer temperatures and reduced fire frequencies, forest taxa would dominate over fynbos. On the other hand, during periods associated with increased winter rainfall, more regular fires and cooler conditions, fynbos communities would have more of an advantage over forest stands.

Future climate change projections for the Western Cape Province/Cape Floristic Region/Fynbos Biome generally predict warmer temperatures and decreased moisture availability (Midgley et al., 2005; Hewitson and Crane, 2006; IPCC, 2007). It is therefore expected that forest extent will be reduced and forest patches will perhaps be confined to isolated refugia where conditions remain favourable. There is, however, considerable uncertainty in the simulations of future rainfall (IPCC,

2007). In addition, while it is likely that winter rainfall will be reduced (e.g. Hewitson and Crane, 2006), the effects of future climate change on the year-round rainfall zone remain largely unknown.

7.3.2 Coastal lowland fynbos

The considerable reductions in Ericaceae percentages in the Pearly Beach and Vankervelsvlei records during interglacial periods suggest that future warming may lead to reductions in cool moist fynbos elements. All three records document the strong association between fynbos and fire providing further substantiation for the maintenance of appropriate fire management practices (e.g. van Wilgen, 1992; Wilgen et al., 1994; Pressey et al., 2003; Kraaij et al., 2012). The overall conclusions drawn from this study indicate that, in general, coastal lowland fynbos communities appear to be susceptible to invasion by other vegetation types (such as coastal thicket and karroid elements) during periods of increased temperatures (curtailing the cool growing season that is necessary for fynbos growth), decreased winter rainfall and reduced fire frequencies.

Significant reductions in the area covered by the Fynbos Biome have been predicted to occur in response to future anthropogenic climate change (Rutherford et al., 1999; Hannah et al., 2002; Midgley et al., 2002; Midgley et al., 2003; Hannah et al., 2005). However more emphasis on the southern Cape region is needed as it is clear from this research that fynbos communities on the SCCP are sensitive to environmental change. Substantial changes in temperatures, moisture availability and fire regimes would mean that the strong edaphic affinities currently constraining the distribution of many fynbos types could play a lesser role in the persistence of species in favour of range shifts and losses, population declines and extinctions. Consequently, coastal thicket elements may invade from the east (Albany Thicket Biome) and encroach further inland with the expansion of coastal dune communities. The Succulent Karoo Biome is predicted to collapse southward, allowing for karroid elements to invade from the north (Hannah et al., 2002). In addition to the threat of future anthropogenic climate change, ongoing habitat transformations (as a result of agricultural, coastal resort and urban development) and the rapid spread of alien vegetation on the SCCP means that the region is particularly vulnerable to significant reductions in biodiversity (Rebelo, 1992; Heijnis et al., 1999; Heydenrych et al., 1999; Rouget et al., 2003).

The findings from this study therefore provide a better understanding of the relation between rates and spatial patterns of past climate change and the distribution of vegetation communities on the SCCP. It supports the prioritisation of the coastal lowlands of the Fynbos Biome for conservation efforts, as advocated by Hannah et al. (2005), Bomhard et al. (2005) and various other researchers.

In addition, the integration of these findings into the assessment of predictive bioclimatic models (Midgley and Thuiller, 2011; West et al., 2011; West et al., 2012) will help refine simulations of how coastal lowland vegetation communities may respond to future climate change.

7.4 Review of the aim and specific objectives

The primarily aim of this research was to investigate the vegetation dynamics and associated environmental conditions on the southern Cape coastal plain over the late Quaternary through the application of pollen analysis. To address this aim a thorough examination of the contemporary environments of the SCCP was undertaken (Chapter 2) along with a review of the existing palaeoenvironmental records for the SCCP and neighbouring regions (Chapter 3). The review highlights the discontinuous nature of the available records, emphasises the lack of an overall cohesive palaeoenvironmental history for the SCCP, presents conceptual climatic models and proposes possible climatic mechanisms for the observed changes. The identification, sampling and analysis of material from Pearly Beach, Rietvlei Still Bay and Vankervelsvlei (Chapter 4) makes it possible to meet the specific objectives outlined in Chapter 1 and generate the results presented in Chapter 5. Through the use of radiocarbon and optically stimulated luminescence (OSL) analyses it proves possible to establish chronologies for the three sequences. Pollen was extracted from the Pearly Beach (PB-1), Rietvlei Still Bay (RVSB-2) and Vankervelsvlei (VVV10.1) sediment cores and pollen records documenting vegetation community changes over the periods: ~25 – 0 cal kBP (PB-1), ~36 – 0 ka (RVSB-2) and ~116 – 7 ka (VVV10.1) were constructed. In addition, sedimentological and geochemical data was generated for the three records, providing additional insight into the nature of the local vlei environments and supplementary insight into the regional vegetation and climate changes. Chapter 6 discusses the results of the study against the backdrop of previous palaeoenvironmental records for the region (as reviewed in Chapter 3) and presents correlations between the new records and other southern African climate proxies, highlighting possible mechanisms for the observed climate change events.

7.5 Future research directions

There is great potential for further work to be conducted on the VVV10.1 sediment core including:

- The establishment of a higher-resolution palynological record by increasing the subsampling resolution and targeting key sections of the record which would benefit most from a high-resolution approach.
- The establishment of a higher-resolution age-depth model by obtaining additional radiocarbon ages for the LGM to the early Holocene section and further OSL ages for the MIS 5 – MIS 3 section (several OSL subsamples were extracted prior to the core being exposed to light and not analysed, therefore appropriate material is available for future analysis).
- The generation of geochemical and plant biomarker data in order to provide supplementary information on the nature of the Vankervelsvlei basin as well as further details on past vegetation and climatic changes at the site over the last ~116 ka.

While many similarities exist between the records presented here and proxies for regional and hemispheric climate change and despite the fact that these proxies provide key evidence of the causal mechanisms responsible for the changes in these records, a linear relationship certainly does not exist between them. This, therefore, highlights that it is not possible to accurately reconstruct SCCP, or for that matter, southern African palaeoenvironments solely by comparison with these climatic proxies, advocating for the establishment of further records to test the conclusions that have been drawn from the data presented within this study.

In general, emphasis should be placed on identifying and analysing more continuous, higher temporally-resolved records from both the western and eastern subregions of the SCCP in order to better resolve key phases such as the LGM. In this regard, the generation and incorporation of hyrax midden records from the southeastern Cape Fold Belt mountain ranges represents a promising avenue. A further option would be to include the analysis of diagnostic graminoid phytolith morphotypes. These phytolith morphotypes appear to hold great potential for the reconstruction of past winter rainfall and therefore could be employed to further explore the changes in rainfall seasonality on the SCCP over the late Pleistocene (c.f. Cordova, 2012; Cordova, 2013).

The bioclimatic analysis conducted for this study represents the first attempt at the creation of bioclimatic envelopes for each pollen taxon. There is scope for more in-depth (the inclusion of several more bioclimatic variables) and finer spatially-resolved analyses of the modern distributions of certain key indicator taxa. Refinements to the bioclimatic analyses will greatly improve the

interpretation of current and future pollen records. In addition, to enable quantitative statistically robust reconstructions of palaeoclimates, the *pdf* (probability density function) method will be investigated. As a comprehensive modern pollen database has yet to be established for the Fynbos Biome but modern climatological and species distribution data are available, the *pdf* approach represents a more appropriate methodology than transfer functions. The *pdf* method focuses on probability density functions as botanical-climatological transfer functions that statistically describe climate (temperature or moisture) - species relationships (Kuhl et al., 2002). This method determines the climate dependencies of individual taxa and enables the use of both modern climate data and fossil pollen data to quantitatively reconstruct past climates. Taxon-specific *pdfs* can be combined to represent the reconstructed most probable climate (Kühl et al., 2007). Therefore this method will make it possible to reconstruct past environments from fossil pollen taxa whose environmental limits have been either previously determined or assumed by correlation of taxon distributions and abundance with climatic variables (e.g. building on the bioclimatic analyses mentioned above).

7.6 Conclusion

This study successfully establishes three valuable new records of vegetation change on the southern Cape coastal plain, documents how glacial – interglacial dynamics have affected the SCCP and provides links as to how changes in Agulhas SSTs, shifts in the STC and the westerly wave belt have modified regional climates. Together with the integration of new proxies and further palaeoenvironmental evidence, this study represents a significant step towards improving our understanding of southern African environments – past, present and future.

REFERENCES

Albert, R.M., Marean, C.W., 2012. The Exploitation of Plant Resources by Early Homo sapiens: The Phytolith Record from Pinnacle Point 13B Cave, South Africa. Geoarchaeology 27, 363-384.

Allott, L., 2006. Archaeological charcoal as a window on the palaeovegetation and wood use during the Middle Stone Age at Sibudu Cave. Southern African Humanities 18, 173-201.

Avery, D.M., 1982. Micromammals as palaeoenvironmental indicators and an interpretation of the late Quaternary in the southern Cape Province, South Africa. Annals of the South African Museum 85, 183-377.

Avery, D.M., 1987. Late Pleistocene coastal environment of the Southern Cape Province of South Africa: micromammals from Klasies River Mouth. Journal of Archaeological Science 14, 405-421.

Avery, G., Cruz-Uribe, K., Goldberg, P., Grine, F.E., Klein, R.G., Lenardi, M.J., Marean, C.W., Rink, W.J., Schwarcz, H.P., Thackeray, A.I., Wilson, M.L., 1997. The 1992-1993 excavations at the Die Kelders Middle and Later Stone Age cave site, South Africa. Journal of Field Archaeology 24, 263-291.

Bailey, C., Shackleton, C., Geldenhuys, C., Moshe, D., Flemming, G., Vink, E., Rathogwa, N., Cawe, S., 1999. Guide to and summary of the meta-database pertaining to selected attributes of South African indigenous forests and woodlands. Report no. ENv-PC 99027.

Bar-Matthews, M., Marean, C.W., Jacobs, Z., Karkanas, P., Fisher, E.C., Herries, A.I.R., Brown, K., Williams, H.M., Bernatchez, J., Ayalon, A., Nilssen, P.J., 2010. A high resolution and continuous isotopic speleothem record of paleoclimate and paleoenvironment from 90 to 53 ka from Pinnacle Point on the south coast of South Africa. Quaternary Science Reviews 29, 2131-2145.

Bard, E., Rickaby, R.E.M., 2009. Migration of the subtropical front as a modulator of glacial climate. Nature 460, 380-383.

Bartram, J., Laurence E., Marean, C.W., 1999. Explaining the "Klasies Pattern": Kua ethnoarchaeology, the Die Kelders Middle Stone Age archaeofauna, long bone fragmentation and carnivore ravaging. Journal of Archaeological Science 26, 9-29.

Bateman, M.D., Carr, A.S., Dunajko, A.C., Holmes, P.J., Roberts, D.L., McLaren, S.J., Bryant, R.G., Marker, M.E., Murray-Wallace, C.V., 2011. The evolution of coastal barrier systems: a case study of the Middle-Late Pleistocene Wilderness barriers, South Africa. Quaternary Science Reviews 30, 63-81.

Bateman, M.D., Carr, A.S., Murray-Wallace, C.V., Roberts, D.L., Holmes, P.J., 2008. A dating intercomparison study on Late Stone Age coastal midden deposits, South Africa. Geoarchaeology 23, 715-741.

Bateman, M.D., Holmes, P.J., Carr, A.S., Horton, B.P., Jaiswal, M.K.M.K., 2004. Aeolianite and barrier dune construction spanning the last two glacial-interglacial cycles from the southern Cape coast, South Africa. Quaternary Science Reviews 23, 1681-1698.

Baxter, A., 1989. Pollen analysis of a Table Mountain cave deposit. Unpublished BSc (Hons) Thesis, University of Cape Town, Cape Town.

Baxter, A., 1996. Late Quaternary Palaeoenvironments of the Sandveld, Western Cape Province, South Africa. Unpublished PhD Thesis, University of Cape Town, Cape Town.

Baxter, A.J., Meadows, M.E., 1999. Evidence for Holocene sea level change at Verlorenvlei, Western Cape, South Africa. Quaternary International 56, 65-79.

Bennett, K.D., 1993 - 2009. Psimpoll and pscomb programs for plotting and analysis, 4.27 ed, Belfast.

Bennett, K.D., 1996. Evolution and ecology: the pace of life. Cambridge University Press.

Bennett, K.D., Willis, K.J., 2001. Pollen, in: Smol, J.P., Birks, H.J.B., Last, W.M. (Eds.), Tracking Environmental Change Using Lake Sediments. Volume 3: Terrestrial, Algal, and Siliceous Indicators. Kluwer Academic Publishers, Dordrecht, The Netherlands, pp. 5-26.

Berger, A., Loutre, M.F., 1991. Insolation values for the climate of the last 10 million years. Quaternary Science Reviews 10, 297-317.

Berger, A., Loutre, M.F., 2004. Theorie astronomique des paleoclimats. Comptes Rendus Geosciences 336, 701-709.

Beuselinck, L., Govers, G., Poesen, J., Degraer, G., Froyen, L., 1998. Grain-size analysis by laser diffractometry: comparison with the sieve-pipette method. CATENA 32, 193-208.

Biastoch, A., Boning, C.W., Schwarzkopf, F.U., Lutjeharms, J.R.E., 2009. Increase in Agulhas leakage due to poleward shift of Southern Hemisphere westerlies. Nature 462, 495-498.

Birch, G.F., 1977. Surficial sediments on the continental margin off the west coast of South Africa. Marine Geology 23, 305-337.

Birks, H.J.B., 1996. Contributions of Quaternary Palaeoecology to Nature Conservation. Journal of Vegetation Science 7, 89-98.

Blaauw, M., 2010. Methods and code for 'classical' age-modelling of radiocarbon sequences. Quaternary Geochronology 5, 512-518.

Blaauw, M., 2012. Out of tune: the dangers of aligning proxy archives. Quaternary Science Reviews 36, 38-49.

Blaauw, M., Christen, J.A., 2005. The problems of radiocarbon dating. Science 308, 1551.

Blaauw, M., van der Plicht, J., van Geel, B., 2004. Radiocarbon dating of bulk peat samples from raised bogs: non-existence of a previously reported 'reservoir effect'? Quaternary Science Reviews 23, 1537-1542.

Blockley, S.P.E., Blaauw, M., Bronk Ramsey, C., van der Plicht, J., 2007. Building and testing age models for radiocarbon dates in Lateglacial and early Holocene sediments. Quaternary Science Reviews 26, 1915-1926.

Blome, M.W., Cohen, A.S., Tryon, C.A., Brooks, A.S., Russell, J., 2012. The environmental context for the origins of modern human diversity: A synthesis of regional variability in African climate 150,000–30,000 years ago. Journal of Human Evolution.

Blunier, T., Brook, E.J., 2001. Timing of millennial-scale climate change in Antarctica and Greenland during the last glacial period. Science 291, 109-112.

Blunier, T., Chappellaz, J., Schwander, J., Daellenbach, A., Stauffer, B., Stocker, T.F., Raynaud, D., Jouzel, J., Clausen, H.B., Hammer, C.U., Johnsen, S.J., 1998. Asynchrony of Antarctic and Greenland climate change during the last glacial period. Nature 394, 739-743.

Bomhard, B., Richardson, D.M., Donaldson, J.S., Hughes, G.O., Midgley, G.F., Raimondo, D.C., Rebelo, A.G., Rouget, M., Thuiller, W., 2005. Potential impacts of future land use and climate change on the Red List status of the Proteaceae in the Cape Floristic Region, South Africa. Global Change Biology 11, 1452-1468.

Bond, P., Goldblatt, P., 1984. Plants of the Cape flora: a descriptive catalogue, in: Eloff, J.N. (Ed.), Journal of South African Botany (suppl. vol.), pp. 1-455.

Bond, W.J., 1984. Fire survival of Cape Proteaceae-influence of fire season and seed predators. Vegetatio 56, 65-74.

Bond, W.J., Midgley, G.F., 2000. A proposed CO_2-controlled mechanism of woody plant invasion in grasslands and savannas. Global Change Biology 6, 865-869.

Bond, W.J., Midgley, G.F., Woodward, F.I., 2003. The importance of low atmospheric CO2 and fire in promoting the spread of grasslands and savannas. Global Change Biology 9, 973-982.

Bond, W.J., Volk, J., Viviers, M., 1984. Variation in Seedling Recruitment of Cape Proteaceae after Fire. Journal of Ecology 72, 209-221.

Boucher, C., Moll, E.J., 1981. South African mediterranean shrublands. Ecosystems of the world 11. Mediterranean-type shrublands, 233-248.

Bowen, B.J., 1991. Fire response within the family Proteaceae: A comparison of plants displaying the seeder and resprouter mode of recovery. University of Western Australia.

Bowman, D., Cook, G., Zoppi, U., 2004. Holocene boundary dynamics of a northern Australian monsoon rainforest patch inferred from isotopic analysis of carbon,(14C and δ13C) and nitrogen (δ15N) in soil organic matter. Austral Ecology 29, 605-612.

Brathauer, U., Abelmann, A., 1999. Late Quaternary variations in sea surface temperatures and their relationship to orbital forcing recorded in the Southern Ocean (Atlantic sector). Paleoceanography 14, 135-148.

Briant, R.M., Bateman, M.D., 2009. Luminescence dating indicates radiocarbon age underestimation in late Pleistocene fluvial deposits from eastern England. Journal of Quaternary Science 24, 916-927.

Brown, K.S., Marean, C.W., Herries, A.I.R., Jacobs, Z., Tribolo, C., Braun, D., Roberts, D.L., Meyer, M.C., Bernatchez, J., 2009. Fire as an engineering tool of early modern humans. Science 325, 859-862.

Brown, K.S., Marean, C.W., Jacobs, Z., Schoville, B.J., Oestmo, S., Fisher, E.C., Bernatchez, J., Karkanas, P., Matthews, T., 2012. An early and enduring advanced technology originating 71,000 years ago in South Africa. Nature 491, 590-593.

Bunting, M.J., Middleton, R., Gaillard, M.-J., Sugita, S., Broström, A., 2004. Vegetation structure and pollen source area. Holocene 14, 651-660.

Bunting, M.J., Tipping, R., 2004. Complex hydroseral vegetation succession and 'dryland'pollen signals: a case study from northwest Scotland. The Holocene 14, 53-63.

Bürger, C., 2011. Charakterisierung der Sedimenteinträge am Vankervelsvlei mit Hilfe der Korngrößenanalyse. Unpublished BSc (Hons) Thesis, Friedrich-Schiller-Universität Jena, Jena, Germany.

Burke, K., Gunnel, Y., 2008. The African Erosion Surface: A Continental-Scale Synthesis of Geomorphology, Tectonics, and Environmental Change over the Past 180 Million Years. The Geological Society of America, Boulder, Colorado.

Butzer, K.W., 1984. Late Quaternary environments in South Africa, in: Vogel, J.C. (Ed.), Late Cainozoic palaeoclimates of the Southern Hemisphere. Proc. SASQUA symposium, Swaziland, 1983. Balkema, pp. 235-264.

Butzer, K.W., 2004. Coastal eolian sands, paleosols, and Pleistocene geoarchaeology of the Southwestern Cape, South Africa. Journal of Archaeological Science 31, 1743-1781.

Butzer, K.W., Stuckenrath, R., Bruzewicz, A.J., Helgren, D.M., 1978. Late Cenozoic paleoclimates of the Gaap Escarpment, Kalahari margin, South Africa. Quaternary Research 10, 310-339.

Caley, T., Kim, J.H., Malaizé, B., Giraudeau, J., Laepple, T., Caillon, N., Charlier, K., Rebaubier, H., Rossignol, L., Castañeda, I.S., Schouten, S., Sinninghe Damsté, J.S., 2011. High-latitude obliquity as a dominant forcing in the Agulhas current system. Clim. Past 7, 1285-1296.

Campbell, B.M., 1985. A classification of the mountain vegetation of the fynbos biome. Botanical Research Institute, Dept. of Agriculture and Water Supply, [Pretoria] South Africa.

Campbell, B.M., Werger, M.J.A., 1988. Plant form in the mountains of the Cape, South Africa. Journal of Ecology 76, 637-653.

Carr, A., 2004. Late Quaternary environmental change on the Agulhas Plain, Winter Rainfall Zone, South Africa. University of Sheffield, Sheffield.

Carr, A., Boom, A., Chase, B., Roberts, D., Roberts, Z., 2010a. Molecular fingerprinting of wetland organic matter using pyrolysis-GC/MS: an example from the southern Cape coastline of South Africa. Journal of Paleolimnology 44, 947-961.

Carr, A.S., Bateman, M.D., Holmes, P.J., 2007. Developing a 150 ka luminescence chronology for the barrier dunes of the southern Cape, South Africa. Quaternary Geochronology 2, 110-116.

Carr, A.S., Bateman, M.D., Roberts, D.L., Murray-Wallace, C.V., Jacobs, Z., Holmes, P.J., 2010b. The last interglacial sea-level high stand on the southern Cape coastline of South Africa. Quaternary Research 73, 351-363.

Carr, A.S., Boom, A., Chase, B.M., 2010c. The potential of plant biomarker evidence derived from rock hyrax middens as an indicator of palaeoenvironmental change. Palaeogeography, Palaeoclimatology, Palaeoecology 285, 321-330.

Carr, A.S., Boom, A., Dunajko, A., Bateman, M.D., Holmes, P.J., Berrio, J.-C., 2010d. New Evidence for the age and palaeoecology of the Knysna Formation, South Africa. South African Journal of Geology 113, 241-256.

Carr, A.S., Thomas, D.S.G., Bateman, M.D., 2006a. Climatic and sea level controls on late Quaternary eolian activity on the Agulhas Plain, South Africa. Quaternary Research 65, 252-263.

Carr, A.S., Thomas, D.S.G., Bateman, M.D., Meadows, M.E., Chase, B., 2006b. Late Quaternary palaeoenvironments of the winter-rainfall zone of southern Africa: palynological and sedimentological evidence from the Agulhas Plain. Palaeogeography, Palaeoclimatology, Palaeoecology 239, 147-165.

Cartwright, C., Parkington, J., 1997. The wood charcoal assemblages from Elands Bay Cave, Southwestern Cape: principles, procedures and preliminary interpretation. South African Archaeological Bulletin 52, 59-72.

Castellani, C., 2000. Strategic conservation interventions: A case study from the Agulhas Plain in southern Africa. ORYX 34, 6.

Cerling, T.E., Quade, J., Ambrose, S.H., Sikes, N.E., 1991. Fossil soils, grasses, and carbon isotopes from Fort Ternan, Kenya: grassland or woodland? Journal of Human Evolution 21, 295-306.

Chambers, F.C., 2002. The environmental applications of pollen analysis, in: Haslett, S. (Ed.), Quaternary Environmental Micropalaeontology. Arnold, London, p. chapter 11.

Chambers, F.M., Booth, R.K., De Vleeschouwer, F., Lamentowicz, M., Le Roux, G., Mauquoy, D., Nichols, J.E., van Geel, B., 2012. Development and refinement of proxy-climate indicators from peats. Quaternary International 268, 21-33.

Charles, C.D., Lynch-Stieglitz, J., Ninnemann, U.S., Fairbanks, R.G., 1996. Climate connections between the hemispheres revealed by deep-sea sediment core/ice core correlations. Earth and Planetary Science Letters 142, 19-27.

Chase, B.M., 2006. Late Quaternary palaeoenvironments of the west coast of South Africa: the aeolian record. Unpublished PhD thesis, University of Oxford, Oxford.

Chase, B.M., 2010. South African palaeoenvironments during marine oxygen isotope stage 4: a context for the Howiesons Poort and Still Bay industries. Journal of Archaeological Science 37, 1359-1366.

Chase, B.M., Meadows, M.E., 2007. Late Quaternary dynamics of southern Africa's winter rainfall zone. Earth-Science Reviews 84, 103-138.

Chase, B.M., Meadows, M.E., Carr, A.S., Reimer, P.J., 2010. Evidence for progressive Holocene aridification in southern Africa recorded in Namibian hyrax middens: Implications for African Monsoon dynamics and the "African Humid Period". Quaternary Research 74, 36-45.

Chase, B.M., Meadows, M.E., Scott, L., Thomas, D.S.G., Marais, E., Sealy, J., Reimer, P.J., 2009. A record of rapid Holocene climate change preserved in hyrax middens from southwestern Africa. Geology 37, 703-706.

Chase, B.M., Quick, L.J., Meadows, M.E., Scott, L., Thomas, D.S.G., Reimer, P.J., 2011. Late-glacial interhemispheric climate dynamics revealed in South African hyrax middens. Geology 39, 19 - 22.

Chase, B.M., Thomas, D.S.G., 2007. Multiphase late Quaternary aeolian sediment accumulation in western South Africa: timing and relationship to palaeoclimatic changes inferred from the marine record. Quaternary International 166, 29-41.

Chiang, J.C., Biasutti, M., Battisti, D.S., 2003. Sensitivity of the Atlantic intertropical convergence zone to last glacial maximum boundary conditions. Paleoceanography 18, 1094.

Chiang, J.H., Bitz, C., 2005. Influence of high latitude ice cover on the marine Intertropical Convergence Zone. Climate Dynamics 25, 477-496.

Clark, J.L., Plug, I., 2008. Animal exploitation strategies during the South African Middle Stone Age: Howiesons Poort and post-Howiesons Poort fauna from Sibudu Cave. Journal of Human Evolution 54, 886-898.

Clark, J.S., 1988. Particle motion and the theory of stratigraphic charcoal analysis: source area, transport, deposition, and sampling. Quaternary Research 30, 67-80.

Clark, P.U., Mix, A.C., 2002. Ice sheets and sea level of the Last Glacial Maximum. Quaternary Science Reviews 21, 1-7.

Clark, R., 1984. The effects on charcoal of pollen preparation procedures. Pollen et Spores 26, 559-576.

Climate Systems Analysis Group, U.C.T., 2012. Climate Information Portal (CIP). http://cip.csag.uct.ac.za/webclient/map. Accessed on: 15 March 2012.

Cockcroft, M.J., Wilkinson, M.J., Tyson, P.D., 1987. The application of a present-day climatic model to the late Quaternary in southern Africa. Climatic Change 10, 161-181.

Cohen, A.L., Parkington, J.E., Brundrit, G.B., van der Merwe, N.J., 1992. A Holocene marine climate record in mollusc shells from the Southwest African coast. Quaternary Research 38, 379-385.

Cole, N., Lombard, A., Cowling, R., Euston-Brown, D., Richardson, D., Heijnis, C., 2000. Framework for a conservation plan for the Agulhas Plain, Cape Floristic Region, South Africa. IPC report 0001 of the CAPE Project, WWF-SA.

Compton, J.S., 2011. Pleistocene sea-level fluctuations and human evolution on the southern coastal plain of South Africa. Quaternary Science Reviews 30, 506-527.

Conedera, M., Tinner, W., Neff, C., Meurer, M., Dickens, A.F., Krebs, P., 2009. Reconstructing past fire regimes: methods, applications, and relevance to fire management and conservation. Quaternary Science Reviews 28, 555-576.

Cook, E.J., van Geel, B., van der Kaars, S., van Arkel, J., 2011. A review of the use of non-pollen palynomorphs in palaeoecology with examples from Australia. Palynology 35, 155-178.

Cordova, C.E., 2012. Biogeographic and climatic patterns of southern African graminoids: an opal-phytolith scheme for paleoenvironmental reconstructions. Quaternary International 279–280, 98.

Cordova, C.E., 2013. C3 Poaceae and Restionaceae phytoliths as potential proxies for reconstructing winter rainfall in South Africa. Quaternary International 287, 121-140.

Cowling, R., Campbell, B., Mustart, P., McDonald, D., Jarman, M., Moll, E., 1988. Vegetation classification in a floristically complex area: The Agulhas Plain. South African Journal of Botany 54, 290-300.

Cowling, R.M., 1983a. The occurrence of C3 and C4 grasses in fynbos and allied shrublands in the South Eastern Cape, South Africa. Oecologia 58, 121-127.

Cowling, R.M., 1983b. Phytochorology and vegetation history in the south-eastern Cape, South Africa (fynbos, renosterveld). Journal of Biogeography 10, 393-419.

Cowling, R.M., 1990. Diversity components in a species-rich area of the Cape Floristic Region. Journal of Vegetation Science 1, 699-710.

Cowling, R.M., 1992. The Ecology of Fynbos: Nutrients, Fire, and Diversity. Oxford University Press, Cape Town.

Cowling, R.M., 1996. Flora and vegetation of Groot Hagelkraal (Bantamsklip site), Agulhas Plain, Unpublished Report. Institute for Plant Conservation, University of Cape Town.

Cowling, R.M., Campbell, B.M., 1983. A comparison of fynbos and non-fynbos coenoclines in the lower Gamtoos River Valley, southeastern Cape, South Africa. Plant Ecology 53, 161-178.

Cowling, R.M., Cartwright, C.R., Parkington, J.E., Allsopp, J.C., 1999. Fossil wood charcoal assemblages from Elands Bay Cave, South Africa: implications for late Quaternary vegetation and climates in the winter-rainfall fynbos biome. Journal of Biogeography 26, 367-378.

Cowling, R.M., Holmes, P.M., 1992a. Endemism and speciation in a lowland flora from the Cape Floristic Region. Biological Journal of the Linnean Society 47, 367-383.

Cowling, R.M., Holmes, P.M., 1992b. Flora and vegetation, in: Cowling, R.M. (Ed.), The Ecology of Fynbos: Nutrients, Fire and Diversity. Oxford University Press, Cape Town, pp. 23-61.

Cowling, R.M., Pierce, S.M., 1988. Secondary succession in coastal dune fynbos: variation due to site and disturbance. Vegetatio 76, 131-139.

Cowling, R.M., Richardson, D.M., J., M.P., 1997a. Fynbos, in: Cowling, R.M., Richardson, D.M., Pierce, S.M. (Eds.), Vegetation of Southern Africa. Cambridge University Press, Cambridge, pp. 99-130.

Cowling, R.M., Richardson, D.M., Paterson-Jones, C., 1995. Fynbos : South Africa's unique floral kingdom. Fernwood Press, Vlaeberg.

Cowling, R.M., Richardson, D.M., Schulze, R.E., Hoffman, M.T., Midgley, J.J., Hilton-Taylor, C., 1997b. Species diversity at the regional scale, in: Cowling, R.M., Richardson, D.M., Pierce, S.M. (Eds.), Vegetation of Southern Africa. Cambridge University Press, Cambridge, pp. 447 - 273.

Crétat, J., Richard, Y., Pohl, B., Rouault, M., Reason, C., Fauchereau, N., 2012. Recurrent daily rainfall patterns over South Africa and associated dynamics during the core of the austral summer. International Journal of Climatology 32, 261-273.

Crosta, X., Sturm, A., Armand, L., Pichon, J.-J., 2004. Late Quaternary sea ice history in the Indian sector of the Southern Ocean as recorded by diatom assemblages. Marine Micropaleontology 50, 209-223.

Daniau, A.L., Bartlein, P.J., Harrison, S.P., Prentice, I.C., Brewer, S., Friedlingstein, P., Harrison-Prentice, T.I., Inoue, J., Izumi, K., Marlon, J.R., Mooney, S., Power, M.J., Stevenson, J., Tinner, W., Andrič, M., Atanassova, J., Behling, H., Black, M., Blarquez, O., Brown, K.J., Carcaillet, C., Colhoun, E.A., Colombaroli, D., Davis, B.A.S., D'Costa, D., Dodson, J., Dupont, L., Eshetu, Z., Gavin, D.G., Genries, A., Haberle, S., Hallett, D.J., Hope, G., Horn, S.P., Kassa, T.G., Katamura, F., Kennedy, L.M., Kershaw, P., Krivonogov, S., Long, C., Magri, D., Marinova, E., McKenzie, G.M., Moreno, P.I., Moss, P., Neumann, F.H., Norström, E., Paitre, C., Rius, D., Roberts, N., Robinson, G.S., Sasaki, N., Scott, L., Takahara, H., Terwilliger, V., Thevenon, F., Turner, R., Valsecchi, V.G., Vannière, B., Walsh, M., Williams, N., Zhang, Y., 2012. Predictability of biomass burning in response to climate changes. Global Biogeochemical Cycles 26, GB4007.

Dansgaard, W., Johnsen, S.J., Clausen, H.B., Dahl-Jensen, D., Gundestrup, N.S., Hammer, C.U., Hvidberg, C.S., Steffensen, J.P., Sveinbjörnsdottir, A.E., Jouzel, J., Bond, G., 1993. Evidence for general instability of past climate from a 250 kyr ice core record. Nature 364, 218-220.

Das, S.K., Routh, J., Roychoudhury, A.N., Klump, J.V., 2008. Elemental (C, N, H and P) and stable isotope (δ 15 N and δ 13 C) signatures in sediments from Zeekoevlei, South Africa: a record of human intervention in the lake. Journal of Paleolimnology 39, 349-360.

Davis, B., Brewer, S., 2009. Orbital forcing and role of the latitudinal insolation/temperature gradient. Clim Dyn 32, 143-165.

Dawson, T.E., Brooks, P.D., 2001. Fundamentals of stable isotope chemistry and measurement, in: Unkovich, M., Pate, J., McNeill, A., Gibbs, J.D. (Eds.), Stable Isotope Techniques in the Study of Biological Processes and Functioning of Ecosystems. Kluwer Academic, Dordrecht.

Deacon, H.J., Deacon, J., Scholtz, A., Thackeray, J.F., Brink, J.S., 1984. Correlation of palaeoenvironmental data from the Late Pleistocene and Holocene deposits at Boomplaas Cave, southern Cape, in: Vogel, J.C. (Ed.), Late Cainozoic Palaeoclimates of the Southern Hemisphere. Balkema, Rotterdam, pp. 339-360.

Deacon, H.J., Jury, M.R., Ellis, F., 1992. Selective regime and time., in: Cowling, R.M. (Ed.), The Ecology of Fynbos: Nutrients, Fire and Diversity. Oxford University Press, Cape Town, pp. 6–22.

Deacon, H.J., Lancaster, N., 1988. Late Quaternary palaeoenvironments of southern Africa. Clarendon Press, Oxford.

Deininger, M., Fohlmeister, J., Scholz, D., Mangini, A., 2012. Isotope disequilibrium effects: The influence of evaporation and ventilation effects on the carbon and oxygen isotope composition of speleothems – A model approach. Geochimica et Cosmochimica Acta 96, 57-79.

Delcourt, H.R., Delcourt, P.A., 1991. Quaternary Ecology: a palaeoecological prespective. Chapman & Hall, London.

Desmarchelier, J.M., Goede, A., Ayliffe, L.K., McCulloch, M.T., Moriarty, K., 2000. Stable isotope record and its palaeoenvironmental interpretation for a late Middle Pleistocene speleothem from Victoria Fossil Cave, Naracoorte, South Australia. Quaternary Science Reviews 19, 763-774.

Di Stefano, C., Ferro, V., Mirabile, S., 2010. Comparison between grain-size analyses using laser diffraction and sedimentation methods. Biosystems Engineering 106, 205-215.

Dingle, R., Rogers, J., 1972. Pleistocene palaeogeography of the Agulhas Bank. Transactions of the Royal Society of South Africa 40, 155-165.

Dingle, R.V., 1973. Post-Palaeozoic stratigraphy of the eastern Agulhas Bank, South African continental margin. Marine Geology 15, 1-23.

Dingle, R.V., Siesser, W.G., Newton, A.R., 1983. Mesozoic and Tertiary geology of southern Africa. A.A. Balkema, Rotterdam.

Dupont, L., 2011. Orbital scale vegetation change in Africa. Quaternary Science Reviews 30, 3589-3602.

Dupont, L., Behling, H., Kim, J.H., 2008. Thirty thousand years of vegetation development and climate change in Angola (Ocean Drilling Program Site 1078). Climate of the Past 4, 107-124.

Dyke, A.S., Andrews, J.T., Clark, P.U., England, J.H., Miller, G.H., Shaw, J., Veillette, J.J., 2002. The Laurentide and Innuitian ice sheets during the Last Glacial Maximum. Quaternary Science Reviews 21, 9-31.

Ehleringer, J.R., Cerling, T.E., 2001. C3 and C4 photosynthesis., in: Mooney, H.A., Canadell, J. (Eds.), Encyclopedia of Global Environmental Change. John Wiley and Sons, New York, pp. 186–190.

Ehleringer, J.R., Cerling, T.E., Helliker, B.R., 1997. C4 photosynthesis, atmospheric CO2, and climate. Oecologia 112, 285-299.

Ehleringer, J.R., Cooper, T.A., 1988. Correlations between carbon isotope ratio and microhabitat of desert plants. Oecologia 76, 562-566.

Ehleringer, J.R., Phillips, S.L., Comstock, J.P., 1992. Seasonal variation in the carbon isotopic composition of desert plants. Functional Ecology 6, 396-404.

Ellery, K., Ellery, W.N., Rogers, K.H., Walker, B.H., 1990. Formation, colonization and fate of floating sudds in the Maunachira river system of the Okavango Delta, Botswana. Aquatic Botany 38, 315-329.

Ellery, W.N., Grenfell, S.E., Grenfell, M.C., Humphries, M.S., Barnes, K., Dahlberg, A., Kindness, A., 2012. Peat formation in the context of the development of the Mkuze floodplain on the coastal plain of Maputaland, South Africa. Geomorphology 141–142, 11-20.

Ellis, A., Van Geel, B., 1978. Fossil zygospores of Debarya glyptosperma (de Bary) Wittr.(Zygnemataceae) in Holocene sandy soils. Acta Botanica Neerlandica 27, 389-396.

Faegri, K., Iversen, J., 1989. Textbook of Pollen Analysis, 4th ed. John Wiley & Sons, Chichester.

Fairbanks, R.G., Mortlock, R.A., Chiu, T.-C., Cao, L., Kaplan, A., Guilderson, T.P., Fairbanks, T.W., Bloom, A.L., Grootes, P.M., Nadeau, M.-J., 2005. Radiocarbon calibration curve spanning 0 to 50,000 years BP based on paired 230Th/234U/238U and 14C dates on pristine corals. Quaternary Science Reviews 24, 1781-1796.

Fairhall, A.W., Young, A.W., 1973. Methodology of radiocarbon dating and radiocarbon dates from Nelson Bay Cave. The South African Archaeological Bulletin 28, 90-93.

Faith, J.T., 2011. Ungulate community richness, grazer extinctions, and human subsistence behavior in southern Africa's Cape Floral Region. Palaeogeography, Palaeoclimatology, Palaeoecology 306, 219-227.

Farmer, E.C., deMenocal, P.B., Marchitto, T.M., 2005. Holocene and deglacial ocean temperature variability in the Benguela upwelling region: implications for low-latitude atmospheric circulation. Paleoceanography 20, doi:10.1029/2004PA001049.

Farquhar, G.D., Ehleringer, J.R., Hubick, K.T., 1989a. Carbon isotope discrimination and photosynthesis. Annual Review of Plant Physiology and Plant Molecular Biology 40, 503-537.

Farquhar, G.D., Hubick, K.T., Condon, A.G., Richards, R.A., 1989b. Carbon isotope fractionation and plant water-use efficiency. Ecological Studies 68, 21-40.

Farquhar, G.D., Richards, R.A., 1984. Isotopic composition of plant carbon correlates with water-use efficiency of wheat genotypes. Australian Journal of Plant Physiology 11, 539-552.

Feathers, J.K., 2002. Luminescence dating in less than ideal conditions: case studies from Klasies River main site and Duinefontein, South Africa. Journal of Archaeological Science 29, 177-194.

Feathers, J.K., Bush, D.A., 2000. Luminescence dating of Middle Stone Age deposits at Die Kelders. Journal of Human Evolution 38, 91-119.

Fey, M., 2010. Soils of South Africa. Cambridge University Press.

Ficken, K.J., Li, B., Swain, D.L., Eglinton, G., 2000. An n-alkane proxy for the sedimentary input of submerged/floating freshwater aquatic macrophytes. Organic Geochemistry 31, 745-749.

Figueiral, I., Mosbrugger, V., 2000. A review of charcoal analysis as a tool for assessing Quaternary and Tertiary environments: achievements and limits. Palaeogeography, Palaeoclimatology, Palaeoecology 164, 397-407.

Finch, J.M., Hill, T.R., 2008. A late Quaternary pollen sequence from Mfabeni Peatland, South Africa: reconstructing forest history in Maputaland. Quaternary Research 70, 442-450.

Fisher, E.C., Bar-Matthews, M., Jerardino, A., Marean, C.W., 2010. Middle and Late Pleistocene paleoscape modeling along the southern coast of South Africa. Quaternary Science Reviews 29, 1382-1398.

Fry, B., 2006. Stable isotope ecology. Springer Verlag, New York.

Gasse, F., Chalié, F., Vincens, A., Williams, M.A.J., Williamson, D., 2008. Climatic patterns in equatorial and southern Africa from 30,000 to 10,000 years ago reconstructed from terrestrial and near-shore proxy data. Quaternary Science Reviews 27, 2316-2340.

Geldenhuys, C.J., 1991. Distribution, size and ownership of forests in the southern Cape. South African Forestry Journal 158, 51–66.

Geldenhuys, C.J., 1993. Floristic composition of the southern Cape forests with an annotated check-list. South African Journal of Botany 59, 26-44.

Geldenhuys, C.J., 1997. Composition and biogeography of forest patches on the inland mountains of the southern Cape. Bothalia 27, 57-74.

Gersonde, R., Abelmann, A., Brathauer, U., Becquey, S., Bianchi, C., Cortese, G., Grobe, H., Kuhn, G., Niebler, H.-S., Segl, M., Sieger, R., Zielinski, U., Fütterer, D.K., 2003. Last glacial sea surface temperatures and sea-ice extent in the Southern Ocean (Atlantic-Indian sector): a multiproxy approach. Paleoceanography 18, 1061.

Gersonde, R., Crosta, X., Abelmann, A., Armand, L., 2005. Sea-surface temperature and sea ice distribution of the Southern Ocean at the EPILOG Last Glacial Maximum--a circum-Antarctic view based on siliceous microfossil records. Quaternary Science Reviews 24, 869-896.

Gersonde, R., Zielinski, U., 2000. The reconstruction of late Quaternary Antarctic sea-ice distribution: the use of diatoms as a proxy for sea-ice. Palaeogeography, Palaeoclimatology, Palaeoecology 162, 263-286.

Geyh, M.A., Eitel, B., 1998. Radiometric dating of young and old calcrete. Radiocarbon 40, 795-802.

Geyh, M.A., Schotterer, U., Grosjean, M., 1998. Temporal changes of the 14C reservoir effect in lakes. Radiocarbon 40, 921-931.

GIBB, A., 2010. Chapter 8: Physical and Biophysical Environment, Revised DEIR - Nuclear-1 Scoping Report. Prepared for Eskom Holdings.

Glew, J.R., Smol, J.P., Last, W.M., 2001. Sediment core collection and extrusion, in: Glew, J.R., Smol, J.P. (Eds.), Tracking Environmental Change Using Lake Sediments Volume 1: Basin Analysis, Coring, and Chronological Techniques. Kluwer Academic Publishers, Dordrecht, The Netherlands, pp. 73 - 106.

Goldblatt, P., Manning, J., 2000. Cape Plants. A conspectus of the Cape flora of South Africa. National Botanical Institute and Missouri Botanical Gardens, Pretoria and St. Louis.

Goldblatt, P., Manning, J.C., 2002. Plant diversity of the Cape Region of southern Africa. Annals of the Missouri Botanical Garden 89, 281-302.

Goos, M., 2009. Bantamsklip: Eskom's extremely bad idea, Village Life. Icon Communications CC, Stanford, Western Cape, pp. 10-15.

Grimm, E., 1987. Coniss: A fortran 77 program for stratigraphically constrained cluster analysis by the method of incremental sum of squares. Computers and Geosciences 13, 13-35.

Grine, F.E., Pearson, O.M., Klein, R.G., Rightmire, G.P., 1998. Additional human fossils from Klasies River Mouth, South Africa. Journal of Human Evolution 35, 95-107.

Grün, R., Shackleton, N.J., Deacon, H.J., 1990 Electron-spin-resonance dating of tooth enamel from Klasies River mouth cave. Current Anthropology 31, 427 - 432.

Grundling, P.L., Mazus, H., Baartman, L., 1998. Peat resources in northern KwaZulu-Natal wetlands: Maputaland, . Department of Environmental Affairs and Tourism, Pretoria, p. 102.

Hall, G., Woodborne, S., Scholes, M., 2008. Stable carbon isotope ratios from archaeological charcoal as palaeoenvironmental indicators. Chemical Geology 247, 384-400.

Hannah, L., Midgley, G.F., Lovejoy, T., Bond, W.J., Bush, M., Lovett, J.C., Scott, D., Woodward, F.I., 2002. Conservation of biodiversity in a changing climate. Conservation Biology 16, 264-268.

Hannah, L.E.E., Midgley, G.U.Y., Hughes, G., Bomhard, B., 2005. The View from the Cape: Extinction Risk, Protected Areas, and Climate Change. BioScience 55, 231-242.

Harrison, M.S.J., 1984. A generalised classification of South African summer rain-bearing synoptic systems. Journal of Climatology 4, 547-560.

Hart, N., Reason, C.J.C., Fauchereau, N., 2012. Cloud bands over southern Africa: Seasonality, contribution to rainfall variability, and modulation by the MJO. Climate Dyn.

Hays, J.D., Imbrie, J., Shackleton, N.J., 1976. Variations in the earth's orbit: pacemaker of the ice ages. Science 194, 1121-1131.

Heaton, T.H.E., Talma, A.S., Vogel, J.C., 1986. Dissolved gas paleotemperatures and 18O variations derived from groundwater near Uitenhage, South Africa. Quaternary Research 25, 79-88.

Heijnis, C.E., Lombard, A.T., Cowling, R.M., Desmet, P.G., 1999. Picking up the pieces: a biosphere reserve framework for a fragmented landscape – The Coastal Lowlands of the Western Cape, South Africa. Biodiversity & Conservation 8, 471-496.

Henshilwood, C.S., d'Errico, F., Watts, I., 2009. Engraved ochres from the Middle Stone Age levels at Blombos Cave, South Africa. Journal of Human Evolution 57, 27-47.

Hewitson, B.C., Crane, R.G., 2006. Consensus between GCM climate change projections with empirical downscaling: precipitation downscaling over South Africa. International Journal of Climatology 26, 1315-1337.

Heydenrych, B.J., Cowling, R.M., Lombard, A.T., 1999. Strategic conservation interventions in a region of high biodiversity and high vulnerability: A case study from the Agulhas Plain at the southern tip of Africa. ORYX 33, 256-269.

Higham, T., 1999. The 14C method. http://www.c14dating.com/int.html. Accessed on: 5 January 2012.

Hijmans, R., Cameron, S.E., Parra, J.L., Jones, P.G., Jarvis, A., 2005. Very high resolution interpolated climate surfaces for global land areas. International Journal of Climatology 25, 1965-1978.

Hjelle, K.L., Sugita, S., 2011. Estimating pollen productivity and relevant source area of pollen using lake sediments in Norway: How does lake size variation affect the estimates? The Holocene.

Holzkämper, S., Holmgren, K., Lee-Thorp, J., Talma, S., Mangini, A., Partridge, T., 2009. Late Pleistocene stalagmite growth in Wolkberg Cave, South Africa. Earth and Planetary Science Letters 282, 212-221.

Hua, Q., 2009. Radiocarbon: A chronological tool for the recent past. Quaternary Geochronology 4, 378-390.

Hughen, K., Southon, J., Lehman, S., Bertrand, C., Turnbull, J., 2006. Marine-derived 14C calibration and activity record for the past 50,000 years updated from the Cariaco Basin. Quaternary Science Reviews

Critical Quaternary Stratigraphy 25, 3216-3227.

Hughen, K.A., Baillie, M.G.L., Bard, E., Beck, J.W., Bertrand, C.J.H., Blackwell, P.G., Buck, C.E., Burr, G.S., Cutler, K.B., Damon, P.E., 2004. Marine04 marine radiocarbon age calibration, 0-26 cal kyr BP. Radiocarbon 46, 1059–1086.

Hunter, I.T., 1987. The Weather of the Agulhas Bank and the Cape South Coast. Unpublished M.Sc thesis, University of Cape Town, Cape Town.

Huntley, D.J., Godfrey-Smith, D.I., Thewalt, M.W.L., 1985. Optical dating of sediments. Nature 313, 105-107.

Huybers, P., Wunsch, C., 2005. Obliquity pacing of the late Pleistocene glacial terminations. Nature 434, 491-494.

Illenberger, W.K., 1996. The geomorphologic evolution of the Wilderness dune cordons, South Africa. Quaternary International 33, 11-20.

Imbrie, J., Berger, A., Boyle, E.A., Clemens, S.C., Duffy, A., Howard, W.R., Kukla, G., Kutzbach, J., Martinson, D.G., McIntyre, A., Mix, A.C., Molfino, B., Morley, J.J., Peterson, L.C., Pisias, N.G., Prell, W.L., Raymo, M.E., Shackleton, N.J., Toggweiler, J.R., 1993. On the structure and origin of major glaciation cycles 2. The 100,000-year cycle. Paleoceanography 8.

Imbrie, J., Boyle, E.A., Clemens, S.C., Duffy, A., Howard, W.R., Kukla, G., Kutzbach, J., Martinson, D.G., McIntyre, A., Mix, A.C., Molfino, B., Morley, J.J., Peterson, L.C., Pisias, N.G., Prell, W.L., Raymo, M.E., Shackleton, N.J., Toggweiler, J.R., 1992. On the structure and origin of major glaciation cycles 1. Linear responses to Milankovitch forcing. Paleoceanography 7.

Imbrie, J., Imbrie, J.Z., 1980. Modeling the climatic response to orbital variations. Science 207, 943-953.

Inskeep, R.R., 1972. Nelson's Bay Cave, Robberg Peninsula, Plettenberg Bay. Palaeoecology of Africa 6, 247-248.

IPCC, 2007. Fourth Assessment Report: Climate Change 2007: Synthesis Report. Intergovernmental Panel on Climate Change.

Irving, S.J.E., 1998. Late Quaternary palaeoenvironments at Vankervelsvlei, near Knysna, South Africa. University of Cape Town, Cape Town.

Irving, S.J.E., Meadows, M.E., 1997. Radiocarbon chronology and organic matter accumulation at Vankervelsvlei, near Knysna, South Africa. South African Geographical Journal 79, 101-105.

Jackson, S.T., 1990. Pollen source area and representation in small lakes of the northeastern United States. Review of Palaeobotany and Palynology 63, 53-76.

Jackson, S.T., Kearsley, J.B., 1998. Quantitative representation of local forest composition in forest-floor pollen assemblages. Journal of Ecology 86, 474-490.

Jacobs, Z., Roberts, R.G., Galbraith, R.F., Deacon, H.J., Grun, R., Mackay, A., Mitchell, P., Vogelsang, R., Wadley, L., 2008a. Ages for the Middle Stone Age of southern Africa: implications for human behavior and dispersal. Science 322, 733-735.

Jacobs, Z., Wintle, A.G., Duller, G.A.T., Roberts, R.G., Wadley, L., 2008b. New ages for the post-Howiesons Poort, late and final Middle Stone Age at Sibudu, South Africa. Journal of Archaeological Science 35, 1790-1807.

Jansen, E., Overpeck, J., Briffa, K.R., Duplessy, J.-C., Joos, F., Masson-Delmotte, V., Olago, D.O., Otto-Bliesner, B., Peltier, W.R., Rahmstorf, S., Ramesh, R., Raynaud, D., Rind, D., Solomina, O., Villalba, R., Zhang, D., 2007. Palaeoclimate, in: Solomon, S.D., Qin, M., Manning, M., Chen, Z., Marquis, M., Averyt, K.B., Tignor, M., Miller, H.L. (Eds.), Climate Change 2007: The Physical Science Basis. Contribution of Working Group I to the Fourth Assessment Report of the Intergovernmental Panel on Climate Change. Cambridge University Press, Cambridge, United Kingdom and New York, NY, USA.

Jansen, J.H.F., Ufkes, E., Schneider, R.R., 1996. Late Quaternary movements of the Angola-Benguela Front, SE Atlantic, and implications for advection in the equatorial ocean, in: Wefer, G., Berger, W.H., Siedler, G., Webb, D.J. (Eds.), The South Atlantic: Present and past circulation. Springer Verlag, Berlin, pp. 553-575.

Jansonius, J., McGregor, D.C., 1996. Chapter 1. Introduction, in: Jansonius, J., McGregor, D.C. (Eds.), Palynology: principles and applications. American Association of Stratigraphic Palynologists Foundation, Salt Lake City, Utah, pp. 1-10.

Jerardino, A., 1993. Mid- to late-Holocene sea-level fluctuations: the archaeological evidence at Tortoise Cave, south-western Cape, South Africa. South African Journal of Science 89, 481-488.

Jerardino, A., 1995. Late Holocene Neoglacial episodes in southern South America and southern Africa: a comparison. Holocene 5, 361-368.

Jerardino, A., Marean, C.W., 2010. Shellfish gathering, marine paleoecology and modern human behavior: perspectives from cave PP13B, Pinnacle Point, South Africa. Journal of Human Evolution 59, 412-424.

Jones, M.G.W., van Nieuwenhuizen, G.D.P., Day, J.A., 2002. Selecting priority wetlands for conservation measures. The Agulhas Plain as a case study, Report to CAPE (Cape Action Plan for the environment).

Joubert, L., Esler, K.J., Privett, S.D.J., 2009. The effect of ploughing and augmenting natural vegetation with commercial fynbos species on the biodiversity of Overberg Sandstone fynbos on the Agulhas Plain, South Africa. South African Journal of Botany 75, 526-531.

Jouzel, J., Masson-Delmotte, V., Cattani, O., Dreyfus, G., Falourd, S., Hoffmann, G., Minster, B., Nouet, J., Barnola, J.M., Chappellaz, J., Fischer, H., Gallet, J.C., Johnsen, S., Leuenberger, M., Loulergue, L., Luethi, D., Oerter, H., Parrenin, F., Raisbeck, G., Raynaud, D., Schilt, A., Schwander, J., Selmo, E., Souchez, R., Spahni, R., Stauffer, B., Steffensen, J.P., Stenni, B., Stocker, T.F., Tison, J.L., Werner, M., Wolff, E.W., 2007. Orbital and millennial Antarctic climate variability over the past 800,000 years. Science 317, 793-797.

Jull, A.J.T., Burr, G.S., 2006. Accelerator mass spectrometry: Is the future bigger or smaller? Earth and Planetary Science Letters 243, 305-325.

Jury, M.R., 1995. A review of research on ocean-atmosphere interactions and South African climate variability., South African Journal of Science. South African Assn. for the Advancement of Science, p. 289.

Jury, M.R., Valentine, H.R., Lutjeharms, J.R.E., 1993. Influence of the Agulhas Current on summer rainfall along the southeast coast of South Africa. Journal of applied meteorology 32, 1282-1287.

Kaplan, J.O., Prentice, I.C., Buchmann, N., 2002. The stable carbon isotope composition of the terrestrial biosphere: modeling at scales from the leaf to the globe. Global Biogeochemical Cycles 16, 1060.

Karkanas, P., Goldberg, P., 2010. Site formation processes at Pinnacle Point Cave 13B (Mossel Bay, Western Cape Province, South Africa): resolving stratigraphic and depositional complexities with micromorphology. Journal of Human Evolution 59, 256-273.

Kawamura, K., Parrenin, F., Lisiecki, L., Uemura, R., Vimeux, F., Raymo, M.E., Matsumoto, K., Nakata, H., Motoyama, H., Fujita, S., Goto-Azuma, K., Fujii, Y., Watanabe, O., 2007. Northern Hemisphere forcing of climatic cycles in Antarctica over the past 360,000 years. Nature 448, 912-916.

Kemper, J., Cowling, R.M., Richardson, D.M., 1999. Fragmentation of South African renosterveld shrublands: Effects on plant community structure and conservation implications. Biological Conservation 90, 103-111.

Kristen, I., Wilkes, H., Vieth, A., Zink, K.G., Plessen, B., Thorpe, J., Partridge, T.C., Oberhänsli, H., 2010. Biomarker and stable carbon isotope analyses of sedimentary organic matter from Lake Tswaing: evidence for deglacial wetness and early Holocene drought from South Africa. Journal of Paleolimnology 44, 143-160.

Kim, J.-H., Schneider, R.R., Müller, P.J., Wefer, G., 2002. Interhemispheric comparison of deglacial sea-surface temperature patterns in Atlantic eastern boundary currents. Earth and Planetary Science Letters 194, 383-393.

King, L.C., 1950. The study of the world's plainlands: a new approach in geomorphology. Quarterly Journal of the Geological Society 106, 101-131.

King, L.C., 1955. Pediplanation and Isostasy: An Example from South Africa. Quarterly Journal of the Geological Society 111, 353-358, NP, 359.

Kitagawa, H., van der Plicht, J., 1998. Atmospheric radiocarbon calibration to 45,000 yr B.P.: late glacial fluctuations and cosmogenic isotope production. Science 279, 1187-1190.

Klein, R.G., 1972a. The late Quaternary mammalian fauna of Nelson Bay Cave (Cape Province, South Africa): its implications for megafaunal extinctions and environmental and cultural change. Quaternary Research 2, 135-142.

Klein, R.G., 1972b. Preliminary report on the July through September 1970 excavations at Nelson's Bay Cave, Plettenberg Bay (Cape Province, South Africa). Palaeoecology of Africa 6, 177-208.

Klein, R.G., 1976. The mammalian fauna of the Klasies River Mouth sites, southern Cape Province, South Africa. South African Archaeological Bulletin 31, 74-98.

Klein, R.G., 1978. A preliminary report on the larger mammals from the Boomplaas stone age cave site, Cango Valley, Oudtshoorn District, South Africa. The South African Archaeological Bulletin 33, 66-75.

Klein, R.G., 1980. Environmental and ecological implications of large mammals from Upper Pleistocene and Holocene sites in southern Africa. Annals of the South African Museum, 223-283.

Klein, R.G., 1983. Palaeoenvironmental implications of Quaternary large mammals in the Fynbos region, in: Deacon, H.J., Hendey, Q.B. and Lambrechts, J.J.N. (Ed.), Fynbos Palaeoecology: a preliminary synthesis, 75 ed, pp. 116-138.

Klein, R.G., 1984. The large animals of southern Africa: late Pliocene to recent, in: Klein, R.G. (Ed.), Southern African Prehistory and Palaeoenvironments. Balkema, Rotterdam, pp. 107-146.

Klein, R.G., 1991. Size variation in the Cape dune molerat (Bathyergues suillus) and late Quaternary climatic change in the southwestern Cape Province, South Africa. Quaternary Research 36, 243-256.

Klein, R.G., Cruz-Uribe, K., 1987. Large mammal and tortoise bones from Elands Bay Cave and nearby sites, western Cape Province, South Africa, in: Parkington, J., and Hall, M. (Ed.), Papers in the Prehistory of the Western Cape, Oxford, pp. 132-163.

Klein, R.G., Cruz-Uribe, K., 2000. Middle and Later Stone Age large mammal and tortoise remains from Die Kelders Cave 1, Western Cape Province, South Africa. Journal of Human Evolution 38, 169-195.

Klein, R.G., Cruz-Uribe, K., Halkett, D., Hart, T., Parkington, J.E., 1999. Paleoenvironmental and human behavioral implications of the Boegoeberg 1 Late Pleistocene hyena den, Northern Cape Province, South Africa. Quaternary Research 52, 393-403.

Konert, M., Vandenberghe, J., 1997. Comparison of laser grain size analysis with pipette and sieve analysis: a solution for the underestimation of the clay fraction. Sedimentology 44, 523-535.

Kouli, K., Gogou, A., Bouloubassi, I., Triantaphyllou, M.V., Ioakim, C., Katsouras, G., Roussakis, G., Lykousis, V., 2012. Late postglacial paleoenvironmental change in the northeastern Mediterranean region: Combined palynological and molecular biomarker evidence. Quaternary International 261, 118-127.

Kraaij, T., Baard, J.A., Cowling, R.M., van Wilgen, B.W., Das, S., 2012. Historical fire regimes in a poorly understood, fire-prone ecosystem: eastern coastal fynbos. International Journal of Wildland Fire.

Kristen, I., Fuhrmann, A., Thorpe, J., Röhl, U., Wilkes, H., Oberhänsli, H., 2007. Hydrological changes in southern Africa over the last 200 Ka as recorded in lake sediments from the Tswaing impact crater. South African Journal of Geology 110, 311-326.

Kuhl, N., Gebhardt, C., Litt, T., Hense, A., 2002. Probability density functions as botanical-climatological transfer functions for climate reconstruction. Quaternary Research 58, 381-392.

Kühl, N., Litt, T., Schölzel, C., Hense, A., 2007. Eemian and Early Weichselian temperature and precipitation variability in northern Germany. Quaternary Science Reviews 26, 3311-3317.

Kutzbach, J., Liu, X., Liu, Z., Chen, G., 2008. Simulation of the evolutionary response of global summer monsoons to orbital forcing over the past 280,000 years. Clim Dyn 30, 567-579.

Kutzbach, J.E., 1981. Monsoon climate of the early Holocene: climate experiment with the Earth's orbital parameters for 9000 years ago. Science 214, 59-61.

Lachniet, M.S., 2009. Climatic and environmental controls on speleothem oxygen-isotope values. Quaternary Science Reviews 28, 412-432.

Lal, D., Charles, C., 2007. Deconvolution of the atmospheric radiocarbon record in the last 50,000 years. Earth and Planetary Science Letters 258, 550-560.

Lamb, A.L., Wilson, G.P., Leng, M.J., 2006. A review of coastal palaeoclimate and relative sea-level reconstructions using d13C and C/N ratios in organic material. Earth-Science Reviews 75, 29-57.

Lancaster, N., 1979. Quaternary environments in the arid zone of southern Africa. Environmental Studies, Occasional Paper 22, 77.

Lancaster, N., 2002. How dry was dry?: Late Pleistocene palaeoclimates in the Namib Desert. Quaternary Science Reviews 21, 769-782.

Lanesky, D.E., Logan, B.W., Brown, R.G., Hine, A.C., 1979. A new approach to portable vibracoring underwater and on land. Journal of Sedimentary Petrology 49, 654–657.

Laskar, A.H., Sharma, N., Ramesh, R., Jani, R.A., Yadava, M.G., 2010. Paleoclimate and paleovegetation of Lower Narmada Basin, Gujarat, Western India, inferred from stable carbon and oxygen isotopes. Quaternary International 227, 183-189.

Laskar, J., Fienga, A., Gastineau, M., Manche, H., 2011. La2010: a new orbital solution for the long-term motion of the Earth. Astronomy and Astrophysics 532, A89.

Laskar, J., Robutel, P., Joutel, F., Gastineau, M., Correia, A.C.M., Levrard, B., 2004. A long-term numerical solution for the insolation quantities of the Earth. Astronomy and Astrophysics 428, 261-285.

Last, W.M., 2001. Textural analysis of lake sediments, in: Last, W.M., Smol, J.P., Birks, H.J.B. (Eds.), Tracking environmental change using lake sediments. Volume 2: Physical and geochemical methods. Kluwer Academic Publishers, Dordrecht.

Laubscher, C.P., Ndakidemi, P.A., 2009. A survey of farm-level practices on endangered Leucadendron species and the future influence of ecotourism development on the Agulhas plain. African Journal of Agricultural Research 4, 1455-1463.

Laubscher, C.P., Ndakidemi, P.A., Bayat, M.S., Slabbert, A., 2009. Conservation and propagation of endangered Proteaceae on the Agulhas plain for sustainable ecotourism development. Scientific Research and Essays 4, 374-380.

Lechmere-Oertel, R.G., Cowling, R.M., 2001. Abiotic Determinants of the Fynbos / Succulent Karoo Boundary, South Africa. Journal of Vegetation Science 12, 75-80.

Lee-Thorp, J.A., Beaumont, P.B., 1995. Vegetation and seasonality shifts during the late Quaternary deduced from 13C/12C ratios of grazers at Equus Cave, South Africa. Quaternary Research 43, 426-432.

Lee, S.Y., Poulsen, C.J., 2005. Tropical Pacific climate response to obliquity forcing in the Pleistocene. Paleoceanography 20, PA4010.

Leps, J., Smilauer, P., 2003. Multivariate Analysis of Ecological Data Using CANOCO. Cambridge University Press, Cambridge.

Lindesay, J.A., 1998. Present Climates of Southern Africa, in: Hobbs, J.E., Lindesay, J.A., Bridgman, H.A. (Eds.), Climates of the Southern Continents: Present, Past and Future. John Wiley & Sons, New York, pp. 5 - 62.

Lisiecki, L.E., 2010. Links between eccentricity forcing and the 100,000-year glacial cycle. Nature Geosci 3, 349-352.

Lisiecki, L.E., Raymo, M.E., 2007. Plio-Pleistocene climate evolution: trends and transitions in glacial cycle dynamics. Quaternary Science Reviews 26, 56-69.

Little, M.G., Schneider, R.R., Kroon, D., Price, B., Bickert, T., Wefer, G., 1997a. Rapid palaeoceanographic changes in the Benguela Upwelling System for the last 160,000 years as indicated by abundances of planktonic foraminifera. Palaeogeography, Palaeoclimatology, Palaeoecology 130, 135-161.

Little, M.G., Schneider, R.R., Kroon, D., Price, B., Summerhayes, C.P., Segl, M., 1997b. Trade wind forcing of upwelling, seasonality, and Heinrich events as a response to sub-Milankovitch climate variability. Paleoceanography 12, 568-576.

Liu, W., Yang, H., Cao, Y., Ning, Y., Li, L., Zhou, J., An, Z., 2005. Did an extensive forest ever develop on the Chinese Loess Plateau during the past 130 ka?: A test using soil carbon isotopic signatures. Applied Geochemistry 20, 519-527.

Lombard, A.T., Cowling, R.M., Pressey, R.L., Mustart, P.J., 1997. Reserve Selection in a Species-Rich and Fragmented Landscape on the Agulhas Plain, South Africa. Conservation Biology 11, 1101-1116.

Lorius, C., Jouzel, J., Ritz, C., Merlivat, L., Barkov, N.I., Korotkevich, Y.S., Kotlyakov, V.M., 1985. A 150,000-year climatic record from Antarctic ice. Nature 316, 591-596.

Lovejoy, T.E., Hannah, L., 2005. Climate change and biodiversity. Yale University Press.

Low, A.B., 2011. Specialist Study Report: Botany and Dune Ecology., Specialist Study for Environmental Impact Report for the proposed Nuclear power station ('Nuclear 1'). Arcus GIBB Pty Ltd prepared on behalf of Eskom Holdings Ltd

Low, A.B., Rebelo, A.G., 1996. Fynbos Biome. Department of Environmental Affairs and Tourism, Pretoria.

Lowe, J.J., Walker, M.J.C., 1997. Reconstructing Quaternary Environments, 2nd ed. Longman.

Lubke, R.A., Avis, A.M., Steinke, T.D., Boucher, C., 1997. Coastal vegetation, in: Cowling, R.M., Richardson, D.M., Pierce, S.M. (Eds.), Vegetation of Southern Africa. Cambridge University Press, Cambridge, pp. 300-321.

Lutjeharms, J., 1996. The exchange of water between the South Indian and the South Atlantic, in: Wefer, G., Berger, W.H., Siedler, G., Webb, D. (Eds.), The South Atlantic: Present and Past Circulation. Springer-Verlag, Berlin pp. 125 -162.

Lutjeharms, J.R.E., Meyer, A.A., Ansorge, I.J., Eagle, G.A., Orren, M.J., 1996. The nutrient characteristics of the Agulhas Bank. South African Journal of Marine Science 17, 253-274.

Lutjeharms, J.R.E., Monteiro, P.M.S., Tyson, P.D., Obura, D., 2001. The oceans around southern Africa and regional effects of global change. South African Journal of Science 97, 119-130.

MacDonald, G.M., Bennett, K.D., Jackson, S.T., Parducci, L., Smith, F.A., Smol, J.P., Willis, K.J., 2008. Impacts of climate change on species, populations and communities: palaeobiogeographical insights and frontiers. Progress in Physical Geography 32, 139 - 172.

Mackie, E.A.V., Leng, M.J., Lloyd, J.M., Arrowsmith, C., 2005. Bulk organic δ13C and C/N ratios as palaeosalinity indicators within a Scottish isolation basin. Journal of Quaternary Science 20, 303-312.

Malan, J., Viljoen, J., 1990. Mesozoic and Cenozoic geology of the Cape South coast, Guidebook Geocongress '90. Geological Society of South Africa, pp. 1 - 81.

Malan, J.A., 1989. Bredasdorp Group, in: Johnson, M.R. (Ed.), Catalogue of South African Lithostratigraphic units., 1st ed. SA Committee for Stratigraphy.

Malan, J.A., 1990. The stratigraphy and sedimentology of the Bredasdorp Group, Southern Cape Province. Unpublished M.Sc. thesis, University of Cape Town,

Manders, P., 1990. Fire and other variables as determinants of forest/fynbos boundaries in the Cape Province. Journal of Vegetation Science 1, 483-490.

Manders, P.T., Richardson, D.M., 1992. Colonization of Cape fynbos communities by forest species. Forest Ecology and Management 48, 277-293.

Manders, P.T., Richardson, D.M., Masson, P.H., 1992. Is fynbos a stage to forest? Analysis of the perceived ecological distinction between two communities., in: van Wilgen, B.W., Richardson, D.M., Kruger, F.J., van Hensbergen, H.J. (Eds.), Fire in South African Mountain Fynbos. Springer-Verlag, Berlin, pp. 81-107.

Manning, M.R., Melhuish, W.H., 1994. Trends: A compendium of data on global change. Carbon Dioxide Information Analysis Centre, Oak Ridge National Laboratory, U.S. Department of Energy, Oak Ridge, TN (United States).

Manten, A.A., 1967. Lennart Von Post and the foundation of modern palynology. Review of Palaeobotany and Palynology 1, 11-22.

Marean, C.W., 2010. Pinnacle Point Cave 13B (Western Cape Province, South Africa) in context: The Cape Floral kingdom, shellfish, and modern human origins. Journal of Human Evolution 59, 425-443.

Marean, C.W., Bar-Matthews, M., Bernatchez, J., Fisher, E., Goldberg, P., Herries, A.I.R., Jacobs, Z., Jerardino, A., Karkanas, P., Minichillo, T., 2007a. Early human use of marine resources and pigment in South Africa during the Middle Pleistocene. Nature 449, 905-908.

Marean, C.W., Bar-Matthews, M., Bernatchez, J., Fisher, E., Goldberg, P., Herries, A.I.R., Jacobs, Z., Jerardino, A., Karkanas, P., Minichillo, T., Nilssen, P.J., Thompson, E., Watts, I., Williams, H.M., 2007b. Early human use of marine resources and pigment in South Africa during the Middle Pleistocene. Nature 449, 905-908.

Marker, M.E., 1987. Relative age of the coastal limestones as determined from the intensity of karst development. South African Journal of Science 83, 505 - 506.

Marker, M.E., Holmes, P.J., 2002. The distribution and environmental implications of coversand deposits in the Southern Cape, South Africa. South African Journal of Geology 105, 135.

Marker, M.E., Holmes, P.J., 2010. The geomorphology of the Coastal Platform in the southern Cape. South African Geographical Journal 92, 105-116.

Martin, A.R.H., 1968. Pollen analysis of Groenvlei lake sediments, Knysna (South Africa). Review of Palaeobotany and Palynology 7, 107-144.

Martínez-Méndez, G., Zahn, R., Hall, I.R., Pena, L.D., Cacho, I., 2008. 345,000-year-long multi-proxy records off South Africa document variable contributions of Northern versus Southern Component Water to the Deep South Atlantic. Earth and Planetary Science Letters 267, 309-321.

Martinson, D.G., Pisias, N.G., Hays, J.D., Imbrie, J., Moore, J., Theodore C., Shackleton, N.J., 1987. Age dating and the orbital theory of the ice ages: development of a high-resolution 0 to 300,000-year chronostratigraphy. Quaternary Research 27, 1-29.

Matthews, T., Rector, A., Jacobs, Z., Herries, A.I.R., Marean, C.W., 2011. Environmental implications of micromammals accumulated close to the MIS 6 to MIS 5 transition at Pinnacle Point Cave 9 (Mossel Bay, Western Cape Province, South Africa). Palaeogeography, Palaeoclimatology, Palaeoecology 302, 213-229.

Mayewski, P.A., Rohling, E.E., Curt Stager, J., Karlen, W., Maasch, K.A., David Meeker, L., Meyerson, E.A., Gasse, F., van Kreveld, S., Holmgren, K., 2004. Holocene climate variability. Quaternary Research 62, 243-255.

McCormac, F.G., Hogg, A.G., Blackwell, P.G., Buck, C.E., Higham, T.F.G., Reimer, P.J., 2004. SHCal04 Southern Hemisphere Calibration, 0-11.0 Cal Kyr BP. Radiocarbon 46, 1087-1092.

McCormac, F.G., Reimer, P.J., Hogg, A.G., Higham, T.F.G., Baillie, M.G.L., Palmer, J., Stuiver, M., 2002. Calibration of the radiocarbon time scale for the Southern Hemisphere: AD 1850–950. Radiocarbon 44, 641 – 651.

McDonald, G.M., 1996. Non-Aquatic Quaternary. Chapter 22., in: Jansonius, J., McGregor, D.C. (Eds.), Palynology: principles and applications. American Association of Stratigraphic Palynologists Foundation, Salt Lake City, Utah, pp. 879-910.

McIntyre, A., Ruddiman, W.F., Karlin, K., Mix, A.C., 1989. Surface water response of the equatorial Atlantic Ocean to orbital forcing. Paleoceanography 4, 19-55.

McPherson, G.R., Boutton, T.W., Midwood, A.J., 1993. Stable carbon isotope analysis of soil organic matter illustrates vegetation change at the grassland/woodland boundary in southeastern Arizona, USA. Oecologia 93, 95-101.

Meadows, M., Sugden, J.M., 1990. Late Quaternary vegetation history of the Cederberg, southwestern Cape Province. Palaeoecology of Africa 21, 269-282.

Meadows, M.E., 2001. The role of Quaternary environmental change in the evolution of landscapes: case studies from southern Africa. Catena 42, 39-57.

Meadows, M.E., 2012. Quaternary environments: Going forward, looking backwards? Progress in Physical Geography.

Meadows, M.E., Baxter, A.J., 1999. Late Quaternary palaeoenvironments of the southwestern Cape, South Africa: a regional synthesis. Quaternary International 57-8, 193-206.

Meadows, M.E., Baxter, A.J., 2001. Holocene vegetation history and palaeoenvironments at Klaarfontein Springs, Western Cape, South Africa. Holocene 11, 699-706.

Meadows, M.E., Baxter, A.J., Parkington, J., 1996. Late Holocene environments at Verlorenvlei, Western Cape Province, South Africa. Quaternary International 33, 81-95.

Meadows, M.E., Linder, H.P., 1993. A paleoecological perspective on the origin of afromontane grasslands. Journal of Biogeography 20, 345-355.

Meadows, M.E., Seliane, M., Chase, B.M., 2010. Holocene palaeoenvironments of the Cederberg and Swartruggens mountains, Western Cape, South Africa: pollen and stable isotope evidence from hyrax dung middens. Journal of Arid Environments 74, 786-793.

Meadows, M.E., Sugden, J.M., 1991. A vegetation history of the last 14,000 years on the Cederberg, southwestern Cape Province. South African Journal of Science 87, 34-43.

Medeanic, S., 2006. Freshwater algal palynomorph records from Holocene deposits in the coastal plain of Rio Grande do Sul, Brazil. Review of Palaeobotany and Palynology 141, 83-101.

Meyers, P.A., 1994. Preservation of elemental and isotopic source identification of sedimentary organic matter. Chemical Geology 114, 289-302.

Meyers, P.A., 1997. Organic geochemical proxies of paleoceanographic, paleolimnologic, and paleoclimatic processes. Organic Geochemistry 27, 213-250.

Meyers, P.A., 2003. Applications of organic geochemistry to paleolimnological reconstructions: a summary of examples from the Laurentian Great Lakes. Organic Geochemistry 34, 261-289.

Meyers, P.A., Lallier-vergés, E., 1999. Lacustrine Sedimentary Organic Matter Records of Late Quaternary Paleoclimates. Journal of Paleolimnology 21, 345-372.

Midgley, G., Chapman, R., Hewitson, B., Johnston, P., De Wit, M., Ziervogel, G., Mukheibir, P., Van Niekerk, L., Tadross, M., Van Wilgen, B., 2005. A status quo, vulnerability and adaptation assessment of the physical and socio-economic effects of climate change in the Western Cape. Report to the Western Cape Government, Cape Town, South Africa. CSIR Report No. ENV-SC 73.

Midgley, G., Thuiller, W., 2011. Potential responses of terrestrial biodiversity in Southern Africa to anthropogenic climate change. Regional Environmental Change 11, 127-135.

Midgley, G.F., Hannah, L., Millar, D., Rutherford, M.C., Powrie, L.W., 2002. Assessing the vulnerability of species richness to anthropogenic climate change in a biodiversity hotspot. Global Ecology and Biogeography 11, 445-451.

Midgley, G.F., Hannah, L., Millar, D., Thuiller, W., Booth, A., 2003. Developing regional and species-level assessments of climate change impacts on biodiversity in the Cape Floristic Region. Biological Conservation 112, 87-97.

Midgley, G.F., Hannah, L., Roberts, R., MacDonald, D.J., Allsopp, J.C., 2001. Have Pleistocene climatic cycles influenced species richness patterns in the greater Cape Mediterranean Region? Journal of Mediterranean Ecology 2, 137-144.

Midgley, J.J., Cowling, R.M., Seydack, A., van Wyk, G.F., 1997. Forest, in: Cowling, R.M., Richardson, D.M., Pierce, S.M. (Eds.), Vegetation of Southern Africa. Cambridge University Press, Cambridge, pp. 278 - 299.

Midgley, J.J., Kruger, L.M., Skelton, R., 2011. How do fires kill plants? The hydraulic death hypothesis and Cape Proteaceae “fire-resisters”. South African Journal of Botany 77, 381-386.

Miller, D.E., Yates, R.J., Jerardino, A., Parkington, J.E., 1995. Late Holocene coastal change in the southwestern Cape, South Africa. Quaternary International 30, 3-10.

Miller, D.E., Yates, R.J., Parkington, J.E., Vogel, J.C., 1993. Radiocarbon-dated evidence relating to a mid-Holocene relative high sea-level on the southwestern Cape coast, South Africa. South African Journal of Science 89, 35-44.

Miller, G.H., Beaumont, P.B., Deacon, H.J., Brooks, A.S., Hare, P.E., Jull, A.J.T., 1999. Earliest modern humans in southern Africa dated by isoleucine epimerization in ostrich eggshell. Quaternary Science Reviews 18, 1537-1548.

Miller, J., Williams, R., Farquhar, G., 2001. Carbon isotope discrimination by a sequence of Eucalyptus species along a subcontinental rainfall gradient in Australia. Functional Ecology 15, 222-232.

Mix, A.C., Bard, E., Schneider, R., 2001. Environmental processes of the ice age: land, oceans, glaciers (EPILOG). Quaternary Science Reviews 20, 627-657.

Mix, A.C., Morey, A.E., 1996. Climate feedback and Pleistocene variations in the Atlantic South Equatorial Current, in: Wefer, G., Berger, W.H., Siedler, G., Webb, D.J. (Eds.), The South Atlantic, Present and Past Circulation. Springer, Berlin, pp. 503-525.

Mooney, S.D., Tinner, W., 2011. The analysis of charcoal in peat and organic sediments. Mires and Peat 7, 1-18.

Moore, P.D., 1989. The ecology of peat-forming processes: a review. International Journal of Coal Geology 12, 89-103.

Moore, P.D., 2000. Wetlands, Revised Edition ed. Facts on File, New York.

Moore, P.D., 2002. The future of cool temperate bogs. Environmental Conservation 29, 3–20.

Moore, P.D., Webb, J.A., Collinson, M.E., 1991. Pollen Analysis, 2nd ed. Blackwell Scientific Publications, Oxford.

Morrison, K.D., 1994. Monitoring Regional Fire History Through Size-Specific Analysis of Microscopic Charcoal: The Last 600 Years in South India. Journal of Archaeological Science 21, 675-685.

Mucina, L., Geldenhuys, C.J., 2006. Afrotemperate, subtropical and azonal forests., in: Mucina, L., Rutherford, M.C. (Eds.), The vegetation of South Africa, Lesotho and Swaziland. South African National Biodiversity Institute, Pretoria, South Africa.

Mucina, L., Rutherford, M.C., 2006. The vegetation of South Africa, Lesotho and Swaziland, Strelitzia. South African National Biodiversity Institute, Pretoria.

Muscheler, R., Beer, J., Wagner, G., Laj, C., Kissel, C., Raisbeck, G.M., Yiou, F., Kubik, P.W., 2004. Changes in the carbon cycle during the last deglaciation as indicated by the comparison of 10Be and 14C records. Earth and Planetary Science Letters 219, 325-340.

Mustart, P.J., Cowling, R.M., Albertyn, J., 2003. Southern Overberg South African Wild Flower Guide 8. Botanical Society of South Africa, Cape Town.

Myers, N., Mittermeier, R.A., Mittermeier, C.G., da Fonseca, G.A.B., Kent, J., 2000. Biodiversity hotspots for conservation priorities. Nature 403, 853-858.

Nakagawa, T., 2007. PolyCounter ver.1.0 & Ergodex DX-1: a cheap and very ergonomic electronic counter board system. Quaternary International 167–168, Supplement, 3-486.

Nakagawa, T., Brugiapaglia, E., Digerfeldt, G., Reille, M., De Beaulieu, J.-L., Yasuda, Y., 1998. Dense media separation as a more efficient pollen extraction method for use with organic sediment/deposit samples: comparison with the conventional method. Boreas 27, 15-24.

Neumann, F.H., Scott, L., Bamford, M.K., 2011. Climate change and human disturbance of fynbos vegetation during the late Holocene at Princess Vlei, Western Cape, South Africa. The Holocene 21, 1137-1149.

Nicholson, S., 2009. A revised picture of the structure of the “monsoon” and land ITCZ over West Africa. Clim Dyn 32, 1155-1171.

Norström, E., Scott, L., Partridge, T.C., Risberg, J., Holmgren, K., 2009. Reconstruction of environmental and climate changes at Braamhoek wetland, eastern escarpment South Africa, during the last 16,000 years with emphasis on the Pleistocene-Holocene transition. Palaeogeography, Palaeoclimatology, Palaeoecology 271, 240-258.

O'Leary, M.H., 1981. Carbon isotope fractionation in plants. Phytochemistry 20, 553-567.

Park, R., Epstein, S., 1961. Metabolic fractionation of 13C and 12C in plants. Plant Physiology 36, 133–138.

Parkington, J., Cartwright, C., Cowling, R.M., Baxter, A., Meadows, M., 2000. Palaeovegetation at the Last Glacial Maximum in the Western Cape, South Africa: wood charcoal and pollen evidence from Elands Bay Cave. South African Journal of Science 96, 543-546.

Parsons, R., 2009. Is Groenvlei really fed by groundwater discharged from the Table Mountain Group (TMG) Aquifer? Water SA 35, 657 - 662.

Partridge, T.C., 1993. Warming phases in southern Africa during the last 150,000 years: an overview. Palaeogeography, Palaeoclimatology, Palaeoecology 101, 237-244.

Partridge, T.C., 1997. Cainozoic environmental change in southern Africa, with special emphasis on the last 200 000 years. Progress in Physical Geography 21, 3-22.

Partridge, T.C., Avery, D.M., Botha, G.A., Brink, J.S., Deacon, J., Herbert, R.S., Maud, R.R., Scholtz, A., Scott, L., Talma, A.S., Vogel, J.C., 1990. Late Pleistocene and Holocene climatic change in southern Africa. South African Journal of Science 86, 302-306.

Partridge, T.C., Maud, R.R., 1987. Geomorphic evolution of southern Africa since the Mesozoic. South African Journal of Geology 90, 179-208.

Partridge, T.C., Maud, R.R., 2000. Macro-Scale Geomorphic Evolution of Southern Africa, in: Partridge, T.C., Maud, R.R. (Eds.), The Cenozoic of South Africa. Oxford University Press, Oxford, pp. 3 - 18.

Partridge, T.C., Scott, L., Hamilton, J.E., 1999. Synthetic reconstructions of southern African environments during the Last Glacial Maximum (21-18 kyr) and the Holocene Altithermal (8-6 kyr). Quaternary International 57-8, 207-214.

Pate, J.S., 2001. Carbon isotope discrimination and plant water-use efficiency: case scenarios for C3 plants, in: Unkovich, M., Pate, J., McNeill, A., Gibbs, D.J. (Eds.), Stable Isotope Techniques in the Study of Biological Processes and Functioning of Ecosystems. Kluwer Academic Publishers, Dordrecht, pp. 19-37.

Patterson, W.A., Edwards, K.J., Maguire, D.J., 1987. Microscopic charcoal as a fossil indicator of fire. Quaternary Science Reviews 6, 3-23.

Pearson, G.W., Stuiver, M., 1986. High-precision calibration of the radiocarbon time scale, 500–2500 BC. Radiocarbon 28, 839–862.

Peeters, F.J.C., Acheson, R., Brummer, G.-J.A., de Ruijter, W.P.M., Schneider, R.R., Ganssen, G.M., Ufkes, E., Kroon, D., 2004. Vigorous exchange between the Indian and Atlantic oceans at the end of the past five glacial periods. Nature 430, 661-665.

Pence, G.Q.K., Botha, M.A., Turpie, J.K., 2003. Evaluating combinations of on-and off-reserve conservation strategies for the Agulhas Plain, South Africa: a financial perspective. Biological Conservation 112, 253-273.

Phillips, J.F.V., 1931. Forest succesion and ecology in the Knysna region. Memoirs of the Botanical Survey of South Africa 14, 1-327.

Phillips, S.J., Anderson, R.P., Schapire, R.E., 2006. Maximum entropy modeling of species geographic distributions. Ecological Modelling 190, 231-259.

Pillans, B., Naish, T., 2004. Defining the Quaternary. Quaternary Science Reviews 23, 2271-2282.

Prentice, I.C., 1985. Pollen representation, source area, and basin size: toward a unified theory of pollen analysis. Quaternary Research 23, 76-86.

Pressey, R.L., Cowling, R.M., Rouget, M., 2003. Formulating conservation targets for biodiversity pattern and process in the Cape Floristic Region, South Africa. Biological Conservation 112, 99-127.

Pyke, C.R., Andelman, S.J., Midgley, G., 2005. Identifying priority areas for bioclimatic representation under climate change: a case study for Proteaceae in the Cape Floristic Region, South Africa. Biological Conservation 125, 1-9.

Quick, L.J., 2009. Late Quaternary vegetation history and palaeoenvironmental in the Cederberg Mountains, South Africa: evidence from hyrax (Procavia capensis) middens. Unpublished MSc thesis, University of Cape Town,

Quick, L.J., Chase, B.M., Meadows, M.E., Scott, L., Reimer, P.J., 2011. A 19.5 kyr vegetation history from the central Cederberg Mountains, South Africa: Palynological evidence from rock hyrax middens. Palaeogeography, Palaeoclimatology, Palaeoecology 309, 253-270.

Rau, A.J., Rogers, J., Lutjeharms, J.R.E., Giraudeau, J., Lee-Thorp, J.A., Chen, M.-T., Waelbroeck, C., 2002. A 450 kyr record of hydrological conditions on the western Agulhas Bank Slope, south of Africa. Marine Geology 180, 183-201.

Raymo, M.E., Nisancioglu, K., 2003. The 41 kyr world: Milankovitch's other unsolved mystery. Paleoceanography 18, 1011.

Reason, C., 1998a. Warm and cold events in the southeast Atlantic/southwest Indian Ocean region and potential impacts on circulation and rainfall over southern Africa. Meteorology and Atmospheric Physics 69, 49-65.

Reason, C.J.C., 2001. Evidence for the Influence of the Agulhas Current on Regional Atmospheric Circulation Patterns. Journal of Climate 14, 2769-2778.

Reason, C.J.C., 2002. Sensitivity of the southern African circulation to dipole sea- surface temperature patterns in the south Indian Ocean. International Journal of Climatology 22, 377-393.

Reason, C.J.C., Landman, W., Tennant, W., 2006. Seasonal to decadal prediction of southern African climate and its links with variability of the Atlantic ocean. Bulletin of the American Meteorological Society 87, 941-955.

Reason, C.J.C., Mulenga, H., 1999. Relationships between South African rainfall and SST anomalies in the southwest Indian Ocean. International Journal of Climatology 19, 1651-1673.

Reason, C.J.C.L., J.R.E., 1998b. Variability of the South Indian Ocean and implications for souther African rainfall., South African Journal of Science. South African Assn. for the Advancement of Science, p. 115.

Rebelo, A.G., 1992. Red Data Book Species in the Cape Floristic Region: Threats, Priorities and Target Species. Transactions of the Royal Society of South Africa 48, 55-86.

Rebelo, A.G., Cowling, R.M., Campbell, B.M., Meadows, M.E., 1991. Plant communities of the Riversdale Plain. . South African Journal of Botany 57, 10–28.

Rector, A.L., Reed, K.E., 2010. Middle and late Pleistocene faunas of Pinnacle Point and their paleoecological implications. Journal of Human Evolution 59, 340-357.

Rector, A.L., Verrelli, B.C., 2010. Glacial cycling, large mammal community composition, and trophic adaptations in the Western Cape, South Africa. Journal of Human Evolution 58, 90-102.

Reimer, P.J., Baillie, M.G.L., Bard, E., Bayliss, A., Beck, J.W., Bertrand, C.J.H., Blackwell, P.G., Buck, C.E., Burr, G.S., Cutler, K.B., Damon, P.E., Edwards, R.L., Fairbanks, R.G., Friedrich, M., Guilderson, T.P., Hogg, A.G., Hughen, K.A., Kromer, B., McCormac, G., Manning, S., Ramsey, C.B., Reimer, R.W., Remmele, S., Southon, J.R., Stuiver, M., Talamo, S., Taylor, F.W., van der Plicht, J., Weyhenmeyer, C.E., 2004a. IntCal04 Terrestrial Radiocarbon Age Calibration, 0-26 Cal Kyr BP. Radiocarbon 46, 1029-1058.

Reimer, P.J., Baillie, M.G.L., Bard, E., Bayliss, A., Beck, J.W., Blackwell, P.G., Ramsey, C.B., Buck, C.E., Burr, G.S., Edwards, R.L., Friedrich, M., Grootes, P.M., Guilderson, T.P., Hajdas, I., Heaton, T.J., Hogg, A.G., Hughen, K.A., Kaiser, K.F., Kromer, B., McCormac, F.G., Manning, S.W., Reimer, R.W., Richards, D.A., Southon, J.R., Talamo, S., Turney, C.S.M., van der Plicht, J., Weyhenmeyer, C.E., 2009. IntCal09 and Marine09 radiocarbon age calibration curves, 0-50,000 years cal BP. Radiocarbon 51, 1111-1150.

Reimer, P.J., Brown, T.A., Reimer, R.W., 2004b. Discussion: reporting and calibration of post-bomb 14C data. Radiocarbon 46, 1299-1304.

Rial, J.A., 2004. Earth's orbital eccentricity and the rhythm of the Pleistocene ice ages: the concealed pacemaker. Global and Planetary Change 41, 81-93.

Richards, M.B., Stock, W.D., Cowling, R.M., 1997. Soil nutrient dynamics and community boundaries in the Fynbos vegetation of South Africa. Plant Ecology 130, 143-153.

Rigaud, J.-P., Texier, P.-J., Parkington, J., Poggenpoel, C., 2006. Le mobilier Stillbay et Howiesons Poort de l'abri Diepkloof. La chronologie du Middle Stone Age sud-africain et ses implications. Comptes Rendus Palevol 5, 839-849.

Rightmire, G.P., Deacon, H.J., 1991. Comparative studies of Late Pleistocene human remains from Klasies River Mouth, South Africa. Journal of Human Evolution 20, 131-156.

Rightmire, G.P., Deacon, H.J., Schwartz, J.H., Tattersall, I., 2006. Human foot bones from Klasies River main site, South Africa. Journal of Human Evolution 50, 96-103.

Roberts, D.L., Bateman, M.D., Murray-Wallace, C.V., Carr, A.S., Holmes, P.J., 2008. Last Interglacial fossil elephant trackways dated by OSL/AAR in coastal aeolianites, Still Bay, South Africa. Palaeogeography, Palaeoclimatology, Palaeoecology 257, 261-279.

Roberts, D.L., Bateman, M.D., Murray-Wallace, C.V., Carr, A.S., Holmes, P.J., 2009. West coast dune plumes: climate driven contrasts in dunefield morphogenesis along the western and southern South African coasts. Palaeogeography, Palaeoclimatology, Palaeoecology 271, 24-38.

Roberts, D.L., Botha, G.A., Maud, R.R., Pether, J., 2006. Coastal Cenozoic Deposits, in: Johnson, M.R., Anhaeusser, C.R., Thomas, R.J. (Eds.), The Geology of South Africa. Geological Society of South Africa and Council of Geoscience, Pretoria and Johannesburg, pp. 605 - 628.

Roets, W., Xu, Y., Raitt, L., El-Kahloun, M., Meire, P., Calitz, F., Batelaan, O., Anibas, C., Paridaens, K., Vandenbroucke, T., Verhoest, N., Brendonck, L., 2008. Determining discharges from the Table Mountain Group (TMG) aquifer to wetlands in the Southern Cape, South Africa. Hydrobiologia 607, 175-186.

Rommerskirchen, F., Eglinton, G., Dupont, L., Rullkötter, J., 2006. Glacial/interglacial changes in southern Africa: Compoundspecific δ13C land plant biomarker and pollen records from southeast Atlantic continental margin sediments. Geochemistry, Geophysics, Geosystems 7.

Rouget, M., 2003. Measuring conservation value at fine and broad scales: implications for a diverse and fragmented region, the Agulhas Plain. Biological Conservation 112, 217-232.

Rouget, M., Richardson, D.M., Cowling, R.M., Lloyd, J.W., Lombard, A.T., 2003. Current patterns of habitat transformation and future threats to biodiversity in terrestrial ecosystems of the Cape Floristic Region, South Africa. Biological Conservation 112, 63-85.

Rozendaal, A., Gresse, P.G., Scheepers, R., Le Roux, J.P., 1999. Neoproterozoic to Early Cambrian Crustal Evolution of the Pan-African Saldania Belt, South Africa. Precambrian Research 97, 303-323.

Rutherford, M., Midgley, G., Bond, W., Powrie, L., Roberts, R., Allsopp, J., 1999. Plant biodiversity: vulnerability and adaptation assessment. South African country study on climate change. National Botanical Institute, Cape Town, South Africa.

Rutherford, M.S., Westfall, R.H., 1986. Biomes of southern Africa: an objective categorization. Memoirs of the Botanical Survey of South Africa 54, 1-98.

Sadori, L., Giardini, M., 2007. Charcoal analysis, a method to study vegetation and climate of the Holocene: The case of Lago di Pergusa (Sicily, Italy). Geobios 40, 173–180.

SANBI, 2003. PRECIS (National Herbarium Pretoria (PRE) Computerized Information System) database.

Schalke, H.J.W.G., 1973. The Upper Quaternary of the Cape Flats area. Scripta Geologica 15, 1-57.

Schneider, R.R., Müller, P.J., Ruhland, G., Meinecke, G., Schmidt, H., Wefer, G., 1996. Late Quaternary surface temperatures and productivity in the east equatorial South Atlantic: response to changes in trade/monsoon wind forcing and surface water advection, in: Wefer, G., Berger, W.H., Siedler, G., D.J., W. (Eds.), The South Atlantic: Present and past circulation. Springer Verlag, Berlin, pp. 527 - 551.

Schnyder, H., Schwertl, M., Auerswald, K., Schaufele, R., 2006. Hair of grazing cattle provides an integrated measure of the effects of site conditions and interannual weather variability on d13C of temperate humid grassland. Global Change Biology 12, 1315-1329.

Scholtz, A., 1986. Palynological and Palaeobotanical Studies in the Southern Cape. University of Stellenbosch, Stellenbosch, South Africa.

Scholz, C.A., Johnson, T.C., Cohen, A.S., King, J.W., Peck, J.A., Overpeck, J.T., Talbot, M.R., Brown, E.T., Kalindekafe, L., Amoako, P.Y.O., Lyons, R.P., Shanahan, T.M., Castaneda, I.S., Heil, C.W., Forman, S.L., McHargue, L.R., Beuning, K.R., Gomez, J., Pierson, J., 2007. East African megadroughts between

135 and 75 thousand years ago and bearing on early-modern human origins. Proceedings of the National Academy of Sciences 104, 16416-16421.

Schoville, B.J., 2010. Frequency and distribution of edge damage on Middle Stone Age lithic points, Pinnacle Point 13B, South Africa. Journal of Human Evolution 59, 378-391.

Schulze, E.D., Williams, R., Farquhar, G., Schulze, W., Langridge, J., Miller, J., Walker, B., 1998. Carbon and nitrogen isotope discrimination and nitrogen nutrition of trees along a rainfall gradient in northern Australia. Functional Plant Biology 25, 413-425.

Schulze, R.E., 1997. Atlas of Agro-Hydrology & Agro-Climatology, WRC Report TT82/96. Water Resource Commission, Pretoria.

Schulze, R.E., Maharaj, M., Ghile, Y., 2007. Climatic Zonation, in: Schulze, R.E. (Ed.), South African Atlas of Climatology and Agrohydrology. Water Research Commission, WRC Report 1489/1/06, Pretoria.

Schumann, E., Perrins, L., Hunter, I., 1982. Upwelling along the south coast of the Cape Province, South Africa. South African Journal of Science 78, 238-242.

Schumann, E.H., Cohen, A.L., Jury, M.R., 1995. Coastal sea surface temperature variability along the south coast of South Africa and the relationship to regional and global climate. Journal of Marine Research 53, 231-248.

Schwarcz, H.P., Rink, W.J., 2000. ESR dating of the Die Kelders Cave 1 Site, South Africa. Journal of Human Evolution 38, 121-128.

Schwark, L., Zink, K., Lechterbeck, J., 2002. Reconstruction of postglacial to early Holocene vegetation history in terrestrial Central Europe via cuticular lipid biomarkers and pollen records from lake sediments. Geology 30, 463-466.

Schwartz, D., deForesta, H., Mariotti, A., Balesdent, J., Massimba, J.P., Girardin, C., 1996. Present dynamics of the Savanna-forest boundary in the Congolese Mayombe: a pedological, botanical and isotopic (13C and 14C) study. Oecologia 106, 516-524.

Schweitzer, F.R., Wilson, M.L., 1978. A Preliminary Report on Excavations at Byneskranskop, Bredasdorp District, Cape. The South African Archaeological Bulletin 33, 134-140.

Schweitzer, F.R., Wilson, M.L., 1982. Byneskranskop 1, a late Quaternary living site in the southern Cape Province, South Africa: A Late Quaternary Living Site in the Southern Cape Province, South Africa. South African Museum.

Scott, A.C., Damblon, F., 2010. Charcoal: Taphonomy and significance in geology, botany and archaeology. Palaeogeography, Palaeoclimatology, Palaeoecology 291, 1-10.

Scott, L., 1982. Late Quaternary fossil pollen grains from the Transvaal, South Africa. Review of Palaeobotany and Palynology 36, 241-278.

Scott, L., 1987. Late Quaternary forest history in Venda, Southern Africa. Review of Palaeobotany and Palynology 53, 1-10.

Scott, L., 1994. Palynology of Late Pleistocene hyrax middens, southwestern Cape Province, South Africa: a preliminary report. Historical Biology 9, 71-81.

Scott, L., 2002. Grassland development under glacial and interglacial conditions in southern Africa: review of pollen, phytolith and isotope evidence. Palaeogeography, Palaeoclimatology, Palaeoecology 177, 47-57.

Scott, L., Cooremans, B., 1992. Pollen in recent Procavia (hyrax), Petromus (dassie rat) and bird dung in South Africa. Journal of Biogeography 19, 205-215.

Scott, L., Cooremans, B., de Wet, J.S., Vogel, J.C., 1991. Holocene environmental changes in Namibia inferred from pollen analysis of swamp and lake deposits. Holocene 1, 8-13.

Scott, L., Marais, E., Brook, G.A., 2004. Fossil hyrax dung and evidence of Late Pleistocene and Holocene vegetation types in the Namib Desert. Journal of Quaternary Science 19, 829-832.

Scott, L., Neumann, F.H., Brook, G.A., Bousman, C.B., Norström, E., Metwally, A.A., 2012. Terrestrial fossil-pollen evidence of climate change during the last 26 thousand years in Southern Africa. Quaternary Science Reviews 32, 100-118.

Scott, L., Nyakale, M., 2002. Pollen indications of Holocene palaeoenvironments at Florisbad spring in the central Free State, South Africa. Holocene 12, 497-503.

Scott, L., Woodborne, S., 2007a. Pollen analysis and dating of late Quaternary faecal deposits (hyraceum) in the Cederberg, Western Cape, South Africa. Review of Palaeobotany and Palynology 144, 123-134.

Scott, L., Woodborne, S., 2007b. Vegetation history inferred from pollen in late Quaternary faecal deposits (hyraceum) in the Cape winter-rain region and its bearing on past climates in South Africa. Quaternary Science Reviews 26, 941-953.

Seppa, H., Bennett, K.D., 2003. Quaternary pollen analysis: recent progress in palaeoecology and palaeoclimatology. Progress in Physical Geography 27, 548-579.

Shi, N., Dupont, L.M., Beug, H.-J., Schneider, R., 2000. Correlation between vegetation in southwestern Africa and oceanic upwelling in the past 21,000 years. Quaternary Research 54, 72-80.

Shi, N., Schneider, R., Beug, H.-J., Dupont, L.M., 2001. Southeast trade wind variations during the last 135 kyr: evidence from pollen spectra in eastern South Atlantic sediments. Earth and Planetary Science Letters 187, 311-321.

Siesser, W.G., 1970. Carbonate components and mineralogy of the South African coastal limestones and linstones of the Agulhas Bank. Transactions of the Geological Society of South Africa 73, 49 - 63.

Sievers, C., 2006. Seeds from the Middle Stone Age layers at Sibudu Cave. Southern African Humanities 18, 203-222.

Singer, R., Wymer, J., 1982. The Middle Stone Age of Klasies River Mouth in South Africa. University of Chicago Press, Chicago.

Singleton, A., Reason, C., 2007. A numerical model study of an intense cutoff low pressure system over South Africa. Monthly weather review 135, 1128-1150.

Smith, B.N., 1972. Natural abundance of the stable isotopes of carbon in biological systems. BioScience 22, 226-231.

Smith, B.N., Epstein, S., 1971. Two categories of 13C/12C ratios for higher plants. Plant Physiology 47, 380-384.

Stager, J.C., Mayewski, P.A., White, J., Chase, B.M., Neumann, F.H., Meadows, M.E., King, C.D., Dixon, D.A., 2012. Precipitation variability in the winter rainfall zone of South Africa during the last 1400 yr linked to the austral westerlies. Clim. Past 8, 877-887.

Stenni, B., Jouzel, J., Masson-Delmotte, V., Rothlisberger, R., Castellano, E., Cattani, O., Falourd, S., Johnsen, S.J., Longinelli, A., Sachs, J.P., 2004. A late-glacial high-resolution site and source temperature record derived from the EPICA Dome C isotope records (East Antarctica). Earth and Planetary Science Letters 217, 183-195.

Sternberg, L., DeNiro, M.J., 1983. Isotopic composition of cellulose from C3, C4, and CAM plants growing near one another. Science 220, 947-949.

Stewart, G.R., Turnbull, M., Schmidt, S., Erskine, P., 1995. 13C natural abundance in plant communities along a rainfall gradient: a biological integrator of water availability. Functional Plant Biology 22, 51-55.

Stock, W., Chuba, D., Verboom, G., 2004. Distribution of South African C3 and C4 species of Cyperaceae in relation to climate and phylogeny. Austral Ecology 29, 313-319.

Stockmarr, J., 1973. Determination of spore concentration with an electronic particle counter. Danmarks geologiske undersøgelse Arbog, 87–89.

Stokes, S., 1999. Luminescence dating applications in geomorphological research. Geomorphology 29, 153-171.

Stuiver, M., 1998. INTCAL98 radiocarbon age calibration, 24,000-0 cal BP. Radiocarbon 40, 1041-1083.

Stuiver, M., Becker, B., 1993. High-precision decadal calibration of the radiocarbon time scale, AD 1950–6000 BC. Radiocarbon 35, 35-65.

Stuiver, M., Polach, H.A., 1977. Discussion: reporting of 14C data. Radiocarbon 19, 355-363.

Stuiver, M., Reimer, P.J., 1986-2010. CALIB Radiocarbon Calibration Program, 6.0.1 ed.

Stuiver, M., Reimer, P.J., 1993. Extended 14C data base and revised CALIB 3.0 14C age calibration program. Radiocarbon 35, 215-230.

Stute, M., Talma, A.S., 1998. Glacial temperatures and moisture transport regimes reconstructed from noble gas and d18O, Stampriet aquifer, Namibia, Isotope Techniques in the Study of Past and Current Environmental Changes in the Hydrosphere and the Atmosphere. IAEA Vienna Symposium 1997, Vienna, pp. 307-328.

Stuut, J.-B.W., Crosta, X., Van der Borg, K., Schneider, R.R., 2004. On the relationship between Antarctic sea ice and southwestern African climate during the late Quaternary. Geology 32, 909-912.

Stuut, J.-B.W., Lamy, F., 2004. Climate variability at the southern boundaries of the Namib (southwestern Africa) and Atacama (northern Chile) coastal deserts during the last 120,000 yr. Quaternary Research 62, 301-309.

Stuut, J.-B.W., Prins, M.A., Schneider, R.R., Weltje, G.J., Jansen, J.H.F., Postma, G., 2002. A 300 kyr record of aridity and wind strength in southwestern Africa: inferences from grain-size distributions of sediments on Walvis Ridge, SE Atlantic. Marine Geology 180, 221-233.

Sugden, J.M., 1989. Late Quaternary palaeoecology of the central and marginal uplands of the Karoo, South Africa. Unpublished PhD Thesis, University of Cape Town, Cape Town.

Sugita, S., 1993. A model of pollen source area for an entire lake surface. Quaternary Research 39, 239-244.

Sugita, S., 1994. Pollen representation of vegetation in Quaternary sediments: theory and method in patchy vegetation. Journal of Ecology, 881-897.

Sugita, S., 2007a. Theory of quantitative reconstruction of vegetation I: pollen from large sites REVEALS regional vegetation composition. The Holocene 17, 229-241.

Sugita, S., 2007b. Theory of quantitative reconstruction of vegetation II: all you need is LOVE. The Holocene 17, 243-257.

Sugita, S., Gaillard, M.-J., Broström, A., 1999. Landscape openness and pollen records: a simulation approach. Holocene 9, 409-421.

Summerfield, M.A., 1996. Tectonics, geology and long-term landscape development, in: Adams, W.M., Goudie, A.S., Orme, A.R. (Eds.), The physical geography of Africa. Oxford Univeristy Press, Oxford, pp. 1 - 17.

Swap, R.J., Aranibar, J.N., Dowty, P.R., Gilhooly, W.P., Macko, S.A., 2004. Natural abundance of 13C and 15N in C3 and C4 vegetation of southern Africa: patterns and implications. Global Change Biology 10, 350-358.

Swartz, E., 2010. Final Scoping Report for the proposed extension of Stillbaai Waste Water Treatment Works., DWEA Reference Number 12/9/11/L400/9. prepared by KV3 Engineers for the Hessequa Municipality., Cape Town.

Taljaard, J., 1996. Atmospheric Circulation Systems, Synoptic Climatology and Weather Phenomena of South Africa. South African Weather Service Technical Paper 32. South African Weather Service, Pretoria, South Africa.

Talma, A.S., Vogel, J.C., 1992. Late Quaternary paleotemperatures derived from a speleothem from Cango Caves, Cape Province, South Africa. Quaternary Research 37, 203-213.

Team, R.D.C., 2011. A Language and Environment for Statistical Computing. R Foundation for Statistical Computing, Vienna, Austria. http://www.R-project.org. Accessed on: 10.05.2011.

Telfer, M.W., Thomas, D.S.G., 2006. Complex Holocene lunette dune development, South Africa: implications for paleoclimate and models of pan development in arid regions. Geology 34, 853-856.

Telford, R., Heegaard, E., Birks, H., 2004a. All age–depth models are wrong: but how badly? Quaternary Science Reviews 23, 1-5.

Telford, R.J., Heegaard, E., Birks, H.J.B., 2004b. The intercept is a poor estimate of a calibrated radiocarbon age. The Holocene 14, 296-298.

Teller, J.T., Last, W.M., 1990a. Paleohydrological indicators in playas and salt lakes, with examples from Canada, Australia, and Africa. Palaeogeography, Palaeoclimatology, Palaeoecology 76, 215-240.

Teller, J.T., Last, W.M., 1990b. Paleohydrological indicators in playas and salt lakes, with examples from Canada, Australia, and Africa. Palaeogeography, Palaeoclimatology, Palaeoecology 76, 215-240.

ter Braak, C.J.F., Smilauer, P., 1997. Canoco for Windows, 4.51 ed. Biometris - Plant Research International, Wageningen, The Netherlands.

Texier, P.-J., Porraz, G., Parkington, J., Rigaud, J.-P., Poggenpoel, C., Miller, C., Tribolo, C., Cartwright, C., Coudenneau, A., Klein, R., Steele, T., Verna, C., 2010. A Howiesons Poort tradition of engraving ostrich eggshell containers dated to 60,000 years ago at Diepkloof Rock Shelter, South Africa. Proceedings of the National Academy of Sciences.

Thackeray, J., 1988. Molluscan fauna from Klasies River, South Africa. The South African Archaeological Bulletin, 27-32.

Thackeray, J.F., 1992. Chronology of Late Pleistocene deposits associated with Homo sapiens at Klasies River Mouth, South Africa. Palaeoecology of Africa 23, 177-191.

Thackeray, J.F., 2007. Sea levels and chronology of Late Pleistocene coastal cave deposits at Klasies River in South Africa. Annals of the Transvaal Museum 44, 219-220.

Thamm, A.G., Grundling, P., Mazus, H., 1996. Holocene and recent peat growth rates on the Zululand coastal plain. Journal of African Earth Sciences 23, 119-124.

Thamm, A.G., Johnson, M.R., 2006. The Cape Supergroup, in: Johnson, M.R., Anhaeusser, C.R., Thomas, R.J. (Eds.), The Geology of South Africa. Geological Society of South Africa and Council of Geoscience, Pretoria and Johannesburg, pp. 443 - 460.

Thomas, D.S.G., Burrough, S.L., 2012. Interpreting geoproxies of late Quaternary climate change in African drylands: Implications for understanding environmental change and early human behaviour. Quaternary International 253, 5-17.

Thompson, E., Williams, H.M., Minichillo, T., 2010. Middle and late Pleistocene Middle Stone Age lithic technology from Pinnacle Point 13B (Mossel Bay, Western Cape Province, South Africa). Journal of Human Evolution 59, 358-377.

Thwaites, R.N., Cowling, R.M., 1988a. Soil-vegetation relationships on the Agulhas Plain, South Africa. Catena 15, 333-345.

Thwaites, R.N., Cowling, R.M., 1988b. Soil-vegetation relationships on the Agulhas Plain, South Africa. CATENA 15, 333-345.

Thwaites, R.N., Jacobs, E.O., 1985. The Cenozoic history of the southern Cape coastal landscape. Palaeoecology of Africa 17.

Tinley, K.L., 1985. Coastal dunes of South Africa, South African National Scientific Programmes Report No. 109. Foundation for Research Development Council for Scientific and Industrial Research, Pretoria, p. 300.

Tinner, W., Hu, F.S., 2003. Size parameters, size-class distribution and area number relationship of microscopic charcoal: relevance for fire reconstruction. The Holocene 13, 499–505.

Tinner, W., Hubschmid, P., Wehrli, M., Ammann, B., Conedera, M., 1999. Long-term forest fire ecology and dynamics in southern Switzerland. Journal of Ecology 87, 273-289.

Todd, M., Washington, R., 1998. Extreme daily rainfall in southern African and Southwest Indian Ocean tropical-temperate links. South African Journal of Science 94, 64-70.

Traverse, A., 2008. Paleopalynology, Second ed. Springer, The Netherlands.

Treble, P.C., Chappell, J., Gagan, M.K., McKeegan, K.D., Harrison, T.M., 2005. In situ measurement of seasonal δ18O variations and analysis of isotopic trends in a modern speleothem from southwest Australia. Earth and Planetary Science Letters 233, 17-32.

Tribolo, C., Mercier, N., Valladas, H., Joron, J.L., Guibert, P., Lefrais, Y., Selo, M., Texier, P.-J., Rigaud, J.-P., Porraz, G., Poggenpoel, C., Parkington, J., Texier, J.-P., Lenoble, A., 2009. Thermoluminescence dating of a Stillbay-Howiesons Poort sequence at Diepkloof Rock Shelter (Western Cape, South Africa). Journal of Archaeological Science 36, 730-739.

Tyson, P.D., 1986. Climatic Change and Variability in Southern Africa. Oxford University Press, Cape Town.

Tyson, P.D., 1999. Atmospheric circulation changes and palaeoclimates of southern Africa. South African Journal of Science 95, 194-201.

Tyson, P.D., Preston-Whyte, R.A., 2000. The Weather and Climate of Southern Africa. Oxford University Press, Cape Town.

Valentine, H.R., Lutjeharms, J.R.E., Brundrit, G.B., 1993. The water masses and volumetry of the southern Agulhas Current region. Deep Sea Research 40, 1285-1305.

van Campo, E., Duplessy, J.C., Prell, W.L., Barratt, N., Sabatier, R., 1990. Comparison of terrestrial and marine temperature estimates for the past 135 kyr off southeast Africa: a test for GCM simulations of palaeoclimate. Nature 348, 209-212.

van Daalen, J.C., 1980. The colonisation of fynbos and disturbed sites by indigenous forest communities in the southern Cape. Unpublished M.Sc thesis, University of Cape Town, Cape Town.

Van der Wateren, F.M., Dunai, T.J., 2001. Late Neogene passive margin denudation history—cosmogenic isotope measurements from the central Namib desert. Global and Planetary Change 30, 271-307.

van Wilgen, B.W., 1992. Fire in South African mountain fynbos : ecosystem, community, and species response at Swartboskloof. Springer-Verlag, Berlin ; New York.

van Zinderen Bakker, E.M., 1953. South African pollen grains and spores. Volume I. Balkema, Amsterdam–Cape Town.

van Zinderen Bakker, E.M., 1956. South African pollen grains and spores. Volume II. Balkema, Amsterdam–Cape Town.

van Zinderen Bakker, E.M., 1967. Upper Pleistocene stratigraphy and Holocene ecology on the basis of vegetation changes in Sub-Saharan Africa, in: Bishop, W.W., Clark, J.D. (Eds.), Background to Evolution in Africa. University of Chicago Press, Chicago, pp. 125-147.

van Zinderen Bakker, E.M., 1976. The evolution of late Quaternary paleoclimates of Southern Africa. Palaeoecology of Africa 9, 160-202.

van Zinderen Bakker, E.M., Coetzee, J.A., 1959. South African pollen grains and spores. Volume III. Balkema, Amsterdam–Cape Town.

Vancampenhout, K., Wouters, K., Caus, A., Buurman, P., Swennen, R., Deckers, J., 2008. Fingerprinting of soil organic matter as a proxy for assessing climate and vegetation changes in last interglacial palaeosols (Veldwezelt, Belgium). Quaternary Research 69, 145-162.

Verboom, G.A., Dreyer, L.L., Savolainen, V., 2009. Understanding the origins and evolution of the world's biodiversity hotspots: The biota of the African 'Cape Floristic Region' as a case study. Molecular Phylogenetics and Evolution 51, 1-4.

Vlok, J.H.J., De Villiers, M.E., 2007. Vegetation map for the Riversdale domain, Unpublished 1:50 000 map and report for the CAPE FSP. CAPE FSP task team and CapeNature.

Vogel, J.C., 1978. Isotopic assessment of dietary habits of ungulates. South African Journal of Science 74, 298-301.

Vogel, J.C., Fuls, A., Ellis, R.P., 1978. The geographic distribution of Krantz species in southern Africa. South African Journal of Science 75, 209-215.

von Breitenbach, F., 1974. Southern Cape Forests and Trees. Government Printer, Pretoria.

Wadley, L., Plug, I., Clark, J.L., 2008. The contribution of Sibudu fauna to an understanding of KwaZulu-Natal environments at ~60 ka, ~50 ka and ~37 ka, in: Badenhorst, S., Mitchell, P., Driver, J.C. (Eds.), Animals and People: Archaeozoological Papers in Honour of Ina Plug. Archaeopress, Oxford.

Waelbroeck, C., Labeyrie, L., Michel, E., Duplessy, J.C., McManus, J., Lambeck, K., Balbon, E., Labracherie, M., 2002. Sea-level and deep water temperature changes derived from benthic foraminifera isotopic records. Quaternary Science Reviews 21, 295-305.

Walker, M., 2005. Quaternary Dating Methods. John Wiley & Sons Ltd, Chichester.

Warner, B., 1993. Palaeoecology of floating bogs and landscape change in the Great Lakes drainage basin of North America, in: Chambers, F.C. (Ed.), Climate Change and Human Impact on the Landscape. Chapman and Hall, London, pp. 237 - 245.

Washington, R., Todd, M., 1999. Tropical-temperate links in southern African and southwest Indian Ocean satellite-derived daily rainfall. International Journal of Climatology 19, 1607-1616.

Weijer, W., de Ruijter, W.P.M., Dijkstra, H.A., van Leeuwen, P.J., 1999. Impact of interbasin exchange on the Atlantic overturning circulation. Journal of Physical Oceanography 29, 2266-2284.

Welman, W.G., Kuhn, L., 1970. South African pollen grains and spores. Volume VI. Balkema, Amsterdam–Cape Town.

Weninger, B., Jöris, O., 2008. A 14C age calibration curve for the last 60 ka: the Greenland-Hulu U/Th timescale and its impact on understanding the Middle to Upper Paleolithic transition in western Eurasia. Journal of Human Evolution 55, 772-781.

West, A.G., Dawson, T.E., February, E.C., Midgley, G.F., Bond, W.J., Aston, T.L., 2012. Diverse functional responses to drought in a Mediterranean-type shrubland in South Africa. New Phytologist 195, 396-407.

West, A.G., February, E.C., Dawson, T.E., 2011. Divergent drought responses in a mountain fynbos community: Impacts for biodiversity under future climate. South African Journal of Botany 77, 567-568.

West, J.B., Bowen, G.J., Cerling, T.E., Ehleringer, J.R., 2006. Stable isotopes as one of nature's ecological recorders. Trends in Ecology and Evolution 21, 408-414.

White, F., 1978. The Afromontane Region, in: Werger, M.J.A. (Ed.), Biogeography and Ecology of Southern Africa. Junk, The Hague, pp. 463-513.

Wilgen, B.W., Richardson, D.M., Seydack, A.H.W., 1994. Managing fynbos for biodiversity: constraints and options in a fire-prone environment. South African Journal of Science 90, 322-329.

Williams, C.R., Kniveton, D., Layberry, R., 2011. Extreme Rainfall Events over Southern Africa, in: Williams, C.J.R., Kniveton, D.R. (Eds.), African Climate and Climate Change. Springer Netherlands, pp. 71-100.

Williams, M., Dunkerly, D., De Deckker, P., Kershaw, P., Chappell, J., 1998. Quaternary Environments. Arnold, New York.

Willis, C.K., Cowling, R.M., Lombard, A.T., 1996a. Patterns of endemism in the limestone flora of South African lowland fynbos. Biodiversity and Conservation 5, 55-73.

Willis, C.K., Lombard, A.T., Cowling, R.M., Heydenrych, B.J., Burgers, C.J., 1996b. Reserve systems for limestone endemic flora of the cape lowland fynbos: Iterative versus linear programming. Biological Conservation 77, 53-62.

Willis, K.J., Araújo, M.B., Bennett, K.D., Figueroa-Rangel, B., Froyd, C.A., Myers, N., 2007. How can a knowledge of the past help to conserve the future? Biodiversity conservation and the relevance of long-term ecological studies. Philosophical Transactions of the Royal Society B: Biological Sciences 362, 175-187.

Willis, K.J., Birks, H.J.B., 2006. What is natural? The need for a long-term perspective in biodiversity conservation. Science 314, 1261.

Wunsch, C., 2003. Greenland-Antarctic phase relations and millennial time-scale climate fluctuations in the Greenland ice-cores. Quaternary Science Reviews 22, 1631-1646.

Wyrwoll, K.-H., Hopwood, J.M., Chen, G., 2012. Orbital time-scale circulation controls of the Australian summer monsoon: a possible role for mid-latitude Southern Hemisphere forcing? Quaternary Science Reviews 35, 23-28.

Yates, R.J., Miller, D.E., Halkett, D.J., Manhire, A.H., Parkington, J.E., Vogel, J.C., 1986. A late mid-Holocene high sea-level: a preliminary report on geoarchaeology at Elands Bay, Western Cape Province, South Africa. South African Journal of Science 82, 164-165.

APPENDIX A

POLLEN CONCENTRATION FROM VLEI SEDIMENTS

- Determine the type and amount of spike to be added (1 *Lycopodium* tablet per sample).
- Set up a test tube rack with 2 sets of 50 ml centrifuge tubes.
- Weigh samples (generally at least 1g of material is required to assure sufficient pollen concentrations).
- In clean 50 ml centrifuge tubes, add about 25 ml of sodium pyrophosphate ($Na_4P_2O_7$) to samples and leave overnight.
- The next day allow samples to sit for about 30 minutes in water bath (90^0C) and then with a stirring rod/Vortex mixer gently break up sample.
- Add 2-3 drops of tertiary butyl alcohol (TBA) to wet down any floating particles; centrifuge for 5 minutes at 3000 rpm and decant.

Section A: Material preparation

1. Sieve the sample using 150/160 µm sieve, washing through sieve using distilled water (DW).
2. Pour into 50 ml centrifuge tubes, balance with DW, centrifuge for 5 minutes at 3000 rpm, and decant.
3. Repeat until all sieved liquid has been centrifuged.
4. Add about 1 ml of 30% HCl to each sample initially and stir in very gently. Control foaming by adding 1-2 drops TBA.
5. Add another 5 ml of 10% HCl, do not let the reaction overflow the test tube.
6. Add 1 *Lycopodium* tablet
7. Heat samples for about 10 minutes in gently boiling water bath. When the reaction is complete, centrifuge and decant. This step removes carbonates.
8. Add about 6 ml of 10% KOH to each sample and stir gently. KOH treatment is used to remove humic acids.
9. Heat with occasional stirring in actively boiling water bath for 10 to 20 minutes.
10. Remove from heat: fill with DW, stir, add TBA, centrifuge and decant.
11. Rinse with DW again and check for obvious clumping.

12. Repeat the KOH step.
13. Rinse 6 - 20 times after second KOH treatment, adding TBA when necessary. Stop when clear or almost clear. This removes many < 3 µ particles that interfere with pollen counting.

Section B: Heavy liquid separation

1. Dissolve zinc chloride ($ZnCl_2$) in 10% HCl to achieve a specific gravity (SG) of 2.0.
   The formula for the heavy liquid SG 2.0 = 225g of $ZnCl_2$ per 100 ml 10% HCl (do this step prior to starting section A as it will take several hours to dissolve the zinc chloride).
2. Carefully dilute this solution to exactly 1.88 using a hydrometer.
3. After decanting rinse at the end of Section A., pour in ~20 ml of heavy liquid, cap and mix well.
1. Centrifuge for 20 minutes at 1800 rpm.
2. When centrifuge cycle is finished, check to make sure the liquid is clear below the suspended material, if not clear return tubes to the centrifuge and run another cycle. If the liquid is still not clear, the SG of the heavy liquid may be incorrect.
3. If a distinct skim of suspended material is evident, transfer this lighter portion to a clean centrifuge tube (Figure 1 below).
4. The heavy fraction at the bottom of the first test tube can then be discarded.
5. Balance with DW ensuring that enough is added to reduce the SG of the liquid (~30 ml including sample and residual heavy liquid) and centrifuge for 5 min at 3000 rpm.
6. Decant, refill with DW, and centrifuge again, repeating 2-3 times.

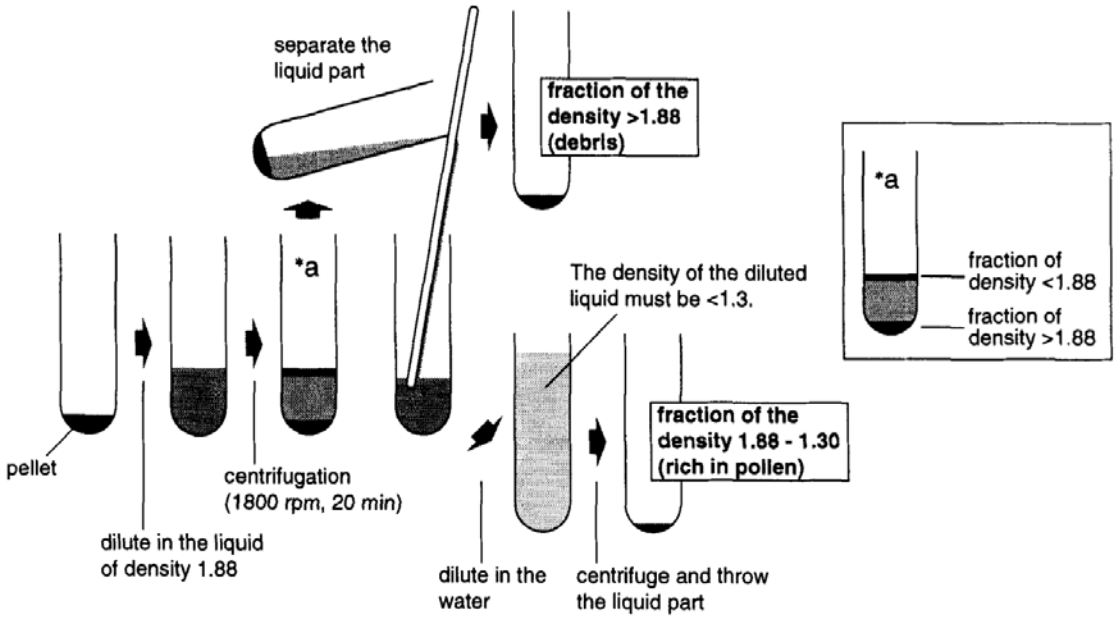

Figure A.1 Dense media separation schematic from Nakagawa et al. (1998).

Section C: HF treatment

Check sample under microscope (wet mount): if pollen grains are obscured from view by silicaceous material such as clay then hydrogen fluoride (HF) digestion will need to be performed.

1. Wear long plastic apron with full sleeves, closed shoes, full face shield and gloves.
2. Place centrifuge tubes with samples in rack for water bath.
3. Add about 8ml 40% HF (direct from bottle) to sample. Avoid drips. Stir carefully.
4. Transfer rack to actively boiling water bath (water bath must be in an effectively drawing fume cupboard/hood).
5. Heat in actively boiling water bath for 20 minutes. Stir 3 or 4 times during the heating using a Vortex mixer.
6. When done, remove rack from water bath, fill with 95% EtOH (ethanol) to cool (no TBA), centrifuge and decant into dedicated HF waste container.
7. Immediately after decant, start the next procedure: Hot 10% HCl rinses. This procedure breaks up siliceous colloidal clumps that formed during silica digestion.
8. Add about 6ml 10% HCl. Stir gently and heat in water bath for about 3 minutes. Add TBA, centrifuge and decant into waste container.

9. Repeat hot HCl rinses 2 – 4 times. High clay samples will need 4 – 5 times and more organic samples 2 – 3 times.
10. Rinse twice with DW.

Section D: Acetolysis

This step removes some organic matter, cleans the surface of the pollen grains and stains the grains a golden brown. This procedure takes about an hour; it must be done efficiently with no interruptions. Water bath must be full and actively boiling during the treatment, acetolysis is only effective near 100^0C. Protective gear must be worn, acetolysis mixture reacts explosively wit h water.

1. Rinse twice with glacial acetic acid using 5/6 ml per rinse (no TBA).
2. Prepare acetolysis mixture which is 9 parts acetic anhydride to 1 part concentrated sulphuric acid.
3. Pour about 6 ml acetolysis mixture into each test tube and stir.
4. Put samples into actively boiling water bath heat for exactly 2 minutes.
5. Remove samples from water bath cool immediately by adding glacial acetic acid (no TBA), centrifuge and decant into waster container.
6. Rinse once with glacial acetic acid.
7. Rinse 3 times with DW (add TBA).
8. Transfer to properly labelled, dry ½ dram shell vials.

Section E: Microscope slide mounting

1. Place glass slides on hot plate
2. Using a pipette extract some of the pollen preparation from the dram shell vials and place 1-2 drops of the pollen sample on each slide.
3. Evenly spread the mixture across the surface of the slides.

4. Allow for the evaporation of the remaining water by leaving the slides on the hot plate for approximately a minute.
5. Take slides off the heat and add 1 - 2 drops of Aquatex mounting medium to each slide, mix, then seal with coverslips.

Method adapted from the Limnological Research Centre, University of Minnesota and Faegri and Iverson, 1989, Moore et al., 1991 and Nakagawa et al., 1998.

APPENDIX B – Modern taxa bioclimatic variables

Pollen Taxa	General ecological affinity*	Climatic Influences^	MAP (mm)			Total winter rainfall~ (mm)			Apan (mm)			MAT (°C)			MTCM (°C)			PDryQ (mm)		
			25 - 75% range	Min	Max	25 - 75% range	Min	Max	25 - 75% range	Min	Max	25 - 75% range	Min	Max	25 - 75% range	Min	Max	25 - 75% range	Min	Max
Apiaceae	aquatic/riparian	spring and autumn potential evaporation and rainfall	450 - 850	13	1782	39 - 138	0	475	1763 - 2161	1075	2965	14.8 - 17.7	5.6	23.5	1.1 - 6.6	-5.6	13.0	31 - 77	0	206
Apongeton	aquatic/riparian	mean annual rainfall	450 - 750	144	1097	10 - 53	0	444	1764 - 2227	1075	2925	15.3 - 19.5	5.2	23.1	0.2 - 6.1	-5.8	11.4	10 - 48	0	190
Araceae	aquatic/riparian	spring rainfall, relative humidity and potential evaporation	600 - 900	223	1438	49 - 127	8	426	1646 - 2085	1511	2676	16.0 - 18.6	12.5	24.4	2.6 - 9.2	-2.3	11.8	39 - 83	0	146
Araliaceae	aquatic/riparian	mean annual rainfall	600 - 900	176	1859	35 - 84	0	397	1753 - 2103	1169	2773	15.9 - 19.1	7.4	23.5	2.3 - 7.9	-4.9	12.9	32 - 79	0	195
Blechnaceae	aquatic/riparian	spring rainfall and potential evaporation	650 - 1000	223	1438	40 - 114	12	444	1700 - 2040	1075	2659	14.7 - 18.1	5.9	21.7	1.8 - 6.5	-5.2	11.1	38 - 73	0	189
Cyperaceae	aquatic/riparian/cosmopolitan	summer rainfall, water availability, potential evaporation and relative humidity	500 - 850	12	1457	18 - 104	0	475	1774 - 2211	1000	3037	15.7 - 19.8	5.9	24.7	1.5 - 6.9	-5.4	13.7	17 - 70	0	214
Gentianaceae	aquatic/riparian	winter rainfall, relative humidity and potential evaporation	450 - 700	52	1395	40 - 193	0	444	1828 - 2163	1075	2889	15.7 - 17.8	6.0	22.8	3.0 - 7.0	-5.2	12.3	29 - 90	0	190
Gunnera	aquatic/riparian	mean annual rainfall	600 - 850	254	1395	37 - 90	13	414	1723 - 2117	1075	2438	13.6 - 17.3	6.0	21.9	0.0 - 4.9	-5.2	11.2	35 - 56	13	176
Haloragaceae	aquatic/riparian	mean annual rainfall	500 - 900	101	1438	22 - 117	0	444	1808 - 2208	1337	2811	16.3 - 19.8	11.3	22.4	2.1 - 7.3	-2.7	11.8	20 - 76	0	234
Ilex	*Aquatic/riparian or forest*	mean annual rainfall	700 - 900	290	1438	26 - 86	12	444	1755 - 2112	1337	2473	15.0 - 17.7	10.3	22.4	1.0 - 5.8	-3.5	12.2	26 - 70	12	195
Juncaceae	aquatic/riparian	mean annual rainfall	500 - 900	11	1438	24 - 98	0	444	1740 - 2227	1075	2905	14.7 - 17.8	5.4	22.8	0.2 - 6.2	-5.4	12.9	23 - 64	0	206
Nymphaea	aquatic/riparian	summer rainfall, potential evaporation and relative humidity	550 - 850	347	1438	11 - 86	0	297	1820 - 2203	1545	2774	18.0 - 22.1	14.2	23.4	4.3 - 10.1	-1.0	12.9	11 - 80	0	185
Onagraceae	aquatic/riparian	mean annual rainfall	550 - 850	49	1438	20 - 55	0	426	1774 - 2208	1075	2932	15.0 - 18.8	5.9	24.4	0.0 - 6.3	-5.2	12.4	40 - 87	0	190
Plantago	aquatic/riparian	mean annual rainfall	500 - 800	48	1380	30 - 116	7	426	1790 - 2262	1116	2881	15.4 - 17.6	8.6	21.1	0.5 - 6.5	-4.6	12.2	23 - 70	5	170
Plumbaginaceae	aquatic/riparian	number and duration of frost days; geology; winter temperatures	200 - 600	17	1395	19 - 129	0	414	1856 - 2452	1337	2932	16.5 - 19.0	10.7	23.5	3.4 - 7.8	-3.5	11.4	11 - 63	0	208
Polygonum	aquatic/riparian	mean annual rainfall; spring water availability; summer potential evaporation	400 - 700	16	1438	17 - 74	0	444	1898 - 2368	1116	2947	15.6 - 18.9	7.2	24.3	0.3 - 6.7	-5.0	11.4	14 - 49	0	189
Potamogeton	aquatic/riparian	summer rainfall, potential evaporation and relative humidity	500 - 800	10	1391	18 - 69	0	426	1778 - 2227	1291	2932	16.1 - 20.2	7.2	24.0	0.4 - 6.8	-4.6	12.9	17 - 62	0	190
Ranunculaceae	aquatic/riparian	mean annual rainfall; summer potential evaporation	550 - 850	84	1620	24 - 69	0	444	1766 - 2232	1075	2912	14.8 - 17.9	6.0	24.4	0.1 - 5.6	-5.2	15.1	23 - 59	0	195
Scabiosa	aquatic/riparian	mean annual rainfall	550 - 850	84	1438	28 - 98	0	486	1766 - 2216	1000	3019	14.9 - 18.1	5.9	24.2	1.0 - 6.1	-5.5	13.4	13 - 53	0	195
Solanum	aquatic/riparian	summer rainfall, potential evaporation and relative humidity	400 - 700	12	1438	15 - 53	0	426	1851 - 2334	1075	3020	16.1 - 19.5	6.0	24.4	1.3 - 6.5	-5.2	12.9	12 - 46	0	195
Typha	aquatic/riparian	mean annual rainfall; summer potential evaporation and relative humidity	500 - 800	29	1391	20 - 101	0	444	1830 - 2211	1291	2953	15.9 - 19.8	9.9	23.4	1.5 - 7.4	-2.8	12.9	20 - 61	0	160
Urticaceae	aquatic/riparian	not correlated strongly to any of the climate variables	150 - 700	12	1438	10 - 53	0	470	1848 - 2367	1075	2932	16.1 - 19.6	6.0	23.6	2.2 - 6.9	-5.2	13.2	8 - 42	0	130
Amaryllidaceae	fynbos	winter rainfall and relative humidity	200 - 650	28	1438	29 - 128	0	505	101 - 2488	1075	3020	15.9 - 18.4	5.9	24.8	2.6 - 6.6	-5.2	13.2	14 - 55	0	189
Anthospermum -type	fynbos	winter rainfall, relative humidity and spring potential evaporation	450 - 800	48	1438	33 - 123	0	508	1774 - 2248	1000	2998	14.8 - 17.7	5.9	22.8	4.0 - 6.3	-5.4	12.6	25 - 73	0	195
Bruniaceae	fynbos	winter rainfall, potential evaporation and relative humidity	450 - 800	134	1237	151 - 353	4	539	1761 - 2066	444	2625	14.3 - 16.4	7.0	24.3	3.5 - 6.8	-2.3	12.5	58 - 90	4	208
Cliffortia	fynbos	winter rainfall, relative humidity and potential evaporation	400 - 800	131	1438	87 - 270	8	497	1803 - 2142	870	2875	14.2 - 16.6	7.3	22.0	4.7 - 8.6	0.7	19.5	47 - 86	7	195
Ericaceae	fynbos	winter rainfall, relative humidity and potential evaporation	500 - 800	131	1782	114 - 293	9	539	1764 - 2065	768	2683	14.3 - 16.6	5.9	22.7	3.1 - 6.8	-5.4	12.6	54 - 90	9	238
Haemodoraceae	fynbos	winter rainfall, relative humidity and potential evaporation	400 - 700	139	944	13 - 297	7	444	1847 - 2164	1620	2615	15.8 -17.1	11.4	20.6	4.4 - 6.9	0.4	9.5	47 - 86	7	190
Iridaceae	fynbos	winter rainfall, relative humidity and potential evaporation	300 - 700	26	1856	66 - 207	0	539	1841 - 2345	444	2998	15.1 - 17.4	5.4	25.4	2.8 - 6.6	-5.4	15.5	26 - 76	0	240
Lobostemon	fynbos	winter rainfall, relative humidity and potential evaporation	300 - 600	95	1057	106 - 232	23	459	1874 - 2321	1116	2681	15.1 - 17.2	8.6	19.9	3.1 - 6.8	-1.9	9.7	36 - 79	7	176
Orchidaceae	fynbos	winter rainfall, relative humidity and potential evaporation	500 - 900	58	1543	46 - 199	0	563	1709 - 2049	674	2918	14.5 - 17.4	5.9	23.7	2.4 - 6.7	-5.2	13.6	40 - 87	0	234
Passerina	fynbos	winter rainfall, relative humidity and potential evaporation	400 - 800	82	1436	55 - 162	2	508	1739 - 2151	1108	2701	14.3 - 17.4	6.6	22.4	1.5 - 6.9	-5.2	12.6	42 - 99	2	195
Phylica	fynbos	winter rainfall, relative humidity and potential evaporation	300 - 600	96	1420	105 - 205	9	487	1836 - 2227	594	2859	14.3 - 17.1	8.0	21.1	2.7 - 6.5	-3.6	11.8	36 - 90	8	206

APPENDIX B – Modern taxa bioclimatic variables

Pollen Taxa	General ecological affinity*	Climatic Influences^	MAP (mm)			Total winter rainfall~ (mm)			Apan (mm)			MAT (°C)			MTCM (°C)			PDryQ (mm)		
			25 - 75% range	Min	Max	25 - 75% range	Min	Max	25 - 75% range	Min	Max	25 - 75% range	Min	Max	25 - 75% range	Min	Max	25 - 75% range	Min	Max
Proteaceae	fynbos	winter rainfall, relative humidity and potential evaporation	400 - 700	125	1420	105 - 267	0	521	1825 - 2165	594	2998	14.7 - 17.1	6.0	22.7	3.1 - 6.7	-5.2	13.0	44 - 87	0	208
Restionaceae	fynbos	winter rainfall, relative humidity and potential evaporation	400 - 700	62	1380	123 - 305	0	563	1821 - 2140	444	2845	14.3 - 16.7	7.9	22.3	3.1 - 6.8	-4.9	12.9	52 - 90	0	206
Rhamnaceae	fynbos	winter rainfall, relative humidity and potential evaporation	400 - 700	49	1438	35 - 161	0	487	1829 - 2227	594	2959	15.2 - 18.2	6.0	24.4	2.5 - 6.6	-5.2	13.1	23 - 79	0	206
Rutaceae	fynbos	winter rainfall, relative humidity and potential evaporation	400 - 700	12	1438	105 - 209	0	543	1804 - 2153	444	2876	15.0 - 17.4	6.0	24.2	3.2 - 7.0	-4.8	12.9	41 - 93	0	239
Stoebe -type	fynbos	winter rainfall, relative humidity and potential evaporation	350 - 700	62	1438	100 - 248	2	444	1857 - 2730	1075	2845	14.7 - 17.2	6.0	21.9	2.7 - 6.5	-5.2	10.6	35 - 82	2	195
Canthium	thicket	summer relative humidity, potential evaporation and rainfall; duration of frost; winter minimum temperatures	700 - 1000	316	1395	37 - 111	11	397	1712 - 1971	1525	2329	16.8 - 19.8	12.5	22.8	5.1 - 9.5	0.0	12.9	37 - 102	11	180
Cardiospermum	thicket	summer potential evaporation and relative humidity; duration of frost; annual minimum temperatures	400 - 700	48	1391	1 - 34	0	414	1889 - 2214	1542	2573	19.0 - 21.8	13.8	23.5	5.0 - 8.7	0.3	12.5	1 - 34	0	169
Celastraceae	thicket	summer and spring relative humidity; summer potential evaporation; spring rainfall	400 - 800	25	1438	31 - 111	0	444	1755 - 2112	1075	2960	16.2 - 19.5	6.0	24.7	3.1 - 8.1	-5.2	13.1	27 - 88	0	199
Diospyros	thicket	summer rainfall and potential evaporation; winter water availability	400 - 800	28	1705	20 - 78	0	444	1825 - 2312	1116	2932	15.8 - 19.4	5.3	24.3	1.6 - 6.7	-5.6	12.9	17 - 55	0	195
Dodonea	thicket	winter rainfall and potential evaporation; spring relative humidity	250 - 600	66	1438	59 - 144	1	426	2032 - 2676	1545	2676	15.6 - 17.9	11.3	22.8	3.0 - 5.9	0.3	11.8	24 - 68	1	190
Euclea	thicket	duration of frost; spring and autumn relative humidity; winter minimum temperatures	350 - 750	25	1438	18 - 90	0	397	1864 - 2316	1172	2949	16.2 - 19.7	5.3	24.4	2.8 - 7.2	-5.6	12.9	14 - 54	0	195
Morella	thicket	winter potential evaporation, rainfall and relative humidity	500 - 750	391	1096	42 - 248	0	397	1777 - 1978	1406	2150	16.0 - 17.6	11.3	22.2	3.5 - 8.3	-3.6	10.6	38 - 79	0	116
Myrtaceae	thicket	spring rainfall; summer potential evaporation; summer relative humidity	600 - 1000	164	1460	31 - 112	0	444	1704 - 2068	1116	2870	16.8 - 20.4	8.6	24.2	4.8 - 9.1	-1.2	12.9	29 - 89	0	190
Olea	thicket	spring and autumn potential evaporation and rainfall	500 - 800	62	1420	26 - 128	1	444	1804 - 2244	1116	2998	16.0 - 18.5	8.6	22.6	2.1 - 7.2	-3.0	12.7	23 - 85	0	195
Santalaceae	thicket	winter rainfall, relative humidity, potential evaporation and water availability	300 - 700	30	1438	44 - 178	0	470	1843 - 2313	962	2998	15.1 - 17.5	5.9	22.7	2.0 - 6.5	-5.4	12.8	25 - 80	0	206
Sapotaceae - sideroxylon inerme	thicket	summer relative humidity; duration of frost; winter minimum temperatures; spring rainfall	550 - 900	350	1391	47 - 119	17	426	1746 - 1947	1000	2998	16.9 - 21.0	6.0	22.8	0.2 - 6.5	-5.2	12.5	23 - 70	0	189
Apocynaceae	forest	geology; winter relative humidity; spring rainfall and potential evaporation	300 - 700	12	1438	16 - 77	0	444	1883 - 2429	1075	3020	16.2 19.6	5.9	24.4	2.2 - 6.9	-5.4	13.2	11 - 53	0	190
Clutia	forest	spring rainfall; summer potential evaporation	500 - 900	64	1438	46 - 149	1	444	1762 - 2112	1116	2802	14.8 - 17.5	6.0	22.7	2.0 - 6.6	-5.2	12.9	38 - 90	1	195
Cunoniaceae	forest	spring potential evaporation; winter rainfall and relative humidity	500 - 850	262	1137	101 - 211	41	418	1738 - 1977	1337	2483	15.1 - 17.3	12.7	20.4	3.9 - 7.0	1.7	11.3	69 - 112	38	195
Grewia	forest	summer potential evaporation, rainfall and humidity; spring minimum temperatures	400 - 700	12	1859	2 - 33	0	414	1925 - 2282	1075	2996	18.3 - 21.6	6.0	24.4	3.0 - 7.6	-5.2	12.9	1 - 32	0	195
Hamamelidaceae	forest	spring rainfall and potentail evaporation; winter water availability	600 - 1000	466	1137	80 - 146	46	241	1623 - 1782	1577	2028	14.9 - 19.0	13.1	21.6	5.2 - 9.2	1.9	12.1	79 - 146	47	190
Kiggelaria	forest	spring rainfall; summer potential evaporation	600 - 900	139	1438	36 - 100	1	444	1753 - 2104	1417	2506	14.6 - 17.7	7.4	21.9	0.2 - 5.9	-4.9	11.8	34 - 70	1	190
Lauraceae	forest	winter rainfall; spring potential evaporation; spring and autumn relative humidity	550 - 1000	178	1438	41 - 149	0	449	1761 - 2040	1417	2523	16.2 - 19.8	12.1	22.8	4.8 - 8.3	-1.4	12.9	39 - 102	0	190
Meliaceae	forest	duration of frost; winter minimum temperatures; spring rainfall	400 - 900	42	1420	16 - 71	0	418	1803 - 2250	1075	3022	17.4 - 21.0	6.0	24.2	3.3 - 8.6	-5.2	13.0	14 - 70	0	192
Moraceae	forest	duration of frost; winter minimum temperatures; spring rainfall	500 - 900	16	1859	13 - 59	0	381	1847 - 2186	1378	2956	17.6 - 21.1	8.8	24.4	3.9 - 8.8	-3.9	13.4	12 - 51	0	195
Myrsine	forest	summer potential evaporation and mean annual rainfall	600 - 900	207	1438	32 - 126	10	521	1769 - 2146	1000	2625	14.4 - 17.1	6.0	22.0	0.4 - 5.6	-5.2	9.8	29 - 62	10	240
Olinia	forest	spring rainfall; spring potential evaporation; winter water availability	500 - 750	315	944	114 - 205	48	414	1769 - 1981	1500	2316	15.2 - 17.3	13.1	18.9	4.8 - 7.1	2.5	10.5	76 - 122	48	190
Phytolaccaceae	forest	spring rainfall and potential evaporation; winter water availability	400 - 900	49	1438	16 - 49	0	414	1803 - 2233	1338	3015	15.7 - 19.4	7.2	23.5	1.2 - 6.1	-4.9	12.0	14 - 49	0	190
Podocarpus	forest	spring rainfall; spring relative humidity; spring potential evaporation	600 - 900	223	1438	43 - 139	5	508	1678 - 2045	1008	2536	15.0 - 17.7	9.9	22.6	2.8 - 6.4	-3.5	12.9	40 - 82	5	195
Aizoaceae	succulent/drought resistant	summer rainfall	150 - 400	9	1278	10 - 83	0	444	2189 - 2681	1116	3010	16.3 - 19.1	8.6	23.5	2.1 - 6.5	-4.4	12.5	7 - 36	0	195
Aloe -type	succulent/drought resistant	spring relative humidity and potential evaporation	250 - 800	18	1438	21 - 78	0	467	1828 - 2350	674	2965	15.8 - 18.9	6.0	24.4	2.3 - 6.6	-5.2	13.4	13 - 54	0	199
ChenoAm-type	succulent/drought resistant	summer rainfall, potential evaporation and relative humidity	300 - 600	11	1438	9 - 43	0	426	1961 - 2562	1116	3037	16.5 - 19.9	7.4	24.4	1.1 - 6.6	-5.0	13.4	7 - 37	0	203

APPENDIX B – Modern taxa bioclimatic variables

Pollen Taxa	General ecological affinity*	Climatic Influences^	MAP (mm)			Total winter rainfall~ (mm)			Apan (mm)			MAT (°C)			MTCM (°C)			PDryQ (mm)		
			25 - 75% range	Min	Max	25 - 75% range	Min	Max	25 - 75% range	Min	Max	25 - 75% range	Min	Max	25 - 75% range	Min	Max	25 - 75% range	Min	Max
Crassula	succulent/drought resistant	winter rainfall, relative humidity and potential evaporation	300 - 800	28	1438	38 - 112	0	445	1804 - 2376	1075	2932	14.9 - 17.6	5.2	24.0	1.3 - 6.2	-5.8	12.8	23 - 69	0	237
Crassulaceae	succulent/drought resistant	winter rainfall, relative humidity and potential evaporation	266 - 747	0	1438	38 - 107	0	445	1844 - 2417	1075	2995	15.2 - 17.7	5.2	23.4	1.4 - 6.1	-5.8	12.8	22 - 65	0	237
Euphorbia	succulent/drought resistant	winter rainfall and relative humidity; spring potential evaporation	200 - 700	9	1438	16 - 79	0	534	1864 - 2459	1075	3005	16.2 - 19.2	5.9	24.6	2.1 - 6.8	-5.4	13.9	10 - 52	0	195
Geraniaceae	succulent/drought resistant	summer rainfall, potential evaporation and relative humidity	250 - 700	9	1420	38 - 143	0	526	1847 - 2400	1075	3006	15.0 - 17.5	5.4	23.8	2.0 - 6.3	-5.4	13.4	19 - 73	0	199
Pentzia -type	succulent/drought resistant	summer rainfall; winter minimum temperatures; geology	200 - 500	12	1125	20 - 45	0	383	2235 - 2642	1169	3020	15.4 - 17.8	6.6	22.9	28.2 – 32.4	16.7	39.1	16 - 40	0	138
Portulacaceae	succulent/drought resistant	summer rainfall	200 - 600	28	1395	11 - 41	0	414	2157 - 2650	1468	3021	16.8 - 19.8	11.1	24.4	1.9 - 6.0	-3.5	11.7	8 - 30	0	180
Ruschia	succulent/drought resistant	summer rainfall and potential evaporation	150 - 450	36	1123	35 - 120	1	486	2162 - 2578	1116	2912	15.7 - 17.7	7.9	22.1	1.8 - 6.1	-4.9	9.6	15 - 47	1	195
Zygophyllaceae	succulent/drought resistant	summer rainfall and potential evaporation	100 - 350	9	1398	6 - 67	0	454	2201 - 2704	1337	3021	16.2 - 19.3	7.7	24.3	2.3 - 6.4	-5.0	13.4	5 - 28	0	195
Acacia	cosmopolitan	spring minimum temperatures; summer relative humidity and rainfall ; duration of frost	400 - 750	12	1438	6 - 43	0	426	1866 - 2304	1075	3020	17.5 - 20.9	5.9	24.4	2.7 - 7.5	-5.2	13.4	6 - 41	0	195
Acanthaceae	cosmopolitan	duration of frost; summer rainfall and water availability	300 - 700	12	1620	3 - 39	0	414	1864 - 2353	1169	3015	17.5 - 20.9	7.8	24.4	2.9 - 7.8	-4.9	13.4	3 - 38	0	191
Artemisia	cosmopolitan	summer rainfall; summer potential evaporation	600 - 800	84	1380	22 - 57	0	411	1774 - 2178	1361	2886	14.4 - 17.6	7.7	21.7	-0.2 - 3.9	-5.0	11.3	22 - 55	0	137
Boraginaceae	cosmopolitan	winter rainfall, relative humidity and potential evaporation	300 - 700	12	1438	12 - 86	0	467	1883 - 2414	1075	3020	16.0 - 19.7	5.9	24.4	1.6 - 6.8	-5.4	13.2	10 - 51	0	191
Brassicaceae	cosmopolitan	winter rainfall, relative humidity and potential evaporation	200 - 700	12	1438	27 - 121	0	508	1886 - 2479	1078	3009	15.1 - 17.7	5.9	23.3	0.7 - 5.9	-5.4	12.8	19 - 56	0	195
Campanulaceae	cosmopolitan	winter rainfall, relative humidity and potential evaporation	400 - 800	25	1438	36 - 149	0	444	1804 - 2320	962	3022	15.0 - 17.6	5.9	24.3	1.4 - 6.4	-5.5	12.9	23 - 70	0	203
Caryophyllaceae	cosmopolitan	spring and autumn potential evaporation and rainfall; winter water availability	400 - 800	11	1438	24 - 87	0	464	1801 - 2319	1075	3006	15.0 - 17.9	5.9	24.3	0.2 - 6.1	-5.5	12.9	20 - 58	0	195
Celtis	cosmopolitan	summer and spring rainfall; summer potential evaporation and relative humidity	600 - 800	311	1438	24 - 69	10	279	1835 - 2227	1408	2889	15.9 -18.4	7.4	22.4	0.6 - 6.9	-4.9	11.8	23 - 63	10	158
Combretaceae	cosmopolitan	summer rainfall, relative humidity and minimum temperatures	500 - 700	26	1438	1 - 32	0	169	1938 - 2244	1495	2932	18.8 - 21.9	12.0	24.4	3.9 - 8.2	-3.0	13.1	1 - 32	0	169
Convolvulaceae	cosmopolitan	mean annual rainfall; summer potential evaporation and relative humidity	450 - 700	18	1581	4 - 39	0	444	1896 - 2305	1408	3020	17.1 - 21.0	7.2	24.4	2.1 - 6.9	-4.5	12.9	4 - 38	0	190
Encephalartos	cosmopolitan	spring rainfall; summer potential evaporation and relative humidity; winter minimum temperatures	550 - 850	271	1420	41 - 114	5	521	1734 - 2059	1361	2463	16.3 - 18.5	7.9	24.2	4.4 - 7.9	-4.2	12.9	40 - 107	5	199
Erythrina	cosmopolitan	summer rainfall, potential evaporation and relative humidity	600 - 900	12	1420	20 - 69	0	177	1709 - 2095	1169	2621	16.5 - 20.0	7.8	23.4	2.3 - 8.5	-4.9	13.0	20 - 69	0	169
Galium	cosmopolitan	spring and autumn potential evaporation and rainfall; winter water availability	400 - 800	62	1278	39 - 136	16	444	1791 - 2233	978	2866	14.0 - 16.7	5.9	19.8	-0.1 - 5.2	-5.4	10.5	29 - 61	7	189
Hermannia	cosmopolitan	winter rainfall, relative humidity and potential evaporation	250 - 600	12	1438	16 - 90	0	490	1928 - 2498	1116	3022	15.7 - 18.7	5.8	24.4	1.3 - 6.1	-5.4	13.4	11 - 52	0	195
Justicia	cosmopolitan	duration of frost; summer potential evaporation and relative humidity	400 - 750	29	1438	5 - 47	0	321	1856 - 2265	1482	2950	17.9 - 21.4	11.6	24.4	3.4 - 8.1	-2.2	12.9	5 - 42	0	158
Lamiaceae	cosmopolitan	winter rainfall, relative humidity and potential evaporation	400 - 800	12	1476	15 - 65	0	490	1851 - 2325	1000	3014	16.2 - 19.7	5.4	24.4	1.6 - 6.6	-5.9	12.9	13 - 49	0	190
Lentibulariaceae	cosmopolitan	mean annual rainfall; summer potential evaporation	550 - 900	88	1438	18 - 118	0	437	1761 - 2157	1291	2811	16.1 - 21.4	10.1	22.8	2.3 - 7.5	-3.6	12.9	16 - 63	0	176
Liliaceae	cosmopolitan	winter rainfall, relative humidity and potential evaporation	300 - 800	24	1420	38 - 118	0	508	1812 - 2402	784	2976	15.3 - 17.7	5.9	23.5	1..2 - 6.2	-5.5	12.9	22 - 69	0	205
Loranthaceae	cosmopolitan	duration of frost; geology; winter minimum temperatures	250 - 700	12	1943	3 - 45	0	417	1891 - 2422	1116	2954	17.4 - 20.8	8.6	24.5	3.3 - 7.9	-2.8	12.9	3 - 39	0	177
Lycium	cosmopolitan	summer rainfall; winter potential evaporation	200 - 500	12	1395	16 - 62	0	397	2151 - 2637	1542	3015	16.1 - 18.6	10.1	24.2	0.7 - 5.6	-4.6	12.9	10 - 39	0	143
Malvaceae	cosmopolitan	winter rainfall, relative humidity and potential evaporation	350 - 700	12	1566	10 - 56	0	490	1901 - 2392	1075	3022	16.5 - 20.3	5.8	24.4	2.0 - 6.7	-5.4	13.4	9 - 43	0	238
Nyctaginaceae	cosmopolitan	summer minimum temperatures; winter potential evaporation; duration of frost	350 - 600	12	1438	2 - 25	0	418	1978 - 2417	1514	2970	18.1 - 21.6	12.0	24.4	2.7 - 7.5	-3.9	13.4	2 - 25	0	185
Oxalis	cosmopolitan	winter rainfall, relative humidity and potential evaporation	200 - 700	12	1438	45 - 157	0	470	1901 - 2476	1075	3020	15.9 - 17.8	6.0	23.5	2.6 - 6.5	-5.2	12.4	16 - 61	0	202
Oxygonum	cosmopolitan	summer rainfall, potential evaporation and relative humidity	400 - 700	17	1395	3 - 23	0	414	1981 - 2690	1468	3006	17.9 - 21.0	11.1	23.0	1.7 - 6.9	-3.8	12.9	3 - 23	0	169

APPENDIX B – Modern taxa bioclimatic variables

Pollen Taxa	General ecological affinity*	Climatic Influences^	MAP (mm)			Total winter rainfall~ (mm)			Apan (mm)			MAT (°C)			MTCM (°C)			PDryQ (mm)		
			25 - 75% range	Min	Max	25 - 75% range	Min	Max	25 - 75% range	Min	Max	25 - 75% range	Min	Max	25 - 75% range	Min	Max	25 - 75% range	Min	Max
Oxygonum	cosmopolitan	summer rainfall, potential evaporation and relative humidity	400 - 700	17	1395	3 - 23	0	414	1981 - 2690	1468	3006	17.9 - 21.0	11.1	23.0	1.7 - 6.9	-3.8	12.9	3 - 23	0	169
Poaceae	cosmopolitan	winter rainfall; winter water availability	300 - 550	9	645	0 - 511	0	539	1075 - 3020	444	3037	6 - 19.8	5.4	26.6	1.6 - 6.7	-5.6	17.5	5 - 44	0	241
Polygala	cosmopolitan	winter rainfall and relative humidity; summer potential evaporation	350 - 800	25	1859	23 - 111	0	444	1802 - 2255	1075	3003	15.3 - 18.3	6.0	23.4	1.6 - 6.4	-5.2	12.9	20 - 73	0	233
Rhus	cosmopolitan	summer potential evaporation; spring rainfall; summer relative humidity	450 - 800	10	1516	21 - 72	0	508	1796 - 2247	1092	3020	15.6 - 18.9	5.9	24.6	1.2 - 6.2	-5.2	13.8	19 - 57	0	195
Rosaceae	cosmopolitan	winter rainfall, relative humidity and potential evaporation	450 - 850	131	1438	50 - 199	0	497	1763 - 2103	870	2889	14.3 - 16.8	6.0	23.4	1.6 - 6.5	-5.2	12.9	43 - 80	0	206
Scrophulariaceae	cosmopolitan	summer relative humidity and rainfall	200 - 600	12	1420	22 - 117	0	490	1918 - 2502	1452	2461	15.3 - 18.0	7.4	22.8	5.7 - 8.0	-4.9	11.4	40 - 78	0	130
Selaginella	cosmopolitan	winter rainfall, relative humidity and potential evaporation; duration of frost	500 - 850	112	1062	47 - 310	0	487	1812 - 2053	1116	2214	16.1 - 19.5	12.7	22.8	6.1 - 10.1	-2.4	12.9	47 - 103	17	160
Stercullariaceae	cosmopolitan	duration of frost and diurnal temperature range	350 - 600	115	1318	1 - 29	0	128	1893 - 2155	1639	2410	19.3 - 21.8	14.9	24.2	5.2 - 8.4	1.3	12.0	1 - 29	0	122
Tarchonanthus	cosmopolitan	summer rainfall	400 - 700	177	1420	16 - 54	0	397	1851 - 2483	1408	2995	16.7 - 19.1	9.5	22.8	0.7 - 6.2	-3.8	12.2	16 - 54	0	169
Verbenaceae	cosmopolitan	summer rainfall, potential evaporation and relative humidity	400 - 800	12	1438	7 - 31	0	267	1799 - 2136	1075	3015	16.7 - 20.0	6.0	24.4	1.6 - 6.6	-5.2	12.4	11 - 42	0	190
Vitaceae	cosmopolitan	summer rainfall, potential evaporation and relative humidity	550 - 900	38	1438	16 - 62	0	414	1799 - 2136	1075	2755	17.4 - 20.8	6.0	24.2	3.4 - 8.5	-5.2	13.4	16 - 62	0	195

***Using inferences from: Scott, 1982; Sugden and Meadows, 1990, Meadows and Sugden, 1991; Geldenhuys, 1992; Scott and Woodborne, 1994; 2007a, b; Baxter, 1996; 1997.**

^Derived from *MaxEnt* jacknife outcomes using Schulze (1997) climate variables as the baseline climate envelopes.

~Sum of June, July August mean rainfall

MAP = Mean annual precipitation

Apan = Mean annual potential evaporation

MAT = Mean annual temperature

MTCM = Mean temperature of coldest month

PDryQ = Precipitation of driest quarter

Taxa distributions data source: (SANBI, 2003)

Climate variables data sources: (Schulze, 1997; Hijmans et al., 2005)

APPENDIX C

PEARLY BEACH 1 GRAIN SIZE DATA

Sample ID	PB-25	PB-24	PB-23	PB-22	PB-21	PB-20	PB-19	PB-18	PB-17	PB-16	PB-15	PB-14	PB-13
Depth (cm)	10	20	30	40	50	60	70	80	90	100	110	120	130
Age (cal kBP)	0.20	0.45	1.61	3.15	4.70	6.25	7.79	9.45	11.13	12.82	13.31	13.73	14.13
Clay	0.58745	0.53047	3.61340	5.10861	4.58993	2.15281	3.64874	3.49406	2.97032	1.66726	0.93930	0.80108	0.76498
Silt	0.61355	0.75649	15.19180	21.36569	21.11856	9.81247	14.67634	18.11507	18.16774	3.15774	1.07796	0.78980	0.83975
Fine Sand	40.22885	25.61745	51.13222	46.78592	46.73023	42.10104	47.53857	51.87041	57.83278	53.94671	55.55373	51.78694	48.23821
Medium Sand	51.95313	59.22245	28.59235	25.03611	25.47344	39.80540	32.12927	25.30999	19.94648	39.93633	40.71376	44.97392	48.46729
Coarse Sand	6.61703	13.87314	1.47023	1.70367	2.08783	6.12828	2.00706	1.21048	1.08268	1.29194	1.71526	1.64827	1.68979
Mean	2.03762	1.73772	3.52360	3.93190	3.84951	2.86072	3.45599	3.67625	3.71612	2.37538	2.34039	2.27132	2.22914
Sorting	0.67147	0.77105	2.08685	2.38386	2.34566	1.83829	2.13718	2.11026	1.95433	0.92180	0.65361	0.57413	0.61223
Skewness	-0.16430	-0.06710	0.64347	0.48387	0.50059	0.50728	0.64408	0.63480	0.62165	0.27476	0.08653	-0.00748	0.03288
Kurtosis	1.15151	0.97835	1.16902	0.89477	0.89569	1.78143	1.24433	0.93930	0.88922	2.42129	1.49238	1.24374	1.27705

Sample ID	PB-12	PB-11	PB-10	PB-09	PB-08	PB-07	PB-06	PB-05	PB-04	PB-03	PB-02	PB-1
Depth (cm)	140	154	160	163	170	180	190	200	210	220	230	240
Age (cal kBP)	14.55	20.53	20.82	20.97	21.28	21.76	22.24	22.72	23.20	23.66	24.11	24.571
Clay	0.46838	0.41157	1.30295	0.61038	1.18994	0.81563	0.98678	1.21624	1.06412	1.13467	0.93359	1.20879
Silt	1.10518	0.36628	1.89375	0.80380	2.65591	1.29952	1.35500	1.80430	1.99511	2.48784	2.17560	3.20072
Fine Sand	11.59315	26.47320	74.01388	40.55166	25.02794	42.37732	49.99731	50.74476	44.95484	43.12845	42.53956	43.89519
Medium Sand	68.13242	66.24744	22.78945	56.07233	55.05991	44.59885	44.60183	44.27810	45.68290	45.37656	46.82042	49.65329
Coarse Sand	18.70087	6.50151	0.00000	1.96180	16.06630	10.90869	3.05907	1.95660	6.30304	7.87248	7.53083	2.04201
Mean	1.43182	1.84739	2.5917	2.12384	1.75501	2.00559	2.26051	2.30773	2.16248	2.12966	2.11187	2.21731
Sorting	0.69231	0.61489	0.61243	0.54151	1.11429	0.91473	0.75499	0.77493	0.88644	1.00837	0.94045	0.95061
Skewness	0.21556	-0.07161	0.34422	-0.02113	0.2206	-0.10345	0.05342	0.13518	0.04962	0.07491	0.04756	0.23545
Kurtosis	1.21256	0.99875	1.61228	1.16822	1.46968	1.08537	1.41538	1.53581	1.56426	1.67296	1.56055	2.04405

Grain size categories	
Clay	0 - 2 µm
Silt	2 - 20 µm
Fine Sand	20 - 200 µm
Medium Sand	200 - 500 µm
Coarse Sand	500 - 2000 µm

APPENDIX D

PEARLY BEACH 1 ABSOLUTE POLLEN, NON-POLLEN PALYNOMORPHS AND MICROSCOPIC CHARCOAL COUNTS

Sample ID	PB-47	PB-46	PB-45	PB-79	PB-44	PB-78	PB-43	PB-77	PB-42	PB-76	PB-41	PB-75	PB-40	PB-74	PB-39	PB-73	PB-38	PB-72	PB-37
Depth (cm)	15	20	25	27.5	30	32.5	35	37.5	40	42.5	45	47.5	50	52.5	55	57.5	60	62.5	65
Age (cal kBP)	0.32	0.45	0.83	1.22	1.61	1.99	2.38	2.77	3.15	3.54	3.93	4.32	4.70	5.09	5.48	5.86	6.25	6.64	7.02
Acacia	2	0	0	0		1	0		1			1	0	1		1	1		
Celastraceae	0	2	1	0		0	0		0			0	0	0		0	0		
Diospyros	2	1	2	1		1	1		3			3	1	0		0	2		
Dodonaea	13	6	0	0		0	0		0			0	0	0		0	0		
Encephalartos	0	0	2	0		1	1		2			1	1	0		0	0		
Euclea	9	4	3	2		5	1		2			3	0	2		1	2		
Grewia	1	1	0	2		0	0		0			0	0	0		0	0		
Ilex	0	1	0	0		0	1		0			0	0	0		0	0		
Lycium	0	0	2	0		0	0		0			0	0	0		0	0		
Myrica	11	1	2	4		2	2		3			3	5	8		1	4		
Myrsine	3	0	4	1		3	0		2			0	2	0		1	1		
Myrtaceae	3	0	3	0		0	0		0			0	0	0		0	0		
Olea	1	0	0	0		1	0		0			0	0	0		1	0		
Podocarpus	4	3	0	0		2	1		0			0	0	2		0	0		
Rhus	0	1	2	1		0	0		0			1	0	0		0	0		
Sapotaceae	3	2	0	0		0	0		0			0	0	0		0	0		
Vitaceae	0	0	0	0		0	0		0			0	0	0		0	0		
Zygophyllaceae	0	0	0	0		0	0		0			0	0	0		0	0		
Proteaceae	130	61	66	49		37	29		26			15	18	21		9	32		
Ericaceae	10	4	10	13		8	15		9			12	3	15		7	10		
Cliffortia	37	5	5	4		4	9		12			9	7	14		3	31		
Bruniaceae	0	1	4	1		5	0		0			0	0	0		0	0		
Stoebe-type	22	8	35	37		40	33		34			23	26	17		4	29		
Asteraceae HS	47	39	122	117		144	64		106			188	43	82		41	101		
Artemisia	2	0	0	5		8	0		1			1	2	2		2	3		
Pentzia-type	2	3	5	2		1	2		0			3	2	2		0	4		
Euphorbiaceae undif	7	2	5	8		5	4		1			8	4	5		4	8		
Euphorbia	3	1	5	3		3	3		0			1	0	4		5	2		
Clutia	1	0	5	6		0	4		4			4	2	5		1	3		
ChenoAm-type	19	14	4	3		10	3		5			5	1	7		5	9		

Sample ID	PB-47	PB-46	PB-45	PB-79	PB-44	PB-78	PB-43	PB-77	PB-42	PB-76	PB-41	PB-75	PB-40	PB-74	PB-39	PB-73	PB-38	PB-72	PB-37
Depth (cm)	15	20	25	27.5	30	32.5	35	37.5	40	42.5	45	47.5	50	52.5	55	57.5	60	62.5	65
Age (cal kBP)	0.32	0.45	0.83	1.22	1.61	1.99	2.38	2.77	3.15	3.54	3.93	4.32	4.70	5.09	5.48	5.86	6.25	6.64	7.02
Crassulaceae	7	1	11	6		3	3		9			2	0	9		2	6		
Ruschia	6	7	8	0		2	7		3			0	0	3		0	7		
Aizoaceae	4	1	7	5		3	4		3			0	3	2		0	2		
Aloe-type	0	0	0	1		0	0		2			0	0	0		0	0		
Geraniaceae	4	2	2	4		3	4		7			4	1	5		3	5		
Brassicaceae	0	0	0	0		1	0		0			0	1	0		0	0		
Anthospermum-type	0	0	2	2		0	1		0			0	0	1		0	4		
Apiaceae	1	0	1	1		0	1		0			4	0	0		0	1		
Fabaceae	4	2	2	4		7	5		3			4	3	3		2	3		
Rhamnaceae	2	2	1	0		0	1		0			0	0	0		0	1		
Rutaceae	3	1	1	5		5	2		4			0	0	5		1	1		
Santalaceae	2	1	0	2		0	1		0			4	0	0		0	0		
Scroph-type	3	1	4	4		3	0		2			3	0	2		0	1		
Thymelaeaceae	3	5	2	5		2	2		0			5	3	6		0	2		
Passerina	2	2	1	0		2	3		4			1	0	1		1	0		
Galium	1	0	0	0		0	0		1			0	0	0		0	0		
Canthium	6	2	2	1		2	3		5			5	9	0		3	7		
Malvaceae	3	1	4	2		2	0		1			1	0	1		0	3		
Onagraceae	0	0	1	0		1	0		0			0	0	1		0	0		
Oxygonum	0	0	0	0		0	0		0			0	0	1		0	0		
Polygonum	0	0	1	0		1	0		1			2	1	2		0	0		
Selaginaceae	0	0	0	0		0	0		2			0	0	0		0	0		
Urticaceae	0	1	1	0		0	4		0			0	0	0		0	0		
Verbenaceae	0	0	0	2		0	0		0			0	0	0		0	0		
Campanulaceae	0	0	0	0		0	0		0			1	0	2		0	0		
Caryophyllaceae	0	0	0	0		0	0		0			0	0	0		0	0		
Polygala	1	1	1	1		1	0		0			0	2	0		1	1		
Cardiospermum	2	0	4	0		0	0		0			0	1	0		0	3		
Rosaceae	2	0	0	0		0	0		1			3	2	1		1	2		
Solanum	2	1	0	1		0	0		0			1	0	1		0	1		

Sample ID	PB-47	PB-46	PB-45	PB-79	PB-44	PB-78	PB-43	PB-77	PB-42	PB-76	PB-41	PB-75	PB-40	PB-74	PB-39	PB-73	PB-38	PB-72	PB-37
Depth (cm)	15	20	25	27.5	30	32.5	35	37.5	40	42.5	45	47.5	50	52.5	55	57.5	60	62.5	65
Age (cal kBP)	0.32	0.45	0.83	1.22	1.61	1.99	2.38	2.77	3.15	3.54	3.93	4.32	4.70	5.09	5.48	5.86	6.25	6.64	7.02
Araliaceae	0	0	0	0		0	0		0			0	0	0		0	0		
Ascelepidaceae	0	0	0	0		0	0		0			0	0	0		0	0		
Orchidaceae	0	0	0	0		0	0		0			0	0	1		0	0		
Combretaceae	0	0	0	0		0	0		1			0	0	1		0	0		
Loranthaceae	0	0	0	0		0	0		0			0	0	0		0	0		
Sterculiaceae	0	0	0	0		1	0		0			0	1	1		0	0		
Acan. Tricolporate	0	0	0	4		0	0		0			0	0	0		0	1		
Acan. Diporate	0	0	0	3		0	0		0			0	0	0		0	0		
Justicia-type	5	1	1	5		0	2		0			1	1	1		3	3		
Oxalis	0	0	0	0		0	0		0			0	0	0		0	0		
Plumbaginaceae	0	0	0	0		0	0		0			0	0	1		0	0		
Boraginaceae	0	0	0	0		0	0		0			0	0	0		0	0		
Bignoniaceae	0	0	0	0		0	0		0			0	0	0		0	1		
Linaceae	0	1	0	1		0	0		0			0	0	3		0	1		
Lamiaceae	0	0	0	0		0	0		0			0	0	0		0	0		
Convolvulaceae	2	1	0	0		0	1		2			2	1	0		0	0		
Hermannia	0	0	0	0		0	0		0			0	0	0		0	1		
Lentibulariaceae	0	0	0	0		0	0		0			0	0	0		0	0		
Haemodoraceae	0	0	0	0		0	0		0			0	0	0		0	0		
Gentianaceae	2	3	2	3		7	1		3			8	2	3		0	2		
Potamogeton	0	0	0	0		0	0		0			0	0	0		0	0		
Ranunculaceae	0	0	0	0		0	0		0			0	1	0		0	0		
Blechnaceae	0	0	2	4		2	1		0			1	0	2		1	3		
Plantago	1	0	0	1		0	3		3			0	0	0		0	4		
Aponogeton	3	3	3	4		6	0		3			0	4	1		0	1		
Haloragaceae	1	1	4	1		4	5		5			7	1	7		2	8		
Typha	1	3	0	0		3	2		6			3	0	0		0	2		
Scabiosa	0	0	0	0		0	0		0			0	0	0		0	0		
Gunneraceae	0	0	0	3		0	0		0			0	0	0		0	0		
Nymphaea	0	0	0	0		0	0		0			0	0	0		0	0		

Sample ID	PB-47	PB-46	PB-45	PB-79	PB-44	PB-78	PB-43	PB-77	PB-42	PB-76	PB-41	PB-75	PB-40	PB-74	PB-39	PB-73	PB-38	PB-72	PB-37
Depth (cm)	15	20	25	27.5	30	32.5	35	37.5	40	42.5	45	47.5	50	52.5	55	57.5	60	62.5	65
Age (cal kBP)	0.32	0.45	0.83	1.22	1.61	1.99	2.38	2.77	3.15	3.54	3.93	4.32	4.70	5.09	5.48	5.86	6.25	6.64	7.02
Araceae	0	0	0	0		0	0		0			0	0	0		0	1		
Juncaceae	1	0	2	1		1	4		1			1	1	2		2	4		
Liliaceae	5	17	13	11		12	8		8			7	11	1		6	17		
Iridaceae	7	7	6	29		11	13		8			51	3	12		2	6		
Amaryllidaceae	1	1	0	4		1	1		0			1	2	1		0	1		
Cyperaceae	17	42	31	20		79	30		48			38	36	41		36	36		
Restionaceae	25	38	52	34		16	41		67			31	51	34		23	45		
Poaceae	33	18	30	52		28	35		46			25	28	37		11	63		
Unknown Type B	0	0	0	0		0	0		0			0	0	2		0	0		
Unknown Tetrad 1	0	0	0	0		0	0		0			0	0	0		0	0		
Unknown Psilate Tricolporate	0	0	0	2		0	0		0			0	0	0		0	0		
Unidentifiable	1	1	1	1		1	1		0			1	2	1		0	0		
Broken	5	7	9	9		7	5		5			1	11	6		4	8		
Unknown	0	1	1	3		2	0		1			1	1	1		0	0		
Total Pollen	500	336	500	500		500	367		466			500	300	392		190	500		
Pollen Concentration	4608	2757	4851	6774		8249	7418		4116			10749	4987	11298		15331	10243		
Monolete	27	14	32	29		16	12		5			14	18	5		6	22		
Trilete	4	2	15	6		9	12		11			5	8	6		2	8		
Ophioglossum	0	0	0	1		0	0		0			0	1	0		0	0		
Mohria	1	0	0	0		0	0		0			0	0	0		0	0		
Riccia	0	0	0	0		0	0		0			0	1	0		0	0		
Pellaea	0	0	0	2		0	0		1			0	0	1		0	0		
Pseudoschizaea	0	0	0	0		0	0		0			0	0	0		0	0		
Debarya glytosperma	0	1	0	1		0	1		2			0	0	0		0	3		
Glomus	0	0	0	2		0	0		1			0	0	0		0	1		
10 - 50 um	3664	1938	2696	4744		4292	1145		1319			1701	1059	1488		799	754		
50 - 100 um	21	22	24	70		59	19		18			42	15	43		18	0		
>100 um	0	0	0	7		0	2		2			2	1	2		1	0		
Total Charcoal	3685	1960	2720	4821		4351	1166		1339			1745	1075	1533		818	754		
Charcoal Concentration	33963	16080	26392	65311		71787	23568		11828			37513	17871	44183		66005	15447		

Sample ID	PB-36	PB-35	PB-34	PB-33	PB-32	PB-71	PB-31	PB-70	PB-30	PB-69	PB-29	PB-68	PB-28	PB-67	PB-27	PB-66	PB-26	PB-25	PB-65
Depth (cm)	70	75	80	85	90	92.5	95	97.5	100	102.5	105	107.5	110	112.5	115	117.5	120	125	127.5
Age (cal kBP)	7.80	8.60	9.45	10.29	11.13	11.55	11.97	12.40	12.82	12.99	13.09	13.20	13.30	13.41	13.51	13.62	13.73	13.92	14.02
Acacia	0						1	0	0	1	1	0	1	0	0	0	0	0	0
Celastraceae	0						2	0	1	0	2	0	1	0	1	0	0	1	0
Diospyros	0						0	0	0	0	1	1	0	0	2	1	1	2	2
Dodonaea	0						2	0	0	0	4	0	2	0	7	0	8	14	14
Encephalartos	0						0	0	0	0	0	0	0	0	0	1	0	0	1
Euclea	1						0	0	1	0	1	0	2	2	4	2	7	4	1
Grewia	0						1	1	0	0	1	0	0	0	1	1	1	0	0
Ilex	1						1	0	0	0	0	0	0	0	0	0	0	0	0
Lycium	0						0	0	0	0	1	0	0	0	0	0	0	0	0
Morella	1						15	7	3	3	3	5	5	2	6	14	5	16	14
Myrsine	1						0	1	0	1	2	0	1	1	1	0	2	1	0
Myrtaceae	0						0	2	0	0	1	0	0	0	0	0	0	0	0
Olea	0						0	2	0	0	0	0	0	0	0	1	0	0	0
Podocarpus	2						1	0	1	0	0	0	0	0	0	0	0	2	0
Rhus	0						0	0	0	1	0	0	0	0	0	1	0	1	1
Sapotaceae	0						0	0	0	0	0	0	0	0	0	0	0	0	0
Vitaceae	0						0	0	0	0	0	0	0	0	0	0	0	0	0
Zygophyllaceae	0						0	0	0	0	0	0	0	0	0	0	0	0	0
Proteaceae	4						19	8	11	11	35	11	12	13	32	42	50	52	26
Ericaceae	4						9	24	7	6	9	21	11	11	19	38	38	16	29
Cliffortia	11						26	15	15	9	30	11	17	3	24	34	21	26	33
Bruniaceae	0						0	0	2	1	1	0	0	0	0	0	1	1	0
Stoebe-type	13						53	20	11	17	30	18	18	8	26	35	16	39	19
Asteraceae HS	32						38	23	21	11	77	19	19	11	48	61	49	38	71
Artemisia	1						3	2	3	0	5	1	1	3	2	5	5	4	1
Pentzia-type	1						0	0	1	0	0	0	1	0	0	1	1	1	3
Euphorbiaceae undif	2						10	14	9	7	7	9	5	3	6	17	5	13	11
Euphorbia	0						4	6	6	2	4	5	1	2	4	6	4	4	5
Clutia	0						11	2	4	0	22	4	9	4	10	12	10	2	4
ChenoAm-type	0						1	5	0	3	4	1	0	2	3	2	7	9	1

Sample ID	PB-36	PB-35	PB-34	PB-33	PB-32	PB-71	PB-31	PB-70	PB-30	PB-69	PB-29	PB-68	PB-28	PB-67	PB-27	PB-66	PB-26	PB-25	PB-65
Depth (cm)	70	75	80	85	90	92.5	95	97.5	100	102.5	105	107.5	110	112.5	115	117.5	120	125	127.5
Age (cal kBP)	7.80	8.60	9.45	10.29	11.13	11.55	11.97	12.40	12.82	12.99	13.09	13.20	13.30	13.41	13.51	13.62	13.73	13.92	14.02
Crassulaceae	4						5	0	5	1	3	0	0	1	0	4	2	6	6
Ruschia	2						2	2	9	0	10	0	6	0	5	2	3	3	0
Aizoaceae	1						8	2	3	2	6	2	4	1	4	5	6	4	4
Aloe-type	0						0	0	0	0	0	0	0	0	0	0	0	0	0
Geraniaceae	3						4	3	1	1	1	0	1	0	3	1	0	0	2
Brassicaceae	1						1	0	1	0	0	0	0	0	3	0	2	0	0
Anthospermum-type	0						3	5	1	0	5	2	1	0	4	8	5	13	4
Apiaceae	0						2	0	0	1	0	0	0	0	0	3	1	1	0
Fabaceae	0						6	5	2	2	3	0	1	4	4	5	7	0	5
Rhamnaceae	0						0	0	0	0	1	0	0	0	0	0	3	0	0
Rutaceae	0						0	0	1	1	0	1	0	1	1	1	4	0	3
Santalaceae	0						1	0	0	0	1	0	1	0	2	0	1	0	0
Scroph-type	0						4	2	0	1	2	0	1	0	4	1	4	3	3
Thymelaeaceae	2						2	5	1	3	3	2	1	2	3	2	4	1	6
Passerina	1						1	0	3	1	1	2	1	0	1	3	2	2	1
Galium	0						1	0	0	0	0	0	1	0	0	0	0	2	0
Canthium	3						8	2	2	5	6	10	2	0	2	7	9	8	3
Malvaceae	0						1	2	2	0	1	1	0	2	0	5	0	1	2
Onagraceae	1						0	0	0	0	0	0	0	0	1	1	1	0	0
Oxygonum	0						0	0	0	0	0	0	0	0	0	0	0	0	0
Polygonum	0						0	0	1	1	0	0	1	0	0	0	1	0	0
Selaginaceae	0						0	1	0	0	0	1	1	0	0	0	0	0	0
Urticaceae	0						0	0	0	0	0	0	0	0	3	0	0	0	0
Verbenaceae	0						0	0	1	0	0	0	0	0	0	0	0	2	0
Campanulaceae	0						0	0	0	0	0	0	0	0	0	0	0	0	0
Caryophyllaceae	0						0	0	0	0	0	0	0	0	0	0	0	0	0
Polygala	0						0	0	0	0	1	0	1	0	2	1	0	1	1
Cardiospermum	0						0	2	0	0	0	0	0	0	3	0	2	7	1
Rosaceae	0						5	3	0	1	6	0	1	0	0	0	0	0	5
Solanum	0						0	0	0	0	0	0	0	0	0	0	0	0	0

Sample ID	PB-36	PB-35	PB-34	PB-33	PB-32	PB-71	PB-31	PB-70	PB-30	PB-69	PB-29	PB-68	PB-28	PB-67	PB-27	PB-66	PB-26	PB-25	PB-65
Depth (cm)	70	75	80	85	90	92.5	95	97.5	100	102.5	105	107.5	110	112.5	115	117.5	120	125	127.5
Age (cal kBP)	7.80	8.60	9.45	10.29	11.13	11.55	11.97	12.40	12.82	12.99	13.09	13.20	13.30	13.41	13.51	13.62	13.73	13.92	14.02
Araliaceae	0						0	0	0	0	0	0	0	0	0	0	0	0	0
Ascelepidaceae	0						0	0	0	0	0	0	0	0	0	0	0	0	0
Orchidaceae	0						0	1	1	0	1	0	0	0	3	0	0	1	0
Combretaceae	0						0	0	0	0	0	0	0	0	0	0	0	0	0
Loranthaceae	0						0	0	0	0	0	0	1	0	0	0	0	0	0
Sterculiaceae	0						0	1	0	1	0	0	0	1	0	0	0	0	0
Acan. Tricolporate	0						0	0	0	0	0	0	0	0	0	1	0	0	0
Acan. Diporate	0						0	0	0	0	0	0	0	0	0	0	0	0	0
Justicia-type	1						11	3	0	3	2	2	0	0	2	6	2	1	5
Oxalis	0						5	0	3	1	0	0	1	0	0	0	2	1	0
Plumbaginaceae	0						0	0	0	0	0	0	0	0	0	0	0	0	0
Boraginaceae	0						0	0	0	0	0	0	0	0	0	0	0	0	0
Bignoniaceae	0						0	0	0	0	0	0	0	0	0	0	0	0	2
Linaceae	0						0	2	0	0	0	0	1	0	1	2	2	0	0
Lamiaceae	0						0	0	1	0	0	0	0	0	6	0	0	0	1
Convolvulaceae	0						0	0	0	0	0	0	0	0	0	0	1	0	1
Hermannia	0						0	0	0	0	0	0	0	0	0	0	0	0	0
Lentibulariaceae	0						0	0	0	0	0	0	0	0	0	0	0	0	0
Haemodoraceae	0						0	0	0	0	0	0	0	0	0	0	0	0	0
Gentianaceae	1						4	0	3	3	5	0	1	0	3	7	4	0	2
Potamogeton	0						0	0	0	0	0	0	0	0	0	0	0	0	0
Ranunculaceae	0						0	0	0	0	0	0	0	0	0	0	0	0	0
Blechnaceae	8						1	0	0	0	1	0	0	0	2	0	2	0	2
Plantago	0						2	2	2	0	4	0	0	0	1	6	0	2	2
Aponogeton	2						3	0	4	0	2	0	3	0	0	0	4	5	0
Haloragaceae	1						3	4	6	2	6	5	3	2	13	6	6	1	6
Typha	1						1	0	1	1	7	0	0	0	2	0	0	0	1
Scabiosa	0						0	0	0	0	0	0	1	0	0	0	1	0	0
Gunneraceae	0						0	0	0	0	0	0	0	0	1	0	0	2	0
Nymphaea	0						0	0	0	0	0	0	0	0	0	0	0	0	0

Sample ID	PB-36	PB-35	PB-34	PB-33	PB-32	PB-71	PB-31	PB-70	PB-30	PB-69	PB-29	PB-68	PB-28	PB-67	PB-27	PB-66	PB-26	PB-25	PB-65
Depth (cm)	70	75	80	85	90	92.5	95	97.5	100	102.5	105	107.5	110	112.5	115	117.5	120	125	127.5
Age (cal kBP)	7.80	8.60	9.45	10.29	11.13	11.55	11.97	12.40	12.82	12.99	13.09	13.20	13.30	13.41	13.51	13.62	13.73	13.92	14.02
Araceae	0						0	0	0	0	0	0	0	0	0	0	0	0	0
Juncaceae	0						1	0	2	0	7	2	1	0	2	0	3	4	0
Liliaceae	16						16	5	7	1	6	5	5	4	6	9	8	21	13
Iridaceae	5						20	2	7	2	3	2	2	3	2	2	1	4	2
Amaryllidaceae	1						1	0	0	1	0	0	0	0	0	1	0	4	0
Cyperaceae	17						66	51	34	24	40	19	27	23	50	40	33	43	63
Restionaceae	28						56	17	26	9	38	13	28	5	58	37	67	56	54
Poaceae	40						49	20	24	17	66	22	30	18	96	48	67	43	55
Unknown Type B	0						0	0	0	0	0	0	0	0	0	0	0	0	0
Unknown Tetrad 1	0						0	0	0	0	0	0	0	0	0	0	0	0	0
Unknown Psilate Tricolporate	0						0	0	0	0	0	0	0	0	0	2	1	0	0
Unidentifiable	1						1	0	0	0	5	1	0	0	0	1	0	1	0
Broken	6						9	1	5	5	16	6	0	3	11	7	8	11	8
Unknown	0						0	0	0	1	0	1	0	0	0	2	0	0	1
Total Pollen	220						500	275	255	164	500	205	234	135	500	500	500	500	500
Pollen Concentration	4965						8173	12106	23348	14895	22353	27629	13835	8208	18020	11494	13251	4883	11655
Monolete	7						9	1	8	2	25	3	4	0	8	14	5	6	8
Trilete	4						14	4	10	2	6	0	8	0	8	3	5	6	4
Ophioglossum	0						0	0	0	0	0	0	0	0	0	0	0	0	0
Mohria	0						1	0	0	0	0	0	0	0	0	0	0	0	0
Riccia	1						0	0	0	0	0	0	0	0	0	0	1	0	0
Pellaea	0						0	0	0	0	0	0	0	0	0	0	0	0	0
Pseudoschizaea	0						0	0	0	0	0	0	0	0	0	0	0	0	0
Debarya glytosperma	0						3	0	0	1	5	0	1	0	5	0	1	2	0
Glomus	0						0	0	0	0	0	0	0	0	0	1	0	2	0
10 - 50 um	73						211	427	202	142	334	90	592	355	715	1732	1070	819	1897
50 - 100 um	1						0	0	0	0	12	2	27	11	28	85	35	3	45
>100 um	0						0	0	0	0	0	0	0	0	3	17	0	0	2
Total Charcoal	74						211	427	202	142	346	92	619	366	746	1834	1105	822	1944
Charcoal Concentration	1670						3449	18798	18495	12897	15468	12399	36598	22253	26886	42159	29285	8028	45314

Sample ID	PB-24	PB-64	PB-23	PB-22	PB-21	PB-80	PB-20	PB-19	PB-18	PB-17	PB-63	PB-16	PB-62	PB-15	PB-61	PB-14	PB-60
Depth (cm)	**130**	**132.5**	**135**	**140**	**145**	**148**	**150**	**155**	**160**	**165**	**166**	**170**	**172.5**	**175**	**177.5**	**180**	**182.5**
Age (cal kBP)	**14.13**	**14.23**	**14.34**	**14.55**	**14.76**	**20.25**	**20.34**	**20.58**	**20.82**	**21.06**	**21.11**	**21.28**	**21.40**	**21.52**	**21.64**	**21.76**	**21.88**
Acacia	2	1	0	0		0	0		0	0	1	0	2	2	0	1	0
Celastraceae	2	1	0	0		0	0		0	0	0	3	0	0	2	0	0
Diospyros	3	2	1	2		2	0		3	1	0	2	2	2	4	1	1
Dodonaea	6	0	4	0		0	0		0	0	0	4	2	12	24	10	2
Encephalartos	0	0	1	0		0	0		0	0	2	0	1	0	2	0	0
Euclea	1	3	3	3		8	0		4	5	2	2	4	8	4	5	13
Grewia	0	1	0	0		0	0		2	0	1	2	2	1	0	1	0
Ilex	0	0	0	1		0	0		0	0	0	0	0	0	0	0	0
Lycium	0	0	0	0		0	0		0	0	0	0	0	0	0	0	0
Morella	25	5	17	10		12	1		7	3	1	5	2	1	16	2	2
Myrsine	0	0	0	1		0	0		0	0	0	0	0	2	0	2	0
Myrtaceae	0	0	0	0		1	0		0	1	0	0	0	1	0	1	0
Olea	0	0	0	0		0	0		0	0	0	1	0	3	0	0	0
Podocarpus	3	0	0	1		0	0		0	0	0	0	0	0	0	0	1
Rhus	0	1	0	1		0	0		0	0	1	0	0	0	1	0	1
Sapotaceae	0	0	0	0		0	0		0	0	0	0	0	0	0	0	0
Vitaceae	0	0	0	0		0	0		0	0	0	1	0	0	0	0	0
Zygophyllaceae	0	0	0	0		0	0		0	1	0	0	0	0	0	0	0
Proteaceae	36	10	15	17		19	5		31	17	29	27	20	19	18	3	6
Ericaceae	30	12	23	11		32	4		21	42	31	43	39	34	10	24	31
Cliffortia	33	5	23	16		41	5		17	15	16	13	15	18	24	14	12
Bruniaceae	0	0	0	1		0	0		0	0	0	0	3	1	4	2	0
Stoebe-type	38	27	22	21		36	9		28	30	42	31	24	34	20	30	46
Asteraceae HS	30	64	30	30		61	10		41	89	78	60	92	72	72	54	84
Artemisia	2	4	7	1		0	0		2	3	1	3	3	7	3	1	0
Pentzia-type	1	2	0	1		4	0		2	2	1	3	3	4	3	4	1
Euphorbiaceae undif	10	5	7	6		7	2		4	9	12	8	11	10	9	13	2
Euphorbia	3	0	2	5		6	1		8	2	3	4	4	7	6	6	0
Clutia	2	4	2	2		8	1		2	16	17	19	8	8	8	4	9
ChenoAm-type	2	5	4	4		4	1		4	4	6	3	5	3	1	5	4

Sample ID	PB-24	PB-64	PB-23	PB-22	PB-21	PB-80	PB-20	PB-19	PB-18	PB-17	PB-63	PB-16	PB-62	PB-15	PB-61	PB-14	PB-60
Depth (cm)	130	132.5	135	140	145	148	150	155	160	165	166	170	172.5	175	177.5	180	182.5
Age (cal kBP)	14.13	14.23	14.34	14.55	14.76	20.25	20.34	20.58	20.82	21.06	21.11	21.28	21.40	21.52	21.64	21.76	21.88
Crassulaceae	1	4	2	0		4	1		8	6	12	2	3	6	7	71	6
Ruschia	2	0	4	1		1	0		9	3	2	0	1	6	9	4	0
Aizoaceae	2	2	1	2		0	0		10	5	7	11	1	7	4	4	8
Aloe-type	0	0	1	0		0	0		2	0	0	0	0	0	0	0	0
Geraniaceae	1	0	0	0		1	0		0	2	2	4	0	1	0	1	2
Brassicaceae	0	0	1	0		3	0		0	0	2	0	1	0	1	0	1
Anthospermum-type	2	1	5	5		13	0		12	3	1	3	1	7	3	8	8
Apiaceae	1	0	0	0		0	0		2	0	0	1	0	0	3	0	0
Fabaceae	4	3	9	2		8	0		1	4	10	3	8	3	14	9	5
Rhamnaceae	4	0	0	0		0	0		2	4	0	0	1	1	0	0	0
Rutaceae	1	0	2	1		8	2		5	1	4	2	5	9	3	5	0
Santalaceae	3	1	0	0		1	0		3	7	3	2	2	1	0	0	0
Scroph-type	3	0	0	3		3	0		0	2	1	3	1	1	0	4	0
Thymelaeaceae	4	1	2	1		5	2		5	0	1	4	5	4	1	3	6
Passerina	3	1	0	0		1	1		1	2	3	1	4	0	1	1	3
Galium	0	0	0	1		0	0		0	3	0	3	0	0	0	0	0
Canthium	6	3	6	1		3	5		5	2	2	2	4	8	2	0	4
Malvaceae	2	0	3	2		1	1		0	0	3	4	0	0	3	1	1
Onagraceae	0	0	0	2		0	0		0	0	0	0	0	0	0	0	1
Oxygonum	0	0	0	0		0	0		0	0	0	0	0	0	0	0	0
Polygonum	0	0	0	0		0	0		0	0	1	0	0	0	0	0	0
Selaginaceae	1	0	0	0		0	0		0	1	0	0	5	0	0	1	0
Urticaceae	2	0	5	0		0	0		0	0	0	0	0	0	0	0	0
Verbenaceae	0	0	0	0		0	0		0	0	0	0	0	0	0	0	0
Campanulaceae	0	0	0	0		0	0		0	0	0	0	0	0	0	0	0
Caryophyllaceae	0	0	0	0		0	0		3	0	0	0	0	0	0	0	0
Polygala	1	1	0	0		0	0		1	0	0	0	2	0	2	1	2
Cardiospermum	3	0	3	0		0	0		0	0	0	2	0	1	0	1	0
Rosaceae	0	0	0	0		0	0		0	1	4	0	0	5	0	4	0
Solanum	0	0	0	0		1	0		0	1	0	0	0	1	0	1	0

Sample ID	PB-24	PB-64	PB-23	PB-22	PB-21	PB-80	PB-20	PB-19	PB-18	PB-17	PB-63	PB-16	PB-62	PB-15	PB-61	PB-14	PB-60
Depth (cm)	130	132.5	135	140	145	148	150	155	160	165	166	170	172.5	175	177.5	180	182.5
Age (cal kBP)	14.13	14.23	14.34	14.55	14.76	20.25	20.34	20.58	20.82	21.06	21.11	21.28	21.40	21.52	21.64	21.76	21.88
Araliaceae	0	0	0	0		0	0		1	0	0	0	0	0	0	0	1
Ascelepidaceae	0	0	1	0		0	0		0	0	0	0	0	0	0	2	0
Orchidaceae	1	1	0	0		0	0		1	2	0	0	1	1	0	3	2
Combretaceae	0	0	0	0		0	0		0	0	2	0	0	0	0	0	0
Loranthaceae	0	0	0	0		0	0		0	0	0	0	0	0	0	0	0
Sterculiaceae	0	0	0	0		0	0		0	0	0	0	0	0	0	0	0
Acan. Tricolporate	0	0	0	0		0	0		0	0	0	0	0	0	0	0	0
Acan. Diporate	0	0	0	0		0	0		0	0	0	0	2	0	0	0	0
Justicia-type	4	0	4	0		5	2		0	0	7	2	1	5	1	3	0
Oxalis	2	0	0	1		0	0		0	0	0	3	0	0	0	0	0
Plumbaginaceae	0	0	0	0		0	0		0	0	0	0	0	0	0	0	0
Boraginaceae	0	0	0	0		0	0		0	0	0	0	0	0	0	0	0
Bignoniaceae	0	0	0	1		0	0		0	0	1	0	0	0	0	0	1
Linaceae	0	0	2	2		0	0		0	1	1	0	3	0	2	2	6
Lamiaceae	2	0	5	2		0	0		0	1	0	4	1	0	2	0	0
Convolvulaceae	1	1	0	0		0	0		0	1	0	0	0	1	1	9	6
Hermannia	0	0	0	0		0	1		0	0	0	0	0	0	0	0	0
Lentibulariaceae	0	0	0	1		0	0		0	0	0	0	0	0	0	0	0
Haemodoraceae	0	0	0	0		0	0		0	0	0	0	0	0	0	0	0
Gentianaceae	1	1	3	1		3	0		0	3	4	5	3	1	0	0	0
Potamogeton	0	0	0	0		0	0		0	0	0	0	0	0	0	0	0
Ranunculaceae	1	0	0	0		0	0		0	0	0	0	0	0	0	0	0
Blechnaceae	1	2	2	0		0	0		3	2	0	1	2	4	2	2	0
Plantago	0	5	2	2		5	0		8	0	1	0	0	2	5	0	1
Aponogeton	2	2	5	6		2	0		1	1	0	1	2	1	0	1	3
Haloragaceae	5	4	14	12		61	5		15	6	1	6	2	0	9	0	0
Typha	1	1	5	4		0	2		3	3	3	5	6	3	1	1	0
Scabiosa	0	0	0	0		1	0		1	0	0	0	0	0	0	1	2
Gunneraceae	0	1	0	0		0	0		1	0	4	0	0	0	0	0	0
Nymphaea	0	0	0	0		0	0		0	0	1	0	0	0	0	0	0

Sample ID	PB-24	PB-64	PB-23	PB-22	PB-21	PB-80	PB-20	PB-19	PB-18	PB-17	PB-63	PB-16	PB-62	PB-15	PB-61	PB-14	PB-60
Depth (cm)	130	132.5	135	140	145	148	150	155	160	165	166	170	172.5	175	177.5	180	182.5
Age (cal kBP)	14.13	14.23	14.34	14.55	14.76	20.25	20.34	20.58	20.82	21.06	21.11	21.28	21.40	21.52	21.64	21.76	21.88
Araceae	0	0	0	0		0	0		0	1	0	0	0	0	0	0	0
Juncaceae	6	2	3	4		2	1		5	4	1	4	2	3	0	4	0
Liliaceae	7	4	12	9		8	1		12	5	18	5	7	13	9	3	8
Iridaceae	8	2	8	2		5	0		2	3	6	6	5	1	1	0	19
Amaryllidaceae	3	1	5	0		2	0		0	0	2	0	1	0	0	0	0
Cyperaceae	40	21	71	39		35	17		19	70	67	52	78	34	91	40	33
Restionaceae	62	5	86	51		23	23		102	40	27	48	36	54	29	53	74
Poaceae	63	28	58	29		42	13		70	63	44	77	49	44	56	58	70
Unknown Type B	0	0	0	0		0	0		0	0	0	0	0	0	0	0	0
Unknown Tetrad 1	0	0	0	1		0	0		0	0	0	0	0	7	0	7	0
Unknown Psilate Tricolporate	0	2	0	0		1	0		2	0	1	0	3	0	0	0	1
Unidentifiable	2	0	0	0		3	0		0	0	0	0	0	2	0	2	4
Broken	12	6	9	5		8	8		9	7	6	0	8	14	7	7	9
Unknown	1	1	0	0		0	0		0	0	1	0	2	0	0	0	0
Total Pollen	500	259	500	327		500	124		500	500	500	500	500	500	500	500	502
Pollen Concentration	6057	3023	2843	1737		13140	1857		33156	32202	22640	19935	17598	32635	24562	11220	12270
Monolete	18	9	13	8		23	10		27	6	7	0	7	8	11	15	34
Trilete	5	5	18	7		15	4		11	6	1	3	3	9	2	10	24
Ophioglossum	0	0	0	0		0	0		0	0	0	0	0	0	0	0	0
Mohria	0	0	0	0		0	0		0	0	0	0	0	0	0	1	0
Riccia	0	1	1	0		0	1		1	0	1	0	2	0	0	0	0
Pellaea	0	1	1	0		0	0		0	0	0	0	0	0	0	0	1
Pseudoschizaea	0	0	1	1		0	0		0	0	0	0	0	0	0	0	0
Debarya glytosperma	0	0	3	0		4	0		0	1	0	1	4	0	0	3	3
Glomus	0	0	0	0		0	0		1	0	0	0	0	4	0	2	0
10 - 50 um	1840	2856	781	251		2884	325		636	55	791	201	705	37	1800	1008	5546
50 - 100 um	47	244	0	0		139	0		23	0	5	0	6	0	104	36	320
>100 um	0	9	0	0		0	0		0	0	1	0	0	0	7	0	12
Total Charcoal	1887	3109	781	251		3023	325		659	55	797	201	711	37	1911	1044	5878
Charcoal Concentration	22858	36287	4440	1333		79443	4866		43699	3542	36088	8014	25024	2415	93878	23427	143672

Sample ID	PB-13	PB-59	PB-12	PB-58	PB-11	PB-57	PB-10	PB-56	PB-9	PB-8	PB-55	PB-7	PB-54	PB-6
Depth (cm)	**185**	**187.5**	**190**	**192.5**	**195**	**197.5**	**200**	**202.5**	**205**	**210**	**212.5**	**215**	**217.5**	**220**
Age (cal kBP)	**22.00**	**22.12**	**22.24**	**22.36**	**22.48**	**22.60**	**22.72**	**22.84**	**22.96**	**23.19**	**23.31**	**23.42**	**23.54**	**23.65**
Acacia	0	2	0	0	0	2	1	0	0	0	2	0	2	0
Celastraceae	3	1	0	0	0	1	0	0	0	1	0	6	0	0
Diospyros	5	2	1	3	2	0	4	2	4	0	4	3	1	2
Dodonaea	3	2	0	0	0	0	0	0	0	0	0	0	0	0
Encephalartos	1	0	0	3	2	1	0	0	0	1	1	0	2	1
Euclea	12	11	2	19	12	6	9	11	17	6	12	10	8	8
Grewia	0	7	0	1	1	0	1	2	2	0	1	0	0	3
Ilex	0	0	0	0	0	0	0	0	0	0	0	0	0	1
Lycium	0	0	0	0	0	0	0	0	0	0	0	1	0	0
Morella	0	0	0	1	1	1	1	4	0	1	1	2	3	3
Myrsine	5	0	3	0	5	0	3	0	3	3	0	2	1	0
Myrtaceae	0	0	0	0	3	0	2	3	0	2	0	0	3	0
Olea	2	0	0	1	0	0	0	0	0	0	0	0	0	0
Podocarpus	0	0	0	0	1	1	0	0	0	0	0	1	0	1
Rhus	0	0	0	2	1	1	0	0	0	0	0	0	1	0
Sapotaceae	0	0	0	0	1	0	0	0	0	0	0	0	0	0
Vitaceae	0	0	0	0	0	0	0	0	0	0	0	0	0	0
Zygophyllaceae	1	0	0	0	2	0	0	0	0	0	0	0	0	0
Proteaceae	9	10	2	11	9	5	17	17	7	10	13	12	8	16
Ericaceae	19	44	8	49	40	9	51	47	49	18	61	45	19	44
Cliffortia	5	2	1	5	16	4	6	14	3	7	12	4	4	11
Bruniaceae	1	0	0	0	0	0	2	2	1	3	3	0	0	2
Stoebe-type	37	98	24	75	35	34	73	59	48	45	60	54	26	51
Asteraceae HS	60	90	24	66	73	62	71	41	52	22	44	42	23	60
Artemisia	0	1	0	1	0	2	0	1	1	1	1	5	0	0
Pentzia-type	0	0	0	0	1	1	0	0	1	0	1	0	0	0
Euphorbiaceae undif	9	5	2	5	5	1	6	5	12	3	2	9	8	8
Euphorbia	7	0	0	0	0	1	0	3	4	1	8	2	1	3
Clutia	5	8	2	9	3	4	7	14	9	1	8	8	5	4
ChenoAm-type	5	7	2	1	6	6	5	6	5	2	4	7	0	7

Sample ID	PB-13	PB-59	PB-12	PB-58	PB-11	PB-57	PB-10	PB-56	PB-9	PB-8	PB-55	PB-7	PB-54	PB-6
Depth (cm)	185	187.5	190	192.5	195	197.5	200	202.5	205	210	212.5	215	217.5	220
Age (cal kBP)	22.00	22.12	22.24	22.36	22.48	22.60	22.72	22.84	22.96	23.19	23.31	23.42	23.54	23.65
Crassulaceae	27	8	7	20	7	4	15	22	16	7	12	7	10	13
Ruschia	2	2	1	2	5	2	2	4	6	8	2	6	3	12
Aizoaceae	24	13	2	9	15	2	13	5	13	6	8	9	2	10
Aloe-type	1	0	0	0	0	0	1	0	0	3	0	0	0	0
Geraniaceae	4	4	0	2	1	2	2	2	2	0	6	9	3	3
Brassicaceae	3	0	0	2	0	1	0	0	1	0	0	0	1	0
Anthospermum-type	1	4	0	0	2	1	1	0	1	2	0	2	0	4
Apiaceae	0	1	0	1	2	0	0	0	0	0	0	0	1	1
Fabaceae	6	6	0	11	7	7	12	8	2	10	5	8	11	8
Rhamnaceae	1	1	2	0	1	0	0	0	0	0	0	1	0	0
Rutaceae	1	4	0	7	1	2	2	7	4	2	3	3	3	5
Santalaceae	4	5	2	5	4	5	4	9	12	4	12	10	5	7
Scroph-type	7	4	2	1	4	0	1	1	4	0	3	5	0	4
Thymelaeaceae	5	9	4	9	6	4	15	10	14	8	8	7	5	12
Passerina	1	3	0	5	6	4	7	8	11	3	13	6	4	4
Galium	0	1	0	0	2	0	0	0	1	0	0	1	0	2
Canthium	2	7	1	4	3	4	0	5	4	4	0	1	1	7
Malvaceae	0	1	0	0	1	0	0	1	0	1	3	3	0	1
Onagraceae	1	3	0	1	0	0	0	0	0	0	1	0	0	0
Oxygonum	0	0	0	0	0	0	0	0	0	0	0	0	0	0
Polygonum	1	0	0	0	0	0	0	0	0	0	0	0	1	0
Selaginaceae	1	0	0	0	0	0	0	3	1	0	0	1	0	0
Urticaceae	0	0	0	0	0	0	0	0	0	0	0	0	0	0
Verbenaceae	0	0	0	0	0	0	0	1	0	0	0	0	0	0
Campanulaceae	0	0	0	0	0	0	1	0	0	0	0	0	0	0
Caryophyllaceae	0	0	0	0	1	0	0	0	0	0	0	0	0	0
Polygala	0	2	0	1	0	0	0	1	0	0	0	0	2	0
Cardiospermum	0	0	0	0	0	0	0	0	0	0	0	0	0	0
Rosaceae	0	0	0	0	0	0	0	0	0	0	0	0	2	1
Solanum	0	2	1	0	3	0	1	1	5	1	0	0	2	0

Sample ID	PB-13	PB-59	PB-12	PB-58	PB-11	PB-57	PB-10	PB-56	PB-9	PB-8	PB-55	PB-7	PB-54	PB-6
Depth (cm)	**185**	**187.5**	**190**	**192.5**	**195**	**197.5**	**200**	**202.5**	**205**	**210**	**212.5**	**215**	**217.5**	**220**
Age (cal kBP)	**22.00**	**22.12**	**22.24**	**22.36**	**22.48**	**22.60**	**22.72**	**22.84**	**22.96**	**23.19**	**23.31**	**23.42**	**23.54**	**23.65**
Araliaceae	0	0	0	3	1	0	0	0	0	0	0	0	0	0
Ascelepidaceae	2	0	0	0	0	0	0	0	0	0	0	0	0	0
Orchidaceae	0	3	0	5	4	0	3	3	2	2	1	1	1	2
Combretaceae	0	0	0	0	0	0	0	0	0	0	0	0	0	0
Loranthaceae	1	0	0	0	0	0	0	0	0	0	0	0	0	0
Sterculiaceae	0	0	0	2	0	1	0	0	0	0	1	0	1	0
Acan. Tricolporate	3	0	0	1	4	0	0	0	0	2	0	0	0	0
Acan. Diporate	0	0	0	0	4	0	0	2	0	0	0	0	0	0
Justicia-type	0	2	0	4	0	2	6	6	0	3	5	11	3	8
Oxalis	0	0	0	1	0	0	0	0	0	0	0	0	0	1
Plumbaginaceae	0	0	0	0	0	0	0	0	0	0	0	0	0	0
Boraginaceae	0	0	0	0	0	0	0	1	0	0	0	0	0	0
Bignoniaceae	0	1	0	1	0	0	0	0	0	2	3	0	0	0
Linaceae	1	3	0	0	2	0	1	2	0	1	2	1	2	0
Lamiaceae	0	0	0	2	0	1	1	0	0	0	1	0	1	0
Convolvulaceae	1	4	0	4	0	0	4	4	0	0	1	1	1	2
Hermannia	0	0	0	0	1	0	1	0	0	0	0	0	0	1
Lentibulariaceae	0	0	0	0	0	0	0	0	0	0	0	0	0	0
Haemodoraceae	0	0	0	0	3	0	0	0	0	0	0	0	0	0
Gentianaceae	2	1	0	1	6	0	3	4	0	0	2	5	1	1
Potamogeton	0	0	0	0	0	0	0	0	0	0	0	0	0	1
Ranunculaceae	1	0	0	0	0	0	0	0	0	0	0	0	0	0
Blechnaceae	8	0	0	0	0	0	3	0	1	2	1	0	1	1
Plantago	0	0	0	1	0	0	0	0	1	0	1	0	1	0
Aponogeton	6	0	3	1	6	0	4	4	3	2	2	2	4	7
Haloragaceae	1	0	0	0	1	0	1	3	3	2	0	0	0	3
Typha	1	5	0	2	7	1	0	3	0	0	0	0	2	0
Scabiosa	1	3	2	1	0	0	1	1	1	0	5	2	0	0
Gunneraceae	1	0	0	0	0	2	2	1	4	0	1	1	0	0
Nymphaea	0	0	0	0	0	0	0	0	0	0	0	0	0	0

Sample ID	PB-13	PB-59	PB-12	PB-58	PB-11	PB-57	PB-10	PB-56	PB-9	PB-8	PB-55	PB-7	PB-54	PB-6
Depth (cm)	**185**	**187.5**	**190**	**192.5**	**195**	**197.5**	**200**	**202.5**	**205**	**210**	**212.5**	**215**	**217.5**	**220**
Age (cal kBP)	**22.00**	**22.12**	**22.24**	**22.36**	**22.48**	**22.60**	**22.72**	**22.84**	**22.96**	**23.19**	**23.31**	**23.42**	**23.54**	**23.65**
Araceae	0	0	0	0	6	0	0	1	0	0	0	0	0	3
Juncaceae	8	3	2	5	7	0	3	4	5	3	2	8	1	2
Liliaceae	20	8	4	13	5	6	9	3	9	10	7	11	7	10
Iridaceae	5	9	2	9	0	1	3	6	3	5	8	5	8	2
Amaryllidaceae	6	4	0	0	4	0	0	0	2	0	1	1	0	0
Cyperaceae	44	22	9	31	32	23	29	51	37	23	46	32	16	41
Restionaceae	45	9	13	16	48	8	27	22	38	30	30	48	12	29
Poaceae	41	41	21	45	63	15	52	51	60	26	57	54	15	43
Unknown Type B	0	0	0	0	0	0	0	0	1	0	0	0	0	0
Unknown Tetrad 1	20	0	0	0	0	0	2	0	3	16	0	2	0	7
Unknown Psilate Tricolporate	2	1	1	0	2	0	0	2	1	1	2	0	1	2
Unidentifiable	5	2	1	0	0	0	0	0	0	4	0	1	0	2
Broken	13	9	7	8	11	6	9	6	11	6	8	11	5	13
Unknown	1	0	0	2	3	1	0	1	1	1	0	1	2	0
Total Pollen	520	500	158	490	510	247	500	500	501	327	501	490	256	500
Pollen Concentration	22671	7426	6684	12081	16768	3731	7801	10514	7884	9185	11036	6145	8091	14532
Monolete	35	63	12	21	33	11	17	11	10	25	7	16	9	17
Trilete	23	26	7	20	25	18	19	19	32	13	18	14	8	10
Ophioglossum	0	0	0	0	0	0	0	0	0	0	0	0	0	0
Mohria	0	0	0	0	1	1	0	0	0	1	0	0	0	0
Riccia	1	0	0	6	1	3	5	2	4	0	1	2	1	0
Pellaea	2	4	0	1	0	4	2	2	0	0	2	0	0	1
Pseudoschizaea	3	0	0	0	0	0	0	0	0	0	0	0	0	0
Debarya glytosperma	0	3	0	6	0	2	5	4	2	0	5	4	2	3
Glomus	3	0	0	1	2	1	3	1	0	1	1	0	0	2
10 - 50 um	753	2480	781	3872	419	4428	1108	1668	267	841	1245	1839	1106	782
50 - 100 um	5	29	5	121	6	66	30	41	0	0	10	21	5	3
>100 um	0	4	0	3	0	0	0	2	0	0	0	0	0	0
Total Charcoal	758	2513	786	3996	425	4494	1138	1711	267	841	1255	1860	1111	785
Charcoal Concentration	33047	37322	33249	98525	13973	67877	17755	35978	4202	23623	27644	23327	35112	22815

Sample ID	PB-53	PB-5	PB-52	PB-4	PB-51	PB-3	PB-50	PB-2	PB-1
Depth (cm)	222.5	225	227.5	230	232.5	235	237.5	240	245
Age (cal kBP)	23.76	23.88	23.99	24.11	24.22	24.34	24.45	24.56	24.79
Acacia		0		0				0	
Celastraceae		0		2				2	
Diospyros		3		5				6	
Dodonaea		0		0				0	
Encephalartos		0		1				2	
Euclea		13		19				16	
Grewia		1		3				0	
Ilex		0		0				0	
Lycium		0		0				0	
Morella		2		0				0	
Myrsine		8		3				4	
Myrtaceae		2		0				2	
Olea		0		0				0	
Podocarpus		0		2				0	
Rhus		0		1				0	
Sapotaceae		0		0				0	
Vitaceae		0		0				0	
Zygophyllaceae		1		2				0	
Proteaceae		9		15				8	
Ericaceae		76		49				30	
Cliffortia		11		4				6	
Bruniaceae		3		0				1	
Stoebe-type		35		39				35	
Asteraceae HS		58		55				45	
Artemisia		1		1				0	
Pentzia-type		0		1				0	
Euphorbiaceae undif		1		9				3	
Euphorbia		1		5				0	
Clutia		4		3				4	
ChenoAm-type		4		2				3	

Sample ID	PB-53	PB-5	PB-52	PB-4	PB-51	PB-3	PB-50	PB-2	PB-1
Depth (cm)	222.5	225	227.5	230	232.5	235	237.5	240	245
Age (cal kBP)	23.76	23.88	23.99	24.11	24.22	24.34	24.45	24.56	24.79
Crassulaceae		5		10				13	
Ruschia		15		2				6	
Aizoaceae		4		10				20	
Aloe-type		0		0				0	
Geraniaceae		2		7				3	
Brassicaceae		0		0				0	
Anthospermum-type		8		5				10	
Apiaceae		0		1				0	
Fabaceae		5		6				9	
Rhamnaceae		0		0				2	
Rutaceae		0		1				2	
Santalaceae		8		12				10	
Scroph-type		2		3				3	
Thymelaeaceae		10		10				5	
Passerina		7		4				15	
Galium		0		0				0	
Canthium		3		3				2	
Malvaceae		1		2				2	
Onagraceae		1		0				0	
Oxygonum		0		0				0	
Polygonum		0		0				0	
Selaginaceae		0		2				0	
Urticaceae		0		3				0	
Verbenaceae		0		3				0	
Campanulaceae		1		0				0	
Caryophyllaceae		0		0				0	
Polygala		0		0				0	
Cardiospermum		0		0				0	
Rosaceae		0		1				0	
Solanum		2		0				0	

Sample ID	PB-53	PB-5	PB-52	PB-4	PB-51	PB-3	PB-50	PB-2	PB-1
Depth (cm)	222.5	225	227.5	230	232.5	235	237.5	240	245
Age (cal kBP)	23.76	23.88	23.99	24.11	24.22	24.34	24.45	24.56	24.79
Araliaceae		0		0				0	
Ascelepidaceae		0		0				0	
Orchidaceae		0		4				4	
Combretaceae		0		0				0	
Loranthaceae		0		0				0	
Sterculiaceae		0		0				1	
Acan. Tricolporate		1		0				1	
Acan. Diporate		0		1				2	
Justicia-type		0		3				1	
Oxalis		2		2				0	
Plumbaginaceae		0		0				0	
Boraginaceae		0		0				0	
Bignoniaceae		0		0				0	
Linaceae		1		0				0	
Lamiaceae		0		0				0	
Convolvulaceae		0		0				0	
Hermannia		0		0				0	
Lentibulariaceae		0		0				0	
Haemodoraceae		1		0				0	
Gentianaceae		0		0				0	
Potamogeton		0		0				0	
Ranunculaceae		0		0				0	
Blechnaceae		0		4				4	
Plantago		0		0				1	
Aponogeton		0		7				7	
Haloragaceae		0		5				5	
Typha		0		0				2	
Scabiosa		2		2				1	
Gunneraceae		0		0				1	
Nymphaea		0		0				0	

Sample ID	PB-53	PB-5	PB-52	PB-4	PB-51	PB-3	PB-50	PB-2	PB-1
Depth (cm)	222.5	225	227.5	230	232.5	235	237.5	240	245
Age (cal kBP)	23.76	23.88	23.99	24.11	24.22	24.34	24.45	24.56	24.79
Araceae		0		0				1	
Juncaceae		5		8				11	
Liliaceae		7		15				15	
Iridaceae		0		10				5	
Amaryllidaceae		2		1				4	
Cyperaceae		48		43				67	
Restionaceae		56		33				23	
Poaceae		51		49				53	
Unknown Type B		0		0				0	
Unknown Tetrad 1		2		0				0	
Unknown Psilate Tricolporate		2		0				1	
Unidentifiable		0		1				3	
Broken		12		6				15	
Unknown		1		0				3	
Total Pollen		500		500				500	
Pollen Concentration		14125		8702				5872	
Monolete		17		18				35	
Trilete		11		35				31	
Ophioglossum		0		1				0	
Mohria		0		0				0	
Riccia		4		3				5	
Pellaea		2		0				1	
Pseudoschizaea		0		0				0	
Debarya glytosperma		0		0				0	
Glomus		0		0				2	
10 - 50 um		148		697				232	
50 - 100 um		0		0				0	
>100 um		0		0				0	
Total Charcoal		148		697				232	
Charcoal Concentration		4181		12131				2725	

APPENDIX E

PEARLY BEACH 1 GEOCHEMICAL DATA

Sample ID	Depth (cm)	Age (cal kBP)	Total Nitrogen	Std deviation	Total Carbon	Std deviation	$\delta^{13}C$ (‰)	Std deviation	Total Organic Carbon (TOC)	$\delta^{13}C_{TOC}$ (‰)	TOC/TN
PB1-227	**23**	**0.53**	0.32	0.00	4.78	0.09	-23.48	0.01	0.28	-25.98	0.89
PB1-222	**28**	**1.30**	0.25	0.03	4.23	0.05	-23.15	0.10	3.95	-24.39	16.05
PB1-217	**33**	**2.07**	0.24	0.01	3.58	0.04	-23.46	0.05	4.29	-23.98	17.57
PB1-212	**38**	**2.85**	0.21	0.01	3.16	0.02	-23.47	0.05	3.52	-24.27	17.10
PB1-207	**43**	**3.62**	0.22	0.02	3.61	0.20	-22.89	0.10	3.06	-23.89	13.95
PB1-202	**48**	**4.39**	0.20	0.01	3.40	0.11	-22.66	0.21	3.12	-24.31	15.33
PB1-197	**53**	**5.17**	0.17	0.01	4.12	0.06	-23.96	0.07	3.16	-23.75	19.00
PB1-192	**58**	**5.94**	0.22	0.01	3.50	0.06	-22.48	0.08	3.25	-24.52	15.08
PB1-187	**63**	**6.71**	0.24	0.01	3.71	0.02	-23.04	0.10	3.53	-24.52	14.79
PB1-182	**68**	**7.49**	0.22	0.00	3.30	0.05	-23.32	0.04	3.64	-24.45	16.60
PB1-177	**73**	**8.27**	0.21	0.01	3.51	0.02	-23.50	0.14	3.38	-24.75	16.12
PB1-172	**78**	**9.11**	0.25	0.01	3.46	0.10	-23.28	0.15	3.32	-24.07	13.24
PB1-167	**83**	**9.95**	0.18	0.01	4.52	0.04	-22.65	0.10	4.40	-22.90	24.44
PB1-162	**88**	**10.80**	0.16	0.00	4.71	0.04	-22.00	0.17	4.65	-22.21	29.61
PB1-157	**93**	**11.64**	0.18	0.01	4.03	0.04	-24.51	0.06	4.06	-24.79	22.75
PB1-152	**98**	**12.48**	0.15	0.01	3.78	0.02	-24.06	0.03	2.66	-24.49	17.18
PB1-147	**103**	**13.01**	0.17	0.00	4.69	0.06	-22.91	0.04	1.72	-24.90	10.21
PB1-142	**108**	**13.22**	0.11	0.00	2.65	0.01	-23.26	0.08	1.46	-25.56	13.76
PB1-137	**113**	**13.43**	0.09	0.00	2.50	0.01	-23.01	0.12	1.24	-25.51	13.87
PB1-132	**118**	**13.64**	0.05	0.00	1.57	0.01	-24.32	0.02	0.87	-25.26	15.83
PB1-127	**123**	**13.83**	0.06	0.01	1.32	0.01	-23.80	0.09	0.54	-25.94	9.82
PB1-122	**128**	**14.04**	0.04	0.01	1.18	0.08	-23.26	0.16	0.50	-24.94	12.07
PB1-117	**133**	**14.25**	0.05	0.00	1.75	0.02	-23.57	0.10	0.33	-24.86	5.97
PB1-112	**138**	**14.46**	0.05	0.01	1.59	0.10	-22.69	0.09	0.40	-25.95	8.19
PB1-107	**143**	**14.68**	0.02	0.00	0.51	0.00	-22.42	0.17	0.24	-25.57	9.82
PB1-102	**148**	**20.25**	0.02	0.00	0.33	0.02	-22.19	0.03	1.29	-25.71	54.45
PB1-97	**153**	**20.49**	0.03	0.00	0.39	0.02	-23.40	0.33	2.62	-25.98	91.77
PB1-92	**158**	**20.73**	0.08	0.01	1.28	0.04	-23.67	0.15	3.62	-25.78	43.28
PB1-87	**163**	**20.97**	0.11	0.00	3.41	0.04	-24.67	0.13	3.25	-26.05	30.04
PB1-82	**168**	**21.18**	0.21	0.00	5.33	0.04	-25.58	0.16	4.39	-25.89	20.58
PB1-77	**173**	**21.42**	0.11	0.00	2.93	0.02	-25.20	0.09	3.47	-25.75	31.00
PB1-72	**178**	**21.66**	0.04	0.00	1.17	0.03	-24.96	0.19	2.74	-25.60	66.09

Sample ID	Depth (cm)	Age (cal kBP)	Total Nitrogen	Std deviation	Total Carbon	Std deviation	$\delta^{13}C$ (‰)	Std deviation	Total Organic Carbon (TOC)	$\delta^{13}C_{TOC}$ (‰)	TOC/TN
PB1-67	**183**	**21.90**	0.23	0.01	4.86	0.07	-24.61	0.07	2.43	-25.64	10.44
PB1-62	**188**	**22.14**	0.13	0.00	2.80	0.02	-25.09	0.07	2.17	-25.29	16.96
PB1-57	**193**	**22.38**	0.17	0.00	2.77	0.03	-23.75	0.32	1.89	-25.84	11.08
PB1-52	**198**	**22.62**	0.10	0.01	2.47	0.20	-24.18	0.07	1.95	-25.62	19.73
PB1-47	**203**	**22.86**	0.09	0.00	2.10	0.05	-24.79	0.09	1.84	-25.54	20.71
PB1-42	**208**	**23.10**	0.08	0.00	1.99	0.01	-24.83	0.06	2.01	-24.45	23.90
PB1-37	**213**	**23.33**	0.13	0.01	2.11	0.04	-23.82	0.09	1.74	-25.69	13.19
PB1-32	**218**	**23.56**	0.08	0.00	1.86	0.02	-24.58	0.03	1.67	-25.91	20.65
PB1-27	**223**	**23.79**	0.07	0.00	1.63	0.07	-24.49	0.15	1.47	-25.15	21.96
PB1-22	**228**	**24.02**	0.08	0.01	1.64	0.02	-23.43	0.03	0.85	-25.96	10.64
PB1-17	**233**	**24.25**	0.04	0.00	0.92	0.01	-24.21	0.31	0.72	-26.05	17.97
PB1-12	**238**	**24.48**	0.02	0.00	0.57	0.01	-24.07	0.06	0.65	-26.31	27.30
PB1-7	**243**	**24.71**	0.02	0.00	0.48	0.00	-24.40	0.31	0.44	-26.33	24.25

APPENDIX F

RIETVLEI STILL BAY 2 GRAIN SIZE DATA

Depth (cm)	10	36	50	70	90	118	130	150	164	180	190	204
Age (ka)	145	472	649	901	1349	4438	5762	6770	7327	7964	8362	8919
% clay	0.03348	0.04060	0.05015	0.05168	0.06362	0.07400	0.05476	0.04038	0.06345	0.05761	0.06871	0.06115
% silt	0.33121	0.18286	0.20019	0.31152	0.14847	0.41747	0.46757	0.27348	0.20310	0.17397	0.17741	0.27651
% sand	0.63531	0.77654	0.74966	0.63680	0.78791	0.50853	0.47767	0.68613	0.73345	0.76842	0.75388	0.66234
Mean	3.46230	3.01979	3.11680	3.61332	3.32943	4.28707	4.17631	3.41047	3.33201	2.95459	2.95674	3.21292
Median	2.73933	2.27801	2.34729	2.94462	2.50914	3.99797	4.15610	2.61080	2.66227	2.25764	2.10332	2.29690
Sorting	1.99426	2.00464	2.13100	2.11553	1.96927	2.16348	2.17386	2.10131	2.09145	2.01284	2.31020	2.26322
Skew	-0.51679	-0.58339	-0.55675	-0.46827	-0.70969	-0.23488	-0.07809	-0.54349	-0.52928	-0.61276	-0.58600	-0.60911
Kurtosis	0.84028	1.42818	1.25988	0.94179	2.06940	0.88548	0.85912	0.91949	1.30755	1.36384	1.28828	0.88386

Depth (cm)	230	246	270	330
Age (ka)	10294	11205	15337	29931
% clay	0.05748	0.09183	0.10702	0.04224
% silt	0.10511	0.13068	0.29858	0.18342
% sand	0.83740	0.77749	0.59440	0.77434
Mean	2.35901	2.73283	3.93442	2.76781
Median	1.80749	1.88629	3.12660	1.96990
Sorting	1.88487	2.46250	2.56513	2.00834
Skew	-0.64611	-0.59144	-0.44404	-0.64924
Kurtosis	2.55002	1.70876	0.80497	1.28491

Grain size categories	
Clay	0 - 2 µm
Silt	2 - 20 µm
Sand	20 - 2000 µm

APPENDIX G

RIETVLEI STILL BAY 2 ABSOLUTE POLLEN, NON-POLLEN PALYNOMORPHS AND MICROSCOPIC CHARCOAL COUNTS

Sample ID	RVSB2-1	RVSB2-2	RVSB2-3	RVSB2-4	RVSB2-5	RVSB2-6	RVSB2-7	RVSB2-8	RVSB2-9	RVSB2-10	RVSB2-11	RVSB2-12	RVSB2-13	RVSB2-14
Depth (cm)	2	6.25	11.25	16.25	21.25	26.25	31.25	36.25	41.25	46.25	51.25	56.25	61.25	66.25
Age (ka)	0.04	0.09	0.16	0.22	0.28	0.35	0.41	0.47	0.54	0.60	0.66	0.73	0.79	0.85
Encephalartos	1	2	2	3	0	1	1	0	0	3	2	0	0	0
Euclea	6	12	18	3	0	3	6	2	0	3	17	3	4	8
Grewia	0	0	3	0	1	0	0	0	0	0	0	0	0	2
Ilex	0	0	0	0	0	0	0	1	0	0	0	1	0	0
Lycium	0	0	0	1	1	0	1	0	0	0	0	0	0	0
Morella	6	2	2	3	5	0	0	2	1	2	3	2	2	0
Myrsine	8	2	5	5	3	4	4	3	2	7	12	2	4	5
Myrtaceae	1	0	0	3	1	0	0	0	0	2	1	1	1	0
Olea	2	18	14	1	7	0	0	0	0	0	3	5	0	2
Acacia	2	3	4	2	2	2	0	7	0	1	1	2	0	0
Blechnaceae	0	0	2	5	5	4	1	7	1	3	0	0	2	0
Celastraceae	10	15	32	3	0	0	0	0	2	1	4	1	0	1
Celtis	0	0	0	0	0	0	0	0	0	0	0	0	0	0
Diospyros	2	4	2	2	0	0	1	1	0	0	7	1	0	5
Dodonaea	13	14	8	7	0	3	6	0	2	5	11	7	5	8
Pinaceae	2	0	0	0	0	0	0	0	0	0	0	0	0	0
Podocarpus	1	1	0	7	18	2	0	44	0	0	0	3	0	0
Rhus	1	5	9	2	2	2	2	0	0	0	4	1	0	0
Sapotaceae	0	0	0	0	0	0	0	0	0	0	0	0	0	1
Vitaceae	1	3	0	0	0	0	0	0	0	0	1	0	0	2
Asteraceae HS	18	19	10	30	12	46	50	25	20	14	63	25	31	73
Pentzia-type	0	2	0	0	1	4	0	1	1	1	7	3	2	9
Artemisia	2	0	0	0	0	0	0	1	0	1	5	0	2	6
Tarchonanthus	1	4	0	2	0	3	0	0	0	0	4	0	0	0
Stoebe-type	12	4	5	14	6	17	8	2	31	9	34	6	8	5
Proteaceae	8	13	5	6	1	12	18	7	19	22	48	18	28	119
Ericaceae	11	7	6	3	2	3	1	3	0	2	1	2	6	0
Cliffortia	9	7	7	10	5	1	4	6	1	1	4	8	1	5
Bruniaceae	21	6	13	4	7	1	3	0	0	1	2	4	2	1
Anthospermum-type	3	6	0	0	1	2	1	2	3	2	5	1	2	2

Sample ID	RVSB2-1	RVSB2-2	RVSB2-3	RVSB2-4	RVSB2-5	RVSB2-6	RVSB2-7	RVSB2-8	RVSB2-9	RVSB2-10	RVSB2-11	RVSB2-12	RVSB2-13	RVSB2-14
Depth (cm)	**2**	**6.25**	**11.25**	**16.25**	**21.25**	**26.25**	**31.25**	**36.25**	**41.25**	**46.25**	**51.25**	**56.25**	**61.25**	**66.25**
Age (ka)	**0.04**	**0.09**	**0.16**	**0.22**	**0.28**	**0.35**	**0.41**	**0.47**	**0.54**	**0.60**	**0.66**	**0.73**	**0.79**	**0.85**
Aizoaceae	13	2	7	5	2	8	8	2	9	1	14	11	2	8
Euphorbiaceae undif	0	0	0	2	0	3	0	0	0	0	4	0	0	7
Aloe-type	0	0	0	3	0	2	10	0	0	7	4	0	0	0
Brassicaceae	3	38	4	1	1	0	0	0	8	0	1	7	0	2
Campanulaceae	8	5	5	4	1	0	1	5	0	0	0	0	0	0
Caryophyllaceae	0	0	0	0	0	0	0	0	0	0	0	0	0	0
Gunneraceae	4	7	9	3	0	1	0	4	1	4	0	1	2	1
Polygala	4	1	0	0	0	1	0	0	0	0	0	0	0	0
Solanum	1	1	3	2	0	0	0	0	0	0	4	0	0	2
Araliaceae	0	0	0	0	0	0	0	0	0	0	0	0	0	0
Ascelepidaceae	0	0	0	0	0	0	0	0	0	0	0	0	0	0
Orchidaceae	0	0	1	0	0	0	0	0	0	0	0	0	0	0
Oxalis	3	3	5	0	0	0	0	0	0	0	1	0	1	0
Plumbaginaceae	0	0	0	0	0	0	0	0	0	0	0	0	0	0
Erythrina	0	0	2	0	0	0	0	0	0	0	0	0	0	0
Boraginaceae	0	0	2	0	0	0	0	0	0	0	0	0	0	0
Portulacaceae	0	0	0	0	0	0	0	0	0	0	0	0	3	0
Bigonaceae	0	2	0	0	0	0	0	0	0	1	0	0	0	1
Kniphofia	0	0	0	0	0	0	0	0	0	0	0	0	0	0
Linaceae	0	0	0	0	0	0	0	0	0	0	0	0	0	0
Lamiaceae	0	0	0	0	1	0	0	0	0	0	0	0	0	0
Convolvulaceae	1	0	0	0	0	0	0	0	0	0	0	0	0	0
Araceae	4	0	0	0	0	0	0	0	0	0	0	0	0	0
Hermannia	3	1	0	0	0	0	0	0	0	0	0	0	0	0
Lentibulariaceae	0	0	0	0	0	0	0	0	0	0	0	0	0	0
Acanthaceae	2	0	0	0	0	0	0	0	0	0	0	0	0	0
Apiaceae	6	12	2	0	0	2	1	0	4	0	6	0	2	1
Gentianaceae	2	4	5	1	0	1	1	0	0	0	0	0	2	2
Potamogetonaceae	0	0	0	0	0	0	0	0	0	0	0	0	0	0
Fabaceae	3	7	17	3	3	0	10	1	2	2	3	8	5	0

Sample ID	RVSB2-1	RVSB2-2	RVSB2-3	RVSB2-4	RVSB2-5	RVSB2-6	RVSB2-7	RVSB2-8	RVSB2-9	RVSB2-10	RVSB2-11	RVSB2-12	RVSB2-13	RVSB2-14
Depth (cm)	**2**	**6.25**	**11.25**	**16.25**	**21.25**	**26.25**	**31.25**	**36.25**	**41.25**	**46.25**	**51.25**	**56.25**	**61.25**	**66.25**
Age (ka)	**0.04**	**0.09**	**0.16**	**0.22**	**0.28**	**0.35**	**0.41**	**0.47**	**0.54**	**0.60**	**0.66**	**0.73**	**0.79**	**0.85**
Rhamnaceae	7	0	9	2	0	0	0	0	0	0	0	1	5	0
Rutaceae	5	8	4	2	2	1	3	2	0	0	11	1	0	10
Santalaceae	3	6	2	1	0	1	1	1	0	1	0	2	4	1
Scroph-type	3	2	6	0	3	2	3	2	1	1	2	1	4	6
Thymelaeaceae	0	2	0	5	7	3	3	6	7	4	5	1	0	3
Passerina	0	8	2	1	0	4	2	2	3	0	4	0	0	9
Galium	1	1	1	0	0	0	0	0	0	0	0	0	3	0
Canthium	6	1	2	4	2	2	0	3	1	1	3	1	1	1
Plantago	18	0	3	9	0	0	3	8	0	0	0	2	2	0
Cyperaceae	14	51	42	66	121	220	103	64	186	42	28	109	192	68
Restionaceae	6	11	0	7	0	15	15	1	14	9	4	26	7	5
Poaceae	116	50	66	126	86	45	130	171	42	68	72	67	89	47
Geraniaceae	1	4	1	3	0	1	1	10	13	1	0	8	3	0
Lobostemon	0	1	1	0	0	0	0	0	1	0	0	0	0	0
Montinaceae	0	2	1	0	0	0	0	1	0	0	0	0	0	0
Onagraceae	1	2	0	0	0	1	0	0	0	1	0	0	0	0
Oxygonum	0	0	0	0	0	0	0	0	0	0	0	0	0	0
Polygonum	1	3	1	0	1	0	2	1	0	1	1	0	1	3
Euphorbia	7	2	2	0	6	2	0	0	1	2	0	3	0	4
Clutia	2	2	1	5	4	1	3	2	1	1	2	1	0	0
ChenAm-type	11	0	1	21	21	7	5	6	18	10	12	11	10	25
Crassula	22	8	30	8	7	5	8	1	9	8	19	10	10	4
Ruschia	6	4	6	4	4	7	5	0	9	6	2	3	8	5
Juncaceae	5	5	7	12	16	4	11	18	11	7	4	20	8	0
Liliaceae	17	31	51	5	25	8	10	6	11	8	6	16	8	2
Iridaceae	6	11	22	3	6	4	3	0	1	4	5	4	3	4
Amaryllidaceae	3	5	4	0	6	0	1	2	1	1	2	7	0	1
Malvaceae	0	3	1	2	3	4	3	1	0	3	4	1	1	0
Scabiosa	0	1	0	0	0	0	0	0	0	1	0	0	0	2
Selaginaceae	0	0	1	0	0	0	0	0	0	0	0	0	0	0

Sample ID	RVSB2-1	RVSB2-2	RVSB2-3	RVSB2-4	RVSB2-5	RVSB2-6	RVSB2-7	RVSB2-8	RVSB2-9	RVSB2-10	RVSB2-11	RVSB2-12	RVSB2-13	RVSB2-14
Depth (cm)	**2**	**6.25**	**11.25**	**16.25**	**21.25**	**26.25**	**31.25**	**36.25**	**41.25**	**46.25**	**51.25**	**56.25**	**61.25**	**66.25**
Age (ka)	**0.04**	**0.09**	**0.16**	**0.22**	**0.28**	**0.35**	**0.41**	**0.47**	**0.54**	**0.60**	**0.66**	**0.73**	**0.79**	**0.85**
Urticaceae	10	6	0	27	18	0	12	16	8	0	4	1	1	0
Verbenaceae	2	1	0	0	5	4	0	4	0	0	3	2	0	0
Aponogeton	12	4	3	1	23	9	7	8	21	0	1	37	4	5
Haloragaceae	0	0	0	0	0	0	0	1	0	0	0	0	0	0
Typha	4	0	2	0	1	4	5	1	10	7	8	10	0	0
Zygophyllaceae	2	2	2	0	0	0	0	0	0	0	0	1	0	0
Loranthaceae	0	1	0	0	2	0	0	0	0	0	0	0	0	0
Sterculiaceae	1	2	5	2	0	2	0	1	0	0	1	1	2	1
Justica-type	0	11	0	1	0	1	0	0	0	0	10	0	1	6
Unknown D	0	0	0	0	0	0	0	0	0	0	0	0	0	0
Unknown E	0	0	0	0	0	0	0	0	0	0	0	0	0	0
Unknown F	0	0	0	0	0	0	0	0	0	0	0	0	0	0
Unknown	0	0	0	25	5	0	0	5	0	0	0	3	0	0
Unkn Tri	0	4	5	1	0	0	2	0	0	2	2	0	0	1
Unidentifiable	4	5	3	2	6	2	7	8	5	3	2	2	3	1
Broken	12	12	9	16	32	14	15	22	18	13	7	25	15	10
Total Unknown Pollen	16	21	17	44	43	16	24	35	23	18	11	30	18	12
Total Pollen	506	504	505	501	500	501	501	500	499	300	500	500	502	502
Pollen concentration	116000	69029	86413	41900	110613	23229	31259	111730	46024	17666	28362	387146	120060	50672
Monolete	28	1	14	57	34	7	62	57	10	49	22	13	32	15
Trilete	10	3	8	15	10	10	24	13	2	15	13	7	13	8
Riccia	1	2	0	1	0	1	5	1	0	5	0	1	1	0
Pellaea	0	0	0	0	0	0	0	0	0	1	0	0	0	0
Pottiaceae	2	0	0	3	0	1	3	0	0	6	0	0	1	0
Pseudoschizaea	0	0	0	0	0	0	0	0	0	0	0	0	0	0
Ophioglossum	0	0	0	2	0	0	1	0	0	0	0	0	0	0
Mohria	0	0	0	0	0	0	0	0	0	0	0	0	0	0
Muriform Spores	0	0	0	0	0	0	0	0	1	0	0	0	0	0
Septated Spores	0	0	0	0	0	0	0	1	0	0	0	0	0	0
Algae cells	1	4	4	10	0	0	15	43	0	21	0	0	7	0

Sample ID	RVSB2-1	RVSB2-2	RVSB2-3	RVSB2-4	RVSB2-5	RVSB2-6	RVSB2-7	RVSB2-8	RVSB2-9	RVSB2-10	RVSB2-11	RVSB2-12	RVSB2-13	RVSB2-14
Depth (cm)	**2**	**6.25**	**11.25**	**16.25**	**21.25**	**26.25**	**31.25**	**36.25**	**41.25**	**46.25**	**51.25**	**56.25**	**61.25**	**66.25**
Age (ka)	**0.04**	**0.09**	**0.16**	**0.22**	**0.28**	**0.35**	**0.41**	**0.47**	**0.54**	**0.60**	**0.66**	**0.73**	**0.79**	**0.85**
Glomus	15	2	2	16	5	3	74	101	1	18	10	0	3	3
10 - 50 um	62	4	10	56	12	96	194	43	113	612	359	74	356	748
50 - 100 um	0	0	0	2	1	2	2	0	1	13	10	1	6	29
>100 um	0	0	0	0	0	0	0	0	0	1	0	0	0	2
Total Charcoal	62	4	10	58	13	98	196	43	114	626	369	75	362	779
Charcoal concentration	14213	548	1711	4851	2876	4544	12229	9609	10515	36863	20931	58072	86577	78632

Sample ID	RVSB2-15	RVSB2-16	RVSB2-17	RVSB2-18	RVSB2-19	RVSB2-20	RVSB2-21	RVSB2-22	RVSB2-23	RVSB2-24	RVSB2-25	RVSB2-26	RVSB2-27	RVSB2-28
Depth (cm)	71.25	76.25	81.25	86.25	91.25	96.25	101.25	106.25	111.25	116.25	122.25	127.25	132.25	137.25
Age (ka)	0.91	0.98	1.04	1.10	1.46	2.01	2.56	3.11	3.67	4.22	4.88	5.43	5.98	6.25
Encephalartos	1	4	0	0	1	1	0	0	0	0	1	0	0	0
Euclea	3	10	0	4	4	1	2	7	13	7	11	10	10	16
Grewia	0	3	0	1	0	0	0	0	0	0	0	0	2	0
Ilex	0	0	0	0	0	0	0	0	0	0	0	0	0	0
Lycium	3	3	0	0	0	1	0	0	0	0	2	0	0	0
Morella	8	7	0	0	0	4	5	0	2	1	0	0	0	0
Myrsine	3	1	2	2	1	1	2	8	4	7	6	0	7	10
Myrtaceae	1	0	3	0	0	0	0	0	0	3	1	0	1	2
Olea	0	1	2	0	0	3	0	1	0	0	1	0	1	1
Acacia	0	5	0	5	0	1	0	2	0	0	0	0	0	0
Blechnaceae	2	8	0	0	0	6	0	0	0	0	4	2	0	0
Celastraceae	1	0	2	2	2	0	1	1	0	3	0	0	3	1
Celtis	0	0	0	0	0	0	0	0	0	0	0	0	0	0
Diospyros	0	1	0	3	0	2	1	5	0	4	5	0	1	5
Dodonaea	3	3	3	7	3	0	1	19	2	7	0	1	2	2
Pinaceae	0	0	0	0	0	0	0	0	0	0	0	0	0	0
Podocarpus	5	3	0	1	1	2	0	1	0	0	0	0	0	0
Rhus	2	0	1	0	0	1	1	3	3	0	0	2	3	2
Sapotaceae	0	0	0	0	0	0	0	0	0	0	0	0	0	0
Vitaceae	1	0	0	0	0	0	0	1	0	0	0	0	0	0
Asteraceae HS	49	40	100	83	110	12	45	71	38	70	90	56	97	120
Pentzia-type	2	2	2	3	9	1	1	2	3	0	3	0	3	4
Artemisia	2	1	1	2	0	3	1	12	0	2	1	1	2	3
Tarchonanthus	0	3	0	6	4	0	0	0	1	0	6	0	0	0
Stoebe-type	22	14	16	13	14	9	16	6	13	5	22	6	8	6
Proteaceae	40	52	112	102	76	145	19	41	36	21	18	9	30	33
Ericaceae	6	7	1	0	1	1	1	13	4	1	7	9	4	3
Cliffortia	5	11	8	26	4	2	2	11	5	13	3	5	13	8
Bruniaceae	3	2	1	3	2	2	0	2	1	2	7	0	0	4
Anthospermum-type	2	5	2	7	1	0	4	26	8	3	0	1	6	9

Sample ID	RVSB2-15	RVSB2-16	RVSB2-17	RVSB2-18	RVSB2-19	RVSB2-20	RVSB2-21	RVSB2-22	RVSB2-23	RVSB2-24	RVSB2-25	RVSB2-26	RVSB2-27	RVSB2-28
Depth (cm)	71.25	76.25	81.25	86.25	91.25	96.25	101.25	106.25	111.25	116.25	122.25	127.25	132.25	137.25
Age (ka)	0.91	0.98	1.04	1.10	1.46	2.01	2.56	3.11	3.67	4.22	4.88	5.43	5.98	6.25
Aizoaceae	2	7	5	3	7	4	4	8	0	33	2	4	23	15
Euphorbiaceae undif	0	1	0	11	1	1	3	12	0	0	3	2	7	4
Aloe-type	0	0	5	2	1	0	0	0	0	1	0	0	2	1
Brassicaceae	0	0	1	0	0	0	0	4	0	1	0	0	2	0
Campanulaceae	0	1	0	0	0	0	0	2	1	0	4	1	0	0
Caryophyllaceae	0	0	0	0	0	0	0	1	0	0	0	1	0	0
Gunneraceae	4	4	1	2	0	0	0	1	2	0	1	1	0	0
Polygala	0	0	0	3	0	0	1	0	0	0	4	0	0	0
Solanum	0	3	2	0	0	0	0	3	0	3	3	3	0	3
Araliaceae	0	0	0	1	0	0	0	0	0	0	0	0	0	0
Ascelepidaceae	0	0	0	0	0	0	0	0	0	0	0	0	0	0
Orchidaceae	0	0	0	0	0	0	0	0	0	0	0	2	0	0
Oxalis	0	0	1	0	0	0	0	0	0	0	0	0	0	0
Plumbaginaceae	0	1	0	0	0	0	0	0	0	0	0	0	0	0
Erythrina	0	0	0	0	0	0	0	0	0	0	0	0	0	0
Boraginaceae	0	0	0	0	0	0	0	0	0	0	0	0	0	0
Portulacaceae	0	0	0	0	0	0	0	0	0	0	0	0	0	0
Bigonaceae	0	0	0	0	0	0	0	0	0	0	0	0	0	0
Kniphofia	0	0	0	2	0	0	0	0	0	0	0	0	0	0
Linaceae	0	0	0	0	0	0	0	1	0	0	0	0	0	0
Lamiaceae	0	0	0	0	0	0	0	0	0	0	0	0	0	0
Convolvulaceae	1	0	0	0	0	0	0	0	0	0	0	0	0	0
Araceae	0	0	0	0	0	0	0	0	0	1	0	0	0	0
Hermannia	0	0	1	0	0	0	0	0	0	0	0	0	1	2
Lentibulariaceae	0	0	0	0	0	0	0	0	0	0	0	0	0	0
Acanthaceae	1	1	0	0	0	0	0	0	0	0	0	0	0	0
Apiaceae	2	2	16	1	0	0	0	0	0	0	2	2	2	2
Gentianaceae	0	2	3	0	0	0	0	0	0	0	9	0	0	0
Potamogetonaceae	0	0	0	0	0	0	0	0	0	0	0	0	0	0
Fabaceae	0	5	3	3	4	9	1	6	9	2	0	9	1	7

Sample ID	RVSB2-15	RVSB2-16	RVSB2-17	RVSB2-18	RVSB2-19	RVSB2-20	RVSB2-21	RVSB2-22	RVSB2-23	RVSB2-24	RVSB2-25	RVSB2-26	RVSB2-27	RVSB2-28
Depth (cm)	71.25	76.25	81.25	86.25	91.25	96.25	101.25	106.25	111.25	116.25	122.25	127.25	132.25	137.25
Age (ka)	0.91	0.98	1.04	1.10	1.46	2.01	2.56	3.11	3.67	4.22	4.88	5.43	5.98	6.25
Rhamnaceae	0	0	2	0	0	0	0	0	2	0	1	1	1	0
Rutaceae	0	1	16	5	1	0	1	0	0	2	0	0	4	12
Santalaceae	1	0	1	0	1	1	0	0	2	2	0	2	1	3
Scroph-type	1	1	0	0	6	3	0	0	0	0	3	0	2	8
Thymelaeaceae	4	2	1	14	7	6	4	4	10	0	8	10	2	2
Passerina	4	3	6	4	4	3	136	32	2	15	5	5	16	10
Galium	1	0	0	0	0	0	0	3	0	0	0	0	0	0
Canthium	3	4	1	2	2	1	0	1	2	0	0	0	3	4
Plantago	6	2	0	0	0	2	0	0	0	0	0	5	0	0
Cyperaceae	85	55	43	42	51	96	161	12	215	94	97	145	103	59
Restionaceae	7	8	6	10	6	10	27	21	32	28	10	12	14	4
Poaceae	80	101	37	44	46	77	17	36	25	68	63	97	43	44
Geraniaceae	6	1	1	0	1	0	4	8	0	6	3	2	3	0
Lobostemon	0	0	0	0	0	0	0	1	0	0	0	1	0	0
Montinaceae	0	0	0	0	0	0	0	0	0	0	0	0	0	0
Onagraceae	3	1	0	0	0	0	1	0	1	0	0	3	0	0
Oxygonum	0	0	1	0	0	0	0	0	0	0	0	0	0	0
Polygonum	0	0	1	0	2	0	4	22	3	3	2	0	3	0
Euphorbia	2	1	0	2	0	0	0	18	5	1	5	8	0	2
Clutia	1	3	0	1	0	0	2	6	3	3	0	2	1	1
ChenAm-type	31	16	54	27	62	3	0	4	0	25	10	15	27	23
Crassula	10	15	7	2	8	2	1	13	7	28	27	9	15	27
Ruschia	13	0	1	2	7	1	2	6	4	8	6	0	4	6
Juncaceae	4	14	2	6	12	11	1	6	4	3	5	12	4	7
Liliaceae	11	5	2	4	7	5	4	3	5	8	8	7	3	4
Iridaceae	1	2	0	3	2	0	3	1	3	2	3	2	0	2
Amaryllidaceae	1	1	0	1	1	0	1	0	2	0	2	0	1	2
Malvaceae	0	0	6	2	2	2	0	3	2	0	6	4	1	2
Scabiosa	1	0	1	0	0	0	0	0	0	0	0	0	0	0
Selaginaceae	0	0	0	1	0	0	0	0	0	0	2	0	0	0

Sample ID	RVSB2-15	RVSB2-16	RVSB2-17	RVSB2-18	RVSB2-19	RVSB2-20	RVSB2-21	RVSB2-22	RVSB2-23	RVSB2-24	RVSB2-25	RVSB2-26	RVSB2-27	RVSB2-28
Depth (cm)	**71.25**	**76.25**	**81.25**	**86.25**	**91.25**	**96.25**	**101.25**	**106.25**	**111.25**	**116.25**	**122.25**	**127.25**	**132.25**	**137.25**
Age (ka)	**0.91**	**0.98**	**1.04**	**1.10**	**1.46**	**2.01**	**2.56**	**3.11**	**3.67**	**4.22**	**4.88**	**5.43**	**5.98**	**6.25**
Urticaceae	7	12	0	0	8	0	3	0	0	0	0	5	0	0
Verbenaceae	6	1	0	0	0	0	0	0	0	0	0	2	0	0
Aponogeton	13	3	0	4	7	12	2	3	4	5	4	0	2	0
Haloragaceae	0	0	0	0	0	0	0	0	0	0	0	0	0	0
Typha	2	5	1	4	2	0	6	0	11	1	6	3	3	2
Zygophyllaceae	2	1	0	0	0	0	0	2	0	0	0	0	0	1
Loranthaceae	0	1	0	0	0	2	0	7	0	0	0	0	0	0
Sterculiaceae	0	2	0	0	1	1	0	2	2	1	0	0	3	1
Justica-type	0	1	3	2	3	0	0	8	1	2	2	2	4	0
Unknown D	0	0	0	1	0	0	0	0	0	0	0	0	0	0
Unknown E	0	0	0	0	0	0	0	0	0	0	0	0	0	0
Unknown F	0	0	0	0	0	0	0	0	0	0	0	0	0	0
Unknown	0	4	0	3	1	2	1	1	0	1	0	0	1	0
Unkn Tri	0	0	2	0	0	0	0	0	2	0	0	4	0	0
Unidentifiable	4	7	1	3	0	6	0	0	1	0	4	2	0	2
Broken	12	15	10	13	6	42	8	7	5	6	11	14	5	9
Total Unknown Pollen	16	26	13	20	7	50	9	8	8	7	15	20	6	11
Total Pollen	496	501	500	500	502	500	500	500	500	502	509	501	500	500
Pollen concentration	112487	99255	42614	32745	84072	73742	95621	73742	140525	35641	38295	38295	64524	48497
Monolete	12	45	26	11	20	41	9	10	13	16	33	14	21	18
Trilete	7	7	7	15	10	6	2	6	7	14	9	7	12	12
Riccia	0	0	0	0	0	1	0	1	0	0	3	0	0	0
Pellaea	0	0	0	0	0	0	0	0	0	0	0	0	0	0
Pottiaceae	4	1	0	0	0	0	0	0	0	0	0	3	0	0
Pseudoschizaea	0	0	0	0	0	0	0	0	0	0	0	0	0	0
Ophioglossum	0	0	0	1	0	0	0	0	0	0	0	0	0	0
Mohria	0	1	2	0	0	0	0	1	0	0	0	1	0	1
Muriform Spores	0	0	0	0	0	0	0	0	0	0	0	0	0	0
Septated Spores	0	0	1	0	0	0	0	0	0	0	0	0	0	0
Algae cells	7	12	0	1	0	25	0	0	2	0	0	3	0	0

Sample ID	RVSB2-15	RVSB2-16	RVSB2-17	RVSB2-18	RVSB2-19	RVSB2-20	RVSB2-21	RVSB2-22	RVSB2-23	RVSB2-24	RVSB2-25	RVSB2-26	RVSB2-27	RVSB2-28
Depth (cm)	**71.25**	**76.25**	**81.25**	**86.25**	**91.25**	**96.25**	**101.25**	**106.25**	**111.25**	**116.25**	**122.25**	**127.25**	**132.25**	**137.25**
Age (ka)	**0.91**	**0.98**	**1.04**	**1.10**	**1.46**	**2.01**	**2.56**	**3.11**	**3.67**	**4.22**	**4.88**	**5.43**	**5.98**	**6.25**
Glomus	6	11	0	3	4	7	0	0	0	0	0	3	0	0
10 - 50 um	578	266	1003	1915	745	792	683	724	47	606	675	121	884	422
50 - 100 um	5	5	0	32	8	22	3	11	0	2	11	0	8	9
>100 um	0	0	0	0	0	3	0	0	0	0	0	0	0	0
Total Charcoal	583	271	1003	1947	753	817	686	735	47	608	686	121	892	431
Charcoal concentration	132217	53689	85483	127510	126108	120495	131192	108401	13209	43339	51611	19553	115111	41804

Sample ID	RVSB2-29	RVSB2-30	RVSB2-31	RVSB2-32	RVSB2-33	RVSB2-34	RVSB2-35	RVSB2-36	RVSB2-37	RVSB2-38	RVSB2-39	RVSB2-40	RVSB2-41	RVSB2-42
Depth (cm)	142.25	147.25	152.25	157.25	162.25	167.25	172.25	177.25	182.25	187.25	192.25	197.25	202.25	207.25
Age (ka)	6.45	6.65	6.85	7.05	7.25	7.45	7.65	7.85	8.04	8.24	8.44	8.64	8.84	9.04
Encephalartos	0	0	0	0	3	0	3	0	1	0	0	6	2	2
Euclea	6	12	1	2	15	6	2	6	5	3	5	1	3	5
Grewia	1	1	0	0	2	2	0	0	0	1	0	0	0	0
Ilex	0	0	0	0	0	0	0	0	0	0	0	0	0	0
Lycium	0	1	0	0	1	0	1	0	1	0	0	0	1	1
Morella	0	1	1	0	1	2	0	0	2	4	0	0	4	4
Myrsine	2	0	2	7	2	7	2	4	2	0	3	2	1	1
Myrtaceae	2	4	1	3	2	0	4	0	1	1	0	0	0	3
Olea	0	2	0	0	2	0	0	1	0	0	0	0	0	0
Acacia	1	1	2	0	1	10	4	0	8	4	0	1	2	1
Blechnaceae	8	2	1	2	3	5	4	0	14	15	4	4	0	5
Celastraceae	1	5	2	0	2	1	0	3	0	2	0	0	0	4
Celtis	0	0	0	0	0	0	0	0	0	0	0	0	0	0
Diospyros	0	3	0	4	2	5	8	2	0	1	7	3	0	0
Dodonaea	1	1	8	2	1	8	3	0	0	6	0	3	8	2
Pinaceae	0	0	0	0	0	0	0	0	0	0	0	0	0	0
Podocarpus	0	0	1	1	2	0	0	1	0	5	0	2	0	0
Rhus	0	1	1	1	0	1	1	0	2	2	0	0	0	0
Sapotaceae	0	0	0	0	0	0	0	0	0	0	0	0	0	0
Vitaceae	0	0	0	1	0	2	0	0	0	0	0	0	0	0
Asteraceae HS	63	44	30	43	27	42	31	83	21	43	127	35	83	83
Pentzia-type	4	1	1	8	0	1	4	6	3	2	15	2	0	2
Artemisia	3	1	0	5	2	3	0	2	3	2	8	0	1	4
Tarchonanthus	0	1	0	0	2	5	3	0	0	0	0	2	0	0
Stoebe-type	3	23	26	1	9	13	9	19	13	6	27	4	58	45
Proteaceae	29	47	34	42	29	36	31	97	9	21	48	10	23	32
Ericaceae	7	2	2	0	5	3	10	1	0	1	1	2	3	0
Cliffortia	0	3	3	2	1	4	3	0	5	0	0	1	4	2
Bruniaceae	1	4	5	3	2	5	0	2	0	0	0	1	1	2
Anthospermum-type	4	5	3	2	2	0	1	1	2	0	1	2	4	2

Sample ID	RVSB2-29	RVSB2-30	RVSB2-31	RVSB2-32	RVSB2-33	RVSB2-34	RVSB2-35	RVSB2-36	RVSB2-37	RVSB2-38	RVSB2-39	RVSB2-40	RVSB2-41	RVSB2-42
Depth (cm)	142.25	147.25	152.25	157.25	162.25	167.25	172.25	177.25	182.25	187.25	192.25	197.25	202.25	207.25
Age (ka)	6.45	6.65	6.85	7.05	7.25	7.45	7.65	7.85	8.04	8.24	8.44	8.64	8.84	9.04
Aizoaceae	9	8	8	2	2	3	1	0	7	4	7	5	3	6
Euphorbiaceae undif	3	0	0	5	0	4	6	3	0	2	4	2	0	0
Aloe-type	1	0	0	1	0	0	0	2	0	0	1	0	0	0
Brassicaceae	0	0	1	0	0	2	7	0	12	1	0	1	1	7
Campanulaceae	0	0	3	0	3	2	2	0	2	7	0	3	10	6
Caryophyllaceae	0	0	0	0	0	2	3	0	0	0	0	0	0	1
Gunneraceae	0	0	1	0	0	2	4	0	1	0	0	3	7	2
Polygala	1	1	1	1	1	0	0	1	1	0	0	2	0	0
Solanum	0	1	0	0	0	4	0	0	0	0	2	0	0	0
Araliaceae	0	0	0	0	0	1	0	1	0	0	1	0	0	0
Ascelepidaceae	0	0	0	0	0	2	3	0	0	0	0	2	0	0
Orchidaceae	0	0	0	0	0	2	0	0	0	0	0	2	0	0
Oxalis	1	0	0	2	1	3	1	5	0	0	0	0	0	0
Plumbaginaceae	0	0	0	0	0	0	0	0	0	0	0	0	0	0
Erythrina	0	0	0	0	0	0	0	0	0	0	0	0	0	0
Boraginaceae	0	0	0	0	0	0	0	0	0	0	0	0	0	0
Portulacaceae	0	0	0	0	0	0	0	0	0	0	0	0	0	0
Bigonaceae	0	0	0	1	1	0	2	0	0	0	0	0	0	0
Kniphofia	0	0	0	0	0	0	0	0	0	0	0	0	0	0
Linaceae	0	0	0	0	0	0	0	0	0	0	0	0	0	0
Lamiaceae	2	0	0	0	0	0	0	0	0	0	0	0	0	0
Convolvulaceae	0	0	0	0	0	0	1	1	0	0	0	0	2	0
Araceae	0	0	0	0	0	0	0	0	0	0	0	1	0	0
Hermannia	3	0	0	0	0	0	0	1	0	0	1	0	0	1
Lentibulariaceae	0	0	0	0	0	0	0	0	0	0	0	0	0	0
Acanthaceae	0	0	0	0	0	0	0	0	2	0	0	0	0	1
Apiaceae	0	0	0	0	1	1	1	0	1	0	0	0	0	1
Gentianaceae	1	3	0	0	2	4	0	0	0	0	0	0	0	0
Potamogetonaceae	0	0	0	0	0	0	0	0	0	0	0	0	0	0
Fabaceae	4	4	3	6	8	4	8	5	1	0	3	0	3	2

Sample ID	RVSB2-29	RVSB2-30	RVSB2-31	RVSB2-32	RVSB2-33	RVSB2-34	RVSB2-35	RVSB2-36	RVSB2-37	RVSB2-38	RVSB2-39	RVSB2-40	RVSB2-41	RVSB2-42
Depth (cm)	**142.25**	**147.25**	**152.25**	**157.25**	**162.25**	**167.25**	**172.25**	**177.25**	**182.25**	**187.25**	**192.25**	**197.25**	**202.25**	**207.25**
Age (ka)	**6.45**	**6.65**	**6.85**	**7.05**	**7.25**	**7.45**	**7.65**	**7.85**	**8.04**	**8.24**	**8.44**	**8.64**	**8.84**	**9.04**
Rhamnaceae	0	0	0	0	0	3	2	0	1	0	0	1	1	3
Rutaceae	2	0	3	8	6	1	2	13	0	1	19	6	1	2
Santalaceae	4	0	0	0	1	1	1	1	0	0	1	3	0	1
Scroph-type	3	3	0	1	5	5	5	3	2	0	0	1	2	2
Thymelaeaceae	0	8	5	2	4	2	9	2	22	1	1	2	0	4
Passerina	4	7	3	7	8	4	3	11	7	3	17	0	1	1
Galium	0	2	0	0	0	0	0	0	0	0	0	0	0	0
Canthium	2	2	0	0	2	3	1	0	1	0	0	0	0	0
Plantago	0	1	6	0	3	13	0	0	7	15	0	0	25	16
Cyperaceae	161	163	162	199	86	69	58	41	67	47	21	107	13	26
Restionaceae	23	8	11	25	7	8	21	5	13	6	15	9	5	4
Poaceae	50	33	60	25	75	59	66	68	47	68	51	125	71	69
Geraniaceae	2	4	7	5	5	2	4	2	11	4	2	0	5	9
Lobostemon	0	4	0	1	1	1	0	0	1	0	0	0	1	2
Montinaceae	0	1	0	0	0	0	0	0	2	0	0	0	2	0
Onagraceae	0	1	0	0	2	0	1	0	0	0	0	0	2	0
Oxygonum	0	0	0	0	0	0	1	0	0	0	0	0	0	0
Polygonum	18	3	0	1	3	0	1	1	0	1	0	0	2	1
Euphorbia	5	0	2	3	1	7	7	1	8	2	4	2	1	2
Clutia	4	2	2	3	1	0	4	1	0	0	4	3	3	2
ChenAm-type	4	12	12	9	15	8	26	52	56	25	42	40	18	23
Crassula	2	17	10	10	14	5	20	8	12	5	14	16	7	23
Ruschia	10	0	8	5	2	9	11	1	3	0	10	3	11	9
Juncaceae	4	6	10	4	20	17	11	10	14	13	7	17	17	7
Liliaceae	2	4	10	6	12	17	12	9	7	3	4	12	10	15
Iridaceae	6	1	2	0	5	5	2	5	0	2	2	0	3	0
Amaryllidaceae	2	2	0	0	4	4	0	3	2	0	3	0	2	0
Malvaceae	1	5	0	4	4	4	2	0	3	5	5	1	3	3
Scabiosa	0	0	0	0	0	0	0	0	0	0	0	0	0	0
Selaginaceae	0	0	0	0	0	0	0	0	0	0	0	0	0	1

Sample ID	RVSB2-29	RVSB2-30	RVSB2-31	RVSB2-32	RVSB2-33	RVSB2-34	RVSB2-35	RVSB2-36	RVSB2-37	RVSB2-38	RVSB2-39	RVSB2-40	RVSB2-41	RVSB2-42
Depth (cm)	142.25	147.25	152.25	157.25	162.25	167.25	172.25	177.25	182.25	187.25	192.25	197.25	202.25	207.25
Age (ka)	6.45	6.65	6.85	7.05	7.25	7.45	7.65	7.85	8.04	8.24	8.44	8.64	8.84	9.04
Urticaceae	0	8	9	0	22	22	21	8	39	111	0	12	9	6
Verbenaceae	0	3	1	0	2	0	0	0	3	2	0	0	6	3
Aponogeton	5	5	8	17	15	9	15	0	13	19	1	7	17	9
Haloragaceae	0	0	0	0	1	0	0	0	0	0	2	1	0	0
Typha	11	3	1	1	7	0	0	0	18	0	0	3	4	6
Zygophyllaceae	1	1	0	0	0	0	0	0	0	0	0	0	3	1
Loranthaceae	0	0	0	0	0	1	0	0	0	0	0	0	0	0
Sterculiaceae	3	3	1	0	4	5	1	0	0	1	0	4	0	1
Justica-type	1	0	0	2	0	2	0	0	0	0	0	2	0	0
Unknown D	0	0	0	0	0	0	1	0	0	0	0	0	0	0
Unknown E	0	0	0	0	0	0	0	0	0	0	0	0	0	0
Unknown F	0	0	0	0	0	0	0	0	0	0	0	0	0	0
Unknown	1	1	0	2	1	0	0	0	2	8	0	0	1	0
Unkn Tri	1	0	0	2	0	6	2	0	0	0	0	3	0	0
Unidentifiable	0	3	5	0	3	3	2	3	4	3	2	4	5	5
Broken	7	5	21	11	14	12	12	6	17	22	8	14	25	17
Total Unknown Pollen	9	9	26	15	18	21	17	9	23	33	10	21	31	22
Total Pollen	500	503	500	500	492	504	487	501	501	500	500	500	500	500
Pollen concentration	30568	84438	130682	92379	35520	135973	64075	16552	111578	58759	14121	33332	51100	35190
Monolete	50	27	14	52	27	15	28	16	13	35	31	46	33	29
Trilete	21	6	8	14	11	15	26	13	8	11	15	42	22	8
Riccia	3	0	0	0	6	1	3	2	0	0	1	4	3	1
Pellaea	0	0	0	0	1	0	3	0	0	0	0	0	1	0
Pottiaceae	0	0	0	0	10	19	13	0	0	0	0	5	0	0
Pseudoschizaea	0	0	0	0	0	0	0	0	0	0	0	0	0	0
Ophioglossum	0	1	0	0	0	0	0	0	0	0	0	0	0	0
Mohria	0	0	0	0	1	0	0	1	0	0	0	0	0	0
Muriform Spores	11	0	0	2	0	0	0	0	0	0	2	2	0	0
Septated Spores	10	0	0	7	0	0	0	1	0	0	17	0	0	0
Algae cells	0	12	20	0	16	9	13	0	5	1	0	18	14	24

Sample ID	RVSB2-29	RVSB2-30	RVSB2-31	RVSB2-32	RVSB2-33	RVSB2-34	RVSB2-35	RVSB2-36	RVSB2-37	RVSB2-38	RVSB2-39	RVSB2-40	RVSB2-41	RVSB2-42
Depth (cm)	**142.25**	**147.25**	**152.25**	**157.25**	**162.25**	**167.25**	**172.25**	**177.25**	**182.25**	**187.25**	**192.25**	**197.25**	**202.25**	**207.25**
Age (ka)	**6.45**	**6.65**	**6.85**	**7.05**	**7.25**	**7.45**	**7.65**	**7.85**	**8.04**	**8.24**	**8.44**	**8.64**	**8.84**	**9.04**
Glomus	0	5	2	9	8	1	6	10	6	2	9	8	18	16
10 - 50 um	2446	286	402	346	85	93	248	504	282	169	1675	366	457	253
50 - 100 um	51	11	7	0	2	5	15	16	1	1	18	11	7	2
>100 um	5	1	0	0	0	0	0	0	0	0	0	0	0	0
Total Charcoal	2502	298	409	346	87	98	263	520	283	170	1693	377	464	255
Charcoal concentration	152963	50025	106898	63926	6281	26439	34603	17180	63027	19978	47813	25132	47421	17947

Sample ID	RVSB2-43	RVSB2-43B	RVSB2-44	RVSB2-44B	RVSB2-45	RVSB2-45B	RVSB2-46	RVSB2-47	RVSB2-47B	RVSB2-48	RVSB2-48B	RVSB2-49	RVSB2-49B
Depth (cm)	212.25	215	217.25	219	222.25	225	227.25	232.25	235	237.25	238	242.25	244
Age (ka)	9.31	9.47	9.58	9.69	9.86	10.02	10.14	10.41	10.58	10.69	10.74	10.96	11.07
Encephalartos	1		0									0	
Euclea	0		1									7	
Grewia	0		0									0	
Ilex	0		0									0	
Lycium	0		0									0	
Morella	0		2									0	
Myrsine	4		2									4	
Myrtaceae	0		0									1	
Olea	0		0									0	
Acacia	1		2									0	
Blechnaceae	0		3									0	
Celastraceae	0		0									0	
Celtis	0		0									0	
Diospyros	1		2									1	
Dodonaea	0		0									0	
Pinaceae	0		0									0	
Podocarpus	1		0									2	
Rhus	0		0									0	
Sapotaceae	0		0									0	
Vitaceae	0		0									1	
Asteraceae HS	70		36									7	
Pentzia-type	1		1									0	
Artemisia	6		0									2	
Tarchonanthus	0		6									0	
Stoebe-type	51		9									0	
Proteaceae	24		3									0	
Ericaceae	3		2									4	
Cliffortia	1		1									25	
Bruniaceae	3		4									3	
Anthospermum-type	2		0									23	

Sample ID	RVSB2-43	RVSB2-43B	RVSB2-44	RVSB2-44B	RVSB2-45	RVSB2-45B	RVSB2-46	RVSB2-47	RVSB2-47B	RVSB2-48	RVSB2-48B	RVSB2-49	RVSB2-49B
Depth (cm)	212.25	215	217.25	219	222.25	225	227.25	232.25	235	237.25	238	242.25	244
Age (ka)	9.31	9.47	9.58	9.69	9.86	10.02	10.14	10.41	10.58	10.69	10.74	10.96	11.07
Aizoaceae	6		4									1	
Euphorbiaceae undif	0		4									14	
Aloe-type	0		1									7	
Brassicaceae	2		0									2	
Campanulaceae	5		1									0	
Caryophyllaceae	0		0									0	
Gunneraceae	0		0									0	
Polygala	0		0									0	
Solanum	0		1									0	
Araliaceae	0		0									0	
Ascelepidaceae	0		0									0	
Orchidaceae	0		1									0	
Oxalis	0		0									1	
Plumbaginaceae	0		0									0	
Erythrina	0		0									0	
Boraginaceae	0		0									0	
Portulacaceae	0		0									0	
Bigonaceae	0		0									0	
Kniphofia	0		0									4	
Linaceae	0		0									0	
Lamiaceae	0		0									0	
Convolvulaceae	0		0									0	
Araceae	0		0									0	
Hermannia	0		0									1	
Lentibulariaceae	0		0									0	
Acanthaceae	0		0									2	
Apiaceae	0		1									0	
Gentianaceae	0		0									4	
Potamogetonaceae	0		0									0	
Fabaceae	1		0									9	

Sample ID	RVSB2-43	RVSB2-43B	RVSB2-44	RVSB2-44B	RVSB2-45	RVSB2-45B	RVSB2-46	RVSB2-47	RVSB2-47B	RVSB2-48	RVSB2-48B	RVSB2-49	RVSB2-49B
Depth (cm)	212.25	215	217.25	219	222.25	225	227.25	232.25	235	237.25	238	242.25	244
Age (ka)	9.31	9.47	9.58	9.69	9.86	10.02	10.14	10.41	10.58	10.69	10.74	10.96	11.07
Rhamnaceae	0		0									0	
Rutaceae	3		1									0	
Santalaceae	3		0									0	
Scroph-type	1		0									2	
Thymelaeaceae	13		3									2	
Passerina	3		0									1	
Galium	1		0									2	
Canthium	1		0									5	
Plantago	0		0									0	
Cyperaceae	76		20									26	
Restionaceae	4		14									88	
Poaceae	61		283									139	
Geraniaceae	6		1									2	
Lobostemon	2		0									0	
Montinaceae	0		0									0	
Onagraceae	0		1									0	
Oxygonum	0		0									0	
Polygonum	1		0									0	
Euphorbia	4		1									7	
Clutia	1		2									4	
ChenAm-type	5		4									0	
Crassula	6		5									2	
Ruschia	4		4									11	
Juncaceae	16		25									9	
Liliaceae	8		8									40	
Iridaceae	2		2									6	
Amaryllidaceae	0		0									2	
Malvaceae	10		0									0	
Scabiosa	0		0									0	
Selaginaceae	0		0									0	

Sample ID	RVSB2-43	RVSB2-43B	RVSB2-44	RVSB2-44B	RVSB2-45	RVSB2-45B	RVSB2-46	RVSB2-47	RVSB2-47B	RVSB2-48	RVSB2-48B	RVSB2-49	RVSB2-49B
Depth (cm)	212.25	215	217.25	219	222.25	225	227.25	232.25	235	237.25	238	242.25	244
Age (ka)	9.31	9.47	9.58	9.69	9.86	10.02	10.14	10.41	10.58	10.69	10.74	10.96	11.07
Urticaceae	3		14									0	
Verbenaceae	1		0									0	
Aponogeton	47		11									9	
Haloragaceae	0		0									0	
Typha	0		0									2	
Zygophyllaceae	0		0									0	
Loranthaceae	2		0									0	
Sterculiaceae	0		0									0	
Justica-type	0		1									2	
Unknown D	0		0									0	
Unknown E	0		0									0	
Unknown F	0		0									0	
Unknown	2		0									0	
Unkn Tri	0		1									1	
Unidentifiable	6		3									3	
Broken	35		9									10	
Total Unknown Pollen	43		13									14	
Total Pollen	510		500									500	
Pollen concentration	52705		4350									28965	
Monolete	30		26									58	
Trilete	16		13									16	
Riccia	3		0									1	
Pellaea	0		0									0	
Pottiaceae	0		2									0	
Pseudoschizaea	0		0									0	
Ophioglossum	0		0									0	
Mohria	0		0									0	
Muriform Spores	0		0									0	
Septated Spores	0		0									0	
Algae cells	14		0									0	

Sample ID	RVSB2-43	RVSB2-43B	RVSB2-44	RVSB2-44B	RVSB2-45	RVSB2-45B	RVSB2-46	RVSB2-47	RVSB2-47B	RVSB2-48	RVSB2-48B	RVSB2-49	RVSB2-49B
Depth (cm)	**212.25**	**215**	**217.25**	**219**	**222.25**	**225**	**227.25**	**232.25**	**235**	**237.25**	**238**	**242.25**	**244**
Age (ka)	**9.31**	**9.47**	**9.58**	**9.69**	**9.86**	**10.02**	**10.14**	**10.41**	**10.58**	**10.69**	**10.74**	**10.96**	**11.07**
Glomus	3		2									1	
10 - 50 um	129		228									31	
50 - 100 um	2		0									0	
>100 um	0		0									0	
Total Charcoal	131		228									31	
Charcoal concentration	13538		14339									1796	

Sample ID	RVSB2-50	RVSB2-51	RVSB2-52	RVSB2-52B	RVSB2-53	RVSB2-53B	RVSB2-54	RVSB2-55	RVSB2-56	RVSB2-56B	RVSB2-57	RVSB2-58	RVSB2-58B
Depth (cm)	247.25	252.25	257.25	259	262.25	264	267.25	272.25	277.25	279	282.25	287.25	289
Age (ka)	11.29	11.67	12.36	12.82	13.50	13.96	14.65	15.79	16.98	17.47	18.20	19.42	19.91
Encephalartos				0	2	0	0	0		0	0	0	
Euclea				1	5	0	0	11		2	1	1	
Grewia				0	0	0	0	0		0	1	2	
Ilex				0	0	0	0	0		0	0	0	
Lycium				0	0	0	0	0		0	0	0	
Morella				0	4	1	0	0		0	1	11	
Myrsine				1	7	0	0	9		1	0	7	
Myrtaceae				1	1	1	0	1		0	0	0	
Olea				0	0	1	0	1		1	0	0	
Acacia				0	0	0	0	1		0	0	0	
Blechnaceae				0	0	0	0	2		0	4	0	
Celastraceae				0	1	0	0	2		0	0	1	
Celtis				0	0	0	0	0		0	1	0	
Diospyros				0	2	0	0	1		0	0	0	
Dodonaea				0	0	0	0	0		0	1	12	
Pinaceae				0	0	0	0	0		0	0	0	
Podocarpus				1	4	0	0	1		0	0	0	
Rhus				0	0	0	0	0		0	0	0	
Sapotaceae				0	0	0	0	0		0	0	0	
Vitaceae				0	0	0	0	0		0	0	0	
Asteraceae HS				73	62	30	46	43		26	24	55	
Pentzia-type				2	3	0	0	1		1	2	4	
Artemisia				2	0	1	2	6		0	0	2	
Tarchonanthus				0	2	0	0	0		0	0	0	
Stoebe-type				21	16	7	35	17		8	17	55	
Proteaceae				10	7	3	8	9		4	3	47	
Ericaceae				0	2	0	1	1		1	2	3	
Cliffortia				0	3	0	2	6		3	1	71	
Bruniaceae				0	9	0	0	0		0	0	3	
Anthospermum-type				1	1	0	0	2		0	0	2	

Sample ID	RVSB2-50	RVSB2-51	RVSB2-52	RVSB2-52B	RVSB2-53	RVSB2-53B	RVSB2-54	RVSB2-55	RVSB2-56	RVSB2-56B	RVSB2-57	RVSB2-58	RVSB2-58B
Depth (cm)	247.25	252.25	257.25	259	262.25	264	267.25	272.25	277.25	279	282.25	287.25	289
Age (ka)	11.29	11.67	12.36	12.82	13.50	13.96	14.65	15.79	16.98	17.47	18.20	19.42	19.91
Aizoaceae				11	3	1	8	6		3	0	3	
Euphorbiaceae undif				0	1	0	0	8		0	1	8	
Aloe-type				0	0	0	0	0		0	1	0	
Brassicaceae				0	0	0	0	5		0	1	0	
Campanulaceae				0	0	0	0	0		0	3	1	
Caryophyllaceae				0	0	0	0	0		0	0	0	
Gunneraceae				1	0	0	0	2		0	0	0	
Polygala				0	1	0	0	1		0	0	2	
Solanum				0	0	0	0	1		0	1	2	
Araliaceae				0	0	0	0	1		0	0	0	
Ascelepidaceae				0	0	0	0	0		0	1	0	
Orchidaceae				0	0	0	0	0		0	1	0	
Oxalis				0	0	0	0	0		0	0	1	
Plumbaginaceae				0	0	0	0	0		0	0	0	
Erythrina				0	0	0	0	0		0	0	0	
Boraginaceae				0	0	0	0	0		0	0	0	
Portulacaceae				0	0	0	0	0		0	0	0	
Bigonaceae				0	0	0	0	0		0	0	0	
Kniphofia				0	0	0	0	0		0	0	0	
Linaceae				0	0	0	0	0		0	0	0	
Lamiaceae				0	0	0	0	0		0	0	0	
Convolvulaceae				0	1	0	0	1		0	0	0	
Araceae				0	0	0	0	2		0	0	0	
Hermannia				0	0	0	0	0		0	0	0	
Lentibulariaceae				0	0	0	0	1		0	0	0	
Acanthaceae				1	0	0	0	0		3	0	0	
Apiaceae				0	0	0	0	0		0	0	0	
Gentianaceae				0	2	0	0	1		1	0	2	
Potamogetonaceae				0	0	0	0	0		0	0	0	
Fabaceae				3	2	1	1	3		0	0	1	

Sample ID	RVSB2-50	RVSB2-51	RVSB2-52	RVSB2-52B	RVSB2-53	RVSB2-53B	RVSB2-54	RVSB2-55	RVSB2-56	RVSB2-56B	RVSB2-57	RVSB2-58	RVSB2-58B
Depth (cm)	247.25	252.25	257.25	259	262.25	264	267.25	272.25	277.25	279	282.25	287.25	289
Age (ka)	11.29	11.67	12.36	12.82	13.50	13.96	14.65	15.79	16.98	17.47	18.20	19.42	19.91
Rhamnaceae				0	1	0	0	0		0	0	0	
Rutaceae				1	1	0	2	0		0	0	0	
Santalaceae				0	0	0	1	0		0	0	0	
Scroph-type				0	1	0	2	3		0	0	0	
Thymelaeaceae				0	3	0	0	8		1	1	5	
Passerina				0	0	0	2	1		0	0	4	
Galium				0	0	0	0	0		0	0	1	
Canthium				1	0	2	0	1		0	0	1	
Plantago				0	2	0	0	0		2	0	0	
Cyperaceae				4	6	1	7	6		7	4	18	
Restionaceae				2	0	1	5	0		1	7	33	
Poaceae				5	56	3	24	57		22	78	40	
Geraniaceae				1	4	1	2	5		3	1	1	
Lobostemon				0	0	0	0	0		0	0	0	
Montinaceae				0	0	0	0	0		0	0	0	
Onagraceae				0	0	0	0	0		0	1	0	
Oxygonum				0	0	0	0	0		0	0	0	
Polygonum				0	1	0	0	0		0	0	0	
Euphorbia				2	4	1	0	1		1	1	0	
Clutia				0	3	0	1	4		0	1	6	
ChenAm-type				127	131	70	80	46		2	14	36	
Crassula				12	17	4	7	8		1	6	2	
Ruschia				4	1	1	1	10		0	5	9	
Juncaceae				4	17	1	2	10		5	14	13	
Liliaceae				2	9	0	3	8		2	7	7	
Iridaceae				0	1	0	2	8		0	2	2	
Amaryllidaceae				0	1	0	1	1		0	0	4	
Malvaceae				3	4	1	0	0		0	1	4	
Scabiosa				0	0	0	0	0		0	0	0	
Selaginaceae				0	0	0	0	0		0	1	0	

Sample ID	RVSB2-50	RVSB2-51	RVSB2-52	RVSB2-52B	RVSB2-53	RVSB2-53B	RVSB2-54	RVSB2-55	RVSB2-56	RVSB2-56B	RVSB2-57	RVSB2-58	RVSB2-58B
Depth (cm)	247.25	252.25	257.25	259	262.25	264	267.25	272.25	277.25	279	282.25	287.25	289
Age (ka)	11.29	11.67	12.36	12.82	13.50	13.96	14.65	15.79	16.98	17.47	18.20	19.42	19.91
Urticaceae				0	14	0	0	3		0	3	0	
Verbenaceae				0	0	0	0	0		0	0	0	
Aponogeton				0	7	0	0	6		0	6	2	
Haloragaceae				0	0	0	0	0		0	0	0	
Typha				0	0	2	0	5		6	7	4	
Zygophyllaceae				0	0	0	0	0		0	0	0	
Loranthaceae				0	0	0	0	0		0	0	0	
Sterculiaceae				0	4	0	0	1		0	0	0	
Justica-type				0	1	0	0	1		0	0	0	
Unknown D				0	0	0	0	0		0	0	0	
Unknown E				0	0	0	0	1		0	0	0	
Unknown F				0	0	0	0	0		0	0	0	
Unknown				1	0	0	0	5		0	0	2	
Unkn Tri				0	0	0	0	5		0	0	0	
Unidentifiable				1	5	0	0	4		0	2	2	
Broken				4	10	2	5	9		0	6	8	
Total Unknown Pollen				6	15	2	5	24		0	8	12	
Total Pollen				303	445	136	250	363		107	235	500	
Pollen concentration				4605	15160	4294	4918	5472		1808	3466	9234	
Monolete				37	32	12	13	54		10	93	27	
Trilete				6	19	2	9	22		20	19	11	
Riccia				1	3	0	2	9		0	4	1	
Pellaea				2	0	0	0	0		0	0	0	
Pottiaceae				0	1	0	0	0		0	14	1	
Pseudoschizaea				0	0	0	0	0		0	0	1	
Ophioglossum				0	0	0	0	5		0	2	2	
Mohria				0	0	0	0	2		0	0	0	
Muriform Spores				0	0	0	1	4		0	1	0	
Septated Spores				0	0	0	0	5		0	0	0	
Algae cells				0	23	0	0	0		0	0	0	

Sample ID	RVSB2-50	RVSB2-51	RVSB2-52	RVSB2-52B	RVSB2-53	RVSB2-53B	RVSB2-54	RVSB2-55	RVSB2-56	RVSB2-56B	RVSB2-57	RVSB2-58	RVSB2-58B
Depth (cm)	**247.25**	**252.25**	**257.25**	**259**	**262.25**	**264**	**267.25**	**272.25**	**277.25**	**279**	**282.25**	**287.25**	**289**
Age (ka)	**11.29**	**11.67**	**12.36**	**12.82**	**13.50**	**13.96**	**14.65**	**15.79**	**16.98**	**17.47**	**18.20**	**19.42**	**19.91**
Glomus				0	7	0	0	7		0	11	5	
10 - 50 um				3994	571	1836	1013	1001		940	586	312	
50 - 100 um				28	4	15	0	12		9	0	5	
>100 um				0	0	0	0	0		0	0	0	
Total Charcoal				4022	575	1851	1013	1013		949	586	317	
Charcoal concentration				61125	19588	58449	19929	15270		16035	8643	5854	

Sample ID	RVSB2-59	RVSB2-60	RVSB2-61	RVSB2-62	RVSB2-63	RVSB2-64	RVSB2-65	RVSB2-66	RVSB2-67	RVSB2-68	RVSB2-68B	RVSB2-69	RVSB2-69B
Depth (cm)	292.25	297.25	302.25	307.25	312.25	317.25	322.25	327.25	332.25	337.25	339	342.25	345
Age (ka)	20.65	21.87	23.09	24.32	25.54	26.76	27.98	29.21	30.43	31.65	32.14	32.88	33.61
Encephalartos												0	0
Euclea												3	0
Grewia												1	0
Ilex												1	0
Lycium												0	0
Morella												2	4
Myrsine												2	2
Myrtaceae												0	0
Olea												0	2
Acacia												0	0
Blechnaceae												0	0
Celastraceae												0	5
Celtis												0	0
Diospyros												3	0
Dodonaea												0	0
Pinaceae												0	0
Podocarpus												4	0
Rhus												1	0
Sapotaceae												0	0
Vitaceae												0	0
Asteraceae HS												18	27
Pentzia-type												0	1
Artemisia												1	13
Tarchonanthus												0	0
Stoebe-type												23	1
Proteaceae												4	2
Ericaceae												2	4
Cliffortia												7	18
Bruniaceae												3	0
Anthospermum-type												12	30

Sample ID	RVSB2-59	RVSB2-60	RVSB2-61	RVSB2-62	RVSB2-63	RVSB2-64	RVSB2-65	RVSB2-66	RVSB2-67	RVSB2-68	RVSB2-68B	RVSB2-69	RVSB2-69B
Depth (cm)	292.25	297.25	302.25	307.25	312.25	317.25	322.25	327.25	332.25	337.25	339	342.25	345
Age (ka)	20.65	21.87	23.09	24.32	25.54	26.76	27.98	29.21	30.43	31.65	32.14	32.88	33.61
Aizoaceae												11	19
Euphorbiaceae undif												8	20
Aloe-type												3	1
Brassicaceae												1	1
Campanulaceae												0	0
Caryophyllaceae												0	0
Gunneraceae												6	0
Polygala												0	0
Solanum												1	2
Araliaceae												0	0
Ascelepidaceae												0	0
Orchidaceae												0	0
Oxalis												0	0
Plumbaginaceae												0	0
Erythrina												0	0
Boraginaceae												0	0
Portulacaceae												0	0
Bigonaceae												0	0
Kniphofia												0	0
Linaceae												0	1
Lamiaceae												0	1
Convolvulaceae												0	0
Araceae												0	0
Hermannia												0	0
Lentibulariaceae												0	0
Acanthaceae												0	0
Apiaceae												0	1
Gentianaceae												1	13
Potamogetonaceae												1	0
Fabaceae												5	9

Sample ID	RVSB2-59	RVSB2-60	RVSB2-61	RVSB2-62	RVSB2-63	RVSB2-64	RVSB2-65	RVSB2-66	RVSB2-67	RVSB2-68	RVSB2-68B	RVSB2-69	RVSB2-69B
Depth (cm)	292.25	297.25	302.25	307.25	312.25	317.25	322.25	327.25	332.25	337.25	339	342.25	345
Age (ka)	20.65	21.87	23.09	24.32	25.54	26.76	27.98	29.21	30.43	31.65	32.14	32.88	33.61
Rhamnaceae												0	0
Rutaceae												0	0
Santalaceae												0	0
Scroph-type												0	0
Thymelaeaceae												4	1
Passerina												2	3
Galium												0	3
Canthium												5	10
Plantago												0	6
Cyperaceae												38	23
Restionaceae												28	73
Poaceae												39	58
Geraniaceae												14	25
Lobostemon												0	0
Montinaceae												0	0
Onagraceae												0	0
Oxygonum												0	0
Polygonum												0	2
Euphorbia												3	9
Clutia												1	0
ChenAm-type												3	2
Crassula												12	8
Ruschia												12	32
Juncaceae												12	4
Liliaceae												19	6
Iridaceae												2	6
Amaryllidaceae												5	1
Malvaceae												0	0
Scabiosa												2	1
Selaginaceae												0	1

Sample ID	RVSB2-59	RVSB2-60	RVSB2-61	RVSB2-62	RVSB2-63	RVSB2-64	RVSB2-65	RVSB2-66	RVSB2-67	RVSB2-68	RVSB2-68B	RVSB2-69	RVSB2-69B
Depth (cm)	**292.25**	**297.25**	**302.25**	**307.25**	**312.25**	**317.25**	**322.25**	**327.25**	**332.25**	**337.25**	**339**	**342.25**	**345**
Age (ka)	**20.65**	**21.87**	**23.09**	**24.32**	**25.54**	**26.76**	**27.98**	**29.21**	**30.43**	**31.65**	**32.14**	**32.88**	**33.61**
Urticaceae												3	0
Verbenaceae												0	0
Aponogeton												14	0
Haloragaceae												0	3
Typha												6	19
Zygophyllaceae												0	2
Loranthaceae												0	0
Sterculiaceae												0	0
Justica-type												1	0
Unknown D												0	0
Unknown E												0	0
Unknown F												35	5
Unknown												1	4
Unkn Tri												3	1
Unidentifiable												3	2
Broken												7	13
Total Unknown Pollen												49	25
Total Pollen												398	500
Pollen concentration												7034	6816
Monolete												25	37
Trilete												15	12
Riccia												0	2
Pellaea												0	1
Pottiaceae												0	0
Pseudoschizaea												0	0
Ophioglossum												0	0
Mohria												0	0
Muriform Spores												1	0
Septated Spores												0	0
Algae cells												1	0

Sample ID	RVSB2-59	RVSB2-60	RVSB2-61	RVSB2-62	RVSB2-63	RVSB2-64	RVSB2-65	RVSB2-66	RVSB2-67	RVSB2-68	RVSB2-68B	RVSB2-69	RVSB2-69B
Depth (cm)	**292.25**	**297.25**	**302.25**	**307.25**	**312.25**	**317.25**	**322.25**	**327.25**	**332.25**	**337.25**	**339**	**342.25**	**345**
Age (ka)	**20.65**	**21.87**	**23.09**	**24.32**	**25.54**	**26.76**	**27.98**	**29.21**	**30.43**	**31.65**	**32.14**	**32.88**	**33.61**
Glomus												2	0
10 - 50 um												120	6040
50 - 100 um												0	13
>100 um												0	0
Total Charcoal												120	6053
Charcoal concentration												2121	82511

Sample ID	RVSB2-70	RVSB2-70B	RVSB2-71	RVSB2-71B	RVSB2-72
Depth (cm)	347.25	349.25	352.25	354.25	357.25
Age (ka)	34.10	34.59	35.32	35.81	36.55
Encephalartos	3	5		0	
Euclea	1	4		6	
Grewia	3	0		1	
Ilex	0	0		0	
Lycium	1	0		0	
Morella	0	0		3	
Myrsine	3	4		0	
Myrtaceae	0	0		1	
Olea	3	3		1	
Acacia	0	0		0	
Blechnaceae	0	5		0	
Celastraceae	2	6		4	
Celtis	0	0		0	
Diospyros	0	1		0	
Dodonaea	0	2		3	
Pinaceae	0	0		0	
Podocarpus	0	0		0	
Rhus	0	0		1	
Sapotaceae	0	0		0	
Vitaceae	2	0		0	
Asteraceae HS	15	26		10	
Pentzia-type	0	0		1	
Artemisia	0	8		9	
Tarchonanthus	0	0		0	
Stoebe-type	9	34		5	
Proteaceae	8	1		1	
Ericaceae	5	1		2	
Cliffortia	8	2		4	
Bruniaceae	2	1		1	
Anthospermum-type	6	9		22	

Sample ID	RVSB2-70	RVSB2-70B	RVSB2-71	RVSB2-71B	RVSB2-72
Depth (cm)	347.25	349.25	352.25	354.25	357.25
Age (ka)	34.10	34.59	35.32	35.81	36.55
Aizoaceae	10	11		30	
Euphorbiaceae undif	19	6		23	
Aloe-type	0	0		0	
Brassicaceae	2	0		0	
Campanulaceae	1	0		0	
Caryophyllaceae	0	0		0	
Gunneraceae	0	2		2	
Polygala	0	0		0	
Solanum	0	3		0	
Araliaceae	0	0		0	
Ascelepidaceae	0	0		0	
Orchidaceae	0	0		0	
Oxalis	2	0		1	
Plumbaginaceae	2	0		0	
Erythrina	0	0		0	
Boraginaceae	0	0		0	
Portulacaceae	0	0		0	
Bigonaceae	0	0		0	
Kniphofia	0	0		0	
Linaceae	0	0		0	
Lamiaceae	0	0		0	
Convolvulaceae	0	1		0	
Araceae	0	0		0	
Hermannia	0	0		0	
Lentibulariaceae	0	0		0	
Acanthaceae	0	0		0	
Apiaceae	0	0		0	
Gentianaceae	2	4		5	
Potamogetonaceae	0	0		0	
Fabaceae	11	6		1	

Sample ID	RVSB2-70	RVSB2-70B	RVSB2-71	RVSB2-71B	RVSB2-72
Depth (cm)	347.25	349.25	352.25	354.25	357.25
Age (ka)	34.10	34.59	35.32	35.81	36.55
Rhamnaceae	0	0		0	
Rutaceae	0	0		1	
Santalaceae	0	1		0	
Scroph-type	0	5		2	
Thymelaeaceae	2	7		3	
Passerina	4	0		1	
Galium	0	0		0	
Canthium	2	1		3	
Plantago	0	0		0	
Cyperaceae	24	11		6	
Restionaceae	51	22		3	
Poaceae	55	48		19	
Geraniaceae	149	192		30	
Lobostemon	0	0		0	
Montinaceae	0	0		0	
Onagraceae	0	0		0	
Oxygonum	0	0		0	
Polygonum	0	0		0	
Euphorbia	8	1		7	
Clutia	6	0		5	
ChenAm-type	1	1		3	
Crassula	9	13		27	
Ruschia	12	9		20	
Juncaceae	8	4		4	
Liliaceae	11	5		1	
Iridaceae	3	2		3	
Amaryllidaceae	1	0		1	
Malvaceae	0	0		0	
Scabiosa	0	1		1	
Selaginaceae	0	0		1	

Sample ID	RVSB2-70	RVSB2-70B	RVSB2-71	RVSB2-71B	RVSB2-72
Depth (cm)	347.25	349.25	352.25	354.25	357.25
Age (ka)	34.10	34.59	35.32	35.81	36.55
Urticaceae	0	0		0	
Verbenaceae	1	0		2	
Aponogeton	7	3		6	
Haloragaceae	0	0		0	
Typha	6	0		0	
Zygophyllaceae	0	0		0	
Loranthaceae	0	0		0	
Sterculiaceae	0	0		0	
Justica-type	1	0		0	
Unknown D	0	0		0	
Unknown E	0	0		0	
Unknown F	1	0		0	
Unknown	3	5		0	
Unkn Tri	4	5		1	
Unidentifiable	0	3		4	
Broken	11	16		9	
Total Unknown Pollen	19	29		14	
Total Pollen	500	500		300	
Pollen concentration	15652	6078		8332	
Monolete	19	35		13	
Trilete	16	17		3	
Riccia	2	2		1	
Pellaea	1	0		0	
Pottiaceae	0	0		0	
Pseudoschizaea	0	88		0	
Ophioglossum	0	0		0	
Mohria	0	0		0	
Muriform Spores	2	0		0	
Septated Spores	1	0		0	
Algae cells	0	0		0	

Sample ID	RVSB2-70	RVSB2-70B	RVSB2-71	RVSB2-71B	RVSB2-72
Depth (cm)	**347.25**	**349.25**	**352.25**	**354.25**	**357.25**
Age (ka)	**34.10**	**34.59**	**35.32**	**35.81**	**36.55**
Glomus	1	0		2	
10 - 50 um	3499	118		102	
50 - 100 um	60	1		2	
>100 um	0	0		0	
Total Charcoal	3559	119		104	
Charcoal concentration	111409	1447		2888	

APPENDIX H

RIETVLEI STILL BAY 2 GEOCHEMICAL DATA

Depth (cm)	Age (cal kBP)	TOC	$\delta^{13}C_{TOC}$ (‰)	TN	TOC/TN
0.2	**0.02**	9.90	-21.21	0.96	10.31
2	**0.04**	8.64	-20.50	0.86	10.05
4	**0.07**	10.55	-21.32	1.12	9.42
6	**0.09**	7.42	-21.77	1.11	6.68
8	**0.12**	11.70	-21.88	1.09	10.74
10	**0.15**	16.33	-22.43	0.78	20.94
12	**0.17**	9.90	-21.59	0.91	10.88
14	**0.20**	10.37	-21.52	0.82	12.65
16	**0.22**	9.62	-21.50	0.85	11.31
18	**0.25**	9.64	-21.17	0.76	12.68
20	**0.27**	9.81	-21.02	0.79	12.41
22	**0.30**	10.56	-21.26	0.84	12.57
24	**0.32**	7.29	-21.16	0.65	11.21
26	**0.35**	7.32	-20.48	0.55	13.31
28	**0.37**	7.73	-20.46	0.54	14.31
32	**0.42**	11.57	-21.23	0.44	26.30
34	**0.45**	7.75	-20.67	0.30	25.83
36	**0.47**	3.62	-19.78	0.25	14.48
40	**0.50**	6.09	-20.57	0.23	26.50
42	**0.52**	3.93	-19.61	0.26	15.12
44	**0.55**	4.15	-19.71	0.28	14.83
46	**0.57**	4.78	-20.37	0.36	13.29
48	**0.60**	4.86	-20.46	0.35	13.88
50	**0.62**	6.49	-20.71	0.40	16.22
52	**0.65**	7.31	-19.95	0.52	14.06
54	**0.67**	9.65	-19.64	0.73	13.21
56	**0.70**	17.30	-20.05	1.38	12.54
62	**0.78**	12.30	-20.51	0.86	14.30
64	**0.80**	12.45	-19.51	0.83	15.00
66	**0.83**	12.00	-21.30	0.89	13.49
68	**0.85**	10.49	-22.19	0.76	13.80
70	**0.88**	10.27	-21.13	0.76	13.52

Depth (cm)	Age (cal kBP)	TOC	$\delta^{13}C_{TOC}$ (‰)	TN	TOC/TN
72	**0.90**	10.34	-21.79	0.77	13.43
74	**0.93**	12.06	-21.98	0.81	14.89
76	**0.95**	12.20	-21.43	0.88	13.86
78	**0.98**	12.04	-22.07	0.74	16.26
80	**1.00**	12.51	-21.69	0.82	15.26
82	**1.03**	12.71	-21.99	0.83	15.31
84	**1.05**	13.69	-22.78	0.95	14.41
90	**1.13**	11.68	-25.11	0.65	17.97
92	**1.35**	15.31	-26.70	1.01	15.15
94	**1.57**	17.70	-27.82	1.08	16.39
96	**1.79**	15.89	-26.73	1.08	14.71
98	**2.01**	29.73	-25.69	2.06	14.43
102	**2.23**	9.02	-22.56	0.48	18.80
104	**2.67**	20.70	-23.25	1.21	17.10
106	**2.89**	21.59	-23.71	1.41	15.31
108	**3.11**	22.46	-23.47	1.58	14.22
110	**3.34**	16.74	-23.70	1.16	14.43
112	**3.56**	2.85	-23.79	0.20	14.25
114	**3.78**	8.27	-21.65	0.56	14.77
116	**4.00**	7.86	-22.25	0.52	15.11
118	**4.22**	2.77	-22.52	0.25	11.09
120	**4.44**	3.56	-21.95	0.39	9.13
122	**4.66**	14.01	-21.69	0.73	19.19
124	**4.88**	17.00	-21.10	0.90	18.89
126	**5.10**	15.85	-21.24	0.92	17.22
128	**5.32**	16.80	-21.68	1.00	16.80
130	**5.54**	16.25	-22.62	0.86	18.89
142	**6.37**	18.80	-26.13	0.65	28.92
144	**6.45**	9.63	-25.35	0.42	22.92
146	**6.53**	8.64	-25.35	0.59	14.64
148	**6.61**	10.71	-25.27	0.62	17.28
150	**6.69**	9.47	-25.01	0.51	18.56

Depth (cm)	Age (cal kBP)	TOC	$\delta^{13}C_{TOC}$ (‰)	TN	TOC/TN
151	**6.81**	9.86	-25.17	0.62	15.90
152	**6.77**	8.98	-24.97	0.52	17.27
154	**6.85**	9.00	-25.03	0.55	16.36
156	**6.93**	10.22	-25.04	0.59	17.33
158	**7.01**	9.93	-25.18	0.64	15.51
160	**7.09**	6.97	-25.42	0.42	16.60
162	**7.17**	6.33	-25.98	0.31	20.41
164	**7.22**	4.94	-24.86	0.30	16.47
166	**7.33**	4.93	-26.03	0.28	17.62
170	**7.41**	4.56	-25.00	0.35	13.02
172	**7.57**	4.89	-24.92	0.30	16.31
178	**7.80**	7.06	-25.14	0.34	20.76
180	**7.88**	6.39	-25.13	0.39	16.39
182	**7.96**	9.00	-23.84	0.50	18.01
184	**8.04**	8.21	-24.12	0.47	17.46
186	**8.12**	9.28	-22.50	0.48	19.34
188	**8.20**	7.77	-24.43	0.39	19.92
190	**8.28**	5.13	-24.94	0.36	14.25
192	**8.36**	7.51	-25.11	0.37	20.31
194	**8.44**	6.48	-25.79	0.28	23.13
196	**8.52**	11.86	-25.83	0.56	21.17
198	**8.60**	6.83	-25.26	0.30	22.78
202	**8.68**	5.18	-26.34	0.18	28.76
204	**8.84**	2.18	-24.06	0.14	15.60
212	**8.92**	2.08	-22.42	0.11	18.89
214	**9.31**	1.65	-21.63	0.09	18.37
220	**9.42**	1.74	-21.66	0.09	19.37
222	**9.75**	1.58	-21.83	0.07	22.60
228	**9.86**	1.61	-21.80	0.08	20.13
230	**10.19**	1.48	-22.76	0.08	18.52
232	**10.30**	1.61	-22.17	0.08	20.18
234	**10.41**	1.55	-22.04	0.08	19.31

Depth (cm)	Age (cal kBP)	TOC	$\delta^{13}C_{TOC}$ (‰)	TN	TOC/TN
238	**10.52**	1.64	-21.80	0.08	20.53
240	**10.74**	1.66	-21.70	0.09	18.50
242	**10.85**	1.55	-21.47	0.08	19.36
244	**10.96**	1.67	-21.59	0.09	18.58
246	**11.07**	2.06	-22.36	0.31	6.65
248	**11.21**	3.38	-22.42	0.18	18.75
250	**11.36**	3.99	-22.26	0.13	30.72
252	**11.52**	3.04	-21.63	0.15	20.26
258	**11.67**	4.80	-23.09	0.19	25.26
260	**12.59**	4.36	-21.82	0.24	18.18
262	**13.04**	4.33	-22.08	0.31	13.95
264	**13.50**	4.39	-22.03	0.30	14.62
266	**13.96**	4.23	-22.23	0.27	15.67
268	**14.42**	3.77	-22.11	0.26	14.49
270	**14.87**	3.97	-23.49	0.21	18.89
272	**15.33**	3.94	-22.51	0.19	20.72
274	**15.79**	3.58	-22.35	0.15	23.89
276	**16.25**	4.09	-22.78	0.14	29.24
278	**16.73**	3.84	-22.57	0.14	27.40
286	**18.68**	1.48	-24.53	0.07	21.09
288	**19.17**	2.52	-22.19	0.09	28.03
290	**19.66**	2.41	-22.31	0.10	24.10
292	**20.15**	1.84	-22.74	0.07	26.24
294	**20.64**	1.56	-22.39	0.06	25.99
296	**21.12**	1.31	-22.28	0.04	32.84
298	**21.61**	1.35	-22.67	0.04	33.73
300	**22.10**	1.16	-22.10	0.05	23.29
301	**22.59**	1.15	-23.00	0.04	28.75
302	**22.83**	1.28	-21.89	0.04	31.96
304	**23.08**	1.25	-22.68	0.04	31.25
306	**23.57**	1.20	-21.98	0.03	39.97
308	**24.06**	0.96	-22.62	0.04	23.90

Depth (cm)	Age (cal kBP)	TOC	$\delta^{13}C_{TOC}$ (‰)	TN	TOC/TN
310	**24.54**	0.53	-22.22	0.02	26.25
312	**25.03**	0.55	-21.95	0.02	27.33
320	**25.52**	0.78	-20.25	0.03	25.98
322	**27.48**	1.01	-19.75	0.03	33.51
324	**27.96**	1.37	-20.31	0.04	34.20
326	**28.45**	2.54	-20.59	0.08	31.80
328	**28.94**	4.73	-21.91	0.17	27.79
330	**29.43**	3.26	-23.26	0.11	29.62
334	**29.92**	4.72	-23.15	0.14	33.68
336	**30.90**	7.26	-23.77	0.18	40.32
338	**31.38**	5.69	-23.13	0.14	40.64
340	**31.87**	5.89	-24.01	0.12	49.06
342	**32.36**	14.56	-25.36	0.25	58.22
344	**32.85**	15.74	-25.31	0.36	43.71
348	**33.34**	18.61	-25.25	0.37	50.29
354	**34.32**	12.35	-21.77	0.47	26.29
359	**36.76**	8.01	-20.35	0.48	16.69
360	**37.00**	10.14	-19.07	0.68	14.91

APPENDIX I

VANKERVELSVLEI 2010 #1 GRAIN SIZE DATA

Sample ID	VVV10.1-1	VVV10.1-2	VVV10.1-3	VVV10.1-4	VVV10.1-5	VVV10.1-6	VVV10.1-7	VVV10.1-8	VVV10.1-9	VVV10.1-10
Depth (cm)	1	5	9	13	17	21	25	29	33	37
Age (ka)	6.08	6.92	7.75	8.59	9.43	10.26	11.10	11.94	12.78	13.61
Clay	20.80913	21.30846	23.20654	21.13587	26.21936	24.26352	28.20106	17.92790	22.62359	8.07045
Silt	55.32544	52.38693	47.91045	47.19582	50.97842	45.20292	45.34780	33.20183	47.42257	36.18844
Fine Sand	23.86543	27.51600	31.51705	35.49609	27.82668	37.06864	33.91288	57.44780	40.29765	55.66582
Medium Sand	0.00000	0.00000	0.14547	0.00000	0.00272	0.00001	0.42171	0.83527	0.27923	0.21283
Coarse Sand	0.00000	0.00000	0.00000	0.00000	0.00000	0.00000	0.00000	0.00000	0.00000	0.00000
Mean	7.21670	7.09002	6.98547	6.83340	7.24601	6.88525	7.08910	5.91261	6.76287	5.52536
Sorting	1.94243	2.12071	2.38802	2.30197	2.34429	2.53048	2.66450	2.71365	2.64648	2.17629
Skewness	-0.01437	-0.02364	0.02170	0.10930	0.01797	0.11404	0.00592	0.34886	0.09697	0.25868
Kurtosis	0.79842	0.82139	0.87596	0.81472	0.88347	0.84742	0.87463	0.90392	0.92554	0.81567

Sample ID	VVV10.1-11	VVV10.1-12	VVV10.1-13	VVV10.1-14	VVV10.1-15	VVV10.1-16	VVV10.1-17	VVV10.1-18	VVV10.1-19	VVV10.1-20
Depth (cm)	41	45	49	53	57	61	65	69	73	77
Age (ka)	14.45	15.29	16.12	16.96	17.80	18.63	19.47	20.31	21.15	21.98
Clay	8.94828	7.08704	8.23546	9.80647	12.77238	21.45956	19.16992	23.40854	23.47920	24.77230
Silt	39.36334	39.61676	36.58005	39.77837	43.48314	44.68299	44.50035	47.51600	46.69387	47.62272
Fine Sand	51.87559	52.38546	54.28286	49.54084	42.94075	33.46854	35.98626	29.88250	30.81797	28.68080
Medium Sand	0.00110	1.14514	1.18305	1.21049	1.20251	0.87571	1.01677	0.00000	0.01538	0.26725
Coarse Sand	0.00000	0.00000	0.00000	0.00000	0.00000	0.00000	0.00000	0.00000	0.00000	0.00000
Mean	5.80923	5.64835	5.51137	5.79372	6.13457	6.84433	6.61146	7.08197	7.04853	7.12787
Sorting	2.10073	2.00597	2.17967	2.21112	2.31027	2.42838	2.47132	2.20850	2.30262	2.38996
Skewness	0.24197	0.19185	0.21313	0.17416	0.08118	0.02423	-0.02510	0.06940	0.04533	-0.06123
Kurtosis	0.80767	0.98210	0.89643	0.87889	0.87592	0.86370	0.84380	0.76880	0.80579	0.86149

Sample ID	VVV10.1-21	VVV10.1-22	VVV10.1-23	VVV10.1-24	VVV10.1-25	VVV10.1-26	VVV10.1-27	VVV10.1-28	VVV10.1-29	VVV10.1-30
Depth (cm)	**81**	**85**	**89**	**93**	**101**	**105**	**109**	**113**	**117**	**121**
Age (ka)	**22.82**	**23.66**	**24.49**	**25.33**	**26.83**	**27.31**	**27.79**	**28.27**	**28.75**	**29.23**
Clay	25.61887	22.87445	25.52518	26.43962	18.93440	17.20392	21.06986	10.52225	12.37003	12.06866
Silt	50.35233	45.75865	54.29184	51.34116	53.89340	53.88950	54.56730	47.58941	49.38435	54.62266
Fine Sand	25.56321	33.02543	22.08222	24.31320	29.44557	31.00895	26.85302	44.00345	40.55018	35.72983
Medium Sand	0.00000	0.07836	0.00000	0.00000	0.00000	0.29190	0.01358	0.52445	0.39702	0.50901
Coarse Sand	0.00000	0.00000	0.00000	0.00000	0.00000	0.00000	0.00000	0.00000	0.00000	0.00000
Mean	7.28186	6.90270	7.38858	7.34971	6.94338	6.78286	7.05324	6.10623	6.25039	6.31197
Sorting	2.17570	2.46415	2.07765	2.10458	2.04865	2.17835	2.14634	2.01595	2.05480	2.01883
Skewness	0.01785	-0.04868	0.03300	0.02776	0.14302	0.07885	0.07985	0.17551	0.18477	0.18027
Kurtosis	0.79574	0.83946	0.83328	0.78031	0.86537	0.99108	0.90166	1.10685	1.18571	1.37484

Sample ID	VVV10.1-31	VVV10.1-32	VVV10.1-33	VVV10.1-34	VVV10.1-35	VVV10.1-36	VVV10.1-37	VVV10.1-38	VVV10.1-39	VVV10.1-40
Depth (cm)	**125**	**129**	**133**	**137**	**141**	**145**	**149**	**153**	**157**	**161**
Age (ka)	**29.71**	**30.18**	**30.66**	**31.14**	**31.62**	**32.10**	**32.58**	**33.06**	**33.54**	**34.02**
Clay	15.76945	16.77808	11.94857	11.72250	22.37404	12.43334	23.85041	19.73310	14.10676	22.32407
Silt	55.23887	46.33018	50.77741	58.83087	49.08763	55.00808	47.31599	56.02016	58.62466	56.34065
Fine Sand	31.98902	39.24389	40.43126	32.66719	31.80886	35.70236	32.08007	27.30120	30.82863	25.01809
Medium Sand	0.00160	0.71820	0.00000	0.00000	0.01469	0.26183	0.23052	0.57439	0.19142	0.26093
Coarse Sand	0.00000	0.00000	0.00000	0.00000	0.00000	0.00000	0.00000	0.00000	0.00000	0.00000
Mean	6.65462	6.49857	6.26679	6.44462	6.96874	6.36427	6.95835	6.92091	6.58682	7.14018
Sorting	2.03289	2.33877	1.91493	1.79272	2.32729	2.01261	2.48311	2.38873	2.04829	2.34430
Skewness	0.23367	0.14582	0.27454	0.23899	0.00650	0.16233	-0.00088	-0.03140	0.16781	-0.05257
Kurtosis	0.96796	0.95261	1.15800	1.23796	0.85527	1.27832	0.87877	1.08758	1.26335	1.06192

Sample ID	VVV10.1-41	VVV10.1-42	VVV10.1-43	VVV10.1-44	VVV10.1-45	VVV10.1-46	VVV10.1-47	VVV10.1-48	VVV10.1-49	VVV10.1-50
Depth (cm)	165	169	173	177	181	185	189	197	201	205
Age (ka)	34.50	34.98	35.46	37.08	39.09	41.09	43.09	47.09	49.09	51.09
Clay	21.49015	25.75441	19.81480	15.55708	15.33777	15.61490	21.10937	16.59481	20.88059	21.19366
Silt	54.76757	49.21566	57.62870	46.42106	54.86727	49.65632	50.45070	57.84103	58.32166	58.39955
Fine Sand	27.59031	29.15477	26.78376	42.00348	34.30170	39.34834	33.13202	30.20095	25.63283	25.47122
Medium Sand	0.22292	0.06648	0.11979	0.48237	0.03606	0.00087	0.00081	0.17786	0.06425	0.11117
Coarse Sand	0.00000	0.00000	0.00000	0.00000	0.00000	0.00000	0.00000	0.00000	0.00000	0.00000
Mean	7.05112	7.13970	6.99328	6.43424	6.63374	6.50308	6.89677	6.73270	7.06767	7.08267
Sorting	2.35124	2.45438	2.19941	2.28233	2.11951	2.14836	2.23853	2.12006	2.18850	2.23617
Skewness	-0.03174	-0.02760	0.11511	0.22656	0.18766	0.28983	0.24296	0.28612	0.19163	0.16328
Kurtosis	1.00874	0.91009	1.04198	1.09241	1.09349	1.04789	0.91550	1.21613	1.05082	1.07393

Sample ID	VVV10.1-51	VVV10.1-52	VVV10.1-53	VVV10.1-54	VVV10.1-55	VVV10.1-56	VVV10.1-57	VVV10.1-58	VVV10.1-59	VVV10.1-60
Depth (cm)	209	213	217	221	225	229	233	237	241	245
Age (ka)	53.09	55.10	57.10	59.10	61.10	63.10	65.10	67.10	69.10	71.11
Clay	23.92758	28.50048	23.57726	26.52483	23.52134	24.03363	27.83759	23.88770	23.18612	19.81225
Silt	50.10644	51.50644	60.66343	59.06645	56.52367	58.11485	51.48849	59.15951	54.87434	52.83786
Fine Sand	30.72262	25.43080	21.37073	20.15280	25.60860	23.83647	26.80086	23.24397	28.35182	34.01008
Medium Sand	0.54056	0.00000	0.00000	0.00000	0.23437	0.01692	0.00000	0.00000	0.00000	0.00329
Coarse Sand	0.00000	0.00000	0.00000	0.00000	0.00000	0.00000	0.00000	0.00000	0.00000	0.00000
Mean	6.99868	7.37744	7.31052	7.47076	7.14018	7.24024	7.32778	7.29515	7.11738	6.80935
Sorting	2.55961	2.31320	2.09284	2.14235	2.42225	2.23270	2.28608	2.18855	2.29228	2.40059
Skewness	0.02976	0.04125	0.20894	0.08340	0.00943	0.11198	0.09804	0.08795	0.12308	0.13656
Kurtosis	0.98617	0.86721	0.97296	0.95336	1.08647	0.99574	0.83593	0.99624	0.94213	1.03622

Sample ID	VVV10.1-61	VVV10.1-62	VVV10.1-63	VVV10.1-64	VVV10.1-65	VVV10.1-66	VVV10.1-67	VVV10.1-68	VVV10.1-69	VVV10.1-70
Depth (cm)	249	253	257	261	269	273	277	281	285	289
Age (ka)	73.11	75.11	77.11	79.11	83.11	85.11	87.12	89.12	91.12	93.12
Clay	20.98178	26.25813	20.56372	21.18076	24.12784	21.98619	26.74301	26.89563	28.24242	28.14234
Silt	51.16577	46.24504	44.92803	39.73243	51.98382	48.27127	41.58624	50.55936	47.20499	44.90249
Fine Sand	33.93180	34.08145	40.24148	44.48162	31.01091	36.78502	38.79316	29.81775	32.11007	34.00233
Medium Sand	0.68819	0.28656	1.27432	1.71683	0.08939	0.29430	0.32358	0.31422	0.17423	0.98596
Coarse Sand	0.00000	0.00000	0.00000	0.00000	0.00000	0.00000	0.00000	0.00000	0.00000	0.00000
Mean	6.78015	7.00428	6.44822	6.22849	7.06179	6.81166	6.87434	7.18804	7.14986	6.98213
Sorting	2.57140	2.62241	2.76246	2.91435	2.45205	2.52425	2.70232	2.56369	2.63065	2.79445
Skewness	0.07546	0.01813	0.08941	0.08473	0.08532	0.17556	0.06827	-0.01429	-0.01854	-0.10338
Kurtosis	1.03852	0.89169	0.94805	0.85861	0.94631	1.00446	0.82554	0.93870	0.88278	0.85980

Sample ID	VVV10.1-71	VVV10.1-72	VVV10.1-73	VVV10.1-74	VVV10.1-75	VVV10.1-76	VVV10.1-77	VVV10.1-78	VVV10.1-79	VVV10.1-80
Depth (cm)	293	297	301	305	309	313	317	321	325	329
Age (ka)	95.12	97.12	99.12	101.12	103.13	105.13	107.13	109.13	111.13	113.13
Clay	27.20462	32.45486	30.90137	32.31975	30.04417	23.15106	26.82501	20.71653	21.54697	24.19982
Silt	50.22969	51.43107	48.41492	50.12786	53.00347	45.00729	39.64746	39.96715	38.05424	38.37137
Fine Sand	30.72971	24.41849	29.13846	26.20513	25.76735	40.80112	42.61005	46.59920	48.00399	46.84739
Medium Sand	0.00178	0.00000	0.03069	0.00227	0.02995	0.03853	0.02197	1.94256	1.71549	0.05043
Coarse Sand	0.00000	0.00000	0.00000	0.00000	0.00000	0.00000	0.00000	0.00000	0.00000	0.00000
Mean	7.20727	7.56331	7.35597	7.49188	7.44237	6.76732	6.84110	6.38596	6.40372	6.62510
Sorting	2.39447	2.31322	2.53133	2.40888	2.40924	2.60024	2.65884	2.76326	2.75725	2.68701
Skewness	0.10838	0.02298	0.00230	0.03075	0.01411	0.15966	0.13903	0.20347	0.22435	0.23876
Kurtosis	0.84086	0.82493	0.86824	0.83050	0.90615	0.88497	0.78722	0.94737	0.89557	0.82758

Sample ID	VVV10.1-81	VVV10.1-82	VVV10.1-83	VVV10.1-84	VVV10.1-85	VVV10.1-86	VVV10.1-87	VVV10.1-88	VVV10.1-89	VVV10.1-90
Depth (cm)	333	336	342	346	350	354	358	362	366	370
Age (ka)	115.13	116.63	119.64	121.64	123.64	125.64	127.64	129.64	131.64	133.64
Clay	16.73023	19.30388	19.39178	28.32342	28.91124	28.33447	32.88258	28.52800	29.39210	31.40596
Silt	17.77827	23.99039	22.37479	38.87131	40.39385	42.71608	47.00180	46.81126	49.63297	50.17373
Fine Sand	47.43004	43.68899	37.61557	41.65715	39.74208	38.23641	30.30236	34.66340	31.44566	29.12692
Medium Sand	26.71734	22.11809	29.21725	0.90567	0.85761	0.76486	0.00281	0.35352	0.01586	0.00144
Coarse Sand	0.92193	0.52518	1.08581	0.00000	0.00000	0.00000	0.00000	0.00000	0.00000	0.00000
Mean	4.81074	5.22633	5.11431	6.84056	6.93875	6.97354	7.40565	7.12538	7.27322	7.41387
Sorting	3.22455	3.26569	3.38428	2.81912	2.78018	2.75285	2.53703	2.66429	2.48999	2.45582
Skewness	0.50774	0.37140	0.37011	0.10907	0.08586	0.06689	-0.00788	0.03303	0.08420	0.07513
Kurtosis	0.87045	0.71401	0.74342	0.80594	0.81196	0.83308	0.80557	0.86320	0.83118	0.81291

Sample ID	VVV10.1-91	VVV10.1-92	VVV10.1-93	VVV10.1-94	VVV10.1-95	VVV10.1-96	VVV10.1-97
Depth (cm)	374	378	382	386	390	394	397
Age (ka)	135.65	137.65	139.65	141.65	143.65	145.65	147.15
Clay	32.52181	36.34220	25.87063	26.26573	35.52800	25.32559	26.08088
Silt	56.98530	49.85841	53.04658	51.72411	52.28082	58.28070	60.37915
Fine Sand	21.36175	24.80981	32.02373	33.33862	23.61974	27.97544	25.22473
Medium Sand	0.00115	0.00000	0.28116	0.00000	0.00000	0.00552	0.00000
Coarse Sand	0.00000	0.00000	0.00000	0.00000	0.00000	0.00000	0.00000
Mean	7.67840	7.68016	7.13040	7.11339	7.73152	7.26066	7.37104
Sorting	2.27488	2.40170	2.57754	2.52997	2.38794	2.30636	2.25801
Skewness	0.01740	0.01552	0.05958	0.07900	-0.08944	0.20826	0.17223
Kurtosis	0.91240	0.78804	0.96138	0.88662	0.86810	0.95551	0.95626

Grain size categories	
Clay	0 - 2 µm
Silt	2 - 20 µm
Fine Sand	20 - 200 µm
Medium Sand	200 - 500 µm
Coarse Sand	500 - 2000 µm

APPENDIX J

VANKERVELSVLEI 2010 #1 ABSOLUTE POLLEN, NON-POLLEN PALYNOMORPHS AND MICROSCOPIC CHARCOAL COUNTS

Sample ID	VVV10.1-1	VVV10.1-2	VVV10.1-3	VVV10.1-4	VVV10.1-5	VVV10.1-6	VVV10.1-7	VVV10.1-8	VVV10.1-9	VVV10.1-10	VVV10.1-11	VVV10.1-12
Depth (cm)	5	10	15	20	25	30	35	40	45	50	55	60
Age (ka)	6.85	7.90	8.95	9.99	11.04	12.09	13.13	14.18	15.23	16.27	17.32	18.37
Encephalartos	0	0										
Euclea	0	5										
Grewia	0	3										
Ilex	1	0										
Morella	0	1										
Myrsine	0	1										
Myrtaceae	1	1										
Olea	3	5										
Acacia	0	0										
Blechnaceae	3	5										
Celastraceae	1	0										
Celtis	1	3										
Diospyros	0	0										
Podocarpus	9	8										
Rhus	3	0										
Hamamelidaceae	12	9										
Pittosporaceae	0	0										
Cunoniaceae	0	0										
Kiggelaria	0	0										
Artemisia	6	4										
Pentzia-type	6	4										
Proteaceae	2	0										
Ericaceae	22	17										
Cliffortia	0	0										
Bruniaceae	0	0										
Anthospermum-type	1	4										
Apiaceae	0	2										
Fabaceae	0	1										
Rhamnaceae	0	0										
Rutaceae	5	6										
Scroph-type	4	3										
Thymelaeaceae	2	0										
Passerina	3	0										
Galium	0	0										
Canthium	2	1										
Plantago	0	0										
Cyperaceae	159	238										
Restionaceae	3	7										
Poaceae	39	28										

Sample ID	VVV10.1-1	VVV10.1-2	VVV10.1-3	VVV10.1-4	VVV10.1-5	VVV10.1-6	VVV10.1-7	VVV10.1-8	VVV10.1-9	VVV10.1-10	VVV10.1-11	VVV10.1-12
Depth (cm)	5	10	15	20	25	30	35	40	45	50	55	60
Age (ka)	6.85	7.90	8.95	9.99	11.04	12.09	13.13	14.18	15.23	16.27	17.32	18.37
Asteraceae HS	70	37										
Stoebe-type	13	17										
Geraniaceae	1	2										
Onagraceae	0	0										
Oxygonum	0	2										
Polygonum	39	29										
Euphorbia	6	4										
Clutia	0	0										
ChenAm-type	0	2										
Crassula	0	0										
Ruschia	0	0										
Juncaceae	13	5										
Liliaceae	8	8										
Iridaceae	6	4										
Amaryllidaceae	1	1										
Malvaceae	1	0										
Scabiosa	0	0										
Selaginaceae	1	1										
Aponogeton	0	3										
Haloragaceae	1	1										
Typha	0	0										
Zygophyllaceae	0	2										
Loranthaceae	0	0										
Sterculiaceae	1	1										
Justica-type	6	1										
Aizoaceae	13	16										
Euphorbiaceae undif	13	7										
Brassicaceae	10	3										
Campanulaceae	0	2										
Gunneraceae	2	1										
Polygala	0	0										
Apocynaceae	0	0										
Cardiospermum	1	0										
Rosaceae	0	0										
Nyctaginaceae	0	0										
Moraceae	3	3										
Lauraceae	0	0										
Orchidaceae	0	0										
Combretaceae	1	0										

Sample ID	VVV10.1-1	VVV10.1-2	VVV10.1-3	VVV10.1-4	VVV10.1-5	VVV10.1-6	VVV10.1-7	VVV10.1-8	VVV10.1-9	VVV10.1-10	VVV10.1-11	VVV10.1-12
Depth (cm)	5	10	15	20	25	30	35	40	45	50	55	60
Age (ka)	6.85	7.90	8.95	9.99	11.04	12.09	13.13	14.18	15.23	16.27	17.32	18.37
Phytolaccaceae	7	3										
Oxalis	1	1										
Plumbaginaceae	0	0										
Portulaceae	0	0										
Gardenia	1	0										
Meliaceae	0	0										
Bigoniaceae	0	2										
Lamiaceae	0	0										
Convolvulaceae	1	0										
Acan. Tricolporate	0	0										
Acan. Diporate	0	0										
Gentianaceae	0	0										
Potamogetonaceae	0	0										
Rannuculaceae	0	0										
Unidentifiable	0	0										
Broken	3	2										
Unknown	4	0										
Total Pollen	515	516										
Pollen concentration	102795	41360										
Botryococcus (1= present, 5= high concentration)												
	1	1										
Monolete	15	18										
Trilete	75	53										
Riccia	1	6										
Ophioglossum	1	0										
Mohria	1	0										
Pellaea	1	3										
Debarya glyptosperma	0	0										
Other zygospores	0	0										
10 - 50 um	1546	661										
50 - 100 um	22	23										
>100 um	4	0										
Total Charcoal	1572	684										
Charcoal concentration	313775	54826										

Sample ID	VVV10.1-13	VVV10.1-14	VVV10.1-15	VVV10.1-16	VVV10.1-17	VVV10.1-18	VVV10.1-19	VVV10.1-20	VVV10.1-21	VVV10.1-22	VVV10.1-23
Depth (cm)	65	70	75	80	85	90	95	100	105	110	115
Age (ka)	19.41	20.46	21.50	22.55	23.60	24.64	25.69	26.65	27.25	27.85	28.44
Encephalartos									0	0	0
Euclea									0	1	1
Grewia									0	0	0
Ilex									0	0	1
Morella									2	10	9
Myrsine									4	8	2
Myrtaceae									1	0	0
Olea									0	2	0
Acacia									0	0	0
Blechnaceae									0	0	0
Celastraceae									0	2	0
Celtis									3	2	1
Diospyros									0	0	0
Podocarpus									7	2	1
Rhus									0	0	0
Hamamelidaceae									0	0	0
Pittosporaceae									0	0	0
Cunoniaceae									0	0	0
Kiggelaria									0	0	0
Artemisia									1	6	10
Pentzia-type									0	1	1
Proteaceae									0	1	0
Ericaceae									115	253	236
Cliffortia									20	13	13
Bruniaceae									0	0	0
Anthospermum-type									0	0	0
Apiaceae									0	0	0
Fabaceae									1	3	1
Rhamnaceae									0	2	0
Rutaceae									0	0	0
Scroph-type									0	0	0
Thymelaeaceae									4	0	5
Passerina									8	8	19
Galium									0	0	0
Canthium									2	4	9
Plantago									0	2	2
Cyperaceae									2	1	3
Restionaceae									2	4	6
Poaceae									20	15	23

Sample ID	VVV10.1-13	VVV10.1-14	VVV10.1-15	VVV10.1-16	VVV10.1-17	VVV10.1-18	VVV10.1-19	VVV10.1-20	VVV10.1-21	VVV10.1-22	VVV10.1-23
Depth (cm)	**65**	**70**	**75**	**80**	**85**	**90**	**95**	**100**	**105**	**110**	**115**
Age (ka)	**19.41**	**20.46**	**21.50**	**22.55**	**23.60**	**24.64**	**25.69**	**26.65**	**27.25**	**27.85**	**28.44**
Asteraceae HS									7	3	1
Stoebe-type									59	77	82
Geraniaceae									0	0	3
Onagraceae									2	1	0
Oxygonum									0	0	0
Polygonum									0	0	0
Euphorbia									9	34	23
Clutia									0	2	2
ChenAm-type									3	2	0
Crassula									1	0	3
Ruschia									0	0	5
Juncaceae									5	3	3
Liliaceae									0	2	0
Iridaceae									0	0	1
Amaryllidaceae									0	0	0
Malvaceae									1	0	0
Scabiosa									0	0	1
Selaginaceae									0	0	0
Aponogeton									0	0	0
Haloragaceae									5	0	2
Typha									0	0	0
Zygophyllaceae									0	0	0
Loranthaceae									0	0	0
Sterculiaceae									0	0	0
Justica-type									0	0	1
Aizoaceae									0	0	0
Euphorbiaceae undif									6	14	23
Brassicaceae									0	0	0
Campanulaceae									0	0	0
Gunneraceae									0	0	0
Polygala									0	0	0
Apocynaceae									0	0	1
Cardiospermum									0	0	0
Rosaceae									0	0	0
Nyctaginaceae									0	0	0
Moraceae									0	0	0
Lauraceae									0	0	0
Orchidaceae									0	0	0
Combretaceae									0	0	0

Sample ID	VVV10.1-13	VVV10.1-14	VVV10.1-15	VVV10.1-16	VVV10.1-17	VVV10.1-18	VVV10.1-19	VVV10.1-20	VVV10.1-21	VVV10.1-22	VVV10.1-23
Depth (cm)	65	70	75	80	85	90	95	100	105	110	115
Age (ka)	19.41	20.46	21.50	22.55	23.60	24.64	25.69	26.65	27.25	27.85	28.44
Phytolaccaceae									5	6	3
Oxalis									0	0	0
Plumbaginaceae									0	0	0
Portulaceae									0	0	0
Gardenia									0	5	3
Meliaceae									0	0	0
Bigoniaceae									0	0	0
Lamiaceae									2	1	0
Convolvulaceae									0	0	0
Acan. Tricolporate									0	0	0
Acan. Diporate									0	0	0
Gentianaceae									0	2	1
Potamogetonaceae									0	0	0
Rannuculaceae									2	3	1
Unidentifiable									1	0	0
Broken									3	3	1
Unknown									2	2	0
Total Pollen									305	500	503
Pollen concentration									92115	338119	77250
Botryococcus (1= present, 5= high concentration)									1	1	0
Monolete									37	7	10
Trilete									5	1	2
Riccia									0	0	0
Ophioglossum									0	0	0
Mohria									0	0	0
Pellaea									7	0	0
Debarya glyptosperma									0	0	0
Other zygospores									8	14	0
10 - 50 um									64	48	71
50 - 100 um									0	4	1
>100 um									0	0	0
Total Charcoal									64	52	72
Charcoal concentration									19329	35164	11058

Sample ID	VVV10.1-24	VVV10.1-25	VVV10.1-26	VVV10.1-27	VVV10.1-28	VVV10.1-29	VVV10.1-30	VVV10.1-31	VVV10.1-32	VVV10.1-33	VVV10.1-34
Depth (cm)	120	125	130	135	140	145	150	155	160	165	170
Age (ka)	29.04	29.64	30.24	30.84	31.44	32.04	32.64	33.24	33.83	34.43	35.03
Encephalartos	0	0	0	0	0	0	0			0	
Euclea	0	0	2	1	2	1	0			1	
Grewia	0	0	0	0	0	0	0			0	
Ilex	0	0	0	0	0	0	0			0	
Morella	23	7	19	7	12	18	5			4	
Myrsine	2	0	1	0	1	0	0			0	
Myrtaceae	0	0	0	0	0	0	0			0	
Olea	1	2	1	0	0	1	4			1	
Acacia	0	0	0	0	0	1	0			0	
Blechnaceae	0	2	0	0	0	1	0			0	
Celastraceae	0	0	0	0	0	0	2			0	
Celtis	1	2	0	0	4	1	1			0	
Diospyros	0	0	0	0	0	0	2			0	
Podocarpus	1	2	0	0	3	0	0			3	
Rhus	1	0	0	0	2	2	0			0	
Hamamelidaceae	0	113	0	0	0	0	0			0	
Pittosporaceae	0	0	0	0	0	0	0			0	
Cunoniaceae	0	0	0	0	0	0	0			0	
Kiggelaria	0	3	0	0	0	0	0			0	
Artemisia	8	1	6	5	6	4	2			1	
Pentzia-type	2	5	4	0	2	13	7			48	
Proteaceae	0	0	1	0	0	1	0			2	
Ericaceae	186	296	262	107	242	238	101			224	
Cliffortia	4	15	33	1	12	17	30			29	
Bruniaceae	0	0	1	0	0	0	0			0	
Anthospermum-type	0	2	4	1	0	4	0			0	
Apiaceae	0	0	0	0	0	0	0			0	
Fabaceae	0	0	1	0	0	1	5			0	
Rhamnaceae	0	1	2	0	0	0	0			0	
Rutaceae	0	1	0	0	0	0	0			0	
Scroph-type	0	0	0	0	0	0	0			0	
Thymelaeaceae	4	4	3	0	1	2	1			6	
Passerina	19	15	10	1	14	3	2			0	
Galium	0	0	0	0	0	0	0			0	
Canthium	16	8	0	2	4	15	1			5	
Plantago	0	3	17	0	0	4	6			2	
Cyperaceae	8	2	0	0	3	0	2			0	
Restionaceae	2	3	6	1	2	5	7			3	
Poaceae	27	4	15	5	19	17	36			11	

Sample ID	VVV10.1-24	VVV10.1-25	VVV10.1-26	VVV10.1-27	VVV10.1-28	VVV10.1-29	VVV10.1-30	VVV10.1-31	VVV10.1-32	VVV10.1-33	VVV10.1-34
Depth (cm)	**120**	**125**	**130**	**135**	**140**	**145**	**150**	**155**	**160**	**165**	**170**
Age (ka)	**29.04**	**29.64**	**30.24**	**30.84**	**31.44**	**32.04**	**32.64**	**33.24**	**33.83**	**34.43**	**35.03**
Asteraceae HS	0	4	4	2	3	7	17			6	
Stoebe-type	114	32	76	41	93	77	60			115	
Geraniaceae	1	4	0	0	4	2	0			0	
Onagraceae	1	0	0	0	0	0	0			2	
Oxygonum	0	0	0	0	0	0	0			0	
Polygonum	0	1	0	1	0	0	0			0	
Euphorbia	12	30	8	6	19	20	7			5	
Clutia	0	0	0	0	0	0	0			0	
ChenAm-type	1	6	1	2	2	1	0			0	
Crassula	1	0	1	0	0	0	3			0	
Ruschia	4	0	0	0	0	1	0			0	
Juncaceae	10	1	0	0	3	0	0			1	
Liliaceae	0	2	1	0	6	1	0			0	
Iridaceae	1	8	0	0	1	5	0			1	
Amaryllidaceae	0	0	0	0	0	0	0			0	
Malvaceae	0	1	0	0	0	1	0			0	
Scabiosa	0	2	0	0	0	0	0			1	
Selaginaceae	0	1	0	0	0	0	0			1	
Aponogeton	4	0	0	0	0	0	3			0	
Haloragaceae	0	1	1	1	8	6	4			8	
Typha	0	2	0	0	1	0	0			0	
Zygophyllaceae	0	0	0	0	0	0	0			0	
Loranthaceae	0	0	0	0	0	0	0			0	
Sterculiaceae	0	0	0	0	0	0	0			0	
Justica-type	0	0	1	0	0	0	0			0	
Aizoaceae	0	0	0	0	0	0	7			0	
Euphorbiaceae undif	24	14	8	5	19	4	5			3	
Brassicaceae	0	1	0	0	0	0	0			0	
Campanulaceae	0	0	0	0	0	0	0			0	
Gunneraceae	1	0	0	0	0	0	0			1	
Polygala	0	0	0	0	0	0	0			0	
Apocynaceae	0	0	1	0	0	1	0			0	
Cardiospermum	0	0	0	0	0	0	0			0	
Rosaceae	1	0	0	0	2	2	0			1	
Nyctaginaceae	0	2	0	0	0	0	0			0	
Moraceae	0	1	0	0	0	1	0			0	
Lauraceae	0	0	0	0	0	0	0			0	
Orchidaceae	1	0	0	0	1	0	0			0	
Combretaceae	0	0	0	0	0	1	0			0	

Sample ID	VVV10.1-24	VVV10.1-25	VVV10.1-26	VVV10.1-27	VVV10.1-28	VVV10.1-29	VVV10.1-30	VVV10.1-31	VVV10.1-32	VVV10.1-33	VVV10.1-34
Depth (cm)	**120**	**125**	**130**	**135**	**140**	**145**	**150**	**155**	**160**	**165**	**170**
Age (ka)	**29.04**	**29.64**	**30.24**	**30.84**	**31.44**	**32.04**	**32.64**	**33.24**	**33.83**	**34.43**	**35.03**
Phytolaccaceae	0	4	3	1	2	5	2			4	
Oxalis	0	0	0	0	0	0	0			0	
Plumbaginaceae	1	0	0	0	0	0	0			0	
Portulaceae	0	0	0	0	0	0	0			0	
Gardenia	2	3	3	0	5	5	3			2	
Meliaceae	0	1	3	0	2	2	4			1	
Bigoniaceae	0	0	0	0	0	0	0			0	
Lamiaceae	2	0	0	3	1	1	0			0	
Convolvulaceae	0	0	0	0	0	0	0			0	
Acan. Tricolporate	0	0	0	0	1	0	0			0	
Acan. Diporate	0	0	0	0	0	0	0			0	
Gentianaceae	6	1	0	2	1	2	1			0	
Potamogetonaceae	0	0	0	0	0	0	0			0	
Rannuculaceae	3	1	4	0	4	0	3			8	
Unidentifiable	1	0	0	0	0	1	1			0	
Broken	5	0	2	0	1	6	4			0	
Unknown	1	0	1	0	0	1	1			0	
Total Pollen	502	614	506	195	508	502	339			500	
Pollen concentration	57091	136614	126249	82733	56225	42511	277762			169801	
Botryococcus (1= present, 5= high concentration)											
	1	1	1	1	1	1	5			5	
Monolete	1	6	0	2	28	19	28			104	
Trilete	4	3	3	0	4	6	6			23	
Riccia	2	0	0	0	0	0	0			1	
Ophioglossum	0	0	0	0	0	0	0			0	
Mohria	0	0	0	0	0	0	0			0	
Pellaea	0	0	1	0	0	1	0			1	
Debarya glyptosperma	0	0	1	0	1	5	2			6	
Other zygospores	2	0	0	0	2	2	4			13	
10 - 50 um	27	96	0	97	109	107	184			86	
50 - 100 um	0	0	0	2	5	1	7			0	
>100 um	0	0	0	0	0	0	0			0	
Total Charcoal	27	96	0	99	114	108	191			86	
Charcoal concentration	3071	21360	0	42003	12617	9146	156497			29206	

Sample ID	VVV10.1-35	VVV10.1-36	VVV10.1-37	VVV10.1-38	VVV10.1-39	VVV10.1-40	VVV10.1-41	VVV10.1-42	VVV10.1-43	VVV10.1-44	VVV10.1-45
Depth (cm)	**175**	**180**	**185**	**190**	**195**	**200**	**205**	**209**	**215**	**220**	**225**
Age (ka)	**35.85**	**37.54**	**39.23**	**40.92**	**42.62**	**44.31**	**46.00**	**47.35**	**49.38**	**51.07**	**52.76**
Encephalartos	0	0	0	0	0	0	0		0	0	
Euclea	1	1	4	0	0	0	0		1	1	
Grewia	0	0	0	0	0	0	0		0	0	
Morella	0	1	0	0	0	0	0		0	0	
Myrica	2	22	12	2	0	1	3		11	16	
Myrsine	0	0	0	0	0	0	1		1	0	
Myrtaceae	0	3	0	0	0	0	0		1	0	
Olea	0	1	2	1	3	0	0		1	2	
Acacia	0	0	1	0	0	0	0		0	0	
Blechnaceae	0	0	0	0	0	0	0		0	2	
Celastraceae	0	0	0	1	0	0	0		0	0	
Celtis	0	1	2	0	0	0	0		0	0	
Diospyros	0	0	0	1	2	0	2		0	0	
Podocarpus	0	4	0	2	0	0	0		2	1	
Rhus	0	2	0	0	0	0	0		1	0	
Hamamelidaceae	0	0	0	0	0	0	0		0	0	
Pittosporaceae	0	0	0	0	0	0	0		0	0	
Cunoniaceae	0	0	0	0	0	0	0		0	1	
Kiggelaria	0	0	0	0	0	0	0		0	0	
Artemisia	1	14	4	2	0	0	3		7	6	
Pentzia-type	2	2	0	0	0	0	1		2	5	
Proteaceae	0	2	0	2	0	0	0		1	0	
Ericaceae	20	149	252	194	63	80	210		345	305	
Cliffortia	14	7	15	7	1	1	7		8	7	
Bruniaceae	0	0	0	0	0	0	0		0	0	
Anthospermum-type	0	0	0	0	0	0	1		0	0	
Apiaceae	0	0	0	0	0	0	0		0	1	
Fabaceae	2	3	2	0	0	0	0		0	1	
Rhamnaceae	0	2	0	0	0	0	0		0	0	
Rutaceae	0	0	1	0	0	0	0		0	0	
Scroph-type	0	0	0	0	0	0	0		0	0	
Thymelaeaceae	1	8	1	0	0	0	1		2	0	
Passerina	0	17	4	3	0	0	6		3	5	
Galium	0	0	0	0	0	0	0		0	0	
Canthium	2	19	7	4	1	5	0		13	4	
Plantago	0	0	5	0	0	1	3		0	7	
Cyperaceae	0	7	0	0	0	0	0		1	1	
Restionaceae	1	3	14	7	0	0	0		7	8	
Poaceae	8	18	24	17	4	9	11		16	27	

Sample ID	VVV10.1-35	VVV10.1-36	VVV10.1-37	VVV10.1-38	VVV10.1-39	VVV10.1-40	VVV10.1-41	VVV10.1-42	VVV10.1-43	VVV10.1-44	VVV10.1-45
Depth (cm)	175	180	185	190	195	200	205	209	215	220	225
Age (ka)	35.85	37.54	39.23	40.92	42.62	44.31	46.00	47.35	49.38	51.07	52.76
Asteraceae HS	1	4	2	5	0	1	0		0	1	
Stoebe-type	21	76	93	29	12	8	49		35	42	
Geraniaceae	0	11	1	2	0	0	0		1	2	
Onagraceae	1	2	0	0	0	0	1		0	0	
Oxygonum	0	0	0	0	0	0	0		0	0	
Polygonum	0	1	0	1	0	0	0		0	0	
Euphorbia	4	16	5	5	0	3	0		13	17	
Clutia	1	0	0	0	0	0	0		0	0	
ChenAm-type	0	1	2	1	0	1	1		1	1	
Crassula	0	1	1	1	0	0	4		0	1	
Ruschia	0	2	0	0	0	0	0		0	0	
Juncaceae	0	19	2	0	1	0	0		3	0	
Liliaceae	0	2	0	0	0	1	0		0	0	
Iridaceae	0	0	0	0	0	1	0		0	2	
Amaryllidaceae	0	0	0	0	0	0	0		0	0	
Malvaceae	1	0	0	0	0	0	0		0	0	
Scabiosa	0	0	0	0	0	0	0		0	1	
Selaginaceae	0	1	0	0	0	0	0		0	0	
Aponogeton	1	0	0	0	0	0	0		0	0	
Haloragaceae	0	0	2	2	0	0	0		5	2	
Typha	0	7	2	0	0	0	0		2	2	
Zygophyllaceae	0	0	0	0	0	0	0		0	0	
Loranthaceae	0	0	0	0	0	0	0		0	0	
Sterculiaceae	0	0	0	0	0	0	0		0	0	
Justica-type	0	2	0	1	0	0	0		0	3	
Aizoaceae	1	1	1	0	0	0	0		1	2	
Euphorbiaceae undif	3	48	6	7	4	1	0		3	8	
Brassicaceae	0	0	0	0	0	0	0		0	0	
Campanulaceae	0	1	0	0	0	0	0		0	0	
Gunneraceae	0	0	1	0	0	0	2		1	2	
Polygala	0	0	0	0	0	0	0		0	1	
Apocynaceae	0	0	0	1	0	0	0		0	0	
Cardiospermum	0	0	0	0	0	0	0		0	0	
Rosaceae	0	0	0	0	0	0	0		0	0	
Nyctaginaceae	0	0	0	0	0	0	0		0	0	
Moraceae	0	0	0	0	0	0	0		0	0	
Lauraceae	0	0	0	0	0	0	0		0	0	
Orchidaceae	0	0	0	0	0	0	0		0	0	
Combretaceae	0	0	0	0	0	0	2		0	0	

Sample ID	VVV10.1-35	VVV10.1-36	VVV10.1-37	VVV10.1-38	VVV10.1-39	VVV10.1-40	VVV10.1-41	VVV10.1-42	VVV10.1-43	VVV10.1-44	VVV10.1-45
Depth (cm)	**175**	**180**	**185**	**190**	**195**	**200**	**205**	**209**	**215**	**220**	**225**
Age (ka)	**35.85**	**37.54**	**39.23**	**40.92**	**42.62**	**44.31**	**46.00**	**47.35**	**49.38**	**51.07**	**52.76**
Phytolaccaceae	3	4	9	4	1	4	7		1	11	
Oxalis	0	0	1	0	0	0	0		0	0	
Plumbaginaceae	0	0	0	0	0	0	0		0	0	
Portulaceae	0	0	0	0	0	0	0		0	0	
Gardenia	0	1	5	0	0	0	4		4	1	
Meliaceae	0	0	1	1	0	0	0		0	0	
Bigoniaceae	0	0	0	0	0	0	0		0	0	
Lamiaceae	0	4	4	0	2	0	1		1	4	
Convolvulaceae	1	0	0	0	0	0	0		0	0	
Acan. Tricolporate	1	0	3	0	0	0	0		0	0	
Acan. Diporate	0	0	0	0	0	0	0		0	0	
Gentianaceae	0	3	4	0	0	0	0		0	0	
Potamogetonaceae	0	0	0	0	0	0	0		0	1	
Rannuculaceae	0	0	2	0	1	1	8		6	9	
Unidentifiable	0	0	0	0	0	0	0		0	0	
Broken	1	5	3	4	2	0	0		0	2	
Unknown	0	2	1	1	0	0	0		0	2	
Total Pollen	94	500	501	308	97	118	328		500	517	
Pollen concentration	11302	47415	217678	245016	165069	263874	273820		575325	370656	
Botryococcus (1= present, 5= high concentration)	1	0	1	1	1	1	5		5	1	
Monolete	12	25	19	7	17	22	51		48	7	
Trilete	2	6	2	2	3	3	3		14	1	
Riccia	0	0	0	0	0	0	1		0	0	
Ophioglossum	0	0	0	0	0	0	0		0	0	
Mohria	0	0	0	0	0	1	0		0	0	
Pellaea	0	0	0	0	1	0	0		0	2	
Debarya glyptosperma	2	4	7	1	3	5	7		31	1	
Other zygospores	1	3	4	4	0	2	11		9	2	
10 - 50 um	269	61	132	81	111	84	415		63	22	
50 - 100 um	4	8	3	7	0	8	18		1	2	
>100 um	1	0	0	1	0	0	3		0	0	
Total Charcoal	274	69	135	89	111	92	436		64	24	
Charcoal concentration	32943	6543	58656	70800	188893	205732	363980		73642	17206	

Sample ID	VVV10.1-46	VVV10.1-47	VVV10.1-48	VVV10.1-49	VVV10.1-50	VVV10.1-51	VVV10.1-52	VVV10.1-53	VVV10.1-54	VVV10.1-55	VVV10.1-56
Depth (cm)	230	235	240	245	250	255	260	265	270	275	280
Age (ka)	54.46	56.15	57.84	59.53	61.22	62.91	64.60	66.30	69.07	72.55	76.04
Encephalartos	0	0	0	0		0	0	0	0	0	0
Euclea	2	0	1	2		1	0	0	0	1	0
Grewia	0	0	1	0		0	0	0	0	0	0
Ilex	1	0	0	0		1	0	2	0	0	0
Morella	30	20	4	38		14	10	30	20	14	29
Myrsine	1	0	0	0		1	0	0	0	1	2
Myrtaceae	0	0	0	0		0	0	0	2	1	0
Olea	2	1	1	1		2	6	2	1	2	6
Acacia	0	4	0	0		0	0	0	0	0	0
Blechnaceae	0	0	2	0		0	0	0	0	3	0
Celastraceae	0	0	0	0		2	0	1	0	0	0
Celtis	0	0	0	1		0	0	0	0	0	1
Diospyros	1	0	0	0		0	0	0	0	0	0
Podocarpus	2	1	2	1		0	3	0	1	9	6
Rhus	0	0	0	0		2	3	1	1	0	1
Hamamelidaceae	0	0	0	1		0	0	0	0	0	0
Pittosporaceae	0	0	1	0		0	0	0	0	0	0
Cunoniaceae	0	0	1	0		0	0	0	0	0	0
Kiggelaria	0	0	0	0		2	0	0	0	0	0
Artemisia	5	6	4	5		4	3	2	5	8	10
Pentzia-type	3	1	2	1		1	4	0	0	0	2
Proteaceae	0	0	0	0		0	0	0	0	0	0
Ericaceae	321	265	320	277		147	200	345	346	227	264
Cliffortia	1	1	6	6		4	8	0	2	3	2
Bruniaceae	0	1	0	0		0	0	0	0	0	0
Anthospermum-type	1	1	0	1		0	0	0	0	2	1
Apiaceae	0	0	0	0		1	0	0	0	0	0
Fabaceae	0	0	2	0		1	3	0	0	0	0
Rhamnaceae	0	1	1	0		0	0	0	0	0	0
Rutaceae	0	0	0	0		2	0	0	0	1	0
Scroph-type	0	1	0	0		0	0	0	0	0	0
Thymelaeaceae	0	4	1	0		0	17	1	1	2	3
Passerina	4	4	5	8		3	7	22	12	14	22
Galium	0	4	0	0		1	1	0	0	0	0
Canthium	2	13	7	9		6	5	8	5	7	4
Plantago	1	0	3	2		1	2	0	0	0	2
Cyperaceae	2	0	4	2		0	10	0	2	8	0
Restionaceae	4	1	1	17		10	17	5	5	6	9
Poaceae	26	13	39	9		11	28	4	14	39	17

Sample ID	VVV10.1-46	VVV10.1-47	VVV10.1-48	VVV10.1-49	VVV10.1-50	VVV10.1-51	VVV10.1-52	VVV10.1-53	VVV10.1-54	VVV10.1-55	VVV10.1-56
Depth (cm)	**230**	**235**	**240**	**245**	**250**	**255**	**260**	**265**	**270**	**275**	**280**
Age (ka)	**54.46**	**56.15**	**57.84**	**59.53**	**61.22**	**62.91**	**64.60**	**66.30**	**69.07**	**72.55**	**76.04**
Asteraceae HS	8	2	2	2		12	14	0	0	6	1
Stoebe-type	25	13	19	17		184	49	7	24	95	62
Geraniaceae	0	15	4	6		2	8	10	3	0	1
Onagraceae	0	0	0	0		0	0	0	0	0	0
Oxygonum	0	0	0	0		0	0	0	0	0	0
Polygonum	0	0	0	0		1	0	1	1	0	0
Euphorbia	22	18	7	24		14	14	16	20	20	21
Clutia	0	0	0	0		0	0	0	0	0	0
ChenAm-type	1	4	1	1		0	3	1	0	1	0
Crassula	0	0	2	1		0	1	2	3	1	0
Ruschia	0	0	0	0		0	1	1	0	0	0
Juncaceae	0	4	3	2		2	5	0	2	5	1
Liliaceae	0	2	1	0		2	1	0	0	1	0
Iridaceae	1	6	0	0		3	3	0	0	0	0
Amaryllidaceae	0	0	0	1		0	0	0	0	0	0
Malvaceae	0	1	0	0		0	1	1	0	0	0
Scabiosa	1	3	3	7		2	12	6	3	0	1
Selaginaceae	0	3	0	0		2	0	0	0	0	0
Aponogeton	0	0	0	1		2	3	0	1	0	0
Haloragaceae	8	0	3	2		4	3	0	0	7	2
Typha	7	6	0	9		22	5	12	2	3	3
Zygophyllaceae	0	0	0	0		0	0	0	0	0	0
Loranthaceae	0	0	0	0		0	0	0	0	0	0
Sterculiaceae	0	0	0	0		0	0	0	0	0	0
Justica-type	2	0	1	2		2	0	1	1	0	0
Aizoaceae	1	1	1	0		0	0	0	0	0	0
Euphorbiaceae undif	2	26	13	19		12	18	48	13	5	8
Brassicaceae	0	1	1	0		0	0	0	3	3	9
Campanulaceae	1	1	0	0		0	0	0	0	0	1
Gunneraceae	1	0	2	0		0	0	0	0	4	1
Polygala	0	0	0	0		0	0	0	0	0	0
Apocynaceae	0	0	0	0		0	0	0	1	0	0
Cardiospermum	0	0	0	0		0	0	0	0	0	0
Rosaceae	0	1	0	0		0	1	0	0	0	1
Nyctaginaceae	0	2	0	0		0	0	0	0	0	0
Moraceae	0	3	0	0		0	0	0	0	0	0
Lauraceae	0	2	1	0		0	4	0	0	0	0
Orchidaceae	0	5	3	2		1	3	1	0	0	0
Combretaceae	0	0	0	0		0	0	0	0	0	1

Sample ID	VVV10.1-46	VVV10.1-47	VVV10.1-48	VVV10.1-49	VVV10.1-50	VVV10.1-51	VVV10.1-52	VVV10.1-53	VVV10.1-54	VVV10.1-55	VVV10.1-56
Depth (cm)	**230**	**235**	**240**	**245**	**250**	**255**	**260**	**265**	**270**	**275**	**280**
Age (ka)	**54.46**	**56.15**	**57.84**	**59.53**	**61.22**	**62.91**	**64.60**	**66.30**	**69.07**	**72.55**	**76.04**
Phytolaccaceae	4	0	11	2		0	11	0	0	4	4
Oxalis	0	3	0	0		0	3	4	0	1	1
Plumbaginaceae	0	0	0	0		0	0	0	0	0	0
Portulaceae	0	0	1	0		0	0	0	0	0	0
Gardenia	6	6	7	0		2	0	2	0	0	3
Meliaceae	0	2	0	0		0	3	0	0	0	2
Bigoniaceae	0	0	0	0		0	0	0	0	0	0
Lamiaceae	0	9	0	0		0	0	0	1	1	3
Convolvulaceae	0	0	0	2		0	0	2	1	0	0
Acan. Tricolporate	0	0	0	0		3	0	0	0	0	0
Acan. Diporate	0	0	0	0		0	0	0	0	0	0
Gentianaceae	0	9	1	1		2	4	2	3	0	5
Potamogetonaceae	0	0	0	0		0	0	0	0	0	0
Rannuculaceae	5	8	4	14		8	0	0	0	0	0
Unidentifiable	0	0	0	1		0	1	0	0	0	0
Broken	2	3	1	3		3	5	0	1	1	0
Unknown	0	1	0	1		0	2	0	1	1	0
Total Pollen	506	502	500	501		502	505	540	501	507	512
Pollen concentration	466419	214206	1155659	286552		1689976	108616	66210	166251	2075238	444187
Botryococcus (1= present, 5= high concentration)											
	5	1	1	1		1	1	1	1	1	1
Monolete	41	68	39	28		7	23	3	11	17	32
Trilete	5	8	12	8		5	7	0	1	5	8
Riccia	0	0	0	1		0	0	0	0	0	1
Ophioglossum	0	0	0	0		0	0	0	0	0	0
Mohria	3	1	1	1		0	11	4	1	1	0
Pellaea	0	1	1	0		0	0	1	0	0	0
Debarya glyptosperma	1	1	0	1		0	0	1	0	1	1
Other zygospores	5	0	3	0		1	1	0	0	0	0
10 - 50 um	39	21	15	27		53	37	6	59	27	17
50 - 100 um	0	0	0	2		0	0	0	0	0	0
>100 um	0	0	0	0		0	0	0	0	0	0
Total Charcoal	39	21	15	29		53	37	6	59	27	17
Charcoal concentration	35949	8961	34670	16587		178424	7958	736	19579	110516	14748

Sample ID	VVV10.1-57	VVV10.1-58	VVV10.1-59	VVV10.1-60	VVV10.1-61	VVV10.1-62	VVV10.1-63	VVV10.1-64	VVV10.1-65	VVV10.1-66	VVV10.1-67
Depth (cm)	**285**	**290**	**295**	**300**	**305**	**310**	**315**	**320**	**325**	**330**	**335**
Age (ka)	**79.53**	**83.02**	**86.51**	**90.00**	**93.49**	**96.97**	**100.46**	**103.95**	**107.44**	**110.93**	**114.42**
Encephalartos	0	0	0	1	0	0	0	0	0	0	0
Euclea	0	0	0	0	3	1	5	9	2	2	1
Grewia	0	0	0	0	0	0	0	0	0	0	0
Ilex	0	2	0	0	0	0	0	0	1	0	3
Morella	20	16	5	5	2	3	3	9	12	8	4
Myrsine	0	0	2	0	0	1	1	0	0	1	2
Myrtaceae	0	1	0	0	1	1	1	0	0	0	0
Olea	0	0	2	0	3	2	8	6	11	10	3
Acacia	0	0	0	0	0	0	0	0	0	0	1
Blechnaceae	0	0	0	0	0	0	0	2	3	0	2
Celastraceae	0	0	0	0	0	1	0	0	1	0	0
Celtis	0	0	0	1	0	0	0	0	0	0	0
Diospyros	0	0	0	0	0	0	0	0	0	0	0
Podocarpus	2	9	27	47	15	74	94	29	41	55	70
Rhus	0	0	2	0	0	0	3	3	0	0	2
Hamamelidaceae	0	0	0	0	0	0	0	0	0	0	0
Pittosporaceae	0	0	1	0	0	0	0	0	0	0	0
Cunoniaceae	0	0	0	0	0	0	0	0	0	0	0
Kiggelaria	0	0	0	0	0	0	2	0	0	0	0
Artemisia	3	4	2	4	4	9	6	2	7	3	5
Pentzia-type	0	1	0	1	0	9	18	0	12	6	3
Proteaceae	0	0	0	0	0	0	1	0	0	0	0
Ericaceae	362	375	366	260	321	124	99	243	197	79	172
Cliffortia	2	7	7	10	12	14	22	20	25	30	16
Bruniaceae	0	0	0	0	0	0	0	0	0	1	0
Anthospermum-type	0	0	0	0	0	0	0	0	0	0	1
Apiaceae	0	0	0	0	0	1	0	0	0	0	0
Fabaceae	2	3	2	1	3	1	0	0	2	0	2
Rhamnaceae	0	0	0	0	0	0	0	0	2	0	1
Rutaceae	0	0	0	0	0	1	0	0	0	0	0
Scroph-type	0	0	0	0	0	0	0	0	0	0	0
Thymelaeaceae	0	0	1	7	6	0	2	1	0	0	0
Passerina	8	4	4	13	13	6	6	4	5	10	4
Galium	0	0	0	0	0	0	1	0	0	0	0
Canthium	1	5	5	1	1	2	1	4	8	6	0
Plantago	2	1	0	0	0	0	7	2	4	0	1
Cyperaceae	0	0	1	0	1	7	14	2	1	11	6
Restionaceae	4	12	11	5	5	10	7	0	2	14	2
Poaceae	25	5	7	25	5	56	29	18	31	51	45

Sample ID	VVV10.1-57	VVV10.1-58	VVV10.1-59	VVV10.1-60	VVV10.1-61	VVV10.1-62	VVV10.1-63	VVV10.1-64	VVV10.1-65	VVV10.1-66	VVV10.1-67
Depth (cm)	285	290	295	300	305	310	315	320	325	330	335
Age (ka)	79.53	83.02	86.51	90.00	93.49	96.97	100.46	103.95	107.44	110.93	114.42
Asteraceae HS	2	0	0	1	1	18	23	5	6	16	1
Stoebe-type	36	19	22	79	53	112	57	50	18	95	26
Geraniaceae	1	2	2	1	3	1	5	5	1	1	1
Onagraceae	0	0	0	0	0	0	0	0	1	0	0
Oxygonum	0	0	0	0	0	0	0	0	0	0	0
Polygonum	0	0	1	1	3	0	4	5	7	5	7
Euphorbia	1	7	7	7	7	17	28	44	50	32	34
Clutia	0	0	0	1	0	0	0	0	0	0	0
ChenAm-type	0	0	1	1	2	2	0	2	3	4	2
Crassula	2	1	0	4	0	1	1	6	0	0	1
Ruschia	0	0	1	0	0	1	0	0	0	0	3
Juncaceae	1	0	2	0	1	6	15	1	4	5	9
Liliaceae	2	0	3	0	0	2	2	3	0	0	0
Iridaceae	0	1	0	2	0	0	0	1	0	0	2
Amaryllidaceae	1	0	0	0	0	0	1	0	0	0	0
Malvaceae	0	0	1	1	0	2	2	2	7	1	9
Scabiosa	0	0	2	0	2	0	0	1	0	0	2
Selaginaceae	0	0	0	0	1	1	2	1	0	0	0
Aponogeton	0	0	0	1	0	0	0	0	0	0	0
Haloragaceae	0	0	0	1	0	5	23	8	5	13	5
Typha	0	0	0	0	1	3	5	4	12	7	32
Zygophyllaceae	0	0	0	0	0	0	0	0	0	0	0
Loranthaceae	0	0	0	0	0	0	0	0	1	0	0
Sterculiaceae	0	0	0	0	0	0	0	0	0	0	0
Justica-type	0	0	1	1	0	0	0	0	2	1	3
Aizoaceae	0	0	1	0	0	0	0	0	0	0	0
Euphorbiaceae undif	10	17	9	3	5	11	11	13	13	15	6
Brassicaceae	0	0	0	0	0	0	3	0	0	1	0
Campanulaceae	0	0	0	0	0	0	0	0	0	0	0
Gunneraceae	0	0	0	0	0	2	0	1	1	1	0
Polygala	0	0	0	1	0	0	0	0	1	0	0
Apocynaceae	0	0	0	0	0	0	0	0	0	0	0
Cardiospermum	0	0	0	0	0	0	0	0	0	0	0
Rosaceae	0	0	0	1	0	0	0	0	0	2	0
Nyctaginaceae	0	1	0	0	1	0	0	0	0	1	0
Moraceae	0	0	0	0	0	0	1	2	0	0	0
Lauraceae	0	0	2	0	2	0	1	3	0	0	0
Orchidaceae	2	0	0	0	1	0	0	0	0	0	0
Combretaceae	0	0	0	0	0	0	0	0	0	0	0

Sample ID	VVV10.1-57	VVV10.1-58	VVV10.1-59	VVV10.1-60	VVV10.1-61	VVV10.1-62	VVV10.1-63	VVV10.1-64	VVV10.1-65	VVV10.1-66	VVV10.1-67
Depth (cm)	**285**	**290**	**295**	**300**	**305**	**310**	**315**	**320**	**325**	**330**	**335**
Age (ka)	**79.53**	**83.02**	**86.51**	**90.00**	**93.49**	**96.97**	**100.46**	**103.95**	**107.44**	**110.93**	**114.42**
Phytolaccaceae	1	2	0	0	9	2	0	2	0	1	2
Oxalis	0	0	2	0	1	0	0	0	0	0	0
Plumbaginaceae	0	0	0	0	0	0	0	0	0	0	0
Portulaceae	0	0	0	0	0	0	0	0	0	0	0
Gardenia	8	8	9	6	4	1	1	0	0	1	0
Meliaceae	0	0	1	1	0	0	1	1	0	0	0
Bigoniaceae	0	0	0	0	0	0	0	0	0	1	0
Lamiaceae	0	0	0	0	2	0	0	0	4	0	0
Convolvulaceae	0	0	0	0	0	0	0	1	0	0	0
Acan. Tricolporate	0	0	0	0	0	0	0	0	0	0	0
Acan. Diporate	0	0	0	0	0	0	0	0	0	2	1
Gentianaceae	1	1	0	0	4	1	1	0	0	0	0
Potamogetonaceae	0	0	0	0	0	0	0	0	0	0	0
Rannuculaceae	1	1	2	1	0	1	5	7	1	7	6
Unidentifiable	0	0	0	0	0	0	0	0	0	0	0
Broken	0	2	1	4	2	0	1	0	2	2	1
Unknown	0	1	1	1	0	0	0	0	1	2	2
Total Pollen	500	508	516	500	500	512	523	522	507	503	501
Pollen concentration	231708	754007	3376348	185237	1843552	689456	278319	3099146	1397861	323099	2476086
Botryococcus (1= present, 5= high concentration)	1	1	1	1	1	1	0	0	0	0	0
Monolete	51	14	29	80	28	9	9	14	12	7	5
Trilete	6	5	11	8	13	9	5	4	6	3	5
Riccia	1	0	0	3	1	0	2	0	0	2	0
Ophioglossum	0	1	1	2	0	0	0	0	0	0	0
Mohria	8	0	3	1	0	0	0	0	0	0	0
Pellaea	3	1	2	4	10	0	0	0	1	0	0
Debarya glyptosperma	0	0	0	5	0	0	0	1	1	0	0
Other zygospores	3	1	1	7	2	0	4	7	8	3	3
10 - 50 um	49	16	4	51	25	3	14	7	25	85	9
50 - 100 um	0	0	0	0	0	0	1	0	1	2	0
>100 um	0	0	0	0	0	0	0	0	0	0	0
Total Charcoal	49	16	4	51	25	3	15	7	26	87	9
Charcoal concentration	22707	23748	26173	18894	92178	4040	7982	41559	71685	55884	44481

Sample ID	VVV10.1-68	VVV10.1-69	VVV10.1-70	VVV10.1-71	VVV10.1-72	VVV10.1-73	VVV10.1-74	VVV10.1-75	VVV10.1-76	VVV10.1-77	VVV10.1-78
Depth (cm)	340	345	350	355	360	365	370	375	380	385	390
Age (ka)	117.91	121.39	124.88	128.37	131.86	135.35	138.84	142.33	145.82	149.30	152.79
Encephalartos											
Euclea											
Grewia											
Ilex											
Morella											
Myrsine											
Myrtaceae											
Olea											
Acacia											
Blechnaceae											
Celastraceae											
Celtis											
Diospyros											
Podocarpus											
Rhus											
Hamamelidaceae											
Pittosporaceae											
Cunoniaceae											
Kiggelaria											
Artemisia											
Pentzia-type											
Proteaceae											
Ericaceae											
Cliffortia											
Bruniaceae											
Anthospermum-type											
Apiaceae											
Fabaceae											
Rhamnaceae											
Rutaceae											
Scroph-type											
Thymelaeaceae											
Passerina											
Galium											
Canthium											
Plantago											
Cyperaceae											
Restionaceae											
Poaceae											

Sample ID	VVV10.1-68	VVV10.1-69	VVV10.1-70	VVV10.1-71	VVV10.1-72	VVV10.1-73	VVV10.1-74	VVV10.1-75	VVV10.1-76	VVV10.1-77	VVV10.1-78
Depth (cm)	340	345	350	355	360	365	370	375	380	385	390
Age (ka)	117.91	121.39	124.88	128.37	131.86	135.35	138.84	142.33	145.82	149.30	152.79
Asteraceae HS											
Stoebe-type											
Geraniaceae											
Onagraceae											
Oxygonum											
Polygonum											
Euphorbia											
Clutia											
ChenAm-type											
Crassula											
Ruschia											
Juncaceae											
Liliaceae											
Iridaceae											
Amaryllidaceae											
Malvaceae											
Scabiosa											
Selaginaceae											
Aponogeton											
Haloragaceae											
Typha											
Zygophyllaceae											
Loranthaceae											
Sterculiaceae											
Justica-type											
Aizoaceae											
Euphorbiaceae undif											
Brassicaceae											
Campanulaceae											
Gunneraceae											
Polygala											
Apocynaceae											
Cardiospermum											
Rosaceae											
Nyctaginaceae											
Moraceae											
Lauraceae											
Orchidaceae											
Combretaceae											

Sample ID	VVV10.1-68	VVV10.1-69	VVV10.1-70	VVV10.1-71	VVV10.1-72	VVV10.1-73	VVV10.1-74	VVV10.1-75	VVV10.1-76	VVV10.1-77	VVV10.1-78
Depth (cm)	340	345	350	355	360	365	370	375	380	385	390
Age (ka)	117.91	121.39	124.88	128.37	131.86	135.35	138.84	142.33	145.82	149.30	152.79
Phytolaccaceae											
Oxalis											
Plumbaginaceae											
Portulaceae											
Gardenia											
Meliaceae											
Bigoniaceae											
Lamiaceae											
Convolvulaceae											
Acan. Tricolporate											
Acan. Diporate											
Gentianaceae											
Potamogetonaceae											
Rannuculaceae											
Unidentifiable											
Broken											
Unknown											
Total Pollen											
Pollen concentration											
Botryococcus (1= present, 5= high concentration)											
Monolete											
Trilete											
Riccia											
Ophioglossum											
Mohria											
Pellaea											
Debarya glyptosperma											
Other zygospores											
10 - 50 um											
50 - 100 um											
>100 um											
Total Charcoal											
Charcoal concentration											